UNITED KINGDOM • CHINA • MALAYSIA

Division of Molecular Therapeutics and Formulation

In-vitro investigations into endocytosis and silencing of siRNA-liposomes

Abdullah Ali D Alshehri, BSc, MRes

Thesis submitted to the University of Nottingham

for the degree of Doctor of Philosophy

August 2017

List of published abstracts

1. In Vitro Study of Lipid-based Nanocarrier for siRNA Delivery in Lung Cancer Cells. Alshehri A, Grabowska A, Stolnik S. *RDD Europe 2015. Volume 2, 2015: 497-500.*

2. Liposome-mediated delivery of siRNA in Lung cancer: formulation design parameters. Abdullah Alshehri, Anna Grabowska and Snow Stolnik. *Journal of Aerosol Medicine and Pulmonary Drug Delivery, August 2015, 28(4): A-1-A25.*

3. Cationic Liposome-Mediated Delivery of siRNA in Lung Cancer. Abdullah Alshehri, Anna Grabowska, and Snow Stolnik. *Proceedings of the Eighth Saudi Students Conference in the UK, 2016: pp. 571-579.*

Abstract

Recent research has focused on exploiting the small interfering ribonucleic acid (siRNA) molecule in cancer therapy. However, the main bottleneck in applying siRNA clinically is its effective delivery to the cytosol of target cell. To design and develop a well-characterised non-viral delivery system to transport siRNA efficiently into A549 (human epithelial lung cancer) cell culture, an siRNA delivery system based on cationic liposomes comprising cationic lipid, 3ß-[N-(N',N'-dimethylaminoethane)-carbamoyl] cholesterol (DC-Chol), and neutral lipid, dioleoylphosphatidylethanolamine (DOPE) was used. Initially, toxicity assays showed that cell viability and cell membrane integrity are highly dependent on the total lipid concentration applied. At the optimised dose of 1.0 mM, liposome formulations did not show considerable, irreversible cellular damage, while dramatically reduced cell metabolic activity (as measured by the MTS assay), marked cell membrane disruption (as measured by the LDH assay) and cell necrosis (as measured by the Annexin V/propidium iodide assay) were found to be associated with exposure to higher doses of cationic liposome formulations. No significant effect was observed for the different ratios of cationic lipid to nucleic acid in the tested range.

The classical film hydration method resulted in a high level of siRNA liposomal encapsulation and stability within RNase, even at relatively low levels of cationic lipid, 3.125:1, as confirmed by gel retardation and the ultrafiltration centrifugation method. In A549 cell culture, siRNA-liposome formulations prepared at different lipid compositions and at selected lipid-siRNA ratios, showed a reasonable cellular

uptake, as observed by flow cytometry and confocal microscopy. A dose response relationship between the siRNA concentration and silencing efficiency was observed. It was noticed that level of luciferase protein silencing is not necessary directly proportional to the extent of cellular uptake; rather the mechanism of endocytosis was suggested to dictate the level of silencing. Cell internalisation pathways were hence probed using a panel of pharmacological inhibitors. Clathrin-mediated, dynamin-dependent pathway, and macropinocytosis - all seem to be involved in the transport of the siRNA-cationic liposomes. It appears that the caveolae-mediated pathway had no important role in the uptake of this delivery system, although the 'non-specificity' in action of inhibitors that cause cholesterol depletion from the plasma membrane, and which significantly affected the internalisation process, makes the difficult to make definitive conclusions.

The level of luciferase silencing in A549-Luc cells, where siRNA uptake is dominated by the clathrin pathway, can almost be doubled using the endosomolytic agent, chloroquine. This indirectly confirms involvement of clathrin-mediated pathway, and is probably due to this cationic liposome system lacking the capacity to escape from the acidic environment of the endosomes/lysosomes. Liposome-siRNA formulations targeting *EGFR* were used to examine the effect on cell proliferation in NSCLC using an *in vitro* model. The siRNA-liposome formulations were able to mediate *EGFR* silencing and to improve cell proliferation. This work therefore contributes to the understanding of the cellular mechanisms involved in the transfer of cationic siRNA-liposome across the cell membrane and has important implications in the area of nanotoxicology and nanocarrier-mediated drug delivery.

Acknowledgements

In the name of Allah, the most gracious and the most merciful. All praises to Allah for the strengths and his blessing in completing this thesis.

First of all, I would like to express my deepest gratefulness to my supervisor, Dr Snow Stolnik-Trenkic, for her supervision, outstanding guidance from the very early stage of this research and providing me with an excellent atmosphere for doing research. Above all and the most needed, she provided me unlimited encouragement and support.

I extend my sincere thanks to my co-supervisor Dr Anna Grabowska and my internal assessor Dr Cynthia Bosquillon for their encouragement, guidance and detailed and constructive comments throughout the work. Not forget, great appreciation go to the rest of Snow's group members who help me from time to time during the lab work. My thanks are also extended to Dr David Onion (flow cytometry) and Dr Hilary Collins (confocal microscopy).

My parents deserve special mention for their inseparable support and prayers. My Father, Ali, in the first place is the person who put the fundament of my learning character and showing me the joy of intellectual pursuit ever since I was a child. My Mother, Zinah, is the one who sincerely raised me with her caring and gently love.

Finally, words fail to express my appreciation to my wife, Amani and my little son, Laith. They were always there cheering me up and stood by me through the good times and bad.

King Abdulaziz City for Science and Technology (KACST) is acknowledged for funding this PhD.

Table of Contents

List of Figures

List of Tables

List of Abbreviations

%	Percentage
°C	Degree centigrade
µg	Micrograms
µl	Microliter
µm	Micrometer
µM	Micromolar
m^2	Meter square
A549	Human lung adenocarcinoma cell line
A549-Luc	Human lung adenocarcinoma-luciferase cell line
AAVs	Adenoviruses, adeno-associated viruses
ABCC1	ATP-binding cassette, sub-family C (CFTR/MRP), member 1
Ago2	Argonaute protein
AKT1	v-akt murine thymoma viral oncogene homolog 1
ALK	Anaplastic Lymphoma Kinase
ANOVA	Analysis of variance
AP2	Adaptor protein complex
ARF6	ADP-ribosylation factor 6
ARH	Autosomal recessive hypercholesterolemia protein
ATCC	American Type Culture Collection
ATPase	Adenylpyrophosphatase
BAR	Bin Amphiphysin Rvs
BCL2	B-cell lymphoma 2
BHQ	Black Hole Quencher
bp	Base pair
BRAF	v-raf murine sarcoma viral oncogene homolog B1
$Ca2^+$	Calcium
CDC42	Cell division control protein 42 homolog
cm^2	Centimetre square
CHCs	Clathrin heavy chains

CMV	Cytomegalovirus
CLCs	Clathrin light chains
CLIC	Clathrin-independent carrier
CPPs	Cell penetrating peptides
CO_2	Carbon dioxide
CSF-1	Colony-stimulating factor-1
CTß	Cholera toxin B subunit
Cy3	Cyanine
dab2	Disabled Homolog 2
DC-Chol	3β-[N-(dimethylaminoethane)carbamoyl] cholesterol
DDR2	Discoidin domain receptor tyrosine kinase 2
DLS	Dynamic Light Scattering
DMEM	Dulbecco's Modified Eagle's Medium
DMSO	Dimethylsulphoxide
DNA	Deoxyribonucleic acid
DOPC	1,2-dioleoyl-sn-glycero-3-phosphocholine
DOPE	Dioleoylphosphatidylethanolamine
DPhyPE	1,2-diphytanoyl-snglycero-3-phosphoethanolamine
DOTAP	N-[1-(2,3-dioleoyloxy)]-N,N,Ntrimethyl ammonium propane
DOTMA	N-[1-(2,3-dioleyloxy)propyl]-N,N,N-trimethylammonium chloride
DPPE	1,2-dipalmitoyl-sn-glycero-3-phosphoethanolamine
dsRNA	double-stranded ribonucleic acid
EDTA	Ethylenediaminetetraacetic acid
EE	Encapsulation efficiency
EGFR	Epidermal Growth Factor Receptor
EIPA	5-(N-Ethyl-N-isopropyl) amiloride
EML4	Echinoderm microtubule associated protein like 4
EPHA2	Epithelial cell receptor protein tyrosine kinase
ERBB2	v-erb-b2 erythroblastic leukemia viral oncogene homolog 2
EtBr	Ethidium bromide
FAM	Fluorescein dye
FBS	Foetal bovine serum
FDA	Food and Drug Administration

FR	Folate receptor
G	Gravity
GEEC	Enriched early endosomal compartment
GEO	Gene Expression Omnibus
GFP	Green fluorescent protein
GTPase	Guanosine triphosphatase
HEPES	Hydroxyethyl piperazineethanesulfonic acid
HII	Inverted hexagonal phase
H^+	Hydrogen ion
Hrs	Hours
IFN	Interferon
IV	Intravenous
K^+	Potassium
kDa	Kilo Dalton
KRAS	v-Ki-ras2 Kirsten rat sarcoma viral oncogene homolog
KSP	Kinesin spindle protein
LDL	Low-density lipoprotein
LDH	Lactate Dehydrogenase
l	Litre
Luc	Luciferase
MßCD	Methyl-β-cyclodextrin
MAPK	Mitogen-activated protein kinase
MB	Molecular Beacon
Mcl1	Myeloid cell leukemia sequence 1
MDR	Multidrug resistance
MET	Met proto-oncogene (hepatocyte growth factor receptor)
MFI	Mean fluorescence intensity
miRNAs	microRNAs
mg	Milligram
min	Minute
mM	Millimolar
mm	Millimeter
mol	Mole

mRNA	Messenger ribonucleic acid
MTS	3-(4,5-dimethylthiazol-2-yl)-5-(3-carboxymethoxyphenyl)-2-(4-sulfophenyl)-2H-tetrazolium
mV	Millivolt
mW	Milliwatt
MYC	V-Myc Avian Myelocytomatosis Viral Oncogene Homolog
N_2	Nitrogen
N/P ratio	Nitrogen to Phosphate ratio
Na^+	Sodium ion
NAD^+	Nicotinamide adenine dinucleotide
NCBI	National Center for Biotechnology Information
nm	Nanometer
NSCLC	Non-small cell lung carcinoma
PBS	Phosphate buffered saline
PEG	Polyethylene glycol
PEI	Polyethylenimine
PES	Phenazine ethosulfate
PDI	Polydispersity index
PI	Propidium iodide
PIK3CA	Phosphatidylinositol-4,5-bisphosphate 3-kinase, catalytic subunit alpha
PKN3	Protein kinase C-related molecule
PLK1	Polo-like kinase 1
pmol	Picomole
PTGS	Post-transcriptional gene silencing
R2D2	Small dsRNA-binding protein
RAC1	Ras-related C3 botulinum toxin substrate 1
RES	Reticuloendothelial system
RISC	RNA-induced silencing complex
RHOA	Ras homolog gene family, member A
RNA	Ribonucleic acid
RNAi	RNA interference
RNase	Ribonuclease
RPS29	Ribosomal Protein S29

RRM2	Ribonucleotide Reductase Regulatory Subunit M2
RT-qPCR	Real-time quantitative polymerase chain reaction
SNARE	soluble N-ethylmaleimide-sensitive-factor attachment receptors
SCLC	Small cell lung carcinoma
SD	Standard deviation
siRNA	Small interfering ribonucleic acid
TAT	Trans-activating transcriptional activator
T*f*	Transferrin receptor
TAE	Tris-acetate-EDTA
TK	Tyrosine kinase
TRL	Toll like receptor
U	Unit
UK	United Kingdom
USA	United State of America
UV	Ultra violet
VEGFA	Vascular endothelial growth factor A
v	Volume
w	Weight

Chapter 1 - Delivery of siRNA Therapeutics

1.1 RNA Interference and Therapeutic Potential

RNA silencing or RNA interference (RNAi) is a gene regulatory mechanism that in nature serves to limit the 'invasion' of 'alien' genetic elements, such as viruses and transposons, before these elements can integrate into the host genome or subvert cellular processes [1]. Basically, the RNAi mechanism is a process in which the expression of a specific protein can be supressed through the degradation of targeted messenger RNA (mRNA) of the gene of interest using RNA molecules such as double stranded RNA (dsRNA) or small interfering RNA (siRNA) [1]. It has been reported that the endogenous, regulatory RNAi mechanism can occur in many organisms, including plants [2], worms, and flies [3].

Napoli and Jorgensen were the first to report an RNAi type of phenomenon in 1990, they referred to as 'co-suppression', following their experiment with *Petunia hybrida* plants [2]. These plants were modified to overexpress chalcone synthase with the aim of intensifying the purple coloration of the flowers. However, the flowers of these modified plants expressed a wide range of pigmentation, and this observation revealed that both the introduced and endogenous forms of the chalcone synthase gene were turned off or silenced to different degrees [2].

RNA silencing was first documented in animals as a biological response to dsRNA by Guo and Kemphues in 1995, following experiments with dsRNA in the nematode *Caenorhabditis elegans* [4]. Injecting dsRNAs into *C. elegans* was found to silence genes whose sequences were complimentary to those of the introduced dsRNAs [4]. However, there were substantial barriers to the acceptance of the idea that dsRNA could trigger sequence-specific gene silencing and how it could induce protein expression silencing.

Subsequently, the American scientists Andrew Fire and Craig Mello were awarded the Noble Prize for Medicine in 2006 for their discovery of the RNAi mechanism of gene silencing by dsRNA, which had been originally published in 1998 [5], and their attempts to use anti-sense RNA as an approach to inhibit gene expression in the nematode worm *C. elegans*, as illustrated in Figure 1.1.

An mRNA molecule encoding a muscle protein was injected into the nematode worm *C. elegans* and no changes were observed in the behaviour of the worm [6]. The genetic code in mRNA is described as being the 'sense' sequence, and injecting 'anti-sense' RNA, which can pair with the mRNA, also had no effect. But when Fire and Mello injected sense and anti-sense RNA together, they observed that the worms displayed peculiar, twitching movements [5]. This illustrates that the mechanism of RNA interference is activated when RNA molecules occur as double stranded pairs in the cell.

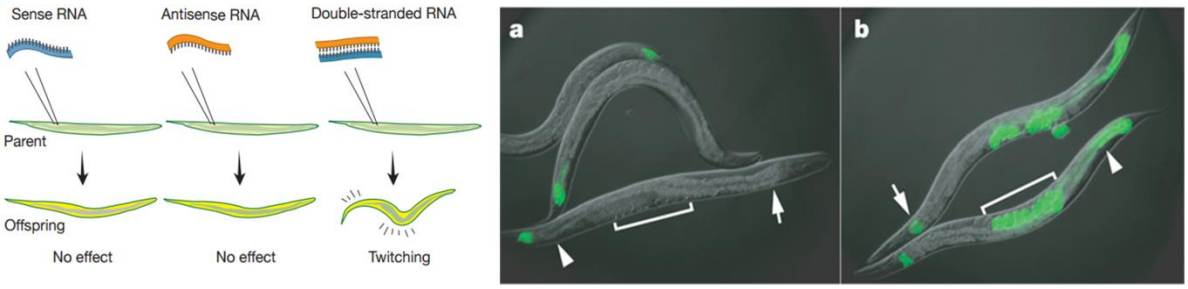

Figure 1.1: Schematic of the experiment performed in the nematode worm C. elegans by Andrew Fire and Craig Mello that led to the discovery of the RNAi mechanism

Silencing of a green fluorescent protein (GFP) reporter in C. elegans occurs when animals feed on bacteria expressing GFP dsRNA (a) but not in animals that are defective for RNAi (b). Adapted from [7].

The RNAi mechanism is initiated when RNA molecules occur as double-stranded pairs in the cell. The dsRNA triggers biochemical machinery which degrades those mRNA molecules that carry a genetic code identical to that of the dsRNA and induce robust suppression of specific genes of interest [8]. The genetic code in DNA determines how proteins are built. The instructions contained in the DNA are copied to mRNA and subsequently used to synthesise proteins. When such mRNA molecules disappear, the corresponding gene is silenced and no protein of the encoded type is made.

In mammalian cells, the delivery of exogenous, long dsRNAs is associated with the activation of the interferon (IFN) pathway, which is part of the defence mechanism against viral infection [9]. The direct introduction of synthetic siRNAs, instead of the long dsRNAs offered the advantage of 'escaping' from the dicer cleavage reaction [1], and leads to effective RNAi without the complication of activating the IFN response [10].

The RNAi mechanism can be induced by endogenous and exogenous small RNAs, including siRNAs and microRNAs (miRNAs), leading to mRNA degradation in the cytosol [11]. siRNAs and miRNAs have similar physicochemical properties but distinct functions. Both are short RNA duplexes that target mRNA to produce a gene silencing effect, yet their mechanisms of action and their requirements for sequence design and therapeutic applications are different [12]. The major difference between siRNAs and miRNAs is that the former inhibit the expression of one specific target mRNA while the latter regulate the expression of multiple mRNAs [13]. The main advantages of exploiting siRNA over miRNA molecules is the lower off-target effect as the siRNA sequence is usually designed to be fully complementary to the targeted mRNA and therefore siRNAs knock-down specific genes, with minor off-target exceptions [14].

siRNA is typically a 21 base pair RNA molecule, which plays a significant function in post-transcriptional gene silencing (PTGS) [15]. Therapeutic approaches based on siRNA involve the introduction of a synthetic siRNA into the target cells to elicit RNAi, thereby inhibiting the expression of a specific mRNA to produce a gene silencing effect, as illustrated in Figure 1.2. The basic steps in the knockdown of expression of siRNA target genes is known as silencing [16]. siRNA is produced in the cytoplasm of a cell as a result of cleavage of dsRNA via an RNase III-like enzyme termed endoribonucleases dicer, or alternatively, siRNA can be introduced directly into the cell. siRNA is then incorporated into a multiprotein complex termed the RNA-induced silencing complex (RISC) [16]. The passenger strand (the sense strand) of an siRNA molecule is released, while the guide strand (the anti-sense strand) binds, with the help of the small dsRNA-binding protein (R2D2), to the RISC, which contains the critical enzymatic component of the RISC, an Argonaute protein (Ago2) that is characterised by PAZ and PIWI domains [16]. Once the

Ago2 is associated with the small RNA, the enzymatic activity conferred by the PIWI domain cleaves only the passenger strand of the siRNA [17]. Strand selection by Ago2 relies on thermodynamic differences of the siRNA duplex; the strand with the less thermodynamically stable, 5' end is favoured as the guide strand towards a complementary mRNA [17]. The guide strand is bound within the catalytic, RNase H-like PIWI domain of Ago2 at the 5′ end, whilst the PAZ domain forms a binding module for the characteristic two nucleotide 3' overhang of the siRNA created by dicer [18]. The anti-sense strand of siRNA then guides the RISC-Ago2 complex to the complimentary target mRNA sequences to be cleaved and therefore inhibits gene expression. The cleavage of mRNA takes place between bases 10 and 11 relative to the 5′ end of the siRNA guide strand resulting in subsequent degradation of the cleaved mRNA [19]. After cleavage, the target RNA lacks those elements which are typically responsible for stabilising mRNAs, namely the 5' end cap and the poly-A tail at the 3' end, so that the cleaved mRNA is rapidly degraded by RNases and the coded protein can no longer be synthesised [20]. On activation by the siRNA guide strand, the RISC can undergo multiple rounds of mRNA cleavage, further propagating gene silencing.

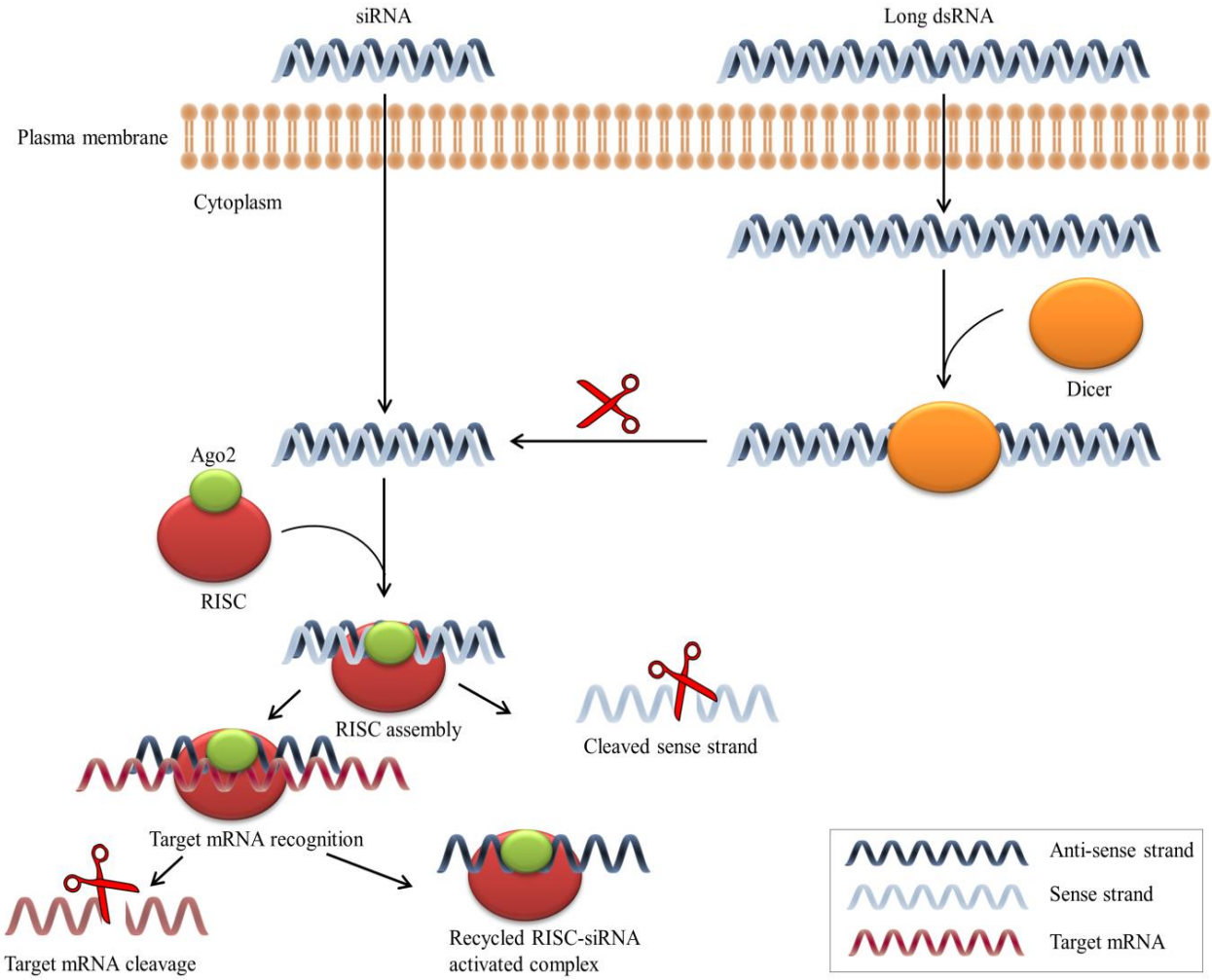

Figure 1.2: RNA interference (RNAi) mechanism

The long dsRNA is introduced into the cell cytoplasm, where it is cleaved into siRNA by dicer. Alternatively, siRNA can be introduced directly into the cell. The siRNA is then incorporated into the RISC, resulting in the cleavage of the sense strand of RNA by Ago2. The anti-sense strand of siRNA binds to the RISC with the help of the protein R2D2 and guides the RISC-Ago2 complex to the complimentary target mRNA sequences to be cleaved. The cleaved mRNA is rapidly degraded by RNases and the coded protein can no longer be synthesised. The activated RISC–siRNA complex can then be recycled for the degradation of multiple mRNA targets. Redrawn from [21].

In 2001, one of the first reports was published to show that mammalian cells can be transfected using siRNA to achieve expression knockdown of a target protein of the gene of interest [1]. The potential advantage of siRNA therapy may be a long(er)-term effect, which is achieved due to the knockdown of protein synthesis [22]. This advantage should have a significant impact on disease treatment through the reduction of dosing frequency [23]. The ability to effectively 'switch off ' any target gene makes RNAi a promising strategy for cancer, viral infections and neurodegenerative disorders [24].

Since its discovery, siRNA has become a highly promising bio therapeutic, which may be utilised as an alternative to chemotherapy in cancer treatment. Atu027 is one of the promising siRNA therapeutics in clinical trials that used as an anti-protein kinase N3 (PKN3) for advanced pancreatic cancer [25]. It is a liposomal formulation that is composed of three lipids: the positively charged lipid β-L-arginyl-2,3-L-diaminopropionic acid-N-palmityl-N-oleyl-amide trihydrochloride (AtuFect01), the fusogenic lipid 1,2-diphytanoyl-snglycero-3-phosphoethanolamine (DPhyPE) and the PEGylated lipid 1,2-distearoyl-sn-glycero-3-phosphoethanol amine-N (methoxy (polyethylene glycol)-2000 (mPEG-2000-DSPE)) complexed with anti-PKN3 siRNA [26]. The siRNAs bind to PKN3 mRNAs, which results in the inhibition of translation and expression of the PKN3 protein and, so, growth inhibition of tumour cells that overexpress PKN3 [26], [27]. In January 2016, Silence Therapeutics completed a phase I/II trial in pancreatic cancer in combination with gemcitabine for patients with locally advanced or metastatic pancreatic adenocarcinoma, and currently Atu027 is available for licensing.

ALN-VSP02 is a stable nucleic acid lipid particle (SNALP) – siRNA delivery system that is formulated by Alnylam Pharmaceuticals to target vascular endothelial growth factor (VEGF) and kinesin spindle protein (KSP1) [27]. SNALP contained the ionisable cationic lipid DLinDMA (1,2-dilinoleyloxy-3-dimethylaminopropane), cholesterol, and ApoE lipoprotein targeting ligand [28]. Targeting of VEGF is proposed to modulate tumour angiogenesis, whereas KSP is essential for mitotic spindle formation in proliferative cells [29]. Both proteins show increased expression in various tumour types. ALN-VSP02 is the first dual targeted siRNA drug used in clinical trial [30].

EphA2 is a tyrosine kinase receptor in the ephrin family that plays a key role in neuronal development [31]. It is expressed to a low degree, primarily in epithelial cells, however overexpression in human cancers has been reported and associated with poor clinical outcome; down-regulation of EphA2 has reduced tumorigenicity in preclinical studies of breast and pancreatic cancer [32]. siRNA formulated with DOPC (1,2-dioleoyl-sn-glycero-3-phosphocholine) neutral liposomes to target EphA2 is currently advancing into phase I clinical trials.

Currently, there are a number of RNAi-based therapeutic agents under investigation in cancer treatment clinical trials, as shown in Table 1.1.

Table 1.1: RNAi-based investigational therapeutics in clinical trials for cancer. *Information collected from (clinicaltrials.gov).*

Drug	Company	Target and Disease	Delivery System	Clinical Trials Gov. Identifier (start date; current status)
siG12D LODER	Silenseed	KRAS, V-Ki-ras2 Kirsten rat sarcoma viral oncogene homolog (Pancreatic Ductal Adenocarcinoma)	Biodegradable polymer matrix	NCT01676259 (December 2015; Phase II not yet recruiting)
DCR-MYC	Dicerna Pharmaceuticals	MYC, V-Myc Avian Myelocytomatosis Viral Oncogene (Hepatocellular Carcinoma)	Lipid	NCT02314052 (June 2016; Phase Ib/II recruiting)
siRNA-EphA2-DOPC	M.D. Anderson Cancer Center	EPHA2, Epithelial Cell Receptor Protein Tyrosine Kinase (Advanced Cancers)	Lipid	NCT01591356 (May 2016; Phase I recruiting)
Atu027	Silence Therapeutics	PKN3, protein kinase N3 (advanced pancreatic cancer)	Lipid	NCT01808638 (March 2016; Phase I/II completed)
TKM-080301	Tekmira Pharmaceuticals	PLK1, polo-like kinase 1 (advanced hepatocellular carcinoma)	Lipid	NCT02191878 (July 2016; Phase I/II completed)
ALN-VSP02	Alnylam Pharmaceuticals	VEGFA, vascular endothelial growth factor and KSP, kinesin spindle protein (Solid Tumors)	Lipid	NCT01158079 (October 2012; Phase I completed)
CALAA-01	Calando Pharmaceuticals	RRM2, M2 subunit of ribonucleotide reductase (R2) (Solid Tumor cancers)	Polymer	NCT00689065 (October 2013; Phase I terminated)
PNT2258	ProNAi Therapeutics	BCL2 (Diffuse Large B-Cell Lymphoma)	Lipid	NCT02226965 (July 2016; Phase II recruiting)
SNS01-T	Senesco Technologies	eIF5A siRNA (B cell lymphoma or plasma cell leukemia)	Polyethylenimine	NCT01435720 (September 2014; Phase II active, not recruiting)
MRX34	Mirna Therapeutics	miR-34 (primary liver cancer)	Lipid	NCT01829971 (June 2016; Phase I recruiting)

1.2 Lung Cancer as a Target for siRNA Delivery

Lung cancer is considered a highly worthwhile target disease in clinical and pharmaceutical research, due to the high rate of incidence and death worldwide [33]. In the UK, more than 45,000 patients are diagnosed with lung cancer each year [34], whilst in Europe, more than 410,000 new cases of lung cancer have been diagnosed in 2012 alone [35]. Cancer statistics feature lung cancer as the main source of cancer related mortality in both males and females [36]. Globally, nearly 1.83 million new cases of lung cancer were diagnosed in 2013, with incidence rates varying across the world [37]. In comparative terms, lung cancer causes more cases of cancer related deaths than any other type of cancer, as shown in Figure 1.3, and three times as many deaths as the next two most lethal forms of cancers, colo-rectal and breast [38].

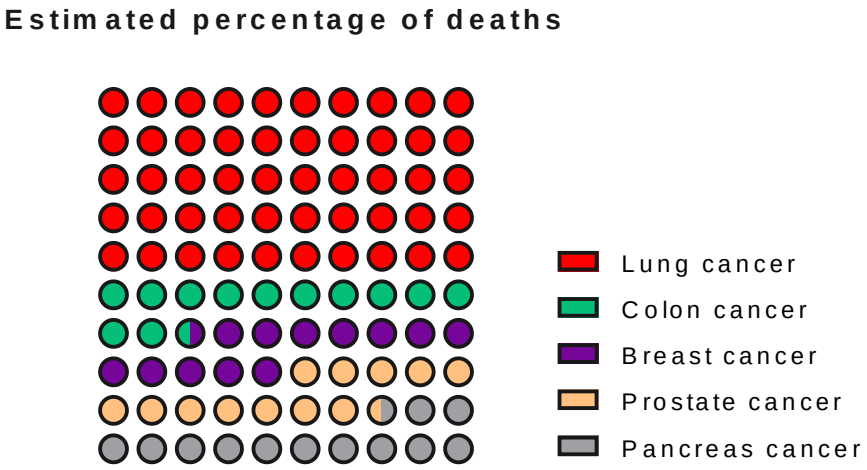

Figure 1.3: Estimated deaths from lung cancer compared to colon cancer, breast cancer, prostate cancer, and pancreatic cancer. *Data taken from* [33], [39].

Lung cancer is defined as a malignancy arising from the cells of the respiratory epithelium and can be divided into two broad categories according to their histology type [40]; small cell lung carcinoma (SCLC) and non-small cell lung carcinoma (NSCLC) [34]. SCLC is a highly malignant tumour type derived from cells exhibiting neuroendocrine characteristics and constitutes a highly aggressive variant, accounting for approximately 15% of cases [41]. NSCLC is the most common type, accounting for more than 85% of all lung cancers and can be further divided into three key subtypes; adenocarcinoma, squamous-cell lung carcinoma, and large-cell lung carcinoma [42], with adenocarcinoma the most prevalent type of NSCLC [40]. Figure 1.4 shows main types of lung cancer.

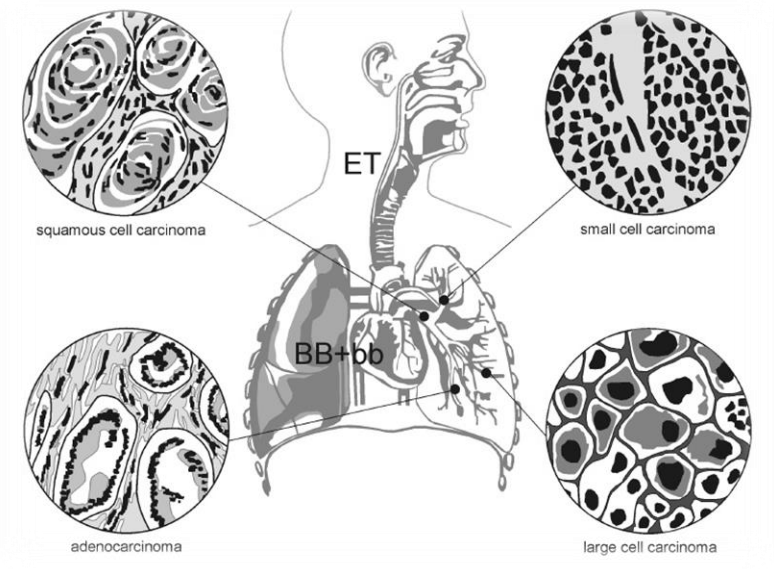

Figure 1.4: Main types of lung cancer and their preferential sites of formation in the human respiratory tract. *Adapted from* [43].

Cigarette smoking has been identified as one of the main causes of lung cancer, especially in males [44], while the contribution of other factors, such as genetic alteration, in the development of the disease remains under investigation [45]. It has been reported that the progression of NSCLC may be a result of changes in the expression profile of some proteins, such as *EGFR* (Epidermal Growth Factor Receptor) [46], *KRAS* (V-Ki-ras2 Kirsten rat sarcoma viral oncogene homolog) [45] and *ERBB2* (Erb-B2 Receptor Tyrosine Kinase 2) [47].

Despite developments in the treatment of cancer and improvements in health care, death rates from lung cancers have not changed significantly over the last 50 years, with a 5-year survival rate of less than 15% [33], [48]. Patients with NSCLC are usually treated by surgery, radiation, and/or chemotherapy [49]; only a low number of lung cancer cases are cured by surgical therapy, and most, especially the metastatic cancers, are chemotherapy dependent [50]. Several chemotherapeutic agents are commercially available and the US Food and Drug Administration (FDA) has approved use of drugs such as Erlotinib, Gefitinib and Cetuximab for the treatment of NSCLC [46]. However, using chemotherapy in lung cancer treatment is usually associated with cytotoxicity, due to very low differences between the effective and lethal dose and the non-specific action of anti-cancer agents [51].

The efficacy of chemotherapy in lung cancer is often limited by the rapid development of multidrug resistance (MDR) during treatment and toxicity to healthy tissue [52], [53]. The severe cytotoxicity of current anti-cancer drugs has prompted research into finding solutions that would reduce the non-specific toxicity and provide higher efficacy of treatment [52]. Whilst conventional chemotherapy is usually limited in its range of

targets, an RNAi based approach can be used to down-regulate almost any gene, including those involved in oncogenesis pathways, cell cycle regulation, angiogenesis and resistance to traditional chemotherapy drugs [54].

Several siRNA-based therapeutics are being evaluated in preclinical trials to be used for lung cancer therapy. So far, there have already been significant developments in siRNAs for primary or metastatic lung cancer *in vivo* models by targeting various types of genes [55]. The delivery of N-[1-(2,3-Dioleoyloxy)propyl]-N,N,N-trimethylammonium chloride (DOTAP) liposomes loaded with doxorubicin/siRNA targeted multidrug resistance-associated protein 1 (MRP1) mRNA as suppressors of cancer cell resistance *via* inhalation resulted in tumour volume reduction of more than 90% in nude mice [56]. Intratracheal administration of liposomes composed of dioleoyl-sn-glycero-3-ethylphosphocholine and cholesterol complexed with siRNA targeted myeloid cell leukemia sequence 1 (siMcl1) significantly silenced Mcl1 mRNA and protein levels in metastatic lung cancer mouse models and reduced the formation of melanoma tumour nodules in the lung [57]. The only siRNA formulation that have been evaluated in clinical trials to treat metastatic lung cancer is CALAA-01, a cationic cyclodextrin-based polymer. It has been designed to be used as a carrier for siRNA to target the M2 subunit of ribonucleotide reductase (RRM2) [58]. RRM2 is a key enzyme in nucleic acid metabolism and is upregulated in many tumour types including lung cancer. RRM2 suppression has been proposed to result in cell cycle arrest and cell death [59]. However, adverse events, related to dose-limiting toxicity have led to CALAA-01 being currently withdrawn from trials.

1.3 Barriers to siRNA Delivery

Synthetic siRNA has shown great potential as a new class of therapeutic nucleic acid for treating many diseases, including cancer, based on its ability to silence gene expression in a sequence specific manner [60]. However, there are multiple barriers to siRNA delivery depending upon the targeted organs and the administration routes. To achieve the full therapeutic potential of siRNA as a therapeutic agent, either 'naked' or when associated with a delivery system, better understanding about the biological processes underlying these barriers will help in the design of more effective delivery systems [61].

1.3.1 Reticuloendothelial System (RES)

The human immune defence system provides excellent protection against any foreign or potentially harmful substances. Recognition of 'foreign' nanoparticles (including siRNA delivery systems) by the RES is one of the main concerns, potentially leading to immune activation. The RES is composed of monocytes and macrophages located in reticular connective tissues, e.g. the spleen, liver and bone marrow [62]. Nanoparticles are rapidly internalised by the cells of the RES upon systemic administration, particularly by macrophages in the liver (Kupffer cells) or spleen [63]. As the RES rapidly eliminates nanoparticles from systemic circulation, it is a major barrier to long term circulation of nanoparticles and their potential targeting to other cellular/tissue targets. The first step of clearance of nanoparticles by the RES is opsonisation, in which nanoparticles are 'coated' with opsonin proteins such as immunoglobulins, which consequently makes them more recognisable to phagocytic cells [64].

Extensive research has been focused on establishing a correlation between surface properties of injected nanoparticles, their opsonisation properties, and *in vivo* biodistribution, including those from our research group [65], [66]. Modification of the nanoparticle surface with chains of hydrophilic and flexible polymers, such as polyethylene glycol (PEG), has been shown to shield nanoparticles from opsonins (e.g. 'stealth' liposomes like Doxil) [67] and, therefore, prevent elimination by the cells of the RES and also reduce complement activation [68]. Addition of PEG and PEG-containing copolymers to the surface of nanoparticles results in an increase in the blood circulation half-life of the particles by several orders of magnitude [69]. This method creates a hydrophilic protective layer around the nanoparticles that is able to repel the absorption of opsonin proteins via steric repulsion forces, thereby blocking and delaying the first step in the opsonisation process [69].

1.3.2 Extracellular Barriers

In order to achieve a gene silencing effect by siRNA therapeutics applied *via* the lung route, multiple extracellular barriers need to be overcome, such as the mucus layer, mucociliary clearance, and the presence of alveolar fluid [70]. Ciliated epithelial cells on mucosal surfaces of the airway are usually covered by a mucus layer secreted by goblet cells and submucosal glands [71]. Mucus is composed of ions, lipids and linear glycoproteins (mucins) that form a dense network of polymeric fibres, with the success of nanoparticle-based siRNA delivery dependent on movement through the pores of the mucin glycoprotein layer [72].

The main function of the mucociliary clearance mechanism is as a defence mechanism to clear any 'trapped' particles from the mucosal surfaces [72]. The mucus layer constitutes

a physical barrier as it increases viscosity at the apical side of lung epithelial cells [73], thereby reducing the diffusion rate of a permeant and hence presenting a considerable hindrance to the ability of a permeant (for example siRNA molecules or a delivery system) to access the targeted pulmonary epithelial cells [72]. Cilia are motile hair-like appendages extending from the surface of epithelial cells and provide the driving force for the mucociliary clearance mechanism [74], where mucus acts as a sticky, fluidic belt that collects and removes foreign particles. Mucin polymers, containing hydrophilic glycosylated amino acid sequences along with hydrophobic cysteine-rich domains, can interact with siRNA nanoparticle carriers through electrostatic interactions, as well as hydrogen bonding and hydrophobic interactions [75]. Consequently, these can become trapped in the mucus and form aggregates or dissociates and release the siRNA 'cargo'.

Alveolar epithelium is an additional defence mechanism and immunological barrier of the respiratory system [76], and are normally covered by a thin layer of surfactant-associated proteins and phospholipids that are produced by the alveolar type-II (AT-II) cells of the lungs [77]. Particle size and surface properties of particulate carriers affect efficient entrapment and uptake by alveolar macrophages, and the particle-macrophage interactions and subsequent uptake can be reduced by optimizing the size and the hydrophilic/lipophilic properties of particulate carriers [78]. It has been reported for example that liposomes with 1–5 μm particle size were taken up at a greater extent by rat alveolar macrophages compared with liposomes that are smaller than 1 μm in an *in vivo* setting [78]. Additionally, surface coating with the hydrophilic polymer (i.e. PEG) makes particles more resistant to opsonisation by serum proteins and hence reduces the chances of their recognition by macrophages [78].

In order to penetrate mucus, synthetic nanoparticles must avoid adhesion to mucin fibres and be small enough to avoid significant steric inhibition by the dense fibre mesh [72]. Recently, it has been demonstrated that nanoparticles as large as 500 nm, if sufficiently coated with a low molecular weight PEG, can rapidly cross physiological human mucus [75]. Coating nanoparticles with low molecular weight PEG is a widely studied mucus penetrating strategy. It has been shown that surface modifying nanoparticles with a high density of low molecular weight PEG (of 2 kDa) can reduce the interactions between particle and mucus [79]. It is hypothesized that coating particles with a high density of low molecular weight (2-5 kDa) PEG may reduce adhesive interactions between nanoparticles and mucus, provided that the molecular weight of the PEG is low enough as to not entangle with mucin fibres and that the PEG density is sufficient to effectively shield the hydrophobic core of the nanoparticle [79] and enables their penetration through the mucus layer.

Treatment of mucus with mucolytics agents may improve the penetration rates of siRNA therapeutics. A novel mucolytic agent Mucinex® (N-acetyl-L-cysteine), a lysine salt of N-acetylcysteine, has the ability to break both hydrogen and disulphide bonds, both of which are important in maintaining the three-dimensional structure of the mucus gel [72]. N-acetyl-L-cysteine has been shown to alter the rheological properties of mucus in a clinical trial of cystic fibrosis patients, either alone or in combination with recombinant human DNase [80]. Recombinant human DNase (Dornase alfa) hydrolyses DNA in cystic fibrosis patient mucus and reduces viscosity in the lungs, promoting increased clearance of secretions [72].

1.3.3 Enzymatic Degradation and Immune System Recognition

Naked, unmodified, and 'unprotected' siRNA molecules are unstable and susceptible to degradation by RNase, resulting in a short biological half-life ($t_{1/2}$ = 2-6 min). RNase is an endoribonuclease with a role in RNA metabolism and the regulation of gene expression [81]. RNase is present in intracellular and extracellular, endosomal and lysosomal environments and can rapidly catalyse RNA hydrolysis. The extra hydroxyl group (2`-OH) on RNA makes it more prone to hydrolysis by serum nucleases than DNA [82]. Serum nucleases cleave the phosphodiester backbone of nucleic acids to facilitate the process of hydrolysis in plasma and cytoplasm [83].

In addition to degradation of siRNA by serum nuclease, it stimulates the innate immune system, resulting in reduced activity. Mammalian immune cells express a sub-family of pattern-recognition Toll-like receptors (TLRs) that recognise pathogen-associated molecules, including viral dsRNA [84]. Several TLRs are involved in the recognition of siRNA, including TLR3, TLR7 and TLR8 [84].

Consequently, these barriers are major obstacles to efficient RNAi therapeutics. One approach that can be applied to increase stability is chemical modification of the siRNA backbone, as illustrated in Figure 1.5. Addition of a 3' phosphorothioate backbone linkage protects against exonucleases and 2' modifications such as 2'-O-methyl or 2'-fluoro protect against endonucleases and abrogate immune-stimulatory activity of siRNA without loss of silencing [85].

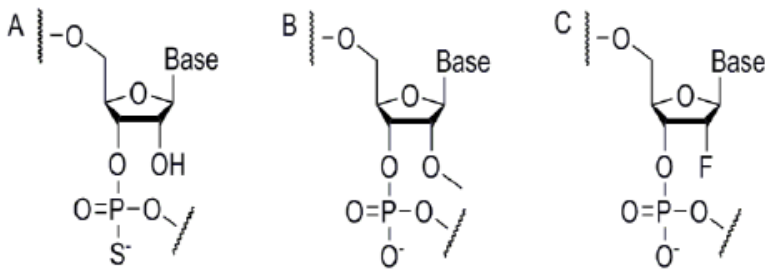

Figure 1.5: Structure of some chemically modified RNAs

(A) 3'-phosphorothioate, (B) 2'-O-methyl, and (C) 2'- fluoro modified RNAs.

In addition to chemical modification of siRNA, the enzymatic degradation and the low serum stability of siRNA molecules can be overcome by the use of nano-sized carriers. Cyclodextrin polymer complexed with siRNA has been reported to fully protect the nucleic acid from nuclease degradation in serum [86]. Non-covalent complexation of synthetic siRNA with low-molecular-weight Polyethylenimine stabilises siRNA and enhances its intracellular delivery [63]. The siRNAs encapsulated in liposomes composed of egg phosphatidylcholine, DOTAP, cholesterol, 1,2-dipalmitoyl-sn-glycero-3-phosphoethanolamine (DPPE) and distearoylsn-glycero-3-phosphoethanolamine-n-[methoxy(polyethyleneglycol)-2000] (PEG-PE), showed a very high stability in serum and remained intact even after 24 hrs incubation [87].

1.3.4 Cellular Uptake

If/once an siRNA therapeutic has successfully passed the extracellular barriers and reached the plasma membrane of the target cells, it then needs to be able to cross the cellular membrane and gain access into the cytoplasm and RISC, the final target of siRNA [21]. However, siRNA is not able to cross the biological membrane on its own

due to its physiochemical properties. siRNA is a negatively charged hydrophilic macromolecule and any siRNA delivery system has to address the issue of cellular uptake [21].

Using high affinity ligands is one of the strategies that can be exploited to improve the interaction of nanoparticles, including siRNA delivery system, with cells facilitating the cellular uptake and subsequent internalisation. The overexpression of receptors on the surface of target disease cells has been widely explored and representative examples of receptors known for active disease cell targeting include folate receptor (FR) and transferrin receptor (T*f*R).

The FR has been reported to be overexpressed in different types of cancer such as lung and colorectal cancer [88]. The natural high affinity of folate for the folate receptor protein allows the selective delivery of folate-drug conjugates to FR-expressing disease cells and trigger cellular uptake via endocytosis [89]. The use of folic acid has many advantages include easy scale-up for clinical applications, facile chemical modification, and low risk of toxicity or immune reactions due to its function as a vitamin [88].

The T*f*R is a cell membrane glycoprotein that plays an important function in facilitating the cellular uptake of iron from the plasma membrane [90]. It is needed for the import of iron into the cell and is regulated in response to the intracellular iron concentration. It imports iron by internalising the transferrin-iron complex through receptor-mediated endocytosis [91]. The receptor is highly expressed in cancer cells making it one of the most attractive targets for cancer therapy by receptor-mediated endocytosis of drug nanoparticles [90].

One of the major pathways that is involved in the cellular uptake of nanoparticles is endocytosis [92]. There are different types of endocytosis mechanisms, which in turn affect the set of barriers that a 'cargo' (e.g. siRNA) may encounter, and each type has its own mechanism of internalisation that leads to different intracellular trafficking of the 'cargo' [92]. Clathrin-mediated endocytosis is the best characterised endocytic pathway, and occurs constitutively in all mammalian cells [93]. The mechanism of endocytosis will be discussed in detail later in Section 1.6.

1.3.5 Endosomal Escape

Once a 'cargo' (e.g. siRNA therapeutic) is internalised by a cell, it eventually be located in the endosomal compartment, particularly if clathrin-mediated endocytosis is the mechanism of uptake [94]. At this stage, siRNA needs to be released from endosomal vesicles into the cytoplasm and then target complimentary mRNA to carry out its RNAi function [94]. During endosomal 'maturation', the pH inside the vesicles gradually decreases from weakly acidic (pH 6.8 - 5.9) in early endosomes to a lower pH and highly acidic environment (pH 6.0 - 4.9) in late endosomes/lysosomes where degradative enzymes, including nucleases are present [95]. Endosomal escape is considered a major bottleneck for the development of an efficacious siRNA delivery system. Therefore, a delivery system must have the ability to escape from endosomal vesicles.

There are several types of endosomolytic agents that can be employed to facilitate endosomal escape, and the common agent is chloroquine, an anti-malarial drug [96]. It prevents the acidification of endosomes, promotes swelling of endosomal vesicle, and destabilises endosomal membranes, thus enhancing endosomal release of the delivery

system [96]. However, due to toxicity problems with chloroquine *in vivo*, the applicability of this agent is limited to the enhancement of transfection *in vitro*. Alternatively, fusogenic lipid such as 1,2-Dioleoyl-sn-glycero-3-phosphoethanolamine (DOPE) can be used to facilitate the endosomal escape, and will be discussed in detail later in Section 1.5.

1.4 Vectors for siRNA Delivery

To overcome the myriad barriers to efficient siRNA delivery, different systems have been designed and studied. There are several generally acknowledged requirements for a good candidate system for siRNA delivery. The optimal siRNA delivery system should be non-toxic, be able to bind and 'condense' siRNA, protect siRNA from RNase, facilitate cell internalisation followed by endosomal escape into the cell cytoplasm, and finally promote efficient gene silencing [58]. In the field of nucleic acids/gene delivery, two classes of delivery systems/vectors/carriers have typically been used: viral vectors, as 'biological' vectors (such as retroviruses, herpes simplex virus, and adenoviruses) [97]; and non-viral carriers, as 'chemical' vectors (such as polymeric nanoparticles and liposomes) [98]. The safety, effectiveness, ease of manipulation or engineering, and the cost of a system's development and potential therapy depend upon the selection of the most suitable delivery vector.

1.4.1 Viral Vectors

To overcome the difficulty of siRNA delivery and to facilitate cellular uptake, viruses can be used. Viruses are extremely efficient vectors for the delivery of siRNA molecules into target cells as they have evolved to specifically enter cells and exploit the cellular

machinery for their own replication [99]. The viral vectors can be classified into two main groups: integrating and non-integrating. Integrating viruses have the ability to integrate their viral genome into the chromosomal DNA of the host cell such as retrovirus and adeno associated virus [100]. The non-integrating viruses deliver their genomes into the nucleus of the target cell such as adenovirus and herpes simplex virus [100].

Viral vectors were shown a promising carrier for gene therapy because of their high delivery effectiveness and *in vivo* tissue specific replication. One of the main advantages of using viral vectors is that a single administration can lead to long-term expression of RNAi therapeutic [101]. However, *in vivo* delivery options become limited in clinical trials due to toxicity and safety concerns, high production costs, low capacity to incorporate nucleic acids, immunogenicity, carcinogenicity and mutagenicity to host cells [97]. The engineered second-generation of viruses show reduced antigenicity *in vivo* by removal of certain coding regions of the viral genome, but the therapeutic efficacy also appears to be reduced [102].

One of the early clinical trials that used engineered adenovirus vector as delivery vehicle for gene therapy resulted in the death of Jesse Gelsinger in 1999 [103]. However, in 2004 China's State Food and Drug Administration approved the first gene therapy for the treatment of head and neck squamous cell carcinoma Gendicine (SiBiono, Shenzen, China), which consists of an adenovirus designed to insert a p53 tumour suppressor gene [104].

1.4.2 Non-viral Vectors

Non-viral delivery vectors for siRNA delivery have recently received great interest because of their potential for large scale production, ease in handling, and reduced specific immune responses relative to viral vectors [105]. Non-viral vectors, such as liposomes, polymers and other non-viral delivery systems could provide effective alternative systems for the efficient delivery of siRNA to targeted cells [105]. The delivery efficiency and toxicity of non-viral vectors is currently under intensive investigation [105].

1.4.2.1 Lipid Based Vectors - Liposomes

One of the non-viral vectors commonly used in the literature are liposomes. Liposomes are able to encapsulate hydrophilic molecules, such as siRNA, which become entrapped in the core, while lipophilic molecules are localised to the bilayer membrane [106]. The efficacy of liposomes, i.e. high levels of tumour cell uptake, can be achieved by modulating the lipid composition, particle size, and surface charge of liposomes [107]. Many commercial transfection reagents (for *in vitro* research use) are lipid based systems, such as Lipofectamine, a cationic liposome-based reagent composed of a 3:1 formulation of the cationic lipid, 2,3-dioleyloxy-N-[2(sperminecarboxamido)ethyl]-nN,N-dimethyl-1-propanaminium trifluoroacetate (DOSPA) and the zwitterionic lipid DOPE [107].

Numbers of cationic lipids have been developed to be used as non-viral carriers of nucleic acid, and all of them share the chemical features of positively charged head group, hydrophobic domain, and linker to connect both. The positive charge of cationic lipid is very important in the interaction with the ‘encapsulated’ nucleic acid. Moreover, the

positive charge electrostatically interacts with the negatively charged glycoproteins and proteoglycans of the cell membrane which may facilitate cellular uptake of such formulated nucleic acids [105]. However, the positive surface charge brings about issues of opsonisation, complement activation, and toxicity limiting feasibility of this approach beyond *in vitro* conditions. As discussed above, PEG is typically used to shield surface charge and its consequences *in vivo* [105]. Liposomes as non-viral vector of siRNA will be discussed in detail later in Section 1.5.

1.4.2.2 Polymers

Polymer based delivery of siRNA has also attracted significant interest to improve therapeutic delivery of siRNA. One of the most common cationic polymers used in research for the delivery of siRNA is polyethylenimine (PEI) [108]. PEI cationic polymer can be synthesised as linear or branched molecules of different molecular weights, and can be substituted with a number of chemical functional groups [108]. Cationic polymers can facilitate endosomal escape via the proton sponge effect [109]. PEIs is considered to have a buffering capability in the low pH environment of the endosome, and in that way assist in releasing the siRNA cargo into the cytoplasm [109]. Increasing the density of the positively charged amino groups in PEI was shown to result in a stronger interaction with the negatively charged phosphate groups of RNA, and better protection of siRNA from degradation [110]. However, PEI has been reported to induce necrosis or cell apoptosis and this tends to increase with higher molecular weight and increased branching [111].

Chitosans belong to the family of natural polysaccharides derived from the common biopolymer chitin and are composed of β-1,4 linked N-acetylated D-glucosamine and D-

glucosamine [112]. They can be chemically produced from chitin by the process of deacetylation with widely varying content of N-acetylated D-glucosamine and chain lengths [112]. Chitosans are considered one of the potential candidates for making polyelectrolyte complexes with siRNA because they show low toxicity both *in vitro* and *in vivo* [110]. One of the main features of chitosans in siRNA delivery is their biodegradability and biocompatibility [113]. The fraction of deacetylated primary amine group of chitosans determine the positive charge density, molecular weight, ratio of chitosan amino groups to RNA phosphate groups, and pKa of the chitosans, and determine the overall charge and size of the chitosan based siRNA polyplexes and eventually the transfection efficiency in target tissues [114]. However, chitosan lacks the buffering capacity at low pH, causing endosomal escape to be a major limiting factor for this polymer [114].

1.4.2.3 Peptides

Cell penetrating peptides (CPPs) are often considered in designing siRNA delivery systems. These short amphipathic or purely cationic peptides of less than 30 amino acids in length possess a positive net charge, and have been demonstrated to be able to penetrate biological membranes and transfer covalently or non-covalently attached bioactive cargos into cells [115]. A wide range of cargos such as proteins, DNA and siRNA can be delivered to cells using CPPs [116]. The most commonly studied CPPs for gene delivery include VP22 and Trans-activating transcriptional activator (TAT).

Peptide VP22 is obtained from herpes simplex virus and exhibits the unusual property of intracellular transport [117]. VP22 appears to be involved in different functions such as

intercellular transport, binding and bundling of microfilaments, inducing cytoskeleton collapse, nuclear translocation during mitosis, and binding to chromatin and nuclear membrane [117]. The TAT peptide is derived from the transactivator of transcription of human immunodeficiency virus type-I [118], and both have been used for DNA and siRNA delivery.

Cationic CPPs are usually non-covalently linked to siRNA via electrostatic interaction, and are being exploited to enhance the cellular uptake of siRNA molecules [119]. The density of cationic charge of CPPs is critical for interaction with cell membrane components prior to internalisation. The peptide/siRNA molar ratio is an essential parameter for the package of siRNA into stable nanoparticles that are capable of crossing the cell membrane [120]. CPPs have significant therapeutic potential; however, overcoming the rate-limiting step of endosomal escape into the cytoplasm remains a major challenge [121].

1.4.2.4 Carbon Nanotubes

Carbon nanotubes are linear elongated cylindrical layers of graphene nanometers in diameter [122]. The graphene layer can be easily modified using various biomolecules, and thereby complexed with siRNA via a covalent or non-covalent bond [123]. Due to their nano-needle structure, they are designed to cross the plasma membrane and enter directly into the cytoplasm via an endocytosis-independent mechanism without inducing cell death [124]. However, the cytotoxicity is the main concern with using carbon nanotubes as drug/gene delivery system. Shvedova *et al*. investigated adverse effects of single-wall carbon nanotubes using a cell culture of immortalized human epidermal

keratinocytes (HaCaT). After 18 hrs of exposure of HaCaT cells to carbon nanotubes, oxidative stress and cellular toxicity were indicated by formation of free radicals, accumulation of peroxidative products, antioxidant depletion, and loss of cell viability [125].

1.5 Liposomes-mediated Delivery of siRNA

One of the non-viral delivery systems that could be a potential carrier of siRNA is liposomes. The advantages of using liposomes as an siRNA delivery carrier are that they can protect the loaded nucleic acid from enzymatic degradation [126], they can deliver a high concentration of therapeutic agents to the target cells [127], they can be designed to accumulate preferentially in tumour tissues [128], they can retain a high plasma concentration of drugs with poor bioavailability [129], and there is the ability to control the efficacy and cytotoxicity by selection of the lipid composition of the liposomes [130].

The biodegradability and biocompatibility of the lipid content are vital advantages of liposomes. Liposomes can be formulated with different types of lipids, such as phosphatidylcholine and phosphatidylethanolamine, which are the main components of the cell membrane [131]. When phospholipids are exposed to water, they form a phospholipid bilayer with the hydrophobic tails facing each other and the hydrophilic heads facing water on both sides [132].

Liposomes have been one of the most extensively studied delivery systems due to their high degree of biocompatibility. Liposome delivery has been considered an option in the delivery of a variety of medicines, including chemo-agents, oligonucleotides, DNA, siRNA, antigens, and proteins. The first liposome pharmaceutical product to be used

clinically to deliver a chemotherapeutic drug was doxorubicin (Doxil®), which was approved by the FDA in 1995 [133], and subsequently more toxic agents, such as daunorubicin [134] and amphotericin B [135], have been successfully entrapped into liposomes, and approved by the FDA. The most recent approved liposomal therapeutic is Marqibo® (vincristine sulfate liposome injection) that was designed to overcome the dosing and pharmacokinetic limitations of standard vincristine [136].

Generally, despite the many benefits of using cationic lipid-based formulations as an siRNA delivery system, the potential toxicity issues need to be addressed before their translation into clinical trials [137]. The chemical structure of cationic lipid plays a key function in predicting the quality of siRNA delivery and cytotoxicity of a liposome [130]. They are usually composed of three main parts: the positive head group, the hydrophobic domain, and the linker moiety, which links the polar and the non-polar parts [63]. The positive head group can be a primary, secondary, or tertiary amine, quaternary ammonium salt, polyamine (spermine), guanidinium, imidazolinium or pyridinium [138], while the linker may be an ether, ester, peptide or carbamate moiety [139], and this determines the chemical stability and biodegradation of a lipid [140]. The lipophilic domain is usually composed of a saturated or un-saturated fatty acyl chain or cholesterol [141].

Studies on entrapment and delivery of siRNA using liposomes have shown that these depend on the physiochemical characterisation of lipids [142]. Using positively charged lipids typically increases siRNA entrapment through the creation of a siRNA/liposome complex (lipoplex) *via* electrostatic interactions with the negative charge of nucleic acid

molecules [60]. The polar and hydrophobic domains of cationic lipids may have dramatic effects on both transfection and toxicity levels.

The most challenging aspect of using liposomes as a delivery system is how to tackle the cytotoxicity of cationic liposomes. Positively charged head groups of cationic liposomes interact with negatively-charged components *in vivo* (e.g. opsonins, serum proteins and enzymes) resulting in haemolysis [143]. The use of cationic liposomes in *in vivo* mouse models produced dose-dependent toxicity and a systemic interferon type I response, attributed in part to activation of TLR4 [144]. Cationic lipids may also activate the complement system and result in their rapid clearance by macrophages of the RES [145]. Careful selection of lipids and formulation strategies may help reduce potential toxicities.

The first cationic lipid based delivery system, N-[1-(2,3-dioleyloxy)propyl]-N,N,N-trimethylammonium chloride (DOTMA) was introduced by Felgner *et al*. in 1987 and is marketed as Lipofectin [146]. The hydrophilic head group of DOTMA is quaternary ammonium, which is more toxic than their tertiary amine counterparts. The ether linker group is too stable to be biodegraded thus causing toxicity [147]. The hydrophobic domain of DOTMA is two unsaturated oleoyl chains (C18), but the effect of the hydrophobic chain on toxicity has not been adequately addressed to date [147]. Traditionally, for aliphatic chains, single-tailed cationic lipids are more toxic and less efficient than their double-tailed counterparts [148]. The initial success of *in vitro* transfection of multiple cell lines with DOTMA sparked a number of attempts to improve the lipid formulation and resulted in the creation of many effective formulations including DOTAP, DOSPA and 3β-[N-(dimethylaminoethane)carbamoyl] cholesterol (DC-Chol).

DOTAP was developed with quaternary ammonium head group and a biodegradable ester bonds which showed lower toxicity than its homologue with ether bonds [149]. The only difference between DOTAP and DOTMA is that the linker is ester rather than ether [147]. DOTAP is completely protonated at pH 7.4, so it is possible that more energy is required to separate the nucleic acid from the lipoplex for successful transfection [150]. Thus, for DOTAP to be more effective in gene delivery, it should be combined with a zwitterionic lipid, as seems to be the case for most cationic lipid formulations [148].

The third cationic lipid that commonly used as a derivative of DOTMA is DOSPA [150]. The main difference between DOSPA and DOTMA is the spermine polyamine group, that is bound to the hydrophobic domain via a peptide bond. The addition of polyamine head group allows for more efficient packing of nucleic acid [150]. DOSPA is usually used with DOPE lipid at a 3:1 ratio to formulate the commercially available transfection reagent Lipofectamine that used in *in vitro* research [151].

One of the most attractive lipids for siRNA delivery is DC-Chol, and was first synthesised by Gao and Huang in 1991. The main advantage of using DC-Chol is the low level of cytotoxicity [152] in comparison to the former lipids, due to the presence of a carbamate group that links the amine head group and the steroid hydrophobic domain [153] (Figure 1.6). This has been shown to be biodegradable and less cytotoxic than other linkers, for example ether [154]. The positive charge functionality plays a significant function in siRNA/lipid complex formation *via* electrostatic interactions [147], and it has also been demonstrated that the tertiary amine group in DC-Chol is less cytotoxic than the quaternary cationic lipids typically used, such as DOTMA and DOTAP [155]. The lipophilic group in DC-Chol is cholesterol, which play an important role in improving the

stability of the liposome lipid bilayer by interaction with the first few alkyl groups of the hydrophobic tail of the combined lipid (such as DOPE). The cholesterol has been reported to be involved in causing the toxic effect of DC-Chol due to the inhibition of protein kinase C [155]. However, the cytotoxicity related to cholesterol-based lipids is significantly lower when the linker moiety is biodegradable [154], as is the case in DC-Chol. DC-Chol was found to have a four-fold reduction in *in vitro* cytotoxicity *versus* Lipofectin [150]. In contrast to cationic liposomes containing fully charged quaternary amines (e.g. DOTMA and DOTAP), DC-Chol, in a 1 : 1 lipid ratio with DOPE, contains a tertiary amine that is charged on 50% of the liposome surface at pH 7.4 [150]. This feature is thought to reduce the aggregation of lipoplexes leading to higher transgene expression. For this reason DC-Chol will be used in this project as a cationic lipid.

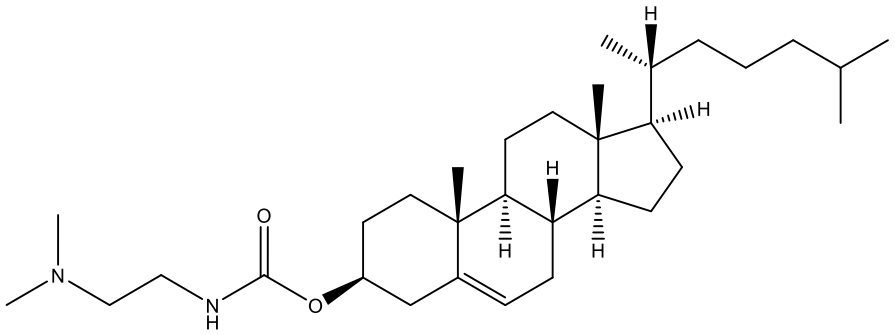

Figure 1.6: Chemical structure of the cationic lipid DC-Chol

Summary of the chemical features of cationic lipids commonly used to formulate liposomes is shown in Table 1.2.

Table 1.2: List of cationic lipids commnly used to formulate liposomes

Cationic lipid	Head group	Linker	Hydrophobic domain
DOTMA	Quaternary ammonium	ether	Fattay acyl chain (C_{18})
DOTAP	Quaternary ammonium	ester	Fattay acyl chain (C_{18})
DOSPA	Polyamine (spermine)	peptide	Fattay acyl chain (C_{18})
DC-Chol	Tertiary amine	carbamate	Cholesterol

To increase the transfection efficiency and the stability of liposome bilayer formation, cationic lipid is usually combined with a zwitterionic helper lipid, such as DOPE, which is the most widely used helper lipid, or DOPC. Lipids are known to adopt a number of different structural phases when suspended in an aqueous media [156]. These phases including micellar, lamellar and inverted hexagonal phase, as illustrated in Figure 1.7.

The specific phase adopted is mainly dependent on the packing parameter ($P = \frac{v}{aLc}$), and defined as the ratio of the hydrophobic tail volume, v, and the product of the hydrophilic headgroup area, *a*, and the hydrophobic tail length, *Lc* [150]. When P is greater than 1 (i.e., the area occupied by the hydrophobic region is larger than head group), the lipid will adopt the inverted hexagonal phase, which is a bilayer destabilising structure. However, when P is less than ½, the lipid monomer will be cone-like shaped and will assemble into micellar phases. Thus, when P possesses a value between ½ and 1, lipid monomers will adopt lamellar phases [157].

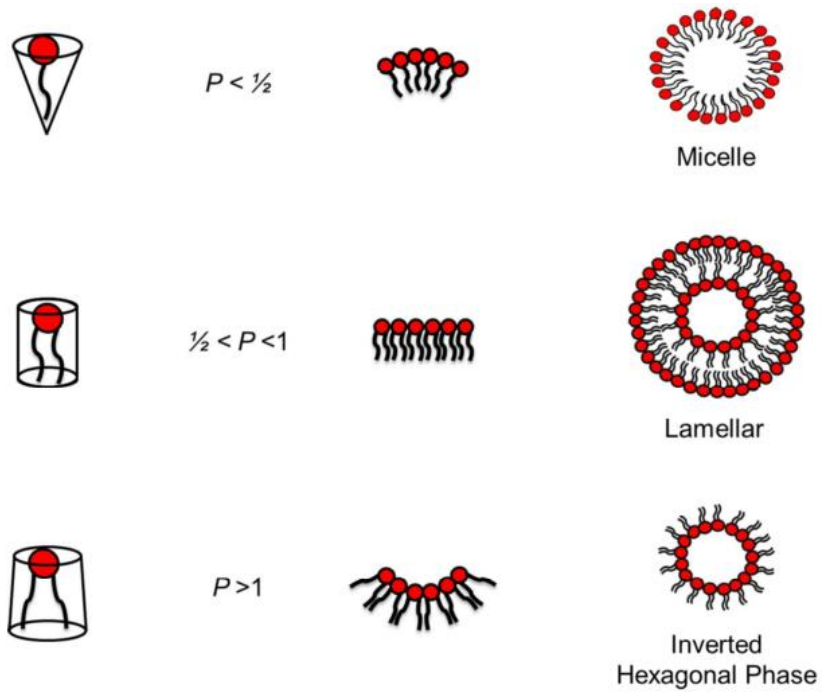

Figure 1.7: Schematic representation of the packing efficiency of lipids and their resulting phase structures

A packing parameter less than ½ confers a cone-like shaped structure that assembles into micellar phases. Values between ½ and 1 allow formation of the lamellar phase (bilayers). For P > 1, the negative curvature leads to the formation of the inverted hexagonal phase. Adapted from [158].

Results have shown that the use of DOPE *versus* DOPC as the zwitterionic helper lipid yields higher transfection efficiencies in many cell types, thought to be due to a conformational shift to an inverted hexagonal packing structure that is imparted by DOPE (Figure 1.8) in endosomes at pH lower than neutral [150]. Studies have suggested that a hexagonal conformation allows the escape of the system/complexed nucleic acids from endosomal vesicles *via* destabilisation of the vesicle membrane [150].

DOPE lipid is shown to help in increasing liposome transport across the cell membrane and therefore improves transfection of a target cell [159]. The hydrophobic region of DOPE contains two unsaturated aliphatic tails, which is reported to have lower cytotoxicity and show more efficient transfection than single-tailed molecules [155]. However, the relationship between the nature of the hydrophobic moiety in lipids and the cytotoxic effects remain unclear [155]. Furthermore, the linker in DOPE is ester, which is biodegradable and a non-toxic group [147].

A primary amine head group is reported to be safer and more efficient in the transfection of human cancer cell lines than a secondary, tertiary and quaternary amine [147]. The zwitterionic property of DOPE is due to the presence of a phosphate group alongside the amine. Due to the important structural and membrane destabilizing features of DOPE, it will be combined with cationic lipid DC-Chol to formulate our cationic liposome delivery system in this project.

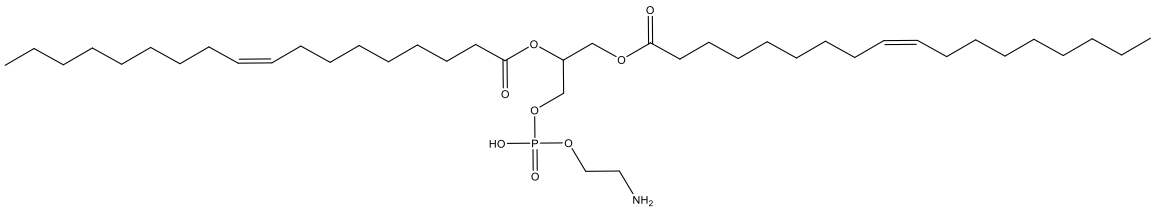

Figure 1.8: Chemical structure of the zwitterionic lipid DOPE

In fact, the most important barrier in the delivery of siRNA molecules using cationic liposomes is how to transfer the siRNA out of the endosomal compartment, as this requires both endosome escape and sufficient de-assembling of the formulation [160], as illustrated in Figure 1.9. The positive charge head groups of cationic liposomes can potentially interact with the anionic lipid present in the endosomal membrane to form ion pairs [161], which form the inverted hexagonal phase and thus destabilise the endosomal membrane by excluding surface bound water [162]. The inverted hexagonal phase is an intermediate structure formed when two lipid bilayers 'fuse' with each other. This interaction leads to the fusion of a liposome formulation with an endosome vesicle and the release of the encapsulated nucleic acid molecules into the cytosol of the targeted cells.

Liposomes formulated with a helper lipid, such as DOPE, have been reported to facilitate the endosomal escape of the delivery system [109], [163]. The ethanolamine head group of DOPE displays a high tendency to form the inverted hexagonal phase, especially within late endosomes where the pH is more acidic [164]. Zuhorn *et al.* hypothesised that the formation of the hexagonal phase of DOPE containing lipoplexes plays a prominent role both in the dissociation of nucleic acids from lipoplexes and in the efficient destabilisation of the endosomal membrane [165].

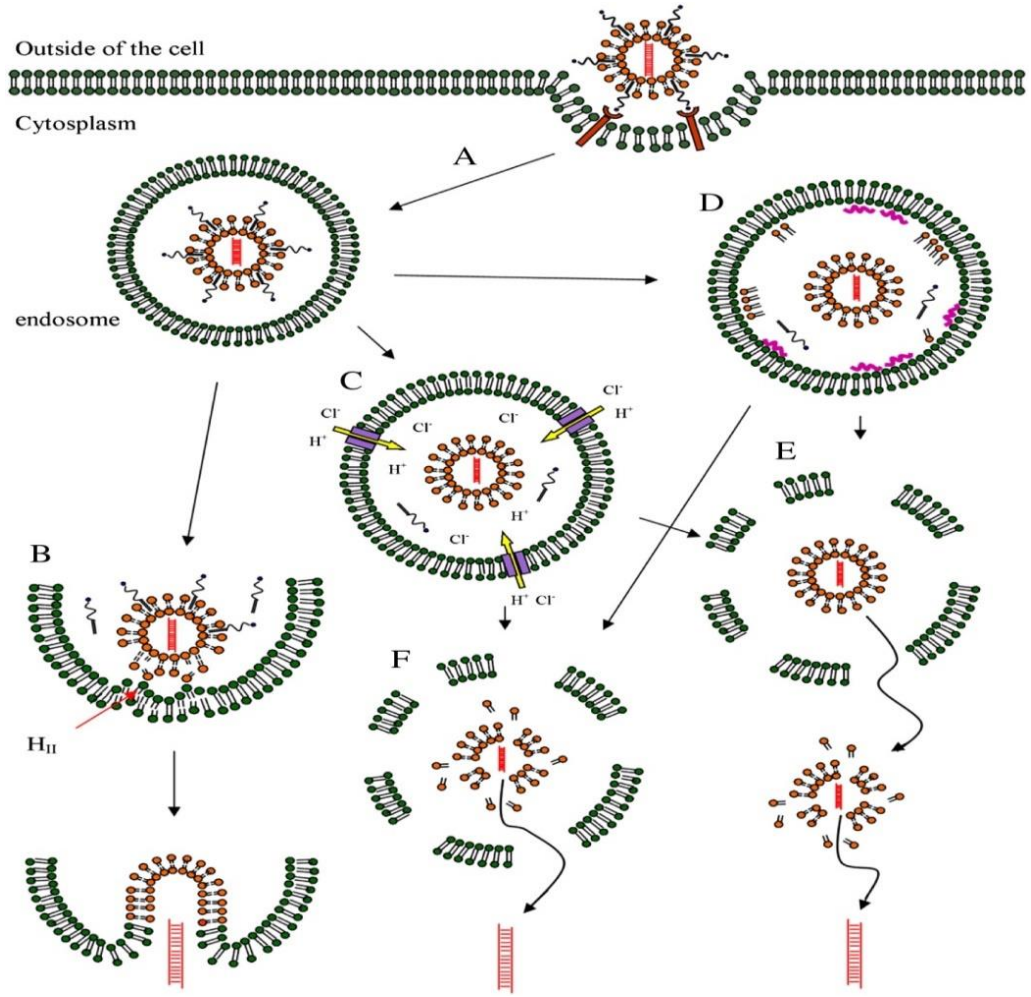

Figure 1.9: Endosome escape in liposomes-mediated siRNA delivery

A*. Liposomes containing siRNA (shown as orange lipid bilayer and red siRNA) are taken up by the target cell via endocytosis.* ***B****. The cationic lipid of the liposomes forms ion pairs with the anionic endosomal lipid and can further form the inverted hexagonal phase (HII). This leads to the fusion of the liposomes with the endosomal membrane and release of the siRNA into the cytoplasm.* ***C****. Liposomes containing molecules having buffer capacity in endosomal pH range can trigger the proton sponge effect that causes the influx of* Cl^- *and swelling of the endosome.* ***D****. Free highly positively charged molecules (shown with orange coloured cationic lipid) can interact with the anionic endosomal membrane and destabilize it by excluding water.* ***E****. Intact liposomes may escape from the ruptured endosome and de-assemble in the cytoplasm and release siRNA if the particle is not too large for the "holes" of the ruptured endosome.* ***F****. Liposomes may also de-assemble inside the endosome and directly release siRNA out of the ruptured endosome. Adapted from* [166].

1.6 Pathways of Cellular Internalisation and Trafficking

In order to formulate a well-characterised siRNA delivery system and to achieve its effect, an siRNA delivery system must be effectively transported across the cell plasma membrane into the cell interior [167]. The cellular internalisation pathway has received much attention in the nanomedicine field [168]. Eukaryotic cells are able to take up macromolecules and particles from the surrounding medium through the plasma membrane by a distinct process called endocytosis [169]. Endocytosis refers to the cellular uptake of macromolecules and solutes into membrane-bound vesicles derived by the invagination and pinching off of pieces of the plasma membrane [170].

There are different entry pathways into mammalian cells, depending on the cargo and on the protein machinery that facilitates the process. Endocytosis is a basic cellular process that is used by cells to internalise portions of the plasma membrane, including concomitant engulfment of extracellular fluid and extracellular material by vesicular carriers [171]. The cargo and membrane components of the vesicles can subsequently either be sent back to the plasma membrane, thus recycling its content back to the cell surface, or the components can be transported to the late endosomes/lysosomes for degradation [172].

Three modes of endocytosis have been defined: fluid-phase, adsorptive, and receptor-mediated endocytosis. Fluid-phase endocytosis refers to the bulk uptake of solutes in the exact proportion to their concentration in the extracellular fluid [173]. This is a low-efficiency and nonspecific process. In contrast, in adsorptive and receptor-mediated endocytosis, macromolecules are bound to the cell surface and hence concentrated before internalisation [173]. In adsorptive endocytosis, molecules preferentially interact with

generic complementary binding sites (e.g. via lectin or charged interaction). The bound molecules then largely follow the fate of the plasma membrane. In receptor-mediated endocytosis, certain ligands can bind to receptors on the cell surface and become concentrated before internalisation [173]. The efficiency of receptor-mediated endocytosis reflects both the affinity of the ligand-receptor interaction and the concentration of these complexes in clathrin-coated pits.

The term endocytosis was established by Christian de Duve in 1963 [174] to include both the ingestion of large particles which is known as phagocytosis (cell eating) and the uptake of fluids or macromolecules in small vesicles which is known as pinocytosis (cell drinking). Phagocytosis is typically restricted to specialised mammalian cells, whereas pinocytosis occurs in all cells [175]. Endocytic mechanisms can be clathrin-mediated endocytosis, caveolae-mediated endocytosis, macropinocytosis, and clathrin- and caveolae-independent endocytosis, as shown in Figure 1.10. This is a complex and currently much evolving research field.

Different aspects/features have a significant influence on which endocytic pathway is used in specific situations, including the nature of the transported molecule/particle (size, surface properties) [176], the nature of its interactions with the cell membrane (e.g. receptors) [177], and the mechanism of formation of an endocytic vesicle and its size [178]. It is generally believed that nanoparticles with cationic surface nature (e.g. cationic liposomes) are internalised across the plasma membrane through endocytosis [179].

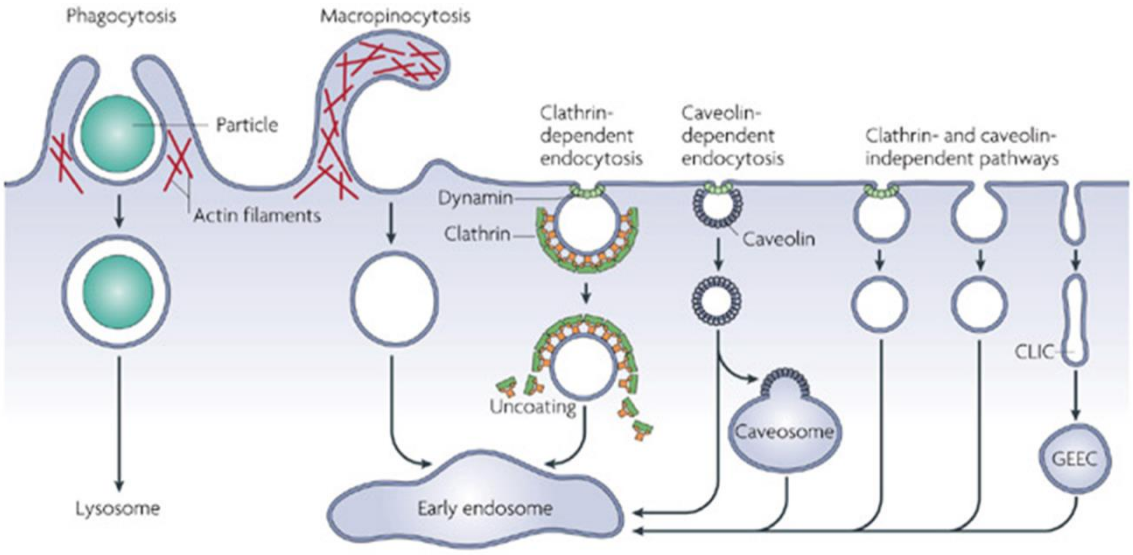

Figure 1.10: Schematic representation of cell endocytosis pathways. *Adapted from* [180].

1.6.1 Clathrin-mediated Endocytosis

Clathrin-mediated endocytosis is the most thoroughly characterised and investigated pathway in the literature. It enables the internalisation of materials, such as pathogens, nutrients, antigens, growth factors and receptors, from the surface into cells via clathrin-coated vesicles [181]. Clathrin-mediated endocytosis was previously referred to as receptor-mediated endocytosis, but it is now clear that this is a misnomer, because most pinocytic pathways involve receptor-ligand interactions [170]. The formation of clathrin coated pits is usually a result of the assembly of the cytosolic-associated protein clathrin, on the intracellular side of the plasma membrane [182].

Structurally, the clathrin coating is a three-dimensional array of triskelia, and each triskelion consists of three clathrin heavy chains (CHCs; 1,675 residues; approximately 190 kDa) and three clathrin light chains (CLCs; 25–29 kDa), each with three-fold

rotational symmetry [183]. The size of clathrin-coated vesicles depends on the size of its cargo, with an observed upper limit of about 200 nm external diameter, as in the case of virus uptake [184].

There are several adaptor proteins required for the formation of clathrin coated pits, such as adaptor protein (AP2), autosomal recessive hypercholesterolemia (ARH) protein and disabled homolog 2 (dab2) protein [185], and these proteins have been demonstrated to be involved in the interaction between cargo and clathrin, and to facilitate their internalisation into the cells [186]. The AP2 complex is essential for linkages between cargo molecules and clathrin [183]. ARH and dab2 have been shown to function as cargo-specific adaptor proteins that facilitate internalisation of low-density lipoprotein receptor (LDLR) [185]. In addition, dynamin guanosine triphosphatase (GTPase) is able to regulate a later conversion of membrane invagination into a vesicle [187]. Epsin-family membrane proteins, such as epsin 1, contribute to membrane curvature-driving proteins in clathrin-coated vesicle budding, via the insertion of an amphipathic helix [188].

Accessory proteins can also contribute in the formation of clathrin coated pits by performing scaffolding/coordination functions or by recruiting other endocytosis-related proteins [189]. For example, BAR (Bin Amphiphysin Rvs) domain proteins and N-BAR domain-containing proteins (such as sorting nexin-9 and amphiphysin) can not only stabilise membrane curvature, but they can also link clathrin to AP2 and recruit dynamin to the neck of the budding vesicle [189].

The formation of a clathrin-coated vesicle is a multi-step process as shown in Figure 1.11. The uptake of cargo molecules by the clathrin-mediated pathway is initiated by cargo-

specific receptors binding to the cell membrane, and subsequently invagination of the membrane to form a coated pit occurs [186]. Clathrin triskelia can assemble into hexagonal and pentagonal lattices, and these lattices then bind to the cell membrane via AP2, leading to invagination of the membrane to form a coated pit. Invaginated coated pits are involved in the engulfment of cargo molecules and their receptors to form clathrin vesicles [190]. Dynamin (GTPase) is then recruited to the neck of the coated pit and assembles into spirals to mediate membrane fission and release of the coated vesicle from the cell membrane [191], [192] which then fuse with early endosomes, and are sorted to either late endosome/lysosomes. Once the clathrin-coated vesicle is released from the cytosol, clathrin coats disassemble to leave the naked transport vesicle ready for fusion with endosomal compartments. The pH environment in early endosomes decreases from a physiological pH of 7.4 to around 6.0, as maturation to late endosomes occurs the pH falls further to around pH 5, followed by fusion with lysosomes containing high concentrations of degradative enzymes [193].The coat components are transported back to the cell membrane to contribute to another round of endocytosis.

In terms of siRNA delivery, clathrin-mediated endocytosis can be targeted by using certain ligands, such as transferrin [194]. This results in an increase in the internalisation of the particles and offers the possibility of targeting specific cells that substantially overexpress the transferrin receptor. However, siRNA delivery systems that are internalised through clathrin-mediated endocytosis are normally trapped in endosomes followed by enzymatic degradation in lysosomes, and the final result is that siRNA molecules have little or no access to their target cytoplasmic sites.

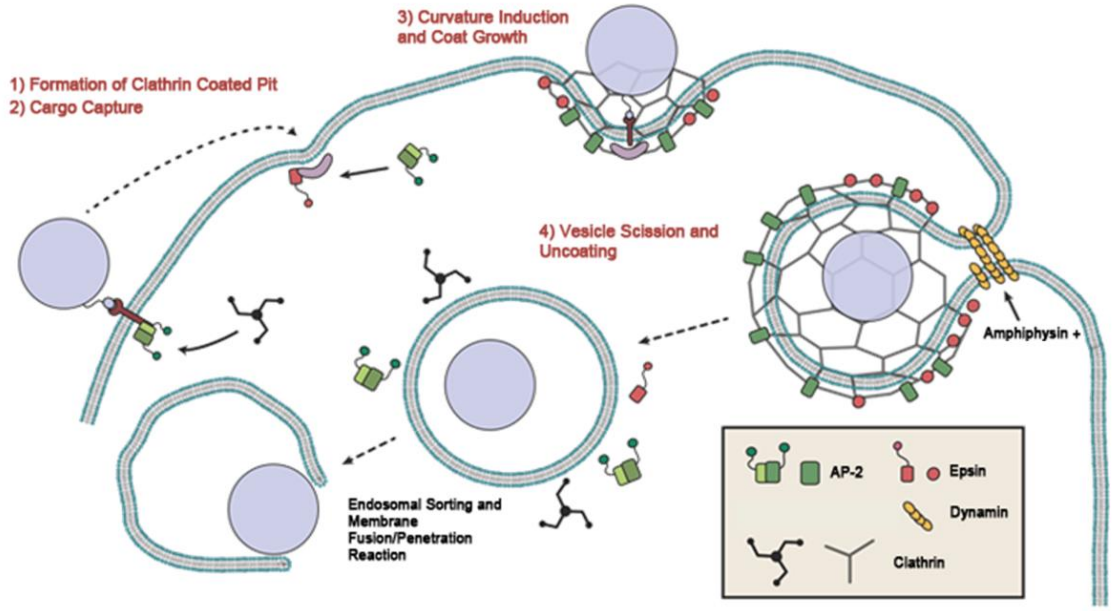

Figure 1.11: Overview of the steps involved in clathrin-mediated endocytosis

Clathrin is first assembled at the intracellular surface of the plasma membrane. After formation of a clathrin-coated pit, invagination occurs. The invaginated pit pinches off from the plasma membrane to form a clathrin-coated vesicle. The vesicle loses its clathrin coat and progresses to an endosome which is acidified. The endosome is then transported to a lysosome where the internalised material is degraded. Adapted from [195].

1.6.2 Caveolae-mediated Endocytosis

Up until the early 1990s, there was controversy over the existence of pathways that may be independent of clathrin. Early studies on the uptake of bacterial toxins using pharmacological perturbations that were considered to interfere with clathrin-dependent uptake did not block all endocytosis [196]. This finding hinted that other endocytic pathways may exist.

Caveolae are inverted omega shaped invaginations of the plasma membrane of around 50–100 nm in diameter, which are involved in endocytosis, transcytosis and signal transduction in mammalian cells [197], [198]. The main component of the caveolae-mediated pathway is a protein called caveolin, whilst cholesterol is required to maintain structural integrity [199]. Caveolin is a dimeric protein that binds cholesterol, and has carboxyl and amino termini that are located in the cytosol and a hydrophobic loop inserts itself into the membrane [200]. From a structural point of view, caveolin-1 presents as a 101 amino acid sequence in the N-terminal domain, a 33 amino acid sequence in the transmembrane domain, and a 44 amino acid sequence in the C-terminal domain [200], [201].

Caveolae are a feature of many mammalian cells, including adipocytes, endothelial cells, smooth muscle cells, and fibroblasts [202]. It has been reported that caveolae-mediated endocytosis contributes to the internalisation of different pathogens, such as Simian virus 40, and cargos, such as membrane components and extracellular ligands [203]. Caveolae, following separation from the cell membrane, are not characterised by a drop in pH, and most pathogens that are internalised by caveolae can be directly transported to the Golgi and/or endoplasmic reticulum, as illustrated in Figure 1.12, thus avoiding normal lysosomal degradation [204].

Christine *et al.* have shown that the dynamin molecular machinery, responsible for the separation of coated vesicles from the cell membrane [205], is shared between the caveolae-mediated and clathrin-mediated pathways. However, the caveolae pathway contrasts with the clathrin pathway in that it seems to be a slower process and ‘uses’ smaller vesicles [206]. The caveolae trafficking process involves invagination of the cell

membrane via caveolin polymerisation, followed by membrane budding inward [207], [208]. Cargo can be delivered by the caveolae pathway to a specific endosomal compartment with a neutral internal pH called a caveosome, or across a cell to the opposite cell membrane surface (transcytosis), rather than leading to a lysosome; therefore, degradation of the cargo is avoided [197]. From siRNA delivery point of view, the caveolae-mediated internalisation can be an attractive option as it may overcome lysosomal degradation issues, if escape of the carrier/siRNA from caveosome can be achieved.

Free caveolar vesicles can dock at specific membranes proteins after transcytosis and fuse with the membrane to release their cargo into the perivascular space, and this is dependent on the presence of members of the SNARE complex (soluble N-ethylmaleimide-sensitive-factor attachment protein receptors) [209]. Studies have shown that clathrin can contribute to transcytosis, but it is responsible for less than 1% of the cargo transported by this route [209]. For this reason, caveolae mediated endocytosis is important process from a drug delivery perspective. It may increase the absorption of nanomedicines across e.g. epithelium. Drug carriers that target caveolae in the vascular endothelium can pass through this barrier to deliver their load in perivascular space. For example, albumin, which binds to its receptor gp60 with the aid of caveolae, can be delivered from the luminal to the basolateral side of cell monolayer, and also paclitaxel-containing nanoparticles that are coated with albumin can be transported to the tumour tissue via transcytosis [209].

Folate ligands conjugated with nanoparticles have been shown to achieve cellular uptake via caveolae-mediated endocytosis. During the uptake of folic acid, it is thought that the

ligand binds to folate receptors that are clustered in invaginated caveolae. Once internalised, the ligand is released from the receptors, and 5-methyltetrahydrofolic acid moves across the caveolar membrane and remains it stays in the cytosol following modification with polyglutamate, and the caveolae begin to reopen again to the extracellular space to repeat the cycle [210].

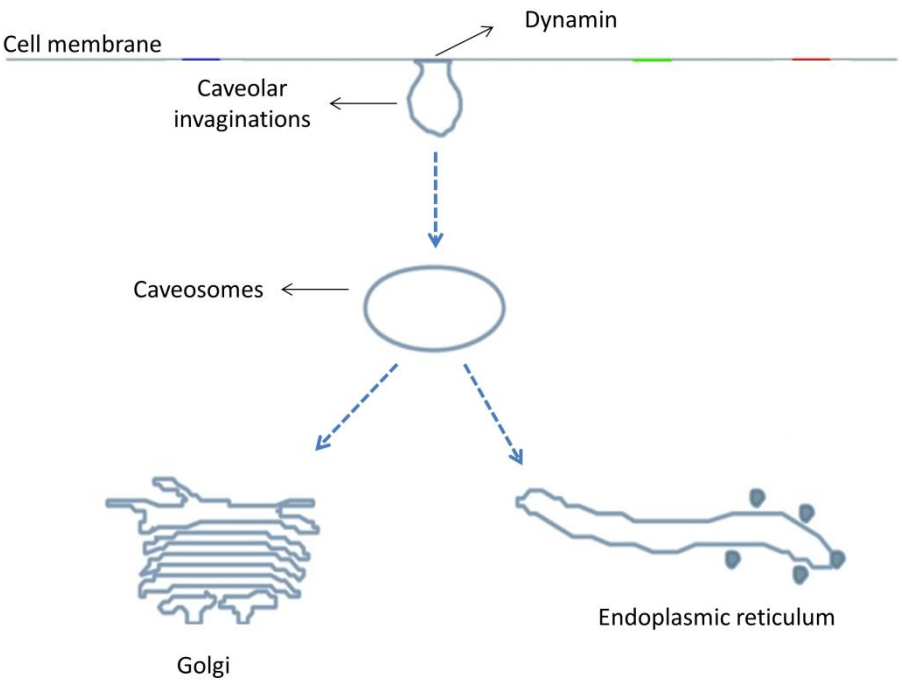

Figure 1.12: Cellular internalisation of nanoparticles via the caveolin-mediated pathway

Caveolae do not suffer a drop in pH, and most pathogens that are internalised by caveolae can be directly transported to the Golgi and/or endoplasmic reticulum.

1.6.3 Macropinocytosis

Macropinocytosis is a form of endocytosis that accompanies plasma membrane ruffling, as illustrated in Figure 1.13, and normally occurs in response to growth factor stimulation, such as macrophage colony-stimulating factor-1 (CSF-1), epidermal growth factor (EGF) and platelet-derived growth factor or tumour-promoting factor, such as phorbol myristate acetate [211]. It is an actin-dependent process initiated from surface membrane ruffles that give rise to large endocytic vacuoles called macropinosomes [172]. Most of the lamellipodia formed will retract back into the cell. However, a subset of lamellipodia may fold back onto themselves and fuse with the basal membrane creating large, irregular shaped vesicles termed macropinosomes [172].

This endocytic pathway offers an efficient route that mediates the non-selective uptake of macromolecules and fluid due to the large diameter of the macropinosomes at around 0.5-10 μm [212]. A study has found that RAC1 (Ras-related C3 botulinum toxin substrate 1) and actin cause formation of membrane ruffles, and macropinocytosis requires cholesterol for the recruitment of activated RAC1 to these sites [213].

Macropinosomes can be pinched off from the cell surface of the plasma membrane by cutting the circular ruffles from the internal cell surface by dynamin GTPase [214]. However, it has been reported that lamellipodia macropinosomes are pinched off from the cell surface without the aid of dynamin. Macropinosomes containing cargo can travel into the cytosol and fuse with lysosomes [209]. After the formation of macropinosomes, these vesicles lose their F-actin and their intracellular fate differs, depending on the cell type.

When cargo and surrounding fluid are internalised to form large endocytic vesicles, the macropinosomes, which range from 0.5 to 10 μm in diameter, can travel into the cytosol and fuse with lysosomes [209]. However, in human epidermoid carcinoma (A431) cells, the macropinosomes return to the cell membrane and the contents are released into the extracellular space, so the destination of macropinosomes depends mainly on the cell type [172]. Macropinosomes are thought to be inherently leaky vesicles compared with other types of endosomes [215].

Macropinocytosis is actin cytoskeleton dependent; therefore, drugs that disrupt the actin cytoskeleton can inhibit this process [216]. Amiloride is an inhibitor of the exchange of Na^+/H^+ in the plasma membrane and can inhibit macropinocytosis [216]. Macropinocytosis has recently received attention as an entry route for gene and drug delivery. Recent reports have established that the uptake of the TAT peptide and its cargos occurs by macropinocytosis [118], [217]. This pathway provides some advantageous aspects such as increased uptake of macromolecules, the avoidance of lysosomal degradation and the ease of escape from macropinosomes because of their relatively leaky nature [218].

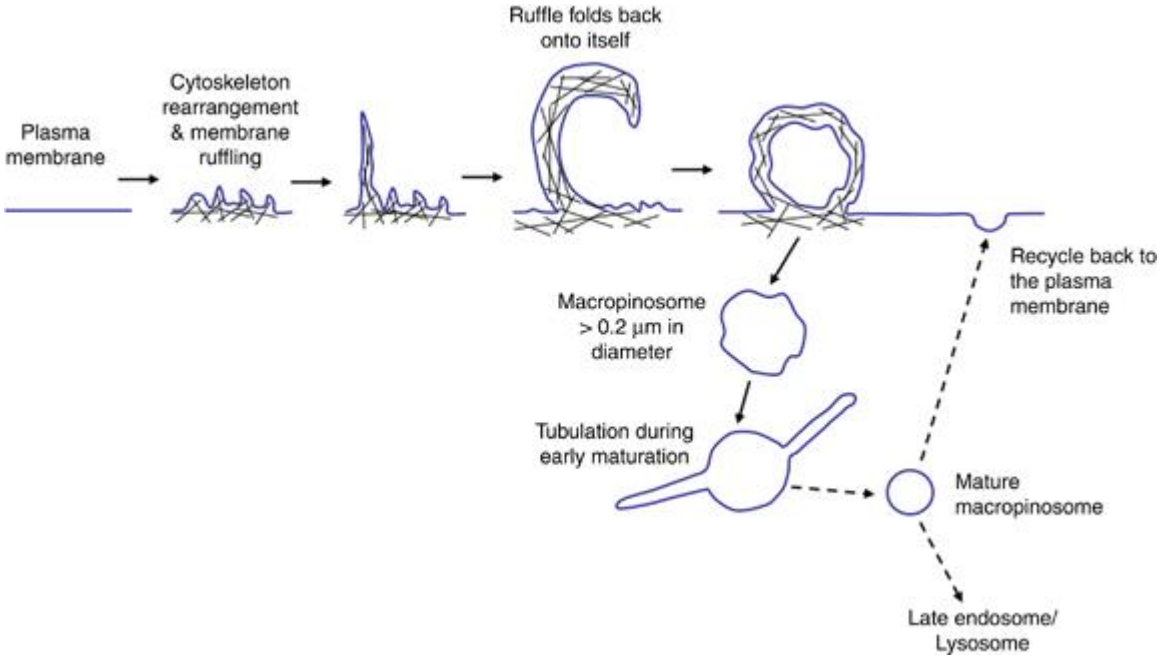

Figure 1.13: Cellular internalisation of nanoparticles via the macropinocytosis pathway. *Adapted from* [172].

1.6.4 Clathrin- and Caveolae-Independent Endocytosis

Cholesterol-rich microdomains in the plasma membrane, such as lipid rafts, could be involved in clathrin- and caveolae-independent endocytosis pathway [219]. In the absence of clathrin and caveolin proteins, cargo can be internalised into cells through lipid rafts, which can diffuse through the plasma membrane [220]. These pathways are classified as ARF6 (ADP-ribosylation factor 6)-dependent, CDC42 (cell division control protein 42 homolog)-dependent or RHOA (Ras homolog gene family, member A)-dependent endocytosis [221]. The associated endocytic apparatus may include the clathrin-independent carrier (CLIC) or phosphatidylinositol (GPI)-anchored protein-enriched early endosomal compartment (GEEC) [221]. The characteristic features of this pathway include the formation of large tubular lipid rafts, pleomorphic invaginations that

internalise large volumes of the membrane and fluids [222], [223], and the process requires actin polymerisation and curvature of the membrane [224]. Investigation into these pathways has recently intensified, but more is required since a thorough understanding of their mechanisms is lacking.

Table 1.3 summaries the main characteristic features of the endocytosis pathways.

Table 1.3: Summary of the main characteristic features of endocytosis pathways

Pathway of Endocytosis	Structure	Size	Protein machinery	Fate of cargo	Comments
Clathrin-mediated	three-dimensional array of triskelia and each triskelion consists of three clathrin heavy chains and three clathrin light chains.	around 200 nm in diameter	AP2, ARH, dab2, dynamin GTPase, Epsin-family membrane proteins, sorting nexin-9 and amphiphysin	fused with early endosomes, and sorted to either late endosome/lysosomes	clathrin-mediated endocytosis can be targeted by using certain ligands, such as transferrin
Caveolae-mediated	inverted omega shaped invaginations of the plasma membrane	around 50–100 nm in diameter	Caveolin-1and dynamin GTPase	delivered to caveosome with a neutral pH and then transported to the Golgi and/or ER, thus avoiding normal lysosomal degradation - across a cell to the opposite cell membrane surface	folate ligands can be conjugated with nanoparticles to achieve the cellular uptake via caveolae-mediated endocytosis
Macropino-cytosis	a form of endocytosis that accompanies plasma membrane ruffling	around 0.5-10 μm in diameter	CSF-1, EGF, platelet-derived growth factor or tumour-promoting factor, RAC1, actin and dynamin GTPase	destination of macropinosomes depends mainly on the cell type	avoidance of lysosomal degradation and the ease of escape from macropinosomes because of their leaky nature can be exploited to increase the uptake of cargos
Clathrin and Caveolae-independent	cholesterol-rich microdomains in the plasma membrane	–	ARF6, CDC42 and RHOA	–	more investigation is required to understand this mechanism

1.7 Methods Used to Study Endocytosis

In order to investigate and understand the cellular trafficking process, different approaches have been used to study the pathways for the cellular uptake and intracellular localisation of nanoparticles. A commonly exploited method to study cellular internalisation is the use of pharmacological inhibitors [225]. For instance, clathrin-mediated endocytosis can be inhibited by concanavalin A through their interaction with coated pits [226], and by chlorpromazine as this prevents their assembly at the cell surface [225]. Caveolae-mediated endocytosis can be inhibited by using tyrosine kinase inhibitor (genistein) [227], or using sterol-binding drugs (filipin, nystatin, and methyl-β-cyclodextrin, MßCD) through cholesterol depletion of the cellular membrane, and inhibiting cholesterol synthesis, and therefore inhibits the formation of caveolae at the cell surface [228], [229]. Dynamin GTPase-dependent pathways can also be inhibited by using a dynasore inhibitor [191], and both 5-(N-Ethyl-N-isopropyl) amiloride (EIPA) [230], and cytochalasin D [231] have been used to block the macropinocytosis process through the inhibition of Na^+/H^+ exchange and actin filament depolymerisation, respectively. It is important to use an appropriate concentration in these experiments, one that is high enough to produce an effect on endocytosis but also low enough not to cause cytotoxicity.

Along with inhibitors, mutated proteins have also been employed to identify which pathways are important for internalisation of the nanoparticles. Although expression of mutant proteins lacking in functionality that is specific to an endocytic pathway has benefits compared to chemical inhibitors [232], the use of such mutated proteins can have side effects and can be less specific. Expression of a mutated protein may result in a

higher concentration than that of the normal endogenous protein and thus give rise to lower-affinity interactions not observed in cells lacking such mutated proteins [233]. For example, the nature of dynamin makes it difficult to employ slow techniques such as immunological depletion and genetic deletion to study them [234]. Temperature-sensitive mutants exhibit an interfering phenotype within minutes, but accumulating a concentration of mutant protein sufficient to produce an observable effect takes several hours [235], [236]. The use of dynamin temperature-sensitive mutants has been instrumental in unravelling the capacity of the endocytic pathway to accommodate perturbation. Research by Damke *et al.* found that the rate of fluid-phase uptake returned to the normal levels in less than 1 hour when the temperature changed [235]. This example indicates the value to examine the influence of rapid perturbations in complex systems.

Together with inhibitors, siRNA knockdown of endocytosis pathway-selective proteins has been advocated as an alternative [225]; however, this approach has been rarely reported in the literature and has its own drawbacks [216]. The treatment of cells with siRNA is usually performed over 2 days, which may cause unwanted cellular changes and lead to observations that are unrelated to the target protein involved in a specific pathway [216].

Some classical ‘probes’ are known to be internalised via a specific endocytic pathway. For example, transferrin (T*f*) [237] and low density lipoprotein (LDL) [238] have been reported to be internalised through clathrin-mediated endocytosis. Shiga toxin [239] and cholera-β-toxin subunit (CβT) [240] enter the cell by caveolae-dependent endocytosis.

1.8 Project Aims and Objectives

The main aim of this project is to design and develop a well-characterised non-viral delivery system to transport siRNA efficiently to NSCLC cells *in vitro*. The delivery system must be capable of protecting, encapsulating, and delivering the siRNA with minimum cytotoxicity but with high efficacy. A cationic liposomal carrier composed of cationic lipid DC-Chol and the zwitterionic lipid DOPE, a composition from previously widely used components, will be used in this work.

Work initially will focus on the biological and physicochemical characterisation of a series of siRNA-liposomes prepared from different total lipid concentrations, different ratios of cationic to zwitterionic lipid, and different ratios of cationic lipid to siRNA (different N/P ratio), such as cytotoxicity, particle size, zeta potential, siRNA encapsulation behaviour, and siRNA protection from RNase degradation, in order to determine the optimum ratios for liposomes formation. The study of uptake and transfection efficiency of siRNA-liposome formulations will be discussed in Chapter 4, and this will be followed by a discussion of the investigation into the mechanism of cellular uptake and intracellular localisation of siRNA-liposomes in A549 cells in order to improve our understanding and to enable the design of more efficient delivery systems, which is the central aim of this thesis. Finally, a screen of the protein expression profiles of candidate genes that could be involved in the progression of NSCLC will be performed, and protein expression of candidate genes will be silenced in an *in vitro* model of NSCLC to validate their involvement and to examine the ability of the delivery system to promote cell proliferation through targeting of the genes of interest.

1.9 References

[1] S. Elbashir, J. Harborth, W. Lendeckel, A. Yalcin, K. Weber, and T. Tuschl, Duplexes of 21-nucleotide RNAs mediate RNA interference in cultured mammalian cells. *Nature*, vol. 411, pp. 494–498, May 2001.

[2] C. Napoli, C. Lemieux, and R. Jorgensen, Introduction of a Chimeric Chalcone Synthase Gene into Petunia Results in Reversible Co-Suppression of Homologous Genes in trans.," *The Plant cell*, vol. 2, no. 4, pp. 279–289, 1990.

[3] J. R. Kennerdell and R. W. Carthew, "Heritable gene silencing in Drosophila using double-stranded RNA.," *Nature biotechnology*, vol. 18, no. 8, pp. 896–898, 2000.

[4] S. Guo and K. J. Kemphues, "par-1, a gene required for establishing polarity in C. elegans embryos, encodes a putative Ser/Thr kinase that is asymmetrically distributed," *Cell*, vol. 81, no. 4, pp. 611–620, 1995.

[5] A. Fire, S. Xu, M. K. Montgomery, S. A. Kostas, S. E. Driver, and C. C. Mello, "Potent and specific genetic interference by double-stranded RNA in Caenorhabditis elegans," *Nature*, vol. 391, no. 6669, pp. 806–811, 1998.

[6] L. Timmons and a Fire, "Specific interference by ingested dsRNA.," *Nature*, vol. 395, no. 6705, p. 854, 1998.

[7] C. C. Mello and D. Conte, "Revealing the world of RNA interference.," *Nature*, vol. 431, no. 7006, pp. 338–342, 2004.

[8] T. M. Rana, "Illuminating the silence: understanding the structure and function of small RNAs," *Nature Molecular Cell Biology*, vol. 8, no. 1, pp. 23–36, 2007.

[9] A. J. Karpala, T. J. Doran, and A. G. D. Bean, "Immune responses to dsRNA: Implications for gene silencing technologies," *Immunology and Cell Biology*, vol. 83, no. 3, pp. 211–216, 2005.

[10] and A. Z. F. Lisa Timmons, Hiroaki Tabara, Craig C. Mello, "Inducible Systemic RNA Silencing in Caenorhabditis elegans," *Molecular biology of the cell*, vol. 14, pp. 2972–2983, 2003.

[11] N. Agrawal, P. V. N. Dasaradhi, A. Mohmmed, P. Malhotra, R. K. Bhatnagar, and S. K. Mukherjee, "RNA interference: biology, mechanism, and applications.," *Microbiology and molecular biology reviews : MMBR*, vol. 67, no. 4, pp. 657–685, 2003.

[12] J. G. Doench, C. P. Petersen, and P. A. Sharp, "siRNAs can function as miRNAs," *Genes and Development*, vol. 17, no. 4, pp. 438–442, 2003.

[13] S. K. Singh, M. Pal Bhadra, H. J. Girschick, and U. Bhadra, "MicroRNAs - Micro in size but macro in function," *FEBS Journal*, vol. 275, no. 20, pp. 4929–4944, 2008.

[14] J. K. W. Lam, M. Y. T. Chow, Y. Zhang, and S. W. S. Leung, "siRNA Versus miRNA as Therapeutics for Gene Silencing," *Molecular Therapy - Nucleic Acids*, vol. 4, no. July, p. e252, 2015.

[15] S. M. Elbashir, J. Martinez, A. Patkaniowska, W. Lendeckel, and T. Tuschl, "Functional anatomy of siRNAs for mediating efficient RNAi in Drosophila melanogaster embryo lysate," *The EMBO*, vol. 20, no. 23, pp. 6877–6888, 2001.

[16] R. C. Wilson and J. A. Doudna, "Molecular Mechanisms of RNA Interference," *Annual*

Review of Biophysics, vol. 42, no. 1, pp. 217–239, 2013.

[17] G. Hutvagner and M. J. Simard, "Argonaute proteins: key players in RNA silencing," *Molecular Cell Biology*, vol. 9, no. 1, pp. 22–32, 2008.

[18] J. B. Ma, Y. R. Yuan, G. Meister, Y. Pei, T. Tuschl, and D. J. Patel, "Structural basis for 5 '-end-specific recognition of guide RNA by the A-fulgidus Piwi protein," *Nature*, vol. 434, no. 2, pp. 356–372, 2015.

[19] E. J. Carthew, Richard W. and Sontheimer, "Origins and Mechanisms of miRNAs and siRNAs," *Cell*, vol. 136, no. 4, pp. 642–655, 2009.

[20] L. P. Ford, P. S. Bagga, and J. Wilusz, "The poly(A) tail inhibits the assembly of a 3'-to-5' exonuclease in an in vitro RNA stability system.," *Molecular and cellular biology*, vol. 17, no. 1, pp. 398–406, 1997.

[21] R. L. Kathryn A. Whitehead and and D. G. Anderson, "Knocking down barriers: advances in siRNA delivery," *Nature Reviews Drug Discovery*, vol. 8, pp. 129–138, 2009.

[22] L. Aagaard and J. J. Rossi, "RNAi therapeutics: principles, prospects and challenges.," *Advanced drug delivery reviews*, vol. 59, no. 2–3, pp. 75–86, Mar. 2007.

[23] A. Gallas, C. Alexander, M. C. Davies, S. Puri, and S. Allen, "Chemistry and formulations for siRNA therapeutics.," *The Royal Society of Chemistry*, vol. 42, no. 20, pp. 7983–7997, Jul. 2013.

[24] D. Cejka, D. Losert, and V. Wacheck, "Short interfering RNA (siRNA): tool or therapeutic?," *Clinical science*, vol. 110, no. 1, pp. 47–58, 2006.

[25] J. E. Zuckerman and M. E. Davis, "Clinical experiences with systemically administered siRNA-based therapeutics in cancer," *Drug Discovery*, vol. 14, no. 12, pp. 843–856, 2015.

[26] B. Schultheis, D. Strumberg, A. Santel, C. Vank, F. Gebhardt, O. Keil, C. Lange, K. Giese, J. Kaufmann, M. Khan, and J. Drevs, "First-in-human phase I study of the liposomal RNA interference therapeutic Atu027 in patients with advanced solid tumors," *Journal of Clinical Oncology*, vol. 32, no. 36, pp. 4141–4148, 2014.

[27] and K. T. John C. Burnett, John J. Rossi, "Current progress of siRNA/shRNA Therapeutics in clinical trials," *Biotechnology Journal*, vol. 6, no. 9, pp. 1130–1146, 2011.

[28] R. W. Esmond and A. K.-H. Chung, "The Patent Landscape of siRNA Nanoparticle Delivery," *Nanotechnology Law & Business*, vol. 11, pp. 15–28, 2014.

[29] A. Daka and D. Peer, "RNAi-based nanomedicines for targeted personalized therapy.," *Advanced drug delivery reviews*, vol. 64, no. 13, pp. 1508–21, Oct. 2012.

[30] C. Xu and J. Wang, "Delivery systems for siRNA drug development in cancer therapy," *Asian Journal of Pharmaceutical Sciences*, vol. 10, no. 1, pp. 1–12, 2015.

[31] R. C. Ireton and J. Chen, "EphA2 receptor tyrosine kinase as a promising target for cancer therapeutics.," *Current cancer drug targets*, vol. 5, no. 3, pp. 149–57, 2005.

[32] M. Tandon, S. V. Vemula, and S. K. Mittal, "Emerging strategies for EphA2 receptor targeting for cancer therapeutics.," *Expert opinion on therapeutic targets*, vol. 15, no. 1, pp. 31–51, 2011.

[33] C. S. Dela Cruz, L. T. Tanoue, and R. a. Matthay, "Lung Cancer: epidemiology, etiology and prevention," *Clinics Chest Medicine*, vol. 32, no. 4, pp. 1–61, 2011.

[34] C. M. Free, M. Ellis, L. Beggs, D. Beggs, S. a Morgan, and D. R. Baldwin, "Lung cancer outcomes at a UK cancer unit between 1998-2001.," *Lung Cancer*, vol. 57, no. 2, pp. 222–228, Aug. 2007.

[35] M. O'Brien, "Lung cancer screening: Is there a future?," *Indian Journal of Medical and Paediatric Oncology*, vol. 35, no. 4, pp. 249–252, 2014.

[36] R. Siegel, D. Naishadham, and A. Jemal, "Cancer Statistics , 2013," *Cancer Journal for Clinicians*, vol. 63, no. 1, pp. 11–30, 2013.

[37] A. Aggarwal, G. Lewison, S. Idir, M. Peters, C. Aldige, W. Boerckel, P. Boyle, E. L. Trimble, P. Roe, T. Sethi, J. Fox, and R. Sullivan, "The state of lung cancer research: a global analysis," *Journal of Thoracic Oncology*, vol. 11, no. 7, pp. 1040–1050, 2016.

[38] A. J. R. Carter and C. N. Nguyen, "A comparison of cancer burden and research spending reveals discrepancies in the distribution of research funding," *BMC Public Health*, vol. 12, no. 526, pp. 1–12, 2012.

[39] R. Siegel, E. Ward, O. Brawley, and A. Jemal, "Cancer statistics, 2011: the impact of eliminating socioeconomic and racial disparities on premature cancer deaths.," *CA Cancer J Clin*, vol. 61, pp. 212–236, 2011.

[40] J. D. Webb and M. C. Simon, "Novel insights into the molecular origins and treatment of lung cancer," *Cell Cycle*, vol. 9, no. 20, pp. 4098–4105, 2010.

[41] G. Hamilton, B. Rath, and E. Ulsperger, "How to target small cell lung cancer," *Oncoscience*, vol. 2, no. 8, pp. 684–692, 2015.

[42] G. a Otterson, M. a Villalona-Calero, W. Hicks, X. Pan, J. a Ellerton, S. N. Gettinger, and J. R. Murren, "Phase I/II study of inhaled doxorubicin combined with platinum-based therapy for advanced non-small cell lung cancer.," *Clinical Cancer Research*, vol. 16, no. 8, pp. 2466–2473, Apr. 2010.

[43] R. Sturm, "Radioactivity and lung cancer-mathematical models of radionuclide deposition in the human lungs," *Journal of Thoracic Disease*, vol. 3, no. 4, pp. 231–243, 2011.

[44] A. Jemal, F. Bray, and J. Ferlay, "Global Cancer Statistics," *Cancer Journal for Clinicians*, vol. 61, no. 2, pp. 69–90, 2011.

[45] N. Sunaga, D. S. Shames, L. Girard, M. Peyton, J. E. Larsen, H. Imai, J. Soh, M. Sato, N. Yanagitani, K. Kaira, Y. Xie, A. F. Gazdar, M. Mori, and J. D. Minna, "Knockdown of oncogenic KRAS in non-small cell lung cancers suppresses tumor growth and sensitizes tumor cells to targeted therapy.," *Molecular Cancer Therapeutics*, vol. 10, no. 2, pp. 336–346, Feb. 2011.

[46] A. Cavazzoni, R. R. Alfieri, D. Cretella, F. Saccani, L. Ampollini, M. Galetti, F. Quaini, G. Graiani, D. Madeddu, P. Mozzoni, E. Galvani, S. La Monica, M. Bonelli, C. Fumarola, A. Mutti, P. Carbognani, M. Tiseo, E. Barocelli, P. G. Petronini, and A. Ardizzoni, "Combined use of anti-ErbB monoclonal antibodies and erlotinib enhances antibody-dependent cellular cytotoxicity of wild-type erlotinib-sensitive NSCLC cell lines.," *Molecular Cancer*, vol. 11, no. 91, pp. 1–14, Jan. 2012.

[47] Y. Minami, T. Shimamura, K. Shah, T. LaFramboise, K. a Glatt, E. Liniker, C. L. Borgman, H. J. Haringsma, W. Feng, B. a Weir, a M. Lowell, J. C. Lee, J. Wolf, G. I. Shapiro, K.-K. Wong, M. Meyerson, and R. K. Thomas, "The major lung cancer-derived mutants of ERBB2 are oncogenic and are associated with sensitivity to the irreversible EGFR/ERBB2 inhibitor HKI-272.," *Oncogene*, vol. 26, no. 34, pp. 5023–5027, 2007.

[48] J. R. Molina, P. Yang, S. D. Cassivi, S. E. Schild, and A. A. Adjei, "Non-small cell lung cancer: epidemiology, risk factors, treatment, and survivorship.," *Mayo Clinic proceedings*, vol. 83, no. 5, pp. 584–594, 2008.

[49] K. a Jinturkar, C. Anish, M. K. Kumar, T. Bagchi, A. K. Panda, and A. R. Misra, "Liposomal formulations of Etoposide and Docetaxel for p53 mediated enhanced cytotoxicity in lung cancer cell lines.," *Biomaterials*, vol. 33, no. 8, pp. 2492–2507, Mar. 2012.

[50] F. Gagnadoux, J. Hureaux, L. Vecellio, T. Urban, A. Le Pape, I. Valo, J. Montharu, V. Leblond, M. Boisdron-Celle, S. Lerondel, C. Majoral, P. Diot, J. L. Racineux, and E. Lemarie, "Aerosolized Chemotherapy.," *Journal of Aerosol Medicine and Pulmonary Drug Delivery*, vol. 21, no. 1, pp. 61–70, Mar. 2008.

[51] A. Sharma and U. S. Sharma, "Liposomes in drug delivery: progress and limitations," *International Journal of Pharmaceutics*, vol. 154, pp. 123–140, 1997.

[52] and P. C. W. A. Xing-Jie Liang, Chunying Chen, Yuliang Zhao, "Circumventing Tumor Resistance to Chemotherapy by Nanotechnology," *Methods in Molecular Biology*, vol. 596, no. 1, pp. 183–198, 2010.

[53] X. D. and R. J. Mumper, "Nanomedicinal strategies to treat multidrug-resistant tumors: current progress," *Nanomedicine*, vol. 5, no. 4, pp. 597–615, 2010.

[54] J. Guo, L. Bourre, D. M. Soden, G. C. O'Sullivan, and C. O'Driscoll, "Can non-viral technologies knockdown the barriers to siRNA delivery and achieve the next generation of cancer therapeutics?," *Biotechnology Advances*, vol. 29, no. 4, pp. 402–417, 2011.

[55] Y. Fujita, K. Kuwano, and T. Ochiya, "Development of Small RNA Delivery Systems for Lung Cancer Therapy," *International Journal of Molecular Sciences*, vol. 16, no. 3, pp. 5254–5270, 2015.

[56] G. Mainelis, S. Seshadri, O. B. Garbuzenko, T. Han, Z. Wang, and T. Minko, "Characterization and application of a nose-only exposure chamber for inhalation delivery of liposomal drugs and nucleic acids to mice.," *Journal of aerosol medicine and pulmonary drug delivery*, vol. 26, no. 6, pp. 345–54, 2013.

[57] G. Shim, H.-W. Choi, S. Lee, J. Choi, Y. H. Yu, D.-E. Park, Y. Choi, C.-W. Kim, and Y.-K. Oh, "Enhanced intrapulmonary delivery of anticancer siRNA for lung cancer therapy using cationic ethylphosphocholine-based nanolipoplexes.," *Molecular therapy : the journal of the American Society of Gene Therapy*, vol. 21, no. 4, pp. 816–24, 2013.

[58] Y.-K. Oh and T. G. Park, "siRNA delivery systems for cancer treatment.," *Advanced drug delivery reviews*, vol. 61, no. 10, pp. 850–862, Aug. 2009.

[59] K. Tiemann and J. J. Rossi, "RNAi-based therapeutics-current status, challenges and prospects.," *EMBO molecular medicine*, vol. 1, no. 3, pp. 142–151, Jun. 2009.

[60] S. Akhtar and I. F. Benter, "Nonviral delivery of synthetic siRNAs in vivo," *The Journal of Clinical Investigation*, vol. 117, no. 12, pp. 3623–3632, 2007.

[61] M. X. Juliano R, Bauman J, Kang H, "Biological barriers to therapy with antisense and siRNA oligonucleotides," *Molecular Pharmaceutics*, vol. 6, no. 3, pp. 686–695, 2009.

[62] S. Azarmi, W. H. Roa, and R. Löbenberg, "Targeted delivery of nanoparticles for the treatment of lung diseases.," *Advanced drug delivery reviews*, vol. 60, no. 8, pp. 863–875, May 2008.

[63] J. Wang, Z. Lu, M. G. Wientjes, and J. L.-S. Au, "Delivery of siRNA therapeutics: barriers and carriers.," *The American Association of Pharmaceutical Scientists Journal*, vol. 12, no. 4, pp. 492–503, Dec. 2010.

[64] S. Nie, "Understanding and overcoming major barriers in cancer nanomedicine," *Nanomedicine*, vol. 5, no. 4, pp. 523–528, 2010.

[65] S. Stolnik, B. Daudali, A. Arien, J. Whetstone, C. R. Heald, M. C. Garnett, S. S. Davis, and L. Illum, "The effect of surface coverage and conformation of poly(ethylene oxide) (PEO) chains of poloxamer 407 on the biological fate of model colloidal drug carriers," *Biochimica et Biophysica Acta - Biomembranes*, vol. 1514, no. 2, pp. 261–279, 2001.

[66] S. Stolnik, L. Illum, and S. S. Davis, "Long circulating microparticulate drug carriers," *Advanced Drug Delivery Reviews*, vol. 64, no. SUPPL. pp. 290–301, 2012.

[67] P. P. Wibroe, D. Ahmadvand, M. A. Oghabian, A. Yaghmur, and S. M. Moghimi, "An integrated assessment of morphology, size, and complement activation of the PEGylated liposomal doxorubicin products Doxil®, Caelyx®, DOXOrubicin, and SinaDoxosome," *Journal of Controlled Release*, vol. 221, pp. 1–8, 2016.

[68] J. J. F. Verhoef and T. J. Anchordoquy, "Questioning the use of PEGylation for drug delivery," *Drug Delivery and Translational Research*, vol. 3, no. 6, pp. 499–503, 2013.

[69] D. E. Owens and N. A. Peppas, "Opsonization, biodistribution, and pharmacokinetics of polymeric nanoparticles," *International Journal of Pharmaceutics*, vol. 307, no. 1, pp. 93–102, 2006.

[70] X. Murgia, C. De Souza Carvalho, and C. M. Lehr, "Overcoming the pulmonary barrier: New insights to improve the efficiency of inhaled therapeutics," *European Journal of Nanomedicine*, vol. 6, no. 3, pp. 157–169, 2014.

[71] A. G. Beule, "Physiology and pathophysiology of respiratory mucosa of the nose and the paranasal sinuses," *Head and Neck Surgery*, vol. 9, pp. 1–24, 2010.

[72] S. K. Lai, Y. Y. Wang, and J. Hanes, "Mucus-penetrating nanoparticles for drug and gene delivery to mucosal tissues," *Advanced Drug Delivery Reviews*, vol. 61, no. 2, pp. 158–171, 2009.

[73] J. V Fahy and B. F. Dickey, "Airway mucus function and dysfunction.," *The New England journal of medicine*, vol. 363, no. 23, pp. 2233–2247, 2010.

[74] E. K. Vladar, Y. L. Lee, T. Stearns, and J. D. Axelrod, "Observing planar cell polarity in multiciliated mouse airway epithelial cells," *Methods in cell biology*, vol. 127, pp. 37–54, 2015.

[75] L. M. Ensign, C. Schneider, J. S. Suk, R. Cone, and J. Hanes, "Mucus penetrating nanoparticles: Biophysical tool and method of drug and gene delivery," *Advanced Materials*, vol. 24, no. 28, pp. 3887–3894, 2012.

[76] O. D. Chuquimia, D. H. Petursdottir, N. Periolo, and C. Ferńndez, "Alveolar epithelial cells are critical in protection of the respiratory tract by secretion of factors able to modulate the activity of pulmonary macrophages and directly control bacterial growth," *Infection and Immunity*, vol. 81, no. 1, pp. 381–389, 2013.

[77] A. Akella and S. B. Deshpande, "Pulmonary surfactants and their role in pathophysiology of lung disorders," *Indian Journal of Experimental Biology*, vol. 51, no. 1, pp. 5–22, 2013.

[78] B. Patel, N. Gupta, and F. Ahsan, "Particle engineering to enhance or lessen particle

uptake by alveolar macrophages and to influence the therapeutic outcome," *European Journal of Pharmaceutics and Biopharmaceutics*, vol. 89, no. 2015, pp. 163–174, 2015.

[79] Y. Y. Wang, S. K. Lai, J. S. Suk, A. Pace, R. Cone, and J. Hanes, "Addressing the PEG mucoadhesivity paradox to engineer nanoparticles that 'slip' through the human mucus barrier," *Angewandte Chemie - International Edition*, vol. 47, no. 50, pp. 9726–9729, 2008.

[80] J. S. Suk, Q. Xu, N. Kim, J. Hanes, and L. M. Ensign, "PEGylation as a strategy for improving nanoparticle-based drug and gene delivery," *Advanced Drug Delivery Reviews*, vol. 99, no. 2016, pp. 28–51, 2016.

[81] W. Huang, M. Zhao, N. Wei, X. Wang, H. Cao, Q. Du, and Z. Liang, "Site-Specific RNase A Activity Was Dramatically Reduced in Serum from Multiple Types of Cancer Patients," *PLoS ONE*, vol. 9, no. 5, p. 496490, 2014.

[82] H. H. Thorp, "The importance of being r: Greater oxidative stability of RNA compared with DNA," *Chemistry and Biology*, vol. 7, no. 2, pp. 33–36, 2000.

[83] M. S. Draz, B. A. Fang, P. Zhang, Z. Hu, S. Gu, K. C. Weng, J. W. Gray, and F. F. Chen, "Nanoparticle-mediated systemic delivery of siRNA for treatment of cancers and viral infections," *Theranostics*, vol. 4, no. 9, pp. 872–892, 2014.

[84] Y. Zhang, A. Satterlee, and L. Huang, "In Vivo Gene Delivery by Nonviral Vectors: Overcoming Hurdles?," *Molecular Therapy*, vol. 20, no. 7, pp. 1298–1304, 2012.

[85] M. a Behlke, "Chemical modification of siRNAs for in vivo use," *Oligonucleotides*, vol. 18, no. 4, pp. 305–319, 2008.

[86] K. Gao and L. Huang, "Nonviral methods for siRNA delivery," *Molecular Pharmaceutics*, vol. 6, no. 3. pp. 651–658, 2009.

[87] C. Zhang, N. Tang, X. J. Liu, W. Liang, W. Xu, and V. P. Torchilin, "siRNA-containing liposomes modified with polyarginine effectively silence the targeted gene," *Journal of Controlled Release*, vol. 112, no. 2, pp. 229–239, 2006.

[88] L. E. Kelemen, "The role of folate receptor alpha in cancer development, progression and treatment: cause, consequence or innocent bystander?," *International journal of cancer*, vol. 119, no. 2, pp. 243–50, Jul. 2006.

[89] A. S. Wibowo, M. Singh, K. M. Reeder, J. J. Carter, A. R. Kovach, W. Meng, M. Ratnam, F. Zhang, and C. E. Dann, "Structures of human folate receptors reveal biological trafficking states and diversity in folate and antifolate recognition," *Proceedings of the National Academy of Sciences*, vol. 110, no. 38, pp. 15180–15188, 2013.

[90] T. R. Daniels, E. Bernabeu, J. A. Rodríguez, S. Patel, M. Kozman, D. A. Chiappetta, E. Holler, J. Y. Ljubimova, G. Helguera, and M. L. Penichet, "The transferrin receptor and the targeted delivery of therapeutic agents against cancer," *Biochimica et biophysica acta*, vol. 1820, no. 3, pp. 291–317, 2012.

[91] E. L. Mackenzie, K. Iwasaki, and Y. Tsuji, "Intracellular Iron Transport and Storage: From Molecular Mechanisms to Health Implications," *Antioxidants & Redox Signaling*, vol. 10, no. 6, pp. 997–1030, 2008.

[92] A. El-Sayed and H. Harashima, "Endocytosis of gene delivery vectors: from clathrin-dependent to lipid raft-mediated endocytosis.," *Molecular therapy*, vol. 21, no. 6, pp. 1118–1130, 2013.

[93] H. T. Mcmahon and E. Boucrot, "Molecular mechanism and physiological functions of clathrin-mediated endocytosis," *NATURE REVIEWS | MOLECULAR CELL BIOLOGY*, vol. 12, no. 8, pp. 517–533, 2011.

[94] R. Juliano, M. R. Alam, V. Dixit, and H. Kang, "Mechanisms and strategies for effective delivery of antisense and siRNA oligonucleotides," *Nucleic Acids Research*, vol. 36, no. 12, pp. 4158–4171, 2008.

[95] J. Huotari and A. Helenius, "Endosome maturation," *The EMBO journal*, vol. 30, no. 17, pp. 3481–3500, 2011.

[96] B. L. Fredericksen, B. L. Wei, J. Yao, T. Luo, and J. V. Garcia, "Inhibition of endosomal/lysosomal degradation increases the infectivity of human immunodeficiency virus," *J. Virol.*, vol. 76, no. 22, pp. 11440–11446, 2002.

[97] P. D. Robbins and S. C. Ghivizzani, "Viral Vectors for Gene Therapy," *Pharmacology & Therapeutics*, vol. 80, no. 1, pp. 35–47, 1998.

[98] S. N. Uddin, "Cationic lipids used in non-viral gene delivery systems," *Biotechnology and Molecular Biology Review*, vol. 2, no. 3, pp. 58–67, 2007.

[99] D. Bouard, D. Alazard-Dany, and F.-L. Cosset, "Viral vectors: from virology to transgene expression.," *British journal of pharmacology*, vol. 157, no. 2, pp. 153–65, 2009.

[100] C. E. Thomas, A. Ehrhardt, and M. A. Kay, "Progress and problems with the use of viral vectors for gene therapy," *Nature Reviews Genetic*, vol. 4, no. 5, pp. 346–358, 2003.

[101] D. Castanotto and J. J. Rossi, "The promises and pitfalls of RNA-interference-based therapeutics," *Molecular Biology*, vol. 457, no. 7228, pp. 426–433, 2009.

[102] M. A. Kay, "State-of-the-art gene-based therapies: the road ahead.," *Nature reviews. Genetics*, vol. 12, no. 5, pp. 316–328, 2011.

[103] B. Sibbald, "Death but one unintended consequence of gene-therapy trial.," *Canadian Medical Association journal*, vol. 164, no. 11, p. 1612, 2001.

[104] L. S. Young, P. F. Searle, D. Onion, and V. Mautner, "Viral gene therapy strategies: from basic science to clinical application.," *The Journal of pathology*, vol. 208, no. 2, pp. 299–318, 2006.

[105] M. R. and A. Narvekar, "Non Viral Vectors in Gene Therapy- An Overview," *Journal of Clinical and Diagnostic Research*, vol. 9, no. 1, pp. 1–6, 2015.

[106] G. Bozzuto and A. Molinari, "Liposomes as nanomedical devices.," *International journal of nanomedicine*, vol. 10, pp. 975–999, 2015.

[107] M. L. Immordino, F. Dosio, and L. Cattel, "Stealth liposomes: Review of the basic science, rationale, and clinical applications, existing and potential," *International Journal of Nanomedicine*, vol. 1, no. 3, pp. 297–315, 2006.

[108] M. Mahato, P. Kumar, and A. K. Sharma, "Amphiphilic polyethylenimine polymers mediate efficient delivery of DNA and siRNA in mammalian cells.," *Molecular bioSystems*, vol. 9, no. 4, pp. 780–791, 2013.

[109] M. Dominska and D. M. Dykxhoorn, "Breaking down the barriers: siRNA delivery and endosome escape.," *Journal of cell science*, vol. 123, no. 8, pp. 1183–1189, Apr. 2010.

[110] K. Singha, R. Namgung, and W. J. Kim, "Polymers in small-interfering RNA delivery.,"

Nucleic acid therapeutics, vol. 21, no. 3, pp. 133–147, 2011.

[111] S. M. Moghimi, P. Symonds, J. C. Murray, A. C. Hunter, G. Debska, and A. Szewczyk, "A two-stage poly(ethylenimine)-mediated cytotoxicity: Implications for gene transfer/therapy," *Molecular Therapy*, vol. 11, no. 6, pp. 990–995, 2005.

[112] I. Aranaz, M. Mengíbar, R. Harris, I. Paños, B. Miralles, N. Acosta, G. Galed, and Á. Heras, "Functional Characterization of Chitin and Chitosan," *Current Chemical Biology*, vol. 3, pp. 203–230, 2009.

[113] S. Mao, W. Sun, and T. Kissel, "Chitosan-based formulations for delivery of DNA and siRNA," *Advanced Drug Delivery Reviews*, vol. 62, no. 1, pp. 12–27, 2010.

[114] H. Ragelle, G. Vandermeulen, and V. Préat, "Chitosan-based siRNA delivery systems," *Journal of Controlled Release*, vol. 172, no. 1, pp. 207–218, 2013.

[115] E. Eiríksdóttir, K. Konate, Ü. Langel, G. Divita, and S. Deshayes, "Secondary structure of cell-penetrating peptides controls membrane interaction and insertion," *Biochimica et Biophysica Acta - Biomembranes*, vol. 1798, no. 6, pp. 1119–1128, 2010.

[116] F. Milletti, "Cell-penetrating peptides: Classes, origin, and current landscape," *Drug Discovery Today*, vol. 17, no. 15–16, pp. 850–860, 2012.

[117] Z. Lai, I. Han, G. Zirzow, R. O. Brady, and J. Reiser, "Intercellular delivery of a herpes simplex virus VP22 fusion protein from cells infected with lentiviral vectors," *Proceedings of the National Academy of Sciences*, vol. 97, no. 21, pp. 11297–11302, 2000.

[118] I. M. Kaplan, J. S. Wadia, and S. F. Dowdy, "Cationic TAT peptide transduction domain enters cells by macropinocytosis," *Journal of Controlled Release*, vol. 102, no. 1, pp. 247–253, 2005.

[119] P. Boisguérin, S. Deshayes, M. J. Gait, L. O'Donovan, C. Godfrey, C. a. Betts, M. J. a. Wood, and B. Lebleu, "Delivery of therapeutic oligonucleotides with cell penetrating peptides," *Advanced Drug Delivery Reviews*, vol. 87, pp. 52–67, 2015.

[120] B. R. Meade and S. F. Dowdy, "Enhancing the cellular uptake of siRNA duplexes following noncovalent packaging with protein transduction domain peptides," *Advanced Drug Delivery Reviews*, vol. 60, no. 4–5, pp. 530–536, 2008.

[121] P. Lönn, A. D. Kacsinta, X.-S. Cui, A. S. Hamil, M. Kaulich, K. Gogoi, and S. F. Dowdy, "Enhancing Endosomal Escape for Intracellular Delivery of Macromolecular Biologic Therapeutics," *Scientific Reports*, vol. 6, no. 1, p. 32301, 2016.

[122] H. Shima, *Buckling of carbon nanotubes: A state of the art review*, vol. 5, no. 1. 2012.

[123] C. Klumpp, K. Kostarelos, M. Prato, and A. Bianco, "Functionalized carbon nanotubes as emerging nanovectors for the delivery of therapeutics," *Biochimica et Biophysica Acta - Biomembranes*, vol. 1758, no. 3, pp. 404–412, 2006.

[124] A. K. Varkouhi, S. Foillard, T. Lammers, R. M. Schiffelers, E. Doris, W. E. Hennink, and G. Storm, "SiRNA delivery with functionalized carbon nanotubes," *International Journal of Pharmaceutics*, vol. 416, no. 2, pp. 419–425, 2011.

[125] A. a Shvedova, V. Castranova, E. R. Kisin, D. Schwegler-Berry, A. R. Murray, V. Z. Gandelsman, A. Maynard, and P. Baron, "Exposure to carbon nanotube material: assessment of nanotube cytotoxicity using human keratinocyte cells.," *Journal of toxicology and environmental health. Part A*, vol. 66, no. 20, pp. 1909–26, 2003.

[126] Y. Gao, X. L. Liu, and X. R. Li, "Research progress on siRNA delivery with nonviral carriers.," *International journal of nanomedicine*, vol. 6, pp. 1017–1025, 2011.

[127] M. A. Behlke, "Progress towards in vivo use of siRNAs," *Molecular Therapy*, vol. 13, no. 4, pp. 644–670, 2006.

[128] A. Schroeder, C. G. Levins, C. Cortez, R. Langer, and D. G. Anderson, "Lipid-based nanotherapeutics for siRNA delivery," *Journal of Internal Medicine*, vol. 267, no. 1, pp. 9–21, 2010.

[129] H. Kim, Y. Kim, and J. Lee, "Liposomal formulations for enhanced lymphatic delivery," *Asian Journal of Pharmaceutical Sciences*, vol. 8, no. 2, pp. 100–109, 2013.

[130] F. C. Szoka, D. Milholland, and M. Barza, "Effect of lipid composition and liposome size on toxicity and in vitro fungicidal activity of liposome-intercalated amphotericin B," *Antimicrobial Agents and Chemotherapy*, vol. 31, no. 3, pp. 421–429, 1987.

[131] K. A. Melzak, S. A. Melzak, E. Gizeli, and J. L. Toca-Herrera, "Cholesterol organization in phosphatidylcholine liposomes: A surface plasmon resonance study," *Materials*, vol. 5, no. 11, pp. 2306–2325, 2012.

[132] M. J. Ziegler and P. Thomas Vernier, "Interface water dynamics and porating electric fields for phospholipid bilayers," *Journal of Physical Chemistry B*, vol. 112, no. 43, pp. 13588–13596, 2008.

[133] T. M. Allen, "Long-circulating (sterically stabilized) liposomes for targeted drug delivery," *Trends in Pharmacological Sciences*, vol. 15, no. 7. pp. 215–220, 1994.

[134] E. Apostolidou, J. Cortes, A. Tsimberidou, E. Estey, H. Kantarjian, and F. J. Giles, "Pilot study of gemtuzumab ozogamicin, liposomal daunorubicin, cytarabine and cyclosporine regimen in patients with refractory acute myelogenous leukemia," *Leukemia Research*, vol. 27, no. 10, pp. 887–891, 2003.

[135] M. Balasegaram, K. Ritmeijer, M. A. Lima, S. Burza, G. Ortiz Genovese, B. Milani, S. Gaspani, J. Potet, and F. Chappuis, "Liposomal amphotericin B as a treatment for human leishmaniasis.," *Expert opinion on emerging drugs*, vol. 17, no. 4, pp. 493–510, 2012.

[136] J. A. Silverman and S. R. Deitcher, "Marqibo (vincristine sulfate liposome injection) improves the pharmacokinetics and pharmacodynamics of vincristine," *Cancer Chemotherapy and Pharmacology*, vol. 71, no. 3, pp. 555–564, 2013.

[137] M. J. Parnham and H. Wetzig, "Toxicity screening of liposomes," *Chemistry and Physics of Lipids*, vol. 64, no. 1–3, pp. 263–274, 1993.

[138] T. Montier, T. Benvegnu, P.-A. Jaffrès, J.-J. Yaouanc, and P. Lehn, "Progress in cationic lipid-mediated gene transfection: a series of bio-inspired lipids as an example.," *Current Gene Therapy*, vol. 8, no. 5, pp. 296–312, Oct. 2008.

[139] D. Zhi, S. Zhang, Y. Zhao, S. Cui, B. Wang, and H. Chen, "In Vitro Study of Carbamate-Linked Cationic Lipid for Gene Delivery Against Cervical Cancer Cells," *Advances in Materials Physics and Chemistry*, pp. 229–231, 2012.

[140] M. a Maier, M. Jayaraman, S. Matsuda, J. Liu, S. Barros, W. Querbes, Y. K. Tam, S. M. Ansell, V. Kumar, J. Qin, X. Zhang, Q. Wang, S. Panesar, R. Hutabarat, M. Carioto, J. Hettinger, P. Kandasamy, D. Butler, K. G. Rajeev, B. Pang, K. Charisse, K. Fitzgerald, B. L. Mui, X. Du, P. Cullis, T. D. Madden, M. J. Hope, M. Manoharan, and A. Akinc, "Biodegradable lipids enabling rapidly eliminated lipid nanoparticles for systemic delivery of RNAi therapeutics.," *Molecular therapy*, vol. 21, no. 8, pp. 1570–1578, 2013.

[141] X.-X. Zhang, T. J. McIntosh, and M. W. Grinstaff, "Functional lipids and lipoplexes for improved gene delivery.," *Biochimie*, vol. 94, no. 1, pp. 42–58, Jan. 2012.

[142] M. Kapoor, D. J. Burgess, and S. D. Patil, "Physicochemical characterization techniques for lipid based delivery systems for siRNA.," *International Journal of Pharmaceutics*, vol. 427, no. 1, pp. 35–57, May 2012.

[143] A. Sharma, S. V. Madhunapantula, and G. P. Robertson, "Toxicological considerations when creating nanoparticle based drugs and drug delivery systems?," *Expert Opin Drug Metab Toxicol*, vol. 8, no. 1, pp. 47–69, 2012.

[144] B. Ozpolat, A. K. Sood, and G. Lopez-Berestein, "Liposomal siRNA nanocarriers for cancer therapy," *Advanced Drug Delivery Reviews*, vol. 66. pp. 110–116, 2014.

[145] S. D. Li and L. Huang, "Nanoparticles evading the reticuloendothelial system: Role of the supported bilayer," *Biochimica et Biophysica Acta - Biomembranes*, vol. 1788, no. 10, pp. 2259–2266, 2009.

[146] P. L. Felgner, T. R. Gadek, M. Holm, R. Roman, H. W. Chan, M. Wenz, J. P. Northrop, G. M. Ringold, and M. Danielsen, "Lipofection: a highly efficient, lipid-mediated DNA-transfection procedure.," *Proceedings of the National Academy of Sciences of the United States of America*, vol. 84, no. 21, pp. 7413–7417, 1987.

[147] D. Zhi, S. Zhang, S. Cui, Y. Zhao, Y. Wang, and D. Zhao, "The headgroup evolution of cationic lipids for gene delivery.," *Bioconjugate Chemistry*, vol. 24, no. 4, pp. 487–519, Apr. 2013.

[148] D. Zhi, S. Zhang, B. Wang, Y. Zhao, B. Yang, and S. Yu, "Transfection efficiency of cationic lipids with different hydrophobic domains in gene delivery.," *Bioconjugate Chemistry*, vol. 21, no. 4, pp. 563–577, Apr. 2010.

[149] D. R. Sørensen, M. Leirdal, and M. Sioud, "Gene silencing by systemic delivery of synthetic siRNAs in adult mice," *Journal of Molecular Biology*, vol. 327, no. 4, pp. 761–766, 2003.

[150] D. a Balazs and W. Godbey, "Liposomes for use in gene delivery.," *Journal of Drug Delivery*, vol. 2011, pp. 1–12, Jan. 2010.

[151] M. DeCastro, Y. Saijoh, and G. C. Schoenwolf, "Optimized cationic lipid-based gene delivery reagents for use in developing vertebrate embryos," *Developmental Dynamics*, vol. 235, no. 8, pp. 2210–2219, 2006.

[152] and G. L.-B. Bulent Ozpolata, Anil K. Soodb, "LIPOSOMAL SIRNA NANOCARRIERS FOR CANCER THERAPY," *Adv Drug Deliv Rev*, vol. 66, pp. 110–116, 2014.

[153] B. K. Kim, Y. B. Seu, Y. U. Bae, T. W. Kwak, H. Kang, I. J. Moon, G. B. Hwang, S. Y. Park, and K. O. Doh, "Efficient delivery of plasmid DNA using cholesterol-based cationic lipids containing polyamines and ether linkages," *International Journal of Molecular Sciences*, vol. 15, no. 5, pp. 7293–7312, 2014.

[154] Y. Lee, H. Koo, Y. Lim, Y. Lee, H. Mo, and J. S. Park, "New cationic lipids for gene transfer with high efficiency and low toxicity: T-shape cholesterol ester derivatives.," *Bioorganic & Medicinal Chemistry Letters*, vol. 14, no. 10, pp. 2637–2641, May 2004.

[155] H. Lv, S. Zhang, B. Wang, S. Cui, and J. Yan, "Toxicity of cationic lipids and cationic polymers in gene delivery.," *Journal of Controlled Release*, vol. 114, no. 1, pp. 100–109, Aug. 2006.

[156] I. M. Hafez, N. Maurer, and P. R. Cullis, "On the mechanism whereby cationic lipids promote intracellular delivery of polynucleic acids.," *Gene therapy*, vol. 8, no. 15, pp. 1188–1196, 2001.

[157] L. Zhu and R. I. Mahato, "Lipid and polymeric carrier-mediated nucleic acid delivery.," *Expert opinion on drug delivery*, vol. 7, no. 10, pp. 1209–1226, 2010.

[158] C. H. Jones, C.-K. Chen, A. Ravikrishnan, S. Rane, and B. a Pfeifer, "Overcoming Nonviral Gene Delivery Barriers: Perspective and Future.," *Molecular pharmaceutics*, vol. 10, no. 11, pp. 4082–4098, Oct. 2013.

[159] M. Muñoz-Ubeda, A. Rodríguez-Pulido, A. Nogales, A. Martín-Molina, E. Aicart, and E. Junquera, "Effect of lipid composition on the structure and theoretical phase diagrams of DC-Chol/DOPE-DNA lipoplexes.," *Biomacromolecules*, vol. 11, no. 12, pp. 3332–33340, Dec. 2010.

[160] Y.-C. Tseng, S. Mozumdar, and L. Huang, "Lipid-based systemic delivery of siRNA.," *Advanced Drug Delivery Reviews*, vol. 61, no. 9, pp. 721–731, Jul. 2009.

[161] L. Huang and Y. Liu, "In vivo delivery of RNAi with lipid-based nanoparticles.," *Annual review of biomedical engineering*, vol. 13, pp. 507–530, 2011.

[162] A. K. K. Leung, I. M. Hafez, S. Baoukina, N. M. Belliveau, I. V. Zhigaltsev, E. Afshinmanesh, D. P. Tieleman, C. L. Hansen, M. J. Hope, and P. R. Cullis, "Lipid nanoparticles containing siRNA synthesized by microfluidic mixing exhibit an electron-dense nanostructured core," *Journal of Physical Chemistry C*, vol. 116, no. 34, pp. 18440–18450, 2012.

[163] S. Sun, M. Wang, K. A. Alberti, A. Choy, and Q. Xu, "DOPE facilitates quaternized lipidoids (QLDs) for in vitro DNA delivery," *Nanomedicine: Nanotechnology, Biology, and Medicine*, vol. 9, no. 7, pp. 849–854, 2013.

[164] G. Caracciolo and R. Caminiti, "Do DC-Chol/DOPE-DNA complexes really form an inverted hexagonal phase?," *Chemical Physics Letters*, vol. 411, pp. 327–332, Aug. 2005.

[165] I. S. Zuhorn, U. Bakowsky, E. Polushkin, W. H. Visser, M. C. A. Stuart, J. B. F. N. Engberts, and D. Hoekstra, "Nonbilayer phase of lipoplex-membrane mixture determines endosomal escape of genetic cargo and transfection efficiency," *Molecular Therapy*, vol. 11, no. 5, pp. 801–810, 2005.

[166] and L. H. Jing Zhanga, Xiang Lia, "Non-viral nanocarriers for siRNA delivery in breast cancer," *Journal of Controlled Release*, vol. 1, pp. 440–450, 2014.

[167] D. Putnam, "Design and development of effective siRNA delivery vehicles.," *Proceedings of the National Academy of Sciences of the United States of America*, vol. 111, no. 11, pp. 3903–3904, 2014.

[168] A. Panariti, G. Miserocchi, and I. Rivolta, "The effect of nanoparticle uptake on cellular behavior: Disrupting or enabling functions?," *Nanotechnology, Science and Applications*, vol. 5, no. 1, pp. 87–100, 2012.

[169] G. Sahay, D. Y. Alakhova, and A. V. Kabanov, "Endocytosis of nanomedicines," *Journal of Controlled Release*, vol. 145, no. 3, pp. 182–195, 2010.

[170] I. a Khalil, K. Kogure, H. Akita, and H. Harashima, "Uptake pathways and subsequent intracellular trafficking in nonviral gene delivery.," *Pharmacological reviews*, vol. 58, no. 1, pp. 32–45, 2006.

[171] J. Samaj, B. Baluska, FrantisekVoigt, M. Schlicht, D. Volkmann, and D. Menzel, "Endocytosis, Actin Cytoskeleton, and Signaling1," *Plant physiology*, vol. 135, no. July, pp. 1150–1161, 2004.

[172] J. P. Lim and P. a Gleeson, "Macropinocytosis: an endocytic pathway for internalising large gulps," *Immunology and Cell Biology*, vol. 89, no. 8, pp. 836–843, 2011.

[173] M. Amyere, M. Mettlen, P. Van Der Smissen, A. Platek, B. Payrastre, A. Veithen, and P. J. Courtoy, "Origin, originality, functions, subversions and molecular signalling of macropinocytosis.," *International journal of medical microbiology*, vol. 291, no. 6–7, pp. 487–494, 2002.

[174] C. de Duve, "Lysosomes," in *The lysosome concept*, 1963, pp. 362–383.

[175] S. D. Conner and S. L. Schmid, "Regulated portals of entry into the cell.," *Nature*, vol. 422, no. 6927, pp. 37–44, 2003.

[176] J. Rejman, V. Oberle, I. S. Zuhorn, and D. Hoekstra, "Size-dependent internalization of particles via the pathways of clathrin- and caveolae-mediated endocytosis," *Biochem J*, vol. 377, 2004.

[177] A. S. and M. von Zastrow, "Endocytosis and signalling: intertwining molecular networks," *Nat Rev Mol Cell Biol.*, vol. 10, no. 9, pp. 609–622, 2009.

[178] A. F. A. and K. W. Leonga, "Emerging links between surface nanotechnology and endocytosis: impact on nonviral gene delivery," *Nano Today*, vol. 5, no. 6, pp. 553–569, 2010.

[179] D. S. Friend, D. Papahadjopoulos, and R. J. Debs, "Endocytosis and intracellular processing accompanying transfection mediated by cationic liposomes," *Biochimica et Biophysica Acta - Biomembranes*, vol. 1278, no. 1, pp. 41–50, 1996.

[180] S. Mayor and R. E. Pagano, "Pathways of clathrin-independent endocytosis," *NATURE REVIEWS | MOLECULAR CELL BIOLOGY*, vol. 8, no. 8, pp. 603–612, 2007.

[181] K. Takei and V. Haucke, "Clathrin-mediated endocytosis: Membrane factors pull the trigger," *Trends in Cell Biology*, vol. 11, no. 9, pp. 385–391, 2001.

[182] H. T. McMahon and E. Boucrot, "Molecular mechanism and physiological functions of clathrin-mediated endocytosis," *Nat Rev Mol Cell Biol*, vol. 12, no. 8, pp. 517–533, 2011.

[183] M. A. Edeling, C. Smith, and D. Owen, "Life of a clathrin coat: insights from clathrin and AP structures," *Nature Reviews Molecular Cell Biology*, vol. 7, no. 1, pp. 32–44, 2006.

[184] M. Ehrlich, W. Boll, A. Van Oijen, R. Hariharan, K. Chandran, M. L. Nibert, and T. Kirchhausen, "Endocytosis by random initiation and stabilization of clathrin-coated pits," *Cell*, vol. 118, no. 5, pp. 591–605, 2004.

[185] N. V. Popova, I. E. Deyev, and A. G. Petrenko, "Clathrin-mediated endocytosis and adaptor proteins," *Acta Naturae*, vol. 5, no. 18, pp. 62–73, 2013.

[186] T. Kirchhausen, J. S. Bonifacino, and H. Riezman, "Linking cargo to vesicle formation: Receptor tail interactions with coat proteins," *Current Opinion in Cell Biology*, vol. 9, no. 4, pp. 488–495, 1997.

[187] S. M. Sweitzer and J. E. Hinshaw, "Dynamin undergoes a GTP-dependent conformational change causing vesiculation," *Cell*, vol. 93, no. 6, pp. 1021–1029, 1998.

[188] M. G. J. Ford, I. G. Mills, B. J. Peter, Y. Vallis, G. J. K. Praefcke, P. R. Evans, and H. T. McMahon, "Curvature of clathrin-coated pits driven by epsin," *Nature*, vol. 419, no. 6905, pp. 361–366, 2002.

[189] B. Pyrzynska, I. Pilecka, and M. Miaczynska, "Endocytic proteins in the regulation of nuclear signaling, transcription and tumorigenesis," *Molecular Oncology*, vol. 3, no. 4, pp. 321–338, 2009.

[190] M. S. Robinson and C. Watts, "Membrane Dynamics in Endocytosis," *Cell*, vol. 84, pp. 13–21, 1996.

[191] E. Macia, M. Ehrlich, R. Massol, E. Boucrot, C. Brunner, and T. Kirchhausen, "Dynasore, a Cell-Permeable Inhibitor of Dynamin," *Developmental Cell*, vol. 10, no. 6, pp. 839–850, 2006.

[192] J. E. Hinshaw and S. L. Schmid, "Dynamin self-assembles into rings suggesting a mechanism for coated vesicle budding.," *Nature*, vol. 374, no. 6518. pp. 190–192, 1995.

[193] H. Xu and D. Ren, "Lysosomal physiology," *Annu Rev Physiol*, vol. 77, no. 1, pp. 57–80, 2015.

[194] S. AL Stoorvogel W, Strous GJ, Ciechanover A, "Trafficking of the transferrin receptor," *Targeted Diagnosis and Therapy*, no. 4, pp. 267–304, 1991.

[195] R. Tourdot and R. Radhakrishnan, "Clathrin Mediated Endocytosis and its Role in Viral Entry," *Atlas of Genetics and Cytogenetics in Oncology and Haematology*, vol. 17, no. 8, pp. 583–588, 2013.

[196] K. Sandvig and B. Van Deurs, "Selective Modulation of the Endocytic Uptake of Ricin and Fluid Phase Markers without Alteration in Transferrin Endocytosis," *Journal of Biological Chemistry*, vol. 265, no. 11, pp. 6382–6388, 1990.

[197] A. L. Kiss and E. Botos, "Endocytosis via caveolae: Alternative pathway with distinct cellular compartments to avoid lysosomal degradation?," *Journal of Cellular and Molecular Medicine*, vol. 13, no. 7, pp. 1228–1237, 2009.

[198] L. Pelkmans and A. Helenius, "Endocytosis via caveolae," *Traffic*, vol. 3, no. 13, pp. 311–320, 2002.

[199] J. Pohl, A. Ring, and W. Stremmel, "Uptake of long-chain fatty acids in HepG2 cells involves caveolae: analysis of a novel pathway," *J. Lipid Res*, vol. 43, no. 9, pp. 1390–1399, 2002.

[200] S. Suetsugu, S. Kurisu, and T. Takenawa, "Dynamic Shaping of Cellular Membranes by Phospholipids and Membrane-Deforming Proteins," *Physiological Reviews*, vol. 94, no. 4, pp. 1219–1248, 2014.

[201] S. C. P.- Scp-, D. Mir, A. B. Kier, J. M. Ball, and F. Schroeder, "A New N-terminal Recognition Domain in Caveolin-1 Interacts with Sterol Carrier Protein-2 (SCP-2)," *Biochemistry*, vol. 46, no. 28, pp. 8301–8314, 2007.

[202] T. M. Williams and M. P. Lisanti, "The caveolin proteins.," *Genome biology*, vol. 5, no. 214, 2004.

[203] L. von Kleist and V. Haucke, "At the Crossroads of Chemistry and Cell Biology: Inhibiting Membrane Traffic by Small Molecules," *Traffic*, vol. 13, no. 4, pp. 495–504, 2012.

[204] L. K. Medina-Kauwe, "'Alternative' Endocytic Mechanisms Exploited by Pathogens: New Avenues for Therapeutic Delivery?," *Adv Drug Deliv Rev*, vol. 59, no. 8, pp. 798–809, 2007.

[205] C. Le Roy and J. L. Wrana, "Clathrin- and non-clathrin-mediated endocytic regulation of cell signalling.," *Nature reviews. Molecular cell biology*, vol. 6, pp. 112–126, 2005.

[206] B. Razani, "Caveolae: From Cell Biology to Animal Physiology," *Pharmacological Reviews*, vol. 54, no. 3, pp. 431–467, 2002.

[207] and B. R. James H. Hurley1, Evzen Boura1, Lars-Anders Carlson1, "Membrane Budding," *Cell*, vol. 143, no. 6, pp. 875–887, 2010.

[208] I. R. Nabi and P. U. Le, "Caveolae/raft-dependent endocytosis," *Journal of Cell Biology*, vol. 161, no. 4, pp. 673–677, 2003.

[209] L. Kou, J. Sun, Y. Zhai, and Z. He, "The endocytosis and intracellular fate of nanomedicines: Implication for rational design," *Asian Journal of Pharmaceutical Sciences*, vol. 8, no. 1, pp. 1–8, 2013.

[210] L. S. Anderson RG, Kamen BA, Rothberg KG, "Potocytosis: sequestration and transport of small molecules by caveolae," *Science*, vol. 255, no. 5043, pp. 410–411, 1992.

[211] J. a Swanson and C. Watts, "Macropinocytosis.," *Trends in cell biology*, vol. 5, no. 11, pp. 424–428, 1995.

[212] M. C. Kerr and R. D. Teasdale, "Defining macropinocytosis," *Traffic*, vol. 10, no. 4, pp. 364–371, 2009.

[213] S. Grimmer, B. van Deurs, and K. Sandvig, "Membrane ruffling and macropinocytosis in A431 cells require cholesterol.," *Journal of cell science*, vol. 115, no. Pt 14, pp. 2953–62, 2002.

[214] J. D. Orth, E. W. Krueger, H. Cao, and M. a McNiven, "The large GTPase dynamin regulates actin comet formation and movement in living cells.," *Proceedings of the National Academy of Sciences of the United States of America*, vol. 99, no. 1, pp. 167–172, 2002.

[215] and M. G. Xiao-Xiang Zhang, Phillip G. Allen, "Macropinocytosis is the Major Pathway Responsible for DNA Transfection in CHO cells by a Charge-Reversal Amphiphile," *Molecular Pharmaceutics*, vol. 8, no. 3, 2011.

[216] D. Dutta and J. G. Donaldson, "Search for inhibitors of endocytosis: Intended specificity and unintended consequences," *Cellular Logistics*, vol. 2, no. 4, pp. 203–208, 2012.

[217] I. Nakase, M. Niwa, T. Takeuchi, K. Sonomura, N. Kawabata, Y. Koike, M. Takehashi, S. Tanaka, K. Ueda, and J. C. Simpson, "Cellular uptake of arginine-rich peptides: roles for macropinocytosis and actin rearrangement," *Molecular Therapy*, vol. 10, no. 6, pp. 1011–1022, 2004.

[218] A. Prokop and J. Davidson, "Nanovehicular intracellular delivery systems," *Journal of pharmaceutical sciences*, vol. 97, no. 9, pp. 3518–3590, 2008.

[219] E. M. Damm, L. Pelkmans, J. Kartenbeck, A. Mezzacasa, T. Kurzchalia, and A. Helenius, "Clathrin- and caveolin-1-independent endocytosis: Entry of simian virus 40 into cells devoid of caveolae," *Journal of Cell Biology*, vol. 168, no. 3, pp. 477–488, 2005.

[220] L. Pelkmans, "Secrets of caveolae- and lipid raft-mediated endocytosis revealed by

mammalian viruses," *Biochimica et Biophysica Acta - Molecular Cell Research*, vol. 1746, no. 3, pp. 295–304, 2005.

[221] N. M. Zaki and N. Tirelli, "Gateways for the intracellular access of nanocarriers: a review of receptor-mediated endocytosis mechanisms and of strategies in receptor targeting," *Expert Opinion on Drug Delivery*, vol. 7, no. 8, pp. 895–913, 2010.

[222] A. Laude and I. Prior, "Plasma membrane microdomains: organization, function and trafficking," *Molecular membrane biology*, vol. 21, no. 3, pp. 193–205, 2004.

[223] M. Jovic, M. Sharma, J. Rahajeng, and S. Caplan, "The early endosome: A busy sorting station for proteins at the crossroads," *Histology and Histopathology*, vol. 25, no. 1, pp. 99–112, 2010.

[224] J. L. Gallop, A. Walrant, L. C. Cantley, and M. W. Kirschner, "Phosphoinositides and membrane curvature switch the mode of actin polymerization via selective recruitment of toca-1 and Snx9.," *Proceedings of the National Academy of Sciences of the United States of America*, vol. 110, no. 18, pp. 7193–8, 2013.

[225] D. Vercauteren, R. E. Vandenbroucke, A. T. Jones, J. Rejman, J. Demeester, S. C. De Smedt, N. N. Sanders, and K. Braeckmans, "The use of inhibitors to study endocytic pathways of gene carriers: optimization and pitfalls," *Molecular Therapy*, vol. 18, no. 3, pp. 561–569, 2010.

[226] S. Guo, X. Zhang, M. Zheng, X. Zhang, C. Min, Z. Wang, S. H. Cheon, M. H. Oak, S. Y. Nah, and K. M. Kim, "Selectivity of commonly used inhibitors of clathrin-mediated and caveolae-dependent endocytosis of G protein-coupled receptors," *Biochimica et Biophysica Acta - Biomembranes*, vol. 1848, no. 10, pp. 2101–2110, 2015.

[227] P. U. Le and I. R. Nabi, "Distinct caveolae-mediated endocytic pathways target the Golgi apparatus and the endoplasmic reticulum.," *Journal of cell science*, vol. 116, no. 6, pp. 1059–1071, 2003.

[228] and J. A. Jan E. Schnitzer, Phil Oh, Emmett Pinney, "Filipin-sensitive Caveolae-mediated Transport in Endothelium: Reduced Transcytosis, Scavenger Endocytosis, and Capillary Permeability of Select Macromolecules," *The Journal of Cell Biology*, vol. 127, no. 5, pp. 1217–1232, 1994.

[229] S. K. Rodal, G. Skretting, O. Garred, F. Vilhardt, B. van Deurs, and K. Sandvig, "Extraction of cholesterol with methyl-beta-cyclodextrin perturbs formation of clathrin-coated endocytic vesicles.," *Molecular biology of the cell*, vol. 10, no. 4, pp. 961–974, 1999.

[230] M. Koivusalo, C. Welch, H. Hayashi, C. C. Scott, M. Kim, T. Alexander, N. Touret, K. M. Hahn, and S. Grinstein, "Amiloride inhibits macropinocytosis by lowering submembranous pH and preventing Rac1 and Cdc42 signaling," *Journal of Cell Biology*, vol. 188, no. 4, pp. 547–563, 2010.

[231] S. Gold, P. Monaghan, P. Mertens, and T. Jackson, "A clathrin independent macropinocytosis-like entry mechanism used by bluetongue virus-1 during infection of BHK cells," *PLoS ONE*, vol. 5, no. 6, 2010.

[232] G. Ter-Avetisyan, G. Tünnemann, D. Nowak, M. Nitschke, A. Hermann, M. Drab, and M. C. Cardoso, "Cell entry of arginine-rich peptides is independent of endocytosis," *Journal of Biological Chemistry*, vol. 284, no. 6, pp. 3370–3378, 2009.

[233] T. G. Iversen, T. Skotland, and K. Sandvig, "Endocytosis and intracellular transport of

nanoparticles: Present knowledge and need for future studies," *Nano Today*, vol. 6, no. 2, pp. 176–185, 2011.

[234] N. B. Cole, C. L. Smith, N. Sciaky, M. Terasaki, M. Edidin, and J. Lippincott-Schwartz, "Diffusional mobility of Golgi proteins in membranes of living cells.," *Science*, vol. 273, no. 5276, pp. 797–801, 1996.

[235] H. Damke, T. Baba, A. M. Van Der Bliek, and S. L. Schmid, "Clathrin-independent pinocytosis is induced in cells overexpressing a temperature-sensitive mutant of dynamin," *Journal of Cell Biology*, vol. 131, no. 1, pp. 69–80, 1995.

[236] Q. Guo, E. Vasfle, A. Fisher, and M. Krieger, "Disruptions in Golgi Structure and Membrane Traffic in a Conditional Lethal Mammalian Cell Mutant Are Corrected by e-COP," *The Journal of CeU Biology*, vol. 125, no. 6, pp. 1213–1224, 1994.

[237] A. P. Liu, F. Aguet, G. Danuser, and S. L. Schmid, "Local clustering of transferrin receptors promotes clathrin-coated pit initiation," *Journal of Cell Biology*, vol. 191, no. 7, pp. 1381–1393, 2010.

[238] S. Duit, H. Mayer, S. M. Blake, W. J. Schneider, and J. Nimpf, "Differential functions of ApoER2 and very low density lipoprotein receptor in Reelin signaling depend on differential sorting of the receptors," *Journal of Biological Chemistry*, vol. 285, no. 7, pp. 4896–4908, 2010.

[239] K. Sandvig, J. Bergan, A. B. Dyve, T. Skotland, and M. L. Torgersen, "Endocytosis and retrograde transport of Shiga toxin," *Toxicon*, vol. 56, no. 7, pp. 1181–1185, 2010.

[240] I. H. L. Hamelers, R. W. H. M. Staffhorst, J. Voortman, B. De Kruijff, J. Reedijk, P. M. P. Van Bergen En Henegouwen, and A. I. P. M. De Kroon, "High cytotoxicity of cisplatin nanocapsuies in ovarian carcinoma cells depends on uptake by caveolae-mediated endocytosis," *Clinical Cancer Research*, vol. 15, no. 4, pp. 1259–1268, 2009.

Chapter 2 - Materials and General Methods

2.1 Materials

2.1.1 Cells and Cell Culture Consumables

A549 human non-small lung adenocarcinoma cells were purchased from the American Type Culture Collection (ATCC number; CCL-185). A549-Luciferase (A549-Luc) cells are derived from A549 cells by stable transfection of the firefly luciferase gene, and were a generous gift from Dr Anna Grabowska (Faculty of Medicine and Health Science, University of Nottingham). Both cells were used between passages 15-45 and routinely cultured in Dulbecco's Modified Eagle's Medium (DMEM), supplemented with 1% (v/v) antibiotic/antimycotic solution (100 U/ml penicillin, 0.1 mg/ml streptomycin, and 0.25 μg/ml amphotericin B), 1% (v/v) L-glutamine (200 mM), 1% (v/v) non-essential amino acids, and 10% (v/v) foetal bovine serum (FBS). All media and supplements were purchased from Sigma-Aldrich (Poole, UK). Trypsin/ethylenediaminetetraacetic acid (EDTA) solution (used to detach adherent cells in the processes of cell 'splitting' or 'passaging') was purchased from Sigma-Aldrich. Phosphate buffered saline (PBS) tablets (pH 7.4) composed of sodium chloride (8.0 g/l), potassium chloride (0.2 g/l), disodium hydrogen phosphate (1.15 g/l) and potassium dihydrogen phosphate (0.2 g/l) were obtained from Oxoid (Basingstoke, UK).

2.1.2 Plasticware and Glassware

24-well plates and 75 cm^2 cell culture flasks, and sterile pipettes, which were used for the maintenance of cells, were obtained from Corning Life Sciences (Amsterdam, The Netherlands). Clear, treated tissue culture 96-well plates, clear bottom 96-black well plates (used for luminescence measurements), black 96-well microplates (used for fluorescence measurements), were supplied by Nunc™ (ThermoFisher Scientific, Loughborough, UK). 8-well ibidi® micro–chamber slides used for confocal microscopy were supplied by Thistle Scientific Ltd (Glasgow, UK). 50 ml and 15 ml volume sterile centrifuge tubes were obtained from Greiner (Stonehouse, UK) and 30 ml and 7 ml universal and bijou tubes were supplied by Sterilin (Newport, UK). Haemocytometer (improved Neubauer, to British Standard 748) was supplied by Scientific Laboratory Supplies (SLS; Nottingham, UK). PD-10 desalting columns and Mr. Frosty™ freezing container were purchased from Fisher scientific. Ultrafiltration centrifugation tubes (Vivaspin®) were obtained from ThermoFisher Scientific. Extruder was purchased from Avanti-polar lipids (Alabama, USA).

2.1.3 Chemical and Biological Reagents

3-(4,5-dimethylthiazol-2-yl)-5-(3-carboxymethoxyphenyl)-2-(4-sulfophenyl)-2H-tetrazolium MTS reagent (commercially known as 'CellTiter 96® AQueous One Solution Cell Proliferation Assay') and the Luciferase assay kit were purchased from Promega (Southampton, UK). Lactate Dehydrogenase (LDH) assay kit (known commercially as 'In Vitro Toxicology Assay Kit') was supplied by Sigma Aldrich. The Annexin V-cy3 apoptosis detection reagent was purchased from Autogen Bioclear (Wiltshire, UK). DRAQ5™ fluorescent probe solution was obtained from Fisher Scientific. All assays were performed as per supplier's instructions.

Cationic lipid 3ß-[N-(N′,N′-dimethylaminoethane)-carbamoyl] cholesterol (DC-Chol) and dioleoylphosphatidylethanolamine (DOPE), with molecular weights 537.26 g/mol and 744.02 g/mol, respectively, were purchased from Avanti-polar Lipids. OptiMEM media and Lipofectamine® RNAiMAX™ transfection reagents were procured from ThermoFisher Scientific. Transferrin-Alexa Fluor® 488 Conjugate (T*f*) and cholera toxin B subunit-Alexa Fluor® 488 Conjugate (CTß) were purchased from Fisher scientific. Agarose powder was obtained from MP Biomedicals (USA). Triton X-100, dimethylsulfoxide (DMSO), tris-acetate-EDTA (TAE) buffer, ethidium bromide (EtBr, 10 mg/ml solution), heparin (sodium), mounting medium, propidium iodide (PI) and RNase A solution were obtained from Sigma-Aldrich. Pharmacological inhibitors; concanavalin A, chlorpromazine, dynasore, genistein, MßCD, nystatin, filipin, EIPA, cytochalasin D and chloroquine were obtained from Sigma-Aldrich. Accutase solution used to detach cells from well plate before flow cytometry analysis was obtained from Sigma-Aldrich.

2.1.4 Nucleic Acids

Silencer® Cy™3-labeled negative control siRNA was obtained from Fisher Scientific. Unlabelled negative control siRNA with a nonsense/scrambled sequence was purchased from Eurogentec (Southampton, UK). The luciferase siRNA was purchased from Eurogentec and had the following sequence: 5`-CCGCAAGAUCCGCGAGAUU-3` with dTdT overhang. 5' 6-FAM-3'BHQ-1™/BHQ-2™ siRNA based Molecular Beacon (MB) used for flow cytometry and confocal microscopy was designed with the same sequence as that of luciferase siRNA to target luciferase mRNA and was purchased from Eurogentec. The mechanism of the MB will be described in Chapter 4. All nucleic acids

were obtained as lyophilized powders and were diluted with nuclease free water and stored at -20°C as 20 μM stock solution for further use.

For cell viability assay on selected gene, ON-TARGETplus siRNA with dTdT overhang and the following sequence: *EGFR* 5`-CACAGUGGAGCGAAUUCCU-3` was used as obtained from ThermoFisher Scientific.

2.2 Methods

2.2.1 Maintenance of Cells

2.2.1.1 Maintenance of Cells in Culture Flasks

A549 and A549-Luc cell lines were cultured in DMEM medium and incubated at 37°C in a 5% CO_2 air-humidified atmosphere in 75 cm^2 flasks until semi-confluent (approximately 80-95%). Cell growth was monitored regularly using an optical inverted microscope. Culture medium was changed every 2-3 days by aspirating the spent medium and replacing it with approximately 12 ml of fresh pre-warmed (37°C) medium. Cells were passaged by aspirating the culture medium, washing with approximately 5 ml of warmed (37°C) PBS to remove any residual medium and dead cells, followed by the addition of approximately 3 ml 2.5% trypsin/EDTA solution. Cells were incubated with trypsin/EDTA solution for 10-15 min until the cells detached from the flask surface. Thereafter, approximately 8 ml of cell culture medium was added to the suspension of cells in trypsin/EDTA to inhibit the action of trypsin. The cell suspension was transferred to a sterile 15 ml centrifuge tube and the cells were pelleted by centrifugation at 500 x g for 5 min. The supernatant was discarded and fresh culture medium added to the pelleted cells to produce a cell suspension. The cells were split between 1:10 and 1:20 into a new flask containing 12 ml of fresh culture medium (warmed to 37°C).

2.2.1.2 Frozen Storage of Cells

Cells were cultured in the tissue culture 75 cm^2 flask until confluence, and then detached from the flask as described in Section 2.2.1.1. After the cell suspension was centrifuged, the supernatant was aspirated. The cell pellet was re-suspended in 1 ml 90% supplemented DMEM, 10% DMSO and transferred to a sterile cryovial, clearly labelled with the user name, cell type, passage number, and date, and placed into a Mr. Frosty™ freezing container containing 250 ml propan-2-ol and left in a -80°C freezer overnight for a gradual, controlled temperature decrease. The system is designed to achieve a rate of cooling very close to -1°C/min, the optimal rate for cell preservation. After that, the vials were transferred into a liquid nitrogen cell storage tank.

2.2.1.3 Cell Revival

Cryovials containing frozen cells were thawed by placing the cryovial in a water bath at 37°C for approximately 5 min. Then the entire contents of the cryovial (DMSO-containing medium and cells) were removed and transferred into a centrifuge tube which contained approximately 10 ml of pre-warmed culture medium. The cell suspension was then centrifuged at 500 x g for 5 min. The supernatant was aspirated and the cell pellet re-suspended in approximately 5 ml of pre-warmed culture medium and transferred to a 75 cm^2 tissue culture flask containing fresh pre-warmed supplemented medium, as described in Section 2.1.1, and incubated under standard conditions.

2.2.2 Preparation of Empty and siRNA-Liposomes

The formulations of empty and siRNA-liposomes were prepared using the classical thin-film hydration method with different total lipid concentrations, different molar ratios of DC-Chol (cationic lipid) to DOPE (zwitterionic lipid) and with different ratios of cationic lipid to siRNA (N/P ratios).

Cationic and helper lipids were dissolved separately in chloroform (1.0 mg/ml), and the solutions mixed in a round bottom flask to achieve different lipid molar ratios and different total lipid concentrations. N_2 gas was used for the evaporation of the solvent until a thin film was formed, which was then hydrated with the addition of an appropriate volume of warmed PBS (10 mM, pH 7.4) containing either scrambled siRNA, cy3-labeled siRNA, FAM-siRNA based MB, or luciferase siRNA. The free, non-encapsulated siRNA was removed from the liposomal formulations using a PD-10 desalting column (containing Sephadex G-25 gel filtration resin) that separates molecules on the basis of differences in size. The formulation was then passed through an extruder, as shown in Figure 2.1, equipped with 0.2 μm polycarbonate membrane filters for 21 times to produce unilamellar liposomes.

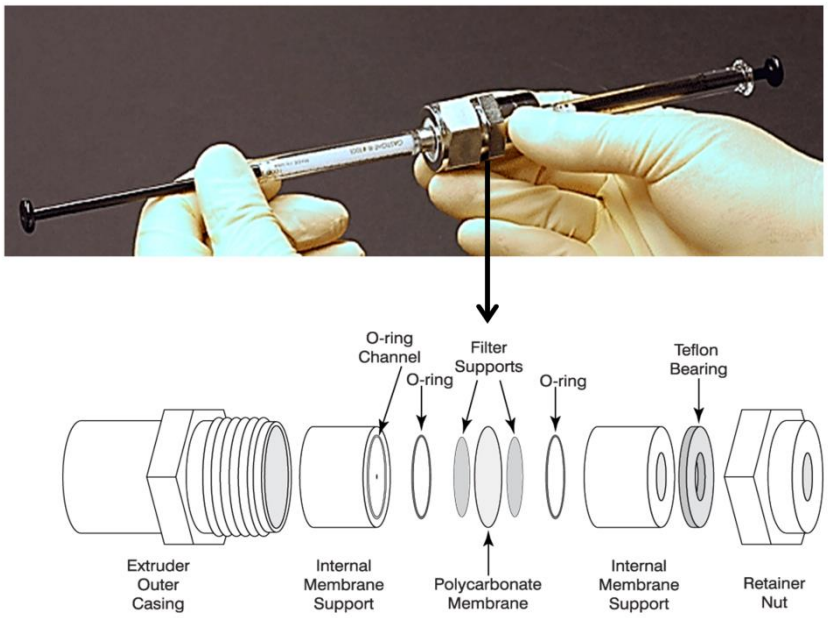

Figure 2.1: Schematic diagram of the extruder apparatus

Liposomes were loaded into one of the syringes and placed into one end of the mini-extruder equipped with a 0.2 μm polycarbonate membrane filter. The plunger of the filled syringe was pushed until the content was completely transferred to the alternate syringe. This cycle was repeated for 21 times. Adapted from [1].

2.2.3 Cell Toxicity Studies

2.2.3.1 MTS Assay

The cytotoxicity of empty and siRNA-liposomes was examined using the MTS assay. This is a colorimetric method, normally used to determine the number of viable cells in proliferation or cytotoxicity assays [2]. It is based on tetrazolium compound, 3-(4,5-dimethylthiazol-2-yl)-5-(3 carboxymethoxyphenyl)- 2- (4-sulfophenyl)-2H tetrazolium (inner salt), and an electron coupling reagent (phenazine ethosulfate; PES). PES has ability to enhance chemical stability allowing its combination with MTS to form a stable solution [2]. The tetrazolium compound is bioreduced by dehydrogenase enzymes inside metabolically active cells to a formazan product, which is soluble in tissue culture

medium [3]. The quantity of formazan product is measured spectrophotometrically and is proportional to the presence of metabolically active (live) cells.

The experiment was conducted as follows: cells were seeded in 96-well plates at a density of 1×10^4 cells per well and were incubated at 37°C, 5% CO_2 in the culture growth medium overnight. Culture medium was removed and replaced with fresh serum-free medium contains the test samples, applied at different concentrations. Cells incubated with serum-free medium only were used as the positive control, whereas cells incubated with 0.2% (v/v) Triton X-100 were used as the negative control. Cells were incubated with the test samples and controls solutions at 37 °C under standard conditions for 4 hrs. After this interval, test samples and controls were removed, and cells washed with PBS. 100 µl of culture medium was then added into each well, followed by 20 µl of the MTS reagent; cells were then incubated for 2 hrs at 37°C under standard conditions. MTS absorbance was thereafter measured at 492 nm using a Dynex absorbance microplate reader (Dynex Technologies, USA). Relative cell viability was calculated using the following equation:

$$Relative\ cell\ viability\ (\%) = \frac{S - T}{H - T} x\ 100$$

Where:

S = absorbance obtained with the test samples

T = absorbance obtained with Triton X-100

H = absorbance obtained with serum-free medium.

2.2.3.2 LDH Assay

The cytotoxicity of empty and siRNA-liposomes was also examined by the LDH assay, which is normally employed as an indicator of relative cell viability, as well as an indicator of the membrane integrity of cells [4]. The latter is a function of the amount of cytoplasmic LDH released into the culture medium [5]. LDH is a soluble enzyme located in the cytosol, and is released into culture medium upon cell membrane damage. This assay is based on two steps. In the first step, LDH catalyses the reduction of nicotinamide adenine dinucleotide ($NAD^{+)}$ to NADH and H^+ by oxidation of lactate to pyruvate [6]. In the second step of the reaction, electron coupling agents or diaphorase uses the newly-formed NADH and H^+ to catalyse the reduction of a tetrazolium salt to highly-coloured formazan which absorbs at 492 nm [5]. The quantity of formazan product is proportional to cell membrane damage.

The assay was conducted in the following steps: cells were cultured in 96-well plate at a density of 1×10^4 cells per well overnight in DMEM at 37°C under standard conditions. Culture growth medium was then removed and replaced with test samples in serum-free medium. 0.2% (v/v) Triton X-100 was used to induce LDH release (positive control), whereas serum-free DMEM was used as the negative control. Cells were incubated with the test samples and controls for 4 hrs. After this period, 50 µl of the test sample solution was removed from each well and placed into a new 96-well plate. 100 µl LDH reagent was applied to the test samples and incubated for 30 min at room temperature. After this period, absorbance at 492 nm was measured using a Dynex absorbance microplate reader. LDH release was calculated using the following equation:

$$LDH\ release\ of\ sample\ (\%) = \frac{S - H}{T - H} x\ 100$$

Where:

S = absorbance obtained with the test samples

T = absorbance obtained with Triton X-100

H = absorbance obtained with serum-free medium.

2.2.3.3 Annexin V-Propidium Iodide Assay

Annexin V/PI assay was performed on the A549 cells to differentiate between the apoptotic, necrotic and live cells. The mechanism of the Annexin V/PI assay will be described in Chapter 3. A549 cells were seeded into a 24-well plate at a density of 5×10^4 cells per well and incubated overnight in 0.5 ml of DMEM. The medium was then aspirated and the cells incubated with empty or siRNA-liposome samples suspended in serum-free DMEM for 4 hrs. Cells incubated with serum-free medium alone were used as negative controls. Annexin V/PI assay was conducted on cells which were detached by trypsin/EDTA treatment (as described in section 2.2.1.1) and collected by centrifugation at 500 x g for 5 min. Cell pellets were resuspended in 0.5 ml binding buffer (0.1 M 4-(2-hydroxyethyl)-1-piperazineethanesulfonic acid (HEPES-pH 7.4), 1.4 M NaCl, and 25 mM $CaCl_2$). Next, 5 µl Annexin V and 5 µl propidium iodide (100 µg/ml) were added to the cells in the dark and incubated at room temperature for 5 min, as instructed by the supplier. The cells were then immediately assessed by flow cytometry using Beckman Coulter MoFlo (measuring a minimum of 10,000 cells/sample), and data was analysed using Weasel Software Version 3.0.2 (The Walter and Eliza Hall Institute of Medical Research, Melbourne, Australia).

2.2.4 Particle Size and Zeta Potential Measurements

The mean diameter and size determination of empty and siRNA-liposome formulations were measured by Dynamic Light Scattering (DLS) using a Viscotek DLS 802 system at 25°C at 40.6 mW of laser power and a fixed scattering angle of 90°. The measurements were performed at room temperature and results represent the mean of 10 measurements. In essence, DLS measurements of the particle size of small colloids in suspension is based on their Brownian motion, and their scattering of incident light; the intensity of the light scattering fluctuates at a rate that is dependent on the size of the particles [7]. From the scattering profiles obtained, particle diameters can be calculated according to the equation below:

$$D = kt/3\pi\eta d$$

Where:

D = diffusion coefficient

k = Boltzmann's constant

t = absolute temperature

η = solvent viscosity

d = diameter of particle.

The zeta potential measurements of empty and siRNA-liposome formulations were assessed using Zetasizer Nano Series (Malvern Instruments, UK). The measurements were carried out at 25°C in 10 mM PBS solution at pH 7.4. Values reported are the mean of three measurements ± SD.

2.2.5 Assessment of Encapsulation Efficiency

2.2.5.1 Gel Retardation Assay

Agarose gel electrophoresis is a technique used to separate molecules such as nucleic acids and proteins according to their size and charge by application of an electric field. As nucleic acids possess a negatively charged phosphate group in every base, different sized fragments have a constant size/charge ratio and so would migrate in a solution at the same rate. An agarose gel matrix has the ability to separate migrating molecules by size; smaller nucleic acid fragments will migrate further. On application of an electric field, free negatively charged siRNA will migrate towards the anode and free positively charged liposomes will migrate towards the cathode. EtBr fluoresces on binding to free siRNA allowing visualisation of siRNA bands in the gel under UV light.

The siRNA encapsulation into liposomes was confirmed by gel electrophoresis. Formulations prepared at different N/P ratios ranging from 0.78:1 to 50:1 were assayed. Naked siRNA and empty liposomes were used as positive and negative controls, respectively. The siRNA-liposome formulations (20 µl) containing 0.4 µg siRNA were mixed with 2.0 µl loading buffer (bromophenol blue and xylene cyanol FF) and separated on a 1.2% (w/v) agarose gel containing EtBr (4 µg, 1 µg/ml) in 1x TAE buffer (40 mM Tris, 20 mM acetic acid, 1mM EDTA) and visualised using a UV transilluminator (GENE, GENIUS, The Bioimaging company, UK) by using Syncgene software.

2.2.5.2 Ultrafiltration Centrifugation Method

Ultrafiltration centrifugation (Vivaspin®) method was used to separate free siRNA from liposome-encapsulated siRNA using centrifugation at 500 x g for 5 min and 4°C as illustrated in Figure 2.2. The liposomal entrapment of siRNA was determined for formulations at different ratios of DC-Chol:DOPE, prepared with 1.0 mM total lipid and 0.4 μg siRNA. The filtrate was collected to determine the free siRNA concentration. The liposome-associated siRNA was assessed by collecting material remaining on the membrane and using 0.2% (v/v) Triton X-100 to disrupt the liposomes and liberate the encapsulated siRNA. The Cy3-labelled siRNA used was then quantified using a fluorimeter, and the encapsulation efficiency (EE %) calculated using following equation:

$$EE\ (\%) = \frac{c_1}{c_0} x\ 100$$

Where:

C_1 = concentration of entrapped siRNA

C_0 = total or initial siRNA concentration.

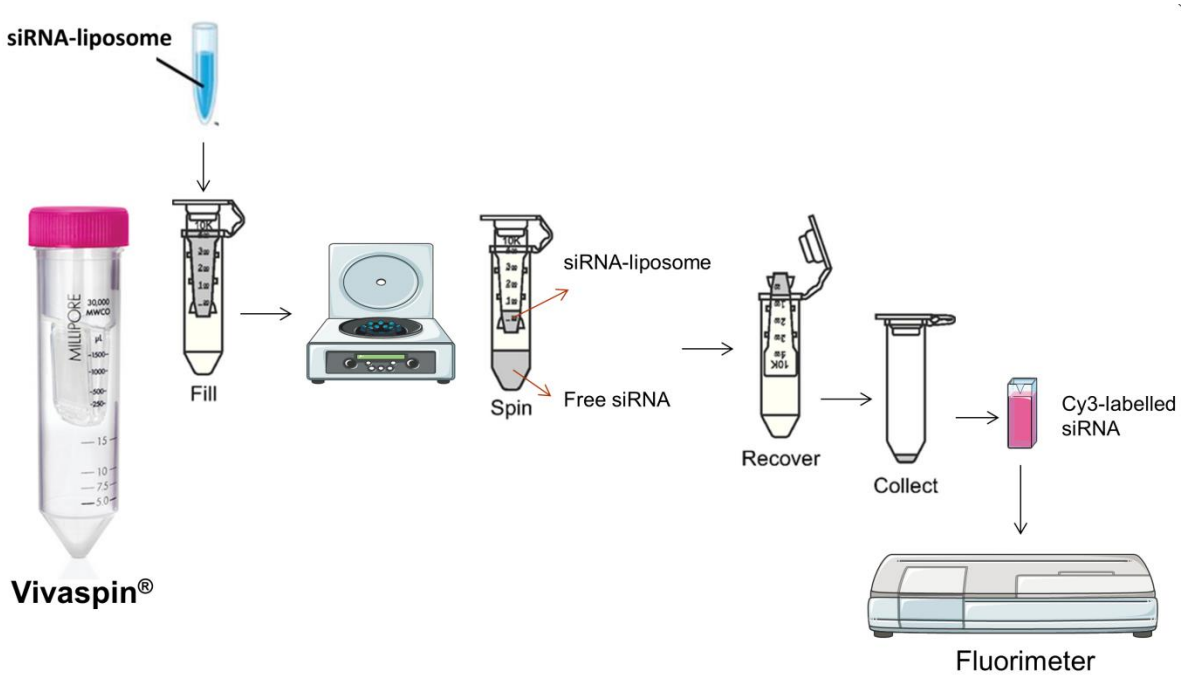

Figure 2.2: Schematic of ultrafiltration centrifugation (Vivaspin®) method

The siRNA-liposome samples were loaded into a Vivaspin® tube and centrifuged at 500 x g for 5 min at 4°C. The filtrate was collected to determine the free siRNA concentration and the liposome-associated siRNA was assessed in the material remaining on the membrane following treatment with 0.2% (v/v) Triton X-100 to liberate the entrapped Cy3-labelled siRNA.

2.2.6 RNase Stability Study

The siRNA-liposome preparations (20 µl containing 0.4 µg siRNA) were incubated with 4 µl RNase A (20 µg/ml) for different time intervals at 37°C to investigate the ability of liposomes to protect the incorporated siRNA from enzymatic degradation. RNase A is an endoribonuclease that attacks at the 3` phosphate of a pyrimidine nucleotide, with functions in RNA metabolism and regulation of gene expression [8]. After the incubation of siRNA-liposomes with RNase enzyme, deionised formamide (denaturing agent) was added to stop the enzymatic activity of RNase. Next, 0.2% (v/v) Triton X-100 (10 µl) was applied to the liposome suspension to disrupt the lipid bilayer and release the incorporated siRNA. Heparin was incubated with the liposome formulations as a

negatively charged competitor for 10 min, at a concentration of 1.7 units per μg of siRNA to ensure the complete release of nucleic acids from the formulations before loading onto a 1.2% (w/v) agarose gel and electrophoresis for 60 min. 'Naked' siRNA not exposed to RNase A was used as a reference and 'naked' siRNA incubated with RNase A was used as a control. Samples were analysed after 30 min, 1, 2, 3, and 4 hrs incubation with RNase A.

2.2.7 Assessment of the Cellular Uptake of Cy3-labelled siRNA

2.2.7.1 Flow Cytometry

Flow cytometry is a laser-based technology employed in cell counting, cell sorting and biomarker detection. Flow cytometry allows simultaneous analysis of physical and chemical characteristics of single cells in a high throughput manner, unlike traditional spectrophotometer techniques where fluorescence is measured for a bulk sample. As the cells pass through the laser source, the scattered and emitted light is converted into electrical pulses, which are then processed and analysed. Typically, 2-3 detectors are used with different wavelength bandpass filters, allowing the simultaneous detection of emissions at different wavelengths from different fluorophores in a single cell.

Cells were seeded in a 24-well plate at a density of 5×10^4 cells per well and incubated overnight in 0.5 ml DMEM. Cells were then washed with PBS and incubated for 4 hrs with serum-reduced OptiMEM containing the liposome–siRNA samples, cy3-siRNA-liposomes (in A549 cells) or 6-FAM 'luc-siRNA based MB' containing liposomes (in A549-Luc cells). The transfection reagent Lipofectamine RNAiMAX® was used as positive control, following the protocol suggested by the supplier. The sample was prepared by mixing 50 μl OptiMEM containing 6 pmol siRNA with another 50 μl

OptiMEM containing 1 µl Lipofectamine RNAiMAX® in an Eppendorf tube and incubation at room temperature for 10-20 min and then applied to the cells for 4 hrs. Cells without cy3-siRNA-liposomes (in A549 cells) or 6-FAM 'luc-siRNA based MB' liposomes (in A549-Luc cells) were used as negative controls.

For investigation of the cellular uptake of Alexa Fluor® 488-labelled T*f* and Alexa Fluor® 488-labelled CTß, cells were incubated with the predetermined concentrations of endocytosis inhibitors (see Sections 5.3.1.1 and 5.3.1.2) for 30 min prior to the application of T*f* (100 µg/ml) or CTß (5 µg/ml). Cells incubated with T*f* or CTß in the absence of endocytosis inhibitors were used as controls. After incubation, the cells were collected and assessed by flow cytometry, using a Beckman Coulter MoFlo instrument with a minimum 10,000 cells/sample, and data were analysed using Weasel Software Version 3.0.2.

2.2.7.2 Confocal Microscopy

A549 and A549-Luc cells were cultured overnight in 0.2 ml DMEM in an ibidi® micro-slide eight-well microscopy chamber at a density of 3×10^4 cells per chamber. Cells were then treated with cy3-siRNA-liposomes (A549 cells) or 6-FAM 'luc-siRNA based MB' liposomes (A549-Luc cells) for 4 hrs, in the presence or absence of endocytosis inhibitors. Cells were then washed gently with PBS and then fixed with 50 µl 4% (w/v) paraformaldehyde for 10 min at room temperature. The cells were washed with PBS before incubation for 10 min at room temperature with DRAQ5 (1:5000) to stain the nuclei. Finally, the cells were washed with PBS and one drop of mounting media was added. Slides were stored at 4°C until viewed using a Zeiss LSM510 confocal microscope.

2.2.8 Silencing of Luciferase Gene Expression

For *in vitro* gene expression studies, A549-Luc cells were seeded in 24-well plates at a density of 5×10^4 cells per well and cultured overnight in 0.5 ml DMEM. The siRNA-liposome samples (containing 0.5 and 1 µg of luciferase siRNA) were prepared as indicated in Section 2.2.2, and added to the cells in OptiMEM® serum-reduced medium and incubated for 4 hrs. The transfection reagent Lipofectamine RNAiMAX® was used as a positive control and prepared by mixing 50 µl OptiMEM containing 6 pmol luciferase siRNA with another 50 µl OptiMEM containing 1 µl transfection reagent in an Eppendorf tube and incubated at room temperature for 10-20 min and then applied to the cells for 4 hrs. A549-Luc cells were also treated with scrambled siRNA-liposomes, under corresponding conditions, as non-targeting control. The medium was then removed, and the cells washed with PBS. After that, cells were incubated in DMEM and the luciferase activity was measured after 24, 48, 72, and 96 hrs to assess time dependence of luciferase knockdown.

To measure luciferase activity, cells were collected at predetermined time points and cell lysates collected to carry out a luciferase assay using the Promega® lysis buffer and luciferase assay reagent. 100 µl Promega lysis buffer was added to each well, and plates were then incubated on a rocker for 20 min at room temperature. In the next stage, 5 µl cell lysate was pipetted into wells of a clear bottom 96-black well plate and 25 µl luciferase assay substrate added into each well. Luciferase activity was measured immediately using a MicroLumi XS luminometer (Hartalabs, USA).

2.2.9 Endocytosis Mechanism of siRNA-Liposomes

To study the endocytic mechanism employed by siRNA-liposomes to gain entry to the cells, the cytotoxicity of endocytosis inhibitors was initially examined using the MTS assay, as described in Section 2.2.3.1, to identify the non-toxic doses of pharmacological inhibitors. A wide range of concentrations of endocytosis inhibitors was applied to the cells: concanavalin A (50-500 μg/ml), chlorpromazine (5-100 μg/ml), dynasore (5-100 μg/ml), genistein (1-75 μg/ml), filipin (5-100 μg/ml), MßCD (100-10,000 μg/ml), nystatin (5-100 μg/ml), EIPA (0.1-50 μg/ml), cytochalasin D (2-75 μg/ml) and chloroquine (25-750 μg/ml).

The effect of selected inhibitors was investigated to determine the lowest concentration of endocytosis inhibitor that can produce maximum inhibition of the particular pathway. To this end, endocytosis of a specific ligand in the presence of endocytosis inhibitors at sub-EC_{50} concentrations was measured. The ligands known to be internalised by the cells via the clathrin pathway, transferrin (T*f*) [9], and via the caveolin pathway, cholera toxin ß (CTß) [10], were used. Cells were incubated with the inhibitors for 30 min prior to the application of Alexa Fluor® 488-labelled T*f* (100 μg/ml) and Alexa Fluor® 488-labelled CTß (5 μg/ml), as described in Section 2.2.7.1. Cells incubated with ligands in the absence of inhibitors were used as controls. After defining the effective concentration of each inhibitor, the mechanisms of endocytosis were always studied by applying the selected concentration of inhibitors for 30 min before treating the cells with siRNA-liposomes samples.

The effect of inhibitors (i) on cellular internalisation was measured by flow cytometry using cy3-labelled siRNA cellular uptake, (ii) on knockdown by luciferase assay in A549-

Luc cells, and (iii) on engagement of siRNA in silencing process in A549-Luc cells using 6-FAM 'luc-siRNA based MB' by flow cytometry. In addition, confocal microscopy, in the case of cy3-labelled siRNA and 6-FAM 'luc-siRNA based MB', was conducted. Cells incubated with cy3-siRNA-liposomes (A549 cells) or 6-FAM 'luc-siRNA based MB' liposomes (A549-Luc cells) in the absence of inhibitors were used as controls.

2.2.10 Candidate Target Gene in NSCLC

Two studies on human lung cancer samples were chosen from Gene Expression Omnibus (GEO) database to perform the gene expression analysis of selected genes. Next to dataset selection, the probe set information for each Affymetrix array for the two studies were collected from the GeneCards database for all candidate genes. Moreover, similar information was collected for the reference gene (Ribosomal Protein S29, RPS29), which will be used in the data analysis stage to normalise the expression intensity.

GeneCards is a searchable, integrative database that provides comprehensive information on all annotated and predicted human genes. The Affymetrix array for each candidate gene was collected according to each study platform. After collecting complete information about candidate genes from GEO and GeneCards databases, the analysis of gene expression microarray for each gene was performed to compare the expression microarray in case of lung cancer and normal lung condition. The expression microarray of each gene was normalised by the reference gene. Then, t-test was performed to confirm that the up- or down-regulation of gene expression of each gene is statistically significant in comparison to healthy lung. More details about the data analysis will be described in Chapter 6.

2.2.11 Statistical Analysis

All data are displayed as mean ± standard deviation from three or four repeats. Student's t-tests were performed for comparisons of two group means, whilst one-way analysis of variance (ANOVA) followed by Bonferroni post-hoc test was applied for comparison of three or more group means. P value of <0.05 was considered statistically significant. ****, ***, ** and * display $p<0.0001$, $p<0.001$, $p<0.01$ and $p<0.05$, respectively, and 'ns' indicates non-significant ($p>0.05$).

2.3 References

[1] Avanti Mini Extruder. [Online]. Available: https://avantilipids.com/divisions/equipment/.

[2] G. Malich, B. Markovic, and C. Winder, The sensitivity and specificity of the MTS tetrazolium assay for detecting the in vitro cytotoxicity of 20 chemicals using human cell lines. *Toxicology*, vol. 124, no. 3, pp. 179–192, Dec. 1997.

[3] P. Twentyman and M. Luscombe, A study of some variables in a tetrazolium dye (MTT) based assay for cell growth and chemosensitivity. *British Journal of Cancer*, vol. 56, no. 1987, pp. 279–285, 1987.

[4] X. Han, R. Gelein, N. Corson, P. Wade-Mercer, J. Jiang, P. Biswas, J. Finkelstein, A. Elder, and G. Oberdörster, Validation of an LDH assay for assessing nanoparticle toxicity. *Toxicology*, vol. 287, no. 1–3, pp. 99–104, 2011.

[5] K. Abe and N. Matsuki, Measurement of cellular 3-(4,5-dimethylthiazol-2-yl)-2,5-diphenyltetrazolium bromide (MTT) reduction activity and lactate dehydrogenase release using MTT. *Neuroscience Research*, vol. 38, no. 4, pp. 325–329, 2000.

[6] D. Lobner, Comparison of the LDH and MTT assays for quantifying cell death: Validity for neuronal apoptosis?. *Journal of Neuroscience Methods*, vol. 96, no. 2, pp. 147–152, 2000.

[7] W. Goldburg, Dynamic light scattering. *American Journal of Physics*, vol. 67, no. 12, pp. 1152–1160, 1999.

[8] W. Huang, M. Zhao, N. Wei, X. Wang, H. Cao, Q. Du, and Z. Liang, Site-specific RNase A activity was dramatically reduced in serum from multiple types of cancer patients. *PLoS ONE*, vol. 9, no. 5, p. 496490, 2014.

[9] K. Mayle, A. Le, and D. Kamei, The intracellular trafficking pathway of transferrin. *Biochimica et Biophysica Acta*, vol. 1820, no. 3, pp. 264–281, 2012.

[10] H. Higgs and K. Peterson, Selective stimulation of caveolar endocytosis by glycosphingolipids and cholesterol. *Molecular Biology of the Cell*, vol. 16, no. 8, pp. 3114–3122, 2004.

Chapter 3 - Biophysical Characterisation of Cationic Liposomes

3.1 Introduction

Delivery of siRNA efficiently to the cytoplasm of target cells is a promising therapeutic approach for the treatment of a wide range of diseases [1]. However, the therapeutic potential of siRNA has not yet been recognised due to the requirement for an appropriate delivery system [2]. Unfavourable properties of siRNA, such as its large size and negative charge, mean that it is difficult for siRNA molecules to cross cell membranes unaided [3]. Naked siRNA has poor cellular uptake, which is attributed to high hydrophilicity and the repulsion of negative charges present on the mammalian cell membrane and 'approaching' siRNA molecules [3]. Moreover, unmodified and unprotected siRNAs are susceptible to enzymatic degradation by RNase within plasma, with a reported half-life of only 2-6 minutes, resulting in a short circulation time and thus limiting its *in vivo* delivery [4].

To overcome the problem of siRNA delivery, a number of systems have been developed. The optimal siRNA delivery system should be non-toxic, protect siRNA from RNase, facilitate intracellular uptake followed by escape from endosome vesicles into the cytosol, and finally encourage effective gene silencing [5]. Cationic liposomes have been considered as siRNA delivery formulations. They have been extensively

investigated and widely used as a delivery system in different biomedical fields, such as the delivery of hydrophilic and hydrophobic molecules, and medical imaging [6], [7].

The evaluation of the *in vitro* cytotoxicity of any biomaterial is an early step in estimating biosafety and biocompatibility that could limit clinical applications [8]. Studying the mechanism of cytotoxicity of cationic liposomes is a critical stage in understanding if and how these particles interact with a variety of cellular targets to produce undesirable effects [9].

The biodegradability and biocompatibility of the lipid content is a vital advantage of liposomes [10]. Studies on entrapment and delivery of siRNA molecules using liposomes have shown that these depend on the physiochemical characteristics of the lipid content [11]. Several factors could contribute to the toxicity of nanoparticles in general, as well as liposomes, including particle size, surface charge and the chemistry of lipid compositions used to prepare liposomes [12]. Using positively charged lipids typically promotes siRNA-liposomes interaction with the cell membrane and cellular internalisation [13]. However, the high cytotoxicity of positively charged lipids remains the main drawback of using cationic liposomes for gene therapy [14], and the chemical structure of these lipids has been reported to be implicated in cellular toxic effects [3]. Cationic liposomes often have cytotoxic effects that arise from their compromising the integrity of the cell membrane, as well as other intracellular effects [15].

For many cationic liposomes (or cationic lipids in general) there is frequently a connection between gene transfection ability and cytotoxicity [16]. A number of studies have reported that positively charged liposomes show higher internalisation by cells,

relative to neutral or anionic liposomes [17]; however, an ideal delivery system should be able to generate maximum transfection activity with minimum cytotoxicity [18]. Both the transfection efficiency and level of cellular toxicity are highly dependent upon the chemistry of the lipid composition of liposomes [19], but also on the type of cultured cells utilised [15]. Optimising the positive and zwitterionic lipid ratio within the liposome formulation may be able to increase the siRNA encapsulation efficiency, improve formulation stability, and decrease cytotoxicity related to highly charged particles [20].

To understand the cytotoxicity of cationic liposomes used in this project, three different assays were employed. The first is the colorimetric MTS assay, which is used to evaluate the metabolic activity of viable cells after applying cationic liposomes [21]. It has been shown in a research by Delikatny *et al*. that cationic lipids could cause mitochondrial damage of cells in culture [22]. The second used test is the LDH assay, which is typically applied to detect defects in the cellular membrane by measuring the release of cytoplasmic lactate dehydrogenase enzyme [23]. Cationic lipid particles are believed to disrupt the plasma membrane of the cells via interaction with membrane bound proteins [15]. Both MTS and LDH were described in detail previously in Chapter 2.

The third assay is a more recent strategy that was introduced to explore the mechanism of cytotoxicity, the Annexin V/Propidium iodide (PI) assay. This technique is commonly used to determine whether cells are still viable, apoptotic or necrotic by following a change in cell membrane permeability and integrity [24]. In the case of early apoptosis, one of the main plasma membrane components, phosphatidylserine,

translocates from the internal to the external surface of the plasma membrane [25], and this translocation can be identified using Annexin V, which is a Ca^{2+} dependant protein that has high affinity to phosphatidylserine [26]. In the case of late apoptosis or cell necrosis, the intercalating agent and membrane non-permeant dye, PI, has the ability to pass through damaged cell and nuclear membranes and bind to DNA, emitting fluorescence [27]. Figure 3.1 summarises the mechanism of Annexin V/PI assay.

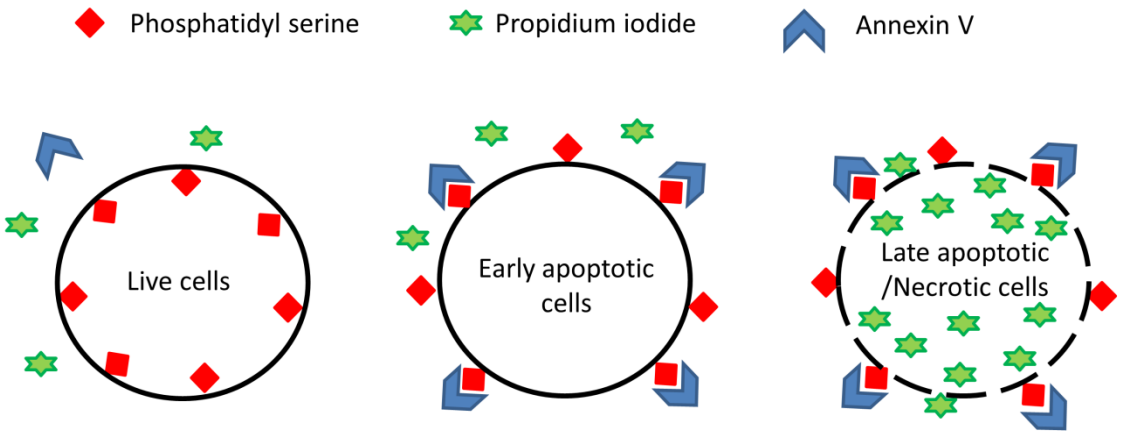

Figure 3.1: Schematic of Annexin V/PI assay mechanism

The surface charge of a liposome particle plays a significant function in cellular uptake and biological activity [28]. To establish a physically stable cationic liposome formulation with efficient encapsulation of siRNA, the electrostatic charge properties of the outer liposomal surface should be optimised [29]. It has been suggested that an ideal liposomal 'charge morphology' could be achieved by controlling the surface charge density, which typically depends on the cationic lipid to zwitterionic lipid ratio [29]. Particle size, zeta potential, encapsulation efficiency of siRNA and the stability of siRNA-liposome preparations have a significant impact on cellular uptake and

transfection efficiency. It has been reported that cellular endosomal compartments have specific size and excessively large sized complexes are unlikely to be taken up by these pathways [30]. Moreover, recent research has demonstrated the important influence of the surface charge of nanoparticles on the downstream biological response such as cellular uptake, biodistribution and the pathway of cellular uptake [31]. Positively charged lipid nanoparticles are usually taken up by cells at a faster rate than anionic or neutral nanoparticles [32], and it has been suggested that cationic nanoparticles can interact with the negatively charged cell membrane and promote lipid bilayer destruction [32].

siRNA is capable of forming different sized complexes with positively charged liposomes which protect siRNA from enzymatic degradation and facilitate cellular uptake [33]. The stability of a siRNA delivery system from the administration site until it reaches the cytoplasm of targeted cells is a crucial factor. It has been stated that extracellular components, such as components of serum, interact with cationic particles and disturb the stability of siRNA-liposome nanoparticles [34].

The nano-scale size (100-200 nm) and overall positive charge of these liposomes allows their endocytosis across cell membrane to reach intracellular space, a cytoplasm [35]. However, physiochemical properties, such as particle size, zeta potential, encapsulation efficiency, and biological stability in the presence of extracellular components, all have a direct influence on the behaviour and efficacy of a siRNA delivery system.

3.2 Aims and Objectives

The aim of work presented in this chapter focuses on formulation optimisation and characterisation of resultant siRNA-liposomes in terms of their cytotoxicity, particle size, zeta potential, siRNA encapsulation efficiency, and siRNA protection from RNase degradation for a series of formulations prepared from different total lipid concentrations, different ratios of cationic to zwitterionic lipid, and different ratios of cationic lipid to siRNA (different N/P ratio). This study adopts a systematic approach to assess the toxicity of empty cationic liposomes and liposomes encapsulating siRNA, presented to the cells in a physiological medium. The formulations will be examined for their cytotoxicity using the MTS, LDH and Annexin V/PI assays. The studies will be conducted using the epithelial NSCLC cell line A549, which is commonly used as an *in vitro* model of lung cancer. The physiochemical characterisation studies will be performed using standard colloidal characterisation techniques, including dynamic light scattering for particle size analysis, zeta potential measurement, and gel electrophoresis, results of which will provide a characteristics of delivery system designed and its potentials for further biological investigation.

3.3 Results

3.3.1 Cytotoxicity of Empty Liposomes

3.3.1.1 Effect on the Metabolic Activity of A549 Cells: MTS Assay

The MTS assay was used to assess the influence of increasing the concentration of total lipids from 1.0 mM to 50.0 mM (log mM from 0 to 1.7) and different molar ratio of DC-Chol:DOPE on the metabolic activity of A549 cells. Cells incubated with serum-free medium only were used as the positive control, whereas cells incubated with 0.2%

(v/v) Triton X-100 were used as the negative control. The concentration of Triton X-100 used in this assay is similar to the concentration that usually used in the literature to cause complete loss of cell viability [36], and it is also similar to the concentration that is usually used in our research group with A549 cells. The results presented in Figure 3.2 show the dose-response profile for DC-Chol:DOPE liposomes towards A549 cells, which demonstrates a typical sigmoidal shape and indicates that the effects of the liposomes on the viability of the epithelial cells were concentration dependant.

Figure 3.2 shows that applying total lipid concentrations of 25.0 and 50.0 mM (log mM of 1.4 and 1.7) resulted in a significant loss of A549 metabolic activity for all liposomes compositions, with relative cell viability less than the EC_{50} values (the concentration of liposome that causes a 50% reduction in cellular metabolic activity). The lower concentrations applied (1.0 - 10.0 mM, log mM 0 - 1) show dramatically reduced cell toxicity, particularly for liposomes prepared with DC-Chol:DOPE ratios of 0.33:1-0.66:1. It is important to note for further work in this project that for concentrations of cationic liposome equal or lower than 5 mM (log mM = 0.7), relatively high cell viability was achieved in A549 cells at > 80%.

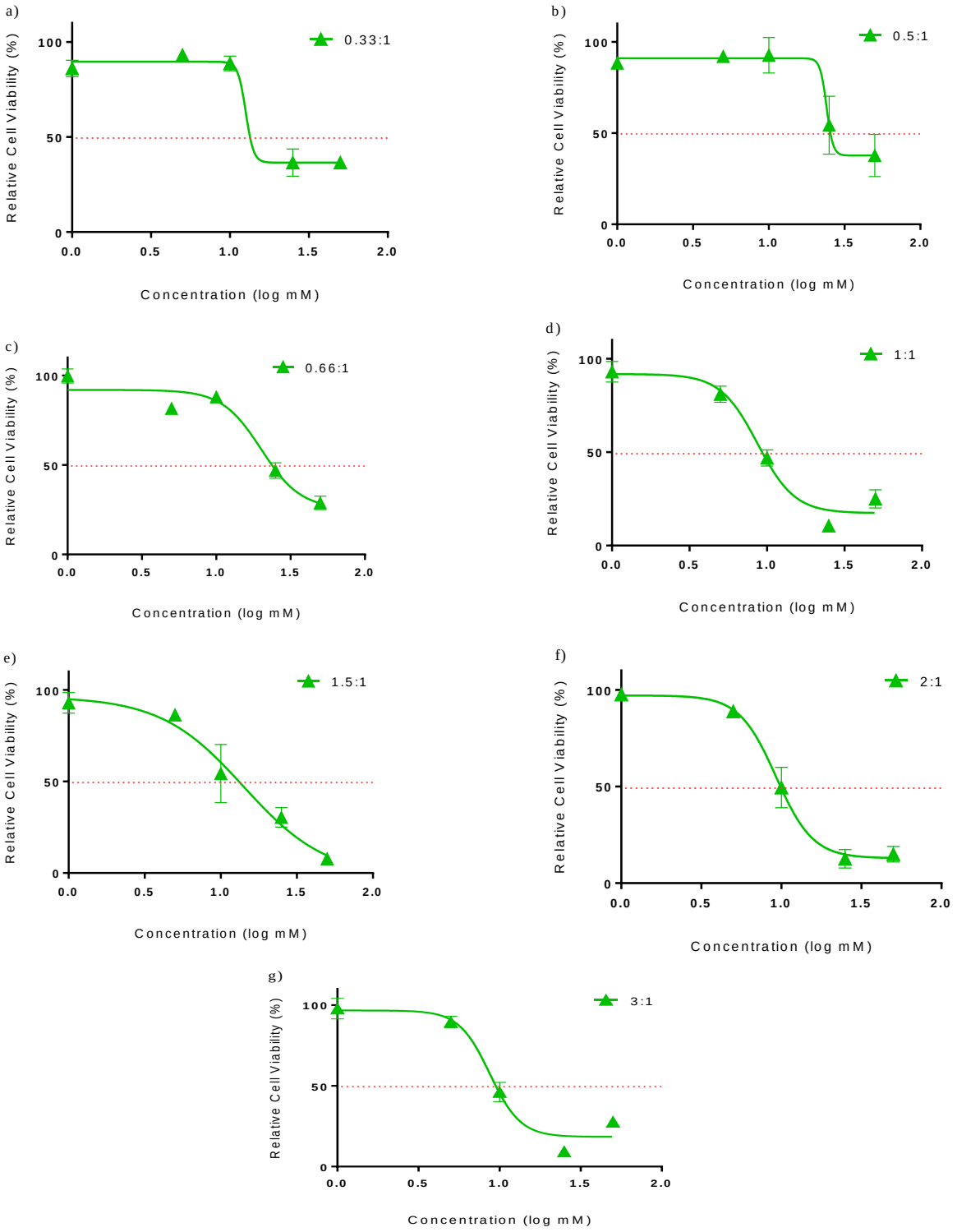

Figure 3.2: Dose-response profiles showing relative cell viability on incubation of empty liposomes with A549 cells

Data from the MTS assay; expressed as relative cell viability, calculated using the equation shown in Section 2.2.3.1 and presented as the mean ± SD (N=3, n=6). Different concentrations of cationic liposomes (1.0, 5.0, 10.0, 25.0, and 50.0 mM) were used at different ratios of a DC-Chol:DOPE and incubated with cells for 4 hrs: a) 0.33:1, b) 0.5:1, c) 0.66:1, d) 1:1, e) 1.5:1, f) 2:1 and g) 3:1. Dose-response curves were generated using GraphPad Prism (v6).

3.3.1.2 Effect on the Membrane Integrity of A549 Cells: LDH Assay

The LDH assay was used to assess the influence of increasing the concentration of total lipids from 1.0 mM to 50.0 mM (log mM from 0 to 1.7) and different molar ratios of DC-Chol:DOPE on the membrane integrity of A549 cells. 0.2% (v/v) Triton X-100 was used to induce LDH release (positive control), whereas serum-free DMEM was used as the negative control. The concentration of Triton X-100 used in this assay is similar to the concentration that usually used in the literature to cause complete loss of cell membrane integrity and release of LDH [36], and it is also similar to the concentration that is usually used in our research group with A549 cells. The results presented in Figure 3.3 show the dose-response trend for DC-Chol:DOPE liposomes towards A549 cells, which has a typical sigmoidal shape and indicates that the effects of the liposomes on the integrity of the epithelial cell membranes were concentration dependant.

Figure 3.3 shows that applying concentrations of 10.0 and 50.0 mM (log mM of 1 and 1.7) total lipid resulted in a significant release of LDH for all liposomes compositions, with the percentages of LDH released more than the EC_{50} values (the concentration of liposome that causes a 50% LDH release). The lower concentrations applied (1.0 - 5.0 mM, log mM 0 - 0.7) show dramatically reduced LDH release. It is important to note that for concentrations of cationic liposome equal or lower than 5 mM (log mM = 0.7), relatively high membrane integrity and the low release of LDH were achieved in A549 cells at < 8%.

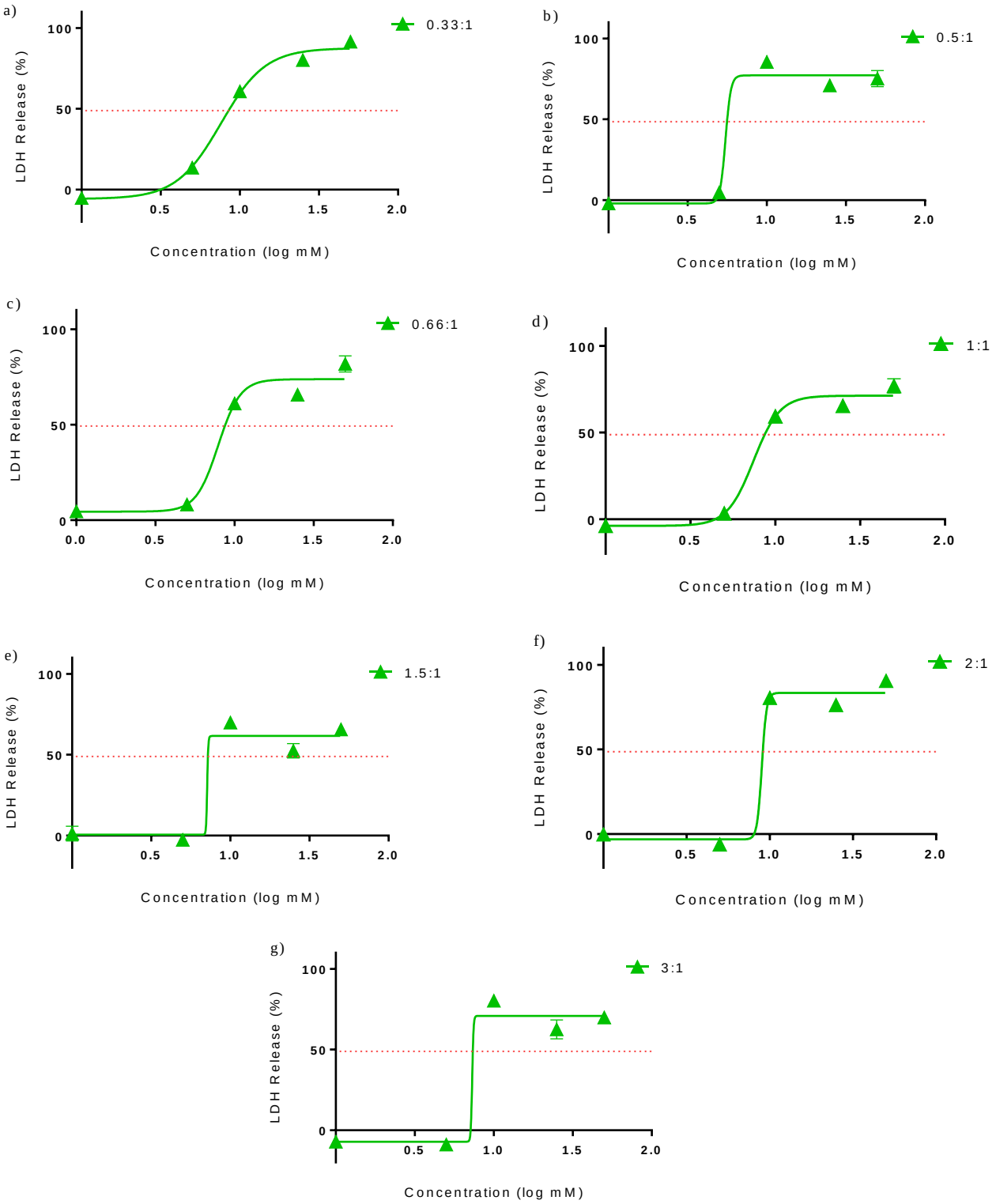

Figure 3.3: Dose-response profiles showing LDH release from A549 cells on exposure to empty liposomes

Data from the LDH assay; expressed as LDH release, calculated using the equation shown in Section 2.2.3.2 and presented as the mean ± SD (N=3, n=6). Different concentrations of cationic liposomes (1.0, 5.0, 10.0, 25.0, and 50.0 mM) were used at different ratios of a DC-Chol:DOPE and incubated with cells for 4 hrs: a) 0.33:1, b) 0.5:1, c) 0.66:1, d) 1:1, e) 1.5:1, f) 2:1 and g) 3:1. Dose-response curves were generated using GraphPad Prism (v6).

3.3.1.3 Cy3-Annexin V/Propidium Iodide Cytotoxicity Study

The Annexin V/PI assay is a rapid and reliable technique used to differentiate between necrotic, apoptotic and viable cells. Figure 3.4 shows the results of the treatment of A549 cells with five empty liposome formulations prepared at different total lipid concentrations, ranging from 1.0 mM to 50.0 mM, and a constant ratio of DC-Chol/DOPE at 1:1. A549 cells without the application of liposomes were used as negative control. The apoptotic effects were assessed using the Annexin V/PI apoptosis assay after 4 hrs liposomes incubation and analysed by flow cytometry. Applying concentrations of 5.0, 10.0, 25.0, and 50.0 mM of the total lipid content resulted in positive cell staining with PI, at percentages of approximately 26%, 43%, 52%, and 63% of cell population, respectively. Interestingly, low percentages of cells stained with Annexin V were observed for the five different concentrations applied, indicating a lack of an increased phosphatidylserine exposure at the cell surface. The results potentially indicate that the toxicity observed was related to the effect of the liposomes on the cell membrane, as confirmed by the LDH assay (Section 3.3.1.2). The lower concentrations applied (1.0 mM) show lower positive cell staining with PI, at percentages of approximately 15% cell population. The proportion of necrotic cells in all treated cells increased in a dose-dependent manner.

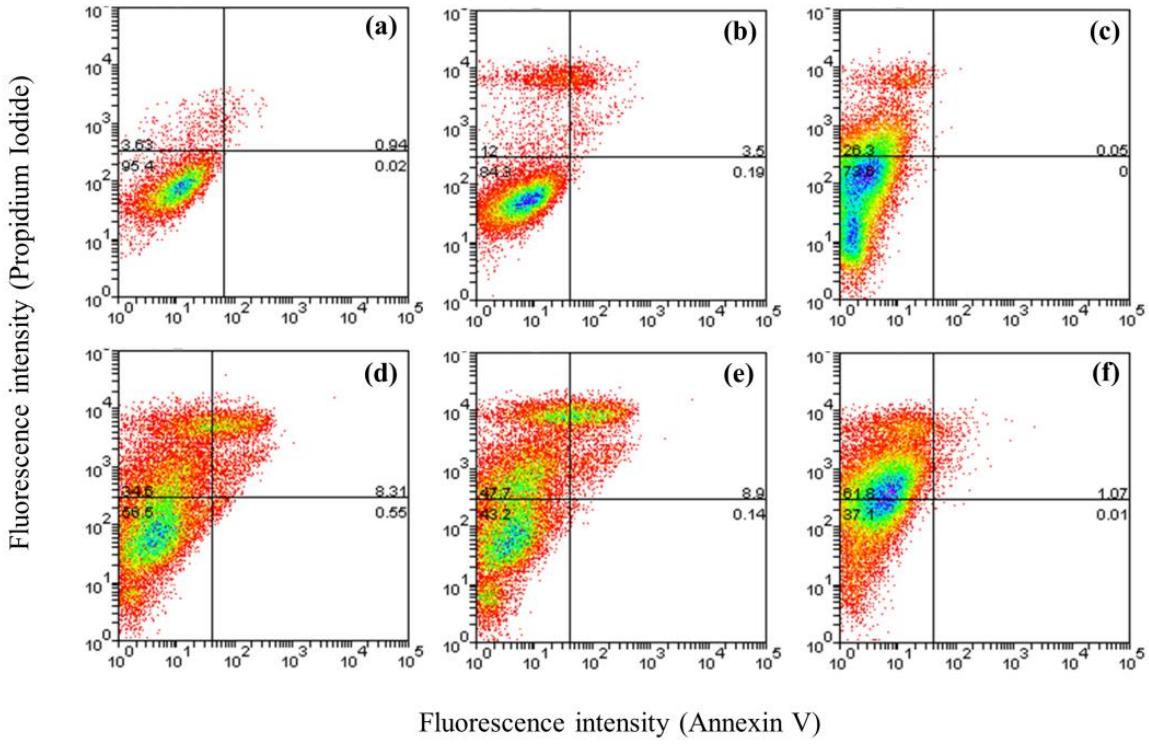

Figure 3.4: Flow cytometry dot plots showing cy3-Annexin V/PI cytotoxicity results for empty cationic liposomes in A549 cells

Result shows dot plots of A549 cells after 4 hrs incubation with empty liposomes at a total lipid concentration of (b) 1.0, (c) 5.0, (d) 10.0, (e) 25.0 and (f) 50.0 mM and a constant ratio of DC-Chol/DOPE at 1:1. A549 cells without the liposomes exposure were used as negative controls (a). The cells were assessed using a Beckman Coulter MoFlo (minimum 10,000 cells/sample), and data were analysed using Weasel software.

3.3.2 Particle Size and Zeta Potential Measurements

3.3.2.1 Empty Liposomes

Following the initial cytotoxicity screening experiments, the optimised preparation conditions were identified at a total lipid concentration of 1.0 mM, the concentration that demonstrated a low level of cytotoxicity. Empty liposomes colloidal properties, hydrodynamic particle diameter, polydispersity index (PDI), and zeta potential, were assessed.

Figure 3.5A shows that the average particle size diameters of empty liposome samples were in the range between approximately 70 nm and 80 nm for all measured formulations. Increasing the ratio of cationic lipids in the formulation had no significant impact on the particle size measurements, as the lowest DC-Chol:DOPE ratio 0.33:1 showed hydrodynamic diameter of around 79 nm, while the highest ratio 3:1 showed 81 nm. The PDI was also determined as a measurement of the level of homogeneity of cationic liposomes particle size (Table 3.1). A PDI value from 0.1 to 0.4 indicates a narrow size distribution, and a PDI value greater than 0.4 indicates a broad distribution. High value of PDI indicates the distribution of NPs with variable size range which results in the formation of aggregates and could result in low stability of particle suspension and low homogeneity. The results in Table 3.1 show that the particle size distributions of empty liposomes were homogenous, judged from the PDI measurements (PDI values <0.27).

Figure 3.5B shows that the zeta potential measurements of empty liposomes samples increased with increase the content of cationic lipid in the formulation. The lowest DC-Chol:DOPE molar ratio 0.33:1 showed zeta potential around + 40 mV, and with increase the cationic lipid ratio to 3:1 the zeta potential was reached to around + 90 mV.

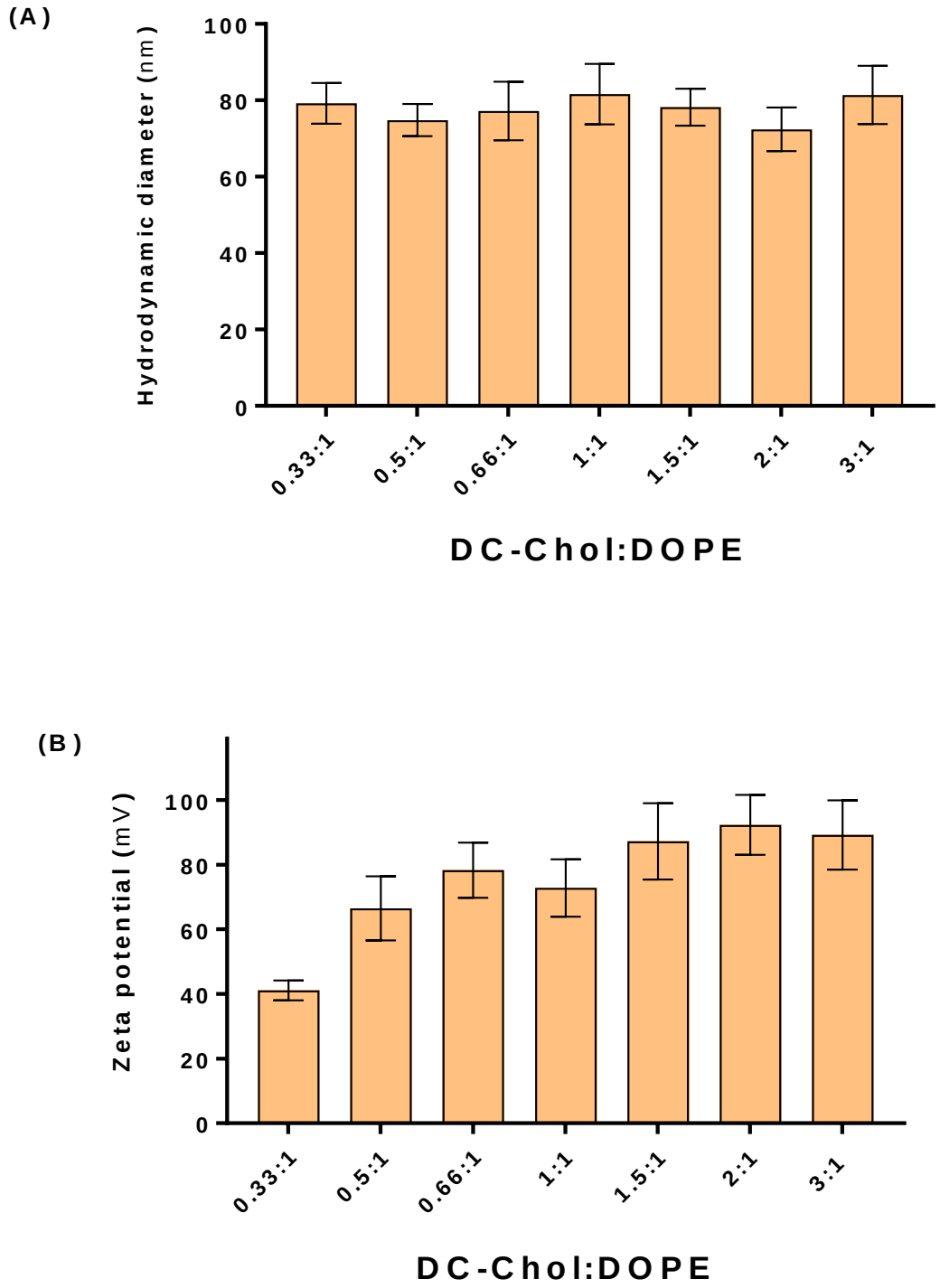

Figure 3.5: (A) Average hydrodynamic diameter (nm) and (B) zeta potential (mV) for empty liposomes prepared at different compositions

Empty liposomes were prepared with different DC-Chol:DOPE ratios at 1.0 mM total lipid concentration. ***(A)*** *Mean hydrodynamic diameter (n = 10 ± SD) of the formulations were determined at 25.0ºC and a fixed scattering angle of 90º.* ***(B)*** *Zeta potential measurements (n = 3 ± SD) were carried out at 25.0°C in 10 mM PBS solution (pH 7.4).*

Table 3.1: Summary of polydispersity index (PDI) of empty liposomes

DC-Chol:DOPE	PDI
0.33:1	0.24
0.5:1	0.22
0.66:1	0.26
1:1	0.26
1.5:1	0.24
2:1	0.25
3:1	0.27

3.3.2.2 siRNA-Liposomes

The next step was to evaluate the hydrodynamic diameter and surface charge of siRNA-containing liposomes prepared at the total lipid concentration of 1.0 mM, as *per* above toxicity study, at different ratios of cationic to zwitterionic lipid, and different N/P ratios.

In comparison to the DLS results of empty liposomes presented in Figure 3.5A, the encapsulation of siRNA during the cationic liposomes preparation led to an increase in the liposomes average size of siRNA-liposomes formulations. Figure 3.6 shows that all measured siRNA-liposome formulations possess hydrodynamic diameters above approximately 170 nm, a dramatic increase relative to hydrodynamic diameter size of empty liposomes of approximately 80 nm.

Results further show that no significant effect of different molar ratio of DC-Chol:DOPE on the hydrodynamic diameter of siRNA-liposomes. For example, in case of 0.78:1 N/P ratio the lowest molar DC-Chol:DOPE ratio of 0.33:1 shows an average hydrodynamic

diameter of approximately 307 nm and the highest molar DC-Chol:DOPE ratio of 3:1 shows diameter of around 314 nm.

In contrast, N/P ratio has a significant effect on the particle size of siRNA-liposomes formulations. The average particle size of the siRNA-liposome formulations decreased significantly with an increase in the ratio of cationic lipid to siRNA (N/P ratio). In case of 0.33:1 molar ratio of DC-Chol:DOPE for example, the particle size of siRNA-liposomes dropped from 307 nm to 210 nm when the N/P ratio increased from 0.78:1 to 50:1, respectively.

The PDI values of siRNA-liposomes formulation were also measured and summarised in Table 3.2. Results of PDI show that no significant effect of different molar ratio of DC-Chol:DOPE on the PDI values of siRNA-liposomes formulations. For example, in case of 0.78:1 N/P ratio the lowest and the highest molar ratios of DC-Chol:DOPE (0.33:1 and 3:1, respectively) show a PDI value of 0.20. Moreover, N/P ratio has no significant influence on the PDI values of siRNA-liposomes formulations. For example, in case of 0.33:1 molar ratio of DC-Chol:DOPE the PDI values of siRNA-liposomes were 0.20 and 0.22 at 0.78:1 and 50:1, respectively.

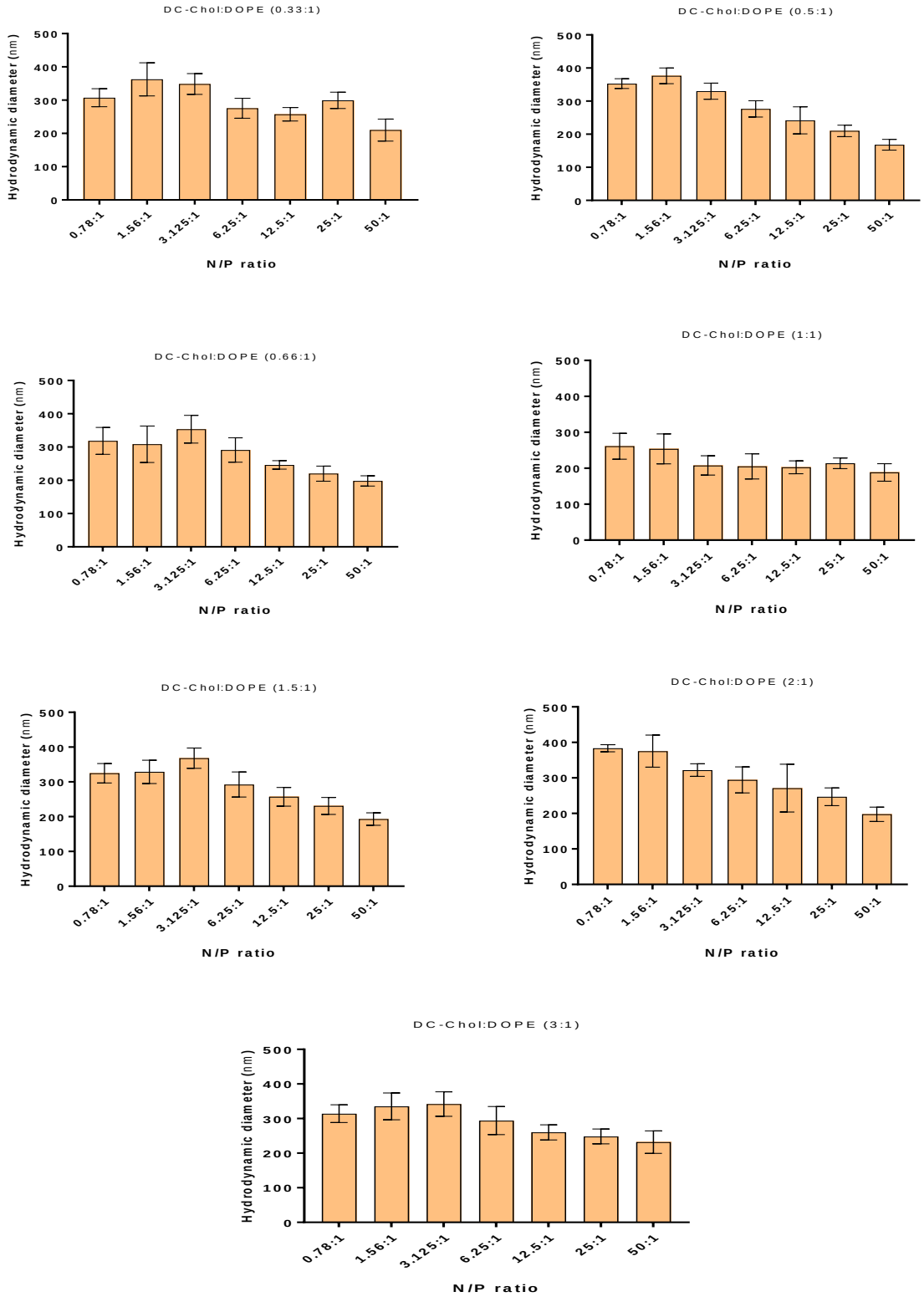

Figure 3.6: Hydrodynamic diameter (nm) for siRNA-liposomes prepared at different compositions and N/P ratios

siRNA-liposomes were prepared with different DC-Chol:DOPE composition at different N/P ratios (0.78:1, 1.56:1, 3.125:1, 6.25:1, 12.5:1, 25:1, and 50:1). Mean hydrodynamic diameter (n = 10 ± SD) of the formulations were determined at 25.0ºC and a fixed scattering angle of 90º.

Table 3.2: Summary of polydispersity index (PDI) of siRNA-liposomes prepared at different compositions and N/P ratios

DC-Chol:DOPE	N/P ratio						
	0.78:1	**1.56:1**	**3.125:1**	**6.25:1**	**12.5:1**	**25:1**	**50:1**
0.33:1	0.20	0.28	0.21	0.22	0.20	0.23	0.22
0.5:1	0.19	0.20	0.20	0.24	0.26	0.18	0.18
0.66:1	0.29	0.31	0.29	0.28	0.19	0.22	0.19
1:1	0.24	0.26	0.24	0.26	0.19	0.19	0.22
1.5:1	0.22	0.23	0.24	0.25	0.24	0.23	0.20
2:1	0.16	0.29	0.20	0.24	0.30	0.24	0.21
3:1	0.20	0.22	0.22	0.23	0.20	0.20	0.22

In comparison to zeta potential values of empty liposomes (Figure 3.5B), the loading of negatively charged siRNA into liposomes has apparent effect on increasing the positive zeta potential values of the formulations as the ratio of N/P is increased (Figure 3.7).

The zeta potential of siRNA-liposomes inverted from negative to positive values upon increasing the ratio of cationic lipid to siRNA, typically at N/P ratio of 1.56:1. It is also important to notice that the zeta potential of siRNA-liposomes did not, as expected, increase with the increase in the proportion of cationic lipid used in the formulations (compositions from 0.33:1 to 3:1 molar ratios of DC-Chol:DOPE), when measured at the same N/P ratio. The ratio between cationic lipid and siRNA is found to be the main determinant in the zeta potential of siRNA-liposomes; the zeta potential increased significantly with increasing the ratio of cationic lipid to siRNA (N/P ratio). For example, at 0.33:1 molar ratio of DC-Chol:DOPE, the zeta potential of siRNA-liposomes increased from around -16 mV at 0.78:1 N/P ratio to around +37 mV when the N/P ratio was 50:1.

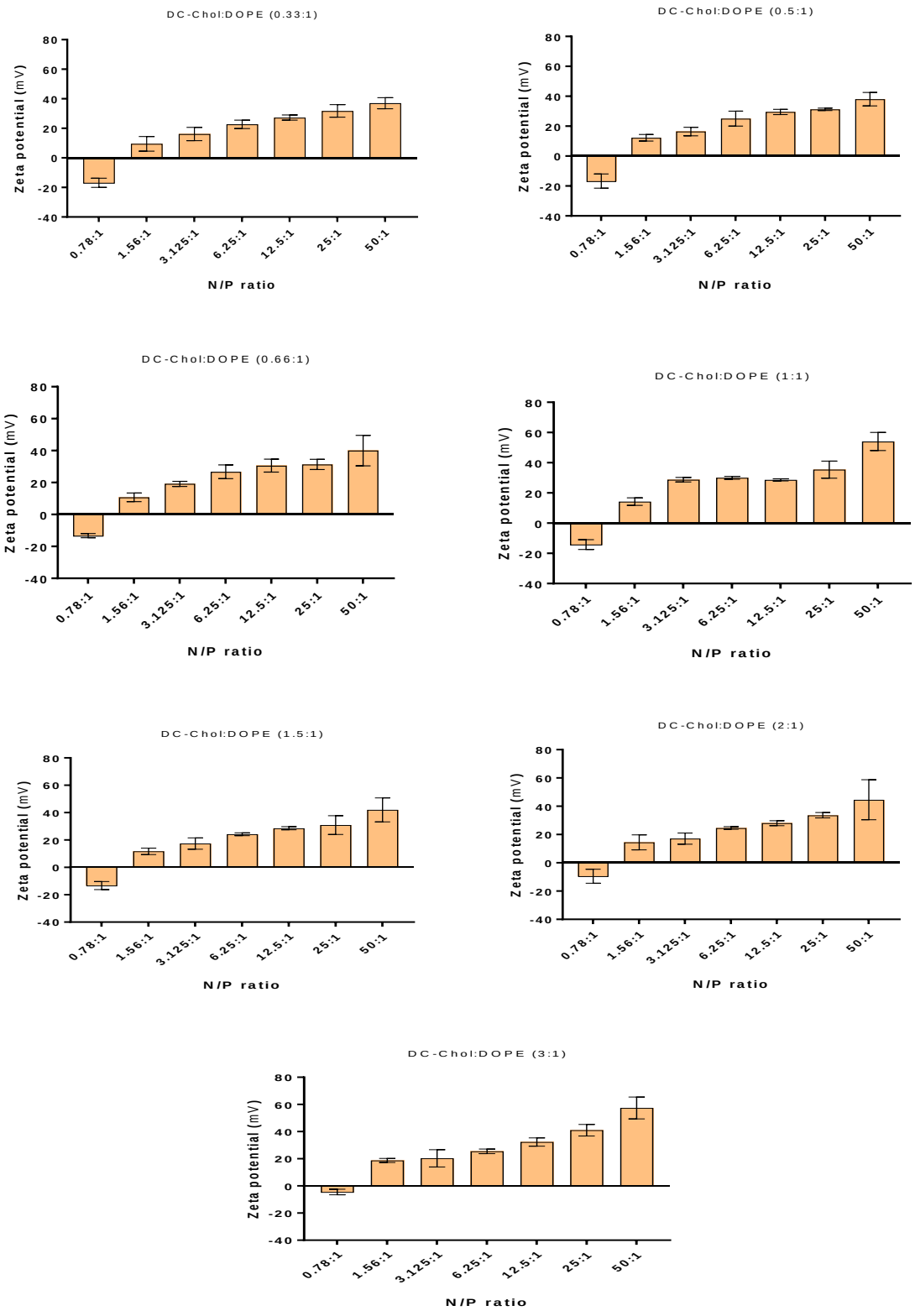

Figure 3.7: Zeta potential (mV) for siRNA-liposomes prepared at different compositions and N/P ratios

siRNA-liposomes were prepared with different DC-Chol:DOPE composition at different N/P ratios (0.78:1, 1.56:1, 3.125:1, 6.25:1, 12.5:1, 25:1, and 50:1).Zeta potential measurements (n = 3 ± SD) were carried out at 25.0°C in 10 mM PBS solution (pH 7.4).

3.3.3 Assessment of siRNA Encapsulation Efficiency

3.3.3.1 Gel Retardation Assay

Gel retardation is a simple technique that is widely used to investigate binding or encapsulation of nucleic acid in different formulations, including cationic liposomes. siRNA-liposome formulations were prepared with 1.0 mM total lipid and 0.4 μg siRNA, and at different composition of DC-Chol:DOPE and different N/P ratios. The formulations were analysed by agarose gel electrophoresis to investigate encapsulation efficiency.

The increased encapsulation of anionic siRNA was achieved by increasing the N/P ratio within the liposome formulations, as illustrated in Figure 3.8. The absence of ethidium bromide stained, migrating siRNA in the gel indicates its complete incorporation (encapsulation). A general trend of a decrease in the migration pattern of free siRNA in the gel is seen with an increase in the N/P ratio, with a complete absence of detectable siRNA at N/P ratio of 50:1. Interestingly, gel electrophoresis showed a relatively high level of siRNA incorporation for liposomal formulations with a relatively low DC-Chol content and low N/P ratio, such as 3.125:1.

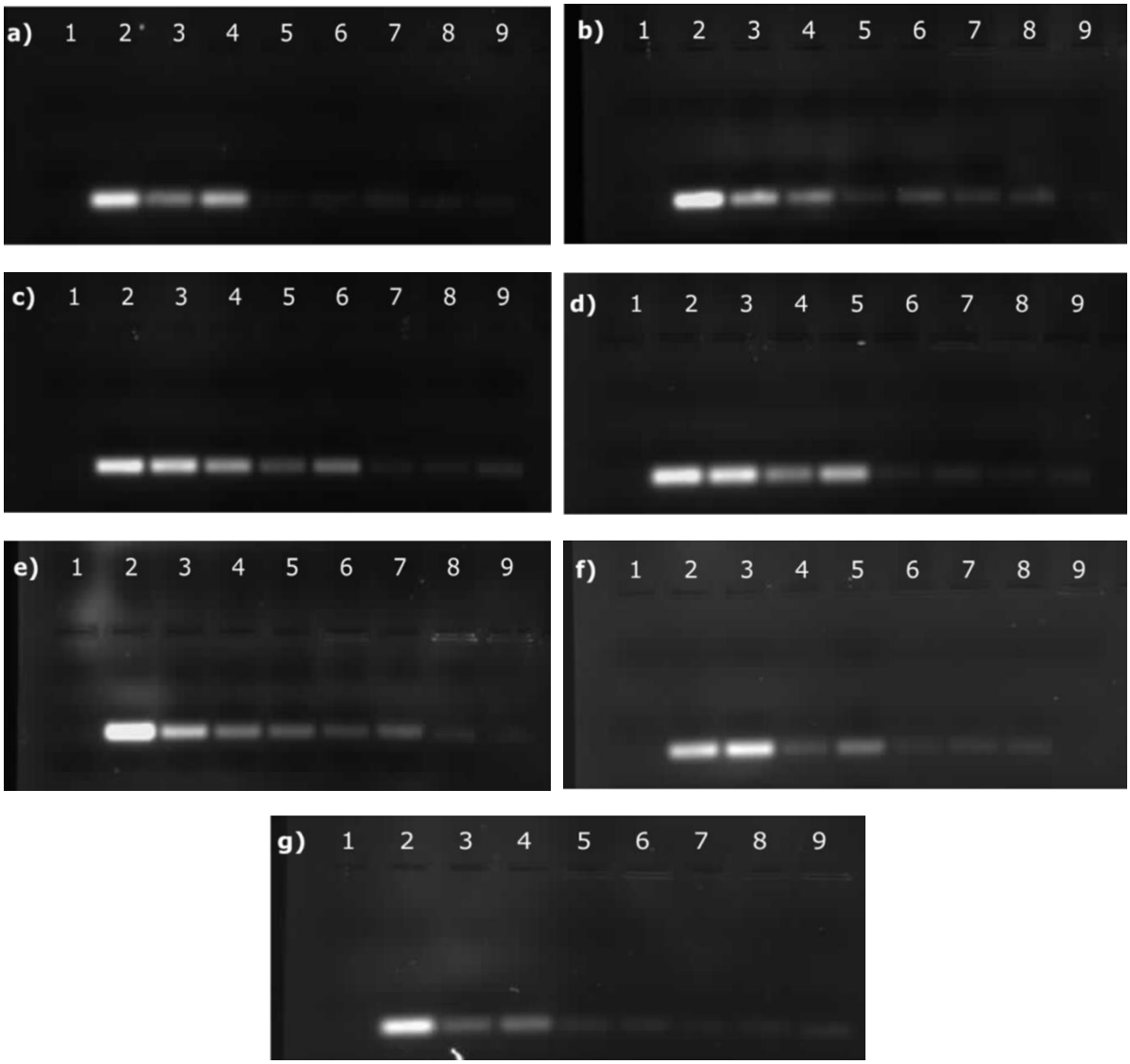

Figure 3.8: Encapsulation efficiency of siRNA into liposomes, as assessed by gel retardation assay

Cationic liposomes were prepared with different DC-Chol:DOPE composition of (a) 0.33:1, (b) 0.5:1, (c) 0.66:1, (d) 1:1, (e) 1.5:1, (f) 2:1 and (g) 3:1. In each gel, liposome–siRNA formulations were tested at various N/P ratios: 0.78:1, 1.56:1, 3.125:1, 6.25:1, 12.5:1, 25:1, and 50:1 (lanes 3, 4, 5, 6, 7, 8 and 9, respectively). Lanes 1 and 2 represent the controls and contain empty liposomes and naked siRNA (0.4 μg), respectively.

3.3.3.2 Ultrafiltration Centrifugation Method

To confirm the encapsulation efficiency of siRNA within the liposome formulations, the ultrafiltration-centrifugation method was performed to determine the effect of main formulation parameters (liposomes composition and N/P ratio). The liposomal entrapment of siRNA was determined for formulations at different ratios of DC-Chol:DOPE, prepared with 1.0 mM total lipid and 0.4 μg siRNA.

The results shown in Figure 3.9 indicate that a high level of siRNA association with liposomes was achieved even at low N/P ratios. The encapsulation of siRNA was increased with an increase in the content of cationic lipid within the formulation. It is interesting to notice that applying this method of analysis, no positive effect can be seen of increased DC-Chol composition of DC-Chol:DOPE liposomes at low N/P ratios. On the contrary, reduced encapsulation was observed at low N/P ratios for higher DC-Chol:DOPE compositions.

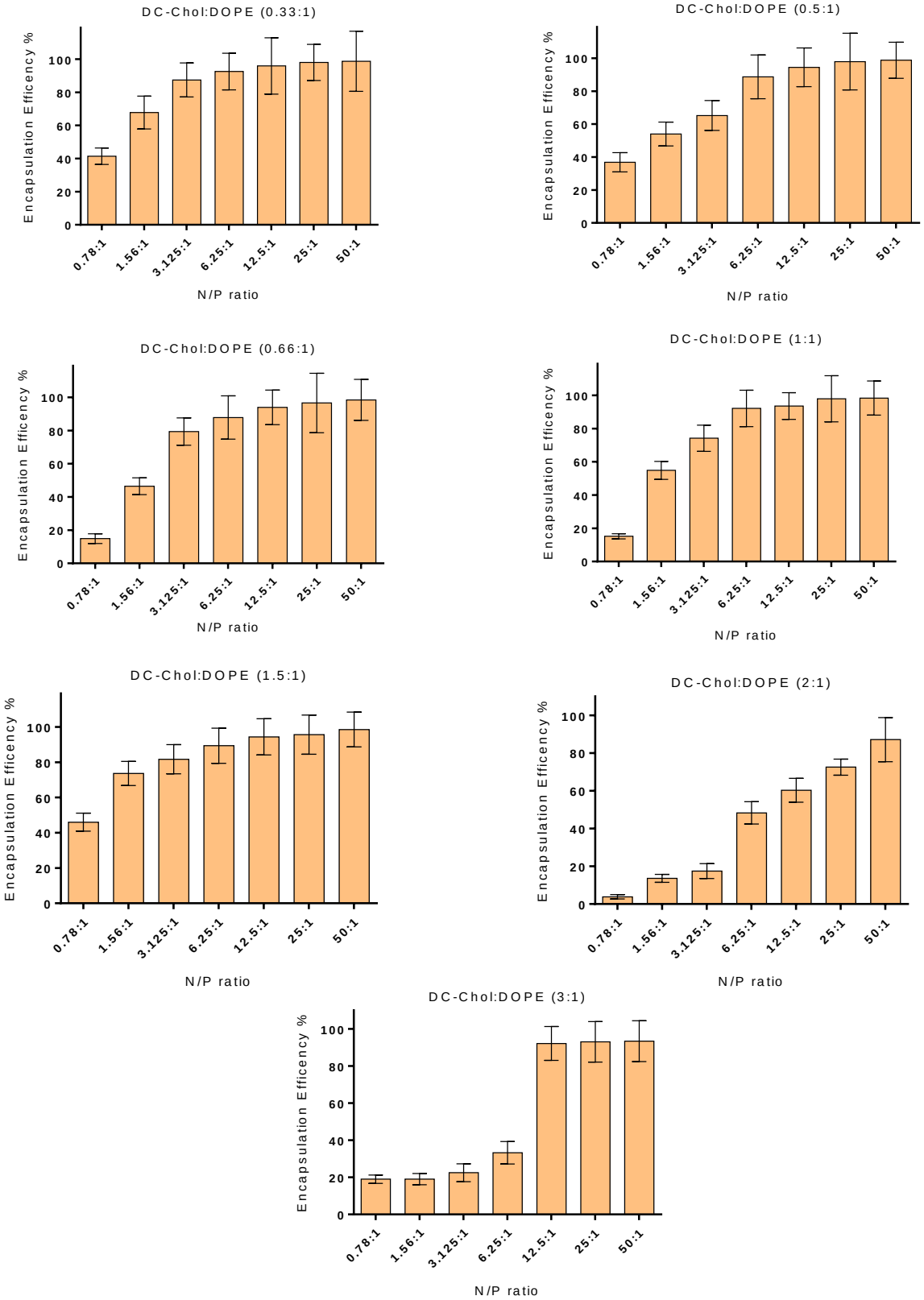

Figure 3.9: Encapsulation efficiency of siRNA-liposomes as assessed by ultrafiltration centrifugation

Cationic liposomes were prepared with a total lipid concentration of 1.0 mM and different DC-Chol:DOPE ratios of 0.33:1, 0.5:1, 0.66:1, 1:1, 1.5:1, 2:1 and 3:1 and different N/P ratios. Data are presented as the mean ± SD (n=3, N=2).

3.3.4 Cytotoxicity of siRNA-Liposomes

3.3.4.1 Effect on the Metabolic Activity of A549 Cells: MTS Assay

The metabolic activity of A549 cells was investigated after applying siRNA-liposome formulations at different N/P ratios and different ratios of DC-Chol:DOPE. Liposomes were prepared at a total lipid concentration of 1.0 mM, as *per* metabolic activity assay in Section 3.3.1.1. The results presented in Figure 3.10 show high cells metabolic activity, > 93%, for all treatment conditions, and no significant effects were observed by increasing the N/P ratio from 0.78:1 to 50:1. Similar toxicity profiles were obtained with different DC-Chol:DOPE ratios; the cell viability did not decrease as the ratio was increased.

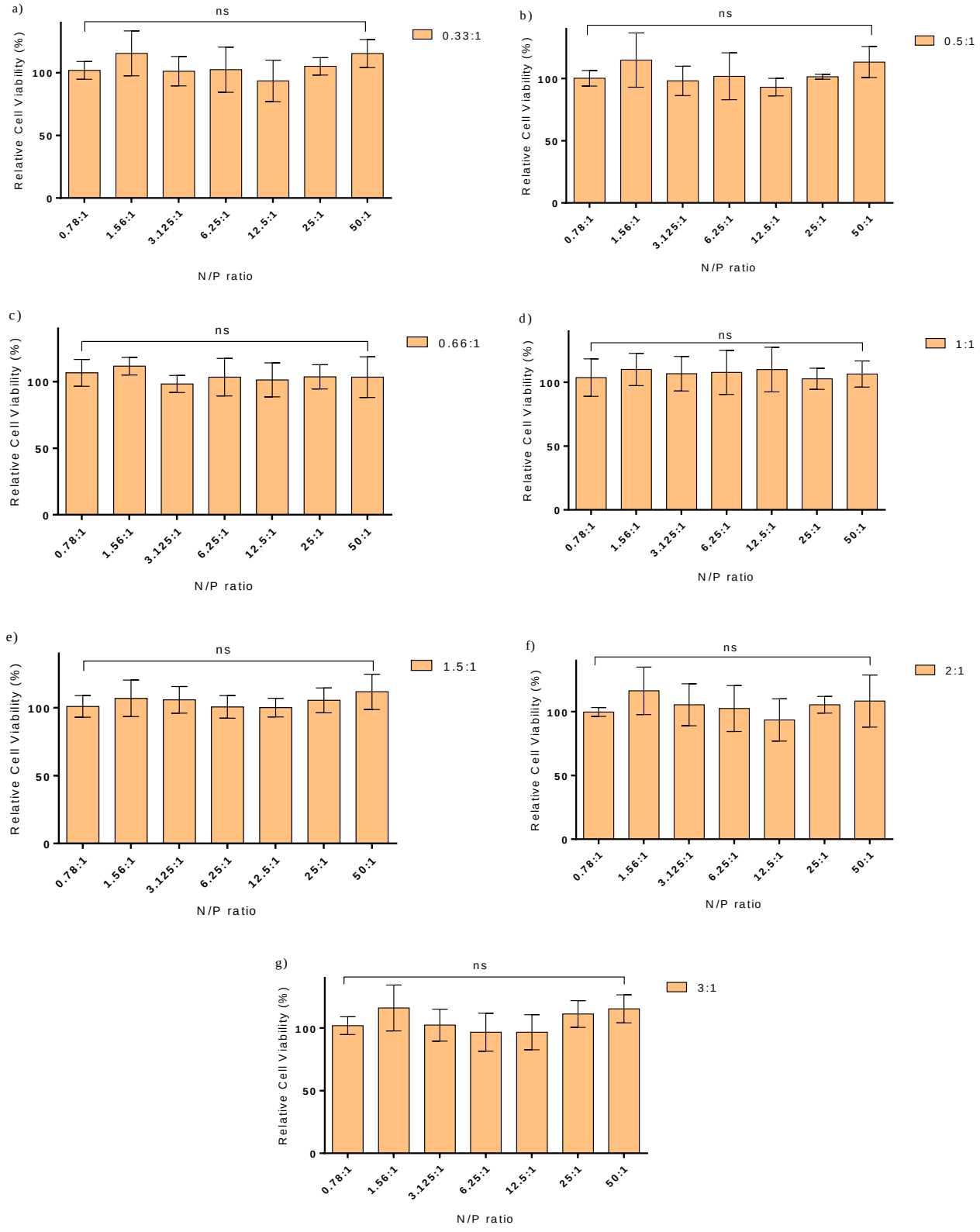

Figure 3.10: Relative cell viability of different siRNA-liposomes after incubation for 4 hrs with A549 cells

calculated using the equation shown in Section 2.2.3.1 and presented as the mean ± SD (N=3, n=6). Different siRNA-liposomes were prepared at an N/P ratios ranging from 0.78:1 to 50:1 and at different ratios of DC-Chol-DOPE: a) 0.33:1, b) 0.5:1, c) 0.66:1, d) 1:1, e) 1.5:1, f) 2:1 and g) 3:1 at 1.0 mM total lipid concentration.

3.3.4.2 Effect on the Membrane Integrity of A549 Cells: LDH Assay

The effect of siRNA-liposomes on the epithelial membrane integrity of A549 cells was investigated using different N/P ratios and different ratios of DC-Chol:DOPE. All formulations were prepared at a total lipid concentration of 1.0 mM. The results presented in Figure 3.11 were obtained from treatment of A549 cells with siRNA-liposomes in the same experimental conditions, and show the low release of LDH from the cells under all treatment conditions, with the maximum release of LDH obtained at a DC-Chol:DOPE ratio of 0.33:1 and a high N/P ratio of 50, at around 12%. No significant effects were observed with an increase in the N/P ratio from 0.78:1 to 50:1 in the reminder of the siRNA-liposomes. Similar toxicity profiles for the membrane integrity of A549 cells were also noted for different molar ratios of cationic and zwitterionic lipids that did not affect the membrane integrity.

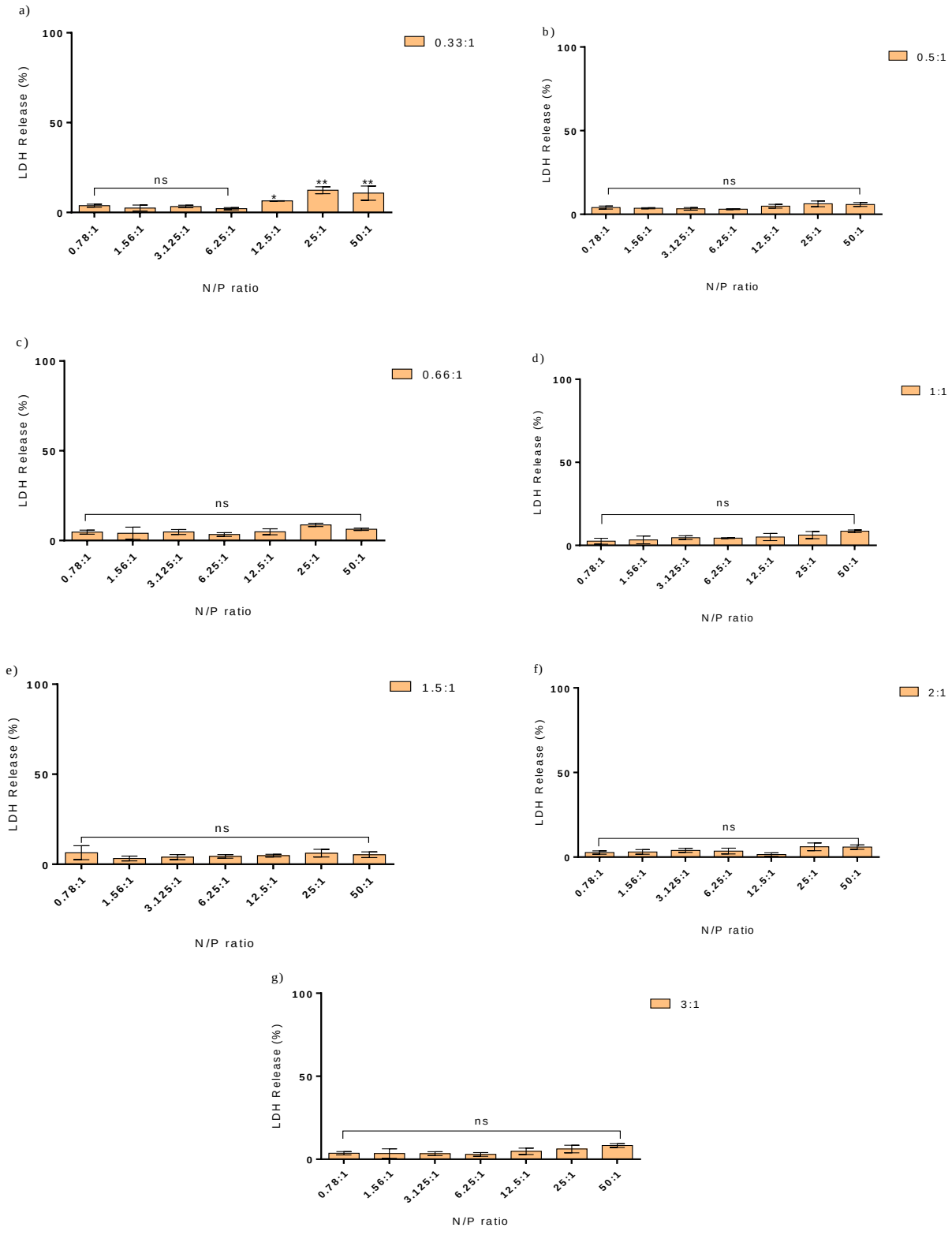

Figure 3.11: LDH release of different siRNA-liposomes after incubation for 4 hrs with A549 cells

Data are the results of an LDH assay and are expressed as LDH release, calculated using the equation shown in Section 2.2.3.2 and presented as the mean ± SD (N=3, n=6). Different siRNA-liposomes were prepared at an N/P ratios ranging from 0.78:1 to 50:1 and at different molar ratio of DC-Chol-DOPE: a) 0.33:1, b) 0.5:1, c) 0.66:1, d) 1:1, e) 1.5:1, f) 2:1 and g) 3:1 at 1.0 mM total lipid concentration.

3.3.4.3 Cy3-Annexin V/Propidium Iodide Cytotoxicity Study

Figure 3.12 shows the results of the treatment of A549 cells with siRNA-liposomes prepared at an N/P ratio of 3.125:1 and different ratios of DC-Chol:DOPE. The flow cytometry dot plot profiles show that a low percentage of the cells were positively stained with PI in all the applied formulations, in comparison to the control cells not exposed to siRNA-liposomes, and most of the cell population remained viable. Interestingly, there seems to be somewhat separate sub-population of cells showing PI staining, rather than a whole cell population shift. It should be noted that no significant staining with Annexin V was seen, suggesting no involvement of an apoptosis mechanism.

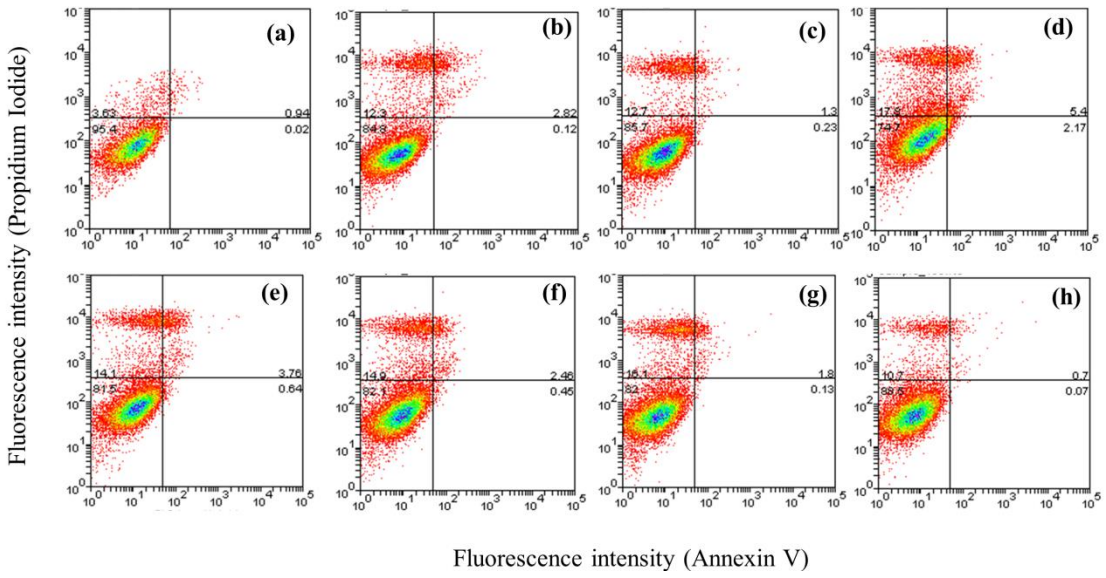

Figure 3.12: Flow cytometry dot plots showing cy3-Annexin/PI cytotoxicity results for siRNA-liposomes in A549 cells

Flow cytometry dot plots showing cell apoptosis and necrosis in A549 cell line after 4 hrs incubation with siRNA-liposomes at total lipid concentration of 1.0 mM and different DC-Chol:DOPE ratios: (b) 0.33:1, (c) 0.5:1, (d) 0.66:1, (e) 1:1, (f) 1.5:1, (g) 2:1 and (h) 3:1, and at fixed N/P ratios of 3.125:1. A549 cells without siRNA-liposomes were used as negative controls (a). The cells were assessed by a Beckman Coulter MoFlo (minimum 10,000 cells/sample), and data were analysed using Weasel software.

3.3.5 RNase Stability of siRNA-Liposomes

siRNA is susceptible to enzymatic hydrolysis within biological fluids. Consequently, an efficient siRNA-delivery system would be one that protects intact siRNA from enzymatic degradation. To achieve this, the delivery system should prevent dissociation of siRNA from its complex/delivery system by anionic components in plasma and extracellular medium between the time of administration and entry into the cytoplasm. In order to study the ability of the liposomes to protect siRNA, different formulations were exposed to RNase A for different time periods and then analysed by gel electrophoresis. Naked siRNA with and without incubation with RNase A was used as the reference to evaluate the magnitude of siRNA protection. The liposomal protection of siRNA was assessed for formulations at different compositions of DC-Chol:DOPE prepared with 1.0 mM total lipid and 0.4 μg siRNA at N/P ratio of 3.125:1. This ratio was determined as the lowest cationic lipid ratio at which high incorporation of siRNA occurred, as *per* the gel retardation assay and ultrafiltration centrifugation experiment (see Section 3.3.3). Nuclease stability can be assumed from the relative intensity of the bands for different time intervals.

Naked siRNA, as shown in Figure 3.13, was degraded completely after 30 min incubation with RNase at 37ºC in PBS buffer. There was no evidence of degradation of siRNA not treated with RNase, at any time point. Furthermore, the results indicate that a high level of siRNA protection was achieved at 30 min incubation, with the intensity of the fluorescent bands for siRNA incorporated into liposomes gradually disappearing with increasing time intervals from 30 min to 4 hrs.

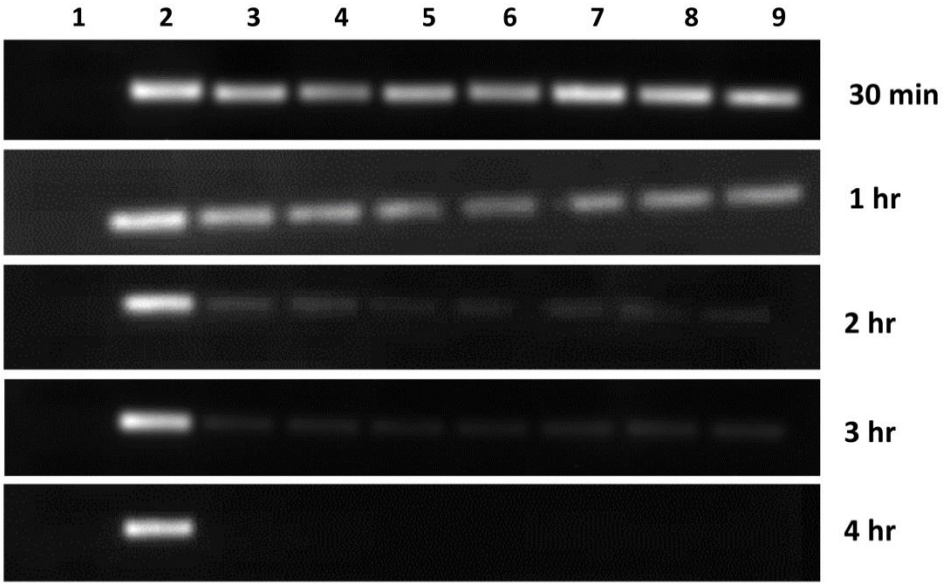

Figure 3.13: RNase stability profile for siRNA-liposomes

siRNA-liposomes prepared with 0.4 μg of siRNA and 1.0 mM total lipid, at a fixed N/P ratio of 3.125:1 and different ratios of DC-Chol:DOPE. Lane 1 indicates naked siRNA with RNase A as the control; Lane 2 indicates naked siRNA without RNase A as a reference, and Lanes 3, 4, 5, 6, 7, 8 and 9 indicate siRNA-liposome samples with DC-Chol:DOPE ratios of 0.33:1, 0.5:1, 0.66:1, 1:1, 1.5:1, 2:1 and 3:1, respectively.

3.4 Discussion

Understanding the biological behaviour in the process of liposomes interacting with epithelial membranes and their internalisation is highly desirable, as it informs both toxicology and nanomedicine design. Liposome based formulations have been extensively used as a non-viral system for the delivery of nucleic acids/genes [20]. Positively charged lipid (DC-Chol) is commonly used to formulate cationic liposomes to incorporate siRNA as has been reported in a number of earlier studies [37]. The zwitterionic lipid (DOPE) used in the formulations in this study, is believed to help to increase liposomes transport across cell membranes and therefore improves cell transfection [38]. The cytotoxicity that can be generated by the presence of cationic lipids in siRNA-liposomes formulations is a major concern [39], and the ideal siRNA-liposome formulation should be able to deliver siRNA efficiently, while not causing cytotoxic effects.

One of the key aims of this chapter was to optimise siRNA-liposome formulations, in terms of their cytotoxicity and also to obtain initial information with regards to the potential mechanisms involved in liposome cytotoxicity. To this end, initial toxicity screening of liposomes prepared with different total lipid concentrations and different molar ratios of DC-Chol:DOPE was conducted to identify ‘safe’ doses and liposome compositions for further studies. Three different methods were used to test liposome toxicity in A549 cell line, a well characterised and widely used in the literature as an *in vitro* model of NSCLC [40]. Cytotoxic effects mediated by free liposomes and siRNA-liposome formulations are a crucial issue for clinical applications. Therefore, the cytotoxicity of selected siRNA-liposome preparations was analysed in comparison to liposomal counterpart without siRNA.

The experimental work presented here showed an important corroboration between cell metabolic activity (MTS assay), increased LDH release, and induced cellular necrosis/apoptosis tests undertaken on exposure to liposome preparations. The application of the combination of these assays in this study ensures that the probable toxic effects of cationic liposome formulations are measured from different perspectives; metabolic activity, cell membrane integrity, and induction of cellular apoptosis/necrosis. It should be noted that both the MTS and LDH assays are generally used to assess cell viability, but that the LDH assay in more informative on cell membrane disruption, the effect that may be expected on the application of cationic liposomes [41]. The data obtained revealed that the toxicity exhibited is essentially associated with free liposomes (empty of siRNA). Moreover, it has been reported that the increased cytotoxicity of liposomes is generally associated with the increase dose of liposomes administered [16]. Similar is observed in the present study, as shown in Figures 3.2 and 3.3, and discussed below.

Measuring the impact of empty liposomes on cell viability *via* the MTS assay revealed a concentration dependent effect. Application of high dose of total lipid (as liposomes) was associated with notably higher toxicity and significantly reduced cell viability (Figure 3.2). Previous studies have reported that cationic liposomes exhibit a toxic effect at high total lipid concentrations [16], while the toxicity is reduced at lower total lipid doses [42]. The probable reasons behind this observation may be that at higher applied concentrations the interactions between positively charged lipid and negatively charged cell membranes would be increased due to the increased amount of cationic charges present, therefore leading to disruption of cellular membrane. Interestingly, the EC_{50} results for the empty liposomes indicated that increasing the ratio of cationic lipid to zwitterionic lipid within

the formulation from 0.33:1 (EC_{50} 12.5 mM) to 3:1 (EC_{50} 8.7 mM) did not significantly reduce the metabolic activity of the cells, if all other conditions remained the same.

The LDH assay was hence performed in this study to examine adverse effects that the liposomes may have on the membrane integrity of A549 cells. LDH is an intracellular enzyme that is released from cells on a damage to cellular membrane and can then be detected [36]. The application of a high dose of liposomes (high total lipid content) to A549 cells in culture was associated with a significant release of LDH enzyme, which indicates damage to the cell membrane integrity (Figure 3.3). Similar to the observations of effects on cell viability in the MTS assay, the LDH assay showed that epithelial membrane integrity was damaged with an increase in the applied dose of liposomes; in a concentration dependent manner. It should be noted that no significant influence on membrane integrity of different DC-Chol:DOPE ratios (applied at one selected total lipid dose) was seen; the lowest ratio of 0.33:1 has an EC_{50} value of around 7.6 mM, while the EC_{50} value of the highest ratio of cationic lipid 3:1 was approximately 7.3 mM. However, in some occasions the highest total lipid concentration produced complete loss of metabolic activity of A549 cells as measured by MTS, while the LDH assay showed around 60% of lactated dehydrogenase release at the same concentration (such as panel e of Figures 3.2 and 3.3). The reason behind the variation between the MTS and LDH results is might be due to that these two assays are usually used to evaluate different phenomena. The MTS assay measures the mitochondrial activity of the cells, while the LDH assay measures the membrane integrity of the cells. Therefore, the complete loss of metabolic activity should not be associated with complete damage of plasma membrane and 100% release of LDH, as toxicants may disrupt cellular metabolic activity, but leave membranes intact. In addition, it should be noted that the LDH release of empty

liposomes formulations plateaus at less than 100% for most of tested formulations. The reason behind this observation is might be that our cationic liposomes were caused partial loss of the membrane integrity of A549 cells, which lead to incomplete release of LDH. However, the effect of highest total lipid concentration applied (50 mM) was lower than the effect of Triton-X, which produced 100% of LDH release and complete loss of membrane integrity.

Phosphatidylserine is an essential component of the cell membrane typically located at the cytoplasmic surface of the membrane, and during cell apoptosis phosphatidylserine translocates to the external side of the cellular membrane [27]. Annexin V is a Ca^{2+} dependent cellular protein that tightly binds to the phosphatidylserine residue. Through conjugation of an appropriate fluorescent dye with Annexin V, a rapid and reliable technique for detecting cell apoptosis was developed [43]. PI is an intercalating probe used to differentiate between necrotic, apoptotic and viable cells. In the case of a damaged cell membrane, otherwise impermeable PI can enter cell and bind to double-stranded DNA, emitting fluorescence [44]. To distinguish between viable and non-viable cells after the application of different concentrations of cationic liposome, the Annexin V/PI assay was performed in this study.

The data obtained reveal that the application of liposomes to A549 cells at concentrations greater than 5.0 mM was associated with a significant decrease in cell survival. The flow cytometry dot plots showed that A549 cells were positively stained with PI at high concentrations of liposomes, as compared to untreated cells (Figure 3.4). For the lowest applied concentration of 1.0 mM, the population of stained cells was fairly similar to the negative control cells, untreated with liposomes, indicating high cell viability. It has been

reported that a cationic delivery system including cationic liposomes could induce cell necrosis through the interaction with Na^+/K^+-ATPase and impair their activity [45].

From the cytotoxicity experiments, the main cause of cell death could be identified as late apoptosis/necrosis, whereas less than 6% of the cells tested were positive for early apoptosis and stained with Annexin V. The PI detected toxicity at the higher concentrations of applied liposomes, corroborate with the results obtained from the MTS and LDH assays.

Further cytotoxicity investigations were performed to examine the influence of siRNA incorporation into liposomes. This could help to understand the mechanism of toxicity and whether it arises from the liposome itself or the siRNA-liposome system. To this end, the safe dose of liposomes at total lipid concentration of 1.0 mM was used to prepare liposomes at different compositions of DC-Chol:DOPE liposome with different N/P ratios. The data obtained for the effect of siRNA-liposome formulations on the metabolic activity of A549 cells showed that the incorporation of siRNA has no significant effect on the cytotoxicity of the liposomes, as *per* data in Figure 3.10.

The data obtained concerning the effect of siRNA-liposome formulations on membrane integrity (Figure 3.11) also showed that following siRNA incorporation into liposomes, no significant effect on membrane integrity was observed for different N/P ratios and different lipid compositions, relative to empty liposomes applied at the same conditions. Also, no significant effect of siRNA incorporation has been observed in the Annexin V/PI assay for application of siRNA-liposome formulations. The dot plots indicated only a small population of cells positively stained with Annexin V/PI (Figure 3.12).

In a summary, the toxicity assays performed indicated that incorporation of siRNA into cationic liposomes composed of DC-Chol:DOPE has no effect on the cytotoxicity of the liposomes. Moreover, no significant influence of different N/P ratios were detected on cytotoxicity under the experimental conditions used (total lipid content and DC-Chol:DOPE composition). This observation contradicts the results of some published studies that demonstrated that the molar ratio between the positive charge of cationic lipid and negative charge of siRNA was important for cytotoxicity [3], [17], [46], although it should be noted that total lipid concentration applied and DC-Chol content were both 'optimised' in our study to be at a low toxic levels. The data hence indicate complexity in the interplay of total lipid applied, DC-Chol to helper lipid composition, and N/P ratio when assessing the formulations toxicity.

Based on the cytotoxicity results obtained in this chapter, it would be reasonable to speculate that the toxicity effect of designed liposomes results from their effect on the cell plasma membrane, leading to compromised integrity of the A549 cell membrane. Cell membrane disruption, as evident from LDH, and necrosis indicated by PI assay, both points to this. The significant toxic effects were noted at a high concentrations applied, higher than typically used in the literature, and data corroborate with limited toxicity of low doses of cationic liposomes [42]. In the scope of the project described in this thesis, liposomes formulations with low toxicity at the optimised conditions were used in subsequent chapters.

During development of a drug delivery system, it is important to establish a connection between the physiochemical properties and biological effect of the system. In this study, siRNA-liposome formulations were prepared at different lipid compositions (different

molar ratios of DC-Chol:DOPE) and different cationic lipid and nucleic acid (N/P) ratios, with the aim at optimising the physiochemical properties of the delivery system and its ability to protect siRNA in biologically relevant conditions. To this end, several techniques were applied to assess the systems performance, in terms of particle size, zeta potential, encapsulation efficiency, and RNase stability.

Initially, the hydrodynamic particle size of empty liposomes and siRNA-liposome formulations was measured to assess the potential of lipid composition and N/P ratio on the size of the particles and particle size distribution and also the effect of siRNA encapsulation on the size of liposomes and PDI values. One of the important factors that could have an effect on the polydispersity of particle size distribution is the buffer used to suspend the siRNA-liposomes. The ionic strength and composition of a buffer affects the electrical double-layer surrounding charged particles, and responsible for electrostatic repulsion to produce a stable colloidal suspension [47]. The DLS results presented in Figure 3.5A showed that average particles hydrodynamic diameter of empty liposomes was between approximately 70 and 80 nm for all samples measured with an acceptable mono-modal particle size distribution profiles, in terms of samples polydispersity. No significant effect of different ratios of DC-Chol:DOPE was observed. PDI values showed monodisperse distribution of liposomes as all PDI values were less than 0.27. However, the hydrodynamic diameter of siRNA-liposomes showed a significant increase to the sizes above approximately 170 nm for all tested formulations (Figure 3.6). The observed increase in particle size of siRNA-liposomal formulations in comparison to empty liposomes could be a result of loading a high amount of siRNA molecules into the liposomes leading a reduction in positive charges and their repulsions which influence the lipids formation process during the dry layer hydration. This would also explain the

observation that diameters of liposomes prepared at high N/P ratios were smaller, declining towards the empty liposomes size. Extrusion of the siRNA-liposome preparations through polycarbonate filters improved the size heterogeneity, and the PDI values indicated that uniform liposomal particles were formed in the solution. Liposomes with particle size of 207 nm and PDI of 0.24 were used in all subsequent experiments.

The electrostatic properties of liposome formulations can be characterised using the zeta potential measurements. When particles are suspended in liquid medium a double layer is formed around each particle; this consists of the stern (inner) layer, where solvent ions are strongly bound to the particle surface, and a diffuse (outer) layer, where they are less firmly associated [48]. The diffuse layer has a notional boundary called the slipping plane, within which ions are bound sufficiently strongly to remain associated with a particle as it moves through the surrounding bulk liquid (dispersion medium) [47]. The zeta potential is the potential difference between the slipping plane and the bulk. The magnitude of the zeta potential provides an indication of the potential stability of a colloidal dispersion [48]. Particles with low zeta potentials will aggregate because there is no repulsive force to prevent their association. Particles with zeta potentials more negative than − 30 mV or more positive than + 30 mV will normally form a stable colloidal suspension in low ionic strength buffer [11]. When measuring and interpreting the zeta potential data, the pH and ionic strength of the solution are the most important factors to be considered.

The results of the zeta potential measurements of the empty liposome (Figure 3.5B) showed that increase in the ratio of cationic lipid (DC-Chol) in the formulation increased the values of positive zeta potential. The encapsulation of negative charges siRNA

molecules into liposomes has significant effect on the zeta potential of the formulations, leading to decrease the positive values. The siRNA-liposome formulations suspended in 10 mM PBS at pH 7.4 become more positively charged with an increase in the ratio of cationic lipids (and in the case of increased N/P ratio). High surface charge values were obtained for liposomes with increasing N/P ratios, arising from the presence of an amino group from the cationic lipid on the liposome surface.

The magnitude of the zeta potential of the empty liposome formulations was highly dependent upon the cationic lipid content whilst for the siRNA-liposomes it inverted from a negative charge for the lowest N/P ratio of 0.78:1, to a positive charge for the N/P ratio of 1.56:1 clearly indicated an excess of siRNA negative charge in the system at low N/P ratios, and charge neutralisation at theoretical N/P ratio >1. At higher N/P ratios, an excess of positive charge is clearly reflected in increasing positive zeta potential values.

To evaluate the siRNA-liposome encapsulation efficiency, different qualitative and quantitative methods are usually used. Gel retardation is a simple qualitative or semi-quantitative technique that is commonly exploited to examine the entrapment behaviour of siRNA for different ratios of cationic lipid and different lipid compositions. The disappearance of ethidium bromide stained migrating siRNA from the gel indicated the complete encapsulation of the nucleic acid. The ultrafiltration centrifugation technique can also be used to quantify and confirm the encapsulation efficiency and to detect the amount of siRNA that is encapsulated by the liposomes [11].

Gel electrophoresis data in Figure 3.8 indicated that the condensation of anionic siRNA was achieved by increasing the ratios of cationic lipid DC-Chol to siRNA within the

liposomes. A general trend of a decrease in the migration pattern of free siRNA in the gel was seen with an increase in the N/P ratio, with a complete absence of detectable siRNA in the gel at N/P ratio of 50:1. Interestingly, gel electrophoresis showed a relatively high level of siRNA incorporation for liposomal formulations with a relatively low DC-Chol content and a low N/P ratio, such as formulation at DC-Chol:DOPE of 1:1 and at N/P ratio of 3.125:1.

At N/P ratios below 3.125:1, siRNA-liposome samples showed high amounts of free or non-entrapped siRNA on the gels migrating away from the loading wells for different DC-Chol:DOPE compositions. A lower content of cationic lipid required for the good encapsulation of siRNA would be expected to reduce the overall toxicity of the system.

With the aim to confirm the results of the gel retardation assay, an ultrafiltration method was performed on siRNA-liposome formulations with different lipid compositions and different N/P ratios. The results presented in Figure 3.9 showed that the encapsulation efficiency is increased with an increase in the cationic lipid content within the formulation. Low encapsulation efficiency has been achieved at DC-Chol:DOPE ratio of 3:1, especially with low N/P ratio. In agreement with the gel retardation results, very high encapsulation of siRNA was observed for an N/P ratio of 50:1, of approximately 98% for all the different lipid compositions.

Taken together, the results of the zeta potential measurements and gel retardation assay of siRNA-cationic liposomes at low N/P ratios indicate presence of excess free siRNA in excess to positive charges present in the system (zeta potential values of liposomes are negative under these conditions while counterpart empty liposomes have positive charge)

resulting in the free siRNA in the system, as seen in gel electrophoresis. With increased N/P ratio, excess of positive charge is achieved, as reflected in positive zeta potential, which results in absence of free siRNA, as seen by gel electrophoresis. This may indicate that despite the encapsulation of siRNA during the liposomes production which aimed at achieving incorporation of siRNA inside the liposomal aqueous core, the electrostatic interactions and the presence of excess of positive charge remains an essential prerequisite for efficient siRNA incorporation.

siRNA is a molecule that has very low stability and is susceptible to hydrolysis within biological fluids by enzymes [4]. In addition, the low stability of siRNA in comparison to DNA in aqueous media is due to RNA possessing a 2'OH. The result is that under basic conditions, this hydroxyl group may be deprotonated and can act as a nucleophile and hydrolyse the phosphate bond [49]. Hence, an efficient siRNA-delivery system would be one that can protect siRNA.

In order to study the ability of the liposomes designed in this study to protect siRNA from enzymatic degradation, the prepared siRNA-liposome formulations were exposed to RNase A solution for different time periods and then analysed by gel electrophoresis. The liposomal protection of siRNA was assessed for formulations with different molar composition of DC-Chol:DOPE prepared with 1.0 mM total lipid and 0.4 μg siRNA at a fixed N/P ratio of 3.125:1.

Nuclease stability can be assumed from the relative intensity of the bands for different time intervals. Naked siRNA, shown in Figure 3.13, was completely degraded after 30 min of RNase incubation at 37°C, while siRNA protection was achieved at 30 min

incubation for all tested DC-Chol:DOPE formulations. Prolonged nuclease resistance was observed for all formulations at time points less than 4 hrs. If such stability would be achieved *in vivo*, the 4 hrs period should be sufficient for siRNA-liposomes to taken up by cells, relative to 30 min time required for complete hydrolysis of free siRNA RNase A solution. No significant difference was observed for the different lipid compositions in terms of siRNA protection. Research by Kim *et al.* stated the cationic liposomes formulated with DSPE-PEG blocked degradation of siRNA partially from nuclease when incubated with RNAse enzyme (0.1 mg/ml) for 30 min [50].

3.5 Conclusions

This chapter illustrates that the cytotoxicity of DC-Chol:DOPE liposomes was highly dependent on the total lipid concentration applied. At the optimised dose of 1.0 mM, liposome formulations did not show considerable, irreversible cellular damage, while significantly reduced cell metabolic activity (as measured by the MTS assay), marked cell membrane disruption (as measured by the LDH assay) and cell necrosis (as measured by the Annexin V/PI assay) were found to be associated with exposure to higher doses of total lipids i.e. cationic liposome formulations. Interestingly, at 1.0 mM total lipid dose, no significant effect was observed for the toxicity of different N/P ratios of cationic lipid to nucleic acid.

Based on the results obtained in this chapter in terms of particle size, zeta potential, gel electrophoresis, and encapsulation efficiency, different N/P ratios were found to play a significant role to influence the physiochemical properties of siRNA-liposome formulations. The present work also demonstrates that the classical film hydration (encapsulation) method resulted in a high level of siRNA liposomal incorporation and

protection, even at relatively low levels of cationic lipid, 3.125:1, as confirmed by gel retardation and the ultrafiltration centrifugation method. siRNA-liposomes prepared with a total lipid concentration of 1.0 mM and a N/P ratio of 3.125:1 have been selected for further biological investigation in the next chapter due to their high level of cell viability, good physiochemical properties, and siRNA protection towards degradation.

3.6 References

[1] L. D. Kumar and A. R. Clarke, "Gene manipulation through the use of small interfering RNA (siRNA): from in vitro to in vivo applications.," *Advanced drug delivery reviews*, vol. 59, no. 2–3, pp. 87–100, Mar. 2007.

[2] J. Hughes, P. Yadava, and R. Mesaros, "Liposomal siRNA Delivery," *Methods in Molecular Biology*, vol. 605, no. 1, pp. 445–459, 2010.

[3] H. Y. Xue, S. Liu, and H. L. Wong, "Nanotoxicity: a key obstacle to clinical translation of siRNA-based nanomedicine.," *Nanomedicine*, vol. 9, no. 2, pp. 295–312, 2014.

[4] A. Gallas, C. Alexander, M. C. Davies, S. Puri, and S. Allen, "Chemistry and formulations for siRNA therapeutics.," *The Royal Society of Chemistry*, vol. 42, no. 20, pp. 7983–7997, Jul. 2013.

[5] Y.-K. Oh and T. G. Park, "siRNA delivery systems for cancer treatment.," *Advanced drug delivery reviews*, vol. 61, no. 10, pp. 850–862, Aug. 2009.

[6] V. P. Torchilin, "Recent advances with liposomes as pharmaceutical carriers.," *Nature reviews. Drug discovery*, vol. 4, no. 2, pp. 145–60, Feb. 2005.

[7] A. D. Miller, "Nonviral liposomes.," *Methods in Molecular Medicine*, vol. 90, pp. 107–137, Jan. 2004.

[8] R. Cortesi, E. Esposito, E. Menegatti, R. Gambari, and C. Nastruzzi, "Effect of cationic liposome composition on in vitro cytotoxicity and protective effect on carried DNA," *International Journal of Pharmaceutics*, vol. 139, no. 1–2, pp. 69–78, 1996.

[9] D. Cipolla, B. Shekunov, J. Blanchard, and A. Hickey, "Lipid-based carriers for pulmonary products: Preclinical development and case studies in humans.," *Advanced drug delivery reviews*, vol. 75, pp. 53–80, May 2014.

[10] A. Akbarzadeh, R. Rezaei-sadabady, S. Davaran, S. W. Joo, and N. Zarghami, "Liposome : classification , preparation , and applications," *Nanoscale Research Letters*, vol. 8, no. 102, pp. 1–9, 2013.

[11] M. Kapoor, D. J. Burgess, and S. D. Patil, "Physicochemical characterization techniques for lipid based delivery systems for siRNA.," *International Journal of Pharmaceutics*, vol. 427, no. 1, pp. 35–57, May 2012.

[12] W. H. De Jong and P. J. a Borm, "Drug delivery and nanoparticles:applications and hazards.," *International journal of nanomedicine*, vol. 3, no. 2, pp. 133–149, 2008.

[13] Y. Li, J. Wang, Y. Gao, J. Zhu, M. G. Wientjes, and J. L.-S. Au, "Relationships between Liposome Properties, Cell Membrane Binding, Intracellular Processing, and Intracellular Bioavailability," *The AAPS Journal*, vol. 13, no. 4, pp. 585–597, 2011.

[14] R. Kedmi, N. Ben-Arie, and D. Peer, "The systemic toxicity of positively charged lipid nanoparticles and the role of Toll-like receptor 4 in immune activation," *Biomaterials*, vol. 31, no. 26, pp. 6867–6875, 2010.

[15] E. Fröhlich, "The role of surface charge in cellular uptake and cytotoxicity of medical nanoparticles," *International Journal of Nanomedicine*, vol. 7, pp. 5577–5591, 2012.

[16] K. Romøren, B. J. Thu, N. C. Bols, and Ø. Evensen, "Transfection efficiency and cytotoxicity of cationic liposomes in salmonid cell lines of hepatocyte and macrophage

origin," *Biochimica et Biophysica Acta - Biomembranes*, vol. 1663, no. 1–2, pp. 127–134, 2004.

[17] M. L. Immordino, F. Dosio, and L. Cattel, "Stealth liposomes: Review of the basic science, rationale, and clinical applications, existing and potential," *International Journal of Nanomedicine*, vol. 1, no. 3, pp. 297–315, 2006.

[18] T. K. Kim and J. H. Eberwine, "Mammalian cell transfection: The present and the future," *Analytical and Bioanalytical Chemistry*, vol. 397, no. 8, pp. 3173–3178, 2010.

[19] V. L. C. Peetla, A. Stine, "Biophysical interactions with model lipid membranes: applications in drug discovery and drug delivery," *Mol Pharm.*, vol. 6, no. 5, pp. 1264–1276, 2009.

[20] D. a Balazs and W. Godbey, "Liposomes for use in gene delivery.," *Journal of Drug Delivery*, vol. 2011, pp. 1–12, Jan. 2010.

[21] G. Malich, B. Markovic, and C. Winder, "The sensitivity and specificity of the MTS tetrazolium assay for detecting the in vitro cytotoxicity of 20 chemicals using human cell lines.," *Toxicology*, vol. 124, no. 3, pp. 179–192, Dec. 1997.

[22] E. J. Delikatny, W. A. Cooper, S. Brammah, N. Sathasivam, and D. C. Rideout, "Nuclear Magnetic Resonance-visible Lipids Induced by Cationic Lipophilic Chemotherapeutic Agents Are Accompanied by Increased Lipid Droplet Formation and Damaged Mitochondria 1," *CANCER RESEARCH*, vol. 62, pp. 1394–1400, 2002.

[23] and M. J. D. R. Francis Ka-Ming Chan, Kenta Moriwaki, "Detection of Necrosis by Release of Lactate Dehydrogenase (LDH) Activity," *Methods Mol Biol*, vol. 979, pp. 65–70, 2013.

[24] A. M. Rieger, K. L. Nelson, J. D. Konowalchuk, and D. R. Barreda, "Modified annexin V/propidium iodide apoptosis assay for accurate assessment of cell death.," *Journal of visualized experiments*, no. 50, pp. 37–40, Jan. 2011.

[25] S. Elmore, "Apoptosis: a review of programmed cell death.," *Toxicologic pathology*, vol. 35, no. 4, pp. 495–516, 2007.

[26] R. a Schlegel and P. Williamson, "Phosphatidylserine, a death knell.," *Cell death and differentiation*, vol. 8, no. 2001, pp. 551–563, 2001.

[27] I. Vermes, C. Haanen, H. Steffens-Nakken, and C. Reutelingsperger, "A novel assay for apoptosis. Flow cytometric detection of phosphatidylserine expression on early apoptotic cells using fluorescein labelled Annexin V," *Journal of Immunological Methods*, vol. 184, no. 1, pp. 39–51, 1995.

[28] S. Honary and F. Zahir, "Effect of Zeta Potential on the Properties of Nano - Drug Delivery Systems," *Tropical Journal of Pharmaceutic al Research*, vol. 12, no. 2, pp. 265–273, 2013.

[29] Y. Xia, J. Tian, and X. Chen, "Effect of surface properties on liposomal siRNA delivery," *Biomaterials*, vol. 79, no. 2016, pp. 56–68, 2016.

[30] S. Zhang, J. Li, G. Lykotrafitis, G. Bao, and S. Suresh, "Size-dependent endocytosis of nanoparticles," *Advanced Materials*, vol. 21, no. 4, pp. 419–424, 2009.

[31] C. He, Y. Hu, L. Yin, C. Tang, and C. Yin, "Effects of particle size and surface charge on cellular uptake and biodistribution of polymeric nanoparticles," *Biomaterials*, vol. 31, no. 13, pp. 3657–3666, 2010.

[32] S. Ahn, E. Seo, K. Kim, and S. J. Lee, "Controlled cellular uptake and drug efficacy of nanotherapeutics.," *Scientific reports*, vol. 3, p. 1997, 2013.

[33] M. S. Draz, B. A. Fang, P. Zhang, Z. Hu, S. Gu, K. C. Weng, J. W. Gray, and F. F. Chen, "Nanoparticle-mediated systemic delivery of siRNA for treatment of cancers and viral infections," *Theranostics*, vol. 4, no. 9, pp. 872–892, 2014.

[34] S.-E. Han, H. Kang, G. Y. Shim, M. S. Suh, S. J. Kim, J.-S. Kim, and Y.-K. Oh, "Novel cationic cholesterol derivative-based liposomes for serum-enhanced delivery of siRNA.," *International journal of pharmaceutics*, vol. 353, no. 1–2, pp. 260–269, Apr. 2008.

[35] A. Prokop and J. Davidson, "Nanovehicular intracellular delivery systems," *Journal of pharmaceutical sciences*, vol. 97, no. 9, pp. 3518–3590, 2008.

[36] K. Abe and N. Matsuki, "Measurement of cellular 3-(4,5-dimethylthiazol-2-yl)-2,5-diphenyltetrazolium bromide (MTT) reduction activity and lactate dehydrogenase release using MTT," *Neuroscience Research*, vol. 38, no. 4, pp. 325–329, 2000.

[37] S. Li, X. Gao, K. Son, F. Sorgi, H. Hofland, and L. Huang, "controlled release DC-Chol lipid system in gene transfer," *Journal of Controlled Release*, vol. 39, pp. 373–381, 1996.

[38] A. Congiu, D. Pozzi, C. Esposito, C. Castellano, and G. Mossa, "Correlation between structure and transfection efficiency: a study of DC-Chol-DOPE/DNA complexes.," *Colloids and surfaces B: Biointerfaces*, vol. 36, no. 1, pp. 43–48, Jul. 2004.

[39] C. Wan, T. M. Allen, and P. R. Cullis, "Lipid nanoparticle delivery systems for siRNA-based therapeutics," *Drug Delivery and Translational Research*, vol. 4, no. 1, pp. 74–83, 2014.

[40] A. F. Gazdar, L. Girard, W. W. Lockwood, W. L. Lam, and J. D. Minna, "Lung cancer cell lines as tools for biomedical discovery and research," *Journal of the National Cancer Institute*, vol. 102, no. 17, pp. 1310–1321, 2010.

[41] X. Han, R. Gelein, N. Corson, P. Wade-Mercer, J. Jiang, P. Biswas, J. N. Finkelstein, A. Elder, and Günter Oberdörster, "Validation of an LDH assay for assessing nanoparticle toxicity," *Toxicology*, vol. 287, no. 1–3, pp. 99–104, 2011.

[42] K. B. Knudsen, H. Northeved, E. K. Pramod Kumar, A. Permin, T. Gjetting, T. L. Andresen, S. Larsen, K. M. Wegener, J. Lykkesfeldt, K. Jantzen, S. Loft, P. Møller, and M. Roursgaard, "In vivo toxicity of cationic micelles and liposomes," *Nanomedicine: Nanotechnology, Biology, and Medicine*, vol. 11, no. 2, pp. 467–477, 2015.

[43] C. Tong, B. Shi, X. Xiao, H. Liao, Y. Zheng, G. Shen, D. Tang, and X. Liu, "An Annexin V-based biosensor for quantitatively detecting early apoptotic cells.," *Biosensors & bioelectronics*, vol. 24, no. 6, pp. 1777–1782, Feb. 2009.

[44] M. Van Engeland, F. C. S. Ramaekers, M. van Engeland, L. J. W. Nieland, F. C. S. Ramaekers, B. Schutte, C. P. M. Reutelingsperger, L. Casciola-Rosen, a Rosen, M. Petri, and M. Schlissel, "A review on an apoptosis detection system based on phosphatidyserine exposure," *Proceedings of the National Academy of Sciences of the United States of America*, vol. 93, no. 4, pp. 1–9, 1996.

[45] X. Wei, B. Shao, Z. He, T. Ye, M. Luo, Y. Sang, X. Liang, W. Wang, S. Luo, S. Yang, S. Zhang, C. Gong, M. Gou, H. Deng, Y. Zhao, H. Yang, S. Deng, C. Zhao, L. Yang, Z. Qian, J. Li, X. Sun, J. Han, C. Jiang, M. Wu, and Z. Zhang, "Cationic nanocarriers induce cell necrosis through impairment of Na(+)/K(+)-ATPase and cause subsequent inflammatory response.," *Cell research*, vol. 25, no. 2, pp. 237–253, 2015.

[46] A. Sharma and U. S. Sharma, "Liposomes in drug delivery: progress and limitations," *International Journal of Pharmaceutics*, vol. 154, pp. 123–140, 1997.

[47] S. Salgin, U. Salgin, and S. Bahadir, "Zeta potentials and isoelectric points of biomolecules: The effects of ion types and ionic strengths," *International Journal of Electrochemical Science*, vol. 7, no. 12, pp. 12404–12414, 2012.

[48] S. Bhattacharjee, "DLS and zeta potential – What they are and what they are not?," *Journal of Controlled Release*, vol. 235, pp. 337–351, 2016.

[49] Y. Shu, F. Pi, A. Sharma, M. Rajabi, F. Haque, D. Shu, M. Leggas, B. M. Evers, and P. Guo, "Stable RNA nanoparticles as potential new generation drugs for cancer therapy.," *Advanced drug delivery reviews*, vol. 66, pp. 74–89, Nov. 2013.

[50] H.-K. Kim, E. Davaa, C.-S. Myung, and J.-S. Park, "Enhanced siRNA delivery using cationic liposomes with new polyarginine-conjugated PEG-lipid.," *International Journal of Pharmaceutics*, vol. 392, pp. 141–147, Jun. 2010.

Chapter 4 - Cellular Uptake and Silencing Efficiency of siRNA-Liposomes

4.1 Introduction

In addition to evaluating the physiochemical and biological characterisations of siRNA delivery systems, it is important to consider the ability and efficacy of the delivery system to facilitate the entry of siRNA molecules into the target cells. The transfection efficiency is the prime interest in determining the potential of a non-viral delivery system to become a therapeutic. The main obstacle in the potential clinical application of siRNA at the present is considered to be the efficient and safe delivery [1].

The DC-Chol:DOPE liposomes have been shown to be relatively efficient non-viral delivery system in carrying siRNA into several cell types both *in vitro* as well as *in vivo* [2]. In this context, DOPE is believed to aid to the elasticity of the liposomal lipid bilayer and facilitates particle uptake across the cell membrane, thereby improving transfection of the target cells [3]. In the previous chapter, the physicochemical properties and biological stability of DC-Chol:DOPE liposomes prepared on this project were evaluated and the preliminary results suggest that certain compositions of DC-Chol:DOPE liposomes appear to be promising candidates for further investigation.

In the process of developing a candidate delivery system, it is very important to carry out an *in vitro* screening initially, that is valuable in indicating whether delivery systems has

potential attributes for further developments. Examining and optimising liposome formulations *in vitro* are therefore essential steps in order to determine the 'lead' candidate for further therapeutic developments. In this chapter, siRNA-liposome formulations characterised and optimised during the first part of this project (Chapter 3) are the basis for further biological investigations to evaluate their gene silencing efficiency *in vitro*, as a measure of their potentials as a therapeutic siRNA delivery vector. The *in vitro* model used in this project is based on A549 cells, human adenocarcinoma alveolar epithelial cell line, that is routinely used in research as an *in vitro* model of NSCLC [4]. The same cell line was used in Chapter 3 to evaluate the cytotoxicity of designed liposomes siRNA formulation, and will be exploited in this chapter to investigate the cellular internalisation.

Following the cellular internalisation, the siRNA-liposomes are mainly reported to be retained inside endosomal or lysosomal compartments, whilst the siRNA 'escape' (or the formulation escape) into the cytosol is essential for siRNA to target mRNA and to achieve the silencing effect [5]. One of the techniques that is commonly used in pharmaceutical and biomedical research to evaluate the transfection efficiency of siRNA delivery system and its ability to target the gene of interest is using the reporter genes. Reporter genes are used as indicators to study gene expression and cellular events coupled to gene expression [6]. A reporter gene is usually cloned with a DNA sequence of interest into an expression vector, which is then transferred into cells [7].

The luciferase-based reporter assay is one of the commonly used assay that is considered to be sensitive, relatively inexpensive, and an accurate quantitative approach to study the expression of target gene at the transcriptional level [8]. It has wide applications across

many fields of cell and molecular biology, to measure or track expression of a cloned gene. The luciferase assay is based on the interaction of the luciferase enzyme with the luciferin substrate, which release light by the process of bioluminescence [9]. The light signals are detected by luminometry measurements, therefore cellular process, or signal is 'read' without directly assaying the cellular gene product. A luciferase-expressing A549 human lung carcinoma cell line (A549-Luc) will be used in this project to assess the ability of our siRNA-liposomal formulations to silence the luciferase gene.

One of the novel experimental techniques that will be exploited in this project to confirm the engagement of siRNA with the targeted mRNA is the application of a so called 'Molecular Beacon' (MB). The MB approach was first introduced by Sanjay Tyagi and Fred Russell Kramer in 1996, and was originally defined as a novel nucleic acid probe that recognise and report the presence of specific nucleic acids in homogeneous solutions [10]. The later work developed MB probes for cellular analysis. The MB probe is typically labelled with a fluorescent emitter and its quencher, attached to a hairpin shaped single stranded nucleic acid sequence. This will fluoresce only upon hybridization with its target molecule when a distance between fluorescence emitter and its quencher is changed [11]. Namely, the MB as shown in Figure 4.1 has a stem-loop structure, a fluorophore, and a quencher attached to opposite ends. In the absence of luciferase mRNA (or other target mRNA), the stem brings the fluorophore and quencher together and the fluorescence signal of the emitter compound is quenched via Fluorescence Resonance Energy Transfer (FRET) [12], [13]. In the presence of the target luciferase mRNA, the loop region of MB hybridize with the luciferase mRNA and opens up the hairpin structure into a linear structure, thus causing separation of the fluorophore and the quencher [13], which results in increase in fluorescence and identification of the target luciferase.

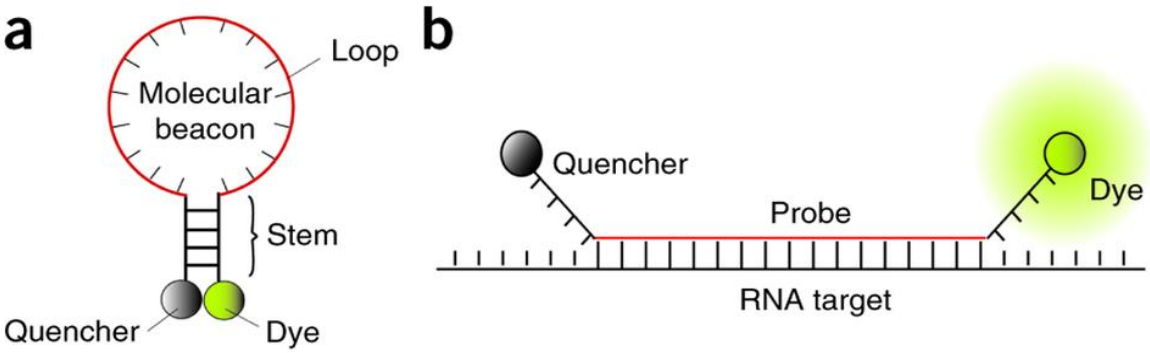

Figure 4.1: Schematic of Molecular Beacon mechanism of action

(a) The stem (which consists of 4-7 base pairs), brings the 5′ dye and 3′ quencher together to quench the fluorescence signal. The loop region with 19–21 bp is complementary to the target sequence of specific mRNA, thus providing specificity. (b) A schematic depicting a MB in an open conformation after hybridizing to its complementary target mRNA sequence. Hybridization induces a conformational change that separates the fluorophore from the quencher, resulting in a more than 10 fold increase in fluorescence signal. Adapted from [14].

4.2 Aims and Objectives

The aims of the work in this chapter are to investigate the cellular uptake of fluorescently labelled siRNA-liposomes in A549 cells using flow cytometry and confocal microscopy. Furthermore, the transfection efficiency of siRNA-liposomes will be evaluated in a luciferase expressing epithelial lung cancer cell line (A549-Luc) using luciferase assay. The 'luc-siRNA based MB' liposomes, which should shows fluorescence when the siRNA binds to the targeted luciferase mRNA, will be exploited in this work to measure the engagement of delivered siRNA molecules with the targeted mRNA.

4.3 Results

4.3.1 Assessment of Cy3-siRNA Cellular Uptake

In order to initiate gene-silencing effect, the liposomal-siRNA formulations need to cross cell plasma membrane into the cytoplasmic compartment of the target cells. To verify this, A549 cells were treated with liposome-siRNA formulations prepared at an optimised N/P ratio of 3.125:1 and at different molar compositions of DC-Chol:DOPE. The cellular uptake and intracellular distribution of the cy3-labelled siRNA-liposomes were investigated quantitatively using flow cytometry (Figure 4.2) and qualitatively using confocal microscopy (Figure 4.3 and Figure 4.4).

4.3.1.1 Flow Cytometry

The cellular association of the cy3-siRNA-liposomes was assessed by analysing ('gating') the cells that show cy3-siRNA fluorescence, and by measuring the mean fluorescence intensity (MFI), a measure of the average fluorescence per cells analysed. To quench the fluorescence of cy3-siRNA that was not internalised by the cells, but was associated to the cell membrane, trypan blue was utilised. A549 cells without the application of cy3-siRNA-liposomes were used as negative controls, and cells treated with cy3-siRNA complexed with the commercially available transfection reagent Lipofectamine® RNAiMAX were used as positive control. This transfection reagent was reported to be able to transfect a broad range of cell types, including A549 cells [15].

The flow cytometry histograms obtained (Figure 4.2 A) shows the A549 cell population with associated fluorescence after 4 hrs incubation and the results are summarised in Figure 4.2 B. The data show that an increase in the cationic lipid ratio within the

liposomal formulations increased the percentage of A549 cells that successfully internalised the cy3-siRNA liposome formulations.

Increasing the ratio of cationic lipid DC-Chol from 0.33 to 1 raised the uptake of siRNA from 20% to around 90% of cell population. Maximum cy3-siRNA cellular uptake was achieved with an equal ratio of DC-Chol to DOPE (1 to 1) liposomes, with uptake more than the cellular uptake of commercially available transfection reagent Lipofectamine® RNAiMAX (80% of cell population).

The MFI data in Figure 4.2 C which were determined relative to the MFI value of negative control (A549 cells not treated with cy3-siRNA liposomes), and results show that a significant proportion of liposomes entry into the cells has been achieved. The highest level of siRNA internalisation obtained when the formulation contained an equal ratio of cationic to zwitterionic lipid (approximately 15 fold increases in fluorescence signal in comparison to negative control). Lipofectamine® RNAiMAX transfection reagent shows MFI value around 5 fold increases in comparison to negative control cells.

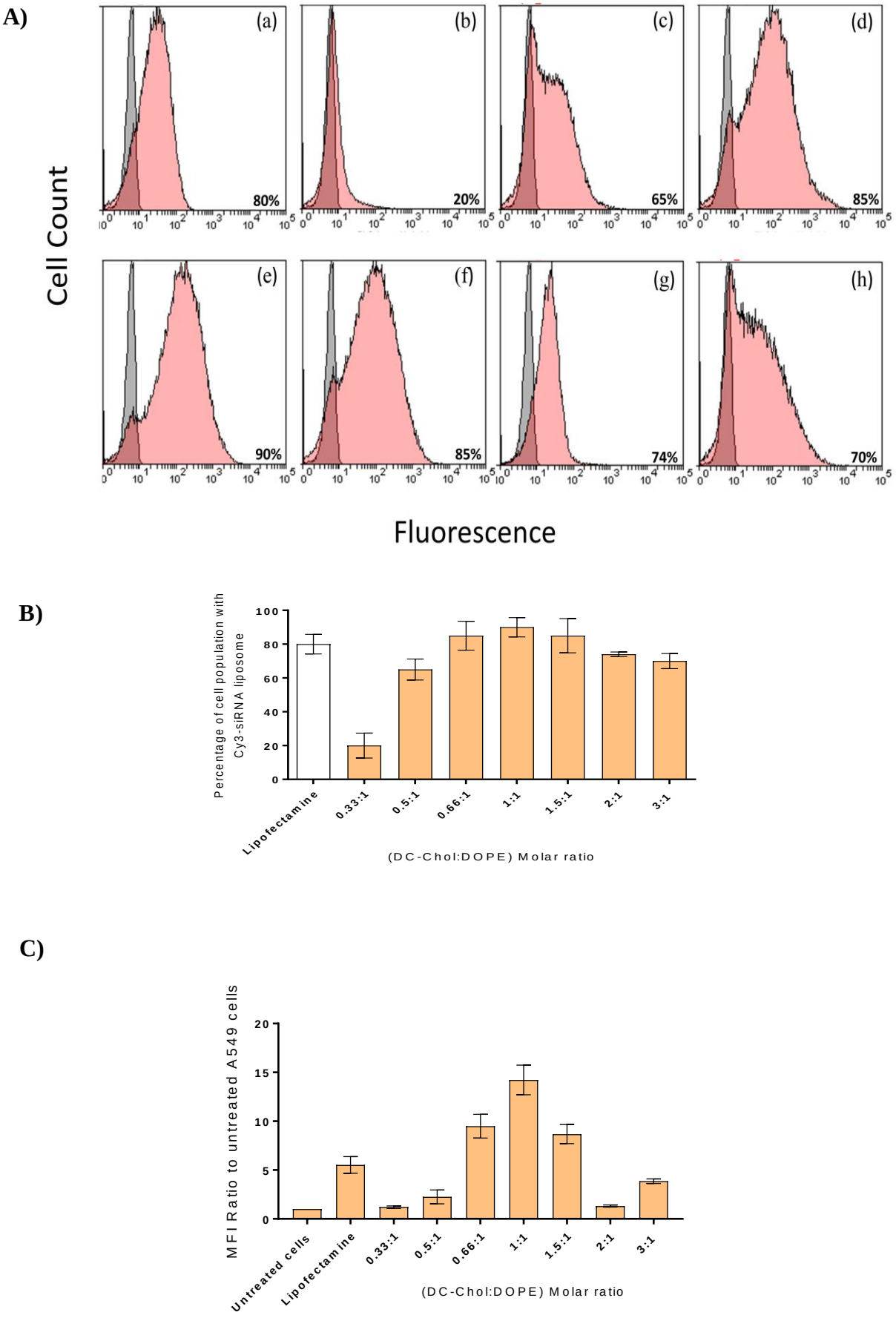

Figure 4.2: Cellular uptake profiles of cy3-siRNA-liposomes by A549 cells

Cells were seeded onto 24-well plates at a density of 5 × 10^4 cells per well and cultured overnight. Liposomes containing 1 μg of siRNA per well were incubated with the cells for 4 hrs. ***(A)*** *Flow cytometry histograms showing cellular uptake after the application of liposomal formulations to A549 cells in culture at an N/P ratio of 3.125:1. Individual red histograms are shown for DC-Chol:DOPE as (b) 0.33:1, (c) 0.5:1, (d) 0.66:1, (e) 1:1, (f) 1.5:1, (g) 2:1 and (h) 3:1, respectively. Cells were assessed by a Beckman Coulter MoFlo (minimum 10,000 cells/sample) and extracellular fluorescence was quenched using trypan blue. Cells without cy3-siRNA-liposomes were used as negative controls (the grey histograms), and cells treated with cy3-siRNA complexed with the commercially available transfection reagent Lipofectamine® RNAiMAX (a) were used as positive control.* ***(B)*** *A summary of the cell population uptake of cy3-siRNA-liposomes.* ***(C)*** *MFI data for all tested formulations calculated as a ratio to negative control (cells without cy3-siRNA-liposomes). Results shown as the mean ± SD, (N=2, n=4).*

4.3.1.2 Confocal Microscopy

Confocal microscopy was carried out in order to visualise the internalisation of cy3-siRNA-liposomes within A549 cells, as well as obtain initial observations on their intracellular trafficking and localisation. Cells were incubated with cy3-siRNA-liposomes at an N/P ratio of 3.125:1, which was found to show optimal encapsulation efficiency (Section 3.3.3), and at DC-Chol:DOPE ratio of 1:1, the ratio that resulted in the highest cellular uptake in the previous experiment. Confocal micrographs (Figure 4.3) indicate the presence of siRNA-liposomes labelled with cy3 (red) in the perinuclear region of the cells. The blue fluorescence is due to DRAQ5 nuclear stain. The micrographs provide a qualitative, initial demonstration of cell internalisation of cy3-siRNA-liposomes, as implied by the presence of fluorescence 'deep' within the A549 cells (as seen in z-stacks in Figure 4.4). Intense red signal appeared as red puncta, distributed typically throughout the endosomes and perinuclear region of the A549 cells, and particularly intense as a 'circular' around blue label of the nuclei. The using of fluorescent co-localisation marker for labeling and tracking acidic organelles such as LysoTracker dye is essential to determine the actual localisation of siRNA-liposomes inside the endosomal/lysosomal comportments.

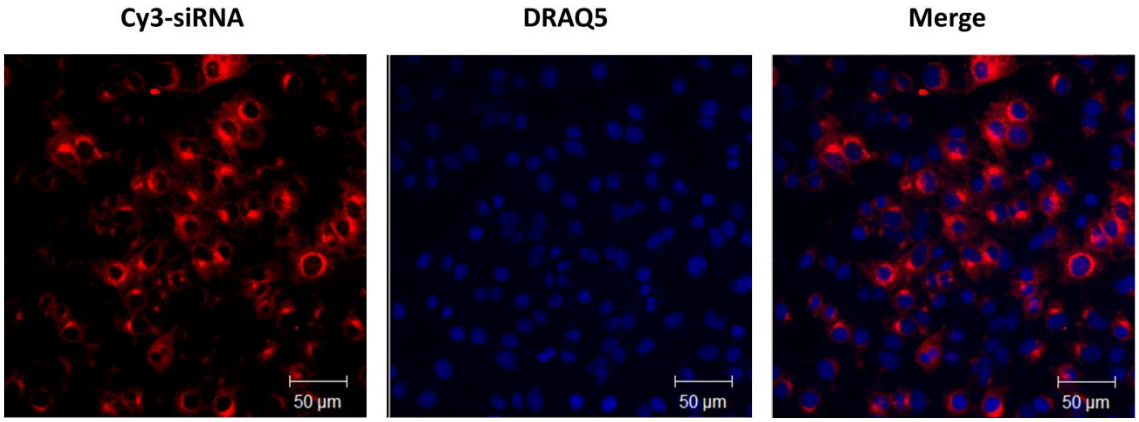

Figure 4.3: Confocal microscopy micrographs of the cellular uptake of cy3-siRNA-liposomes by A549 cells in culture

Cells were incubated with cy3-siRNA-liposomes at an N/P ratio of 3.125:1 and a DC-Chol:DOPE ratio of 1:1 for 4 hrs and then assessed using confocal microscopy. Cy3-siRNA-liposomes appear red, whereas nuclei appear blue as stained with DRAQ5. Scale bar: 50 µm.

Combined, the results from the flow cytometry and confocal microscopy, confirm the cellular internalisation of cy3-siRNA-liposomes and their presence inside cell cytosol, particularly in the perinuclear region.

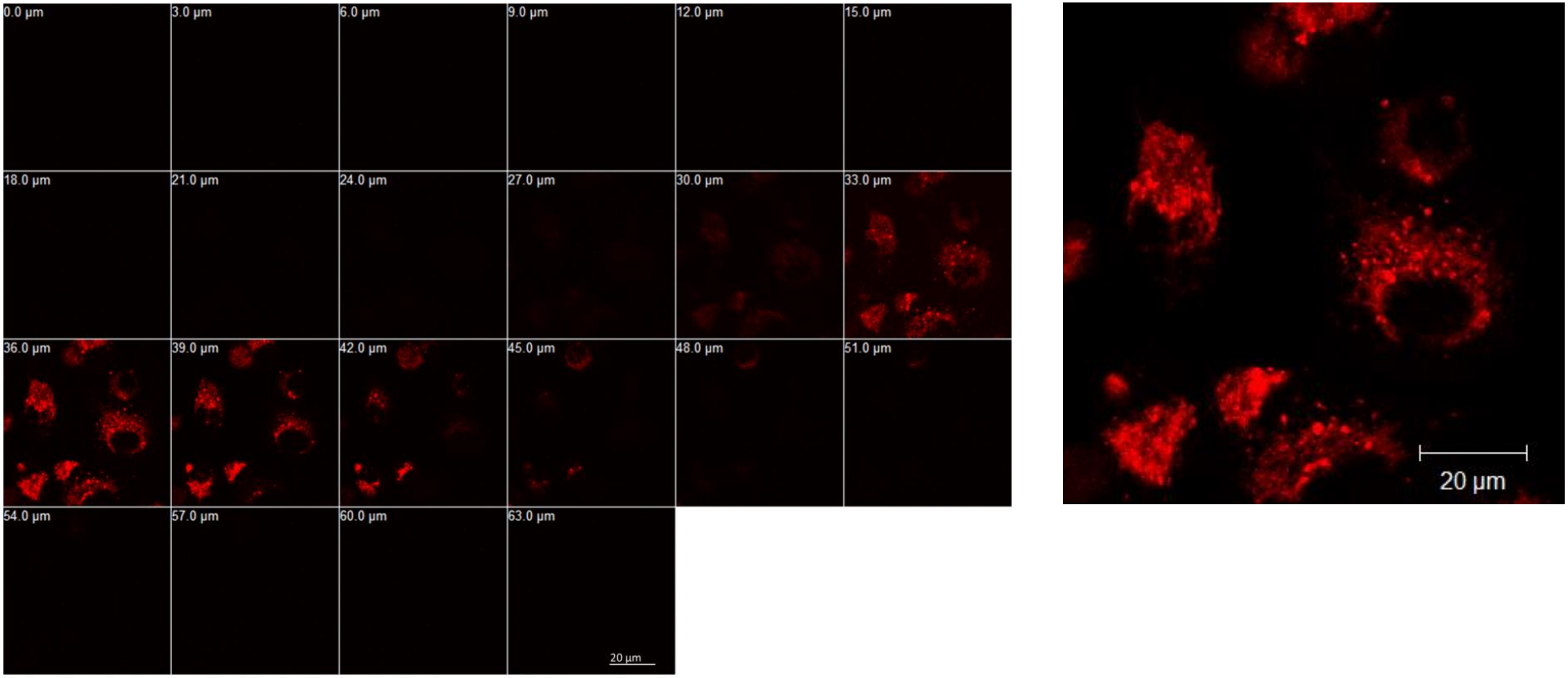

Figure 4.4: Confocal microscopy panel of z-stack micrographs of cy3-siRNA-liposomes cellular uptake in A549 cells

Cells were incubated with cy3-siRNA-liposomes at an N/P ratio of 3.125:1 and a DC-Chol:DOPE ratio of 1:1 for 4 hrs and then assessed using confocal microscopy. The localisation of cy3-siRNA-liposomes (red) is represented as individual image (right micrograph). Z-stack sections images from the top to the bottom of the cells at 63 µm thickness are presented in left panels. Scale bar: 20 µm.

4.3.2 Assessment of Luciferase Expression Silencing

In order to investigate the ability of the optimised siRNA-liposome formulation to produce the gene-silencing effect, a delivery system needs to escape from endosomal vesicles (if this was involved in its cellular internalisation pathway) and ensure that delivered siRNA binds the mRNA of the targeted gene to 'knockdown' the expression of the protein of interest. A gene knockdown study was therefore carried out using a luciferase-expressing A549 human lung carcinoma cell line. To verify luciferase silencing, A549-Luc cells in culture were treated with the siRNA-liposomes formulations at an N/P ratio of 3.125:1, and the relative luciferase protein activity was examined quantitatively using a luciferase assay (Figure 4.5 and Figure 4.6) and flow cytometry (Figure 4.7), and qualitatively using confocal microscopy (Figure 4.8).

4.3.2.1 Luciferase Assay

4.3.2.1.1 Effect of siRNA Amount on Luciferase Activity

Liposome-siRNA formulations with two different amounts of siRNA (0.5 and 1 μg per well) were used to evaluate the luciferase silencing activity and also to examine the effect of different amounts of applied siRNA on the transfection efficiency. Formulations were prepared with different molar ratios of cationic to zwitterionic lipid and at fixed an N/P ratio of 3.125:1, which was found to show optimal encapsulation efficiency (Section 3.3.3) and successful cellular internalisation (Section 4.3.1).

The transfection reagent Lipofectamine® RNAiMAX was used as positive control according to the manufacturer protocol described previously in Chapter 2. Also, siRNA alone (1 μg) was applied to confirm the ability of liposomes to deliver siRNA and

produce the silencing effect. A549-Luc cells were also treated with scrambled siRNA (1 μg) as non-targeting negative control to distinguish between specific and non-specific effects of siRNA activity. The luciferase silencing activity of scrambled siRNA was tested on only one liposomal formulation (prepared at 1:1 molar ratio of DC-Chol:DOPE, N/P ratio of 3.125:1 and applied at 1 μg siRNA/well dose) which was found to show the highest level of cellular uptake (Section 4.3.1), to compare knockdown levels *vs* background, and to assess the off-target effect of siRNA sequence. Results of a pilot study on scrambled non-targeting siRNA-liposome formulations prepared at different molar ratios of DC-Chol:DOPE on A549-Luc cells indicated no statistically significant reduction on the luciferase activity of different ratios tested, $p>0.05$ (see Appendix 1). Additionally, no significant silencing effect of scrambled siRNA-lipofectamine complexes was detected (Appendix 1). The luciferase activity of all liposomal formulations was normalised and presented as a percentage of luciferase activity relative to A549-Luc cells not treated with Luc-siRNA liposomes which was taken as 100% of luciferase protein activity. It should be noted that two formulations with molar ratio of 0.5:1 and 3:1 showed significant increase in luciferase activity in comparison to control A549-Luc cells not treated with siRNA-liposomes which represents 100% luciferase activity.

The results, as shown in Figure 4.5, indicate statistically significant inhibition of relative luciferase activity for all the selected liposome formulations used for cell transfection ($p<0.0001$). Increasing the amount of siRNA from 0.5 μg/well to 1 μg/well, as well as increasing the ratio of cationic lipid in the formulations appeared to have a significant influence on the transfection efficiency. For example, the relative luciferase activity for the lowest cationic lipid ratio of 0.33:1 applied was reduced from 72% with 0.5 μg/well to

56% with 1 μg/well siRNA ($p<0.0001$). Additionally, at the highest cationic lipid ratio of 3:1 the relative luciferase activity was decreased from 59% with 0.5 μg/well to 40% with 1 μg/well siRNA, ($p<0.0001$). However, at the 'middle' ratios of 0.66:1 to 2:1, there is no significant effect of the siRNA increased dose (except 1.5:1 ratio).

Regarding the effect of DC-Chol:DOPE ratio on the luciferase silencing, the silencing effect was lowest at the lowest two ratios of 0.33:1 and 0.5:1 (with relative expression at 72 and 77% of the untreated control), and achieving an apparent plateau, with some variations, at an equal ratio of DC-Chol to DOPE (1 to 1), with a transfection efficiency of approximately 54% and 57% for 0.5 μg/well and 1 μg/well siRNA, respectively; this follows the expectations from the cellular uptake study (Figure 4.2).

The negative control with non-targeting/scrambled siRNA did not produce significant effect on the luciferase activity.

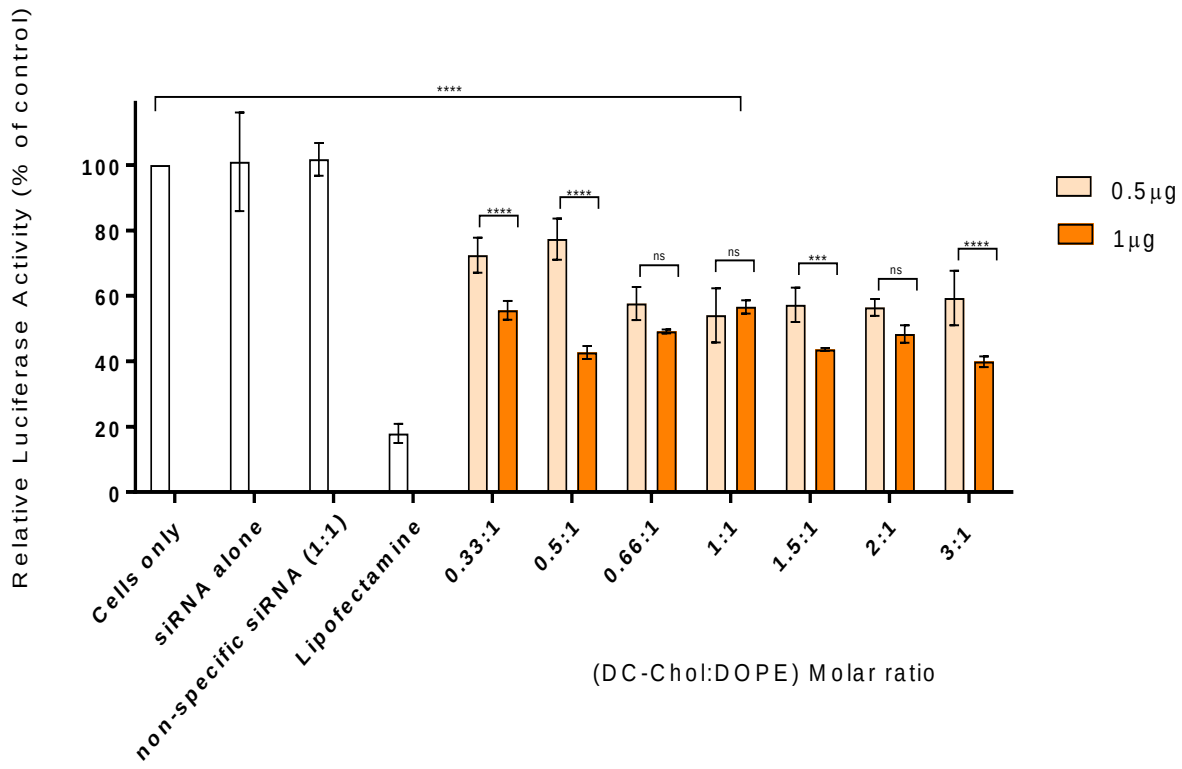

Figure 4.5: Relative luciferase activity of A549-Luc cells after incubation with luc-siRNA-liposomes

*Cells were seeded onto 24-well plates at a density of 5 × 10^4 cells per well and cultured overnight. Liposome-siRNA formulations were prepared at an N/P ratio of 3.125:1 and different DC-Chol:DOPE molar ratios, and applied to the cells for 4 hrs. A549-Luc cells were also treated with scrambled siRNA-liposomes with 1:1 molar ratio of DC-Chol:DOPE, N/P ratio of 3.125:1 and applied at 1 µg siRNA/well dose as non-targeting controls and the transfection reagent Lipofectamine® RNAiMAX was used as positive control. A549-Luc cells not treated with Luc-siRNA liposomes taken as 100% of luciferase protein activity and used to normalise the luciferase activity of all tested formulations. Samples were removed and replaced with fresh medium, and the cells then incubated for a further 48 hrs before analysis. **** and *** indicate a significant difference between the results ($p<0.0001$ and $p<0.001$, respectively) and ns indicates no significant difference ($p>0.05$). Data is shown as the mean ± SD, (N=2, n=4).*

4.3.2.1.2 Effect of Analysis Time on Luciferase Activity

To investigate the effect of analysis time and when maximum knockdown of luciferase activity can be achieved by the liposome-siRNA formulations, these were applied to

A549-Luc cells for 4 hrs and the assessment of luciferase activity conducted at 24, 48, 72, and 96 hrs time points post-transfection (Figure 4.6). The transfection reagent Lipofectamine® RNAiMAX was used as positive control according to the manufacturer protocol described previously in Chapter 2. No negative controls or scrambled siRNA were used in this experiment as no significant effect of non-targeting siRNA or no off-target effect on the luciferase activity have been observed in the previous experiment (Figure 4.5) and in the pilot study (Appendix 1). A549-Luc cells not incubated with siRNA-Luc liposomes were taken as 100% luciferase activity and used to normalise the luciferase activity of all tested formulations.

The results in Figure 4.6 show that luciferase activity was significantly decreased ($p<0.001$) when the analysis was performed 48 hrs post-transfection. Interestingly, an increase of the analysis time to more than 48 hrs post-transfection showed that the cells started to recover from the silencing effect, as indicated by the increase in luciferase activity for A549-Luc cells at 72 and 96 hrs. It should be noted that the transfection reagent Lipofectamine® RNAiMAX shows significant reduction of the luciferase activity at all time points studied. Interestingly, the knockdown effect remained at the same level at the different time points.

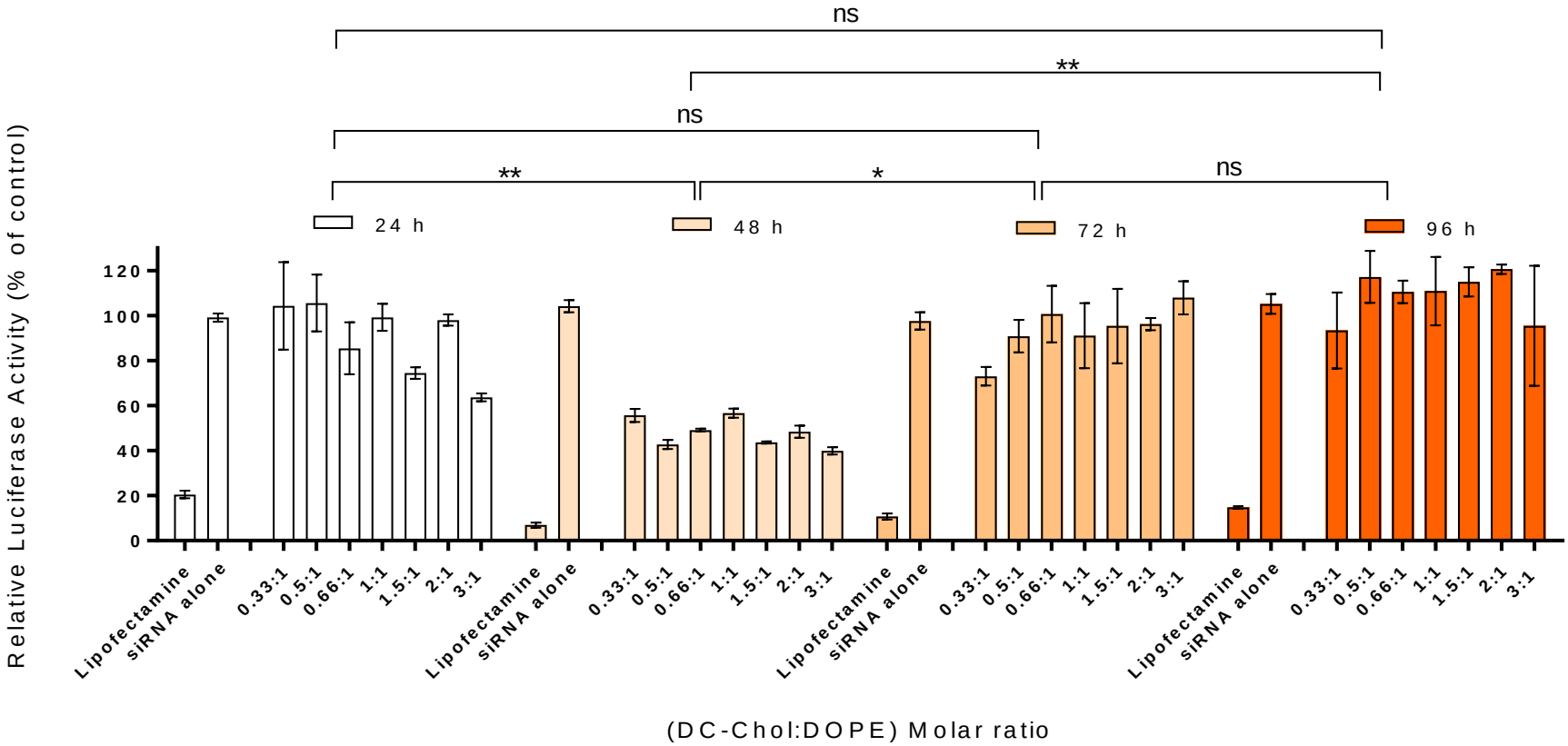

Figure 4.6: Relative luciferase activity of A549-Luc cells after incubation with 1 µg/well of Luc-siRNA

*Cells were seeded onto 24-well plates at a density of 5 × 10^4 cells per well and cultured overnight. Liposome-siRNA formulations were prepared at an N/P ratio of 3.125:1 and different DC-Chol:DOPE molar ratios and applied to the cells for 4 hrs. A549-Luc cells were also treated with the transfection reagent Lipofectamine® RNAiMAX as positive control. A549-Luc cells not incubated with siRNA-Luc liposomes were used as 100% luciferase activity. Samples were removed and replaced with fresh medium, and cells were then incubated for a further 24, 48, 72 and 96 hrs before analysis. * and ** indicate a significant difference between the results ($p<0.05$ and $p<0.01$, respectively) and ns indicates no significant difference ($p>0.05$). Data is shown as the mean ± SD, (N=2, n=4).*

4.3.2.2 Flow Cytometry and Confocal Study

The results of the luciferase assay were further assessed using 'luc-siRNA based MB' liposomes loaded with the siRNA labelled with 6-FAM fluorescent probe and BHQ-1 quencher, which shows green fluorescence when the siRNA binds to the targeted luciferase mRNA. The intracellular presence of these liposomes and MB engagement with target mRNA was evaluated by measuring the fluorescence intensity associated with the cells, and arising from 6-FAM probe 4 hrs post-transfection, quantitatively using flow cytometry (Figure 4.7) and qualitatively using confocal microscopy (Figure 4.8).

A dot plot profile of the flow cytometry data (Figure 4.7 A) shows that the 'luc-siRNA based MB' successfully binds the targeted mRNA in approximately 90% of the whole cell population in comparison to the control (A549-Luc cells without liposomes). The MFI value of the 'luc-siRNA based MB' in Figure 4.7 B shows that around 21 fold increases in the fluorescence signal was detected in comparison to untreated A549-Luc cells.

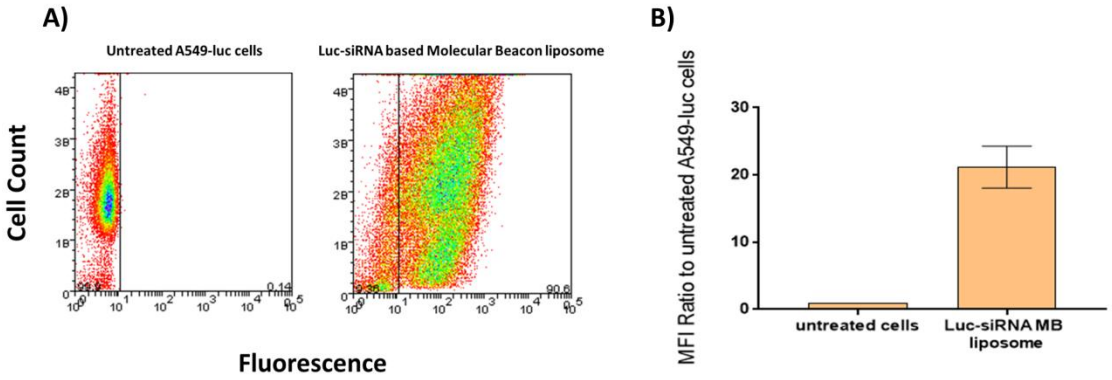

Figure 4.7: The engagement of 'luc-siRNA based MB' liposomes with the targeted luc-mRNA in A549-Luc cells

(A) *Dot plot profile of 'luc-siRNA based MB' liposomes engagement with the targeted Luc-mRNA.* ***(B)*** *MFI data of 'luc-siRNA based MB' liposomes calculated as a ratio to untreated A549-Luc cells. Cells were treated with 'luc-siRNA based MB' liposomes (conjugated to 6-FAM as the fluorophore and BHQ-1 as the quencher) at an N/P ratio of 3.125:1 and a DC-Chol:DOPE ratio of 1:1 for 4 hrs. The fluorescence intensity of FAM-MB was assessed 4 hrs post-transfection using a Beckman Coulter MoFlo (minimum 10,000 cells/sample).*

Confocal microscopy was carried out to visually confirm the ability of the delivery system to target the luciferase mRNA in A549-Luc cells using the 'luc-siRNA based MB'. Confocal micrographs (Figure 4.8) indicate the 'release' and presence of the green 6-FAM-MB in the perinuclear region of the cells, thereby confirming endosomal escape, and binding to Luc-mRNA. The blue fluorescence results from DRAQ5 which stains the cell nuclei. Very intense green signals appeared in the large cytoplasmic areas of A549-Luc cells and most of these signals were distributed throughout the cytoplasmic region of A549-Luc cells.

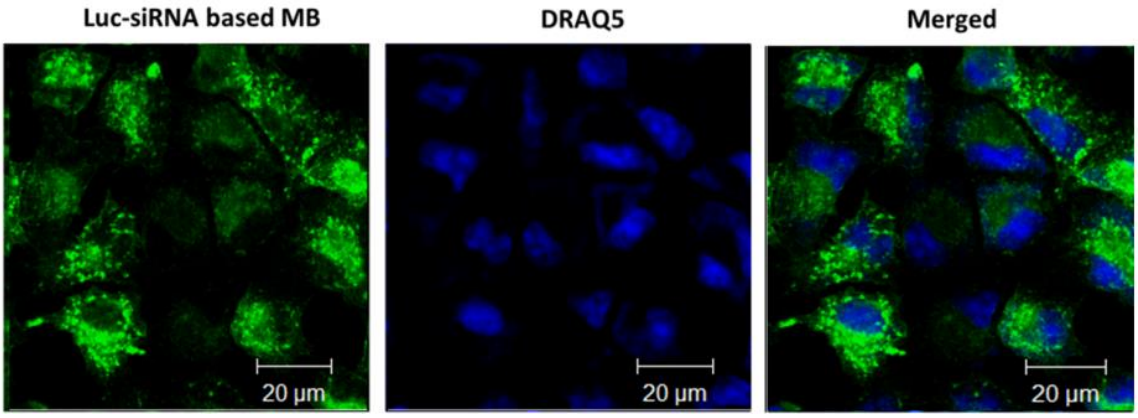

Figure 4.8: Confocal microscopy micrographs of 'luc-siRNA based MB' liposomes in A549-Luc cells

Cells were incubated with 'luc-siRNA based MB' liposomes (conjugated to 6-FAM as the fluorophore and BHQ-1 as the quencher) at an N/P ratio of 3.125:1 and a DC-Chol:DOPE ratio of 1:1 for 4 hrs and then assessed immediately using confocal microscopy. 'Luc-siRNA based MB' liposomes appear green, whereas the nuclei appear blue as stained with DRAQ5. Scale bar: 20 µm.

The flow cytometry and confocal microscopy assessment of MB is limited by non-using of 'scrambled siRNA based MB' liposomes as negative control which is essential to distinguish between specific and non-specific binding effects of 'luc-siRNA based MB' with Luc-mRNA. Moreover, the analysis of non-specific fluorescence of FAM-MB by using the normal A549 cells without the luciferase mRNA is important to confirm that the green fluorescence detected is due to the successful engagement of FAM-MB with the targeted mRNA, not due to the non-specific binding of MB or the degradation by ribonuclease enzyme.

4.4 Discussion

It is believed that effective siRNA delivery into target cells is the main barrier which needs to be overcome if the concept of siRNA therapeutics is to be translated into the clinical setting [16]. A number of studies have demonstrated that cationic liposome delivery system can result in the efficient siRNA transfection [17], [18]. The cellular uptake of siRNA-liposome formulations and intracellular trafficking route dictates the gene silencing efficiency, and may present a major barrier to effective gene silencing [19]. Cationic DC-Chol/DOPE liposomes have been reported as one of the most effective siRNA transfection vectors and one of the least toxic option currently available in preclinical experiments and clinical trials [2], [20].

Positively charged liposomes would be expected to interact electrostatically with the plasma membrane, and this interaction may not only promote the association of siRNA-liposomes with cells but also induce their cellular uptake through endocytic mechanisms [21]. Therefore, there is an important need to evaluate the effect of such parameters on cellular uptake and transfection efficiency, for instance the molar ratio of DC-Chol and DOPE, as well as the ratio between cationic lipid and negatively charge siRNA (N/P ratio).

The effect of N/P ratio on siRNA-liposomes behaviour in gel electrophoresis was examined in Chapter 3, and the results indicated that complete entrapment of siRNA occurred only at a high N/P ratio of 50:1. However, since a high content of cationic lipid would results in increased cytotoxic to cells [22], and could interfere with siRNA release into the cytoplasm due to the excess of positive charges to the negative charge of siRNA,

this could induce the formation of 'non-transfectable aggregates' [23]. An excessive ratio of positively charge lipid to zwitterionic lipid has been reported to affect the stability of the lipid bilayer and the ability of the delivery system to escape from endosomes [24]. Therefore, in this chapter we tested if 'a balanced' option, siRNA-liposomes particles prepared at lower N/P ratio of 3.125:1 with good siRNA encapsulation level and cytotoxicity profile would achieve an acceptable degree of cellular uptake and luciferase-silencing.

The evaluation of siRNA-liposome cellular uptake and luciferase protein knockdown at different molar ratios of cationic to zwitterionic lipid was conducted. The N/P charge ratio is generally considered fundamental for optimising *in vitro* transfection protocols and the efficiency of siRNA-liposomes typically depends on the ratio between cationic and zwitterionic lipids used, and the ratio between the positive charge and siRNA, i.e. N/P ratio. To this end, A549 cells were treated with siRNA-liposomes at an N/P ratio of 3.125:1.

The flow cytometry histograms obtained showed the cellular internalisation of a significant proportion of applied siRNA-liposomes. Trypan blue was used to quench the extracellular fluorescence of cy3-siRNA-liposomes bound to the cell membrane but not internalised. Since trypan blue cannot pass the plasma membrane, the fluorescence remaining after trypan blue quenching must therefore result from the internalized siRNA-liposomes, as only extracellular fluorescence of cy3-siRNA-liposomes is quenched. This method offers a simple and convenient technique for rapidly distinguishing between intracellular and extracellular fluorescence of siRNA-liposomes formulations.

The molar ratio of DC-Chol to DOPE also plays a significant function in the internalisation of siRNA-liposomes; Figure 4.2 shows that an increase in the cationic lipid composition in the formulation enabled higher cell population entry of cy3-siRNA. Interestingly, maximum cellular uptake was achieved with an equal ratio of DC-Chol to DOPE (1 to 1) liposomes. MFI data demonstrated that cy3-siRNA cellular uptake is three times higher than the cellular uptake of siRNA-Lipofectamine transfection reagent. The cellular uptake by A549 cells of a significant amount of cy5-siRNA cationic liposome nanoparticles has also been reported previously [25]. The results of the cy3-siRNA cellular uptake in this study also indicated that at this stage of the system design, the effect of charged lipid on the cellular internalisation was important.

The flow cytometry and confocal microscopy data in A549 cells clearly show that the cy3-siRNA-liposomes were successfully internalised into the cytoplasm of the target cells. Confocal micrographs (Figure 4.3 and Figure 4.4) show the intracellular distribution of the liposomes as puncta, with a significant localisation in the perinuclear region. A number of studies have suggested that liposomes with positive amino groups within their structure can generate a pH-dependent endosomal membrane disruption [26], [27], whereby the disruptive interactions of the increasingly positively charged cationic liposome with the endosomal membrane could play an important role in endosomal escape. The fact that in the presence study the fluorescence in the cytoplasm is primarily seen as puncta, rather than diffused fluorescence, and located in the perinuclear region, indicate that a significant proportion of internalised liposomes are most likely ‘grouped’ in some cytoplasmic vesicles. Presence of some diffused red florescence (in higher magnification image in Figure 4.4) may indicate that some ‘escape’ may have occurred. These assumptions would need further experimental studies.

A gene knockdown study was carried out using a luciferase-expressing A549 human lung carcinoma cell line, A549-Luc. The luciferase gene was selected as a target for knockdown since it is expressed by the CMV promoter by stable transfection of firefly luciferase. The transfection reagent Lipofectamine® RNAiMAX was used for comparison, and siRNA-liposomes were prepared at a fixed N/P ratio of 3.125:1, which was found to show successful cellular internalisation (Figure 4.2 and Figure 4.3). A549-Luc cells were also treated with scrambled siRNA as non-targeting controls to distinctly differentiate between the specific and non-specific effects of the siRNA activity.

The results of the gene silencing study using 0.5 and 1 μg per well of siRNA indicated significant inhibition of the luciferase activity for all the selected liposome formulations used in the cell transfection experiment, in comparison to the negative controls with non-targeting siRNA. An increase in the ratio of cationic lipid in the formulations had a significant influence on the transfection efficiency. For example, the relative luciferase activity of the lowest cationic lipid ratio of 0.33:1 was reduced from 72% with 0.5 μg/well to 56% with 1 μg/well siRNA and, the highest cationic lipid ratio of 3:1 decreased the relative luciferase activity from 59% with 0.5 μg/well to 40% with 1 μg/well siRNA. The highest level of luciferase silencing was achieved with siRNA-liposomes with an equal ratio of DC-Chol to DOPE (1 to 1), with a transfection efficiency of approximately 54% and 57% with 0.5 μg/well and 1 μg/well siRNA, respectively. This finding follows the expectation from the cellular uptake study (Figure 4.2). It has been reported that the luciferase knockdown can increase significantly by increasing the amount of cationic lipid particles [28]. A previous study has suggested that a higher transfection efficiency could be achieved by using a 1:1 molar ratio of cationic to helper

lipid [2], as seen in our study. This has been ascribed to the effect of that the zwitterionic character of DOPE lipid which facilitates the transition from a lamellar to a hexagonal phase [29], [30], of lipid bilayer of cell membrane. This could promote liposomal cellular entry and escape from endosomes following endocytosis, resulting in enhanced knockdown activity [31], [32]. It should be noted that the level of luciferase silencing of DC-Chol:DOPE (1 to 1) formulation is lower than the transfection efficiency of Lipofectamine, although the cellular uptake of cy3-siRNA DC-Chol:DOPE liposome was higher than the transfection reagent. This observation could be a result of poor endosomal escape of the DC-Chol:DOPE liposomes which lead to reduce the silencing efficiency. Similar observation reported with poly (amidoamine)-siRNA lipoplexes which had a higher internalization rate but a lower interference effect than Lipofectamine in HaCat cells [33].

It is important to perform a time course study when initially testing a new target siRNA sequence. Luciferase knockdown was in this study analysed 24, 48, 72, and 96 hrs post-transfection. This provides essential data (Figure 4.6) on the time point which corresponds to maximal knockdown of the target gene and also the duration of the knockdown. Data demonstrated that maximum silencing was obtained 48 hrs post-transfection. Interestingly, luciferase activity began to recover, as demonstrated by an increase in luciferase activity at 72 and 96 hrs, respectively. A study on the transfection of A549 cells using plasmid DNA-DMAEMA polyplexes showed that the peak level of transfection was reached between 12 and 48 hrs. However, from 48 hrs after the transfection point, transfection efficiency significantly decreased at the 72 hrs point [34] and this observation is in agreement with the result presented in this current work. Luciferase silencing effect post-treatment of A549-Luc cells with lipofectamine was

measured at 24, 48, 72, and 96 hrs, and results show that same level of silencing has achieved at the different time points studied. The steady effect of lipofectamine on the luciferase activity is might be due to the cytotoxic effect of this transfection reagent that lead to loss the activity of luciferase at all measured time points. MTS and LDH assay should be performed to assess the effect of lipofectamine on the cell viability and membrane integrity of A549-Luc cells.

The result of the luciferase assay was confirmed using 'luc-siRNA based MB' liposomes loaded with targeted siRNA labelled with the 6-FAM fluorescent probe, which releases green fluorescence when siRNA binds to the targeted Luc-mRNA. Since a MB only shows fluorescence when it combines with the target mRNA, MB can be used as a readout for endosomal release. It has been reported that treat SK-HEP-1 cells with cy3-MB for GAPDH that was complexes with lipid nanoparticles showed the red signal of cy3 in perinuclear site of cytoplasm and the signal reached the maximum at 4 hrs post-transfection [24]. This observation is in agreement with our study that green fluorescence of FAM-MB probe was detected in the cell cytoplasm which confirms Luc-siRNA binding to the targeted Luc-siRNA. The assessment of MB using the flow cytometry and confocal microscopy is limited by non-using of 'scrambled siRNA based MB' liposomes as negative control which is essential to distinguish between specific and non-specific binding effects of 'luc-siRNA based MB' with Luc-mRNA. The assessment of FAM-MB using flow cytometry and confocal microscopy in current chapter is limited by missing of important negative controls (i.e. 'scrambled siRNA based MB' liposomes) that essential to validate the technique and to distinguish between the specific and non-specific binding effects of 'luc-siRNA based MB' with Luc-mRNA. Additionally, the transfection of normal A549 cells that not contain Luc-mRNA using 'luc-siRNA based MB' liposomes is

very important to validate that the measured green fluorescence is due to the binding of FAM-MB with the targeted mRNA and not due to the non-specific engagement of MB or the degradation by RNase.

4.5 Conclusions

Work in this chapter establishes that designed siRNA-liposome systems can efficiently transfect human epithelial non-small cell lung carcinoma cells in culture, which are targets for a number of current gene therapy protocols. Additionally, it demonstrates that the silencing activity of this system mainly depends on the ratio between cationic lipid of the liposome and siRNA. The high level of uptake (relative to commercially available transfecting agent) has not been reflected in equally high silencing effect, which is presumably due to the liposome system tested lacking the ability to efficiently escape from endosomal/lysosomal compartments. A formulation dependent relationship between the siRNA concentration and silencing efficiency was observed. It is difficult to extrapolate the conditions and formulations from *in vitro* experiments to the *in vivo* setting of gene therapy protocols, these results provide important insights into the delivery of siRNA to human epithelial cells. A further investigation of the siRNA-liposome mechanism of endocytosis and intracellular trafficking is needed to achieve further understanding of the cellular uptake process.

4.6 References

[1] M. Díaz and P. Vivas-Mejia, Nanoparticles as drug delivery systems in cancer medicine: Emphasis on RNAi-containing nanoliposomes. *Pharmaceuticals*, vol. 6, no. 11, pp. 1361–1380, 2013.

[2] Y. Zhang, H. Li, J. Sun, J. Gao, W. Liu, B. Li, Y. Guo, and J. Chen, DC-Chol/DOPE cationic liposomes: a comparative study of the influence factors on plasmid pDNA and siRNA gene delivery. *International Journal of Pharmaceutics*, vol. 390, no. 2, pp. 198–207, May 2010.

[3] S. Yang, J. Chen, D. Zhao, D. Han, and X. Chen, Comparative study on preparative methods of DC-Chol/DOPE liposomes and formulation optimization by determining encapsulation efficiency. *International Journal of Pharmaceutics*, vol. 434, no. 1–2, pp. 155–60, Sep. 2012.

[4] A. Gazdar, L. Girard, W. Lockwood, W. Lam, and J. Minna, Lung cancer cell lines as tools for biomedical discovery and research. *Journal of the National Cancer Institute*, vol. 102, no. 17, pp. 1310–1321, 2010.

[5] J. Zhang, X. Li, and L. Huang, Non-viral nanocarriers for siRNA delivery in breast cancer. *Journal of Controlled Release*, vol. 190, pp. 440–450, Sep. 2014.

[6] S. Welsh and S. Kay, Reporter gene expression for monitoring gene transfer. *Current Opinion in Biotechnology*, vol. 8, no. 5, pp. 617–622, Oct. 1997.

[7] L. Naylor, Reporter gene technology: the future looks bright. *Biochemical Pharmacology*, vol. 58, no. 5, pp. 749–757, Sep. 1999.

[8] D. Mcnabb, R. Reed, and R. Marciniak, Dual luciferase assay system for rapid assessment of gene expression in saccharomyces cerevisiae. *Eukaryotic Cell*, vol. 4, no. 9, pp. 1539–1549, 2005.

[9] J. Li, L. Chen, L. Du, and M. Li, Cage the firefly luciferin: a strategy for developing bioluminescent probes. *Chemical Society Reviews*, vol. 42, no. 2, pp. 662–676, 2013.

[10] S. Tyagi and F. Kramer, Molecular beacons: probes that fluoresce upon hybridization. *Nature Biotechnology*, vol. 14, no. 3, pp. 303–308, 1996.

[11] S. Tyagi and F. Kramer, Molecular beacons in diagnostics. *F1000 Medicine Reports*, vol. 4, no. May 2012, pp. 2–7, 2012.

[12] X. Su, X. Xiao, C. Zhang, and M. Zhao, Nucleic acid fluorescent probes for biological sensing. *Applied Spectroscopy*, vol. 66, no. 11, pp. 1249–1261, 2012.

[13] B. Juskowiak, Nucleic acid-based fluorescent probes and their analytical potential. *Analytical and Bioanalytical Chemistry*, vol. 399, no. 9, pp. 3157–3176, 2011.

[14] B. Wile, K. Ban, Y. Yoon, and G. Bao, Molecular beacon-enabled purification of living cells by targeting cell type-specific mRNAs. *Nature Protocols*, vol. 9, no. 10, pp. 2411–2424, 2014.

[15] Z. Wu, Y. Zeng, M. Zhong, and B. Wang, Targeting A549 lung adenocarcinoma cell growth and invasion with protease-activated receptor-1 siRNA. *Molecular Medicine Reports*, vol. 9, no. 5, pp. 1787–1793, 2014.

[16] B. Shi and M. Abrams, Technologies for investigating the physiological barriers to

efficient lipid nanoparticle-siRNA delivery. *The Journal of Histochemistry and Cytochemistry*, vol. 61, no. 6, pp. 407–420, 2013.

[17] D. Balazs and W. Godbey, Liposomes for use in gene delivery. *Journal of Drug Delivery*, vol. 2011, pp. 1–12, Jan. 2010.

[18] Y. Shen, H. Fang, K. Zhang, R. Shrestha, K. Wooley, and J. Taylor, Efficient protection and transfection of small interfering RNA by cationic shell-crosslinked knedel-like nanoparticles. *Nucleic Acid Therapeutics*, vol. 23, no. 2, pp. 95–108, 2013.

[19] R. Kanasty, K. Whitehead, A. Vegas, and D. Anderson, Action and reaction: the biological response to siRNA and its delivery vehicles. *Molecular Therapy*, vol. 20, no. 3, pp. 513–524, 2012.

[20] V. López-Dávila, H. Welch, M. Dwek, I. Uchegbu, and M. Loizidou, Efficacy of DOPE / DC-cholesterol liposomes and GCPQ micelles as AZD6244 nanocarriers in a 3D colorectal cancer in vitro model. *Nanomedicine*, vol. 11, no. 4, pp. 331–344, 2016.

[21] G. Bozzuto and A. Molinari, Liposomes as nanomedical devices. *International Journal of Nanomedicine*, vol. 10, pp. 975–999, 2015.

[22] K. Romoren, B. Thu, N. Bols, and O. Evensen, Transfection efficiency and cytotoxicity of cationic liposomes in salmonid cell lines of hepatocyte and macrophage origin. *Biochimica et Biophysica Acta - Biomembranes*, vol. 1663, no. 1–2, pp. 127–134, 2004.

[23] A. Colosimo, A. Serafino, F. Sangiuolo, S. Sario, E. Bruscia, P. Amicucci, G. Novelli, B. Dallapiccola, and G. Mossa, Gene transfection efficiency of tracheal epithelial cells by DC-chol-DOPE/DNA complexes. *Biochimica et Biophysica Acta*, vol. 1419, no. 2, pp. 186–194, Jul. 1999.

[24] X. Zhang, T. McIntosh, and M. Grinstaff, Functional lipids and lipoplexes for improved gene delivery. *Biochimie*, vol. 94, no. 1, pp. 42–58, Jan. 2012.

[25] M. Qu, R. Zeng, S. Fang, Q. Dai, H. Li, and J. Long, Liposome-based co-delivery of siRNA and docetaxel for the synergistic treatment of lung cancer. *International Journal of Pharmaceutics*, vol. 474, no. 1–2, pp. 112–122, 2014.

[26] M. Dominska and D. Dykxhoorn, Breaking down the barriers: siRNA delivery and endosome escape. *Journal of Cell Science*, vol. 123, no. 8, pp. 1183–1189, Apr. 2010.

[27] R. Adami, S. Seth, P. Harvie, R. Johns, R. Fam, K. Fosnaugh, T. Zhu, K. Farber, M. McCutcheon, T. Goodman, Y. Liu, Y. Chen, E. Kwang, M. Templin, G. Severson, T. Brown, N. Vaish, F. Chen, P. Charmley, B. Polisky, and M. Houston, An amino acid-based amphoteric liposomal delivery system for systemic administration of siRNA. *Molecular Therapy*, vol. 19, no. 6, pp. 1141–1151, 2011.

[28] P. Pierrat, D. Kereselidze, P. Wehrung, G. Zuber, F. Pons, and L. Lebeau, Bioresponsive deciduous-charge amphiphiles for liposomal delivery of DNA and siRNA. *Pharmaceutical Research*, vol. 30, no. 5, pp. 1362–1379, May 2013.

[29] S. Marrink and A. Mark, Molecular view of hexagonal phase formation in phospholipid membranes. *Biophysical Journal*, vol. 87, no. 6, pp. 3894–3900, 2004.

[30] M. Rappolt, A. Hickel, F. Bringezu, and K. Lohner, Mechanism of the lamellar/inverse hexagonal phase transition examined by high resolution x-ray diffraction. *Biophysical Journal*, vol. 84, no. 5, pp. 3111–3122, 2003.

[31] S. Mochizuki, N. Kanegae, K. Nishina, Y. Kamikawa, K. Koiwai, H. Masunaga, and K.

Sakurai, The role of the helper lipid dioleoylphosphatidylethanolamine (DOPE) for DNA transfection cooperating with a cationic lipid bearing ethylenediamine. *Biochimica et Biophysica Acta*, vol. 1828, no. 2, pp. 412–418, Feb. 2013.

[32] M. Muñoz-Ubeda, A. Rodríguez-Pulido, A. Nogales, A. Martín-Molina, E. Aicart, and E. Junquera, Effect of lipid composition on the structure and theoretical phase diagrams of DC-Chol/DOPE-DNA lipoplexes. *Biomacromolecules*, vol. 11, no. 12, pp. 3332–33340, Dec. 2010.

[33] H. Luo, N. Li, Y. Li, K. Mai, K. Sun, W. Wang, G. Lao, C. Yang, L. Zhang, and M. Ren, Comparison of the cellular transport mechanism of cationic, star-shaped polymers and liposomes in hacat cells. *International Journal of Nanomedicine*, vol. 12, pp. 1085–1096, 2017.

[34] J. Lam, S. Armes, and S. Stolnik, The involvement of microtubules and actin filaments in the intracellular transport of non-viral gene delivery system. *Journal of Drug Targeting*, vol. 19, no. 1, pp. 56–66, 2011.

Chapter 5 - Endocytosis Mechanism of siRNA-Liposomes

5.1 Introduction

In order to prepare an efficient siRNA-liposome formulation, capable of intracellular delivery of siRNA, it is important to understand the cellular internalisation mechanism of delivery system in order to evade the recycling pathways and to achieve successful cellular uptake [1]. siRNA-liposomes can be internalised into cells through different mechanisms (as discussed in Chapter 1), including clathrin-mediated endocytosis, caveolae-mediated endocytosis, or macropinocytosis [2]. However, despite its importance in achieving siRNA silencing effect, the understanding of siRNA-liposome interaction with cells and cellular internalisation mechanism processed remains poorly studies and understood [3].

It is generally believed that siRNA-liposomes are internalised by mammalian cells via different endocytosis pathways [4]. The importance of exploring the cellular uptake pathway is that each mechanism leads to a different intracellular fate, and consequently, different silencing efficiencies [5]. For example, after cellular uptake of a siRNA-liposome system via the clathrin-mediated pathway, liposomes will be retained inside the endosomal or lysosomal compartments [6], yet their escape into the cytosol is essential to enable the siRNA to target the mRNA of interest. Nanoparticles in general taken up by clathrin-mediated pathway undergo endosomal acidification (pH 6.0-6.5 in early endosomes) and trafficking to lysosomes (pH 4.5-5.5 in late endosomes and lysosomes),

where enzymatic and acidic degradation happen [7]. Another endocytosis pathway, the caveolae-mediated mechanism, is thought to avoid the acidic environment of endosomes and lysosomes, although it is important to notice that this process is less understood [8].

The cellular internalisation pathway of siRNA-liposomes mainly depends upon several factors, such as the range of physiochemical properties of the delivery system as well as the nature of the targeted cells [9]. A number of recent reports aimed to establish endocytosis pathway leading to effective cellular effects of internalised nanoparticles [10]–[12]. Understanding the cell entry processes of siRNA delivery systems is essential in enabling the prediction, design, and optimisation of transfection efficiency [13]. The cell entry pathway of a delivery system is likely to affect intracellular processing and hence the silencing efficiency [13]. Despite extensive research in developing siRNA delivery systems, understanding of the cell uptake mechanism of siRNA carriers is often inadequate, leading to an inability to predict or explain transfection efficiencies [13].

To identify internalisation pathways of designed siRNA-liposome in A549 and A549-Luc cell lines, this study applied a panel of different pharmacological endocytosis inhibitors, as shown in Figure 5.1 and Table 5.1, to deplete key endocytic pathways. To inhibit the clathrin-mediated pathway, three different inhibitors were used. Concanavalin A, is a lectin that interferes with the signalling of transmembrane G protein-coupled receptors located on the surface of cells, and therefore prevents the assembly of clathrin coated pits and impairs their movement through the cell membrane [14]. Chlorpromazine is a known clathrin-dependent endocytosis inhibitor which is used to inhibit clathrin coated pit formation through reversible translocation of clathrin and its adapter proteins from the plasma membrane to intracellular vesicles [15]. The third inhibitor is dynasore, an

inhibitor of dynamin GTPase activity, which is crucial for clathrin-coated vesicle formation in clathrin-mediated endocytosis [16]. Moreover, dynasore inhibits dynamin in the caveolae-mediated pathway and therefore prevents caveolar budding or fission from the plasma membrane to form free vesicles [16].

In addition to dynasore, four more inhibitors were used to control the caveolae-mediated pathway. Genestein was used as an inhibitor of the tyrosine kinases involved in caveolae/raft-mediated endocytosis [17]. Filipin was used as it inhibits disassembling of caveolae and unclustering of the receptors found in caveolae by eliminating cholesterol from the plasma membrane [18]. MßCD, a cholesterol-depleting agent, was also used as an inhibitor for caveolae/raft-mediated endocytosis, and it acts by extracting cholesterol from the cell membrane [19]. The final inhibitor of the caveolae-mediated pathway used in this work was nystatin, a cholesterol sequestrating agent that interferes with caveolae/lipid raft-dependent endocytosis without affecting the clathrin-mediated pathway [20].

To inhibit macropinocytosis, EIPA and cytochalasin D were used. The former is a selective inhibitor known to inhibit Na^+/H^+ exchange within membranes, and therefore lowers the sub-membranous pH [21]. Cytochalasin D disrupts actin filaments, and inhibits actin polymerisation [22].

Chloroquine is a lysosomotropic agent that prevents endosome acidification and facilitates endosomal escape of the delivery system [23], and was used in the current work to facilitate the disruption of endosomal vesicles and therefore promote the escape

of siRNA-liposomes from acidic compartments and their release into the cellular cytoplasmic region.

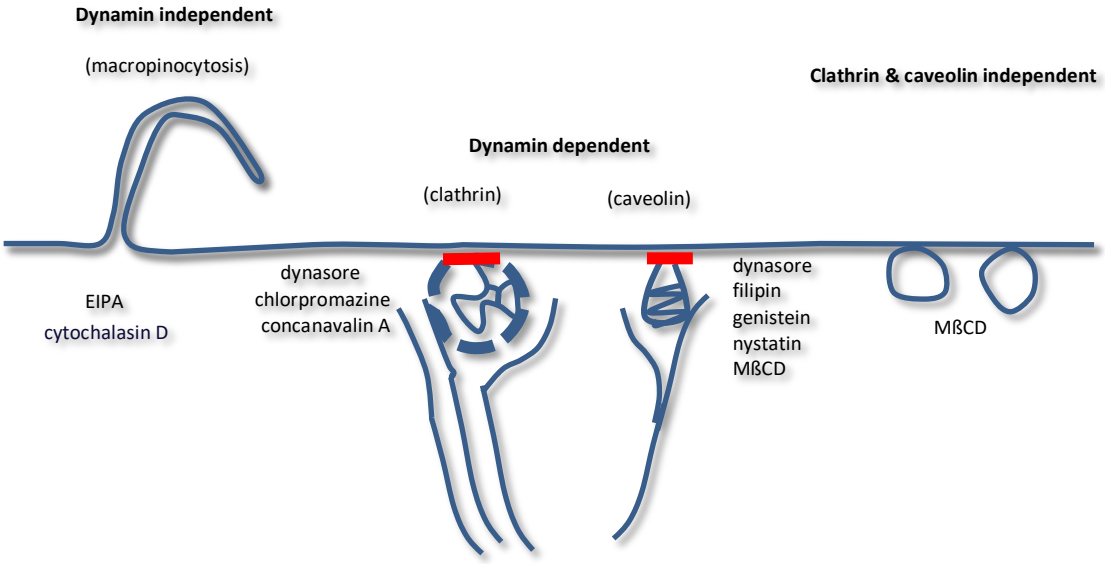

Figure 5.1: Mechanisms of endocytosis inhibition using pharmacological inhibitors to deplete key endocytic pathways

Table 5.1: Summary of pharmacological endocytosis inhibitors used to investigate the endocytosis mechanism of siRNA-liposomes

Inhibitor	Mechanism	References
Concanavalin A	Clathrin-mediated inhibitor, prevents assembly of clathrin coated pits	[14]
Chlorpromazine	Clathrin-mediated inhibitor, interacts with coated pits	[15]
Dynasore	Dynamin inhibitor, blocks dynamin GTPase activity	[16]
Genistein	Inhibition of tyrosine kinase and the caveolae pathway	[17]
Filipin	Caveolin-mediated inhibitor, inhibits cholesterol synthesis	[18]
MßCD	Caveolae/raft-mediated inhibitor through cholesterol depletion of the cellular membrane	[19]
Nystatin	Caveolin-mediated inhibitor through sequestration of cholesterol	[20]
EIPA	Macropinocytosis inhibitor through inhibition of Na^+/H^+ exchange	[21]
Cytochalasin D	Macropinocytosis inhibitor through actin filament depolymerising	[22]
Chloroquine	Endosomolytic agent through buffering the pH in acidic vesicles	[23]

5.2 Aims and Objectives

The aim of this chapter is to investigate the cellular internalisation pathways of the designed siRNA-liposomes (Chapter 3 and 4) and the consequent inhibition of luciferase expression in the presence of different endocytosis inhibitors in order to identify important key regulators of cellular uptake and silencing. The work aims to understand the relationship between the cellular internalisation mechanism of endocytosis and gene silencing efficiency in A549 and A549-Luc cells. Direct probing of endocytosis pathways was achieved using chemical inhibitors, a summary of which are shown in Table 5.1.

5.3 Results

5.3.1 Toxicity of Endocytosis Inhibitors; MTS Assay Assessment

5.3.1.1 MTS on A549 Cells

Before exploring the effect of endocytosis inhibitors on the cellular internalisation of cy3-siRNA-liposomes, MTS cell viability testing was conducted to determine the optimal concentration of the inhibitors with acceptable toxicity profile in A549 cells for the duration of the 4 hrs cells exposure to the liposomes. Figure 5.2 shows the relative cell viability for the nine different pharmacological inhibitors of endocytosis used in this study, as discussed in the introduction above.

Dose response curves indicated that applying clathrin-mediated inhibitors, concanavalin A and chlorpromazine, showed an EC_{50} concentrations of approximately 193 and 74 μg/ml, respectively. Dynasore, a dynamin inhibitor, demonstrated an EC_{50} concentration of around 43 μg/ml, while incubation of A549 cells for 4 hrs with a tyrosine kinase inhibitor, genistein, showed an EC_{50} concentration of about 28 μg/ml. A caveolin-

mediated inhibitor, filipin, and cholesterol sequestering agents, MßCD and nystatin, exhibited EC_{50} concentrations of approximately 66, 951 and 52 μg/ml, respectively. The MTS data for macropincytosis inhibitors, EIPA and cytochalasin D, showed EC_{50} concentrations of 6 and 28 μg/ml, respectively.

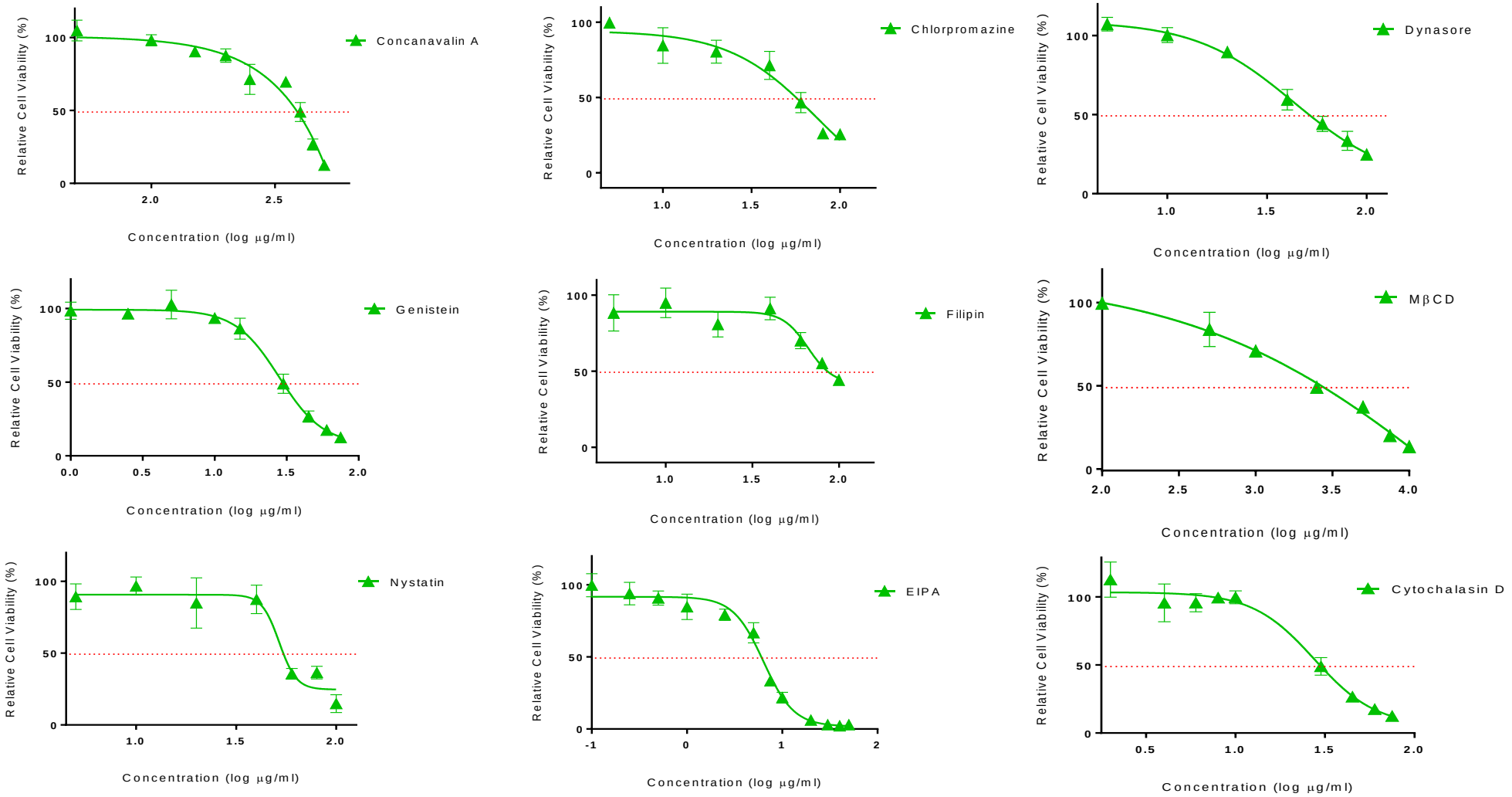

Figure 5.2: Dose-response curves showing relative percentage cell viability of the endocytosis inhibitors after incubation for 4 hrs with A549 cell line

Data are the results of an MTS assay and are expressed as relative cell viability, calculated using the equation shown in Section 2.2.3.1 and presented as the mean ± SD (N=3, n=6). Dose-response curves were generated using GraphPad Prism (v6).

5.3.1.2 MTS on A549-Luc Cells

MTS cell viability assay of the inhibitors also was carried out using A549-Luc cells to determine the optimal concentration of the inhibitors, before examining their effects on luciferase protein silencing via Luc-siRNA-liposomes. Figure 5.3 shows the relative cell viabilities for the different inhibitors that were applied using a wide range of concentrations to determine the EC_{50} concentrations.

Dose response curves indicated that applying clathrin-mediated inhibitors, concanavalin A and chlorpromazine, showed an EC_{50} concentrations of approximately 261 and 48 µg/ml, respectively. Dynasore, a dynamin inhibitor, demonstrated an EC_{50} concentration of around 51 µg/ml, while the tyrosine kinase inhibitor, genistein, gave an EC_{50} concentration of about 28 µg/ml. A caveolin-mediated inhibitor, filipin, and cholesterol sequestering agents, MßCD and nystatin, exhibited EC_{50} concentrations of approximately 72, 473 and 35 µg/ml, respectively. The MTS data for the macropincytosis inhibitors, EIPA and cytochalasin D, showed EC_{50} concentrations of 5 and 48 µg/ml, respectively.

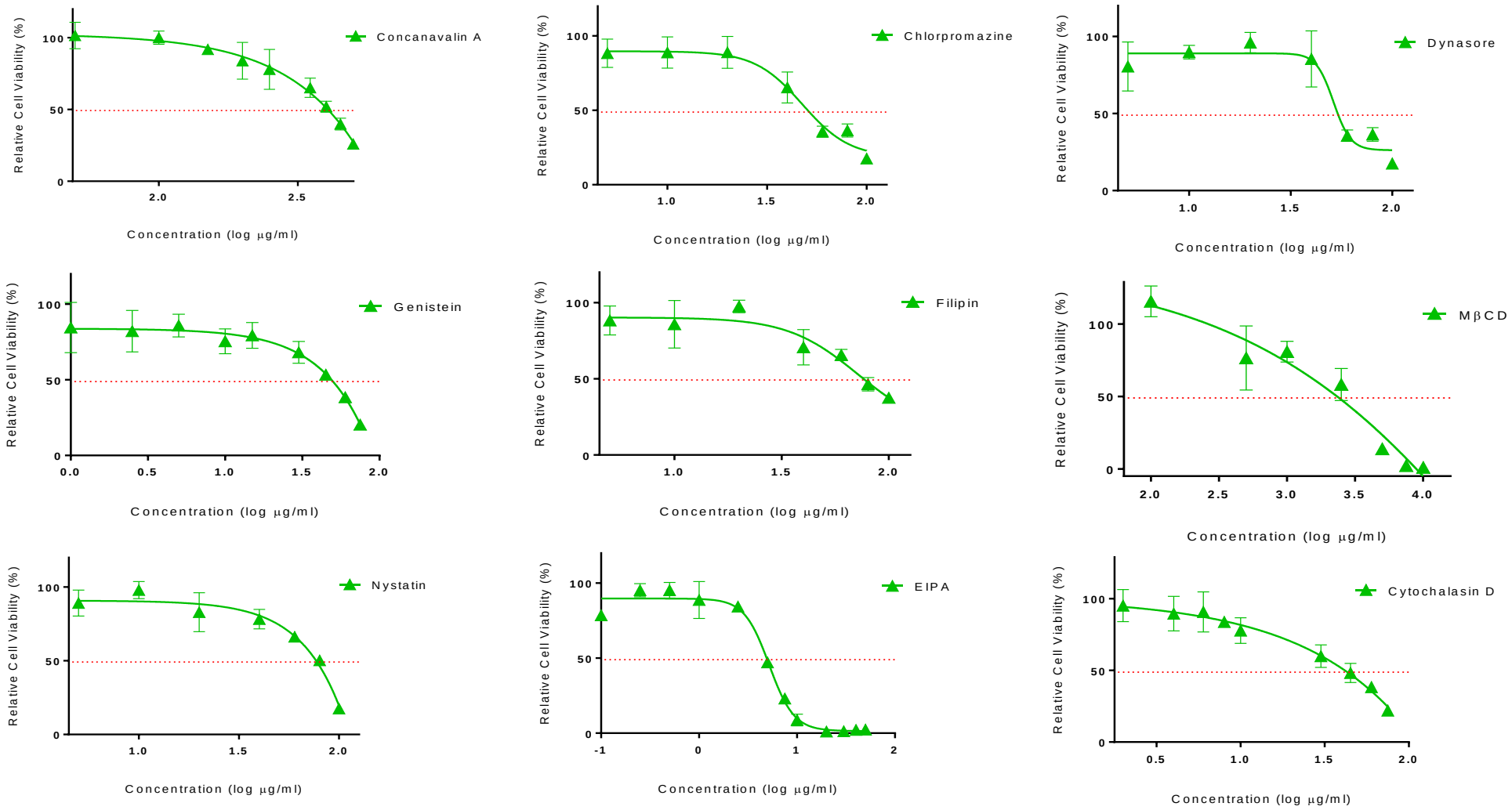

Figure 5.3: Dose-response curves showing relative percentage cell viability of the endocytosis inhibitors after incubation for 4 hrs with A549-Luc cell line

Data are the results of an MTS assay and are expressed as relative cell viability, calculated using the equation shown in Section 2.2.3.1 and presented as the mean ± SD (N=3, n=6). Dose-response curves were generated using GraphPad Prism (v6).

5.3.2 Effect of Endocytosis Inhibitors on the Uptake of Pathway-Specific Ligands: T*f* and CTß

5.3.2.1 Effect on A549 Cells

After optimising the concentrations of the pharmacological inhibitors on the A549 cell line in terms of their cytotoxicity (Figure 5.2), an uptake study of 'classical' endocytosis pathway markers was conducted using sub-EC_{50} concentrations of inhibitors. T*f* and CTß, have been reported to selectively enter cells via the clathrin [24], [25] and caveolae pathways [26], [27], respectively. The application of clathrin-mediated pathway inhibitor (chlorpromazine) and caveolin-mediated pathway inhibitor (MßCD) was reported to generate selective inhibition of T*f* and CTß, respectively, in A549 cells [28]. These ligands were hence used as controls to confirm the specificity of the inhibitory function of the selected concentrations of inhibitors on clathrin and caveolin mediated endocytosis in A549 cells in this study. No markers were used to explore the macropinocytosis pathway as the dextran, commonly used in the literature as a macropinocytosis marker, has been reported not to be a solely specific ligand for this internalisation pathway [29]. T*f* and CTß were used at concentrations of 100 μg/ml and 5 μg/ml, according to the work performed previously on these two markers in our research group on A549 cells.

The uptake study was carried out in the presence of relevant pathway inhibitors to (i) confirm that the selected inhibitors were able to affect the pathways in A549 cells and (ii) to define the optimal concentration of each inhibitor that provides minimum cytotoxic effects and maximum pathway inhibition. T*f* uptake was tested in the presence of concanavalin A (50-150 μg/ml), chlorpromazine (5-20 μg/ml), and dynasore (5-20 μg/ml), while CTß internalisation was tested in the presence of dynasore (5-20 μg/ml),

genistein (5-15 μg/ml), filipin (5-20 μg/ml), MßCD (100-300 μg/ml) and nystatin (5-20 μg/ml) (Figure 5.4).

Applying concanavalin A (50, 100 and 150 μg/ml) showed a T*f* internalisation of approximately 82%, 57% and 50%, respectively, relative to untreated cells. Chlorpromazine application showed a T*f* internalisation of approximately 94%, 80% and 62% relative to untreated cells after incubation for 4 hrs with 5, 10 and 20 μg/ml, respectively. Dynasor, a dynamin inhibitor involved in the formation of coated pits in both the clathrin and caveolae-mediated pathways, demonstrated internalisation of T*f* and CTß at 20 μg/ml, of approximately 50% and 74%, respectively, relative to the untreated cells.

For the caveolae-mediated pathway, A549 cells treated with genistein, filipin, MßCD and nystatin demonstrated CTß internalisation of approximately 72%, 60%, 66% and 40% relative to untreated cells, respectively, after applying the inhibitors at 15, 20, 300 and 20 μg/ml, respectively.

It is of importance to note that in all cases the effect of inhibitors was concertation dependent, with more pronounced effect seen at increased concentrations of inhibitors applied.

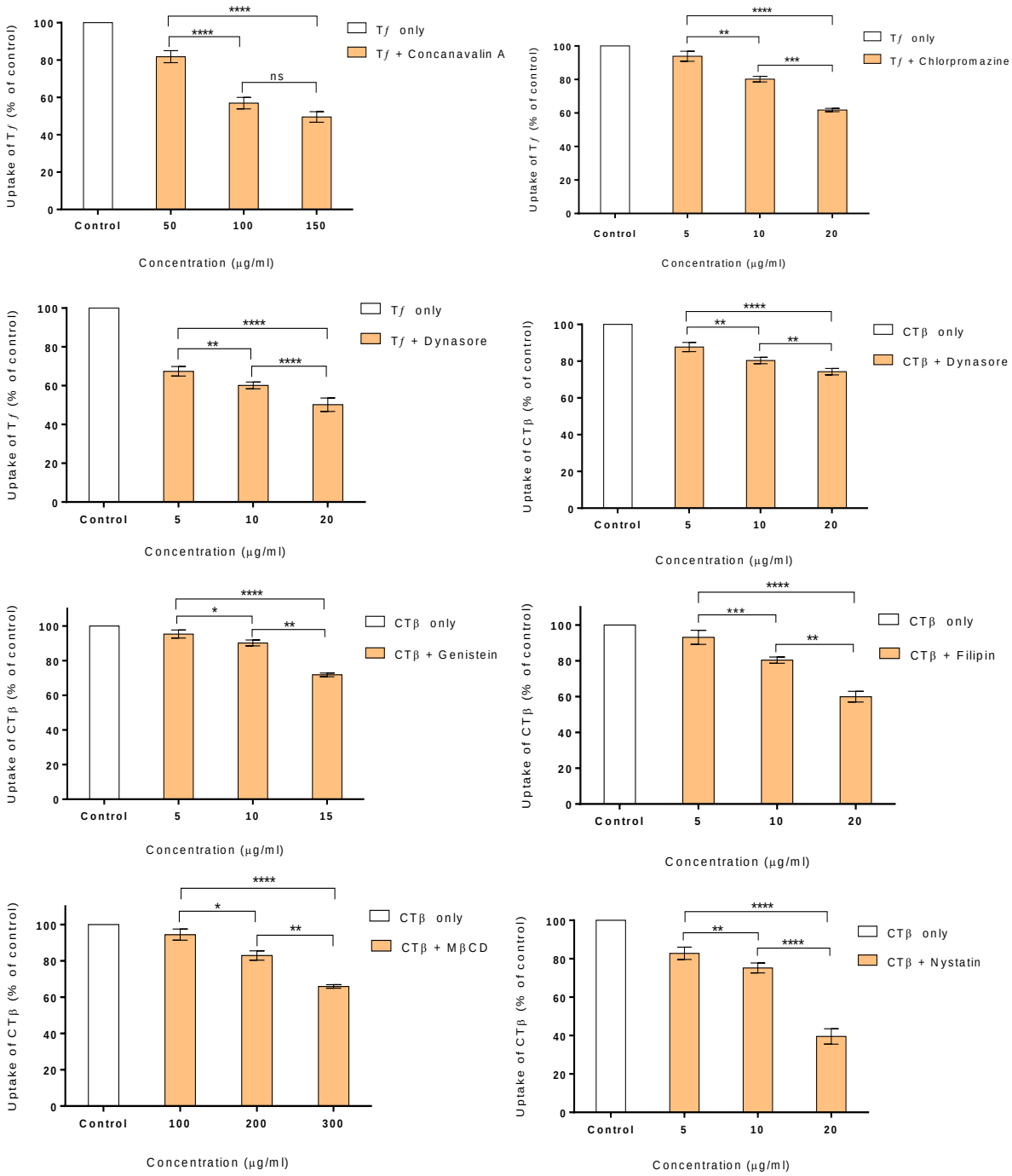

Figure 5.4: Effect of endocytosis inhibitors on the uptake of Tf and CTβ in A549 cells

*Cells were pre-treated with three different concentrations of inhibitors for 30 min, followed by 4 hrs of exposure to Alexa fluor 488 Tf, a clathrin-mediated pathway marker and Alexa fluor 488 CTß, a caveolin-mediated pathway marker. Uptake was assessed using a Beckman Coulter MoFlo (minimum 10,000 cells/sample). ****, ***, ** and * indicate statistical differences at $p<0.05$, $p<0.01$, $p<0.001$ and $p< 0.0001$, respectively, compared to the control (cells incubated with markers in absence of inhibitors), whereas ns indicates a non-significant result, $p>0.05$ (N=2, n=4).*

5.3.2.2 Effect on A549-Luc Cells

After adjusting the concentrations of the pharmacological inhibitors in terms of their cellular viability for the A549-Luc cell line (Figure 5.3), an uptake study using 'classical' endocytosis pathways markers was conducted. All inhibitors were used with concentrations below the EC_{50} concentration. T*f* uptake was tested in the presence of concanavalin A (50-150 µg/ml), chlorpromazine (5-20 µg/ml), and dynasore (5-20 µg/ml), while CTß internalisation was tested in the presence of dynasore (5-20 µg/ml), genistein (5-15 µg/ml), filipin (5-20 µg/ml), MßCD (100-300 µg/ml) and nystatin (5-20 µg/ml) (Figure 5.5).

Applying concanavalin A (50, 100 and 150 µg/ml) resulted in the internalisation of T*f* of around 80%, 53% and 52% relative to untreated cells, respectively. Chlorpromazine application showed a T*f* uptake of approximately 95%, 73% and 55% after incubation with 5, 10 and 20 µg/ml, respectively. In the presence of dynasore, the internalisation of T*f* and CTß at 20 µg/ml was approximately 64% and 54%, respectively, relative to untreated cells.

Looking at the caveolae-mediated pathway, A549-Luc cells treated with genistein, filipin, MßCD and nystatin demonstrated internalisation of CTß of approximately 32%, 54%, 71% and 44%, respectively after applying 15, 20, 300 and 20 µg/ml.

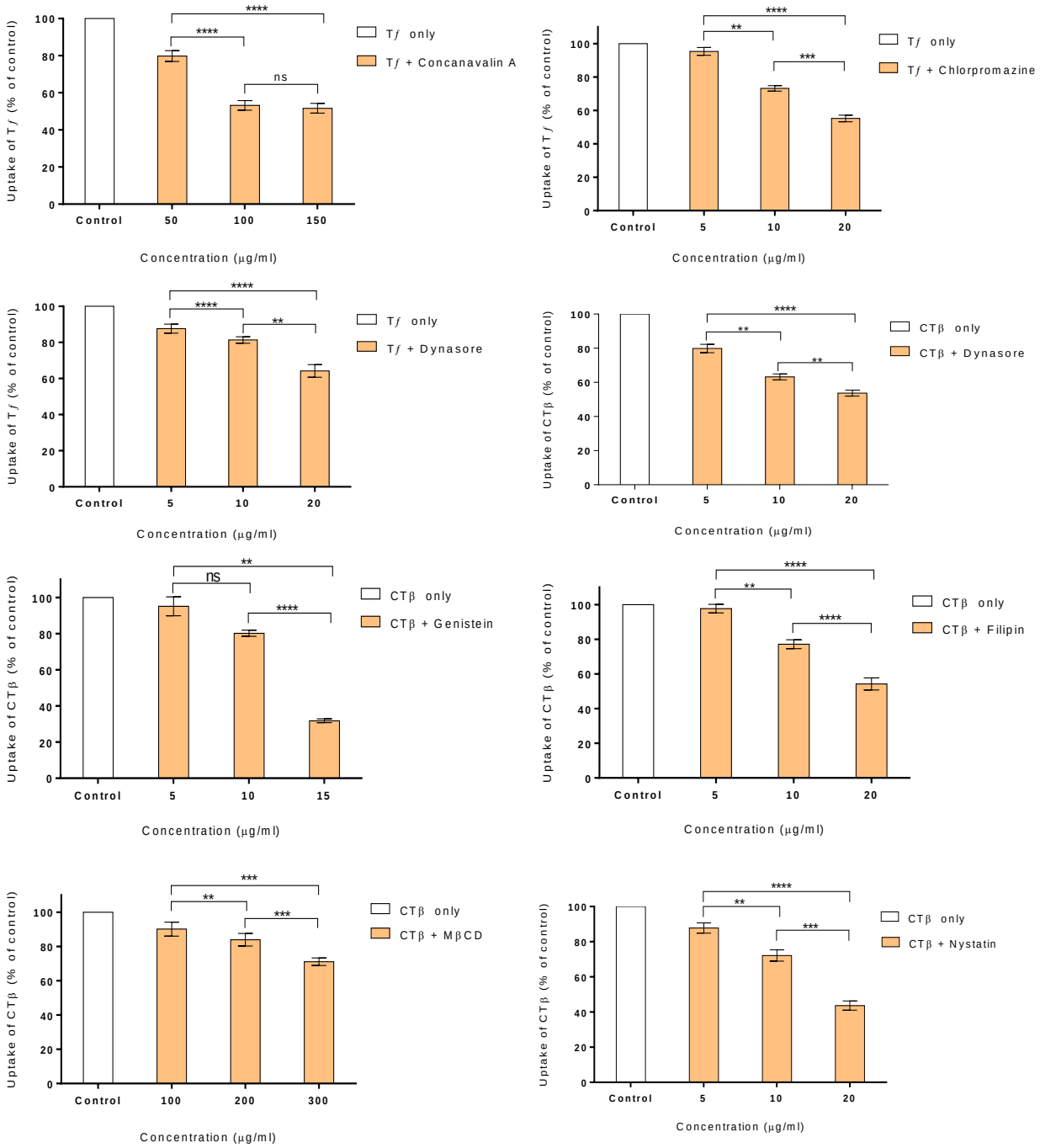

Figure 5.5: Effect of endocytosis inhibitors on the uptake of Tf and CTß in A549-Luc cells

*Cells were pre-treated with three different concentrations of inhibitors for 30 min, followed by 4 hrs of exposure to Alexa fluor 488 Tf, a clathrin-mediated pathway marker and Alexa fluor 488 CTß, a caveolin-mediated pathway marker. Uptake was assessed using a Beckman Coulter MoFlo (minimum 10,000 cells/sample). ****, ***, ** and * indicate statistical differences at p<0.05, p<0.01, p<0.001 and p< 0.0001, respectively, compared to the control (cells incubated with markers in absence of inhibitors), whereas ns indicates a non-significant result, p>0.05 (N=2, n=4).*

Based on the results of the MTS screening (Figure 5.2 and 5.3) and the uptake of pathways markers using A549 and A549-Luc cells (Figure 5.4 and 5.5), concentrations of the inhibitors were selected for use in investigating the mechanism of endocytosis of siRNA-liposomes. These concentrations show a low cytotoxic effect, while significantly inhibiting internalisation of specific ligands, and are summarised in Table 5.2.

Table 5.2: Selected concentrations of inhibitors

Inhibitor	**Concentration** (μg/ml)	**Cell viability (%)** A549	A549-Luc
Concanavalin A	100	98.2	100
Chlorpromazine	20	80.4	88.9
Dynasore	20	89.5	96.1
Genistein	15	86.4	79.3
Filipin	20	80.9	97.5
MβCD	300	91.7	96.12
Nystatin	20	84.9	82.9
EIPA	0.5, 1.0, 2.5	90.8, 84.7, 79.3	95.2, 88.7, 84.3
Cytochalasin D	2, 4, 6	112.8, 95.6, 95.8	95.1, 89.6, 90.7

5.3.3 Role of Clathrin-Mediated Endocytosis

5.3.3.1 Effect of Concanavalin A Inhibitor

5.3.3.1.1 Effect on cy3-siRNA-Liposomes` Cellular Uptake

Concanavalin A is a clathrin-mediated endocytosis inhibitor which prevents the formation of clathrin coated pits [30]. Figure 5.6 shows the effect of this inhibitor on the cellular uptake of cy3-siRNA-liposomes in A549 cells. A549 cells were treated with concanavalin A (100 μg/ml) for 30 min prior to the application of cy3-siRNA-liposomes and incubated with the applied system for a further 4 hrs in the presence of the inhibitor. The effect of inhibitor on the cellular uptake of cy3-siRNA-lipsomes was assessed using flow cytometry and visualized by confocal microscopy. The flow cytometry provides quantification of the internalisation, by measuring the MFI values of cy3-siRNA associated with the treated cells. The values are in this work expressed as a percentage relative to control cells (cells incubated with cy3-siRNA-liposome in the absence of inhibitor and taken as 100% MFI). The flow cytometry data are also displayed as the percentage of cell population, out of total cell population analysed, with associated fluorescence, relative to control cells not incubated with inhibitor. The MFI data (Figure 5.6 a), expressed relative to the control cells without concanavalin A, show that no significant difference in cy3-siRNA-liposomes internalization by the cells has been achieved in comparison to the control. Figure 5.6 b and c show the cell population with associated fluorescence in the presence of the inhibitor, which was approximately 99% relative to the control (cells incubated with cy3-siRNA-liposome in the absence of concanavalin A, taken as 100%). Confocal microscopy was performed to visualise the effect of the inhibitor on cy3-siRNA-liposomes internalisation into cells, as well as intracellular trafficking. It should be noted that the confocal negative control micrographs

treated with cy3-siRNA in the absence of inhibitors were only performed once and the same micrographs will be presented in all used inhibitors. Confocal micrographs (Figure 5.6 d) and z-stack micrographs (Figure 5.6 e) show that siRNA-liposomes labelled with cy3 (red) were internalised into cells in the presence of the clathrin inhibitor, but it appears that there is a lower fluorescence intensity in comparison to the control (without concanavalin A), and this appears to contradict with the data obtained from flow cytometry (Figure 5.6 a and b).

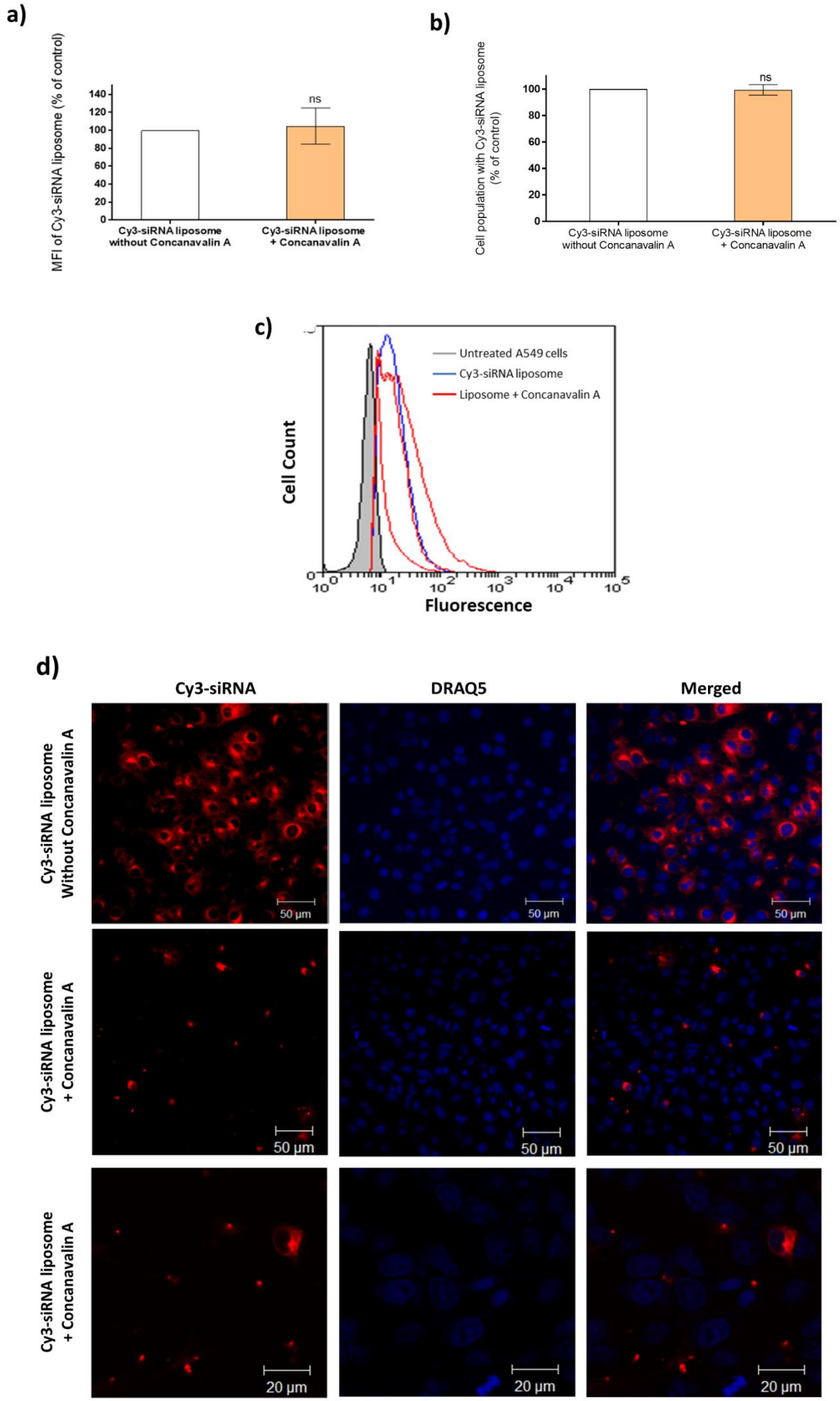
a)
MFI of Cy3-siRNA liposome (% of control)
140
120
100
80
60
40
20
0
ns
Cy3-siRNA liposome without Concanavalin A
Cy3-siRNA liposome + Concanavalin A
b)
Cell population with Cy3-siRNA liposome (% of control)
100
80
60
40
20
0
ns
Cy3-siRNA liposome without Concanavalin A
Cy3-siRNA liposome + Concanavalin A
c)
Untreated A549 cells
Cy3-siRNA liposome
Liposome + Concanavalin A
Cell Count
0
10^0
10^1
10^2
10^3
10^4
10^5
Fluorescence
d)
Cy3-siRNA
DRAQ5
Merged
Cy3-siRNA liposome Without Concanavalin A
Cy3-siRNA liposome + Concanavalin A
Cy3-siRNA liposome + Concanavalin A
50 μm
50 μm
50 μm
50 μm
50 μm
50 μm
20 μm
20 μm
20 μm

e)

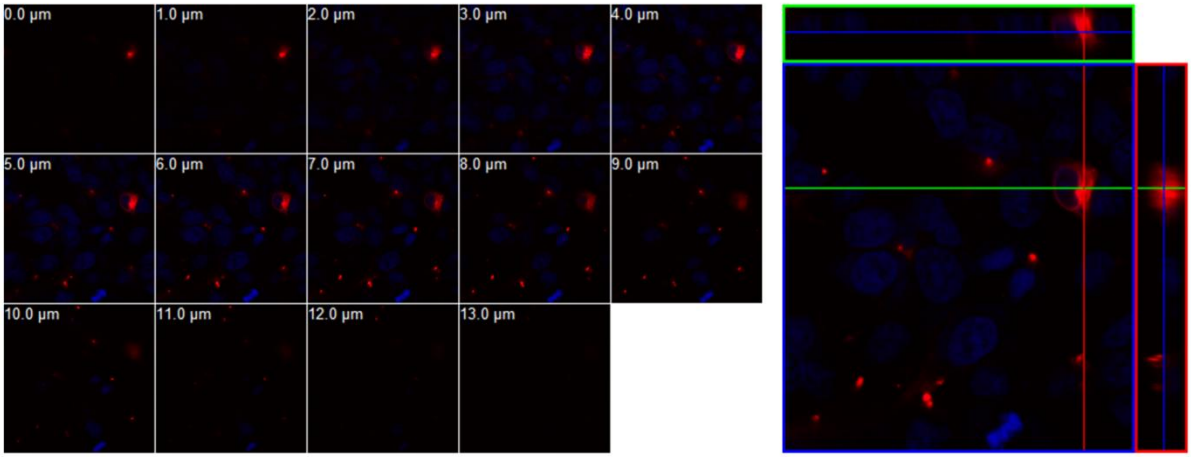

Figure 5.6: The effect of concanavalin A inhibitor on the internalisation of cy3-siRNA-liposomes in A549 cells

Concanavalin A (100 µg/ml) was pre-applied to cells for 30 min followed by exposure to cy3-siRNA-liposomes prepared at an N/P ratio of 3.125:1 and a DC-Chol:DOPE ratio of 1:1 for 4 hrs, in the presence of concanavalin A.
***(a)** MFI and **(b)** Cell population with cy3-siRNA-liposomes presented relative to the control (cells without concanavalin A). Flow cytometry data assessed by a Beckman Coulter MoFlo (minimum 10,000 cells/sample), and data represents the mean ± SD (N=2, n=3), ns indicates the difference is non-statistically significant (p>0.05) compared to the control. **(c)** Histograms cellular uptake profile of cy3-siRNA-liposomes assessed by a Beckman Coulter MoFlo (minimum 10,000 cells/sample). Untreated cells appear grey, cy3-siRNAliposomes appear blue and liposomes treated with concanavalin A appear red for the three repeats. **(d)** Confocal microscopy micrographs of cy3-siRNA-liposomes uptake in A549 cells in the absence (upper micrographs) and presence (middle and lower micrographs) of concanavalin A. **(e)** Z-stack of cy3-siRNA-liposomes internalisation in the presence of concanavalin A. Cy3-siRNA-liposomes appear red, whereas nuclei appear blue as stained with DRAQ5.*

5.3.3.1.2 Effect on luc-siRNA-Liposomes` Luciferase Silencing

The aim of this study was to assess the effect of endocytosis inhibition on silencing of luciferase protein expression in A549-Luc cells, linked to the effect of cellular uptake, in order to better understand the siRNA-liposome mechanism of endocytosis. Figure 5.7 shows the effect of concanavalin A (100 µg/ml) presence on the luciferase knockdown by Luc-siRNA-liposomes in A549-Luc cells. It is clear from the results of the luciferase assay (Figure 5.7 a) that clathrin inhibition by concanavalin A does not significantly

affect the luciferase expression (knockdown was approximately 113% relative to control, $p>0.05$), and hence clathrin does not appear to be the major player in the internalisation of the tested delivery system. The result of the luciferase assay was corroborated using liposome loaded with '6-FAM luc-siRNA based MB'. The MB will release green fluorescence when it (siRNA) binds to the targeted mRNA for luciferase protein. The cells fluorescence arising from MB was evaluated using flow cytometry (Figure 5.7 b, c and d) and green fluorescence was visualised via confocal microscopy (Figure 5.7 e and f). The MFI data in Figure 5.7 b show that the application of concanavalin A has no significant effect on the engagement of FAM-MB with the targeted mRNA in comparison to control cells not incubated with the inhibitor. The flow cytometry data (Figure 5.7 c and d) show that the cell population showing 'luc-siRNA based MB' fluorescence is not statistically different in the presence or the absence of concanavalin A.

Confocal and z-stack micrographs of the 'luc-siRNA based MB' in the A549-Luc cell line (Figure 5.7 e and f) show that the green dye of the FAM-MB appears into the perinuclear region of the cells confirming binding to Luc-mRNA. However, it is appear from the confocal results that the intensity of FAM-MB fluorescence in A549-Luc cells is lower in comparison to results of control (cells treated with 'luc-siRNA based MB' in the absence of concanavalin A). It should be noted that the confocal negative control micrographs treated with 'luc-siRNA based MB' in the absence of inhibitors were only performed once and the same micrographs will be presented in all used inhibitors.

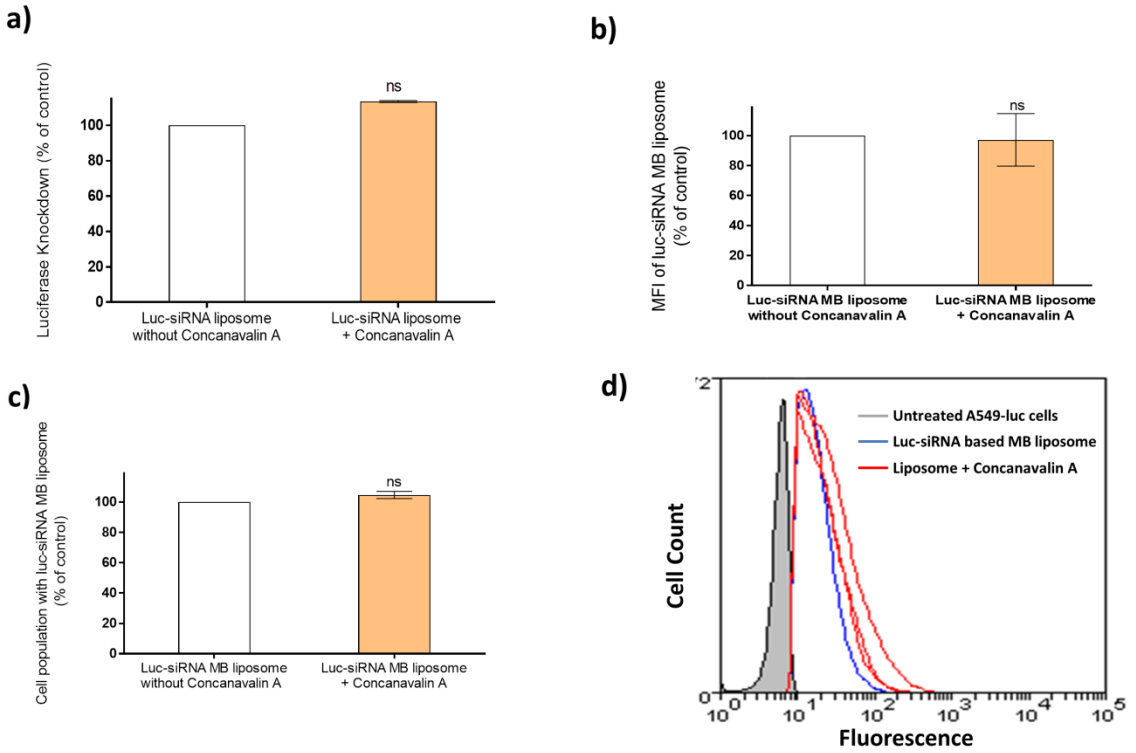
a)
Luciferase Knockdown (% of control)
ns
Luc-siRNA liposome without Concanavalin A
Luc-siRNA liposome + Concanavalin A
b)
MFI of luc-siRNA MB liposome (% of control)
ns
Luc-siRNA MB liposome without Concanavalin A
Luc-siRNA MB liposome + Concanavalin A
c)
Cell population with luc-siRNA MB liposome (% of control)
ns
Luc-siRNA MB liposome without Concanavalin A
Luc-siRNA MB liposome + Concanavalin A
d)
Untreated A549-luc cells
Luc-siRNA based MB liposome
Liposome + Concanavalin A
Cell Count
Fluorescence

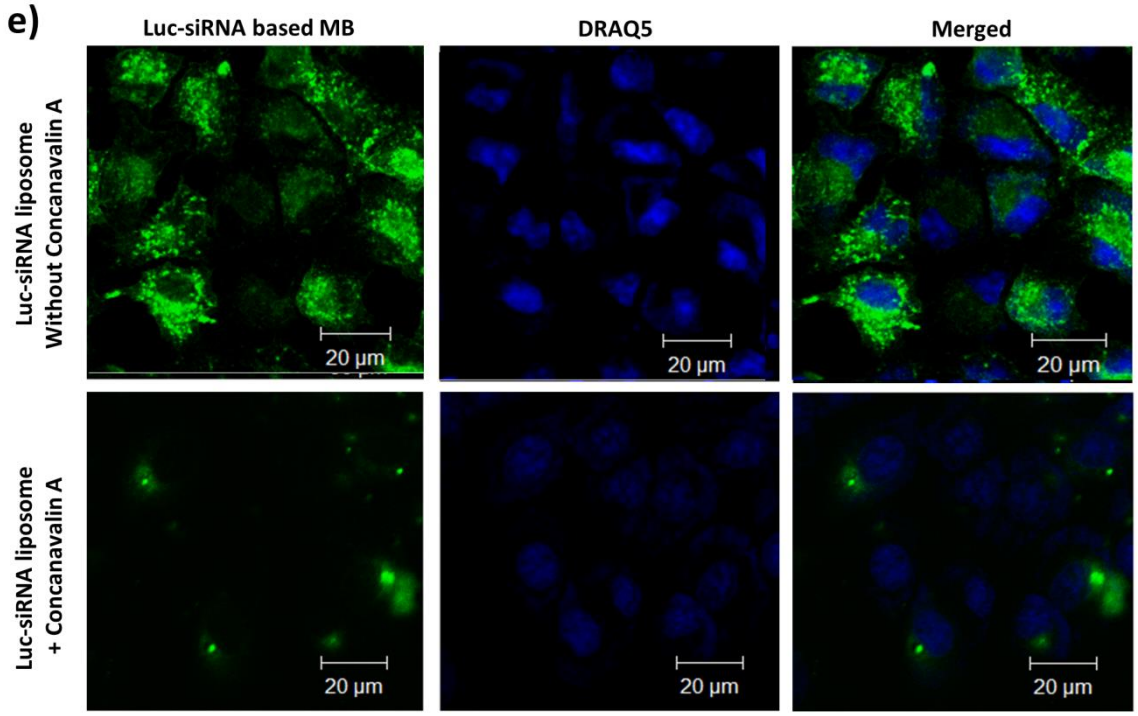
e)
Luc-siRNA based MB
DRAQ5
Merged
Luc-siRNA liposome Without Concanavalin A
Luc-siRNA liposome + Concanavalin A
20 µm

f)

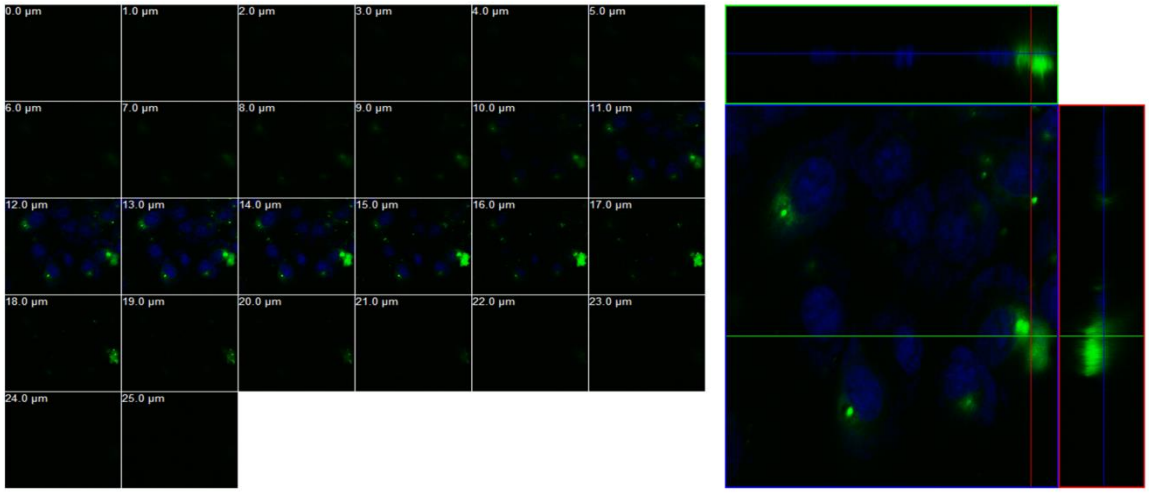

Figure 5.7: The effect of concanavalin A inhibitor on the luciferase knockdown of luc-siRNA-liposomes and 'luc-siRNA based MB' liposomes in A549-Luc cells

Concanavalin A (100 µg/ml) was pre-applied to cells for 30 min followed by exposure to luc-siRNA-liposomes and 'luc-siRNA based MB' liposomes prepared at an N/P ratio of 3.125:1 and a DC-Chol: DOPE ratio of 1:1 for 4 hrs, in the presence of concanavalin A. ***(a)*** *Luciferase knockdown of luc-siRNA-liposomes relative to the control (cells without concanavalin A), data represents the mean ± SD (N=2, n=3), ns indicates the difference is a non-statistically significant (p>0.05) compared to the control.* ***(b)*** *MFI and* ***(c)*** *'Luc-siRNA based MB' liposomes associated with cell population presented relative to the control (cells without concanavalin A). Flow cytometry data assessed by a Beckman Coulter MoFlo (minimum 10,000 cells/sample), and data represents the mean ± SD (N=2, n=3), ns indicates the difference is non-statistically significant (p>0.05) compared to the control.* ***(d)*** *'Luc-siRNA based MB' liposomes fluorescence histograms profile assessed by a Beckman Coulter MoFlo (minimum 10,000 cells/sample). Untreated cells appear grey, luc-siRNA based MB liposomes appear blue and liposomes treated with concanavalin A appear red for three repeats.* ***(e)*** *Confocal microscopy micrographs of 'luc-siRNA based MB' liposomes in A549-Luc cells in the absence (upper micrographs) and presence (lower micrographs) of concanavalin A.* ***(f)*** *Z-stack of 'luc-siRNA based MB' liposomes fluorescence in the presence of concanavalin A. 'Luc-siRNA based MB' liposomes appear green, whereas nuclei appear blue as stained with DRAQ5.*

5.3.3.2 Effect of Chlorpromazine Inhibitor

5.3.3.2.1 Effect on cy3-siRNA-Liposomes` Cellular Uptake

Another inhibitor that is widely reported in the literature to inhibit the clathrin-mediated pathway is chlorpromazine, which prevents formation of clathrin-coated pits at the plasma membrane [15]. Figure 5.8 shows the effect of chlorpromazine inhibitor (20 μg/ml) on the cellular uptake of cy3-siRNA-liposomes in A549 cells. In contrast to the concanavalin A data, the MFI results (Figure 5.8 a) show a significant decrease of cy3-siRNA-liposomes fluorescence level in the presence of inhibitor, relative to control cells without chlorpromazine. The flow cytometry results (Figure 5.8 b and c) demonstrate that chlorpromazine produced a significant reduction in ($p<0.0001$) cell population with cy3-siRNA-liposomes, which was 66%, relative to the control cells (cells without chlorpromazine). In agreement with flow cytometry data, confocal micrographs (Figure 5.8 d) indicates that the fluorescence of the red cy3-siRNA is reduced on chlorpromazine treatment (lower micrographs), in comparison to untreated A549 cells (upper micrographs).

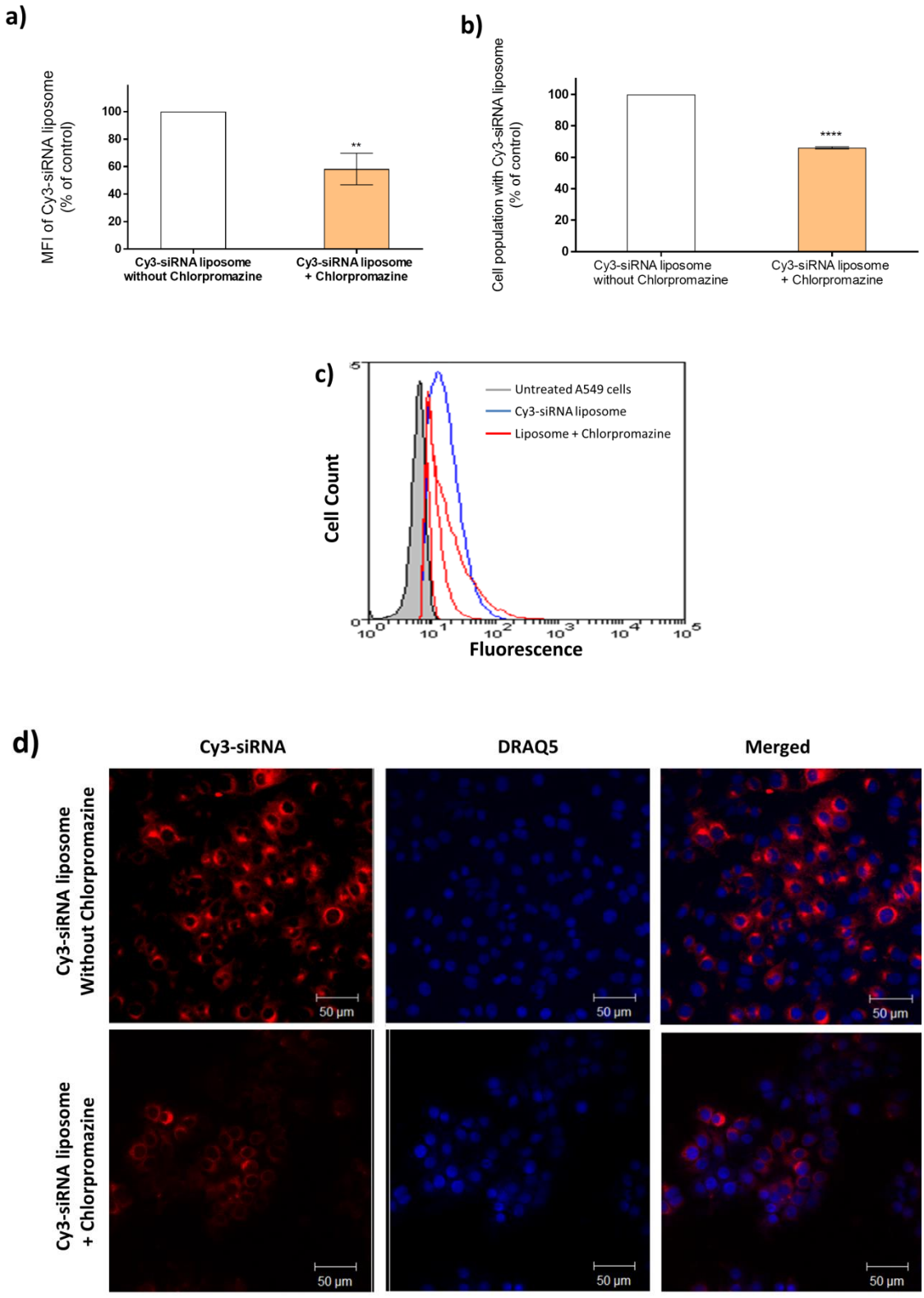

Figure 5.8: The effect of chlorpromazine inhibitor on the internalisation of cy3-siRNA-liposomes in A549 cells

Chlorpromazine (20 μg/ml) was pre-applied to cells for 30 min followed by exposure to cy3-siRNA-liposomes prepared at an N/P ratio of 3.125:1 and a DC-Chol:DOPE ratio of 1:1 for 4 hrs, in the presence of chlorpromazine.
(a) *MFI and* ***(b)*** *Cell population with cy3-siRNA-liposomes presented relative to the control (cells without chlorpromazine). Flow cytometry data assessed by a Beckman Coulter MoFlo (minimum 10,000 cells/sample), and data represents the mean ± SD (N=2, n=3), ** and **** Indicate the difference is statistically significant (p<0.01 and 0.0001, respectively), compared to the control.* ***(c)*** *Histograms cellular uptake profile of cy3-siRNA-liposomes assessed by a Beckman Coulter MoFlo (minimum 10,000 cells/sample). Untreated cells appear grey, luc-siRNA based MB liposomes appear blue and liposomes treated with chlorpromazine appear red for three repeats.* ***(d)*** *Confocal microscopy micrographs of cy3-siRNA-liposomes uptake in A549 cells in the absence (upper micrographs) and presence (lower micrographs) of chlorpromazine. Cy3-siRNA-liposomes appear red, whereas nuclei appear blue as stained with DRAQ5.*

5.3.3.2.2 Effect on luc-siRNA-Liposomes` Luciferase Silencing

Figure 5.9 shows the effect of chlorpromazine inhibitor (20 μg/ml) on the luciferase knockdown by luc-siRNA-liposomes in A549-Luc cells. The result of the luciferase assay (Figure 5.9 a) demonstrates chlorpromazine`s effect on the clathrin pathway, as indicated by reduced silencing effect of the liposomes in the inhibitor's presence. The luciferase knockdown in the presence of the inhibitor was dramatically reduced to only 5%, relative to the silencing effect in control cells (cells without chlorpromazine, taken as 100% silencing). The significant involvement of chlorpromazine inhibitor on the luciferase silencing was confirmed by examine the intensity of green fluorescence of MB into A549-Luc cells using flow cytometry and confocal microscopy. The flow cytometry data of FAM-MB (Figure 5.9 b, c and d) show that the MFI values and association of 'luc-siRNA based MB' fluorescence with the cells were significantly reduced in the presence of the inhibitor, in comparison to control cells (in absence of chlorpromazine). Confocal micrographs of the 'luc-siRNA based MB' in the A549-luc cell line (Figure 5.9 e) show that the green colour of FAM-MB (lower micrographs) appears at a lower level in comparison to untreated A549-Luc cells (upper micrographs).

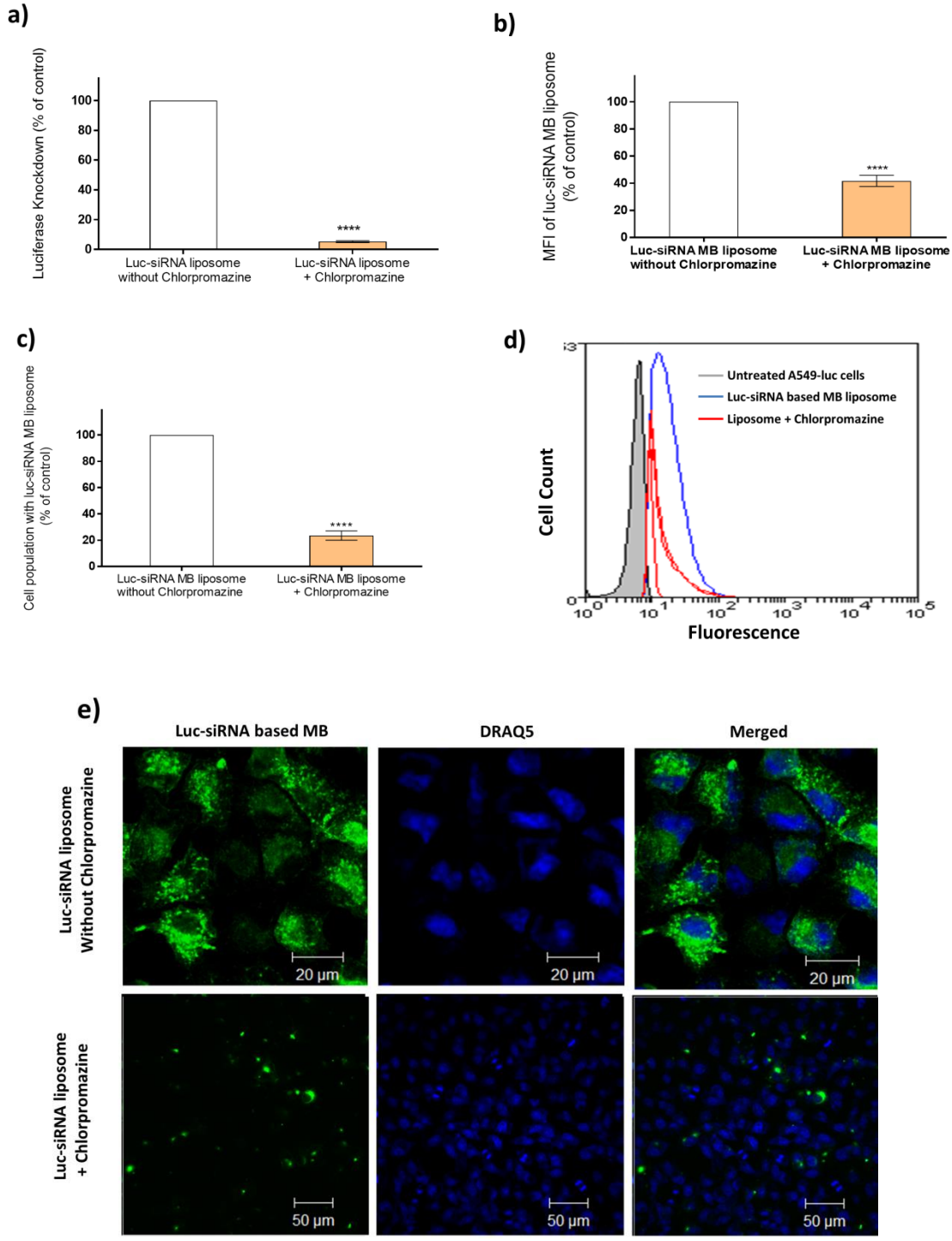

Figure 5.9: The effect of chlorpromazine inhibitor on the luciferase knockdown of luc-siRNA-liposomes and 'luc-siRNA based MB' liposomes in A549-Luc cells

Chlorpromazine (20 µg/ml) was pre-applied to cells for 30 min followed by exposure to luc-siRNA-liposomes and 'luc-siRNA based MB' liposomes prepared at an N/P ratio of 3.125:1 and a DC-Chol:DOPE ratio of 1:1 for 4 hrs, in the presence of chlorpromazine. ***(a)*** *Luciferase knockdown of luc-siRNA-liposomes relative to the control (cells without chlorpromazine), data represents the mean ± SD (N=2, n=3), **** Indicates the difference is a statistically significant ($p<0.0001$) compared to the control.* ***(b)*** *MFI and* ***(c)*** *'Luc-siRNA based MB' liposomes associated with cell population presented relative*

*to the control (cells without chlorpromazine). Flow cytometry data assessed by a Beckman Coulter MoFlo (minimum 10,000 cells/sample), and data represents the mean ± SD (N=2, n=3), **** Indicates the difference is statistically significant (p<0.0001, respectively), compared to the control.* ***(d)*** *'Luc-siRNA based MB' liposomes fluorescence histograms profile assessed by a Beckman Coulter MoFlo (minimum 10,000 cells/sample). Untreated cells appear grey, luc-siRNA based MB liposomes appear blue and liposomes treated with chlorpromazine appear red for three repeats.* ***(e)*** *Confocal microscopy micrographs of 'luc-siRNA based MB' liposome in A549-Luc cells in the absence (upper micrographs) and presence (lower micrographs) of chlorpromazine. 'Luc-siRNA based MB' liposomes appear green, whereas nuclei appear blue as stained with DRAQ5.*

5.3.4 Role of Pathways Involving Dynamin: Dynasore Inhibitor

5.3.4.1 Effect on cy3-siRNA-Liposomes` Cellular Uptake

To investigate influenced by dynamin inhibition, dynasore, a dynamin inhibitor, was used [16]. Figure 5.10 shows the effect of the inhibition of dynamin by dynasore inhibitor (20 μg/ml) on the cellular uptake of cy3-siRNA-liposomes in A549 cells. The flow cytometry results (Figure 5.10 a) indicate that dynasore exhibited no significant effects ($p>0.05$) on the cy3-siRNA fluorescence intensity of the measured cells incubated with inhibitor in comparison to control cells. Moreover, Figure 5.10 b and c show that dynamin inhibition has no significant effect on the population of cells with cy3-siRNA-liposomes, relative to the control cells (cells without dynasore). This is in agreement with the confocal micrographs (Figure 5.10 d) that reveal that cy3-siRNA was internalised into cells in the presence of the dynamin inhibitor (lower micrographs), and that the red fluorescence is of comparable intensity with the results of the control cells without dynasore (upper micrographs).

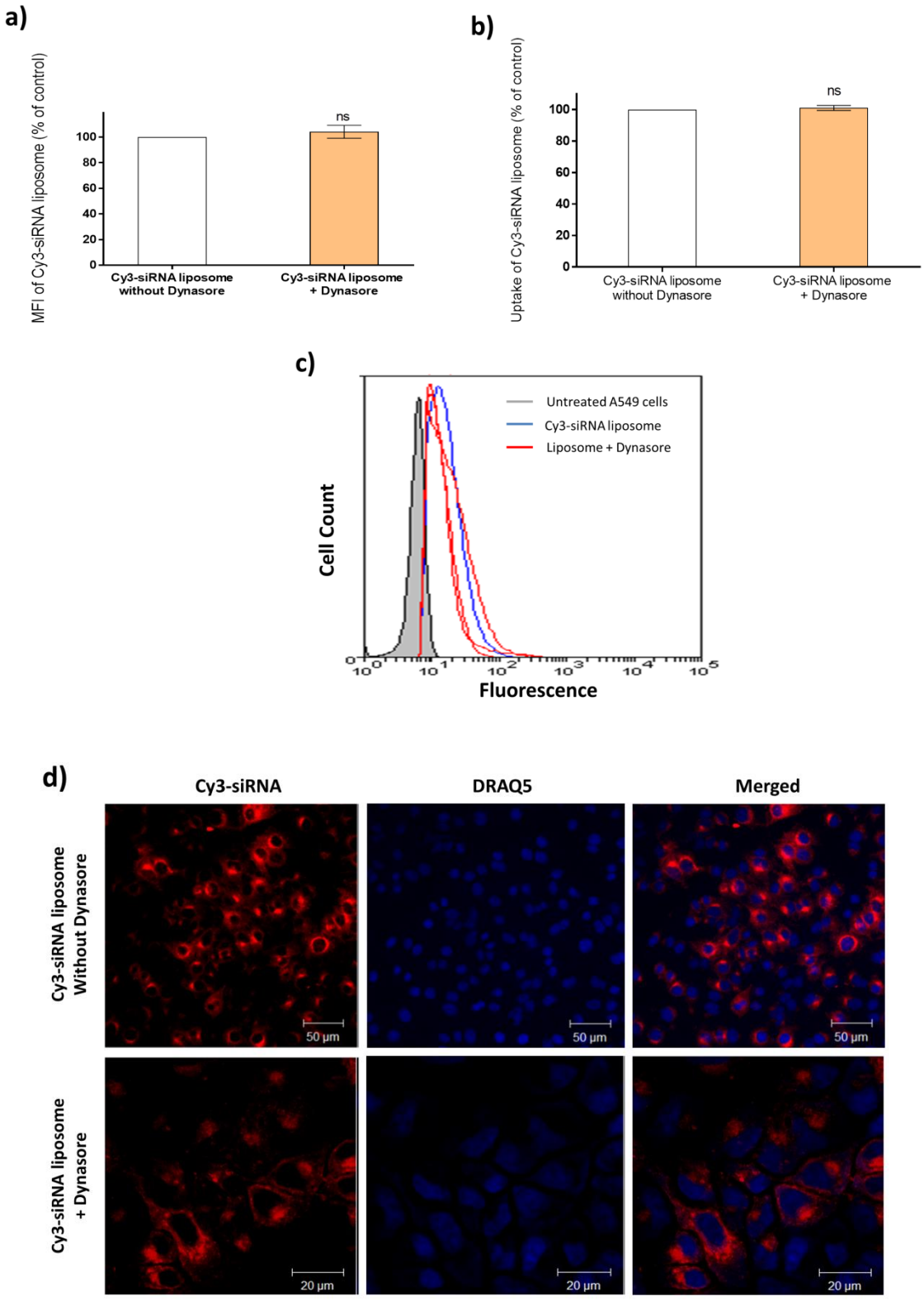

Figure 5.10: The effect of dynasore inhibitor on the internalisation of cy3-siRNA-liposomes in A549 cells

Dynasore (20 μg/ml) was pre-applied to cells for 30 min followed by exposure to cy3-siRNA-liposomes prepared at an N/P ratio of 3.125:1 and a DC-Chol:DOPE ratio of 1:1 for 4 hrs, in the presence of dynasore.
(a) *MFI and* ***(b)*** *Cell population with cy3-siRNA-liposomes presented relative to the control (cells without dynasore). Flow cytometry data assessed by a Beckman Coulter MoFlo (minimum 10,000 cells/sample), and data represents the mean ± SD (N=2, n=3), ns indicates the difference is non-statistically significant (p>0.05) compared to the control. (c) Histograms cellular uptake profile of cy3-siRNA-liposomes assessed by a Beckman Coulter MoFlo (minimum 10,000 cells/sample). Untreated cells appear grey, cy3-siRNA-liposomes appear blue and liposomes treated with dynasore appear red for three repeats.* ***(d)*** *Confocal microscopy micrographs of cy3-siRNA-liposomes uptake in A549 cells in the absence (upper micrographs) and presence (lower micrographs) of dynasore. Cy3-siRNA-liposomes appear red, whereas nuclei appear blue as stained with DRAQ5.*

5.3.4.2 Effect on luc-siRNA-Liposomes` Luciferase Silencing

Figure 5.11 shows the effect of the inhibition of the dynamin-mediated pathway by dynasore inhibitor (20 μg/ml) on the luciferase knockdown by luc-siRNA-liposomes. Data from the luciferase assay (Figure 5.11 a) show that exposure to dynasore significantly reduced the luciferase knockdown of luc-siRNA-liposomes (51% relative to control, $p<0.0001$). The flow cytometry data (Figure 5.11 b, c and d) show a significant reduction in the MFI values and hence the 'involvement' of 'luc-siRNA based MB' with targeted mRNA for cells incubated with dynasore in comparison to the control cells (A549-Luc cells incubated with 'luc-siRNA based MB' liposomes in the absence of dynasore). The population of cells with 'luc-siRNA based MB' is also reduced, relative to untreated control. Confocal and z-stack micrographs of the 'luc-siRNA based MB' in A549-Luc cells (Figure 5.11 e and f) confirm the effect of dynamin inhibition on the luciferase mRNA and shows that the green colour of the FAM-MB appeared in the cytoplasmic region of the cells in the presence of dynasore, confirming binding to Luc-mRNA (lower micrographs), but the fluorescence is appears lower and in fewer cells, compared to untreated A549-Luc cells (upper micrographs).

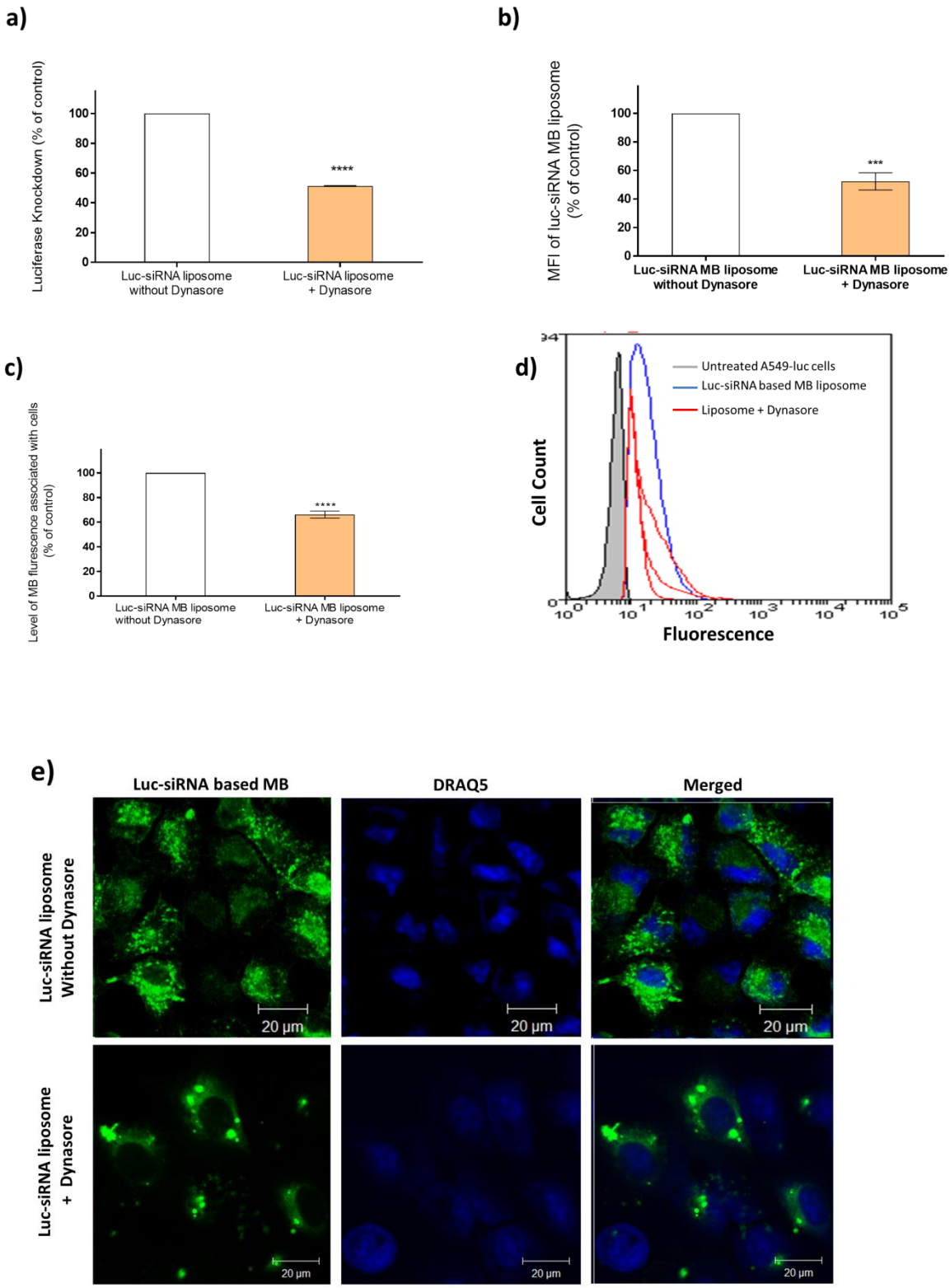
a)
Luciferase Knockdown (% of control)
100
80
60
40
20
0
****
Luc-siRNA liposome without Dynasore
Luc-siRNA liposome + Dynasore
b)
MFI of luc-siRNA MB liposome (% of control)
100
80
60
40
20
0
***
Luc-siRNA MB liposome without Dynasore
Luc-siRNA MB liposome + Dynasore
c)
Level of MB flurescence associated with cells (% of control)
100
80
60
40
20
0
****
Luc-siRNA MB liposome without Dynasore
Luc-siRNA MB liposome + Dynasore
d)
Untreated A549-luc cells
Luc-siRNA based MB liposome
Liposome + Dynasore
Cell Count
Fluorescence
e)
Luc-siRNA based MB
DRAQ5
Merged
Luc-siRNA liposome Without Dynasore
Luc-siRNA liposome + Dynasore
20 µm

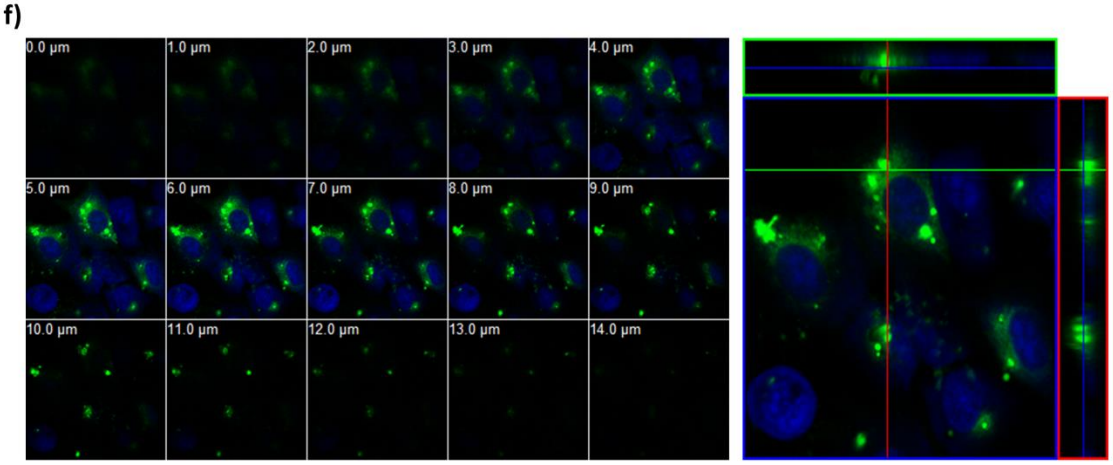

Figure 5.11: The effect of dynasore inhibitor on the luciferase knockdown of luc-siRNA-liposomes and 'luc-siRNA based MB' liposomes in A549-Luc cells

Dynasore (20 µg/ml) was pre-applied to cells for 30 min followed by exposure to luc-siRNA-liposomes and 'luc-siRNA based MB' liposomes prepared at an N/P ratio of 3.125:1 and a DC-Chol: DOPE ratio of 1:1 for 4 hrs, in the presence of dynasore. ***(a)*** *Luciferase knockdown of luc-siRNA-liposomes relative to the control (cells without dynasore), data represents the mean ± SD (N=2, n=3), **** Indicates the difference is a statistically significant ($p<0.0001$) compared to the control.* ***(b)*** *MFI and* ***(c)*** *'Luc-siRNA based MB' liposomes associated with cell population presented relative to the control (cells without dynasore). Flow cytometry data assessed by a Beckman Coulter MoFlo (minimum 10,000 cells/sample), and data represents the mean ± SD (N=2, n=3), *** and **** Indicate the difference is statistically significant ($p<0.001$ and 0.0001, respectively), compared to the control.* ***(d)*** *'Luc-siRNA based MB' liposomes fluorescence histograms profile assessed by a Beckman Coulter MoFlo (minimum 10,000 cells/sample). Untreated cells appear grey, luc-siRNA based MB liposomes appear blue and liposomes treated with dynasore appear red for three repeats.* ***(e)*** *Confocal microscopy micrographs of 'luc-siRNA based MB' liposomes in A549-Luc cells in the absence (upper micrographs) and presence (lower micrographs) of dynasore.* ***(f)*** *Z-stack of 'luc-siRNA based MB' liposomes fluorescence in the presence of dynasore. 'Luc-siRNA based MB' liposomes appear green, whereas nuclei appear blue as stained with DRAQ5.*

5.3.5 Role of Caveolin-Mediated Endocytosis

5.3.5.1 Genistein Inhibitor

5.3.5.1.1 Effect on cy3-siRNA-Liposomes` Cellular Uptake

Figure 5.12 shows the effect of the inhibition of caveolae pathways by genistein as a tyrosine kinase inhibitor [17], on the cellular uptake of cy3-siRNA-liposomes in A549 cells. The flow cytometry results (Figure 5.12 a, b and c) indicate that genistein (15 μg/ml) did not have a significant effect on the MFI values and the cell population with cy3-siRNA-liposomes, relative to the control A549 cells incubated with cy3-siRNA-liposomes in the absence of genistein). The results of the flow cytometry were supported by confocal microscopy (Figure 5.12 d). Confocal micrographs show that the red colour of cy3-siRNA in the cytoplasmic region of the cells is fairly similar in fluorescence level and appearance in both the absence and presence of genistein, upper and lower micrographs, respectively.

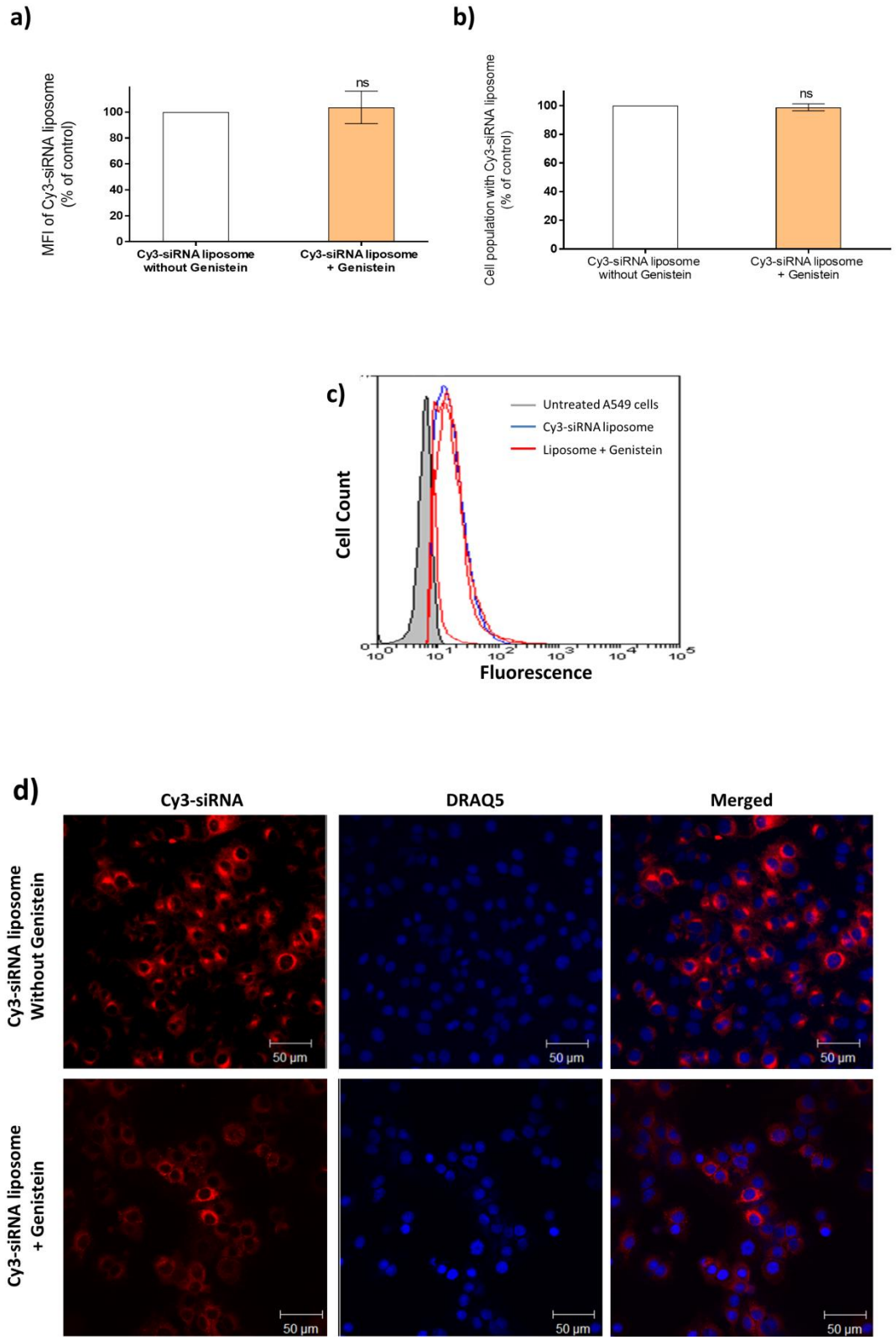

Figure 5.12: The effect of genistein inhibitor on the internalisation of cy3-siRNA-liposomes in A549 cells

Genistein (15 μg/ml) was pre-applied to cells for 30 min followed by exposure to cy3-siRNA-liposomes prepared at an N/P ratio of 3.125:1 and a DC-Chol:DOPE ratio of 1:1 for 4 hrs, in the presence of genistein.
(a) *MFI and* ***(b)*** *Cell population with cy3-siRNA-liposomes presented relative to the control (cells without genistein). Flow cytometry data assessed by a Beckman Coulter MoFlo (minimum 10,000 cells/sample), and data represents the mean ± SD (N=2, n=3), ns indicates the difference is non-statistically significant (p>0.05) compared to the control.* ***(c)*** *Histograms uptake profile of cy3-siRNA-liposomes assessed by a Beckman Coulter MoFlo (minimum 10,000 cells/sample). Untreated cells appear grey, cy3-siRNA-liposomes appear blue and liposomes treated with genistein appear red for three repeats.* ***(d)*** *Confocal microscopy micrographs of cy3-siRNA-liposomes uptake in A549 cells in the absence (upper micrographs) and presence (lower micrographs) of genistein. Cy3-siRNA-liposomes appear red, whereas nuclei appear blue as stained with DRAQ5.*

5.3.5.1.2 Effect on luc-siRNA-Liposomes` Luciferase Silencing

Figure 5.13 shows the effect of the inhibition of tyrosine kinase and caveolae endocytosis by genistein inhibitor (15 μg/ml) on the luciferase knockdown of luc-siRNA-liposomes in A549-Luc cells. It is clear from the result of the luciferase assay (Figure 5.13 a) that genistein did not demonstrate a significant effect ($p>0.05$) on the luciferase knockdown in A549-Luc cells. The luciferase knockdown in the presence of the inhibitor was around 113% relative to the control cells (A549-Luc cells incubated with luc-siRNA-liposomes in the absence of genistein). The flow cytometry data (Figure 5.13 b, c and d) show that genistein has no significant effect on the MFI values and the cell population exhibiting 'luc-siRNA based MB' fluorescence, in comparison to control cells (A549-Luc cells incubated with 'luc-siRNA based MB' liposomes in the absence of genistein). Confocal micrographs of the luc-MB in A549-Luc cells (Figure 5.13 e) show that the green colour of the FAM-MB appeared in the cytoplasmic region of the cells, confirming the binding to luc-mRNA (lower micrographs), and the green fluorescence of FAM-MB is roughly in comparable intensity with the control cells without genistein.

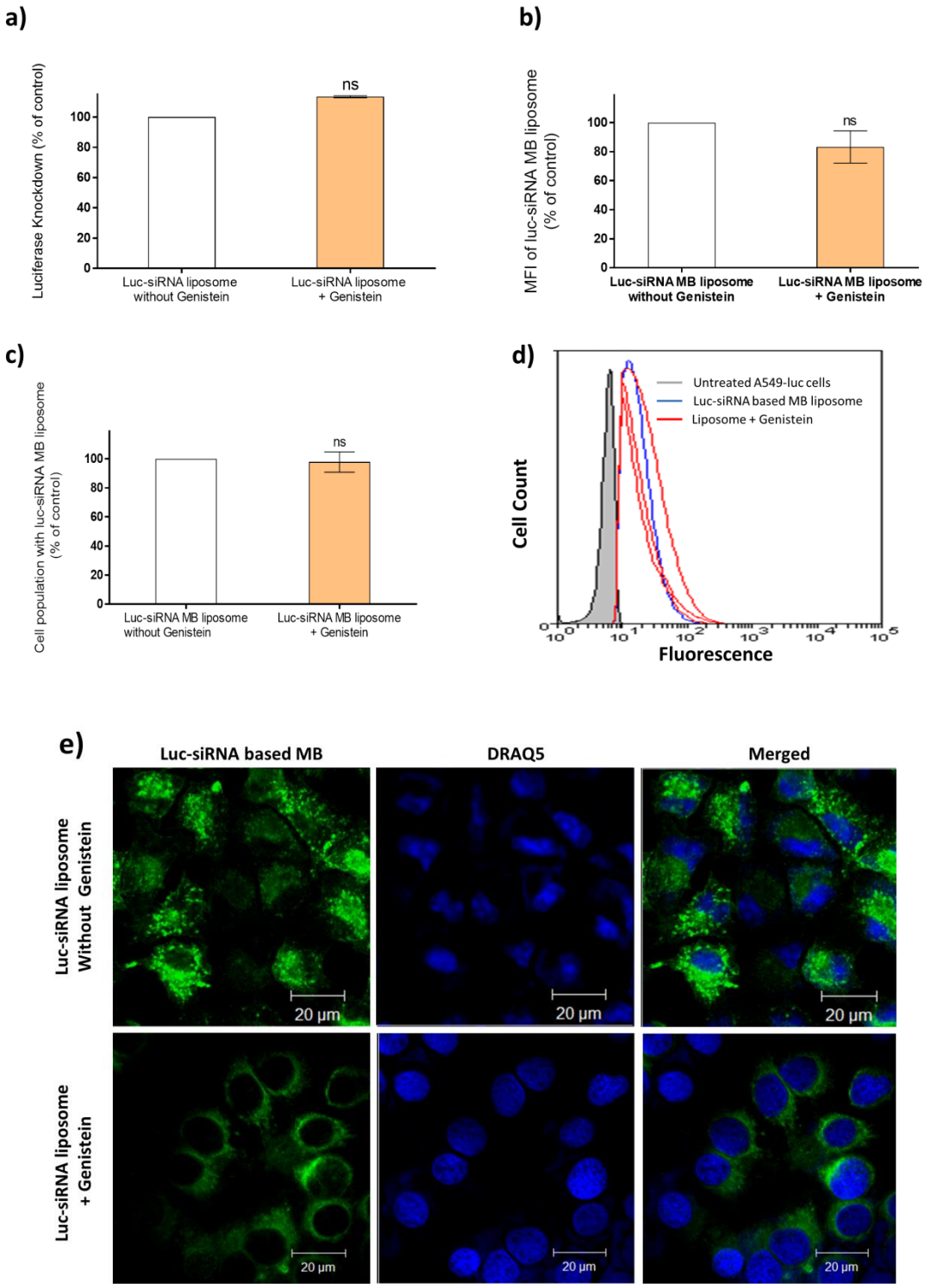

Figure 5.13: The effect of genistein inhibitor on the luciferase knockdown of luc-siRNA-liposomes and 'luc-siRNA based MB' liposomes in A549-Luc cells

Genistein (15 µg/ml) was pre-applied to cells for 30 min followed by exposure to luc-siRNA-liposomes and 'luc-siRNA based MB' liposomes prepared at an N/P ratio of 3.125:1 and a DC-Chol: DOPE ratio of 1:1 for 4 hrs, in the presence of genistein.
***(a)** Luciferase knockdown of luc-siRNA-liposomes relative to the control (cells without genistein), data represents the mean ± SD (N=2, n=3), ns indicates the difference is non-*

statistically significant (p>0.05) compared to the control. ***(b)*** *MFI and* ***(c)*** *'Luc-siRNA based MB' liposomes associated with cell population presented relative to the control (cells without genistein). Flow cytometry data assessed by a Beckman Coulter MoFlo (minimum 10,000 cells/sample), and data represents the mean ± SD (N=2, n=3), ns indicates the difference is non-statistically significant (p>0.05) compared to the control.* ***(d)*** *'Luc-siRNA based MB' liposomes fluorescence histograms profile assessed by a Beckman Coulter MoFlo (minimum 10,000 cells/sample). Untreated cells appear grey, luc-siRNA based MB liposomes appear blue and liposomes treated with genistein appear red for three repeats.* ***(e)*** *Confocal microscopy micrographs of 'luc-siRNA based MB' liposomes in A549-Luc cells in the absence (upper micrographs) and presence (lower micrographs) of genistein. 'Luc-siRNA based MB' liposomes appear green, whereas nuclei appear blue as stained with DRAQ5.*

5.3.5.2 Filipin Inhibitor

5.3.5.2.1 Effect on cy3-siRNA-Liposomes` Cellular Uptake

Filipin is cholesterol sequestering agent that is commonly used to examine the involvement of caveolae-mediated endocytosis in the uptake of siRNA-liposomes [18]. Figure 5.14 shows the effect of inhibition of caveolae-mediated endocytosis by filipin (20 μg/ml) on the cellular uptake of cy3-siRNA-liposomes in A549 cells. It is clear from the flow cytometry results (Figure 5.14 a, b and c) that filipin produced a significant effect on the MFI level and on population of cells with cy3-siRNA-liposomes, relative to untreated control. The effect of filipin on the uptake of liposomes was supported by visualising the red fluorescence of cy3-siRNA under the microscope in the presence and the absence of inhibitor. Confocal micrographs of cy3-siRNA-liposomes cellular uptake in A549 cells (Figure 5.14 d) show that the fluorescence of the red labelled siRNA that appears in the cytoplasmic region of the cells after the application of the inhibitor (lower micrographs) is of lower fluorescence than in the control cells without filipin (upper micrographs).

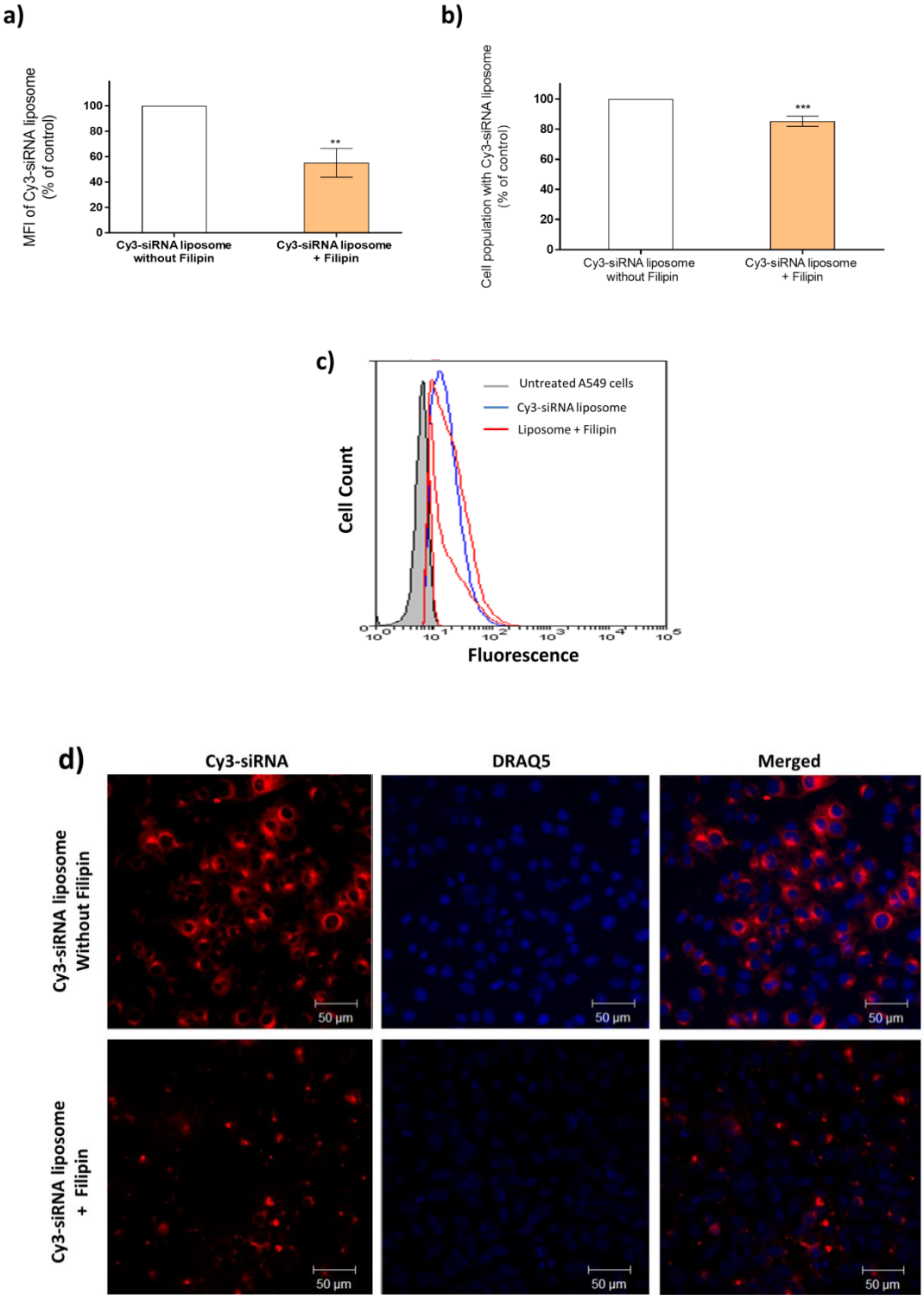

Figure 5.14: The effect of filipin inhibitor on the internalisation of cy3-siRNA-liposomes in A549 cells

Filipin (20 µg/ml) was pre-applied to cells for 30 min followed by exposure to cy3-siRNA-liposomes prepared at an N/P ratio of 3.125:1 and a DC-Chol:DOPE ratio of 1:1 for 4 hrs, in the presence of filipin.

(a) *MFI and* ***(b)*** *Cell population with cy3-siRNA-liposomes presented relative to the control (cells without filipin). Flow cytometry data assessed by a Beckman Coulter MoFlo (minimum 10,000 cells/sample), and data represents the mean ± SD (N=2, n=3), ** and *** Indicate the difference is statistically significant (p<0.01 and 0.001, respectively) compared to the control.* ***(c)*** *Histograms cellular uptake profile of cy3-siRNA-liposomes assessed by a Beckman Coulter MoFlo (minimum 10,000 cells/sample). Untreated A549 cells appear grey, cy3-siRNA-liposomes appear blue and liposomes treated with filipin appear red for three repeats.* ***(d)*** *Confocal microscopy micrographs of cy3-siRNA-liposomes uptake in A549 cells in the absence (upper micrographs) and presence (lower micrographs) of filipin. Cy3-siRNA-liposomes appear red, whereas nuclei appear blue as stained with DRAQ5.*

5.3.5.2.2 Effect on luc-siRNA-Liposomes` Luciferase Silencing

Figure 5.15 shows the effect of filipin inhibitor (20 μg/ml) on the luciferase knockdown of luc-siRNA-liposomes in A549-Luc cells. The luciferase assay (in Figure 5.15 a) shows no significant difference in silencing of untreated and filipin treated cells (filipin knockdown ~ 102% compared to in the control cells ($p>0.05$), indicating that caveolae pathway internalisation may not play a prominent role in the system's silencing effect. The flow cytometry results (Figure 5.15 b, c and d) show that the application of filipin inhibitor has no significant effect on the MFI values and the population of cells with associated 'luc-siRNA based MB' fluorescence, in comparison to control cells (cells without filipin). However, the confocal and z-stack micrographs of the 'luc-siRNA based MB' in A549-Luc cells (Figure 5.15 e and f) show that the green dye of the FAM-MB appears to be highly reduced in the presence of filipin in comparison to control A549-luc cells treated with the 'luc-siRNA based MB' in the absence of inhibitor.

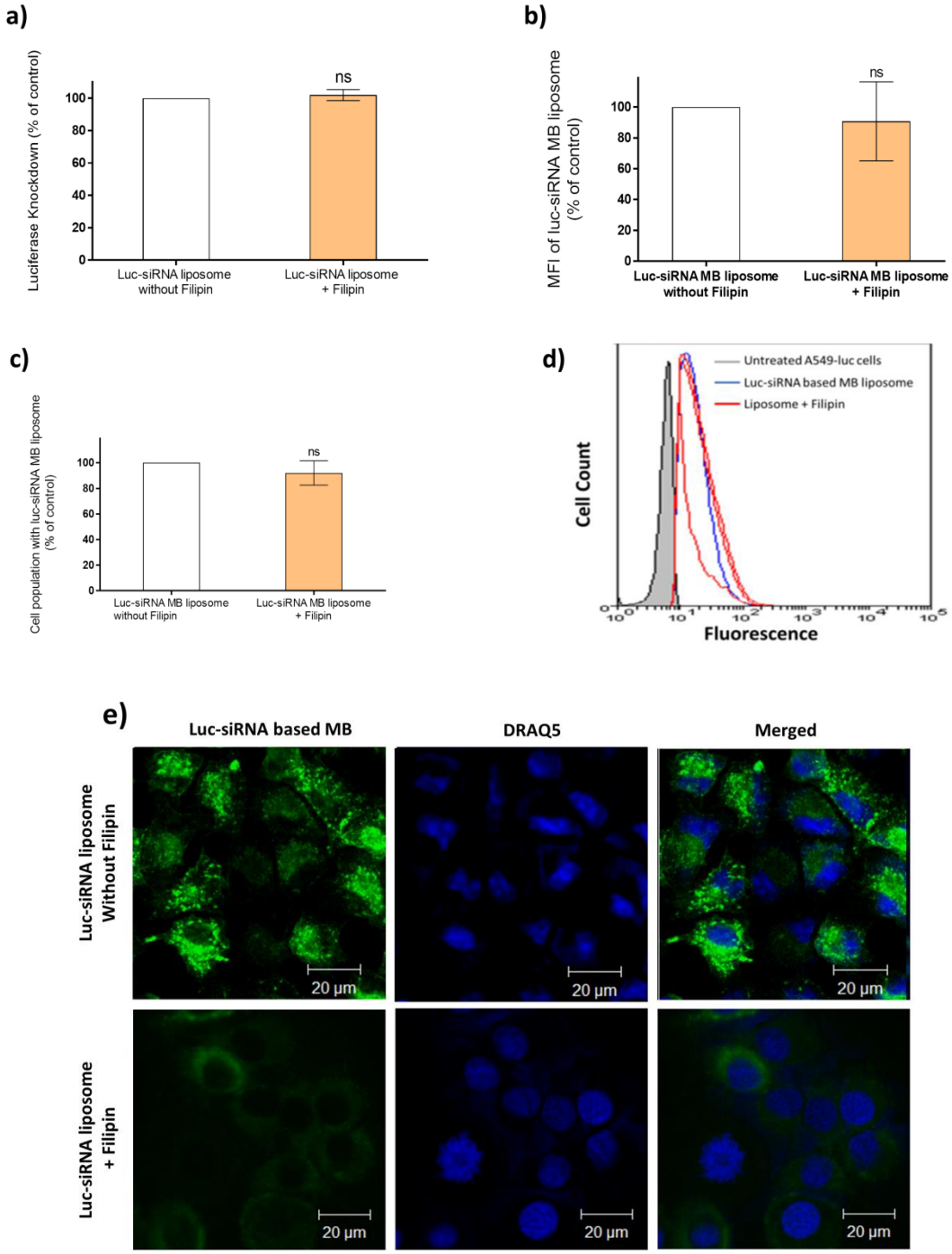
a)
Luciferase Knockdown (% of control)
ns
Luc-siRNA liposome without Filipin
Luc-siRNA liposome + Filipin
b)
MFI of luc-siRNA MB liposome (% of control)
ns
Luc-siRNA MB liposome without Filipin
Luc-siRNA MB liposome + Filipin
c)
Cell population with luc-siRNA MB liposome (% of control)
ns
Luc-siRNA MB liposome without Filipin
Luc-siRNA MB liposome + Filipin
d)
Untreated A549-luc cells
Luc-siRNA based MB liposome
Liposome + Filipin
Cell Count
Fluorescence
e)
Luc-siRNA based MB
DRAQ5
Merged
Luc-siRNA liposome Without Filipin
Luc-siRNA liposome + Filipin
20 µm

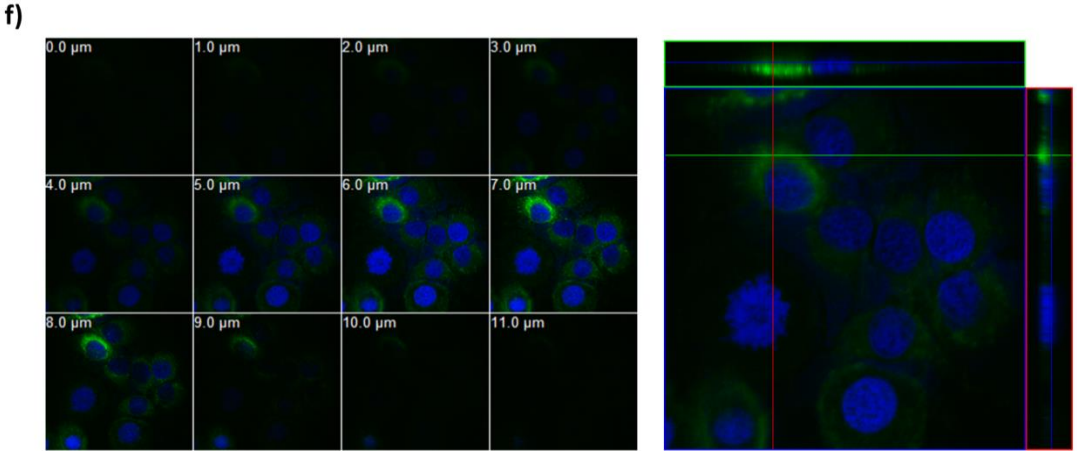

Figure 5.15: The effect of filipin inhibitor on the luciferase knockdown of luc-siRNA-liposomes and 'luc-siRNA based MB' liposomes in A549-Luc cells

Filipin (20 µg/ml) was pre-applied to cells for 30 min followed by exposure to luc-siRNA-liposomes and 'luc-siRNA based MB' liposomes prepared at an N/P ratio of 3.125:1 and a DC-Chol: DOPE ratio of 1:1 for 4 hrs, in the presence of filipin.
(a) *Luciferase knockdown of luc-siRNA-liposomes relative to the control (cells without filipin), data represents the mean ± SD (N=2, n=3), ns indicates the difference is non-statistically significant (p>0.05) compared to the control.* ***(b)*** *MFI and* ***(c)*** *'Luc-siRNA based MB' liposomes associated with cell population presented relative to the control (cells without filipin). Flow cytometry data assessed by a Beckman Coulter MoFlo (minimum 10,000 cells/sample), and data represents the mean ± SD (N=2, n=3), ns indicates the difference is non-statistically significant (p>0.05) compared to the control.* ***(d)*** *'Luc-siRNA based MB' liposomes fluorescence profile assessed by a Beckman Coulter MoFlo (minimum 10,000 cells/sample). Untreated cells appear grey, luc-siRNA based MB liposomes appear blue and liposomes treated with filipin appear red for three repeats.* ***(e)*** *Confocal microscopy micrographs of 'luc-siRNA based MB' liposomes in A549-Luc cells in the absence (upper micrographs) and presence (lower micrographs) of filipin.* ***(f)*** *Z-stack of 'luc-siRNA based MB' liposomes fluorescence in the presence of filipin. 'Luc-siRNA based MB' liposomes appear green, whereas nuclei appear blue as stained with DRAQ5.*

5.3.5.3 MßCD Inhibitor

5.3.5.3.1 Effect on cy3-siRNA-Liposomes` Cellular Uptake

Figure 5.16 shows the effect of cholesterol depletion by MßCD inhibitor (300 μg/ml), which depletes cell membrane associated cholesterol [19], on the cellular uptake of cy3-siRNA-liposomes. The results of the flow cytometry (Figure 5.16 a, b and c) indicate that MßCD treatment reduced the MFI and the population of cy3-siRNA-liposomes associated cells significantly ($p<0.0001$) relative to the control cells (cells without MßCD). The results of the flow cytometry was confirmed using confocal microscopy (Figure 5.16 d) which illustrate that the fluorescence of the red cy3-siRNA is reduced post-MßCD treatment (lower micrographs) when compared to untreated A549 cells (upper micrographs).

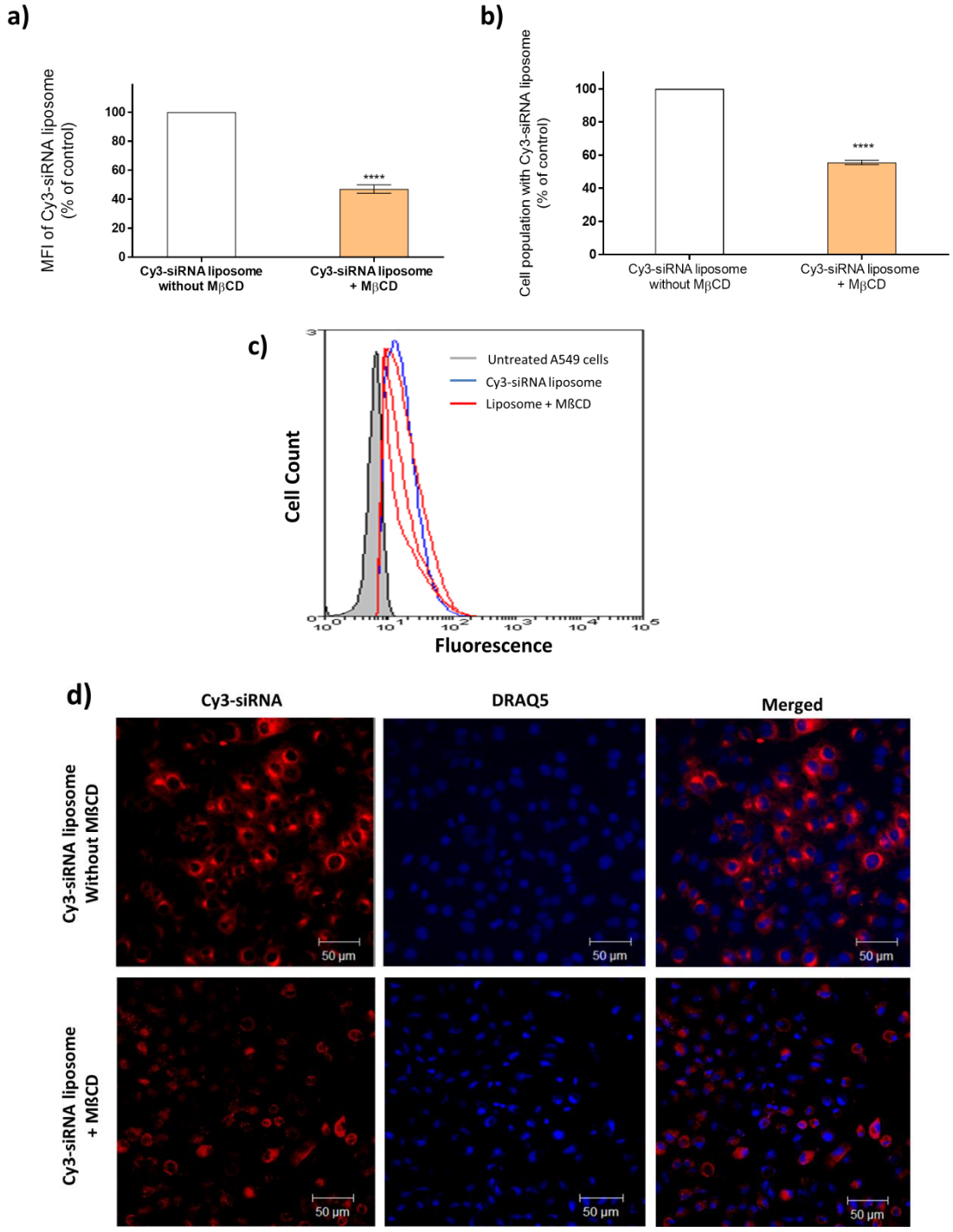

Figure 5.16: The effect of MßCD inhibitor on the internalisation of cy3-siRNA-liposomes in A549 cells

MßCD (300 µg/ml) was pre-applied to cells for 30 min followed by exposure to cy3-siRNA-liposomes prepared at an N/P ratio of 3.125:1 and a DC-Chol:DOPE ratio of 1:1 for 4 hrs, in the presence of the MßCD.
(a)** MFI and **(b)** Cell population with cy3-siRNA-liposomes presented relative to the control (cells without MßCD). Flow cytometry data assessed by a Beckman Coulter MoFlo (minimum 10,000 cells/sample), and data represents the mean ± SD (N=2, n=3), * indicates the difference is statistically significant ($p<0.0001$) compared to the control. **(c)** Histograms cellular uptake profile of cy3-siRNA-liposomes assessed by a*

Beckman Coulter MoFlo (minimum 10,000 cells/sample). Untreated cells appear grey, cy3-siRNA-liposomes appear blue and liposomes treated with MßCD appear red for three repeats. ***(d)*** *Confocal microscopy micrographs of cy3-siRNA-liposomes uptake in A549 cells in the absence (upper micrographs) and presence (lower micrographs) of MßCD. Cy3-siRNA-liposomes appear red, whereas nuclei appear blue as stained with DRAQ5.*

5.3.5.3.2 Effect on luc-siRNA-Liposomes` Luciferase Silencing

Figure 5.17 shows the effect of MßCD inhibitor (300 µg/ml) on the luciferase knockdown achieved by applying luc-siRNA-liposomes in A549-Luc cells. Data from the luciferase activity assay (Figure 5.17 a) demonstrates that the MßCD treatment resulted in a dramatic reduction in the silencing effects by the liposomes. The luciferase knockdown in the presence of the inhibitor was around 11% of the control (cells without MßCD, $p<0.0001$), indicating a pronounced effect of MßCD and inhibit the pathway and prevent luc-siRNA-liposomes from achieving high luciferase knockdown in A549-luc cells. The flow cytometry results (Figure 5.17 b, c and d) show reduced engagement of the 'luc-siRNA based MB' with the target mRNA, in comparison to control cells. The inhibitory effect of MßCD was further investigated using confocal microscopy, and the micrographs of the 'luc-siRNA based MB' in A549-Luc cells (Figure 5.17 e) show the green colour of the FAM-MB present in the perinuclear region of only few cells, although this is absent in the majority of cells in the inspected sample.

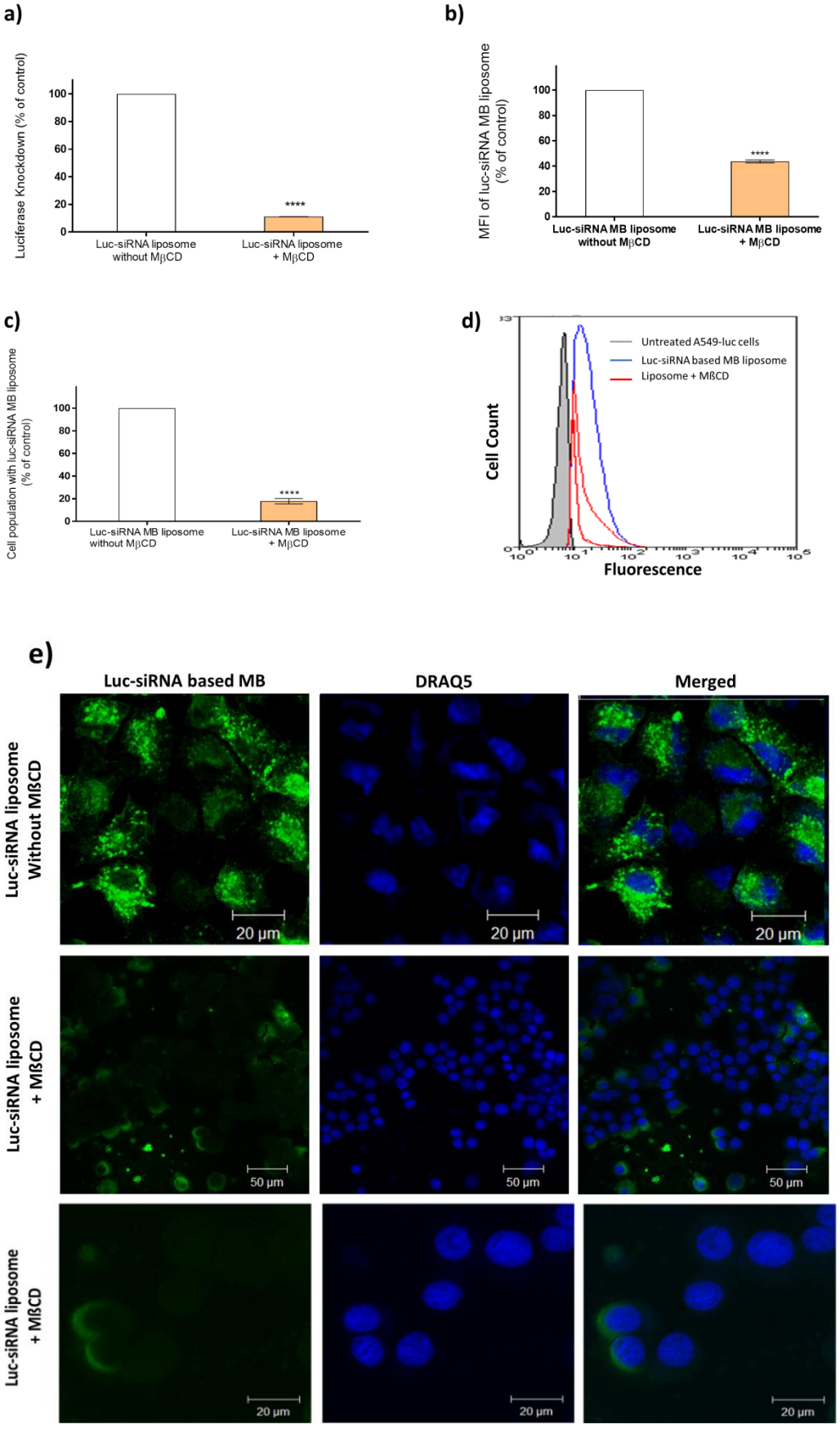
a)
Luciferase Knockdown (% of control)
100
80
60
40
20
0
****
Luc-siRNA liposome without MβCD
Luc-siRNA liposome + MβCD
b)
MFI of luc-siRNA MB liposome (% of control)
100
80
60
40
20
0
****
Luc-siRNA MB liposome without MβCD
Luc-siRNA MB liposome + MβCD
c)
Cell population with luc-siRNA MB liposome (% of control)
100
80
60
40
20
0
****
Luc-siRNA MB liposome without MβCD
Luc-siRNA MB liposome + MβCD
d)
Untreated A549-luc cells
Luc-siRNA based MB liposome
Liposome + MßCD
Cell Count
Fluorescence
e)
Luc-siRNA based MB
DRAQ5
Merged
Luc-siRNA liposome Without MßCD
Luc-siRNA liposome + MßCD
Luc-siRNA liposome + MßCD
20 µm
50 µm

Figure 5.17: The effect of MßCD inhibitor on the luciferase knockdown of luc-siRNA-liposomes and 'luc-siRNA based MB' liposomes in A549-Luc cells

MßCD (300 µg/ml) was pre-applied to cells for 30 min followed by exposure to luc-siRNA-liposomes and 'luc-siRNA based MB' liposomes prepared at an N/P ratio of 3.125:1 and a DC-Chol: DOPE ratio of 1:1 for 4 hrs, in the presence of MßCD. ***(a)*** *Luciferase knockdown of luc-siRNA-liposomes relative to the control (cells without MßCD), data represents the mean ± SD (N=2, n=3), **** Indicates the difference is a statistically significant ($p<0.0001$) compared to the control.* ***(b)*** *MFI and* ***(c)*** *'Luc-siRNA based MB' liposomes associated with cell population presented relative to the control (cells without MßCD). Flow cytometry data assessed by a Beckman Coulter MoFlo (minimum 10,000 cells/sample), and data represents the mean ± SD (N=2, n=3), **** Indicates the difference is a statistically significant ($p<0.0001$) compared to the control.* ***(d)*** *'Luc-siRNA based MB' liposomes fluorescence histograms profile assessed by a Beckman Coulter MoFlo (minimum 10,000 cells/sample). Untreated cells appear grey, luc-siRNA based MB liposomes appear blue and liposomes treated with MßCD appear red for three repeats.* ***(e)*** *Confocal microscopy micrographs of 'luc-siRNA based MB' liposomes in A549-Luc cells in the absence (upper micrographs) and presence (lower micrographs) of MßCD. 'Luc-siRNA based MB' liposomes appear green, whereas nuclei appear blue as they were stained with DRAQ5.*

5.3.5.4 Nystatin Inhibitor

5.3.5.4.1 Effect on cy3-siRNA-Liposomes` Cellular Uptake

Figure 5.18 shows the effect of inhibition of caveolae by sequestration of cholesterol using nystatin inhibitor (20 μg/ml) [20], on the cellular uptake of cy3-siRNA-liposomes in A549 cells. The flow cytometry results (Figure 5.18 a, b and c) demonstrate that nystatin significantly reduced the MFI level and cell population with cy3-siRNA-liposomes, relative to the control cells (cells without nystatin). Confocal micrographs (Figure 5.18 d) reveal the cytoplasmic, diffuse presence of cy3-siRNA fluorescence in some, while some cells show lack of visible cy3-siRNA.

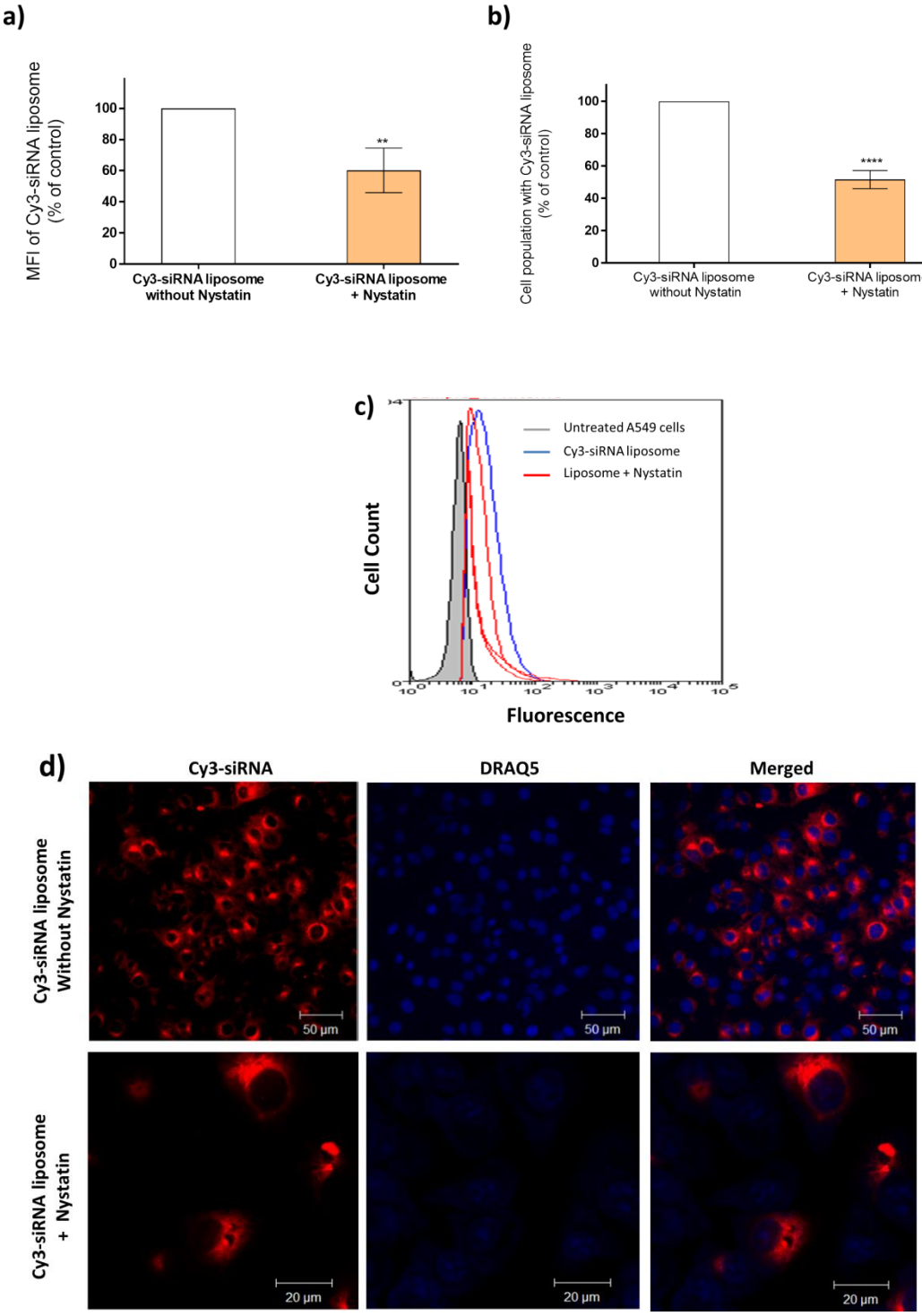

Figure 5.18: The effect of nystatin inhibitor on the internalisation of cy3-siRNA-liposomes in A549 cells

Nystatin (20 µg/ml) was pre-applied to cells for 30 min followed by exposure to cy3-siRNA-liposomes prepared at an N/P ratio of 3.125:1 and a DC-Chol:DOPE ratio of 1:1 for 4 hrs, in the presence of nystatin.
***(a)** MFI and **(b)** Cell population with cy3-siRNA-liposomes presented relative to the control (cells without nystatin). Flow cytometry data assessed by a Beckman Coulter MoFlo (minimum 10,000 cells/sample), and data represents the mean ± SD (N=2, n=3),*

*** and **** indicate the difference is statistically significant (p<0.01 and 0.0001, respectively) compared to the control.* ***(c)*** *Histograms cellular uptake profile of cy3-siRNA-liposomes assessed by a Beckman Coulter MoFlo (minimum 10,000 cells/sample). Untreated cells appear grey, cy3-siRNA-liposomes appear blue and liposomes treated with nystatin appear red for three repeats.* ***(d)*** *Confocal microscopy micrographs of cy3-siRNA-liposomes uptake in A549 cells in the absence (upper micrographs) and presence (lower micrographs) of nystatin. Cy3-siRNA-liposomes appear red, whereas nuclei appear blue as stained with DRAQ5.*

5.3.5.4.2 Effect on luc-siRNA-Liposomes` Luciferase Silencing

Figure 5.19 shows the effect of nystatin inhibitor (20 μg/ml) on the luciferase knockdown of luc-siRNA-liposomes. The results of the luciferase activity assay (Figure 5.19 a) show that the nystatin treatment did not have a significant effect ($p>0.05$) on the luciferase knockdown in A549-Luc cells, as the luciferase knockdown in the presence of the inhibitor was around 106% compared to the control cells (A549-Luc cells without nystatin). The data of flow cytometry (Figure 5.19 b, c and d) show that the 'luc-siRNA based MB' MFI levels and cellular association are similar in nystatin treated cells and the control cells (A549-luc cells incubated with 'luc-siRNA based MB' liposomes in the absence of nystatin). Confocal and z-stack micrographs of 'luc-siRNA based MB' in A549-luc cells (Figure 5.19 e and f) reveal an interesting appearance of green FAM-MB fluorescence. It appears to form 'doted rims' at a distance from cell nuclei. Such morphology was not seen for other inhibitors. The green fluorescence intensity of FAM-MB appears to be reduced post-nystatin application in comparison to control cells without inhibitor.

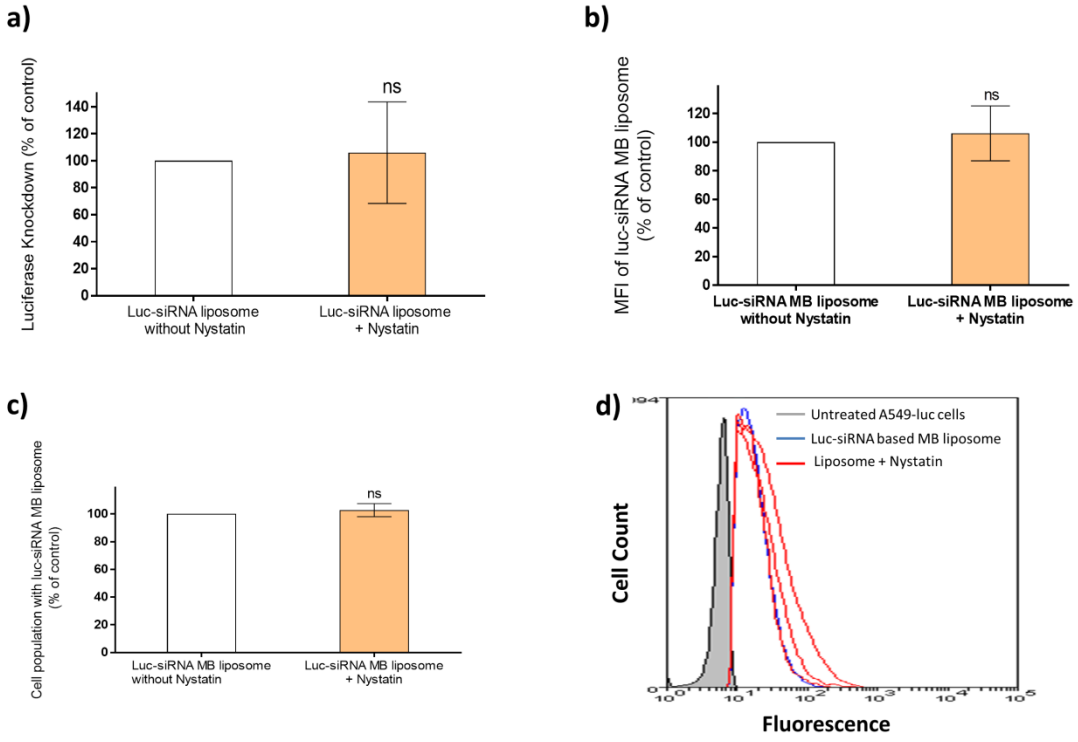
a)
Luciferase Knockdown (% of control)
140
120
100
80
60
40
20
0
ns
Luc-siRNA liposome without Nystatin
Luc-siRNA liposome + Nystatin
b)
MFI of luc-siRNA MB liposome (% of control)
120
100
80
60
40
20
0
ns
Luc-siRNA MB liposome without Nystatin
Luc-siRNA MB liposome + Nystatin
c)
Cell population with luc-siRNA MB liposome (% of control)
100
80
60
40
20
0
ns
Luc-siRNA MB liposome without Nystatin
Luc-siRNA MB liposome + Nystatin
d)
Untreated A549-luc cells
Luc-siRNA based MB liposome
Liposome + Nystatin
Cell Count
Fluorescence

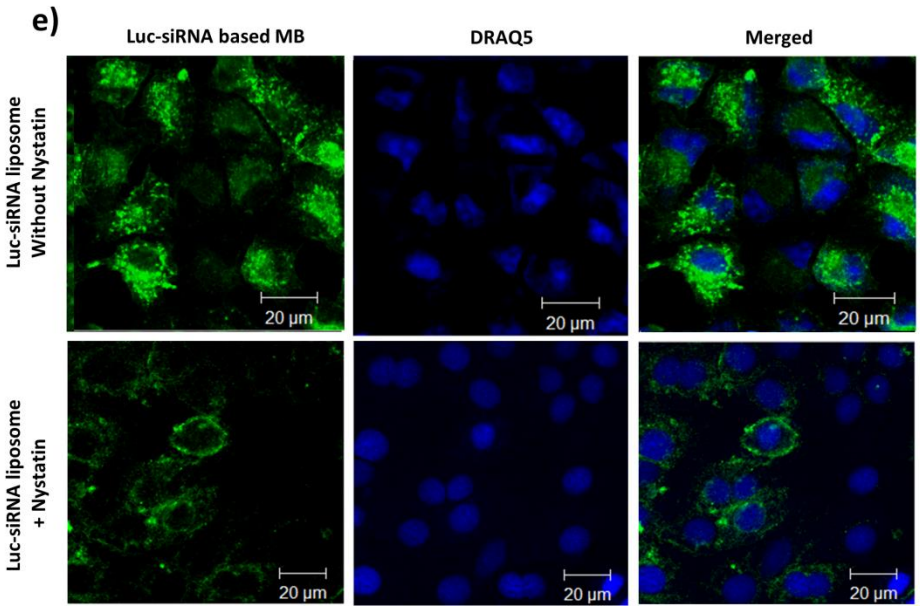
e)
Luc-siRNA based MB
DRAQ5
Merged
Luc-siRNA liposome Without Nystatin
Luc-siRNA liposome + Nystatin
20 µm

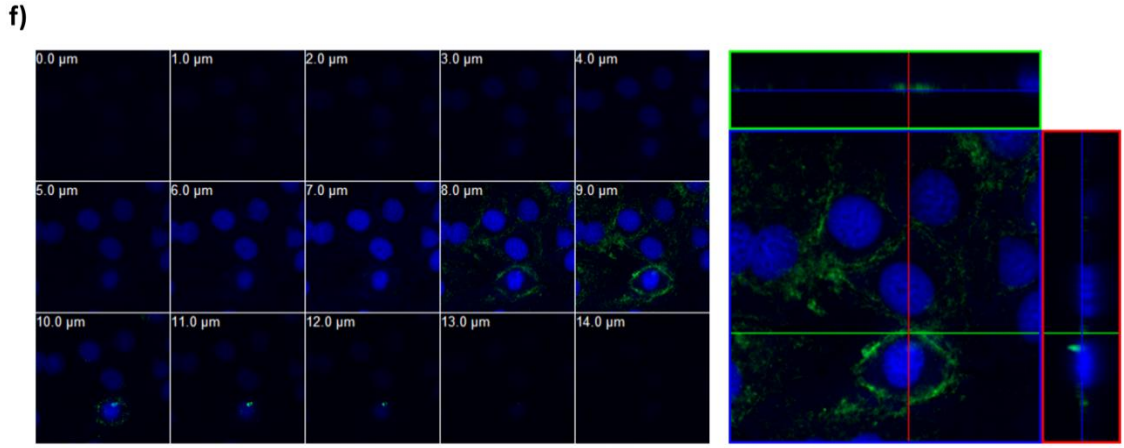

Figure 5.19: The effect of nystatin inhibitor on the luciferase knockdown of luc-siRNA-liposomes and 'luc-siRNA based MB' liposomes in A549-Luc cells

Nystatin (20 µg/ml) was pre-applied to cells for 30 min followed by exposure to luc-siRNA-liposomes and 'luc-siRNA based MB' liposomes prepared at an N/P ratio of 3.125:1 and a DC-Chol: DOPE ratio of 1:1 for 4 hrs, in the presence of nystatin. ***(a)*** *Luciferase knockdown of luc-siRNA-liposomes relative to the control (cells without nystatin), data represents the mean ± SD (N=2, n=3), ns indicates the difference is non-statistically significant (p>0.05) compared to the control.* ***(b)*** *MFI and* ***(c)*** *'Luc-siRNA based MB' liposomes associated with cell population presented relative to the control (cells without nystatin). Flow cytometry data assessed by a Beckman Coulter MoFlo (minimum 10,000 cells/sample), and data represents the mean ± SD (N=2, n=3), ns indicates the difference is non-statistically significant (p>0.05) compared to the control.* ***(d)*** *'Luc-siRNA based MB' liposomes fluorescence histograms profile of 'luc-siRNA based MB' liposomes assessed by a Beckman Coulter MoFlo (minimum 10,000 cells/sample). Untreated cells appear grey, luc-siRNA based MB liposomes appear blue and liposomes treated with nystatin appear red for three repeats.* ***(e)*** *Confocal microscopy micrographs of 'luc-siRNA based MB' liposomes in A549-Luc cells in the absence (upper micrographs) and presence (lower micrographs) of nystatin.* ***(f)*** *Z-stack of 'luc-siRNA based MB' liposomes fluorescence in the presence of nystatin. 'Luc-siRNA based MB' liposomes appear green, whereas nuclei appear blue as stained with DRAQ5.*

5.3.6 Role of Macropinocytosis

5.3.6.1 EIPA Inhibitor

5.3.6.1.1 Effect on cy3-siRNA-Liposomes` Cellular Uptake

EIPA inhibits Na^+/H^+ exchange and, consequently, lowers the sub-membranous pH of the cells [21], and it is used in the literature to investigate the role of macropinocytosis pathway. Figure 5.20 shows the effect of EIPA inhibitor (0.5, 1 and 2.5 μg/ml) on the uptake of cy3-siRNA-liposomes in A549 cells. The flow cytometry results in Figure 5.20 a, b and c show that EIPA was able to significantly reduce the MFI level and cell population with cy3-siRNA-liposomes at all the tested concentrations. Confocal micrographs of cy3-siRNA-liposome cellular uptake in A549 cells (Figure 5.20 d) illustrate that the red siRNA appears in the cytoplasmic region of few cells in the inspected sample, whereby the majority of the cells do not exhibit observable fluorescence.

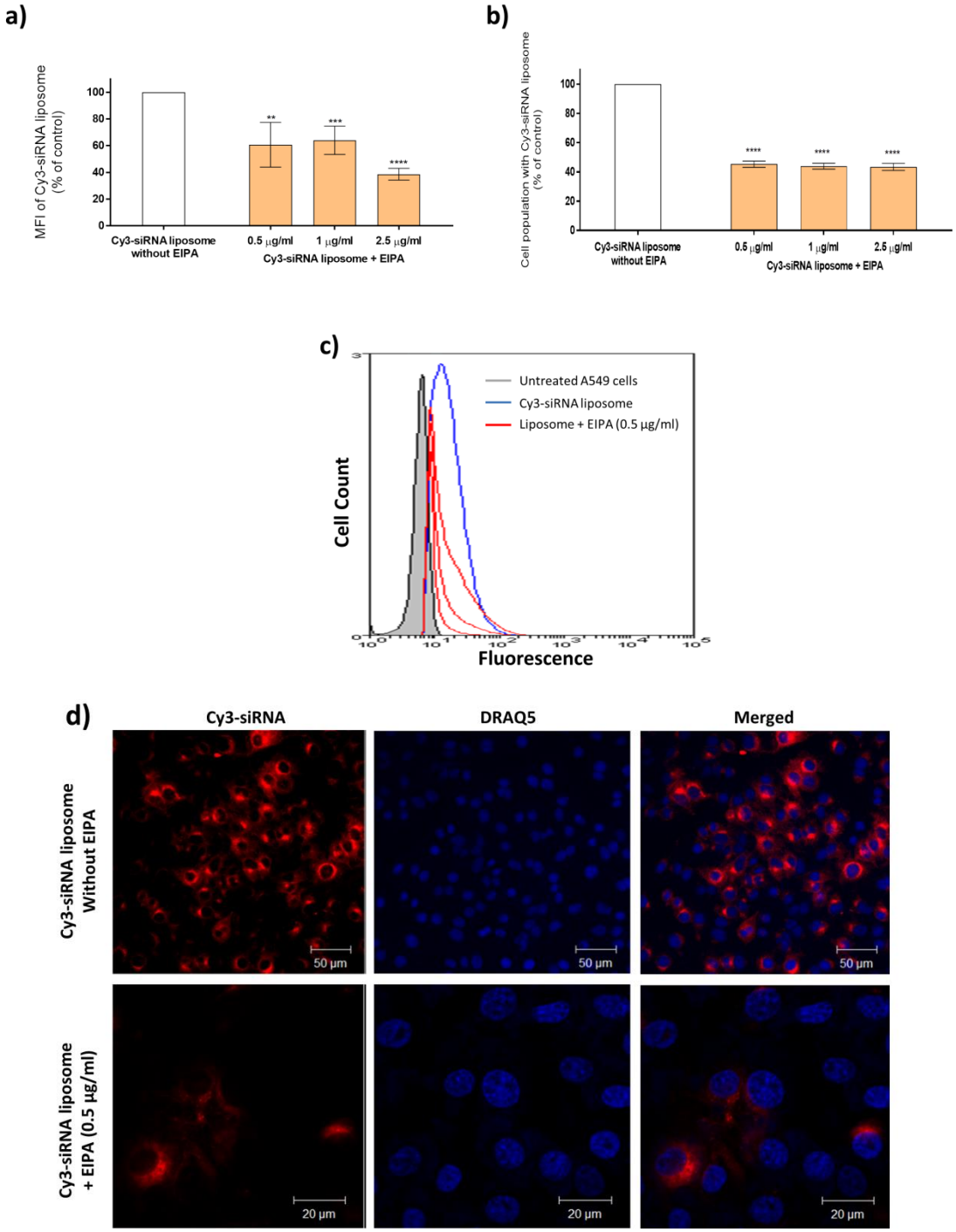

Figure 5.20: The effect of EIPA inhibitor on the internalisation of cy3-siRNA-liposomes in A549 cells

EIPA (0.5, 1 and 2.5 µg/ml) was pre-applied to cells for 30 min followed by exposure to cy3-siRNA-liposomes prepared at an N/P ratio of 3.125:1 and a DC-Chol:DOPE ratio of 1:1 for 4 hrs, in the presence of EIPA.
(a) *MFI and* ***(b)*** *Cell population with cy3-siRNA-liposomes presented relative to the control (cells without EIPA). Flow cytometry data assessed by a Beckman Coulter MoFlo (minimum 10,000 cells/sample), and data represents the mean ± SD (N=2, n=3), **, *** and **** indicate the difference is statistically significant (p<0.01, 0.001 and 0.0001, respectively) compared to the control.* ***(c)*** *Histograms cellular uptake profile of cy3-*

siRNA-liposomes assessed by a Beckman Coulter MoFlo (minimum 10,000 cells/sample). Untreated cells appear grey, cy3-siRNA-liposomes appear blue and liposomes treated with EIPA appear red for three repeats. ***(d)*** *Confocal microscopy micrographs of cy3-siRNA-liposomes uptake in A549 cells in the absence (upper micrographs) and presence (lower micrographs) of EIPA (0.5 μg/ml). Cy3-siRNA-liposomes appear red, whereas nuclei appear blue as stained with DRAQ5.*

5.3.6.1.2 Effect on luc-siRNA-Liposomes` Luciferase Silencing

Figure 5.21 shows the effect of EIPA inhibitor (0.5, 1 and 2.5 μg/ml) on the luciferase knockdown of luc-siRNA-liposomes in A549-Luc cells. At all applied concentrations, the luciferase activity assay (Figure 5.21 a) shows that EIPA had a dramatic effect ($p<0.0001$) on the luciferase knockdown. The luciferase knockdown in the presence of the inhibitor was around 2% (for 0.5 μg/ml) and 1% (for 1 and 2.5 μg/ml) compared to the control cells. The flow cytometry data (Figure 5.21 b, c and d) illustrate that EIPA reduced the MFI values and the cell population with 'luc-siRNA based MB' fluorescence significantly in comparison to the control cells (cells without EIPA). Confocal micrographs of the 'luc-siRNA based MB' in A549-Luc cells (Figure 5.21 e) show very reduced fluorescence of the FAM-MB (lower micrographs) compared to untreated A549-Luc cells (upper micrographs).

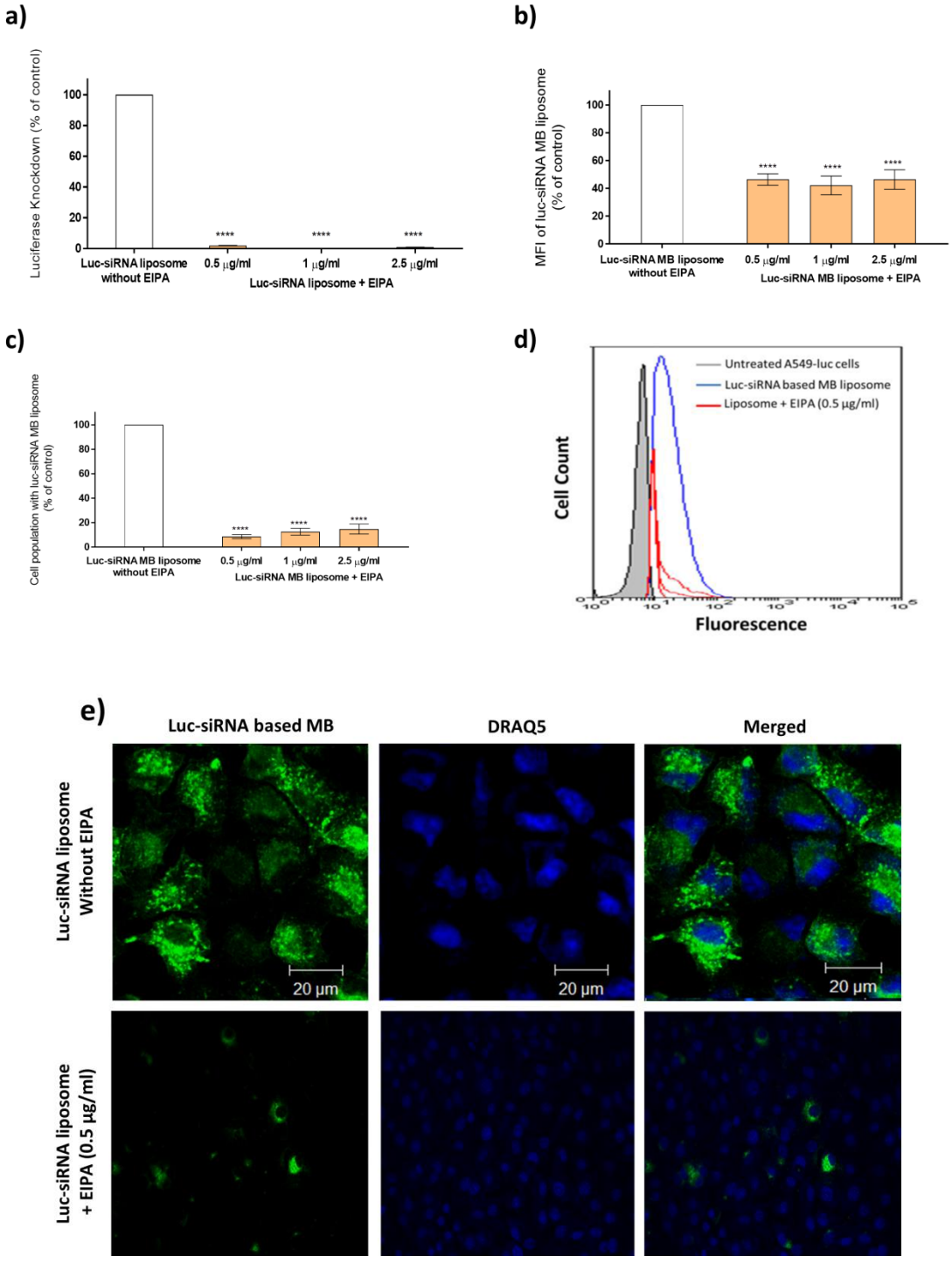

Figure 5.21: The effect of EIPA inhibitor on the luciferase knockdown of luc-siRNA-liposomes and 'luc-siRNA based MB' liposomes in A549-Luc cells

EIPA (0.5, 1 and 2.5 μg/ml) was pre-applied to cells for 30 min followed by exposure to luc-siRNA-liposomes and 'luc-siRNA based MB' liposomes prepared at an N/P ratio of 3.125:1 and a DC-Chol: DOPE ratio of 1:1 for 4 hrs, in the presence of EIPA.
(a)** Luciferase knockdown of luc-siRNA-liposomes relative to the control (cells without EIPA), data represents the mean ± SD (N=2, n=3), * Indicates the difference is a statistically significant ($p<0.0001$) compared to the control. **(b)** MFI and **(c)** 'Luc-siRNA*

*based MB' liposomes associated with cell population presented relative to the control (cells without EIPA). Flow cytometry data assessed by a Beckman Coulter MoFlo (minimum 10,000 cells/sample), and data represents the mean ± SD (N=2, n=3), **** Indicates the difference is a statistically significant (p<0.0001) compared to the control.* ***(d)*** *'Luc-siRNA based MB' liposomes fluorescence histograms profile assessed by a Beckman Coulter MoFlo (minimum 10,000 cells/sample). Untreated cells appear grey, luc-siRNA based MB liposomes appear blue and liposomes treated with EIPA appear red for three repeats.* ***(e)*** *Confocal microscopy micrographs of 'luc-siRNA based MB' liposomes in A549-Luc cells in the absence (upper micrographs) and presence (lower micrographs) of EIPA (0.5 μg/ml). 'Luc-siRNA based MB' liposomes appear green, whereas nuclei appear blue as stained with DRAQ5.*

5.3.6.2 Cytochalasin D Inhibitor

5.3.6.2.1 Effect on cy3-siRNA-Liposomes` Cellular Uptake

Figure 5.22 shows the effect of inhibition of macropinocytosis endocytosis by cytochalasin D (2, 4 and 6 μg/ml), which is an actin filament depolymerising agent [22], on the cellular uptake of cy3-siRNA-liposomes in A549 cells. The flow cytometry results (Figure 5.22 a, b and c) show that cytochalasin D had no significant effect on the MFI of cy3-siRNA-liposomes in A549 cells at a concentration 2 and 6 μg/ml, while at 4 μg/ml the MFI is slightly reduced. Also, cytochalasin D had no significant effect on the population of cy3-siRNA-liposomes associated A549 cells at a concentration of 4 and 6 μg/ml (~ 97% relative to the control cells, $p>0.05$), while at 2 μg/ml the effect is statistically significant, however reduction is only 10% relative to the control ($p<0.01$). The results of the flow cytometry were confirmed using confocal microscopy (Figure 5.22 d). Confocal micrographs show that the red labelled siRNA in the cytoplasmic region of the cells is of lower fluorescence in the presence of cytochalasin D (lower micrographs), compared to the control cells (upper micrographs).

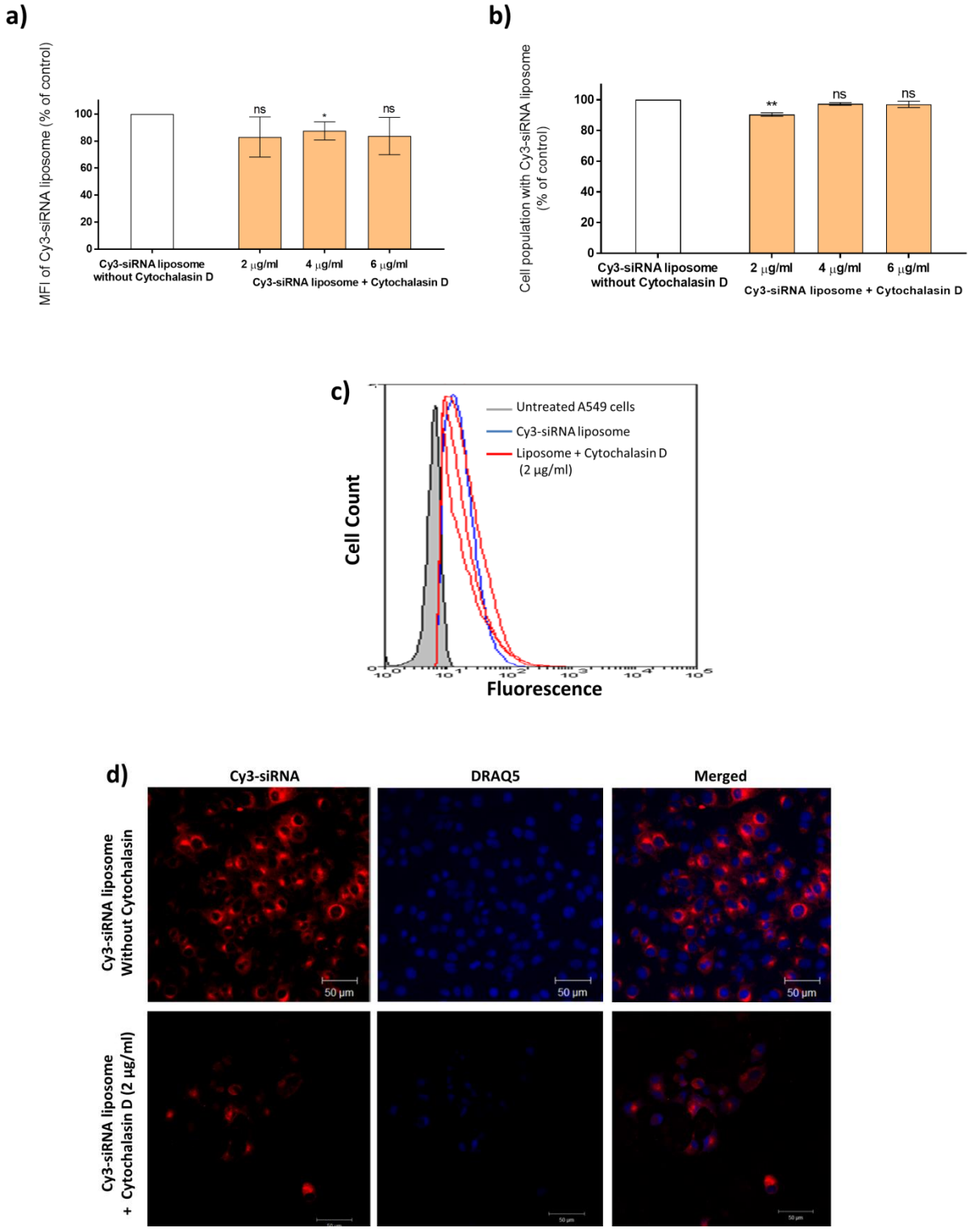

Figure 5.22: The effect of cytochalasin D inhibitor on the internalisation of cy3-siRNA-liposomes in A549 cells

Cytochalasin D (2, 4 and 6 μg/ml) was pre-applied to cells for 30 min followed by exposure to cy3-siRNA-liposomes prepared at an N/P ratio of 3.125:1 and a DC-Chol:DOPE ratio of 1:1 for 4 hrs, in the presence of cytochalasin D.

(a) *MFI and* ***(b)*** *Cell population with cy3-siRNA-liposomes presented relative to the control (cells without cytochalasin D. Flow cytometry data assessed by a Beckman Coulter MoFlo (minimum 10,000 cells/sample), and data represents the mean ± SD (N=2, n=3) ns indicates the difference is non-statistically significant (p>0.05) compared to the control, * and ** indicate the difference is statistically significant (p<0.05and 0.01, respectively) compared to the control.* ***(c)*** *Histograms cellular uptake profile of cy3-siRNA-liposomes assessed by a Beckman Coulter MoFlo (minimum 10,000 cells/sample). Untreated cells appear grey, cy3-siRNA-liposomes appear blue and liposomes treated with cytochalasin D appear red for three repeats.* ***(d)*** *Confocal microscopy micrographs of cy3-siRNA-liposomes uptake in A549 cells in the absence (upper micrographs) and presence (lower micrographs) of cytochalasin D (2 μg/ml). Cy3-siRNA-liposomes appear red, whereas nuclei appear blue as stained with DRAQ5.*

5.3.6.2.2 Effect on luc-siRNA-Liposomes` Luciferase Silencing

Figure 5.23 shows the effect of cytochalasin D inhibition (2, 4 and 6 μg/ml) on the luciferase knockdown of luc-siRNA-liposomes in A549-Luc cells. The luciferase activity assay data (Figure 5.23 a) show that cytochalasin D had no significant effect ($p>0.05$) on the luciferase knockdown. The luciferase silencing in the presence of the inhibitor was around 109% (for 2 μg/ml) and 120% (for 4 and 6 μg/ml) relative to the control cells (not treated with the inhibitor). The flow cytometry results in Figure 5.23 b, c and d illustrate the MFI values and the cell population with 'luc-siRNA based MB' fluorescence are not affected by the presence of inhibitor in comparison to the control cells (cells without cytochalasin D). Interestingly, confocal micrographs of the 'luc-siRNA based MB' in A549-Luc cells (Figure 5.23 e) reveal a very high levels of green fluorescence of the FAM-MB in some cells in the sample, whilst other cells do not seem to show observable fluorescence, indicating heterogeneity in the cell population not seen in the flow cytometry data.

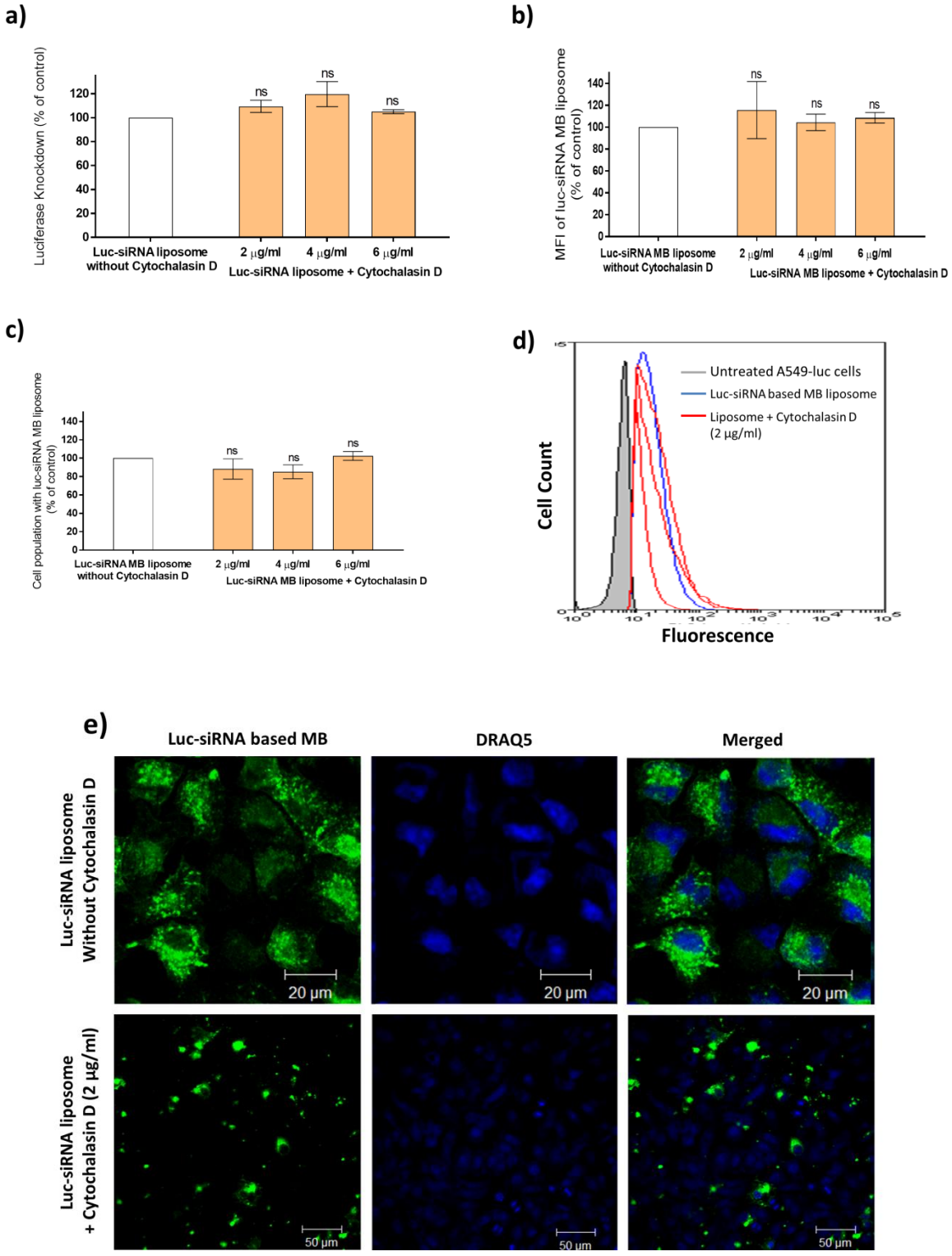

Figure 5.23: The effect of cytochalasin D inhibitor on the luciferase knockdown of luc-siRNA-liposomes and 'luc-siRNA based MB' liposomes in A549-Luc cells

Cytochalasin D (2, 4 and 6 μg/ml) was pre-applied to cells for 30 min followed by exposure to luc-siRNA-liposomes and 'luc-siRNA based MB' liposomes prepared at an N/P ratio of 3.125:1 and a DC-Chol: DOPE ratio of 1:1 for 4 hrs, in the presence of cytochalasin D.

(a) *Luciferase knockdown of luc-siRNA-liposomes relative to the control (cells without cytochalasin D), data represents the mean ± SD (N=2, n=3), ns indicates the difference is non-statistically significant (p>0.05) compared to the control.* ***(b)*** *MFI and* ***(c)*** *'Luc-siRNA based MB' liposomes associated with cell population presented relative to the control (cells without cytochalasin D). Flow cytometry data assessed by a Beckman Coulter MoFlo (minimum 10,000 cells/sample), and data represents the mean ± SD (N=2, n=3), ns indicates the difference is non-statistically significant (p>0.05) compared to the control.* ***(d)*** *'Luc-siRNA based MB' liposomes fluorescence histograms profile of 'luc-siRNA based MB' liposomes assessed by a Beckman Coulter MoFlo (minimum 10,000 cells/sample). Untreated cells appear grey, luc-siRNA based MB liposomes appear blue and liposomes treated with cytochalasin D appear red for three repeats.* ***(e)*** *Confocal microscopy micrographs of 'luc-siRNA based MB' liposomes in A549-Luc cells in the absence (upper micrographs) and presence (lower micrographs) of cytochalasin D (2 µg/ml). 'Luc-siRNA based MB' liposomes appear green, whereas nuclei appear blue as stained with DRAQ5.*

5.3.7 Role of Endosomolytic Agent: Chloroquine

5.3.7.1 MTS Assay of Cell Viability on A549-Luc Cells

Chloroquine is an endosomolytic agent that inhibits the acidification of endosomal vesicles by its osmotic effect and therefore disrupts vesicles [23]. This agent is commonly used to confirm the involvement of endosomal vesicles in the internalisation process of nanoparticles. Before exploring the effect of chloroquine on the cellular internalisation of luc-siRNA-liposomes, MTS toxicity test was conducted to determine the optimal concentration of chloroquine that is not toxic to A549-Luc cells for the duration of the 4 hrs of the liposomes treatment assay. Dose response curves (Figure 5.24) indicated that the EC_{50} is approximately 286 μg/ml.

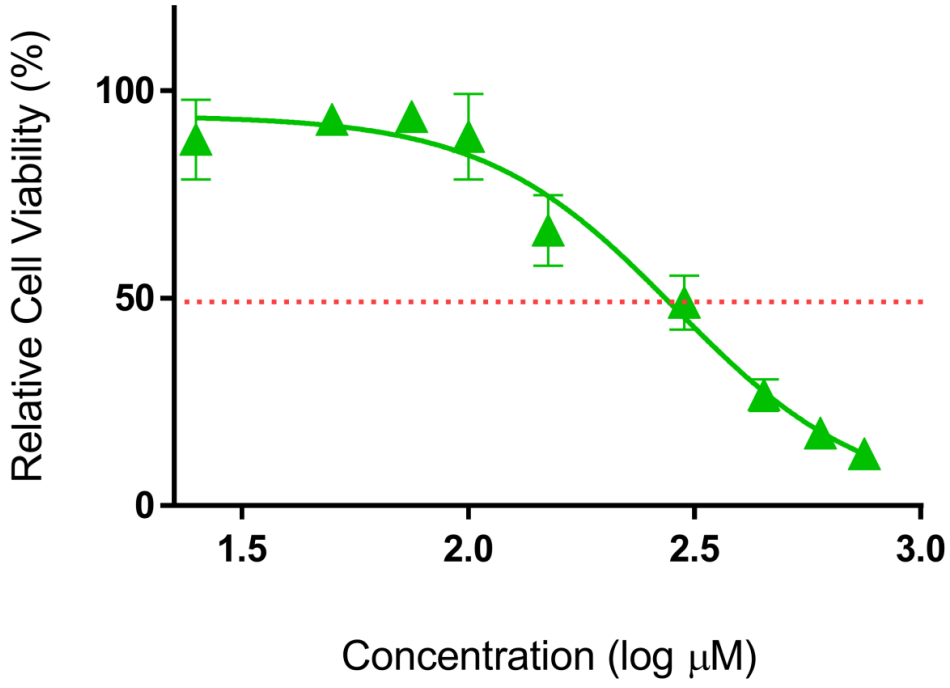

Figure 5.24: Dose-response curves showing percentage relative cell viability of chloroquine after incubation for 4 hrs with A549-Luc cells

Data are the results of an MTS assay and are expressed as relative cell viability and presented as the mean ± SD (N=3, n=6). Dose response curves were generated using GraphPad Prism (v6).

5.3.7.2 Effect on luc-siRNA-Liposomes` Luciferase Silencing

Chloroquine effect is normally investigated in cases of predominately clathrin route of endocytosis leading to entrapment of material in endosomes and consequent lysosomal deposition. Figure 5.25 shows the effect of chloroquine (100 μg/ml) on the luciferase knockdown by luc-siRNA-liposomes in A549-Luc cells. The data (Figure 5.25 a) clearly demonstrate that chloroquine treatment significantly doubled the luciferase knockdown, relative to knockdown in the cells not treated with chloroquine. This would indicate a significant importance of endosomal/ lysosomal trafficking route in the liposomes internalisation in A549 cells. The MFI data in Figure 5.25 b which were determined relative to the MFI value of negative control (A549-luc cells not treated with chloroquine), and results show that approximately 7 fold increases in fluorescence signal of the 'luc-siRNA based MB' in comparison to control. Confocal micrographs of the luc-MB in A549-Luc cells (Figure 5.25 d) show an interesting presentation of the green fluorescence of the FAM-MB in the chloroquine treated cells. The rims of green colour, somewhat removed from the perinuclear region, can be seen together with some punctate fluorescence.

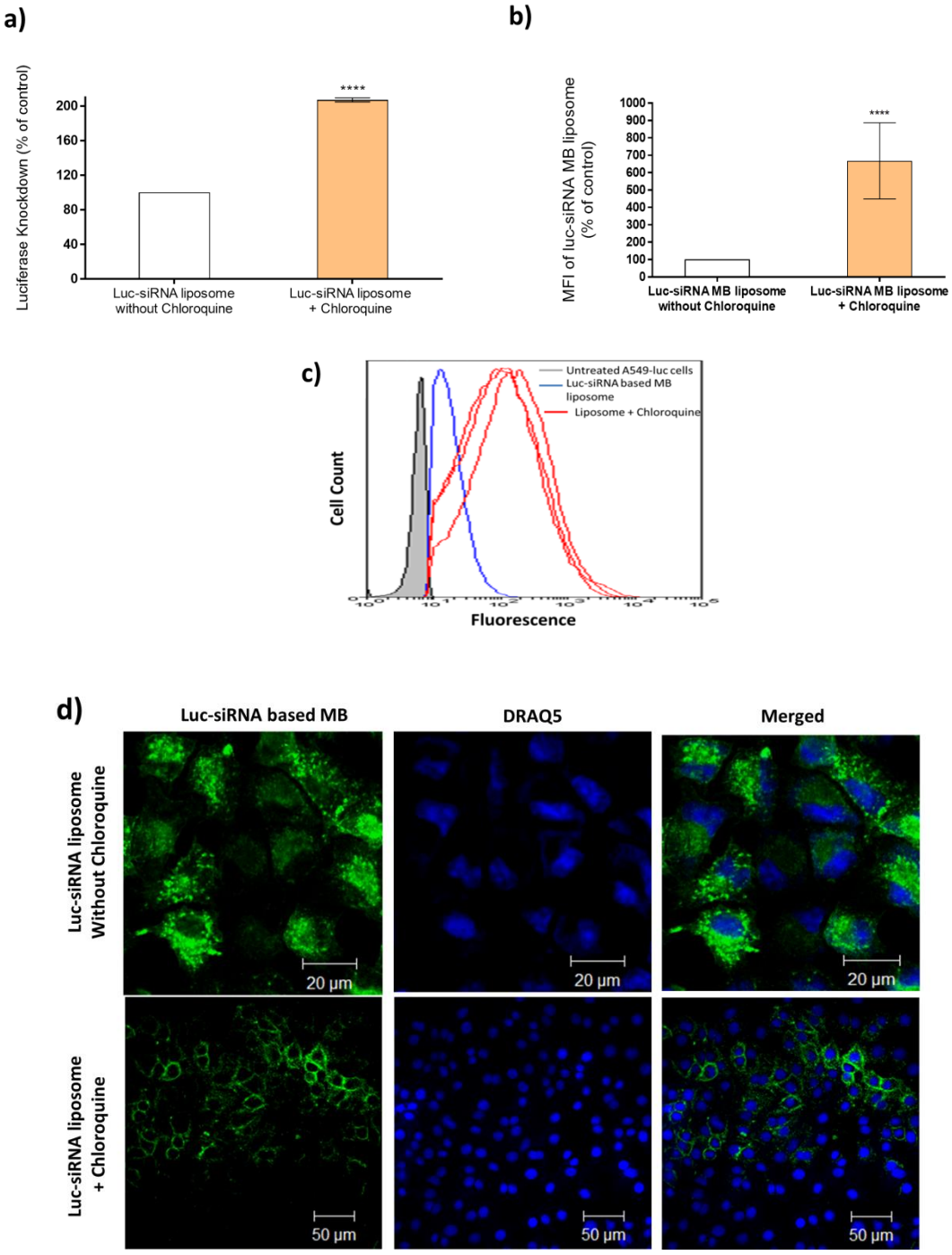

Figure 5.25: The effect of endosomolytic agent, chloroquine on the luciferase knockdown of luc-siRNA-liposomes and 'luc-siRNA based MB' liposomes in A549-Luc cells

Chloroquine (100 µg/ml) was pre-applied to cells for 30 min followed by exposure to luc-siRNA-liposomes and 'luc-siRNA based MB' liposomes prepared at an N/P ratio of 3.125:1 and a DC-Chol: DOPE ratio of 1:1 for 4 hrs, in the presence of chloroquine. ***(a)*** *Luciferase knockdown of luc-siRNA-liposomes relative to the control (cells without chloroquine), data represents the mean ± SD N=2, n=3), **** Indicates the difference is a statistically significant ($p<0.0001$) compared to the control.* ***(b)*** *MFI of 'Luc-siRNA*

*based MB' liposomes presented relative to the control (cells without chloroquine). Flow cytometry data assessed by a Beckman Coulter MoFlo (minimum 10,000 cells/sample), and data represents the mean ± SD (N=2, n=3), **** Indicates the difference is a statistically significant (p<0.0001) compared to the control.* ***(c)*** *'Luc-siRNA based MB' liposomes fluorescence histograms profile of 'luc-siRNA based MB' liposomes assessed by a Beckman Coulter MoFlo (minimum 10,000 cells/sample). Untreated cells appear grey, luc-siRNA based MB liposomes appear blue and liposomes treated with chloroquine appear red for three repeats.* ***(d)*** *Confocal microscopy micrographs of 'luc-siRNA based MB' liposomes in A549-Luc cells in the absence (upper micrographs) and presence (lower micrographs) of chloroquine. 'Luc-siRNA based MB' liposomes appear green, whereas nuclei appear blue as stained with DRAQ5.*

Table 5.3: Summary of the quantitative effect of pharmacoligical inhibitors on endocytosis pathways.

Inhibitors	Effect on cellular uptake (Flow cytometry)	Effect on luciferase silencing (Luciferase assay)	Effect on MB engagement with luc-mRNA (Flow cytometry)
Concanavalin A	ns (p>0.05)	ns (p>0.05)	ns (p>0.05)
Chlorpromazine	↓ (p<0.01)	↓ (p<0.0001)	↓ (p<0.0001)
Dynasore	ns (p>0.05)	↓ (p<0.0001)	↓ (p<0.001)
Genistein	ns (p>0.05)	ns (p>0.05)	ns (p>0.05)
Filipin	↓ (p<0.01)	ns (p>0.05)	ns (p>0.05)
MßCD	↓ (p<0.0001)	↓ (p<0.0001)	↓ (p<0.0001)
Nystatin	↓ (p<0.01)	ns (p>0.05)	ns (p>0.05)
EIPA	↓ 2.5 µg/ml (p<0.0001) ↓ 1 µg/ml (p<0.001) ↓ 0.5 µg/ml (p<0.01)	↓ (p<0.0001)	↓ (p<0.0001)
Cytochalasin D	↓ at 4 µg/ml (p<0. 05)	ns (p>0.05)	ns (p>0.05)
Chloroquine **(Endosomolytic agent)**	-	↑ (p<0.0001)	↑ (p<0.0001)

*** ns (**no significant effect**), ↓ (**significant inhibition**), and ↑ (**significant increase**).**

5.4 Discussion

To date, the cellular internalisation pathways of siRNA-liposomes has not been extensively studies and more systematic studies are needed to provide better understanding [31]. Recent work has reported that siRNA-liposomes enter cells via endocytosis pathways [32]–[34]. More specifically, it has been stated that cationic liposomes (containing helper lipid) are internalised by the clathrin-mediated pathway, leading to successful gene knockdown due to the interaction of positively charged lipids with the anionic components of endosomal membrane that leads to the material escape from endosomal vesicles [35]. However, it has been highlighted that the caveolae-mediated pathway plays an essential role in successful gene delivery due to avoiding the 'entrapment' in endosomes and lysosomes [13], [36]. Another investigations of siRNA-liposomes add to complexity by demonstrating that the internalisation pathway of any delivery system depends on the cell line type used [13], [37], [38]. Therefore, the actual mechanisms by which siRNA-liposomes internalise into the alveolar epithelium are poorly defined in literature.

To explore which mechanism of endocytosis is responsible for the internalisation and trafficking of a gene delivery vectors, pharmacological inhibitors of endocytosis is a commonly used approach [39], [40]. There are a number of advantages in using this approach, such as the ease of application (cells treatment) and the fact that their influence can be simply measured. However, the cytotoxic effect of inhibitors is one of the main draw backs, although this is mainly dependent upon cell type and the concentration applied [15]. Additional approaches that can be used to examine the mechanism of endocytosis include the use of dominant-negative mutants and RNA interference technology to compete with and downregulate the expression of endogenous proteins

involved in endocytosis [41]. These technologies are theoretically advantageous, however they are complex to perform, and very few studies are reported the use of these approaches to study cellular internalisation of nanoparticles. Consequently, multiple inhibitors were used in this work for each pathway in order to be able to consider the selectivity of some inhibitors on the endocytosis pathway.

Before investigating the mechanism of endocytosis of a siRNA-liposome delivery system, it is essential to examine the cytotoxicity effect of the selected inhibitors on A549 and A549-Luc cells in order to determine the non-toxic concentrations of inhibitors. Cell viability was examined after 4 hrs exposure to the endocytosis inhibitors; concanavalin A, chlorpromazine, dynasore, genistein, filipin, MßCD, nystatin, EIPA and cytochalasin D. The concentrations range of inhibitors applied were nearly similar to those reported in other endocytosis studies [15], [42], [43]. It is clear from the results of the MTS screening presented in Sections 5.3.1.1 and 5.3.1.2 that the cellular viability of both cell lines decreased with an increase in the concentration of inhibitors, and non-toxic doses of the inhibitors were used in the subsequent investigations.

It was also necessary to investigate the specificity of clathrin and caveolin pathways inhibitors against the 'classical' pathway ligands and determine the optimal sub-EC_{50} concentrations that produce successful pathway inhibition in A549 and A549-Luc cells. A549 cells are known to express clathrin and caveolin-1 protein, which are essential for the formation of clathrin and caveolae coated pits and invaginations, and hence A549 cells should be capable of clathrin and caveolae-mediated endocytosis [28]. To this end, the inhibitory effect of selected inhibitors were examined in A549 and A549-Luc cells to evaluate the cellular uptake of two classical ligands, T*f* and CTß, which are reported in

the literature as being internalised selectively into cells through clathrin and caveolin-mediated endocytosis, respectively [44]. The cholera toxin ligand used in this work is a recombinant version of the B subunit only, which free of the cytotoxic A subunit. The B subunit has been shown to be non-toxic to cells in culture and possesses no intrinsic adenylate cyclase activity in the absence of the A subunit [45]. Effect of all the selected inhibitors on internalisation of the endocytosis markers was tested, except for EIPA and cytochalasin D, which are reported to be involved in the macropinocytosis mechanism. It should be noted that dextran, commonly used in the literature as a macropinocytosis marker, has been reported not to be a solely specific ligand for this internalisation pathway [46]. Therefore, EIPA and cytochalasin D inhibitors were used at three different sub-EC_{50} concentrations to investigate cy3-siRNA-liposome cellular uptake and luc-siRNA-liposome luciferase knockdown.

The cellular uptake of Alexa fluor 488 T*f* in the presence of concanavalin A (100 μg/ml) and chlorpromazine (20 μg/ml) were inhibited significantly in both A549 and A549-Luc cells. These results are in agreement with published data that have demonstrated that high inhibition of T*f* internalisation can be achieved by clathrin-mediated endocytosis inhibitors, concanavalin A and chlorpromazine in monkey kidney fibroblast-like cell line (Cos-7) [47]. Moreover, it is clear from the current data that the inhibitory effect is increased with a corresponding increase in the concentration of inhibitors; a maximum effect was achieved with the concentrations shown above.

For cells treated with dynasore (20 μg/ml), the internalisation of both T*f* and CTß was decreased significantly in both A549 cells and A549-Luc cells. Dynasore has been identified to be involved in the inhibition of the 'pinch off' of clathrin and caveolin

coated pits from the cell membrane by blocking the GTPase activity of dynamin, and hence dynamin-dependent endocytosis in cells [48], [49]. It has been reported that the uptake, trafficking, and intracellular accumulation of transferrin and cholera toxin were all strongly blocked in HeLa and BSC1 cells, respectively, pre-incubated for 30 min with dynasore inhibitor [16]. Similar to concanavalin A and chlorpromazine, the inhibitory effect is increased with a corresponding increase in the concentration of dynasore; a maximum effect was achieved with 20 μg/ml.

The internalisation of CTß was reduced significantly in the presence of caveolae-mediated endocytosis inhibitors: genistein (15 μg/ml), filipin (20 μg/ml), MßCD (300 μg/ml) and nystatin (20 μg/ml) in both A549 cells and A549-Luc cells. Genistein has been reported to be involved in the inhibition of the caveolae-dependent pathway and is a tyrosine kinase inhibitor, therefore inhibiting caveolae pinching [17]. Research by Torgersen *et al.* stated that when CHC cells were incubated with the tyrosine kinase inhibitor genistein (100 μg/ml), the uptake of CTß was reduced by 35% [26]. Filipin, MßCD and nystatin are also reported to inhibit the same pathway (and lipid rafts) through cholesterol binding and depletion from the cell membrane forming inclusion complexes [30], [40], [44]. Treating Caco-2 cells with filipin inhibitor shows that 33% of CTß was internalised by filipin-treated cells within 1 hr [50]. It has been reported that the treatment of Caco-2 cells with MβCD resulted in a significant reduction in CTß cellular uptake [26]. Nystatin inhibitor demonstrated to inhibit the internalisation of CTß in MDCK, and Calu-1 cells [51]. In agreement with the inhibitors of clathrin and dynamin dependent pathways, the inhibitory effect of caveolae-mediated endocytosis inhibitors is concentration dependent; a maximum effect was achieved with the concentrations shown above.

Based on the results of the MTS screening and the uptake of pathways markers using A549 and A549-Luc cells, concentrations of the inhibitors were selected for use in investigating the mechanism of endocytosis of siRNA-liposomes. These concentrations show a low cytotoxic effect with a significant inhibition of specific ligands, and are summarised in Table 5.2.

To investigate the internalisation and trafficking pathways followed by siRNA-liposomes, a panel of endocytic inhibitors were applied for each endocytosis pathway in order to increase the significance of the study and to enable the consideration of the different mechanisms involved in each pathway. Concanavalin A is a lectin that interferes with the signalling of transmembrane G protein-coupled receptors located on the surface of cells [41], and therefore prevents the assembly of clathrin coated pits and impairs their movement through the cell membrane [14]. Chlorpromazine is clathrin-dependent endocytosis inhibitor which is used to inhibit clathrin coated pit formation through reversible translocation of clathrin and its adapter proteins from the plasma membrane to intracellular vesicles [15], [52]. Applying two clathrin-mediated inhibitors to examine the uptake and trafficking routes followed by cy3-siRNA or luc-siRNA-liposomes in A549 and A549-Luc cells, respectively, showed apparently contradictory results.

Regarding concanavalin A (100 μg/ml) flow cytometry data show that concanavalin A-mediated inhibition of clathrin-dependent endocytosis had no significant effect on the uptake of the liposomes and on luciferase knockdown. However, the confocal micrographs revealed an apparent reduction in the fluorescence intensity of cy3-siRNA and FAM-MB fluorescence on incubation of A549 and A549-Luc cells, respectively, with

concanavalin A. The reason behind the contradiction between flow cytometry data and confocal images is not clear at this stage. It should be emphasized here that confocal microscopy was conducted only on one sample for each inhibitor applied (as *per* work and cost burden of this analysis), and that additional measurements will be essential to validate the results of cellular uptake and MB fluorescence. On the contrary, flow cytometry experiments were repeated on at least three separate occasions and a minimum of 10,000 cells were analysed for each sample, making this analysis more representative.

Regarding chlorpromazine inhibition of clathin, it showed, in contrast to the results of concanavalin A, a significant inhibition of cy3-siRNA cellular uptake, as well as MB fluorescence and luciferase silencing in A549 and A549-Luc cells, respectively. Moreover, lower fluorescence intensity of both cy3-siRNA and FAM-MB has been found on chlorpromazine treatment under confocal microscope examination, in comparison to control cells without inhibitor, confirming the effect of chlorpromazine on clathrin pathway. The chlorpromazine data would therefore suggest that siRNA-liposomes internalization employs clathrin-mediated entry route in A549 cells.

The effect of both inhibitors on the internalisation of nanoparticles has been reported in a number of studies, but variable results depending on applied nanoparticles and cell lines used makes a comparison difficult. Concanavalin A application (100 μg/ml) reduced the cell internalisation of siRNA-polyplexes in A549 cells to approximately 50% of untreated cells [13]. In case of chlorpromazine, it has been reported that the internalisation of FITC-albumin and DOTAP lipoplex was reduced in the presence of inhibitor in A549 cells [44], [53]. However, to the best of our knowledge, there is no report that uses both of these inhibitors in one study that can be compared with the current data. We hypothesise that

the different effects of these two inhibitors shown in this study could possibly be due to different mechanisms they use to affect the clathrin-mediated pathway but a further investigation is needed to confirm that.

Our results suggest that the incorporation of an endosomolytic agent into the siRNA delivery system where the dominant cellular internalisation pathway involves clathrin may be beneficial to supplement the silencing efficiency, but such functionality could be purposeless in non-clathrin cell internalisation pathways. Chloroquine is a endosomolytic agent that prevents endosome acidification and facilitates endosomal escape of delivery systems [23], and it was used in this work to explore its influence on the luciferase knockdown. Chloroquine has been proved to facilitate the disruption of endosomal vesicles and therefore the escape of nanoparticles from acidic compartments into the cytoplasmic region of cells. The level of luciferase silencing increased significantly in the presence of chloroquine in comparison to control A549-Luc cells. Data thus indirectly point to a principally clathrin-mediated internalisation of siRNA-liposomes by A549 cells, whereby the silencing efficiency is enhanced by the endosomolytic action of chloroquine. It has been reported that chloroquine promoted endosomal escape and increases the transfection efficiency of a Tat-lipid nanocarrier in MC3T3-E1 cells (mouse preosteoblasts) [54]. Cellular internalisation of siRNA-polyplexes in Calu-3 post-chloroquine treatment shows a significant increase in the silencing efficiency, from 33% to 66% of the control in Calu-3 [13].

Dynamin protein plays an important function in the regulation of both clathrin and caveolae-mediated pathways of endocytosis. It is involved in the newly formed intracellular invagination to pinch off from the cell membrane and form intracellular

vesicles [55]. Dynasore inhibits the GTPase activity of dynamin and therefore prevents the release of clathrin- and caveolin-coated vesicles [48]. The effect of dynasore (20 μg/ml) on the uptake of siRNA-polyplexes in A549 cells has been investigated and result reported that dynasore reduced the internalisation of polyplexes significantly in A549 cells [13]. The data of flow cytometry and confocal microscopy presented demonstrate no significant reduction in the uptake of cy3-siRNA-liposomes in A549 cells. However, the data for the luciferase knockdown showed that dynasore had a significant effect on the silencing activity, showing by significant reduction of luciferase silencing and lower fluorescence intensity of FAM-MB under the microscope. The apparent contradiction of these results on the effect of dynasore on cy3-siRNA uptake and luciferase silencing may actually indicate the luc-siRNA-liposomes are internalised by the cells but that the formed endosomal vesicles was 'stuck' to the cell membrane, whereby small amount of siRNA/liposomes was able to escape the vesicles and bind the cytoplasmic mRNA to perform the knockdown activity. The data for MB-liposomes indeed indicate engagement of the beacon siRNA to cytoplasmic target mRNA (Figure 5.11). It should be also noted that Andar *et al.* reported that liposomes with a hydrodynamic diameter larger than 40 nm are usually not affected by the inhibition of the dynamin-dependent pathway [56], the phenomenon that was confirmed in the current study (liposomes of approximately 200 nm in diameter).

Inhibition of the caveolae-mediated pathway has been investigated in this work via suppression of the enzyme protein tyrosine kinase using genistein inhibitor, which interferes with lipid raft dependent endocytosis within the caveloin pathway [39]. It is important to note that the intracellular trafficking pathway following caveolae-mediated endocytosis within a cell is much less well understood than the clathrin-mediated

mechanism and is subject to controversy within the literature [30]. The caveolar pathway has been proposed to be advantageous over the clathrin-mediated pathway due to the avoidance of the acidic environment of endosomal vesicles and lysosomes following clathrin uptake [57]. Caveolae 'pinch off' to form pH neutral, non-degradative endocytic organelles known as caveosomes [57]. It has been reported that caveolae pathway is involved in the uptake of liposomes, as judged from decrease the internalisation of lipoplexes in the presence of genistein in Hep-2 cell line [58]. Moreover, the genistein inhibitor exhibited a significant reduction on the internalisation and transfection of PEI polyplexes in both A549 and HeLa cells [53]. Additional study on A549 cells showed significant reduction on the internalisation of siRNA-polyplexes in the presence of genistein by approximately 35% relative to untreated cells [15]. In contrast, a study by Rejman *et al.* reported that genistein had no significant effect on the internalisation and transfection of DOTAP lipoplexes in A549 and HeLa cells [53], and suggested that the caveolae-dependent pathway did not play an essential role in the transmembrane transport of liposome delivery systems. The results from current work show that genistein exhibited no significant reduction in the cellular uptake of cy3-siRNA and in luciferase knockdown by luc-siRNA-liposomes. The data further show similar levels of fluorescence to untreated cells and clear presence of green fluorescence of luc-siRNA-MB-liposomes in cytoplasm of A549-Luc cells indicating luc-siRNA-MB engagement with target mRNA, as confirmed using flow cytometry and confocal microscopy. We hypothesise that the contradictory effects of genistein reported in literature indicate that the involvement of caveolae-mediated pathway on the internalisation of nanoparticles could be mainly dependent on the nature of delivery system applied as well as the type of cells used to perform the *in vitro* study [13].

Caveolae are invaginations of the plasma membrane that are believed to be localised in lipid rafts which are rich in cholesterol [59]. Cholesterol is considered essential for caveolae-mediated endocytosis and is also important for the clathrin-mediated pathway and macropinocytosis. Hence, although cholesterol depletion approach is often used strategy to investigate the caveolae-mediated and lipid raft mediated pathways; one needs to be cautions of other effects on the cells that this treatment may elicit. A number of inhibitors have been reported in the literature as depleting cholesterol from the plasma membrane, through extraction of cholesterol from lipid rafts, such as MβCD [55] or by interacting with cholesterol, such as filipin and nystatin. MβCD is a cyclic hepta-saccharide cholesterol-solubilising agent that can remove cholesterol from the plasma membrane by forming soluble cholesterol inclusion complexes [60], thus changing the structure of cholesterol rich domains within the membrane [61]. Hauth *et al.* reported that cellular uptake of liposomes was significantly reduced in the presence of MβCD in two cell lines, COS-7 and HUVEC [62]. In the current work, cellular internalisation and luciferase silencing effect were both significantly reduced in the presence of MβCD, although the stronger effect on the silencing is evident and further confirmed using luc-siRNA-MB-liposomes which show low levels of siRNA engagement with target siRNA in both flow cytometry and confocal microscopy. The results would hence indicate an important role of cholesterol rich domains within the membrane and lipid raft associated pathway on the endocytosis internalisation mechanism of siRNA-liposomes.

Filipin is a polyene antibiotic and interacts with 3-h-hydroxysterols, such as cholesterol, in the plasma membrane to form filipin-sterol complexes [62]. Filipin is considered a specific inhibitor for the caveolae pathway and its mechanism of action does not involve interference with cholesterol present within clathrin coated pits [63]. Nystatin is a

selective lipid raft/caveolae pathway inhibitor that profoundly disrupts the structure and functions of cholesterol rich membrane domains by binding to cholesterol within the plasma membrane [20]. A study on DOTAP/DNA lipoplexes demonstrated that filipin had no significant effect on internalisation in A549 and HeLa cells [64]. Another study using COS-7 and HUVEC cell lines, indicated that incubating the cells with filipin for 60 min pre-addition of the liposomes decreased uptake in both cell lines, but a 30 min pre-incubation did not result in an equivalent response, implying that the effect of some inhibitors are rapidly reversible and the incubation time may depends on inhibitors applied and the type of cell line [62]. Applying filipin and nystatin inhibitors to A549 cells in the current study showed a statistically significant decrease in cy3-siRNA-liposome internalisation and low fluorescence of red cy3-siRNA, but to a lesser extent when compared to MβCD. Interestingly, no significant influence for either inhibitor was noted on the luciferase knockdown in A549-Luc cells. These inhibitors also did not show significant reduction in level of luc-siRNA-MB fluorescence in the cells (flow cytometry data), although the confocal microscopy images illustrate an interesting fluorescence distribution in the cells. These together would indicate that 'maximum' level of cellular uptake of the liposomes is not crucial to perform similar level of siRNA engagement with target luciferase mRNA and protein silencing activity. The results demonstrate the involvement of cholesterol rich domains within the membrane on the cellular internalisation pathway of siRNA-liposomes.

The macropinocytosis mechanism of endocytosis was investigated in this work using EIPA and cytochalasin D inhibitors [65]. EIPA is a specific inhibitor of macropinocytosis through inhibition of Na^+/H^+ exchange and reducing the sub-membranous pH [66]. EIPA makes the sub-membrane cell cytoplasm more alkaline, and this leads to the

disappearance of ruffles and a decrease in the fluid phase mediated cell uptake [21]. It has been reported that the internalisation of liposomes was reduced significantly after blocking the macropinocytosis pathway in murine bladder tumour cells (MBT-2) using EIPA [66]. In contrast, Ruyar *et al.* demonstrated that the uptake of liposomes in Zebrafish ZFL cells was not affected by the presence of EIPA inhibitor [67]. The data presented here is in agreement with the former two studies and show that the cellular uptake and luciferase silencing of cy3-siRNA-liposomes and luc-siRNA-liposomes, respectively, were both significantly reduced after incubating A549 and A549-Luc cells with EIPA. This finding suggests that macropinocytosis has a significant involvement in the endocytosis pathway of the cationic liposome used in this work.

Cytochalasin D is an actin filament depolymerising agent that inhibits macropinocytosis by binding to the positive termini of actin filaments and preventing the elongation of microfilament [68]. A study conducted by Huth *et al.* demonstrated that the internalisation of pH-sensitive liposomes was significantly inhibited by cytochalasin D in HUVEC cells (human endothelial cells from umbilical cords), whereas uptake in COS-7 cells (monkey kidney carcinoma cells, SV 40 transformed) did not appear to be influenced by cytochalasin D [62]. The effect of cytochalasin D (2 μg/ml) on the uptake of siRNA-polyplexes in A549 cells has been examined and result showed small but significant internalisation reduction of delivery system in the presence of cytochalasin D [13]. The data in current study reveal that the application of cytochalasin D to A549 cells has no significant effect on the cellular uptake of cy3-siRNA-liposomes in A549 cells (although data indicate some reduction) or on the luciferase knockdown and luc-siRNA-MB fluorescence in A549-Luc cells.

It should be mentioned that the assessment of MB in current work using the flow cytometry and confocal microscopy is limited by non-using of 'scrambled siRNA based MB' liposomes as negative control which is essential to distinguish between specific and non-specific binding effects of 'luc-siRNA based MB' with Luc-mRNA. Moreover, the analysis of non-specific fluorescence of FAM-MB by using the normal A549 cells without the luciferase mRNA is important to confirm that the green fluorescence detected is due to the successful engagement of FAM-MB with the targeted mRNA and not due to the non-specific binding of MB or the degradation by ribonuclease enzyme.

It is worth noting that at this time no studies comparing the mechanism of endocytosis in terms of cellular uptake and transfection efficiency of siRNA-liposomes into A549 cells have been published. This fact highlights the value of this present study and the need for further investigation in the future.

5.5 Conclusions

The work in this chapter has focused on the investigation of the actual endocytic mechanism(s) of a siRNA-liposome delivery system into A549 cells using pharmacological inhibitors. The data show a significant role of clathrin-mediated pathway on cellular uptake and consequent luciferase silencing effect of siRNA-liposomes into A549 cells, whereas caveolae dependent pathway does not appear to be significantly involved in the internalisation of tested cationic liposomes.

The level of luciferase silencing in A549-Luc cells can almost be doubled through the use of the endosomolytic agent, chloroquine, indicating that the clathrin-mediated pathway,

leading to lysosomal compartment, is indeed important route for internalisation and silencing of the investigated liposomal system.

In addition to clathrin pathway, depletion of cholesterol from the plasma membrane, through extraction of cholesterol from lipid rafts, significantly affected the internalisation of siRNA-liposomes as well as knockdown process, indicating the importance of lipid rafts for the system internalization. A major involvement of macropinocytosis in the internalisation and silencing of the siRNA-liposomes formulations was confirmed and emphasize that the internalization of the system may be occurring by a combination of different pathways.

Overall, the work in this chapter demonstrates that knowledge on cell trafficking processes is essential in deciding the design parameters of siRNA delivery systems.

5.6 References

[1] S. Vranic, N. Boggetto, V. Contremoulins, S. Mornet, N. Reinhardt, F. Marano, A. Baeza-Squiban, and S. Boland, Deciphering the mechanisms of cellular uptake of engineered nanoparticles by accurate evaluation of internalization using imaging flow cytometry. *Particle and Fibre Toxicology*, vol. 10, p. 2, 2013.

[2] M. Bareford and P. Swaan, Endocytic mechanisms for targeted drug delivery. *Advanced Drug Delivery Reviews*, vol. 59, no. 8, pp. 748–758, 2007.

[3] R. Kanasty, K. Whitehead, A. Vegas, and D. Anderson, Action and reaction: the biological response to siRNA and its delivery vehicles. *Molecular Therapy*, vol. 20, no. 3, pp. 513–524, 2012.

[4] N. Düzgüneş and S. Nir, Mechanisms and kinetics of liposome-cell interactions. *Advanced Drug Delivery Reviews*, vol. 40, no. 1–2, pp. 3–18, 1999.

[5] J. Singh, D. Michel, J. Chitanda, R. Verrall, and I. Badea, Evaluation of cellular uptake and intracellular trafficking as determining factors of gene expression for amino acid-substituted gemini surfactant-based DNA nanoparticles. *Journal of Nanobiotechnology*, vol. 10, no. 1, p. 7, 2012.

[6] X. Zhangb, J. McIntoshc, and W. Grinstaff , Functional lipids and lipoplexes for improved gene delivery. *Biochimie*, vol. 94, no. 1, pp. 42–58, 2012.

[7] L. Huang and S. Guo, Nanoparticles escaping RES and endosome: Challenges for siRNA delivery for cancer therapy. *Journal of Nanomaterials*, vol. 2011, 2011.

[8] A. Kiss and E. Botos, Endocytosis via caveolae: Alternative pathway with distinct cellular compartments to avoid lysosomal degradation?. *Journal of Cellular and Molecular Medicine*, vol. 13, no. 7, pp. 1228–1237, 2009.

[9] F. Pérez-Martínez, J. Guerra, I. Posadas, and V. Ceña, Barriers to non-viral vector-mediated gene delivery in the nervous system. *Pharmaceutical Research*, vol. 28, no. 8, pp. 1843–1858, 2011.

[10] N. Agrawal, P. Dasaradhi, A. Mohmmed, P. Malhotra, R. Bhatnagar, and S. Mukherjee, RNA interference: biology, mechanism, and applications. *Microbiology and Molecular Biology Reviews*, vol. 67, no. 4, pp. 657–685, 2003.

[11] A. Thorley, P. Ruenraroengsak, T. Potter, and T. Tetley, Critical determinants of uptake and translocation of nanoparticles by the human pulmonary alveolar Epithelium. *ACS Nano*, vol. 8, no. 11, pp. 11778–11789, 2014.

[12] A. Bannunah, D. Vllasaliu, J. Lord, and S. Stolnik, Mechanisms of nanoparticle internalization and transport across an intestinal epithelial cell model: effect of size and surface charge. *Molecular Pharmaceutics*, vol. 11, pp. 4363–4373, 2014.

[13] V. Capel, D. Vllasaliu, P. Watts, and S. Stolnik, Insight into the relationship between the cell culture model, cell trafficking and siRNA silencing efficiency. *Biochemical and Biophysical Research Communications*, vol. 477, no. 2, pp. 260–265, 2016.

[14] F. Ferreira, M. Foley, A. Cooke, M. Cunningham, G. Smith, R. Woolley, G. Henderson, E. Kelly, S. Mundell, and E. Smythe, Endocytosis of G protein-coupled receptors is regulated by clathrin light chain phosphorylation. *Current Biology*, vol. 22, no. 15, pp. 1361–1370, 2012.

[15] D. Vercauteren, R. Vandenbroucke, A. Jones, J. Rejman, J. Demeester, S. Smedt, N. Sanders, and K. Braeckmans, The use of inhibitors to study endocytic pathways of gene carriers: optimization and pitfalls. *Molecular Therapy*, vol. 18, no. 3, pp. 561–569, 2010.

[16] E. Macia, M. Ehrlich, R. Massol, E. Boucrot, C. Brunner, and T. Kirchhausen, Dynasore, a cell-permeable inhibitor of dynamin. *Developmental Cell*, vol. 10, no. 6, pp. 839–850, 2006.

[17] P. Le and I. Nabi, Distinct caveolae-mediated endocytic pathways target the Golgi apparatus and the endoplasmic reticulum.. *Journal of Cell Science*, vol. 116, no. 6, pp. 1059–1071, 2003.

[18] J. Jan, E. Schnitzer, P. Oh, and E. Pinney, Filipin-sensitive Caveolae-mediated Transport in Endothelium: Reduced Transcytosis, Scavenger Endocytosis, and Capillary Permeability of Select Macromolecules. *The Journal of Cell Biology*, vol. 127, no. 5, pp. 1217–1232, 1994.

[19] S. Rodal, G. Skretting, O. Garred, F. Vilhardt, B. Deurs, and K. Sandvig, Extraction of cholesterol with methyl-beta-cyclodextrin perturbs formation of clathrin-coated endocytic vesicles. *Molecular Biology of the Cell*, vol. 10, no. 4, pp. 961–974, 1999.

[20] Y. Chen, S. Wang, X. Lu, H. Zhang, Y. Fu, and Y. Luo, Cholesterol sequestration by nystatin enhances the uptake and activity of endostatin in endothelium via regulating distinct endocytic pathways. *Blood*, vol. 117, no. 23, pp. 6392–6403, 2011.

[21] M. Koivusalo, C. Welch, H. Hayashi, C. Scott, M. Kim, T. Alexander, N. Touret, K. Hahn, and S. Grinstein, Amiloride inhibits macropinocytosis by lowering submembranous pH and preventing Rac1 and Cdc42 signaling. *Journal of Cell Biology*, vol. 188, no. 4, pp. 547–563, 2010.

[22] S. Gold, P. Monaghan, P. Mertens, and T. Jackson, A clathrin independent macropinocytosis-like entry mechanism used by bluetongue virus-1 during infection of BHK cells. *PLoS ONE*, vol. 5, no. 6, 2010.

[23] G. Misinzo, P. Delputte, and H. Nauwynck, Inhibition of endosome-lysosome system acidification enhances porcine circovirus 2 infection of porcine epithelial cells. *Journal of Virology*, vol. 82, no. 3, pp. 1128–35, 2008.

[24] A. Liu, F. Aguet, G. Danuser, and S. Schmid, Local clustering of transferrin receptors promotes clathrin-coated pit initiation. *Journal of Cell Biology*, vol. 191, no. 7, pp. 1381–1393, 2010.

[25] K. Mayle, A. Le, and D. Kamei, The intracellular trafficking pathway of transferrin. *Biochimica et Biophysica Acta*, vol. 1820, no. 3, pp. 264–281, 2012.

[26] M. Torgersen, G. Skretting, B. Deurs, and K. Sandvig, Internalization of cholera toxin by different endocytic mechanisms. *Journal of Cell Science*, vol. 114, no. 20, pp. 3737–3747, 2001.

[27] H. Higgs and K. Peterson, Selective stimulation of caveolar endocytosis by glycosphingolipids and cholesterol. *Molecular Biology of the Cell*, vol. 16, no. 8, pp. 3114–3122, 2004.

[28] D. Kuhn, D. Vanhecke, B. Michen, F. Blank, P. Gehr, A. Petri-Fink, and B. Rothen-Rutishauser, Different endocytotic uptake mechanisms for nanoparticles in epithelial cells and macrophages. *Beilstein Journal of Nanotechnology*, vol. 5, pp. 1625–1636, 2014.

[29] V. Weissig and G. Souza, *O*rganelle-Specific Pharmaceutical Nanotechnology. 2010.

[30] J. Lam, S. Armes, and S. Stolnik, The involvement of microtubules and actin filaments in the intracellular transport of non-viral gene delivery system. *Journal of Drug Targeting*, vol. 19, no. 1, pp. 56–66, 2011.

[31] A. Elouahabi and J. Ruysschaert, Formation and intracellular trafficking of lipoplexes and polyplexes. *Molecular Therapy*, vol. 11, no. 3, pp. 336–347, 2005.

[32] J. James, R. Langer, J. Novel, C. Link, J. Lu, and J. Chen, A novel mechanism is involved in cationic lipid-mediated functional siRNA delivery. *Molecular Pharmaceutics*, vol. 6, no. 3, pp. 763–771, 2009.

[33] J. Ziello and Y. Huang, Cellular endocytosis and gene delivery. *Molecular Medicine*, vol. 16, no. 5–6, pp. 222–229, 2010.

[34] A. Schroeder, C. Levins, C. Cortez, R. Langer, and D. Anderson, Lipid-based nanotherapeutics for siRNA delivery. *Journal of Internal Medicine*, vol. 267, no. 1, pp. 9–21, 2010.

[35] M. Kaneda, G. Lanza, Y. Sasaki, J. Milbrandt, and S. Wickline, Mechanisms of nucleotide trafficking during siRNA delivery to endothelial cells using perfluorocarbon nanoemulsions. *Biomaterials*, vol. 31, no. 11, pp. 3079–3086, 2010.

[36] P. Tuma and A. Hubbard, Transcytosis: crossing cellular barriers. *Physiological Reviews*, vol. 83, no. 3, pp. 871–932, 2003.

[37] L. Shang, K. Nienhaus, and G. Nienhaus, Engineered nanoparticles interacting with cells: size matters. *Journal of Nanobiotechnology*, vol. 12, no. 1, p. 5, 2014.

[38] K. Kettler, K. Veltman, D. Meent, A. Wezel, and A. Hendriks, Cellular uptake of nanoparticles as determined by particle properties, experimental conditions, and cell type. *Environmental Toxicology and Chemistry*, vol. 33, no. 3, pp. 481–492, 2014.

[39] T. Iversen, T. Skotland, and K. Sandvig, Endocytosis and intracellular transport of nanoparticles: Present knowledge and need for future studies. *Nano Today*, vol. 6, no. 2, pp. 176–185, 2011.

[40] I. Khalil, K. Kogure, H. Akita, and H. Harashima, Uptake pathways and subsequent intracellular trafficking in nonviral gene delivery. *Pharmacological Reviews*, vol. 58, no. 1, pp. 32–45, 2006.

[41] S. Guo, X. Zhang, M. Zheng, X. Zhang, C. Min, Z. Wang, S. Cheon, M. Oak, S. Nah, and K. Kim, Selectivity of commonly used inhibitors of clathrin-mediated and caveolae-dependent endocytosis of G protein-coupled receptors. *Biochimica et Biophysica Acta - Biomembranes*, vol. 1848, no. 10, pp. 2101–2110, 2015.

[42] T. Santos, J. Varela, I. Lynch, A. Salvati, and K. Dawson, Effects of transport inhibitors on the cellular uptake of carboxylated polystyrene nanoparticles in different cell lines. *PLoS ONE*, vol. 6, no. 9, 2011.

[43] P. Fishman, Filipin-dependent inhibition of cholera toxin: evidence for toxin internalization and activation through caveolae-like domains. *The Journal of Cell Biology*, vol. 141, no. 4, pp. 905–915, 1998.

[44] R. Yumoto, S. Suzuka, K. Oda, J. Nagai, and M. Takano, Endocytic uptake of FITC-albumin by human alveolar epithelial cell line A549. *Drug Metabolism and Pharmacokinetics*, vol. 27, no. 3, pp. 1–2, 2012.

[45] A. Aman, S. Fraser, E. Merritt, C. Rodigherio, M. Kenny, M. Ahn, W. Hol, N. Williams,

W. Lencer, and T. Hirst, A mutant cholera toxin B subunit that binds GM1- ganglioside but lacks immunomodulatory or toxic activity. *Proceedings of the National Academy of Sciences of the United States of America*, vol. 98, no. 15, pp. 8536–8541, 2001.

[46] V. Souza, Organelle-Specific Pharmaceutical Nanotechnology. 2010.

[47] K. Remaut, N. Sanders, B. Geest, K. Braeckmans, J. Demeester, and S. Smedt, Nucleic acid delivery: Where material sciences and bio-sciences meet. *Materials Science and Engineering R*, vol. 58, pp. 117–161, Nov. 2007.

[48] R. Juliano and K. Carver, Cellular uptake and intracellular trafficking of oligonucleotides. *Advanced Drug Delivery Reviews*, vol. 87, pp. 35–45, 2015.

[49] S. Gratton, P. Ropp, P. Pohlhaus, J. Luft, V. Madden, M. Napier, and J. DeSimone, The effect of particle design on cellular internalization pathways. *Proceedings of the National Academy of Sciences of the United States of America*, vol. 105, no. 33, pp. 11613–11618, 2008.

[50] P. Orlandi and P. Fishman, Filipin-dependent Inhibition of Cholera Toxin: Evidence for Toxin Internalization and Activation through Caveolae-like Domains. *The Journal of Cell Biology*, vol. 141, no. 4, pp. 905–915, 1998.

[51] Y. Kimata, Y. Kimata, Y. Shimizu, H. Abe, I. Farcasanu, M. Takeuchi, M. Rose, and K. Kohno, Genetic Evidence for a Role of BiP / Kar2 That Regulates Ire1 in Response to Accumulation of Unfolded Proteins. *Molecular Biology of the Cell*, vol. 14, no. February, pp. 2559–2569, 2003.

[52] K. Hussain, K. Leong, M. Ng, and J. Chu, The essential role of clathrin-mediated endocytosis in the infectious entry of human enterovirus 71. *Journal of Biological Chemistry*, vol. 286, no. 1. 2011.

[53] J. Rejman, A. Bragonzi, and M. Conese, Role of clathrin- and caveolae-mediated endocytosis in gene transfer mediated by lipo- and polyplexes. *Molecular Therapy*, vol. 12, no. 3, pp. 468–474, 2005.

[54] Z. Rehman, I. Zuhorn, and D. Hoekstra, How cationic lipids transfer nucleic acids into cells and across cellular membranes: recent advances. *Journal of Controlled Release*, vol. 166, no. 1, pp. 46–56, Feb. 2013.

[55] P. Boisguérin, S. Deshayes, M. Gait, L. Donovan, C. Godfrey, C. Betts, M. Wood, and B. Lebleu, Delivery of therapeutic oligonucleotides with cell penetrating peptides. *Advanced Drug Delivery Reviews*, vol. 87, pp. 52–67, 2015.

[56] A. Andar, R. Hood, W. Vreeland, D. Devoe, and P. Swaan, Microfluidic preparation of liposomes to determine particle size influence on cellular uptake mechanisms. *Pharmaceutical Research*, vol. 31, no. 2, pp. 401–413, 2014.

[57] A. Wong, S. Scales, and D. Reilly, DNA internalized via caveolae requires microtubule-dependent, Rab7-independent transport to the late endocytic pathway for delivery to the nucleus. *Journal of Biological Chemistry*, vol. 282, no. 31, pp. 22953–22963, 2007.

[58] S. Cui, B. Wang, Y. Zhao, H. Chen, H. Ding, D. Zhi, and S. Zhang, Transmembrane routes of cationic liposome-mediated gene delivery using human throat epidermis cancer cells. *Biotechnology Letters*, Sep. 2013.

[59] K. Ikonen, Functional rafts in cell membranes. *Nature*, vol. 387, pp. 569–572, 1997.

[60] M. Utech, R. Mennigen, and M. Bruewer, Endocytosis and recycling of tight junction

proteins in inflammation. *Journal of Biomedicine and Biotechnology*, vol. 2010, pp. 1–6, Jan. 2010.

[61] A. Fallis, Surface functionality of nanoparticles determines cellular uptake mechanisms in mammalian cells. *Journal of Chemical Information and Modeling*, vol. 53, no. 9, pp. 1689–1699, 2013.

[62] U. Huth, R. Schubert, and R. Peschka-Süss, Investigating the uptake and intracellular fate of pH-sensitive liposomes by flow cytometry and spectral bio-imaging. *Journal of Controlled Release*, vol. 110, no. 3, pp. 490–504, 2006.

[63] Y. Lamberti, J. Hayes, M. Vidakovics, and M. Rodriguez, Cholesterol-dependent attachment of human respiratory cells by Bordetella pertussis. *Immunology and Medical Microbiology*, vol. 56, no. 2, pp. 143–150, 2009.

[64] J. Rejman, A. Bragonzi, and M. Conese, Role of clathrin- and caveolae-mediated endocytosis in gene transfer mediated by lipo- and polyplexes. *Molecular Therapy*, vol. 12, no. 3, pp. 468–474, 2005.

[65] L. Kou, J. Sun, Y. Zhai, and Z. He, The endocytosis and intracellular fate of nanomedicines: Implication for rational design. *Asian Journal of Pharmaceutical Sciences*, vol. 8, no. 1, pp. 1–8, 2013.

[66] A. Homhuan, H. Harashima, and I. Yano, Cellular attachment and internalization of cationic liposomes containing mycobacterial cell wall. *Science Asia*, vol. 34, no. 2, pp. 179–185, 2008.

[67] A. Ruyra, M. Cano-Sarabia, S. MacKenzie, D. Maspoch, and N. Roher, A novel liposome-based nanocarrier loaded with an LPS-dsRNA cocktail for fish innate immune system stimulation. *PLoS ONE*, vol. 8, no. 10, pp. 1–13, 2013.

[68] T. Pollard, Effects of cytochalasin, phalloidin and pH on the elongation of actin filaments. *Biochemistry*, vol. 30, pp. 1973–1980, 1991.

Chapter 6 - Candidate Target Genes in NSCLC

6.1 Introduction

Lung cancer is one of the most common and serious types of cancer, usually stimulated by endogenous and exogenous factors, although through different mechanisms [1]. Lung cancer is the leading cause of cancer related deaths in the US, with a median 5-years survival rate of only 5% [2]. NSCLC accounts for approximately 85% of lung cancers, with diagnosis often made in the advanced stages of the disease [3], when chemotherapy is considered ineffective or excessively toxic. A number of components of the epithelium have been revealed to be involved in the tumour progression mechanism for a wide range of cancer types, including lung cancer [5], [6]. It has been stated that a number of epithelial membrane proteins could be significant constituents of lung cancer development in humans [7], and strategies to develop new therapies involve targeting such proteins in advanced NSCLC.

Epidemiological studies have demonstrated that an alteration in the expression of certain genes in epithelial cells genome may have an essential role in cancer development [8]. Furthermore, there is a solid evidence that the progression of cancer is based mainly on modifications to the protein expression pattern of certain genes [9], hence a good understanding of the involvement of gene up- or down-regulation during the cancer

development process could lead to the discovery of a novel therapeutic strategy with clinical applications.

Recently, various studies have established that the alteration in expression profile of certain 'key' proteins is a central feature of the pathophysiology of lung cancer [10]–[12]. The literature reports several genes, shown in Table 6.1, which may play paramount roles in the development and progression of NSCLC. It can be hypothesised that these genes play vital roles in the modulation of cell behaviour and proliferation.

Epidermal growth factor receptor (EGFR) is a trans-membrane glycoprotein with an extracellular epidermal growth factor binding domain and an intracellular tyrosine kinase domain that regulates signalling pathways to control cellular proliferation [13]. Overexpression of EGFR has been reported and implicated in the pathogenesis of many human malignancies, including NSCLC [14].

The rearrangements in the anaplastic lymphoma kinase (ALK) gene and the echinoderm microtubule-associated protein-like 4 (EML4) gene was first described by Soda and colleagues in 2007 [15], and are found in approximately 4%–7% of NSCLC tumours [16]. EML4–ALK rearrangement was identified as an oncogene and EML4–ALK fusion protein was found to possess transforming activity and oncogenic potential [15].

The Kirsten rat sarcoma viral oncogene homolog (KRAS) is the most frequently mutated oncogene in NSCLC [17]. KRAS is a member of the ras gene family which encodes small G proteins with intrinsic GTPase activity, which normally leads to protein inactivation

and activates downstream effectors involved in multiple pathways including proliferation, differentiation and apoptosis [18].

The Erb-B2 Receptor Tyrosine Kinase 2 gene (ERBB2) has been identified as an oncogenic driver in different types cancers, and somatic mutations in ERBB2 have been reported in 1% to 2% of patients with lung adenocarcinoma [19]. The v-raf murine sarcoma viral oncogene homolog B1 gene (BRAF) is a member of the RAF kinase family, belongs to the group of serine-threonine kinases and plays vital role in mitogen-activated protein kinase (MAPK) pathways. Mutations in BRAF were found in 1–3% of NSCLC patients [20].

Mesenchymal-epidermal transition gene (MET) has been identified as abnormally overexpressed, potentially having activating mutations, and amplified in lung cancers. MET has been implicated in several oncogenic processes including cell proliferation, survival, invasion, motility, and metastasis [21]. MET has recently emerged as a promising target, and ongoing trials will clarify the role of anti-MET strategies in NSCLC [22].

AKT Serine/Threonine Kinase 1 (AKT1) has reported to play an important role in the regulation of the process of cell survival, growth, and migration in NSCLC cells, and the inhibition of AKT1 genes could be used as a strategy for the treatment of NSCLC [23]. The phosphatidylinositol 3-kinases (PI3K) play a pivotal role in cell metabolism and proliferation, affecting both cancer and metabolic disorders [24]. Somatic mutations of the PIK3CA gene have been described in NSCLC, but limited data is available on their biological relevance [25].

Discoidin domain receptor 2 (DDR2) is a receptor tyrosine kinase which binds collagen as its endogenous ligand and has been previously shown to promote cell migration, proliferation and survival when activated by ligand binding and phosphorylation [26]. DDR2 mutations have been reported in several cancer including lung cancer, and suggested that the inhibition of DDR2 may be an important therapeutic target in lung cancer [27]. ATP binding cassette, sub family C, member 1 (ABCC1) is overexpressed in lung cancer tissue and could play an important function on the progression of NSCLC. It appears that ABCC1 may have strong implications for management of NSCLC and design of ABCC1 inhibitors could be used as a therapeutic agent to control NSCLC [28].

Table 6.1: List of genes whose expression profiles could play key roles in the progression of lung cancer

#	Symbol	Name
1	EGFR	Epidermal Growth Factor Receptor
2	ALK	Anaplastic Lymphoma Kinase
3	EML4	Echinoderm Microtubule Associated Protein Like 4
4	KRAS	Kirsten Rat Sarcoma Viral Oncogene Homolog
5	ERBB2	Erb-B2 Receptor Tyrosine Kinase 2
6	BRAF	V-Raf Murine Sarcoma Viral Oncogene Homolog B1
7	MET	Mesenchymal-epidermal transition
8	AKT1	AKT Serine/Threonine Kinase 1
9	PIK3CA	Phosphatidylinositol-4,5-Bisphosphate 3-Kinase Catalytic Subunit Alpha
10	DDR2	Discoidin Domain Receptor Tyrosine Kinase 2
11	ABCC1	ATP Binding Cassette Subfamily C Member 1

The candidate genes shown in Table 6.1 can be also investigated, and analysis corroborated with the data from studies listed in Table 6.2, by using gene expression microarray data from the Gene Expression Omnibus (GEO) database in order to uncover differences in gene expression in normal *versus* lung cancer tissue, enabling the selection of genes of interest for study.

GEO is a public microarray databank which was created in 2000 by the National Centre for Biotechnology Information (NCBI) to archive experimental information for mRNA, protein molecules and genomic DNA, which are used regularly in biomedical and molecular biology research [29], [30]. Currently, many researchers mine the GEO database to identify candidate genes, confirm their results, and to design further studies. The GEO database can be accessed freely (http://www.ncbi.nlm.nih.gov/geo).

In 2013, the GEO database contained more than 40,000 studies, including 33 billion individual measurements, and about a million samples from over 2,200 organisms, submitted by 15,000 laboratories from all around the world [31]. The GEO database contains three types of data; series, platform, and sample [29]. Platform refers to the type of array used in an experiment and is identified by the prefix GPL [32], while sample is the collection of a summary of the materials and general methodology used in an experiment and is known by the GSM prefix [33], and finally, series is a collection of samples which compose part of a study and is known by the prefix GSE [31]. In addition, there is a further tool, called Dataset, which is known by the prefix GDS, and this contains a complete summary of the final values [34].

In an attempt to investigate the contribution of specific genes involved in the development of lung cancer in epithelial tissue, A549 cells were used. This is a well-characterised cell line that represents an *in vitro* model of NSCLC and is widely used in a variety of pharmaceutical research.

6.2 Aims and Objectives

The aim of this chapter is to perform a GEO database search/screen of the expression profiles of candidate genes that could be involved in the progression of NSCLC. Once such candidate genes have been identified, they could be targeted using siRNA, and protein expression silenced in, initially, an *in vitro* model of NSCLC to validate their involvement and to examine the ability of the siRNA delivery system to target and silence the gene(s) of interest.

6.3 Methods

6.3.1 Dataset Collection from the GEO Database

Two studies on human lung cancer samples were chosen from the GEO database for the gene expression analysis of selected genes and available information about these two studies is summarised in Table 6.2.

Table 6.2: Summary of information collected from GEO database of two studies used to perform gene expression data analysis

Study No.	1	2
Title	Non-small cell lung carcinoma in female non-smokers [35]	Cigarette smoking effect on lung adenocarcinoma [36]
Organism	Homo sapiens	Homo sapiens
Platform	Affymetrix Human Genome U133 Plus 2.0 Array	Affymetrix Human Genome U133A Array
Reference Series	GSE19804	GSE10072
Sample count	120	107

6.3.2 Probe Set Collection from the GeneCards Database

Following dataset selection, probe set information for each Affymetrix array for the two selected studies were collected from the GeneCards database for all candidate genes. In addition, similar information was collected for the reference gene *RPS29*, which was used in the data analysis stage to normalise expression intensity. GeneCards is a searchable, integrative database that provides comprehensive information on all annotated and predicted human genes and can be accessed freely (http://www.genecards.org/). The Affymetrix array for each candidate gene was collected according to the study platform and is summarised in Table 6.3.

Table 6.3: Summary of probe set Affymetrix array information collected from GeneCards database of the two studies used to perform gene expression data analysis

#	Genes	Study (1) HG-U133_Plus_2	Study (2) HG-U133A
1	EGFR	201983_s_at	201983_s_at
2	ALK	208211_s_at	208211_s_at
3	EML4	220386_s_at	220386_s_at
4	KRAS	204010_s_at	204010_s_at
5	ERBB2	210930_s_at	210930_s_at
6	BRAF	206044_s_at	206044_s_at
7	MET	203510_at	203510_at
8	AKT1	207163_s_at	207163_s_at
9	PIK3CA	204369_at	204369_at
10	DDR2	205168_at	205168_at
11	ABCC1	202804_at	202804_at
Reference gene	RPS29	200823_x_at	200823_x_at

6.3.3 Gene Expression Microarray Analysis of the Candidate Genes

After collecting complete information about the candidate genes from the GEO and GeneCards databases, the analysis of the gene expression microarray for each gene was performed to compare the expression in lung cancer and normal lung tissue. The expression microarray for each gene was normalised using the reference gene *RPS29*. The full analysis details are shown in Appendices 2 and 3, and a results summary is presented in this chapter.

6.3.4 Cell Viability Assay for Silencing of the Selected Gene

To assess level of silencing of specific gene by liposome-siRNA formulations, cellular proliferation of A549-Luc cells was measured by MTS assay. ON-TARGETplus siRNA

with dTdT overhang and the following sequence: EGFR (5`-CACAGUGGAGCGAAUUCCU-3`) was used.

A549-Luc cells were seeded in a 96-well plate at a density of 1×10^4 cells *per* well and cultured overnight in 100 µl of DMEM. The effect of selected targeted siRNA on the proliferation of A549-Luc was measured by MTS viability assay. Liposome preparations containing ON-TARGETplus siRNA with dTdT overhang and the following sequence: EGFR (5`-CACAGUGGAGCGAAUUCCU-3`), and negative control siRNA-liposomes with a nonsense/scrambled sequence were added to cells in serum reduced media OptiMEM at a concentration of 100 nM siRNA *per* well. After 4 hrs, the liposomes were removed and replaced with fresh serum containing DMEM. After 24, 48, 72 and 96 hrs the cellular viability was measured by an MTS assay as described in Section 2.2.3.1.

6.4 Results

6.4.1 Gene Expression Microarray Analysis of Candidate Genes

The list of candidate genes shown in Table 6.1 whose expression profiles could play a significant role in the progression of lung cancer were analysed by normalising the expression microarray data for each gene against an appropriate reference gene, *RPS29*, in normal lung and lung cancer tissue and the results are summarised in Table 6.4.

In the first analysed study (GSE19804), analyses of changes in gene expression microarray between healthy lung and lung cancer patients did not show a significant difference for the *ALK* and *AKT1* genes, whereas the *EGFR, EML4, ERBB2, BRAF* and *MET* genes were significantly up-regulated in lung cancer compared to the healthy lung. The remaining four genes, *KRAS, PIK3CA, DDR2* and *ABCC1*, were significantly

down-regulated in lung cancer tissue. The reference gene (RPS29) shows similar expression microarray in case of lung cancer patients and healthy lung samples.

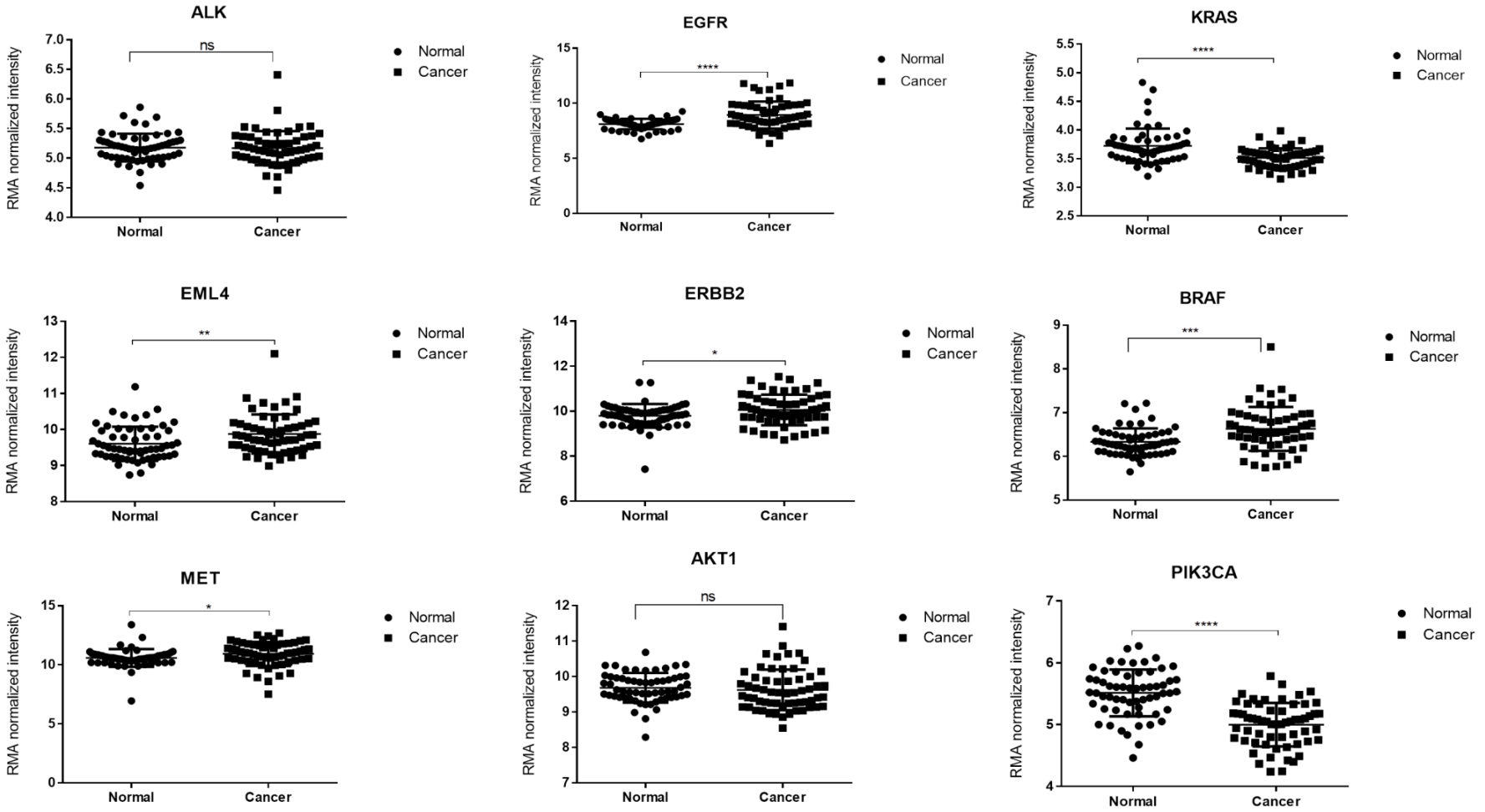
ALK
ns
RMA normalized intensity
Normal
Cancer
EGFR
****
KRAS
****
EML4
**
ERBB2
*
BRAF
***
MET
*
AKT1
ns
PIK3CA
****

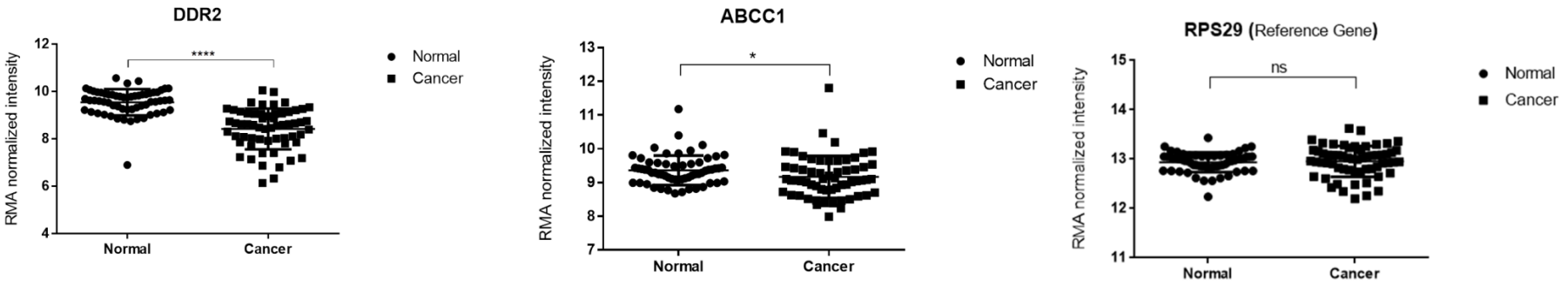

Figure 6.1: Gene expression microarray analysis of candidate genes from the GSE19804 study

*A t-test of significance was applied to determine differences between the expression of normal control (healthy individuals) and diseased tissue (lung cancer patients). P value (ns > 0.05, * < 0.05, ** < 0.01, *** < 0.001, and **** < 0.0001).*

The expression microarray analysis for the GSE10072 study, which contained a lower sample number, indicated a significant increase in protein expression for the genes *EGFR, EML4, ERBB2, BRAF* and *MET*, whilst the expression level of the genes *PIK3CA*, *DDR2* and *ABCC1* decreased in lung cancer tissue. No significant change in expression was observed for the remaining genes *ALK, KRAS* and *AKT1*. The expression profile of the reference gene RPS29 shows no significant change in the expression level in case of lung cancer tissue in comparison to healthy control.

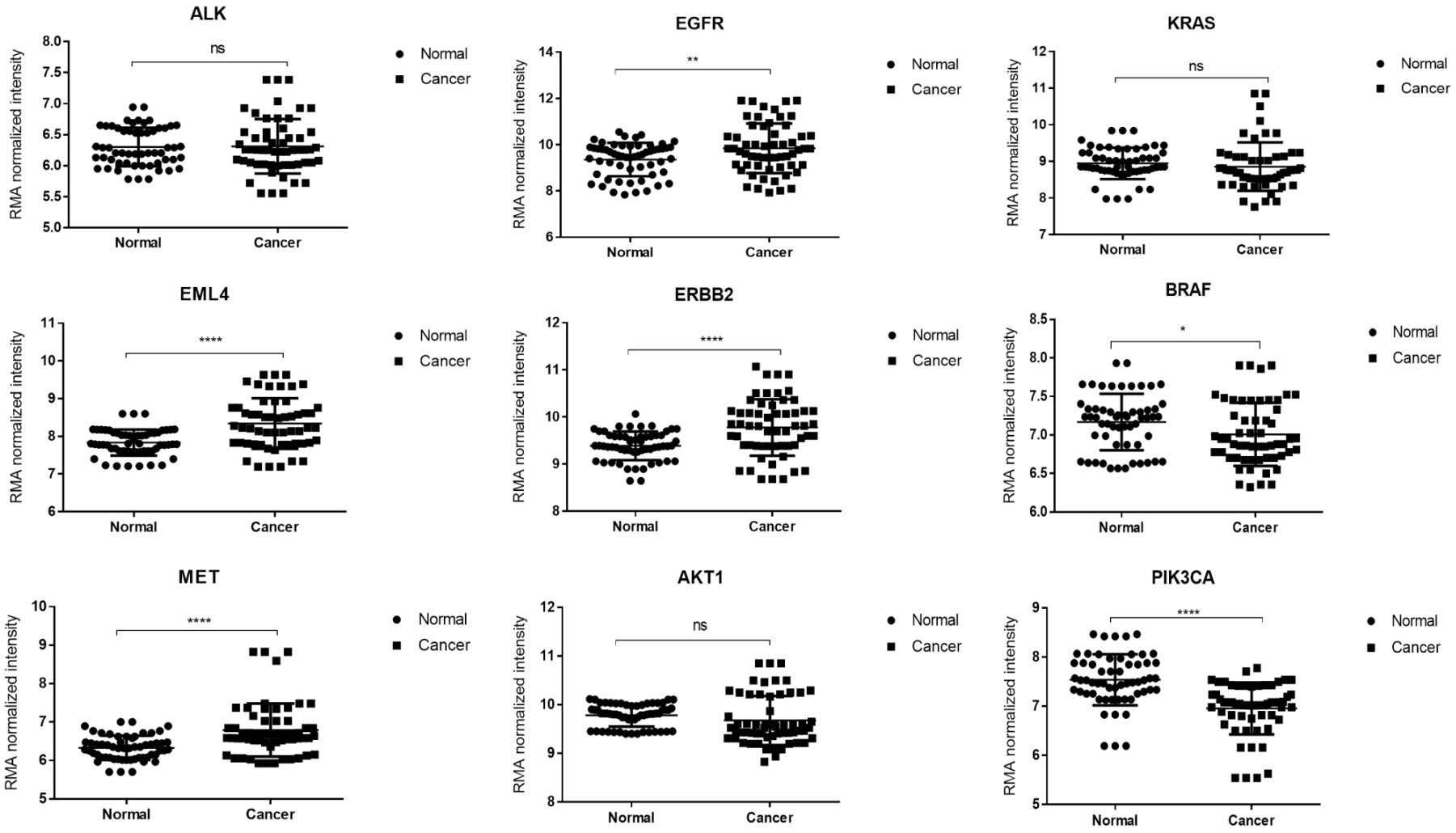
ALK
ns
RMA normalized intensity
Normal
Cancer
EGFR
**
KRAS
ns
EML4
****
ERBB2
****
BRAF
*
MET
****
AKT1
ns
PIK3CA
****

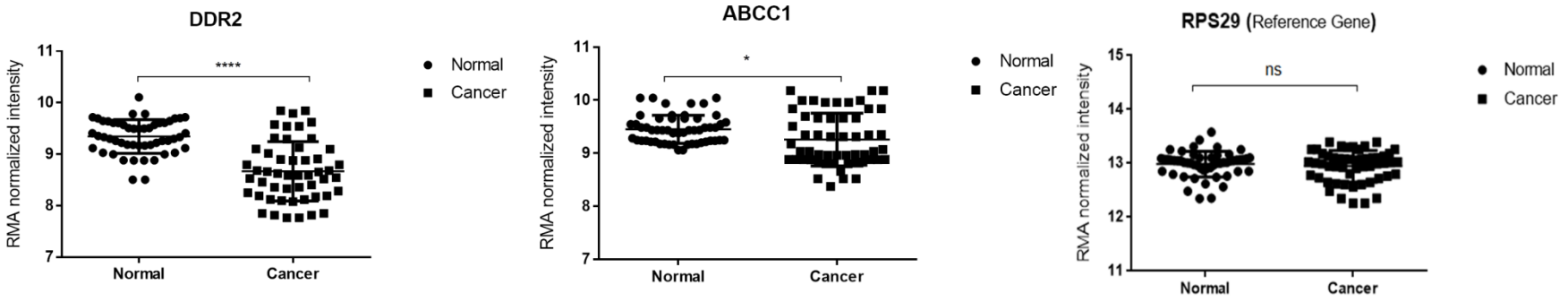

Figure 6.2: Gene expression microarray analysis of candidate genes for the GSE10072 study

*A t-test of significance was applied to determine differences between the expression of normal control (healthy individuals) and diseased tissue (lung cancer patients). P value (ns > 0.05, * < 0.05, ** < 0.01, *** < 0.001, and **** < 0.0001).*

Table 6.4 shows a result summary for the analysed expression data for eleven candidate gene microarrays from two different studies with different sample numbers, which are presented in Figure 6.1 and Figure 6.2 for study 1 and 2, respectively.

Table 6.4: Summary of gene expression microarray analysis of candidate genes

*A significant difference in expression level between lung cancer and healthy control tissue was confirmed by a t-test of significance. (+) represents overexpressed, (-) down-regulated and (ns) no significant difference. P values (**ns** > 0.05, **±** < 0.05, **±±** < 0.01, **±±±**< 0.001, and **±±±±** < 0.0001).*

Gene	Study 1 (GSE19804)	Study 2 (GSE10072)
ALK	**ns**	**ns**
EGFR	+ + + +	+ +
KRAS	- - - -	**ns**
EML4	+ +	+ + + +
ERBB2	+	+ + + +
BRAF	+ + +	+
MET	+	+ + + +
AKT1	**ns**	**ns**
PIK3CA	- - - -	- - - -
DDR2	- - - -	- - - -
ABCC1	-	-
RPS29 (Reference gene)	**ns**	**ns**

From the combined results, five different genes were found to be overexpressed in lung cancer and selected for further investigation; *EGFR, EML4, ERBB2, BRAF* and *MET*. These genes showed interesting expression data in the primary data analysis and all were overexpressed in lung cancer in comparison to healthy lung. Figure 6.1 and Figure 6.2 indicated that these genes showed a significant difference, as determined by performing a

t-test of significance, in expression levels in lung cancer compared to the healthy control. The next step would ideally be to confirm their role in lung cancer development by investigating the effect of silencing their expression on proliferation in an *in vitro* model of lung cancer. In the current study, one of these genes was selected.

6.4.2 Cell Proliferation Assay of *EGFR*-siRNA-Liposomes

In order to assess the role of epidermal growth factor receptor (*EGFR*) in the development of lung cancer, the effect of *EGFR*-targeted siRNA on the proliferation of the cell line that was intended to be used in *in vivo* (A549-Luc cells) experiments was investigated. In the literature, *EGFR* mutations were reported in NSCLC and this has been used in studies to develop siRNA silencing therapy [37]. *EGFR* has been shown to be up-regulated in the epithelial cells of many tumours and silencing of *EGFR* has shown direct and indirect effects on angiogenesis and tumour inhibition [38], [39].

Figure 6.3 shows the cellular proliferation of A549-Luc cells following incubation with *EGFR*-siRNA-liposomes, using ON-TARGETplus siRNA with dTdT overhang and the following sequence: *EGFR* (5`-CACAGUGGAGCGAAUUCCU-3`), and negative control siRNA-liposomes. Cell survival was reduced from 106% at 24 hrs to 89% and 62% at 48 and 72 hrs post-transfection, respectively, with *EGFR*-siRNA-liposomes. Cellular proliferation of A549-Luc cells began to recover after 72 hrs and reached maximum recovery (103%) at 96 hrs post-transfection. Negative control siRNA had no significant effect on cellular proliferation at any time point ($p>0.05$).

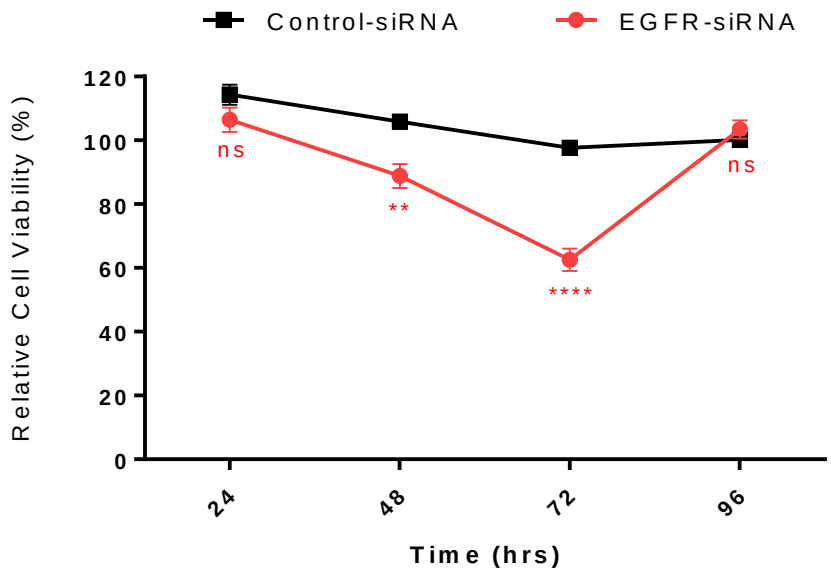

Figure 6.3: Effect of EGFR-siRNA-liposomes on the cellular proliferation of A549-Luc cells

EGFR-siRNA and negative control siRNA-liposomes (100 nM) were incubated with A549-Luc cells for 4 hrs, then removed and replaced with fresh media. A549-Luc cells were incubated in growth medium for further 24, 48, 72 and 96 hrs and cell survival was measured by MTS assay. Data are expressed as the relative cell viability, calculated using the equation shown in Section 2.2.3.1 and presented as the mean ± SD (N=3, n=6).

6.5 Discussion

With progress in cytogenetic and molecular biology, the detection and analysis of both tumour suppressor genes and oncogenes may provide predictive values for prognosis and treatment choice for NSCLC [40], [41]. Recent research has reported that controlling the expression of such encoded proteins could be an effective therapeutic strategy to control cancer [8]. The work in this chapter aimed to investigate the expression features of a panel of genes which have been reported in the literature to be involved in the development of lung cancer. Microarray protein expression of eleven different genes were analysed in lung cancer samples and compared to healthy lung from two studies available in the GEO database. The results provide a primary overview of gene expression features and allowed an initial assumption about the involvement of these genes in the control of lung cancer to be made.

From the results, five different genes were found to show over-expression in lung cancer tissue; *EGFR, EML4, ERBB2, BRAF* and *MET*. Consequently, these genes could be good candidate targets for NSCLC treatment, and knockdown of their protein expression using siRNA therapeutics may be an attractive option for lung cancer treatment.

EGFR is a transmembrane glycoprotein that is a member of the protein kinase superfamily and possesses three functional domains; an extracellular domain, a hydrophobic transmembrane domain, and a cytoplasmic domain containing tyrosine kinase (TK) and a carboxyl autophosphorylation region [40]. It has been demonstrated that *EGFR* is overexpressed in different types of tumours, including NSCLC [42]. The overexpression of *EGFR* usually leads to the deregulation of receptor tyrosine kinases and this can promote cell proliferation, the inhibition of cell death, or the induction of

angiogenesis [39]. Targeting *EGFR* in lung cancer using the tyrosine kinase inhibitor Erlotinib however shows little improvement in lung cancer patient survival [43]; therefore, siRNA approaches could offer a new strategy for the treatment of NSCLC.

EML4 was one of the identified candidate genes that could be involved in the progression of NSCLC. *ALK* protein is usually reported to be fused with *EML4*, and was first identified in 2007 [44]. Abnormal fusion of parts of this gene with portions of the anaplastic lymphoma receptor tyrosine kinase gene, which generates *EML4-ALK* fusion transcripts, is one of the primary mutations associated with NSCLC [45]. It has been suggested that around 5% of all NSCLCs contain an *EML4-ALK* translocation [44], [46]. *ERBB2* is a member of the protein kinase subfamily that is found to be the most mutated gene in human cancers [47]. A mutation of *ERBB2* has been found in 2% of NSCLCs, but the mechanism of involvement in the disease progression remains unclear [48].

BRAF is another member of the protein kinase subfamily that has been demonstrated to be involved in the development of NSCLC [49]. *BRAF* is a proto-oncogene encoding a serine/threonine protein kinase which is a downstream effector protein of *RAS*, and transduces signalling through the mitogen-activated protein kinase pathway to promote cell proliferation and survival [37]. A mutation in *BRAF* has been reported to occur in around 4% of NSCLCs, and if confirmed as a therapeutic target in NSCLC, *BRAF* may expand the number of potential candidates for personalised lung cancer therapy [50]. The *MET* receptor tyrosine kinase has been identified as being mutated and overexpressed in lung cancer [21], and knockdown of *MET* using siRNA has been demonstrated to be important *in vitro* for cell viability and downstream signalling [51].

The involvement of these candidate genes in the progression of NSCLC needed to be validated and the effect of protein silencing using siRNA on cell proliferation within the *in vitro* model of NSCLC investigated. Treatment of A549-Luc cells with anti-*EGFR*-siRNA encapsulated in liposomes showed a significant reduction in cell survival at 48 and 72 hrs post-transfection. From 72 hrs post-treatment time point cellular proliferation started to recover, reaching 'normal growth' at 96 hrs post-transfection, with similar metabolic activity to cells treated with negative control siRNA. Knockdown of the expression of *EGFR* in two established glioma cell lines, U373 MG and LN18, using anti-*EGFR*-siRNA showed successful down-regulation of protein expression by 70%-90%, however, there was no associated significant reduction in cell proliferation [52]. In contrast, A549 and SPC-A1 cells transfected with anti-*EGFR*-siRNA exhibited a decrease in protein expression by around 70%, and this was accompanied by a significant growth inhibition, suggesting that silencing of *EGFR* could be an effective therapeutic strategy for NSCLC [53], [54].

The initial analysis of EGFR knockdown effect on the proliferation of A549-Luc cells should be validated using real-time quantitative RT-qPCR and western blot. The RT-qPCR can be used to quantify the extent of EGFR-mRNA expression knockdown, while the western blot technique is the best way to confirm successful knockdown of the targeted EGFR protein by siRNA.

6.6 Conclusions

In this chapter, the microarray gene expression of eleven different genes was investigated in lung cancer tissue from two different studies available in GEO database, and five genes were found to be significantly up regulated. Silencing of these genes could help to control the progression of lung cancer and provide an attractive approach for lung cancer treatment. Liposome-siRNA formulations targeting *EGFR* gene were used to experimentally examine the effect on cell proliferation in NSCLC using an *in vitro* cell culture model. The liposome formulations were able to mediate *EGFR* silencing and to decrease cell viability. An *in vivo* study should be performed in the future to confirm these results, and to assess if this approach holds promise the *in vivo* situation.

6.7 References

[1] H. Biesalski, B. De Mesquita, A. Chesson, F. Chytil, R. Grimble, R. Hermus, J. Kohrle, R. Lotan, K. Norpoth, U. Pastorino, and D. Thurnham, European consensus statement on lung cancer : risk factors and prevention. *Cancer Journal Clinics*, vol. 48, pp. 316–322, 1998.

[2] A. Schwartz and M. Cote, Epidemiology of lung cancer. *Advances in Experimental Medicine and Biology*, vol. 893, pp. 21–41, 2016.

[3] J. Molina, P. Yang, S. Cassivi, S. Schild, and A. Adjei, Non-small cell lung cancer: epidemiology, risk factors, treatment, and survivorship. *Mayo Clinic Proceedings*, vol. 83, no. 5, pp. 584–594, 2008.

[4] S. Ozkaya, S. Findik, O. Uzun, A. Atici, and L. Erkan, Comparison of vinorelbine-cisplatin with gemcitabine-cisplatin in patients with advanced non-small cell lung cancer. *Clinical Medicine*, vol. 2, pp. 27–34, 2008.

[5] P. Lu, V. Weaver, and Z. Werb, The extracellular matrix: A dynamic niche in cancer progression. *Journal of Cell Biology*, vol. 196, no. 4, pp. 395–406, 2012.

[6] S. Diaz-Cano, Tumor heterogeneity: Mechanisms and bases for a reliable application of molecular marker design. *International Journal of Molecular Sciences*, vol. 13, no. 2, pp. 1951–2011, 2012.

[7] R. Leth-Larsen, R. Lund, H. Hansen, A. Laenkholm, D. Tarin, O. Jensen, and H. Ditzel, Metastasis-related plasma membrane proteins of human breast cancer cells identified by comparative quantitative mass spectrometry. *Molecular and Cellular Proteomics*, vol. 8, no. 6, pp. 1436–1449, 2009.

[8] S. Sharma, T. Kelly, and P. Jones, Epigenetics in cancer. *Carcinogenesis*, vol. 31, no. 1, pp. 27–36, 2009.

[9] B. Sadikovic, K. Al-Romaih, J. Squire, and M. Zielenska, Cause and consequences of genetic and epigenetic alterations in human cancer. *Current Genomics*, vol. 9, no. 6, pp. 394–408, 2008.

[10] W. Cooper, D. Lam, S. Toole, and J. Minna, Molecular biology of lung cancer. *Journal of Thoracic Disease*, vol. 5, no. 5, pp. 479–489, 2013.

[11] R. Blanco, R. Iwakawa, M. Tang, T. Kohno, B. Angulo, R. Pio, L. Montuenga, J. Minna, J. Yokota, and M. Sanchez, A gene-alteration profile of human lung cancer cell lines. *Human Mutation*, vol. 30, no. 8, pp. 1199–1206, 2010.

[12] M. Roh, Molecular pathology of lung cancer: Current status and future directions. *Tuberculosis and Respiratory Diseases*, vol. 77, no. 2, pp. 49–54, 2014.

[13] K. Inamura, H. Ninomiya, Y. Ishikawa, and O. Matsubara, Is the epidermal growth factor receptor status in lung cancers reflected in clinicopathologic features?. *Archives of Pathology and Laboratory Medicine*, vol. 134, no. 1, pp. 66–72, 2010.

[14] G. Selvaggi, S. Novello, V. Torri, E. Leonardo, P. Giuli, P. Borasio, C. Mossetti, F. Ardissone, P. Lausi, and G. Scagliotti, Epidermal growth factor receptor overexpression correlates with a poor prognosis in completely resected non-small-cell lung cancer. *Annals of Oncology*, vol. 15, no. 1, pp. 28–32, 2004.

[15] M. Soda, Y. Choi, M. Enomoto, S. Takada, Y. Yamashita, S. Ishikawa, S. Fujiwara, H. Watanabe, K. Kurashina, H. Hatanaka, M. Bando, S. Ohno, Y. Ishikawa, H. Aburatani, T.

Niki, Y. Sohara, Y. Sugiyama, and H. Mano, Identification of the transforming EML4–ALK fusion gene in non-small-cell lung cancer. *Nature*, vol. 448, no. 7153, pp. 561–566, 2007.

[16] S. Kayaniyil, M. Hurry, J. Wilson, B. Melosky, J. Rothenstein, V. Cohen, C. Koch, J. Zhang, K. Osenenko, and G. Liu, Treatment patterns and survival in patients with ALK-positive non-small-cell lung cancer : a Canadian retrospective study. *Current Oncology*, vol. 23, no. December, pp. 589–597, 2016.

[17] G. Riely, J. Marks, and W. Pao, KRAS mutations in non-small cell lung cancer. *Proceedings of the American Thoracic Society*, vol. 6, no. 2, pp. 201–5, 2009.

[18] Y. Pylayeva-Gupta, E. Grabocka, and D. Bar-Sagi, RAS oncogenes: weaving a tumorigenic web. *Nature Reviews Cancer*, vol. 11, no. 11, pp. 761–774, 2011.

[19] J. Chuang, H. Stehr, Y. Liang, M. Das, J. Huang, M. Diehn, H. Wakelee, and J. Neal, ERBB2-Mutated metastatic non–small cell lung cancer: response and resistance to targeted therapies. *Journal of Thoracic Oncology*, vol. 12, no. 5, pp. 833–842, 2017.

[20] D. Chen, L. Zhang, J. Huang, K. Liu, Z. Chuai, Z. Yang, Y. Wang, D. Shi, Q. Liu, Q. Huang, and W. Fu, BRAF mutations in patients with non-small cell lung cancer: a systematic review and meta-analysis. *PLoS ONE*, vol. 9, no. 6, p. e101354, 2014.

[21] A. Sadiq and R. Salgia, MET as a possible target for non-small-cell lung cancer. *Journal of Clinical Oncology*, vol. 31, no. 8, pp. 1089–1096, 2013.

[22] L. Landi, G. Minuti, A. Incecco, and F. Cappuzzo, Targeting c-MET in the battle against advanced nonsmall-cell lung cancer. *Current Opinion in Oncology*, vol. 25, no. 2, pp. 130–136, 2013.

[23] M. Lee, D. Kim, J. Lee, B. Lee, S. Lee, H. Jung, K. Sung, H. Kim, K. Yoo, and H. Koo, Roles of AKT1 and AKT2 in non-small cell lung cancer cell survival, growth, and migration. *Cancer Science*, vol. 102, no. 10, pp. 1822–1828, 2011.

[24] I. Vivanco and C. Sawyers, The phosphatidylinositol 3-Kinase AKT pathway in human cancer. *Nature Reviews Cancer*, vol. 2, no. 7, pp. 489–501, 2002.

[25] M. Scheffler, M. Bos, M. Gardizi, K. König, S. Michels, J. Fassunke, C. Heydt, H. Künstlinger, M. Ihle, F. Ueckeroth, K. Albus, M. Serke, U. Gerigk, W. Schulte, K. Töpelt, L. Nogova, T. Zander, W. Engel-Riedel, E. Stoelben, Y. Ko, W. Randerath, B. Kaminsky, J. Panse, C. Becker, M. Hellmich, S. Merkelbach-Bruse, L. Heukamp, R. Büttner, and J. Wolf, PIK3CA mutations in non-small cell lung cancer (NSCLC): genetic heterogeneity, prognostic impact and incidence of prior malignancies. *Oncotarget*, vol. 6, no. 2, pp. 1315–1326, 2015.

[26] W. Vogel, G. Gish, F. Alves, and T. Pawson, The discoidin domain receptor tyrosine kinases are activated by collagen. *Molecular Cell*, vol. 1, no. 1, pp. 13–23, 1997.

[27] P. Hammerman, M. Sos, A. Ramos, C. Xu, A. Dutt, W. Zhou, L. Brace, B. Woods, W. Lin, J. Zhang, X. Deng, S. Lim, S. Heynck, M. Peifer, J. Simard, M. Lawrence, R. Onofrio, H. Salvesen, D. Seidel, T. Zander, J. Heuckmann, A. Soltermann, H. Moch, M. Koker, F. Leenders, F. Gabler, S. Querings, S. Ansén, E. Brambilla, C. Brambilla, P. Lorimier, O. Brustugun, Å. Helland, I. Petersen, J. Clement, H. Groen, W. Timens, H. Sietsma, E. Stoelben, J. Wolf, D. Beer, M. Tsao, M. Hanna, C. Hatton, M. Eck, P. Janne, B. Johnson, W. Winckler, H. Greulich, A. Bass, J. Cho, D. Rauh, N. Gray, K. Wong, E. Haura, R. Thomas, and M. Meyerson, Mutations in the DDR2 kinase gene identify a novel therapeutic target in squamous cell lung cancer. *Cancer Discovery*, vol. 1, no. 1, pp. 78–

89, 2011.

[28] J. Wangari-Talbot and E. Hopper-Borge, Drug resistance mechanisms in non-small cell lung carcinoma. *Journal of Cancer Research Updates*, vol. 2, no. 4, pp. 265–282, 2013.

[29] R. Edgar, M. Domrachev, and A. Lash, Gene expression Omnibus: NCBI gene expression and hybridization array data repository. *Nucleic Acids Research*, vol. 30, no. 1, pp. 207–210, Jan. 2002.

[30] T. Barrett and R. Edgar, Gene expression omnibus: microarray data storage, submission, retrieval, and analysis. *Methods in Enzymology*, vol. 411, no. 2005, pp. 352–369, Jan. 2006.

[31] T. Barrett, D. Troup, S. Wilhite, P. Ledoux, C. Evangelista, I. Kim, M. Tomashevsky, K. Marshall, K. Phillippy, P. Sherman, R. Muertter, M. Holko, O. Ayanbule, A. Yefanov, and A. Soboleva, NCBI GEO: archive for functional genomics data sets-10 years on. *Nucleic Acids Research*, vol. 39, pp. 1005–1010, Jan. 2011.

[32] T. Barrett, D. Troup, S. Wilhite, P. Ledoux, D. Rudnev, C. Evangelista, I. Kim, A. Soboleva, M. Tomashevsky, K. Marshall, K. Phillippy, P. Sherman, R. Muertter, and R. Edgar, NCBI GEO: archive for high-throughput functional genomic data. *Nucleic Acids Research*, vol. 37, pp. 885–890, Jan. 2009.

[33] T. Barrett, D. Troup, S. Wilhite, P. Ledoux, D. Rudnev, C. Evangelista, I. Kim, A. Soboleva, M. Tomashevsky, and R. Edgar, NCBI GEO: mining tens of millions of expression profiles-database and tools update. *Nucleic Acids Research*, vol. 35, pp. 760–765, Jan. 2007.

[34] D. Sean and P. Meltzer, GEOquery: a bridge between the Gene Expression Omnibus (GEO) and BioConductor. *Bioinformatics*, vol. 23, no. 14, pp. 1846–1847, Jul. 2007.

[35] T. Lu, M. Tsai, J. Lee, C. Hsu, P. Chen, C. Lin, J. Shih, P. Yang, C. Hsiao, L. Lai, and E. Chuang, Identification of a novel biomarker, SEMA5A, for non-small cell lung carcinoma in nonsmoking women. *Cancer Epidemiology, Biomarkers and Prevention*, vol. 19, no. 10, pp. 2590–2597, 2010.

[36] M. Landi, T. Dracheva, M. Rotunno, J. Figueroa, H. Liu, A. Dasgupta, F. Mann, J. Fukuoka, M. Hames, A. Bergen, S. Murphy, P. Yang, A. Pesatori, D. Consonni, P. Bertazzi, S. Wacholder, J. Shih, N. Caporaso, and J. Jen, Gene expression signature of cigarette smoking and its role in lung adenocarcinoma development and survival. *PLoS ONE*, vol. 3, no. 2, 2008.

[37] P. Luk, B. Yu, C. Ng, B. Mercorella, C. Selinger, T. Lum, S. Kao, S. Toole, and W. Cooper, BRAF mutations in non-small cell lung cancer. *Translational Lung Cancer Research*, vol. 4, no. 2, pp. 142–148, 2015.

[38] I. Paul, S. Bhattacharya, A. Chatterjee, and M. Ghosh, Current understanding on EGFR and Wnt/β-Catenin signaling in glioma and their possible crosstalk. *Genes and Cancer*, vol. 4, no. 11–12, pp. 427–446, 2013.

[39] M. Luo and L. Fu, Redundant kinase activation and resistance of EGFR-tyrosine kinase inhibitors. *American Journal of Cancer Research*, vol. 4, no. 6, pp. 608–628, 2014.

[40] F. Li, Y. Liu, H. Chen, D. Liao, Y. Shen, F. Xu, and J. Wang, EGFR and COX-2 protein expression in non-small cell lung cancer and the correlation with clinical features. *Journal of Experimental and Clinical Cancer Research*, vol. 30, no. 27, pp. 1–8, 2011.

[41] S. Mehta, A. Shelling, A. Muthukaruppan, A. Lasham, C. Blenkiron, G. Laking, and C.

Print, Predictive and prognostic molecular markers for cancer medicine. *Therapeutic Advances in Medical Oncology*, vol. 2, no. 2, pp. 125–148, 2010.

[42] J. Engelman, K. Zejnullahu, C. Gale, E. Lifshits, A. Gonzales, T. Shimamura, F. Zhao, P. Vincent, G. Naumov, J. Bradner, I. Althaus, L. Gandhi, G. Shapiro, J. Nelson, J. Heymach, M. Meyerson, K. Wong, and P. Jonne, PF00299804, an irreversible pan-ERBB inhibitor, is effective in lung cancer models with EGFR and ERBB2 mutations that are resistant to gefitinib. *Cancer Research*, vol. 67, no. 24, pp. 11924–11932, 2007.

[43] M. Siegelin and A. Borczuk, Epidermal growth factor receptor mutations in lung adenocarcinoma. *Laboratory Investigation*, vol. 94, no. 2, pp. 129–137, 2014.

[44] T. Sasaki, S. Rodig, L. Chirieac, and P. Jänne, The biology and treatment of EML4-ALK non-small cell lung cancer. *European Journal of Cancer*, vol. 46, no. 10, pp. 1773–1780, 2010.

[45] S. Nanjo, T. Nakagawa, S. Takeuchi, K. Kita, K. Fukuda, M. Nakada, H. Uehara, H. Nishihara, E. Hara, H. Uramoto, F. Tanaka, and S. Yano, In vivo imaging models of bone and brain metastases and pleural carcinomatosis with a novel human EML4-ALK lung cancer cell line. *Cancer Science*, vol. 106, no. 3, pp. 244–252, 2015.

[46] S. Perner, P. Wagner, F. Demichelis, R. Mehra, C. Lafargue, B. Moss, S. Arbogast, A. Soltermann, W. Weder, T. Giordano, D. Beer, D. Rickman, A. Chinnaiyan, H. Moch, and M. Rubin, EML4-ALK fusion lung cancer: a rare acquired event. *Neoplasia*, vol. 10, no. 3, pp. 298–302, 2008.

[47] A. Tatem, C. Guerra, P. Atkinson, and S. Hay, Intragenic ERBB2 kinase mutations in tumours. *Nature*, vol. 431, no. 7008, pp. 525–525, 2004.

[48] Y. Minami, T. Shimamura, K. Shah, T. LaFramboise, K. Glatt, E. Liniker, C. Borgman, H. Haringsma, W. Feng, B. Weir, M. Lowell, J. Lee, J. Wolf, G. Shapiro, K. Wong, M. Meyerson, and R. Thomas, The major lung cancer-derived mutants of ERBB2 are oncogenic and are associated with sensitivity to the irreversible EGFR/ERBB2 inhibitor HKI-272. *Oncogene*, vol. 26, no. 34, pp. 5023–5027, 2007.

[49] J. Sánchez-Torres, S. Viteri, M. Molina, and R. Rosell, BRAF mutant non-small cell lung cancer and treatment with BRAF inhibitors. *Translational Lung Cancer Research*, vol. 2, no. 3, pp. 244–250, 2013.

[50] J. Melorose, R. Perroy, and S. Careas, Clinical, pathological and biological features associated with BRAF mutations in non-small cell lung cancer. *Clinical Cancer Research*, vol. 19, no. 16, pp. 617–632, 2013.

[51] R. Lawrence and R. Salgia, MET molecular mechanisms and therapies in lung cancer. *Cell Adhesion and Migration*, vol. 4, no. 1, pp. 146–152, 2010.

[52] A. Vollmann, H. Vornlocher, T. Stempfl, G. Brockhoff, R. Apfel, and U. Bogdahn, Effective silencing of EGFR with RNAi demonstrates non-EGFR dependent proliferation of glioma cells. *International Journal of Oncology*, vol. 28, no. 6, pp. 1531–1542, 2006.

[53] M. Zhang, X. Zhang, C. Bai, X. Song, J. Chen, L. Gao, J. Hu, Q. Hong, M. West, and M. Wei, Silencing the epidermal growth factor receptor gene with RNAi may be developed as a potential therapy for non small cell lung cancer. *Genetic Vaccines and Therapy*, vol. 3, no. 5, pp. 1–12, 2005.

[54] M. Wei, M. Zhang, X. Zhang, J. Chen, L. Gao, J. Hu, M. West, C. Bai, and S. Diamond, Inhibition of non-small cell lung cancer by silencing EGFR with RNAi. *Molecular*

Therapy, vol. 9, no. 1, pp. 189–190, 2004.

Chapter 7 - Summary and Future Directions

7.1 Summary

The main challenge in the translation of RNAi therapeutics into clinical trials is a lack of biocompatible siRNA carriers/vectors capable of overcoming the many extracellular and intracellular barriers to the effective siRNA delivery and silencing. These barriers specific to siRNA delivery were discussed in the introduction (Chapter 1). This thesis has explored the potential characteristics of siRNA-liposomal formulations which enable the entry of siRNA into the cells and its cytosolic compartment to achieve the mRNA targeting and the gene silencing effect. The work focused on the study of mechanisms of cellular internalization of the siRNA delivery systems designed and fabricated, and their intracellular localisation, i.e. engagement in mRNA silencing cellular machinery, as a crucial part of improving our understanding of how the siRNA-liposomes internalisation pathways influence the intracellular localisation and a consequent silencing effect.

The first experimental part of this project (Chapter 3) studied the cytotoxicity and the physicochemical characterisations of siRNA-liposomes in order to formulate an optimised delivery system and to provide a fundamental understanding that help in designing an effective delivery system for further biological investigations.

The cytotoxicity of DC-Chol:DOPE liposomes was initially investigated in empty and then siRNA-liposomal formulations to identify the safe doses of liposomes, to highlight

possible mechanisms of toxicity, and assess whether toxic effects arise from the liposome formulation itself or the siRNA-liposome system. The application of a high dose of empty liposomes (high total lipid content) to A549 cells in culture revealed a concentration dependent effect, as confirmed by the MTS, LDH and Annexin V/PI assays. From the MTS and LDH results of empty liposomes, the highest total lipid concentration (50 mM) produced complete loss of metabolic activity of A549 cells as measured by MTS but the LDH assay showed around 60% of lactated dehydrogenase release at the same concentration (such as panel e of Figure 3.2 and 3.3). MTS assay is usually used to measure the mitochondrial activity of the cells, while the LDH assay measures the membrane integrity of the cells. Therefore, the complete loss of metabolic activity should not be associated with complete damage of plasma membrane and 100% release of LDH, as toxicants may disrupt cellular metabolic activity, but leave membranes intact. In addition, it should be noted that the LDH release of empty liposomes formulations plateaus at less than 100% for most of the formulations. It might be that our cationic liposomes were caused partial loss of the membrane integrity of A549 cells at the highest concentration applied, which led to partial release of LDH. However, the effect of highest total lipid concentration applied (50 mM) was lower than the effect of Triton-X, which produced 100% of LDH release and complete loss of membrane integrity.

The minimum cytotoxic effect of liposomes on A549 cells was obtained with the total lipid concentration of 1.0 mM, and no significant effect of different molar ratios of DC-Chol to DOPE on the cytotoxicity has been observed. The safe dose of liposomes at total lipid concentration of 1.0 mM was used to prepare liposomes at different compositions of DC-Chol:DOPE and different N/P ratios of siRNA loaded liposomes. The toxicity assays indicated that the incorporation of siRNA molecules into the cationic liposomes

fabricated showed no significant effect on the cytotoxicity of A549 cells, relative to empty liposomes. The cationic delivery systems, including cationic liposomes, were demonstrated to cause 'pathological' changes in the cells, including cell shrinking, reduced number of mitoses and vacuolization of the cytoplasm [1], cell necrosis through the interaction with Na^+/K^+-ATPase, and impaired activity [2]. Moreover, it has been reported that exposure of the cells in culture to a high total lipid concentration of cationic liposomes is associated with an increase in the toxic effects, and this influence can be reduced applying lower doses [3], [4]. The possible contribution to the observed toxicity at higher applied concentrations of cationic liposomes may be the increased interactions between positively charged lipids and negatively charged cell membrane components, due to the increased content of cationic charges, leading to a cascade of cellular events [3], [5].

The hydrodynamic particle size of empty and siRNA-liposomes was measured to evaluate if the liposomes of size and size homogeneity appropriate for endocytosis were fabricated by the method adopted, and is the siRNA encapsulation had an effect on the size of liposomes. The DLS results showed that particles hydrodynamic diameter of empty liposomes was less than 80 nm for all samples measured, and no significant effect of different ratios of DC-Chol:DOPE was observed. The results in Table 3.1 show that the particle size distributions of empty liposomes were homogenous, judged from the PDI measurements (PDI values <0.27). However, the hydrodynamic diameter of siRNA-liposomes showed a significant increase to approximately 200 nm for all tested formulations. The PDI values of siRNA-liposomes formulation were also measured and summarised in Table 3.2. Results of PDI show that no significant effect of different molar ratio of DC-Chol:DOPE on the PDI values of siRNA-liposomes formulations. It should

be noted here that the liposomes fabrication method included an addition of siRNA during the lipid layer hydration stage, hence promoting encapsulation of siRNA molecules into the 'core'/internal surface of the liposomes, which may have resulted in a formation of larger lipid bilayer vesicles. An increase in the content of cationic lipid to siRNA was observed to reduce the particle size of siRNA-liposomes, possibly due to affecting the overall charge balance of the system and packing of lipids and lipid-siRNA 'complexes' into the vesicles.

The electrostatic properties of liposomal formulations were characterised using the zeta potential. Results of empty liposomes showed that the magnitude of the zeta potential was highly dependent upon the cationic lipid content. The potential of siRNA-liposomes inverted from a negative charge for the lowest tested N/P ratio of 0.78:1, to a positive charge for the N/P ratio of 1.56:1, clearly indicating an excess of siRNA negative charge in the system at low N/P ratios and an excess of positive charge of the liposomes at ratios higher than N/P 1.56:1. This will have consequences to the liposome surface-cell surface interactions in the subsequent experiments.

The encapsulation efficiency of siRNA molecules into liposomes was investigated and the data of gel electrophoresis and Vivaspin filtration both indicated that the increased entrapment of anionic siRNA was achieved by increasing the ratios of cationic lipid, DC-Chol, to siRNA. The classical film hydration method resulted in a high level of siRNA liposomal encapsulation, even at relatively low levels of cationic lipid (N/P ratio of 3.125:1), while in the same time maintaining colloidal stability of the siRNA-liposomes. A lower content of cationic lipid required for the good encapsulation of siRNA would be expected to reduce the overall toxicity of the system.

In terms of RNase A stability, prolonged nuclease resistance was observed for the tested siRNA-liposomal formulations prepared at 1.0 mM total lipid concentration and at N/P ratio of 3.125:1, at time points less than 4 hours, and no significant difference was observed for the different lipid compositions in terms of siRNA protection. It should be noted here that although a protection of siRNA from enzymatic degradation is an essential prerequisite of an ideal siRNA delivery system, this product attribute has is not routinely tested/reported in the literature.

Following the initial biological and physicochemical characterisations, the next step of this project (Chapter 4) aimed to investigate (i) the cellular uptake of fluorescently labelled siRNA-liposomes and (ii) the inhibition of luciferase expression for a series of liposomal formulations in *in vitro* cell model of epithelial lung cancer. In addition, the correlation between cellular internalisation and gene silencing efficiency in A549 and A549-Luc cancer cells was assessed.

The cellular uptake of siRNA-liposomes and intracellular trafficking route dictates the gene silencing efficiency, and may present a major barrier to effective gene silencing [6]. Positively charged liposomes, as the system used in this study, would be expected to interact electrostatically with the plasma membrane of cells in culture [7], and therefore it was important to evaluate the effect of the DC-Chol and DOPE molar ratio, as well as the ratio between cationic lipid and negatively charge siRNA (N/P ratio), on the cellular internalization and trafficking. The data show a bell shaped relationship between level of cellular internalization and DC-Chol:DOPE ratios in the 0.33:1 to 3:1 range with the maxima at 1:1 ratio. At the present it is not clear to why the uptake of liposomes with

highest ratios of DC-Chol:DOPE is lower than the 1:1 ratio (Figure 4.2.C), as would be expected from their higher positive charge.

In addition to flow cytometry data, the uptake visualisation by confocal microscopy indicated the presence of some punctate and some 'diffused' red fluorescence in higher magnification images which may indicate that some endosomal 'escape' may have occurred.

A gene knockdown study was performed using a luciferase-expressing A549 human lung carcinoma cell line, A549-Luc. The siRNA-liposomes were prepared at a fixed N/P ratio of 3.125:1, and the results of gene silencing study using 0.5 and 1 μg *per* well of siRNA indicated significant inhibition of the luciferase activity for all liposome formulations used, in comparison to the negative controls with non-targeting siRNA. An increase in the ratio of cationic lipid in the formulations had a significant influence on the transfection efficiency, whereby the highest level of luciferase silencing was achieved with siRNA-liposomes with an equal ratio of DC-Chol to DOPE (1 to 1), and maximum silencing was obtained 48 hours post-transfection. It has been reported that the luciferase knockdown can increase significantly by increasing the amount of cationic lipid particles [8]. A previous study has suggested that a higher transfection efficiency could be achieved by using a 1:1 molar ratio of cationic to helper lipid [9], as seen in our study. This has been ascribed to the effect of that the molecular character of the 'helper' DOPE lipid - which facilitates the transition from a lamellar to a hexagonal phase [10], [11] of lipid bilayers. This has been ascribed to promote liposomal cellular entry and escape from endosomes following endocytosis, resulting in enhanced silencing activity [12], [13].

In an important aspect of this project, 'luc-siRNA based MB'-liposomes were fabricated and used to assess a level of siRNA involvement in the mRNA silencing cellular machinery. A detection of green molecular beacon fluorescence within the cell cytoplasm, which confirms luc-siRNA binding to the targeted Luc-mRNA, was quantified using flow cytometry and visualised by confocal microscopy. This part of the project clearly demonstrated positive correlation between cellular uptake pathway(s), siRNA engagement and mRNA silencing. The assessment of MB is somewhat limited by not using a 'scrambled siRNA based MB' liposomes as negative control, which would be essential to distinguish between specific and non-specific binding effects of 'luc-siRNA based MB' with target luc-mRNA. In future developments, a quantitative relationship between internalization, engagement and silencing of different siRNA delivery systems could be an important part of their silencing potentials assessment. Moreover, the analysis of non-specific fluorescence of FAM-MB by using the normal A549 cells without the luciferase mRNA is important to confirm that the green fluorescence detected is due to the successful engagement of FAM-MB with the targeted mRNA, not due to the non-specific binding of MB or the degradation by ribonuclease enzyme.

Studying the molecular and functional basis of endocytic mechanisms provides basic concepts for tailoring the design parameters of delivery systems to improve their efficiency and specificity [14]. To date, the cellular internalisation pathways of siRNA-liposomes has not been extensively studied and systematic studies are needed to provide better understanding [15], [16]. The work presented in Chapter 5 provides insight into the mechanisms of the siRNA-liposomes uptake by A549 and A549-Luc cells. Similar studies are rare in the literature, and these results have important implications for the design of therapeutic siRNA delivery systems to improve siRNA therapy potentials. In

this work, pharmacological inhibitors were used as an experimental tool to provide an insight into which endocytic mechanism(s) were responsible for the liposomes uptake and cellular trafficking. The inhibitor concentrations applied were non-toxic to the cells, as determined by the metabolic activity (MTS) assay in the preliminary experiments. The inhibitors were also tested on two 'classical' ligands, T*f* and CTß, which are reported in the literature as being internalised into cells through clathrin and caveolin-mediated endocytosis, respectively [17], [18], to evaluate their inhibitory effect on the cellular internalisation through endocytosis in the A549 cells. The present work revealed that siRNA-liposomes were internalised into the cells *via* multiple endocytosis pathways. The data of clathrin pathway inhibition showed that this pathway is playing an important role on the cellular uptake and luciferase silencing effect of siRNA-liposomes into A549 and A549-Luc cells. The level of luciferase silencing in A549-Luc cells can almost be doubled through the use of the endosomolytic agent, chloroquine, indicating that the clathrin-mediated pathway and intercellular trafficking, leading to lysosomal compartment, is indeed an important route for internalisation and silencing of the investigated liposomal system (Figure 5.25). Caveolae dependent pathway was not found to have a substantial involvement in the internalisation of tested cationic liposomes. On the other hand, the depletion of cholesterol from the plasma membrane, through extraction of cholesterol from lipid rafts, significantly affected the internalisation of siRNA-liposomes as well as knockdown processes. In addition, macropinocytosis was found to have a major involvement in the internalisation of the siRNA-liposomes formulations as seen by the effect of EIPA inhibitor.

The final part of this project (Chapter 6) was to perform a screening of the expression profiles of candidate genes that could be involved in the progression of NSCLC.

Microarray protein expression profiles of eleven different genes were analysed in lung cancer samples and compared to healthy lung from two studies available in the GEO database. The results provide a primary overview of gene expression features and allowed an initial assumption about the involvement of these genes in the control of lung cancer to be made. Only five genes, *EGFR*, *EML4*, *ERBB2*, *BRAF* and *MET*, were found to be significantly up-regulated in lung cancer, and silencing of the proteins they encode could help to control the progression of lung cancer and may provide an attractive approach for lung cancer treatment. The involvement of these candidate genes in the progression of NSCLC needed to be validated, so the effect of protein silencing using siRNA on cell proliferation within the *in vitro* model of NSCLC was investigated.

Liposome-siRNA formulations targeting *EGFR* were used to examine the effect on cell proliferation in NSCLC using an *in vitro* model, and it was found that the liposome formulations were able to mediate *EGFR* silencing and to improve cell proliferation. The preliminary experiments of EGFR silencing effect on the proliferation of A549-Luc cells should be validated using RT-qPCR to quantified EGFR-mRNA knockdown and western blot to confirm successful knockdown of the protein of a target EGFR.

In summary, siRNA-liposomes prepared from DC-Chol and DOPE has the potential to become versatile nucleic acid and drug delivery system with possible clinical translation.

7.2 Future Directions

In this project the main aims and objectives were (i) formulation optimisation and characterisation of the siRNA delivery system, (ii) providing insights regarding the system uptake and intracellular transport mechanisms, and (iii) establishing trend in internalization and siRNA engagement in the cell silencing machinery, to aid in the design of an efficient siRNA formulations. DC-Chol/DOPE liposomes were used in throughout the project, as a 'reasonable' model system based on a body of previous literature.

There remain a number of experiments that would complement the current work as well as ideas that could have been, and could be, tested in the future. For instance, to compare the effect of varying the N/P ratios, to expand confocal microscopy studies, test the influence of liposome surface attributes and to further test intracellular transport and localization of siRNA.

In the future, attachment of different functionalities onto the liposomal surface (e.g. PEG chains and ligands) could be added to the design of the system while the endosomal escape, shown to be an important step, can be enhanced by the use of membrane disrupting peptides [19]. PEG is expected to reduce the liposomes contacts with serum proteins while the covalent coupling of a targeting ligand to one of the liposome components would facilitate the uptake of siRNA, via receptor mediated cellular internalisation. The mechanism of such created system`s cellular internalisation will have to be assess by the protocols developed in the work.

Further research to understand of the complex processes involved in cell internalisation and transport could involve the use of knock-out cell models, to overcome issues of non-specificity of used pharmacological inhibitors. However, these models are not routinely available and their development would be beyond the scope of this work. Alternatively, siRNA knock-down cell models can be used, as suggested in [20], [21], however this would involve repeated cell treatment with siRNA, while potential non-specific effects are also possible.

In the next step, an *in vivo* study should be performed to determine if *in vitro* results in the cell model indeed predict the *in vivo* situation. The siRNA-liposomes formulations will be prepared to be administered 'locally' into the lung (e.g. using nebulization), although it should be appreciated that it is not clear from the literature if this route indeed allows a better access to the lung cancer tissue. It has been shown that the intratracheal aerosolization method to deliver formulations to the mouse can result in a direct access to the lung epithelia [22], while a clear evidence to access to the lung tumour is less clear [23]. Many *in vivo* animal studies are now employing a less invasive intratracheal delivery method, which, while still requiring anaesthesia, eliminates the need for surgery by the use of aerosolizers such as the Penn-Century MicroSprayer®. In the past, MicroMist nebulizer [24], and AeroProbe nebulizing catheter have been used also, but in the recent years, the Penn-Century MicroSprayer® seems to have gained the leadership [25].

7.3 References

[1] H. Lv, S. Zhang, B. Wang, S. Cui, and J. Yan, Toxicity of cationic lipids and cationic polymers in gene delivery. *Journal of Controlled Release*, vol. 114, no. 1, pp. 100–109, Aug. 2006.

[2] X. Wei, B. Shao, Z. He, T. Ye, M. Luo, Y. Sang, X. Liang, W. Wang, S. Luo, S. Yang, S. Zhang, C. Gong, M. Gou, H. Deng, Y. Zhao, H. Yang, S. Deng, C. Zhao, L. Yang, Z. Qian, J. Li, X. Sun, J. Han, C. Jiang, M. Wu, and Z. Zhang, Cationic nanocarriers induce cell necrosis through impairment of Na(+)/K(+)-ATPase and cause subsequent inflammatory response. *Cell Research*, vol. 25, no. 2, pp. 237–253, 2015.

[3] K. Romoren, B. Thu, N. Bols, and O. Evensen, Transfection efficiency and cytotoxicity of cationic liposomes in salmonid cell lines of hepatocyte and macrophage origin. *Biochimica et Biophysica Acta - Biomembranes*, vol. 1663, no. 1–2, pp. 127–134, 2004.

[4] K. Knudsen, H. Northeved, E. Kumar, A. Permin, T. Gjetting, T. Andresen, S. Larsen, K. Wegener, J. Lykkesfeldt, K. Jantzen, S. Loft, P. Moller, and M. Roursgaard, In vivo toxicity of cationic micelles and liposomes. *Nanomedicine*, vol. 11, no. 2, pp. 467–477, 2015.

[5] E. Fröhlich, The role of surface charge in cellular uptake and cytotoxicity of medical nanoparticles. *International Journal of Nanomedicine*, vol. 7, pp. 5577–5591, 2012.

[6] R. Kanasty, K. Whitehead, A. Vegas, and D. Anderson, Action and reaction: the biological response to siRNA and its delivery vehicles. *Molecular Therapy*, vol. 20, no. 3, pp. 513–524, 2012.

[7] G. Bozzuto and A. Molinari, Liposomes as nanomedical devices. *International Journal of Nanomedicine*, vol. 10, pp. 975–999, 2015.

[8] P. Pierrat, D. Kereselidze, P. Wehrung, G. Zuber, F. Pons, and L. Lebeau, Bioresponsive deciduous-charge amphiphiles for liposomal delivery of DNA and siRNA. *Pharmaceutical Research*, vol. 30, no. 5, pp. 1362–1379, May 2013.

[9] Y. Zhang, H. Li, J. Sun, J. Gao, W. Liu, B. Li, Y. Guo, and J. Chen, DC-Chol/DOPE cationic liposomes: a comparative study of the influence factors on plasmid pDNA and siRNA gene delivery. *International Journal of Pharmaceutics*, vol. 390, no. 2, pp. 198–207, May 2010.

[10] S. Marrink and A. Mark, Molecular view of hexagonal phase formation in phospholipid membranes. *Biophysical Journal*, vol. 87, no. 6, pp. 3894–3900, 2004.

[11] M. Rappolt, A. Hickel, F. Bringezu, and K. Lohner, Mechanism of the lamellar/inverse hexagonal phase transition examined by high resolution x-ray diffraction. *Biophysical Journal*, vol. 84, no. 5, pp. 3111–3122, 2003.

[12] S. Mochizuki, N. Kanegae, K. Nishina, Y. Kamikawa, K. Koiwai, H. Masunaga, and K. Sakurai, The role of the helper lipid dioleoylphosphatidylethanolamine (DOPE) for DNA transfection cooperating with a cationic lipid bearing ethylenediamine. *Biochimica et Biophysica Acta*, vol. 1828, no. 2, pp. 412–418, Feb. 2013.

[13] M. Muñoz-Ubeda, A. Rodríguez-Pulido, A. Nogales, A. Martín-Molina, E. Aicart, and E. Junquera, Effect of lipid composition on the structure and theoretical phase diagrams of DC-Chol/DOPE-DNA lipoplexes. *Biomacromolecules*, vol. 11, no. 12, pp. 3332–33340, Dec. 2010.

[14] R. Sahay, W. Querbes, C. Alabi, A. Eltoukhy, S. Sarkar, C. Zurenko, E. Karagiannis, K. Love, D. Chen, R. Zoncu, Y. Buganim, and A. Schroeder, Efficiency of siRNA delivery by lipid nanoparticles is limited by endocytic recycling. *Nature Biotechnology*, vol. 31, no. 7, pp. 653–661, 2013.

[15] A. Elouahabi and J. Ruysschaert, Formation and intracellular trafficking of lipoplexes and polyplexes. *Molecular Therapy*, vol. 11, no. 3, pp. 336–347, 2005.

[16] M. Hirsch and M. Helm, Live cell imaging of duplex siRNA intracellular trafficking. *Nucleic Acids Research*, vol. 43, no. 9, pp. 4650–4660, 2015.

[17] K. Mayle, A. Le, and D. Kamei, The Intracellular trafficking pathway of transferrin. *Biochimica et Biophysica Acta*, vol. 1820, no. 3, pp. 264–281, 2012.

[18] M. Torgersen, G. Skretting, B. Deurs, and K. Sandvig, Internalization of cholera toxin by different endocytic mechanisms. *Journal of Cell Science*, vol. 114, no. 20, pp. 3737–3747, 2001.

[19] A. El-Sayed, S. Futaki, and H. Harashima, Delivery of macromolecules using arginine-rich cell-penetrating peptides: ways to overcome endosomal entrapment. *The American Association of Pharmaceutical Scientists Journal*, vol. 11, no. 1, pp. 13–22, 2009.

[20] P. Pereira, S. Pedrosa, J. Wymant, E. Sayers, A. Correia, M. Vilanova, A. Jones, and F. Gama, siRNA inhibition of endocytic pathways to characterize the cellular uptake mechanisms of folate-functionalized glycol chitosan nanogels. *Molecular Pharmaceutics*, vol. 12, no. 6, pp. 1970–1979, 2015.

[21] M. Al-soraj, C. Watkins, D. Vercauteren, S. Smedt, K. Braeckmans, and A. Jones, siRNA versus pharmacological inhibition of endocytic pathways for studying cellular uptake of cell penetrating peptides. *Journal of Controlled Release*, vol. 148, no. 1, pp. e86–e87, 2000.

[22] A. Rosas-Taraco, D. Higgins, J. Sánchez-Campillo, E. Lee, I. Orme, and M. González-Juarrero, Intrapulmonary delivery of XCL1-targeting small interfering RNA in mice chronically infected with Mycobacterium tuberculosis. *American Journal of Respiratory Cell and Molecular Biology*, vol. 41, no. 2, pp. 136–145, 2009.

[23] O. Garbuzenko, M. Saad, S. Betigeri, M. Zhang, A. Vetcher, V. Soldatenkov, D. Reimer, V. Pozharov, and T. Minko, Intratracheal versus intravenous liposomal delivery of siRNA, antisense oligonucleotides and anticancer drug. *Pharmaceutical Research*, vol. 26, no. 2, pp. 382–394, 2009.

[24] D. Zamora-Avila, P. Zapata-Benavides, M. Franco-Molina, S. Saavedra-Alonso, L. Trejo-Avila, D. Reséndez-Pérez, J. Méndez-Vázquez, J. Isaias-Badillo, and C. Rodríguez-Padilla, WT1 gene silencing by aerosol delivery of PEI–RNAi complexes inhibits B16-F10 lung metastases growth. *Cancer Gene Therapy*, vol. 16, no. 12, pp. 892–899, 2009.

[25] O. Merkel, I. Rubinstein, and T. Kissel, siRNA delivery to the lung: What's new?. *Advanced Drug Delivery Reviews*, vol. 75, pp. 112–128, Jun. 2014.

Appendices

1. Luciferase Activity of scrambled non-targeting siRNA-liposomes:

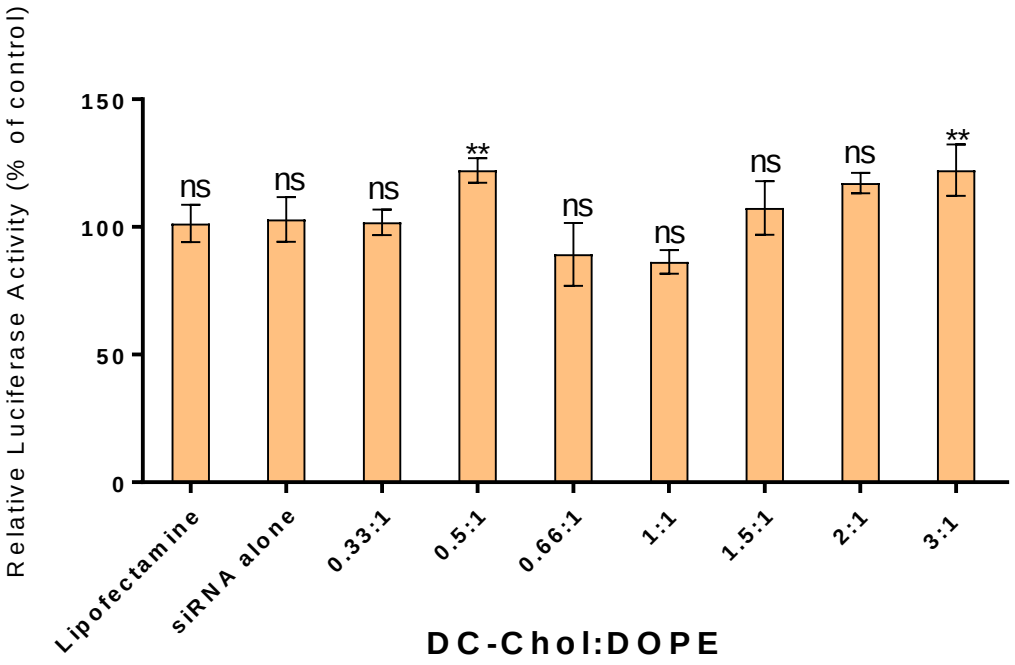

Figure A1. Relative luciferase activity of A549-Luc cells after incubation with non-targeting siRNA-liposomes

*Cells were seeded onto 24-well plates at a density of 5 × 10^4 cells per well and cultured overnight. Liposome-siRNA formulations were prepared at an N/P ratio of 3.125:1 and different DC-Chol:DOPE molar ratios, and applied to the cells for 4 hrs. The transfection reagent Lipofectamine® RNAiMAX was prepared as per manufacturer instruction described previously in Chapter 2. A549-Luc cells not treated with siRNA liposomes accounted as 100% of luciferase protein activity and used to normalise the luciferase activity of all tested formulations. Samples were removed and replaced with fresh medium, and the cells then incubated for a further 48 hrs before analysis. ** indicates a significant difference between the results ($p<0.01$) and ns indicates no significant difference ($p>0.05$).*

2. Normalizing Gene expression Data from GEO database for Study 1:

Series: GSE19804, Platform: Affymetrix Human Genome U133 Plus 2.0 Array, Sample number: 120 samples (60 healthy lung and 60 NSCLC)

		RPL29	DDR2		DDR2		DDR2		ALK	
Patient NO.	Condition	200823_x_at	205168_at		225442_at		227561_at		208211_s_at	
GSM494556	Lung Cancer 2T	12.5196	8.45329	8.45329	8.41711	8.41711	8.64255	8.64255	5.45383	5.45383
GSM494557	Lung Cancer 3T	12.4263	8.03678	8.097122	7.92139	7.980866	7.88373	7.942923	5.38982	5.430288
GSM494558	Lung Cancer 6T	12.9369	9.54722	9.239259	10.3089	9.97637	9.98057	9.658631	5.05212	4.889156
GSM494559	Lung Cancer 17T	12.2582	6.64821	6.78998	8.86074	9.049691	7.07418	7.225033	5.05022	5.157913
GSM494560	Lung Cancer 32T	12.6482	6.69515	6.627077	8.70917	8.62062	7.00431	6.933094	5.23779	5.184535
GSM494561	Lung Cancer 33T	13.0887	6.51601	6.232692	9.62527	9.206761	6.9383	6.636621	5.66506	5.418742
GSM494562	Lung Cancer 37T	13.1324	7.5997	7.245074	7.76545	7.403089	7.9411	7.570543	5.33273	5.083888
GSM494563	Lung Cancer 40T	13.0767	7.18943	6.883142	9.74402	9.3289	7.65497	7.328849	5.28441	5.059281
GSM494564	Lung Cancer 43T	13.026	6.94862	6.678485	9.63712	9.262466	7.40395	7.116113	5.21936	5.016452
GSM494565	Lung Cancer 79T	12.9914	7.8372	7.552582	9.39745	9.056169	9.71166	9.358968	5.06125	4.877444
GSM494566	Lung Cancer 91T	12.9482	8.85927	8.566018	9.59347	9.275915	9.42498	9.113003	4.85905	4.69821
GSM494567	Lung Cancer 92T	13.2565	8.76544	8.278188	8.57822	8.101375	9.14125	8.633108	5.5524	5.243754
GSM494568	Lung Cancer 94T	12.7319	8.89856	8.75018	9.10682	8.954967	9.23673	9.082711	5.38303	5.29327
GSM494569	Lung Cancer 97T	12.804	9.03049	8.829906	9.7515	9.534902	9.69108	9.475824	5.04341	4.931387

EGFR		EGFR		EGFR		EGFR		KRAS		KRAS	
211550_at		211551_at		211607_x_at		224999_at		1559203_s_at		1559204_x_at	
5.31532	5.31532	5.19049	5.19049	6.74348	6.74348	7.8167	7.8167	3.57585	3.57585	6.80175	6.80175
5.38763	5.428082	5.4876	5.528802	9.0848	9.153011	11.8101	11.89877	3.6628	3.690301	7.05594	7.108918
5.19767	5.030011	5.40826	5.233808	6.81549	6.595646	8.99093	8.700913	3.69415	3.574989	7.27742	7.042675
5.29282	5.405687	5.41843	5.533975	7.22838	7.382522	9.62906	9.834395	3.60433	3.681191	6.08683	6.216629
5.37044	5.315836	5.78343	5.724627	7.32724	7.252741	10.827	10.71692	3.92075	3.880886	6.19555	6.132557
4.91831	4.704461	5.38037	5.14643	6.385	6.107379	8.23024	7.872387	3.64896	3.490302	6.28851	6.015084
5.65738	5.393388	6.22453	5.934073	10.4121	9.926238	11.9646	11.40629	3.5864	3.419047	6.6721	6.360758
5.18226	4.961483	5.37398	5.145035	6.16961	5.906769	9.62967	9.219422	3.98663	3.81679	6.37634	6.104692
5.19514	4.993173	5.79353	5.5683	6.17552	5.93544	8.71055	8.371918	3.76326	3.616959	5.96488	5.732989
5.41874	5.221951	5.60569	5.402112	6.55585	6.317766	9.06468	8.735484	3.77345	3.636412	6.65286	6.411253
5.34385	5.166963	5.58598	5.401078	7.45741	7.210561	9.14418	8.841497	3.5207	3.404161	6.22202	6.016064
5.55851	5.249525	5.45835	5.154932	6.30353	5.95313	8.34741	7.883396	3.72444	3.517406	6.48743	6.126808
5.16991	5.083704	5.37486	5.285236	6.76126	6.648518	8.91337	8.764743	4.05382	3.986224	6.58951	6.479632
4.98082	4.870187	5.20784	5.092164	7.35557	7.192189	9.34088	9.133402	3.77646	3.692578	6.51701	6.372255

ALK		EGFR		EGFR		EGFR		EGFR		EGFR	
208212_s_at		1565483_at		1565484_x_at		201983_s_at		201984_s_at		210984_x_at	
5.3078	5.3078	6.74258	6.74258	6.1734	6.1734	9.40519	9.40519	7.99194	7.99194	7.00431	7.00431
4.88516	4.921839	6.88815	6.939868	6.37471	6.422573	13.8107	13.91439	11.3375	11.42262	9.31657	9.386521
5.10299	4.938385	7.46696	7.226101	6.86471	6.643278	11.369	11.00228	8.00172	7.743612	7.58585	7.341157
5.12815	5.237505	7.66057	7.823928	7.1525	7.305023	9.57118	9.775281	9.26872	9.466371	7.41033	7.568352
5.51955	5.46343	6.62962	6.562214	6.16482	6.102139	11.32	11.2049	11.2658	11.15126	7.74485	7.666105
5.70731	5.459155	7.29854	6.981198	6.81034	6.514225	7.8211	7.481037	7.34887	7.029339	6.47877	6.197071
4.84312	4.617124	7.59349	7.239153	7.31812	6.976633	13.252	12.63362	11.7791	11.22945	10.7804	10.27735
5.65892	5.417836	6.51331	6.235827	5.97577	5.721187	9.0746	8.687999	9.25839	8.86396	6.88802	6.594573
5.37673	5.167704	6.69818	6.437781	5.96032	5.728606	7.89587	7.588909	7.75811	7.456505	6.32031	6.074601
5.38862	5.192925	6.33369	6.103674	6.22558	5.99949	10.3146	9.940012	9.2091	8.874659	7.04841	6.792438
5.23299	5.059772	5.68749	5.499228	5.39758	5.218914	10.8653	10.50565	9.40317	9.091914	7.81555	7.556846
5.01436	4.735623	5.8191	5.495629	5.97402	5.641937	10.4807	9.898101	8.19096	7.735642	7.01311	6.623266
5.3091	5.220573	5.5844	5.491282	6.1083	6.006446	10.6713	10.49336	8.85862	8.710906	7.11182	6.993233
4.85453	4.746702	5.60558	5.48107	5.68808	5.561737	11.5024	11.24691	8.70976	8.5163	7.59037	7.421774

EML4		EML4		ERBB2		ERBB2		ERBB2		BRAF	
228674_s_at		232587_at		210930_s_at		216836_s_at		234354_x_at		206044_s_at	
7.82812	7.82812	6.54897	6.54897	5.63934	5.63934	10.9475	10.9475	5.14081	5.14081	6.42611	6.42611
8.99474	9.062275	7.00308	7.055661	5.5487	5.590361	11.0322	11.11503	4.6235	4.658214	6.56498	6.614272
8.20188	7.937315	6.61331	6.399987	4.9834	4.822653	9.59038	9.281027	4.45374	4.310078	6.26692	6.064771
8.11061	8.283565	6.2803	6.414224	4.83724	4.940392	11.0192	11.25418	5.17196	5.282249	6.56477	6.70476
7.91565	7.835168	5.84575	5.786314	5.08819	5.036456	10.8376	10.72741	5.23182	5.178626	6.95025	6.879584
8.32966	7.967484	6.77736	6.482679	5.09627	4.874683	9.6213	9.202963	4.505	4.309121	6.83207	6.53501
8.25712	7.871816	6.50049	6.197156	6.97043	6.645167	10.0806	9.610207	4.40816	4.202461	7.79463	7.430908
7.96418	7.624886	5.74958	5.504634	5.13994	4.920966	9.55605	9.148938	4.64639	4.448442	7.5461	7.224617
8.17407	7.856294	5.9093	5.679569	5.37602	5.167021	10.292	9.891887	4.8893	4.699223	6.82442	6.559113
6.54664	6.30889	6.60277	6.362982	5.03033	4.847647	10.483	10.1023	5.00398	4.822254	7.61362	7.337121
8.07418	7.806916	6.75154	6.528056	7.44741	7.200892	11.7636	11.37421	5.0639	4.896279	6.83416	6.607942
8.54846	8.07327	6.864	6.482445	5.54932	5.240845	10.7915	10.19162	4.75199	4.487837	7.09288	6.698602
9.41082	9.253898	7.15161	7.032359	5.37477	5.285148	9.93788	9.772169	4.58663	4.51015	6.96357	6.847455
7.88613	7.710965	6.68651	6.537991	5.62112	5.496265	9.96603	9.744666	4.49354	4.39373	6.52888	6.383862

BRAF		BRAF		MET		MET		MET		MET	
236402_at		243829_at		203510_at		211599_x_at		213807_x_at		213816_s_at	
5.15374	5.15374	5.57346	5.57346	11.1616	11.1616	7.95219	7.95219	7.41698	7.41698	4.95684	4.95684
5.35264	5.392829	5.94807	5.99273	10.9122	10.99413	7.70796	7.765833	7.5062	7.562559	4.37892	4.411798
4.82657	4.670881	5.24755	5.078282	9.21354	8.916343	7.1387	6.90843	6.98321	6.757956	4.15697	4.02288
6.26948	6.403174	6.05077	6.1798	11.5283	11.77414	6.53464	6.673988	6.92095	7.068536	4.1724	4.261374
7.28815	7.214048	6.32839	6.264046	12.0088	11.8867	6.87502	6.805119	6.41741	6.352161	4.35879	4.314472
6.20615	5.936305	6.42461	6.145266	10.4185	9.965501	6.28429	6.011047	6.72011	6.427918	3.81381	3.647985
6.4841	6.181531	6.30941	6.014993	12.1728	11.60478	10.6279	10.13197	9.67132	9.220025	7.67761	7.319348
7.29713	6.986254	5.6562	5.415232	10.3995	9.956455	6.48008	6.204012	6.26047	5.993758	3.81342	3.650959
7.00213	6.729915	6.56866	6.313296	12.4622	11.97772	7.09198	6.816272	6.58861	6.332471	4.35591	4.186569
6.89954	6.648974	7.13287	6.87383	12.5457	12.09009	6.96345	6.710563	7.01439	6.759653	4.67863	4.508719
5.74205	5.551982	6.47329	6.259017	11.4025	11.02506	9.33766	9.028573	8.56564	8.282108	5.52759	5.344621
5.89218	5.564647	6.5329	6.16975	11.2138	10.59045	7.23517	6.832983	6.88747	6.504611	4.53706	4.284855
6.4841	6.37598	6.29847	6.193445	11.286	11.09781	7.83015	7.699585	7.46063	7.336227	5.1714	5.085169
5.73304	5.605699	6.13764	6.001312	11.5922	11.33472	8.6277	8.436063	8.0497	7.870902	4.51405	4.413785

ABCC1		ABCC1		AKT1		PIK3CA		PIK3CA		PIK3CA	
202804_at		202805_s_at		207163_s_at		204369_at		231854_at		235980_at	
9.90444	9.90444	7.6604	7.6604	9.91709	9.91709	8.60215	8.60215	5.41302	5.41302	6.97407	6.97407
9.6011	9.673188	7.94861	8.00829	10.5608	10.64009	7.71109	7.768987	4.64069	4.675534	5.95897	6.003712
9.6908	9.378208	6.75351	6.535665	9.61323	9.30314	8.29832	8.030645	5.68099	5.497741	7.06499	6.837098
9.53861	9.742016	6.91601	7.06349	9.53671	9.740076	6.91088	7.058251	5.24361	5.355427	6.76231	6.906513
10.018	9.916142	7.9493	7.868476	9.89255	9.791968	7.29179	7.217651	5.15291	5.100518	6.48326	6.417342
9.54999	9.134754	7.60649	7.275758	9.2608	8.858138	7.0834	6.775412	5.01664	4.798515	7.01451	6.709517
8.91751	8.50139	7.38145	7.037008	10.0992	9.627939	8.01856	7.644388	5.14015	4.900294	5.73202	5.464546
12.3264	11.80126	10.6454	10.19188	9.68995	9.277134	8.50481	8.142484	5.41479	5.184106	7.11986	6.816536
10.3223	9.921009	7.37382	7.087155	9.50423	9.134743	8.00383	7.692672	5.5478	5.332123	7.41633	7.128012
9.38275	9.042003	6.87919	6.629363	10.1033	9.736385	7.54177	7.267881	5.37242	5.177313	6.29475	6.066148
9.59468	9.277085	8.14375	7.874183	9.71166	9.390193	8.73508	8.445939	5.40873	5.229695	6.73873	6.51567
9.90615	9.355489	7.41203	7.000011	9.66382	9.126629	7.37288	6.963038	5.179	4.891111	6.31235	5.96146
9.58642	9.42657	7.68553	7.557376	9.76322	9.600422	8.40843	8.268222	5.1709	5.084677	6.73029	6.618065
9.14168	8.938627	7.07823	6.92101	9.46117	9.25102	8.39713	8.210615	5.45469	5.333531	6.57362	6.427608

KRAS 204009_s_at		KRAS 204010_s_at		KRAS 214352_s_at		EML4 220386_s_at		EML4 223068_at		EML4 223069_s_at	
11.061	11.061	4.71175	4.71175	10.8383	10.8383	7.72169	7.72169	9.66146	9.66146	5.95516	5.95516
9.29041	9.360165	4.43674	4.470052	10.4149	10.4931	8.55277	8.616986	10.5484	10.6276	6.99519	7.047712
9.90883	9.589205	4.62312	4.473994	9.33742	9.036227	7.61604	7.370373	10.0069	9.684112	6.58925	6.376703
10.0426	10.25675	4.80959	4.912152	6.62036	6.761536	6.30953	6.444078	10.3371	10.55753	6.95081	7.099033
10.0969	9.99424	4.78679	4.738121	6.87249	6.802614	6.9532	6.882504	10.0287	9.926734	6.80704	6.73783
10.2951	9.847466	4.54098	4.343537	6.0264	5.764371	7.85968	7.517939	10.8309	10.35997	7.24715	6.932042
9.86354	9.403276	4.61678	4.401346	9.45208	9.011016	9.5867	9.139354	9.88711	9.425746	7.94811	7.577226
10.866	10.40308	4.93127	4.721186	7.86292	7.52794	7.50006	7.180539	9.95409	9.530021	7.02996	6.730466
10.9687	10.54228	5.61486	5.396576	7.87358	7.567486	7.1232	6.846278	10.2499	9.851424	6.59965	6.343081
10.588	10.20348	5.22159	5.031961	8.02932	7.737725	5.84814	5.635757	9.74402	9.390153	6.15726	5.933651
9.7413	9.418852	4.65231	4.498313	9.71254	9.391044	8.51906	8.23707	9.79351	9.469334	6.98458	6.753383
9.81466	9.269084	4.924	4.650286	9.76425	9.221477	6.61394	6.246285	9.69767	9.158598	6.02583	5.690867
10.2164	10.04605	4.61337	4.536444	10.6851	10.50693	8.02103	7.887282	10.1056	9.937093	7.09288	6.974609
9.98622	9.764408	4.70575	4.601227	9.55103	9.338884	7.99602	7.818414	9.60028	9.38704	6.67449	6.526238

GSM494570	Lung Cancer 102T	13.2565		7.49343	7.076887	10.6443	10.05261	8.14774	7.694825	4.72006	4.457682	5.23713	4.946009
GSM494571	Lung Cancer 103T	12.7738		10.3432	10.13737	9.64897	9.456954	10.879	10.66251	5.19633	5.092922	5.16329	5.06054
GSM494572	Lung Cancer 106T	13.5775		8.04816	7.421082	7.80073	7.192931	9.09108	8.382742	5.52429	5.093861	4.98228	4.594082
GSM494573	Lung Cancer 109T	13.0808		6.8313	6.53822	8.47463	8.111047	7.14259	6.836154	4.89313	4.683202	5.61424	5.373375
GSM494574	Lung Cancer 114T	12.9181		8.1479	7.896552	9.02632	8.747874	8.6405	8.373956	5.34986	5.184827	5.12784	4.969655
GSM494575	Lung Cancer 115T	12.353		6.94712	7.040813	7.96661	8.074053	7.4086	7.508517	5.31029	5.381908	4.96678	5.033765
GSM494576	Lung Cancer 116T	13.3931		7.8649	7.35195	7.7372	7.232579	7.94489	7.426723	5.56058	5.197918	5.50903	5.14973
GSM494577	Lung Cancer 117T	12.9292		8.98376	8.699152	9.02247	8.736636	9.27297	8.9792	5.42255	5.250762	5.12752	4.965079
GSM494578	Lung Cancer 118T	12.9482		9.2374	8.931632	9.17109	8.867517	9.50028	9.18581	5.40574	5.226804	4.73059	4.574002
GSM494579	Lung Cancer 119T	13.1891		9.49871	9.01654	9.71954	9.22616	9.8767	9.375343	5.1549	4.893229	4.68367	4.445919
GSM494580	Lung Cancer 120T	13.065		9.53563	9.137564	9.45558	9.060856	9.88545	9.472781	5.1694	4.953603	4.76019	4.561475
GSM494581	Lung Cancer 121T	13.2836		7.57897	7.143069	8.32877	7.849745	8.63826	8.141435	5.33331	5.026567	5.19924	4.900208
GSM494582	Lung Cancer 122T	13.1539		6.22346	5.923356	6.65122	6.330489	6.58405	6.266558	5.22946	4.977288	5.01229	4.77059
GSM494583	Lung Cancer 123T	12.4932		8.63881	8.657065	8.5768	8.594924	9.01694	9.035994	5.52722	5.5389	4.93895	4.949387
GSM494584	Lung Cancer 124T	12.8441		8.82175	8.598873	8.60487	8.387472	9.14327	8.91227	5.29461	5.160844	4.88168	4.758347
GSM494585	Lung Cancer 125T	13.325		8.67296	8.148742	8.71148	8.184934	8.85718	8.321827	5.70138	5.356773	4.9291	4.631172
GSM494586	Lung Cancer 126T	13.6218		7.89257	7.253947	7.69678	7.074	8.02225	7.373134	5.2227	4.800108	4.64096	4.265439
GSM494587	Lung Cancer 127T	13.2332		7.42199	7.021759	7.54383	7.137029	7.61983	7.208931	5.4113	5.119496	5.12359	4.847301
GSM494588	Lung Cancer 129T	12.9607		7.15394	6.910465	9.87501	9.538927	7.8061	7.54043	5.19389	5.017123	5.39032	5.206868
GSM494589	Lung Cancer 130T	12.741		6.11053	6.004347	9.31022	9.148437	6.91031	6.79023	5.32651	5.233951	5.56774	5.47099

5.78882	5.467032	6.42901	6.071635	9.01488	8.513762	3.88951	3.673301	6.32215	5.970715	10.2915	9.719418
5.38409	5.276946	6.46979	6.34104	9.04309	8.863132	3.43315	3.36483	6.8409	6.704765	9.22074	9.037246
5.41292	4.991169	6.80211	6.272119	9.70815	8.951733	3.61093	3.329582	7.81959	7.210321	9.71495	8.958003
5.46828	5.233677	6.3438	6.071635	9.43027	9.025687	3.77516	3.613196	6.54054	6.259934	10.19	9.752823
5.46063	5.292179	7.53821	7.30567	9.40341	9.113332	3.5074	3.399203	6.98758	6.772026	9.95696	9.649806
5.4726	5.546407	8.15356	8.263524	10.387	10.52709	3.57632	3.624552	6.84298	6.935269	10.2456	10.38378
5.33943	4.991192	7.39181	6.909715	9.19103	8.59159	3.58111	3.347549	6.66896	6.234009	10.3371	9.662913
5.54173	5.366167	8.05836	7.803069	10.5011	10.16842	3.44818	3.338941	6.80317	6.587644	9.57558	9.272223
5.28194	5.107102	7.42437	7.178615	9.52543	9.210128	3.33421	3.223844	6.5137	6.298089	9.70721	9.38589
5.33644	5.065554	7.84337	7.445228	10.0825	9.570696	3.55907	3.378406	6.43156	6.105084	10.1345	9.620056
5.41361	5.187618	6.96615	6.675347	8.38022	8.030387	3.43629	3.292842	6.79722	6.513469	10.1875	9.762222
5.54827	5.229164	7.24061	6.82417	9.51986	8.97233	3.55069	3.346474	6.51903	6.144091	9.97497	9.401264
5.30824	5.052269	8.06317	7.674352	8.75951	8.337114	3.50446	3.33547	6.69187	6.369178	10.741	10.22305
5.63478	5.646687	6.99218	7.006956	9.17834	9.197735	3.31965	3.326665	6.66113	6.675206	10.121	10.14239
5.60287	5.461316	7.09171	6.912541	9.01839	8.790545	3.56217	3.472173	6.65719	6.488999	10.0199	9.766752
5.3993	5.072951	9.42897	8.859057	10.9829	10.31906	3.59256	3.375416	6.77299	6.363612	9.6914	9.105625
5.47615	5.033051	7.1032	6.528449	8.40809	7.727754	3.51323	3.228959	6.87164	6.315625	10.1933	9.368515
5.28762	5.002485	7.8362	7.413633	9.77032	9.243456	3.55481	3.363117	6.9061	6.533689	9.64342	9.123399
5.59682	5.40634	6.68691	6.45933	9.04891	8.740943	3.68348	3.558118	5.94786	5.745433	10.0548	9.712598
5.20855	5.118041	6.76949	6.651857	10.4637	10.28187	3.64878	3.585375	6.36239	6.251831	10.2678	10.08938

7.17939	6.780303	6.48502	6.124532	8.98613	8.486611	8.32645	7.863601	6.90625	6.522347	5.25523	4.963103
8.15562	7.993322	7.78425	7.629343	12.1348	11.89332	9.24125	9.057348	7.46666	7.318073	5.07783	4.976781
8.13974	7.505527	7.851	7.239284	10.8974	10.04832	8.56865	7.901018	6.86566	6.330718	5.4307	5.007563
6.95334	6.655024	6.49601	6.217314	8.96114	8.576684	8.6154	8.245777	6.38616	6.112177	5.21757	4.993723
6.96053	6.74581	6.50416	6.303518	9.85142	9.547522	8.39713	8.138094	8.26959	8.014488	5.3158	5.151817
6.70964	6.80013	6.47317	6.560471	11.0523	11.20136	9.71616	9.847198	8.54795	8.663233	5.40237	5.47523
7.68694	7.185597	7.10427	6.640928	11.0895	10.36624	7.96693	7.447326	7.68177	7.180764	5.54547	5.183794
7.11956	6.894011	6.41842	6.215083	12.6867	12.28478	10.2159	9.892258	8.44154	8.17411	5.41586	5.244284
6.94505	6.715161	6.57394	6.356335	12.0859	11.68584	9.99675	9.665846	8.02208	7.75654	5.42814	5.248462
6.78141	6.437175	6.53464	6.202931	11.5725	10.98506	9.4763	8.995268	8.3315	7.90858	5.28377	5.015557
7.59579	7.278703	6.92701	6.637841	10.483	10.04539	8.20789	7.865251	7.26305	6.959853	5.38726	5.162368
5.92604	5.585207	6.0659	5.717023	10.8639	10.23907	9.93885	9.367222	7.65437	7.214133	5.33636	5.029442
6.05463	5.762667	5.96271	5.67518	9.5045	9.046179	8.99893	8.564989	8.38852	7.984013	5.42183	5.160382
7.01248	7.027298	6.72268	6.736886	11.0668	11.09019	9.17295	9.192334	7.4622	7.477969	5.35623	5.367549
6.93962	6.764294	6.88998	6.715908	10.9702	10.69304	8.3315	8.121009	7.68786	7.49363	5.46412	5.326072
7.55897	7.102085	6.79225	6.381708	12.7258	11.95662	11.1115	10.43989	9.63069	9.048584	5.38992	5.064138
7.63159	7.014084	7.00173	6.435189	9.91016	9.108285	7.9101	7.270059	7.42295	6.822326	5.68167	5.221941
7.86459	7.440492	7.59532	7.185743	11.1179	10.51837	8.7569	8.284684	8.19901	7.756879	5.52103	5.223309
6.33033	6.114886	6.19757	5.986644	8.30952	8.026717	8.46064	8.172693	6.95153	6.714944	5.19676	5.019895
6.67702	6.560994	6.30468	6.195124	10.0912	9.915846	9.94566	9.772835	7.18088	7.056098	5.36789	5.274612

5.96032	5.628999	4.87797	4.606814	10.3009	9.728295	4.98359	4.706563	6.8522	6.471301	5.98298	5.650399
8.77013	8.595603	4.47588	4.38681	11.1237	10.90234	4.62852	4.536412	7.68944	7.536419	5.85977	5.74316
7.8929	7.277919	4.81314	4.438121	10.5348	9.713974	4.39181	4.049619	7.57085	6.980962	4.80723	4.432671
6.35012	6.077684	4.88799	4.678283	10.3763	9.93113	4.93006	4.718548	7.64092	7.313105	6.01881	5.760588
5.82436	5.644689	6.06251	5.875493	9.23761	8.952646	4.4151	4.278902	6.34819	6.15236	4.74923	4.602725
5.89404	5.973531	7.51703	7.618409	10.5453	10.68752	4.65626	4.719057	6.88012	6.972909	5.5337	5.608331
6.45257	6.031732	6.23369	5.827128	11.0269	10.30772	4.31112	4.029948	6.65861	6.224334	5.88824	5.504208
5.91655	5.729112	5.46828	5.295044	10.187	9.864274	4.16892	4.036848	6.82915	6.612801	5.11963	4.957439
6.65352	6.433281	5.03681	4.870086	9.85002	9.523973	4.34905	4.205092	6.66871	6.447968	5.04445	4.877473
6.21333	5.897931	5.64128	5.35492	9.44876	8.969126	4.26711	4.050505	6.91888	6.567666	5.81004	5.515113
7.06705	6.772035	4.98795	4.779727	10.3911	9.957322	4.3232	4.142727	6.06272	5.809631	4.72626	4.528962
5.72643	5.397077	5.66621	5.340321	10.9265	10.29807	4.54569	4.284247	7.027	6.622845	6.04611	5.698371
5.70411	5.42905	8.98481	8.55155	10.9559	10.42759	5.08493	4.839727	6.86213	6.531228	6.72027	6.396209
6.1787	6.191757	5.46187	5.473412	10.2906	10.31235	4.34242	4.351596	6.74054	6.754784	5.22519	5.236232
6.29149	6.132539	5.99327	5.841853	11.0393	10.7604	4.41453	4.302999	7.19556	7.013768	5.24229	5.109846
6.52553	6.131109	5.83431	5.481668	10.1738	9.558867	4.4522	4.183097	8.04475	7.558503	6.87944	6.463628
6.33343	5.820964	5.71927	5.256499	9.77032	8.97976	4.4564	4.095813	6.45322	5.931061	5.51488	5.068647
6.34615	6.003934	5.68691	5.380244	10.1037	9.558858	4.23661	4.008151	6.61405	6.257388	4.97641	4.708057
6.14545	5.936298	4.96603	4.797018	10.2816	9.93168	4.88428	4.71805	5.94291	5.740651	6.9309	6.695016
7.61279	7.480503	5.05201	4.964221	10.9233	10.73349	5.06378	4.975787	7.09855	6.975199	6.31181	6.20213

5.73663	5.417743	11.2958	10.66789	6.46502	6.105644	6.64712	6.277621	3.79163	3.580862	9.09744	8.591733
6.21599	6.092291	12.1076	11.86666	6.72298	6.589192	6.86713	6.730473	4.85046	4.753935	9.73235	9.538675
5.29666	4.883967	11.2563	10.37926	7.17598	6.616859	7.65437	7.057975	4.94493	4.559642	9.17569	8.46076
6.41288	6.137751	11.7871	11.2814	6.7947	6.50319	6.40896	6.133999	4.19645	4.016411	9.23153	8.835474
4.46788	4.330054	9.97355	9.665884	8.85622	8.583022	8.42433	8.164455	5.23789	5.076311	10.7939	10.46093
4.86897	4.934636	10.8238	10.96978	9.5289	9.657412	8.75932	8.877453	6.42349	6.510121	9.19577	9.31979
5.86964	5.486821	10.7369	10.03664	7.82432	7.314017	7.46334	6.97658	4.04335	3.779642	8.81277	8.238
4.80921	4.656853	10.9156	10.56979	7.56376	7.324138	7.57514	7.335158	4.50445	4.361748	9.0772	8.789632
4.6262	4.473068	10.944	10.58174	7.20295	6.964524	6.70652	6.484527	4.26798	4.126705	9.32067	9.012145
5.80224	5.507709	11.3013	10.72763	8.45642	8.027158	7.85442	7.455717	5.03956	4.783744	9.07639	8.615658
4.53861	4.349145	10.9356	10.47909	7.20252	6.90185	7.06337	6.768509	4.40788	4.223873	9.45789	9.063069
7.08765	6.680007	12.488	11.76976	7.91244	7.45736	7.67123	7.230023	4.90494	4.622835	9.25667	8.724277
4.42029	4.207137	12.2709	11.67918	11.6941	11.13019	10.5528	10.04393	8.82112	8.395753	9.93955	9.460251
4.86679	4.877074	11.5972	11.62171	7.61004	7.626121	7.23643	7.251722	4.93099	4.94141	8.92354	8.942397
4.99514	4.86894	9.51322	9.272873	7.56359	7.3725	7.20469	7.022667	4.37724	4.266651	9.29331	9.058519
6.09353	5.72522	12.8008	12.02708	9.92923	9.32908	9.54395	8.967087	6.16927	5.796382	9.59579	9.015794
4.72006	4.338139	11.5935	10.65542	9.4351	8.671664	8.86536	8.148025	4.64657	4.270595	9.38609	8.62662
5.1295	4.852892	11.1348	10.53436	8.90573	8.425489	8.59541	8.131903	4.84042	4.5794	8.44117	7.98598
6.25189	6.039115	10.8764	10.50624	6.70345	6.475307	6.22689	6.014966	3.79923	3.669928	9.40389	9.083841
7.28437	7.15779	11.6572	11.45463	6.54367	6.429961	6.37773	6.266904	4.15649	4.084263	9.8681	9.696622

5.10329	4.819609	6.31169	5.960837	6.34949	5.996536	10.2646	9.694013	6.92636	6.541339	8.46384	7.993354
4.49717	4.407676	9.84198	9.646124	7.27714	7.132324	10.2381	10.03436	6.85411	6.717712	10.1352	9.933508
5.34473	4.928292	10.7536	9.915726	8.38767	7.734139	10.8336	9.989493	6.97744	6.433788	10.2117	9.416049
4.76028	4.556052	6.94888	6.650755	7.56729	7.242634	11.3623	10.87483	7.09536	6.790951	8.47463	8.111047
4.18996	4.060707	8.53468	8.271401	9.13344	8.85169	10.021	9.71187	8.14674	7.895428	7.5694	7.335898
4.52981	4.590902	9.05646	9.178601	9.19082	9.314773	9.71773	9.848789	8.15973	8.269777	7.54336	7.645094
4.43152	4.142496	9.20145	8.60133	8.5639	8.005361	10.2373	9.569622	7.4729	6.985516	8.25465	7.71628
4.56691	4.422229	9.60855	9.304149	7.77876	7.532327	10.0233	9.70576	7.21762	6.988964	8.72396	8.447583
4.88199	4.720391	9.59808	9.280373	7.62159	7.369307	10.2196	9.88132	6.72858	6.505856	9.18245	8.878501
5.23949	4.973525	10.0676	9.556552	8.99436	8.537792	10.2312	9.711848	7.42425	7.047383	8.83691	8.388334
4.7434	4.545386	9.79099	9.382264	7.44234	7.131659	10.617	10.17379	7.05991	6.765193	9.55664	9.157697
4.68916	4.419465	8.27166	7.795919	7.33187	6.910181	10.0548	9.476503	6.11518	5.763468	7.33532	6.913433
4.49075	4.2742	9.5392	9.079206	10.4587	9.954366	10.4801	9.974734	9.31657	8.867312	7.8372	7.459279
4.98962	5.000164	10.2942	10.31595	6.31671	6.330058	9.26453	9.284107	6.14127	6.154247	8.31992	8.337501
4.83965	4.717379	10.1158	9.860229	8.02513	7.822379	10.0191	9.765972	7.02415	6.846688	8.83252	8.609371
4.46388	4.194071	9.4113	8.842455	10.1548	9.541016	11.0269	10.3604	8.53402	8.0182	9.72164	9.134037
4.24769	3.903991	9.94893	9.143918	9.16399	8.422491	10.1267	9.307304	7.50402	6.896837	8.70424	7.999941
4.90683	4.642229	9.16066	8.666672	9.3656	8.86056	10.3816	9.821772	7.9877	7.556963	8.71912	8.248942
4.7757	4.613165	6.71621	6.487633	7.5015	7.246197	10.683	10.31942	7.16767	6.923728	7.97715	7.705658
4.59665	4.516774	6.09289	5.987014	8.31897	8.174411	10.9538	10.76346	7.062	6.939284	8.26293	8.119345

6.96629	6.579049	9.67543	9.137594	7.269	6.864932	5.12805	4.842993	7.01975	6.629537
6.6784	6.545499	10.8736	10.65721	6.3453	6.219028	4.72843	4.634334	5.64442	5.532095
5.68954	5.246236	9.79903	9.035532	7.90268	7.286937	4.77165	4.399864	6.04125	5.570542
6.85325	6.559228	9.74095	9.323038	7.90645	7.567243	5.27546	5.049129	6.74611	6.456685
9.45378	9.162148	9.33082	9.042981	8.55054	8.286771	5.71244	5.536222	6.55538	6.353158
7.89856	8.005085	9.16131	9.284865	7.99014	8.0979	5.34404	5.416113	5.78155	5.859523
7.21704	6.746344	10.3472	9.672354	7.63672	7.138652	5.0102	4.683434	5.86351	5.481091
7.03658	6.81366	10.6027	10.2668	8.67953	8.404561	5.24716	5.080929	6.25077	6.052744
7.47451	7.227095	10.2247	9.886251	7.88173	7.620836	4.90138	4.739139	6.24513	6.038409
6.99683	6.64166	9.91016	9.407104	8.4686	8.03872	5.27407	5.00635	6.43462	6.107988
7.09757	6.801281	9.83395	9.423431	7.34338	7.03683	4.99189	4.783503	5.6529	5.416919
7.1376	6.727084	9.81635	9.251767	7.29105	6.871709	5.14998	4.853781	6.37061	6.004207
9.19057	8.747387	10.1356	9.646847	9.07309	8.635573	5.93937	5.652965	7.12232	6.778871
6.90208	6.916665	9.97743	9.998514	7.76796	7.784375	5.07399	5.084712	6.04506	6.057834
7.14737	6.966795	10.2329	9.974371	7.19993	7.018027	4.58239	4.466618	5.44186	5.304374
7.95711	7.47616	9.53155	8.955437	7.86692	7.391422	5.01154	4.708629	5.76476	5.416322
7.67502	7.054	9.3	8.547496	8.19278	7.529866	5.22045	4.79804	6.18532	5.684838
6.54833	6.195211	9.77369	9.246644	7.86905	7.444712	4.67222	4.420271	5.76216	5.451436
7.26814	7.020779	9.35821	9.039716	7.88577	7.617388	5.32064	5.139559	6.73336	6.504199
7.90693	7.769531	10.4084	10.22753	6.94699	6.826272	5.09464	5.006111	6.10521	5.99912

GSM494590	Lung Cancer 131T	12.7939	9.27201	9.073219	8.48669	8.304736
GSM494591	Lung Cancer 132T	13.0846	7.26753	6.953714	8.20533	7.851019
GSM494592	Lung Cancer 133T	12.6482	7.38054	7.305499	8.09159	8.009319
GSM494593	Lung Cancer 134T	12.9216	8.74213	8.470156	7.94337	7.696246
GSM494594	Lung Cancer 135T	13.0767	8.63477	8.266907	9.03402	8.649148
GSM494595	Lung Cancer 136T	12.344	8.67481	8.798214	6.04757	6.1336
GSM494596	Lung Cancer 137T	13.0067	8.98442	8.647954	9.20719	8.862381
GSM494597	Lung Cancer 139T	12.4828	7.35073	7.3724	8.00931	8.032922
GSM494598	Lung Cancer 142T	13.2993	8.13925	7.662069	9.09028	8.557343
GSM494599	Lung Cancer 143T	12.7196	5.9416	5.848176	9.27606	9.130205
GSM494600	Lung Cancer 144T	12.9077	8.53384	8.27725	8.85598	8.589704
GSM494601	Lung Cancer 145T	13.307	7.81055	7.348385	8.29704	7.806089
GSM494602	Lung Cancer 146T	12.7939	9.08616	8.891354	9.25448	9.056065
GSM494603	Lung Cancer 148T	13.0574	9.19696	8.818161	9.85324	9.447411
GSM494604	Lung Cancer 149T	13.3135	8.65283	8.136851	9.63684	9.062184
GSM494605	Lung Cancer 152T	12.6085	7.8751	7.819574	6.84454	6.796281
GSM494606	Lung Cancer 154T	13.1825	7.48954	7.112918	8.3335	7.914439
GSM494607	Lung Cancer 156T	13.0967	8.23146	7.868745	8.85092	8.460908
GSM494608	Lung Cancer 157T	13.073	7.13554	6.833482	7.71551	7.388901
GSM494609	Lung Cancer 158T	13.361	8.23364	7.715132	9.04289	8.47342
GSM494610	Lung Cancer 159T	12.8294	8.321	8.120067	8.87988	8.665452
GSM494611	Lung Cancer 165T	13.1739	8.214	7.80604	9.14994	8.695496
GSM494612	Lung Cancer 167T	13.026	6.99939	6.727281	7.14988	6.871921
GSM494613	Lung Cancer 177T	13.113	8.75404	8.357895	9.03069	8.622026
GSM494614	Lung Cancer 179T	12.198	8.1604	8.375549	7.8306	8.037054
GSM494615	Lung Cancer 189T	12.9327	8.46492	8.194531	8.90591	8.621435

8.89141	8.700779	5.63249	5.51173	5.15023	5.03981	9.86569	9.654171	8.9098	8.718775	11.3826	11.13856
7.99975	7.654317	5.19571	4.971356	5.18992	4.965816	5.38437	5.15187	5.97194	5.714068	9.18156	8.785095
8.04056	7.958808	5.58301	5.526245	5.08146	5.029794	6.11728	6.055083	6.04757	5.986082	10.2737	10.16924
8.95099	8.672518	5.19428	5.032682	4.93108	4.777671	9.21244	8.925835	8.47667	8.212955	11.2553	10.90514
9.27743	8.882188	5.44613	5.214111	5.40738	5.177012	5.59345	5.355155	5.81723	5.569402	13.5976	13.01831
7.84151	7.95306	5.72763	5.809109	5.11037	5.183068	9.85354	9.993712	9.25933	9.391049	13.6512	13.8454
9.78193	9.415597	5.56891	5.360355	5.0422	4.85337	7.91975	7.623156	7.37349	7.097353	12.2851	11.82502
7.88765	7.910903	5.5123	5.528551	4.95684	4.971453	5.92118	5.938636	5.93421	5.951704	12.226	12.26204
8.72851	8.216782	5.23172	4.924999	5.07582	4.778239	5.62354	5.293848	5.59886	5.270615	11.2343	10.57567
6.80667	6.699644	5.21596	5.133945	5.75922	5.668663	7.08148	6.970132	6.24147	6.143331	9.69267	9.540265
9.03069	8.759161	5.54374	5.377055	5.23545	5.078034	8.37849	8.126571	7.66858	7.438006	11.085	10.7517
8.17164	7.688109	5.45149	5.128915	5.43588	5.114229	5.25976	4.94853	5.31922	5.004472	10.755	10.11861
9.49633	9.29273	5.16571	5.054958	4.97331	4.866683	6.0981	5.967357	5.88061	5.75453	10.4112	10.18798
9.9757	9.564827	5.35991	5.139149	5.30239	5.083998	5.52419	5.296663	5.28176	5.064218	10.7439	10.30139
9.59633	9.024089	5.32127	5.003956	4.91903	4.625702	5.70781	5.367446	5.2043	4.893961	8.84461	8.317195
7.05624	7.006488	5.28319	5.245939	4.86534	4.831035	9.77495	9.706029	9.01319	8.94964	11.9278	11.8437
8.25902	7.843704	5.37242	5.102261	5.21795	4.955558	5.79951	5.507874	5.96917	5.669002	10.9959	10.44296
8.93653	8.542746	5.49031	5.248382	5.52286	5.279498	5.51651	5.273428	5.31454	5.080357	8.86395	8.473364
7.98738	7.649262	5.13899	4.921449	4.84567	4.640545	6.27859	6.012808	6.37672	6.106784	11.442	10.95764
9.08306	8.51106	5.56616	5.215635	5.59635	5.243924	6.21567	5.824242	6.29898	5.902306	10.5136	9.851513
9.09896	8.879241	5.42215	5.291218	5.17225	5.047352	6.38924	6.234955	5.98615	5.841598	12.8332	12.52331
8.68287	8.251623	6.74361	6.408679	7.85346	7.463407	6.27826	5.966442	6.03224	5.73264	9.75361	9.269183
6.72899	6.467393	5.66212	5.441999	5.16677	4.965906	5.81024	5.584361	5.93101	5.700435	8.89327	8.547534
9.33819	8.915611	5.11305	4.88167	4.74066	4.526132	6.90103	6.588739	6.31426	6.028522	11.8765	11.33906
8.22461	8.441452	5.22759	5.365415	5.01011	5.142201	6.37949	6.547685	6.29091	6.45677	13.0185	13.36173
8.68819	8.410669	5.14215	4.977898	4.60638	4.459242	6.38924	6.185153	6.21366	6.015181	10.8116	10.46625

ALK		ALK		EGFR		EGFR		EGFR		EGFR	
208211_s_at		208212_s_at		1565483_at		1565484_x_at		201983_s_at		201984_s_at	
5.20824	5.20824	4.68244	4.68244	5.83633	5.83633	6.05138	6.05138	10.8982	10.8982	8.23709	8.23709
5.35422	5.362751	5.13181	5.139987	5.90737	5.916783	6.05202	6.061663	10.7176	10.73468	8.26293	8.276096
5.25735	5.392519	4.78532	4.908353	6.30755	6.46972	6.42259	6.587717	11.559	11.85619	8.74514	8.969981
5.17531	5.178002	5.00871	5.011316	9.80572	9.810821	8.80414	8.80872	8.57954	8.584003	8.23827	8.242556
5.23958	5.268815	5.49122	5.521859	6.59319	6.629977	6.27644	6.31146	8.95984	9.009832	8.3515	8.398098
4.9784	4.998883	5.44129	5.463677	7.12878	7.15811	6.46834	6.494953	8.48472	8.519629	8.04725	8.080359
5.65912	5.603029	4.86897	4.820711	7.7631	7.686155	7.36613	7.29312	9.90273	9.804578	7.46203	7.388069
5.22326	5.272978	5.68308	5.737175	6.95997	7.026219	6.11818	6.176416	8.48669	8.567471	8.06844	8.14524
5.17845	5.229134	5.86574	5.923151	6.71168	6.777371	6.18124	6.241739	7.79139	7.867649	8.07372	8.152742
5.14649	5.418907	5.58104	5.876459	6.3219	6.656535	6.18919	6.5168	8.98987	9.465727	8.42036	8.866072
5.232	5.214518	4.86186	4.845615	5.90481	5.88508	5.51601	5.497579	10.7536	10.71767	8.72794	8.698778
5.28099	5.28099	4.6261	4.6261	6.04924	6.04924	5.97717	5.97717	10.9768	10.9768	8.15854	8.15854
5.28713	5.302768	5.35175	5.367579	6.10521	6.123267	5.83849	5.855758	10.475	10.50598	8.29226	8.316786
5.10173	5.192927	5.00754	5.097053	5.79207	5.895607	5.96908	6.075781	11.4936	11.69906	8.22356	8.370561
5.421	5.437033	5.59495	5.611498	6.66208	6.681784	6.21702	6.235408	8.62018	8.645676	8.16255	8.186692
4.97895	4.992316	4.68403	4.696604	7.66072	7.681285	7.20282	7.222156	11.8017	11.83338	9.23007	9.254848
5.24586	5.178784	4.88665	4.824167	7.19366	7.101679	6.44615	6.363727	10.477	10.34304	8.2725	8.166724
5.2612	5.151149	5.55341	5.437247	6.75283	6.611578	6.25925	6.128323	8.88754	8.701636	7.83687	7.672943
5.12673	5.016291	4.71886	4.617207	6.42947	6.290967	6.34053	6.203943	9.12907	8.932413	8.5759	8.391159
4.82551	4.759397	4.68986	4.625606	6.61383	6.523216	6.58536	6.495136	9.69925	9.566363	7.88189	7.773902
4.97533	4.893643	5.12507	5.040924	6.83315	6.72096	6.2524	6.149745	11.128	10.9453	8.12974	7.996262

8.85511	8.665257	7.47661	7.316312	5.91247	5.785707	6.06611	5.936053	7.31107	7.154321	8.59269	8.408464
8.9607	8.573772	7.56142	7.234914	5.28713	5.058829	5.29452	5.0659	7.33936	7.022443	9.14557	8.750659
9.98475	9.883231	8.16436	8.081349	5.51664	5.46055	5.26899	5.215418	7.7578	7.678923	9.66115	9.562921
7.73838	7.497634	7.60649	7.369847	5.89026	5.70701	5.16199	5.001397	6.88789	6.673603	8.58814	8.320957
12.3073	11.78298	11.1884	10.71175	5.56524	5.328147	5.88508	5.634361	10.6719	10.21725	12.4648	11.93377
10.1147	10.25859	8.32457	8.442991	5.92926	6.013607	5.32986	5.40568	7.93979	8.052738	10.1999	10.345
8.68214	8.356994	7.80198	7.509796	5.46553	5.260846	5.35402	5.153512	7.485	7.204687	9.75456	9.389252
11.813	11.84783	9.64023	9.66865	5.48947	5.505653	5.82947	5.846656	9.32902	9.356522	11.2088	11.24184
9.38196	8.831922	8.60648	8.101907	5.15104	4.849049	5.38046	5.065019	8.51301	8.013917	10.4475	9.834993
9.77495	9.621251	6.97394	6.864283	5.01578	4.936913	5.42674	5.341411	6.88124	6.773041	10.4976	10.33254
10.0243	9.722896	8.30037	8.0508	5.52722	5.361031	5.67292	5.50235	8.04916	7.807143	9.69584	9.404312
8.77331	8.254177	8.17969	7.695682	5.22658	4.917314	5.16713	4.861381	7.78638	7.325645	8.95543	8.425521
8.95099	8.759082	6.8455	6.698733	5.24873	5.136198	5.46216	5.345052	6.2771	6.14252	8.47166	8.290028
8.66107	8.304343	7.93829	7.611333	5.44443	5.220188	5.59564	5.36517	7.77623	7.455948	9.36183	8.976241
7.54006	7.090437	6.64821	6.251769	5.33656	5.018335	5.3667	5.046677	6.25823	5.885044	8.47126	7.966109
9.90851	9.838647	7.61969	7.565965	5.87226	5.830856	5.41292	5.374755	7.07667	7.026774	9.28612	9.220645
9.05395	8.59866	8.20704	7.794338	5.20544	4.943677	5.54081	5.262183	7.71519	7.327221	9.0952	8.637835
6.63979	6.347211	7.4186	7.091703	5.5249	5.281448	5.34353	5.10807	6.70233	6.406995	6.98972	6.681721
9.23697	8.845955	7.78269	7.453237	5.43273	5.202754	5.43438	5.204334	7.61279	7.290529	9.43679	9.037316
8.68933	8.142125	7.37349	6.909149	5.51876	5.17122	5.67	5.312936	7.09348	6.646773	8.91358	8.352253
10.2983	10.04962	9.99207	9.750785	5.42551	5.294497	5.96552	5.821467	9.4477	9.21956	11.373	11.09837
8.87674	8.435864	8.0592	7.658929	5.23904	4.978836	5.38718	5.119618	7.94642	7.55175	9.19577	8.739049
8.83922	8.495586	8.03218	7.71992	5.44602	5.2343	5.38216	5.172923	7.45168	7.161988	8.1278	7.811823
10.2537	9.789691	7.93916	7.579891	5.25603	5.01818	5.38603	5.142297	7.58992	7.246455	10.7357	10.24988
11.2755	11.57278	8.44245	8.665035	5.14764	5.283357	5.84408	5.998159	7.83577	8.04236	11.5808	11.88613
9.30048	9.003401	7.328	7.093927	5.20836	5.041993	5.22449	5.057608	7.00041	6.776801	10.1243	9.800907

9.50318	9.299433	6.92935	6.780785	8.6632	8.477462	7.77664	7.60991	5.04915	4.940897	10.0455	9.830125
10.0806	9.645314	8.30482	7.946213	7.41247	7.092396	5.71287	5.466185	7.6823	7.350574	10.5172	10.06306
10.2556	10.15133	8.34222	8.257401	7.18487	7.111818	6.32763	6.263294	7.027	6.955553	11.0322	10.92003
10.1622	9.846047	6.9437	6.727677	9.80821	9.50307	7.09771	6.876895	4.9511	4.797068	10.4092	10.08536
10.3036	9.864641	7.38798	7.073234	7.84996	7.515532	5.67606	5.434246	6.40597	6.13306	10.2737	9.836015
10.5869	10.7375	7.34024	7.444659	10.5625	10.71276	7.20138	7.303823	4.92706	4.99715	11.3759	11.53773
10.474	10.08175	7.19144	6.922121	9.07332	8.733525	8.37281	8.059249	4.98257	4.795973	9.40157	9.049482
10.0297	10.05927	8.21047	8.234675	6.90595	6.926309	5.95667	5.974231	6.49243	6.51157	10.1139	10.14372
10.1662	9.570185	8.19954	7.718824	7.24528	6.82051	5.97827	5.627781	7.52281	7.081769	11.0595	10.41111
11.0835	10.90923	7.16267	7.050046	8.2531	8.12333	7.77876	7.656449	4.91197	4.834735	10.5618	10.39573
9.92092	9.622624	7.8227	7.587492	8.12063	7.876464	5.96869	5.789227	7.07837	6.865542	11.761	11.40738
9.80572	9.225497	7.63255	7.180918	7.59907	7.149419	5.83868	5.493194	7.13508	6.712884	10.477	9.857056
10.0008	9.786384	6.84735	6.700543	9.01023	8.817052	6.62806	6.485955	5.34315	5.228593	10.2816	10.06116
9.59666	9.201399	7.10955	6.816726	7.2967	6.996168	5.68838	5.454091	6.35758	6.095728	9.50968	9.118001
9.83005	9.243872	7.19129	6.762465	7.82289	7.356402	6.38122	6.0007	5.53755	5.207339	9.27862	8.725325
10.6579	10.58275	7.45471	7.402148	9.00574	8.942242	8.86993	8.80739	5.15592	5.119567	10.6378	10.5628
9.89968	9.401861	7.13013	6.771582	7.92218	7.523802	5.75758	5.468052	6.46729	6.142073	10.4412	9.91615
10.0191	9.577613	7.956	7.605423	7.7667	7.424464	5.65746	5.408167	6.40797	6.125606	9.27887	8.870001
9.38881	8.991367	6.75708	6.471043	7.51219	7.194188	5.86742	5.619043	6.01619	5.761516	10.6863	10.23393
10.1387	9.500222	6.79919	6.371016	7.59517	7.116869	6.14268	5.755849	6.15021	5.762905	11.2755	10.56543
10.4437	10.19151	7.93791	7.746228	7.83475	7.645559	5.7877	5.647941	6.36548	6.211769	9.98508	9.743964
9.84169	9.352889	8.22445	7.815971	7.89343	7.501392	5.87855	5.586584	7.42573	7.056921	10.3686	9.853629
10.5099	10.10132	9.19814	8.840552	8.23584	7.915663	5.78409	5.559227	7.28279	6.999664	10.1459	9.751467
10.7137	10.22888	7.37799	7.044115	8.80011	8.40188	7.11268	6.790811	5.26836	5.029952	10.7273	10.24186
11.7928	12.10372	8.85387	9.087302	9.20356	9.446212	6.92154	7.104026	5.22382	5.361546	10.7159	10.99842
10.3625	10.0315	7.33827	7.103869	8.27748	8.013078	6.98361	6.760538	5.01971	4.859369	9.97497	9.656347

7.29435	7.13796	4.25101	4.159869	9.99598	9.781667	7.08298	6.931122	10.3593	10.1372	5.54819	5.429237	4.33157	4.238702	5.31572	5.201751
11.2242	10.73953	9.24261	8.843509	8.76762	8.389029	7.80295	7.466014	10.6869	10.22543	8.33894	7.97886	5.57464	5.333924	6.47602	6.196382
9.80691	9.707199	7.26587	7.191995	8.98725	8.895873	7.75936	7.680467	10.663	10.55458	8.03269	7.951018	5.21855	5.165491	6.54079	6.474287
7.06291	6.843178	4.20106	4.070362	9.95101	9.641427	6.88205	6.667945	9.53861	9.241857	5.18723	5.025852	4.37981	4.243551	5.56069	5.387693
8.15523	7.807797	4.83028	4.624498	9.44483	9.042457	7.87803	7.542406	10.594	10.14267	7.43173	7.11512	4.96271	4.751286	5.54182	5.305725
7.37783	7.482784	4.5005	4.564522	9.32572	9.458383	5.8146	5.897316	9.32549	9.45815	3.83358	3.888115	4.46969	4.533274	4.73151	4.798818
7.56272	7.279497	4.64593	4.47194	9.46958	9.114945	7.07043	6.805643	9.3834	9.031992	7.01043	6.74789	4.66294	4.488313	5.93765	5.715285
9.25283	9.280108	6.60026	6.619718	9.0746	9.101352	7.83774	7.860846	10.6087	10.63998	8.55829	8.58352	5.36141	5.377216	6.58925	6.608675
10.8912	10.25268	8.43724	7.942589	9.34873	8.800641	8.23146	7.748873	10.1548	9.559453	8.37066	7.879912	5.67173	5.339213	7.00504	6.594354
6.78676	6.680047	4.51495	4.443958	10.3551	10.19228	8.18691	8.058181	9.42304	9.274874	7.07194	6.960742	5.08319	5.003263	6.62901	6.524777
8.35899	8.107658	4.56662	4.429314	9.67955	9.388512	8.00527	7.764573	10.1735	9.86761	8.46028	8.205902	4.8741	4.727549	6.07722	5.894494
9.09701	8.558723	6.47013	6.08728	9.49332	8.931583	8.15973	7.676904	9.50113	8.93893	8.64994	8.138107	5.41843	5.097811	6.61835	6.22673
6.76727	6.62218	4.80452	4.701512	9.40055	9.199003	7.40987	7.251003	10.0727	9.856742	8.55367	8.37028	5.33061	5.216322	6.66523	6.522328
7.73304	7.414536	4.68524	4.492267	8.70268	8.344239	7.13478	6.840917	9.55078	9.157408	9.01839	8.646946	6.03368	5.785169	7.00319	6.714747
7.73351	7.272352	4.89999	4.607798	9.00552	8.46851	7.50232	7.054948	9.99864	9.402409	8.85718	8.329016	5.82776	5.480244	7.01149	6.593386
7.26109	7.209894	4.49764	4.465928	9.95509	9.884899	7.9501	7.894045	11.4895	11.40849	6.57856	6.532176	4.64031	4.607592	5.21416	5.177396
8.08119	7.674816	4.98611	4.735377	8.84441	8.399657	6.95153	6.601963	10.0243	9.520214	8.61901	8.185591	5.45119	5.177069	6.44909	6.124789
7.40531	7.078998	5.08599	4.861878	9.17472	8.77044	8.01806	7.664748	9.56324	9.14184	8.68404	8.301382	5.64952	5.400577	6.14357	5.872856
7.75728	7.428903	4.58712	4.39294	9.50577	9.103376	7.73401	7.406618	9.33497	8.939807	7.78795	7.458274	5.28386	5.060186	6.6406	6.359493
8.29976	7.777088	4.53165	4.246272	9.08777	8.515474	7.18147	6.729222	9.78839	9.171973	7.82934	7.336293	5.52158	5.173862	6.5984	6.18287
8.47391	8.269285	5.05156	4.929577	9.53755	9.30724	7.76454	7.577045	9.98302	9.741953	8.25465	8.05532	5.16199	5.03734	6.22018	6.069977
8.24369	7.834256	5.81204	5.523377	9.06334	8.613197	8.07285	7.671901	10.0444	9.545531	8.04251	7.643068	5.17959	4.922338	6.00667	5.70834
10.5412	10.1314	8.83135	8.488022	9.05551	8.703467	7.89955	7.592446	10.6258	10.21271	8.67331	8.336126	5.31812	5.111372	6.20127	5.960189
9.89594	9.448121	6.82332	6.514546	10.1116	9.654022	7.98541	7.624048	10.9517	10.4561	7.61111	7.266686	4.57291	4.365973	6.221	5.939482
7.794	7.999489	4.18232	4.292587	9.39253	9.640164	7.81509	8.021135	10.5811	10.86007	7.66185	7.863855	4.924	5.053821	5.92685	6.083111
7.88815	7.636184	4.8576	4.702437	9.36411	9.064999	7.58217	7.339978	9.85713	9.542271	7.91101	7.658314	5.10784	4.944684	6.61383	6.402569

3.7445	3.664218	7.34917	7.191604	4.37259	4.278842	5.03557	4.927608	10.4744	10.24983	7.45369	7.293884
4.70242	4.499367	6.82655	6.531776	5.64973	5.405772	6.04788	5.786729	13.0067	12.44506	11.837	11.32587
4.38653	4.34193	7.24803	7.174336	5.96488	5.904232	5.79301	5.73411	12.2298	12.10545	10.6835	10.57488
4.11987	3.991698	6.3915	6.192656	3.75392	3.637133	4.46172	4.322913	10.7065	10.37341	7.68019	7.441254
5.13908	4.920142	6.05528	5.79731	5.29789	5.072187	4.55821	4.364019	11.4905	11.00098	8.57331	8.208066
4.16035	4.219533	8.38714	8.506452	4.0041	4.06106	4.67032	4.736758	7.41363	7.519093	6.89325	6.99131
3.91958	3.772792	6.72112	6.469415	4.74731	4.569524	5.92491	5.703023	11.776	11.33499	8.10908	7.805396
4.74519	4.759179	6.82049	6.840597	6.13959	6.15769	5.38184	5.397706	12.0951	12.13076	9.82366	9.852621
4.69356	4.41839	6.56236	6.177628	5.90325	5.557159	6.08767	5.730767	12.9723	12.21177	11.756	11.06678
4.64566	4.572613	6.52038	6.417855	6.57515	6.471764	6.79562	6.688767	12.7227	12.52265	6.65743	6.55275
4.26588	4.137616	6.93757	6.728976	4.72178	4.579809	4.90275	4.755337	11.4014	11.05859	8.87401	8.607192
4.78024	4.497384	7.34069	6.906328	6.0636	5.704805	7.23444	6.806365	11.4482	10.77079	10.0195	9.426628
4.70658	4.605671	6.93393	6.785267	6.12658	5.995227	6.37494	6.238262	11.03	10.79352	7.16002	7.00651
4.49519	4.310045	6.01832	5.770441	5.45816	5.233353	5.14847	4.936418	9.68463	9.285746	8.09268	7.759364
5.02532	4.725654	6.25529	5.88228	5.42763	5.103974	6.0101	5.651711	10.8625	10.21476	8.18163	7.69375
3.77232	3.745722	6.78544	6.737597	4.73811	4.704703	5.86432	5.822972	11.7456	11.66278	7.55439	7.501126
5.00243	4.750876	6.89461	6.547905	5.69336	5.407062	6.30013	5.983319	10.8432	10.29793	8.60374	8.171089
4.53221	4.3325	6.28089	6.004126	5.98413	5.720442	5.55842	5.313491	8.98461	8.588707	8.09633	7.739569
4.6155	4.420119	6.85614	6.565909	5.79035	5.545236	6.82929	6.540196	11.765	11.26697	8.06577	7.724334
4.71744	4.420362	6.79778	6.369694	6.25261	5.858856	6.76444	6.338454	12.1543	11.38889	8.5768	8.036682
4.30503	4.201074	6.55757	6.39922	5.81193	5.671585	5.87524	5.733367	11.1455	10.87636	8.95121	8.735059
4.67425	4.442097	6.5999	6.272107	6.02649	5.727176	4.86058	4.619173	9.53316	9.059682	8.65617	8.226249
4.4421	4.269409	6.88539	6.617713	5.48019	5.267142	5.61179	5.393626	12.2972	11.81913	11.2393	10.80236
4.43769	4.236872	7.13917	6.816103	5.13468	4.902321	6.55396	6.257375	13.2836	12.68248	10.9002	10.40694
4.34434	4.458878	6.74992	6.927881	5.79515	5.947939	5.61898	5.767124	11.2292	11.52526	8.19027	8.406206
4.37715	4.237334	6.65938	6.446664	5.77351	5.589091	6.50416	6.296402	11.7804	11.40411	8.56564	8.292034

3.49274	3.417856	6.97086	6.821405	9.0562	8.862036	4.1462	4.057306	8.41298	8.232607	5.95135	5.823754
3.74615	3.584389	6.47425	6.194688	10.1083	9.671818	4.17716	3.996788	8.38503	8.02296	9.85713	9.431494
3.69915	3.661539	6.30092	6.236856	9.50113	9.404528	4.30362	4.259863	8.21434	8.130821	9.76745	9.66814
3.4018	3.295968	6.82346	6.611177	9.00531	8.725149	4.51527	4.374797	9.66115	9.360585	5.87146	5.688795
3.6453	3.490001	6.46049	6.185257	10.1037	9.673257	4.56258	4.368203	8.83838	8.461843	8.88794	8.509292
3.43716	3.486055	6.69961	6.794916	8.99568	9.123648	4.30097	4.362154	10.1376	10.28181	6.52219	6.614972
3.74731	3.606974	7.5015	7.220569	10.1368	9.757178	4.46078	4.293724	10.2238	9.840919	8.33647	8.02427
3.61814	3.628806	6.40679	6.425678	9.30483	9.332261	4.24889	4.261416	8.07106	8.094854	9.55353	9.581694
3.77562	3.554266	6.63992	6.25064	9.97531	9.390486	4.34795	4.093042	7.96907	7.501866	9.74059	9.169527
3.81096	3.751037	6.44371	6.342391	10.2758	10.11423	3.99916	3.936278	6.16537	6.068427	8.03269	7.906386
3.34263	3.242126	7.12088	6.906774	9.96153	9.662013	4.28207	4.15332	9.19605	8.919549	8.80457	8.53984
3.71333	3.493605	6.44615	6.064719	9.77401	9.195664	4.86249	4.574767	9.51857	8.955338	9.16462	8.622332
3.66326	3.58472	6.40111	6.263871	10.0931	9.876705	4.93252	4.826767	10.1444	9.926905	7.62651	7.462998
3.59599	3.447881	6.72558	6.448571	9.67307	9.274662	4.83883	4.639531	8.86596	8.500794	8.83623	8.472289
3.74189	3.518757	6.27973	5.905262	9.9739	9.379144	4.9857	4.688397	9.14396	8.598695	8.62923	8.114659
3.16904	3.146696	6.97332	6.924153	8.95476	8.891622	3.92156	3.89391	7.68568	7.63149	8.18799	8.130258
3.66799	3.48354	6.55611	6.226427	9.9837	9.481656	5.05549	4.801268	9.85478	9.359219	8.82896	8.384984
3.75294	3.587568	6.26136	5.985456	9.71042	9.282535	4.72043	4.512426	9.43538	9.019614	9.57364	9.151782
3.61005	3.457231	6.63204	6.351296	10.0376	9.612693	4.59021	4.395899	9.20858	8.818767	7.69922	7.3733
3.77883	3.540861	6.62843	6.211009	10.1235	9.485979	4.53748	4.251735	8.89952	8.339079	8.30006	7.777369
3.61093	3.523734	6.85182	6.686365	10.2595	10.01176	4.43378	4.326715	9.37942	9.152929	9.68522	9.451345
3.66643	3.484332	6.62214	6.293242	9.9601	9.465418	4.5464	4.320597	9.06111	8.611077	9.75641	9.271844
3.90379	3.752026	6.53811	6.283934	10.477	10.0697	4.41334	4.241767	9.47006	9.101901	10.2942	9.894002
3.76905	3.59849	7.02632	6.708359	10.6158	10.13541	4.34148	4.145016	9.54611	9.114122	8.85049	8.449981
3.5942	3.688961	6.59965	6.77365	9.95409	10.21653	4.3053	4.418809	8.56711	8.792982	10.5924	10.87167
3.73019	3.611039	6.81136	6.59379	10.179	9.853859	4.40139	4.2608	8.97831	8.691522	8.80414	8.522916

		RPL29 200823_x_at	DDR2 205168_at		DDR2 225442_at		DDR2 227561_at	
GSM494616	Lung Normal 2N	12.886	9.48849	9.48849	9.95441	9.95441	9.84639	9.84639
GSM494617	Lung Normal 3N	12.8655	9.48177	9.496878	10.0444	10.0604	9.73259	9.748098
GSM494618	Lung Normal 6N	12.563	9.68431	9.933298	10.0871	10.34644	9.81013	10.06235
GSM494619	Lung Normal 17N	12.8793	7.44585	7.449723	9.91709	9.922249	8.14929	8.153529
GSM494620	Lung Normal 32N	12.8145	7.51987	7.561828	9.9558	10.01135	8.0192	8.063944
GSM494621	Lung Normal 33N	12.8332	7.64525	7.676705	10.3949	10.43767	7.76422	7.796165
GSM494622	Lung Normal 37N	13.015	9.88058	9.782647	9.96993	9.871112	9.93111	9.832676
GSM494623	Lung Normal 40N	12.7645	7.39875	7.469176	9.81369	9.907102	8.35772	8.437274
GSM494624	Lung Normal 43N	12.7611	6.86373	6.930909	9.67988	9.774622	7.81704	7.89355
GSM494625	Lung Normal 79N	12.2382	6.92519	7.291758	9.61323	10.12208	9.93817	10.46422
GSM494626	Lung Normal 91N	12.9292	9.11641	9.08595	9.84269	9.809803	9.59863	9.566558
GSM494627	Lung Normal 92N	12.886	9.8695	9.8695	9.78907	9.78907	10.2283	10.2283
GSM494628	Lung Normal 94N	12.848	9.51322	9.541357	9.84043	9.869535	10.1807	10.21081
GSM494629	Lung Normal 97N	12.6597	9.39614	9.564102	9.45613	9.625164	9.89804	10.07497
GSM494630	Lung Normal 102N	12.848	6.99891	7.01961	9.72223	9.750985	8.12959	8.153635
GSM494631	Lung Normal 103N	12.8515	10.043	10.06996	9.85573	9.882188	9.94375	9.970444
GSM494632	Lung Normal 106N	13.0529	8.52391	8.41492	9.07191	8.955913	9.33181	9.212489
GSM494633	Lung Normal 109N	13.1613	7.25214	7.100444	9.95829	9.749989	8.13749	7.967275
GSM494634	Lung Normal 114N	13.1697	8.72205	8.534161	10.192	9.972445	9.67027	9.461954
GSM494635	Lung Normal 115N	13.065	9.53943	9.408733	10.2686	10.12791	10.1585	10.01932
GSM494636	Lung Normal 116N	13.1011	9.84878	9.687078	10.1368	9.970369	10.5764	10.40275

KRAS 1559204_x_at		KRAS 204009_s_at		KRAS 204010_s_at		KRAS 214352_s_at		EML4 220386_s_at		EML4 223068_at	
6.22401	6.22401	9.92434	9.92434	4.56501	4.56501	9.6624	9.6624	7.73417	7.73417	9.4775	9.4775
6.45561	6.465896	9.92092	9.936728	4.91423	4.92206	9.31408	9.328921	8.76316	8.777123	9.45253	9.467592
6.75141	6.924992	10.4523	10.72103	4.48394	4.599224	9.72569	9.975742	8.19132	8.401922	9.54342	9.788785
6.6681	6.671569	10.5912	10.59671	4.19958	4.201765	7.79008	7.794133	6.69418	6.697662	9.60316	9.608156
6.25483	6.28973	10.5618	10.62073	5.41177	5.441966	6.80992	6.847917	6.84652	6.884721	9.34922	9.401385
6.35791	6.384069	10.5738	10.6173	5.03257	5.053276	6.53701	6.563905	7.36092	7.391205	9.92676	9.967602
6.98972	6.92044	10.0467	9.947121	4.91235	4.863661	9.61754	9.522214	8.90532	8.817054	10.1158	10.01554
6.76066	6.825012	10.757	10.85939	4.84654	4.892672	8.32861	8.407887	8.0899	8.166904	10.4617	10.56128
6.45713	6.52033	10.8263	10.93226	5.05109	5.100528	7.32724	7.398956	7.34184	7.413699	10.3063	10.40717
6.57071	6.918515	10.894	11.47065	5.13331	5.40503	7.82451	8.238682	6.26006	6.591421	9.52033	10.02427
6.49257	6.470877	9.85875	9.825809	4.67007	4.654466	8.94809	8.918192	8.09022	8.063188	9.42843	9.396927
6.65898	6.65898	10.1041	10.1041	4.67996	4.67996	9.98922	9.98922	6.92993	6.92993	9.45815	9.45815
6.61777	6.637343	10.195	10.22515	5.2849	5.300531	9.92166	9.951005	7.94145	7.964938	9.99283	10.02239
6.46741	6.583019	10.1009	10.28146	4.98795	5.077113	10.7207	10.91234	6.3639	6.477659	9.32617	9.492881
6.49082	6.510018	10.1316	10.16157	5.57409	5.590576	5.72246	5.739385	6.63705	6.65668	9.65818	9.686746
6.54886	6.56644	9.8966	9.923168	4.65956	4.672069	9.77811	9.804359	8.08186	8.103556	9.93615	9.962824
6.82951	6.742185	10.4724	10.3385	5.25763	5.190404	9.91918	9.792349	8.23827	8.132932	9.69201	9.568084
6.30081	6.169014	10.2646	10.04989	5.56069	5.444375	6.71196	6.571563	7.10955	6.960837	10.0214	9.811779
6.66778	6.524144	9.65699	9.44896	4.43443	4.338904	8.10293	7.928378	8.95887	8.765879	9.47273	9.26867
6.7013	6.609487	9.94783	9.811537	4.33488	4.275489	8.31897	8.204994	7.70229	7.596763	9.37755	9.249071
6.68203	6.572321	9.9623	9.798734	4.94656	4.865345	9.57855	9.421285	7.3114	7.191358	9.4682	9.312747

EGFR 210984_x_at		EGFR 211550_at		EGFR 211551_at		EGFR 211607_x_at		EGFR 224999_at		KRAS 1559203_s_at	
7.14752	7.14752	5.02946	5.02946	5.32478	5.32478	6.58137	6.58137	9.20833	9.20833	3.84883	3.84883
7.60466	7.616777	5.19534	5.203618	5.25223	5.260599	7.18645	7.197901	9.19082	9.205465	3.63526	3.641052
7.78975	7.990028	5.37673	5.514968	5.25773	5.392908	7.20194	7.387105	9.71462	9.964387	3.77692	3.874026
7.19144	7.195181	5.32829	5.331062	5.70657	5.709539	7.11325	7.11695	8.9173	8.921939	3.84752	3.849522
6.59158	6.628358	5.10339	5.131865	5.34033	5.370127	6.8743	6.912656	9.31999	9.371992	4.06207	4.084735
6.46669	6.493296	5.06696	5.087807	5.52111	5.543826	6.33772	6.363795	8.90879	8.945444	3.7524	3.767839
6.98523	6.915995	5.36074	5.307606	5.21807	5.16635	6.78936	6.722066	8.13404	8.053418	3.43119	3.397181
6.59468	6.657452	5.15913	5.208238	5.45509	5.507015	6.7027	6.7665	8.73235	8.81547	4.65892	4.703266
6.71735	6.783096	5.15394	5.204384	5.37398	5.426578	6.653	6.718117	8.71979	8.805135	4.26871	4.31049
6.93447	7.30153	5.32508	5.60695	5.37262	5.657007	6.53528	6.881209	8.95229	9.426158	4.58834	4.831213
7.20403	7.179959	5.44958	5.431371	5.4726	5.454315	6.95363	6.930396	9.3938	9.362413	3.58715	3.575164
6.90075	6.90075	5.4647	5.4647	5.34404	5.34404	6.52491	6.52491	8.90279	8.90279	3.67459	3.67459
7.0324	7.053199	5.33331	5.349084	5.22743	5.242891	6.76231	6.782311	8.85839	8.88459	3.56262	3.573157
6.89154	7.014731	5.31764	5.412696	5.09025	5.181241	6.2622	6.374141	8.96158	9.121774	3.56582	3.629561
6.83489	6.855105	4.85963	4.874003	5.35047	5.366295	6.48719	6.506377	8.56785	8.593191	3.76476	3.775895
8.00311	8.024594	5.47007	5.484754	5.31649	5.330762	7.61017	7.6306	9.52543	9.551001	3.52681	3.536278
7.5062	7.410222	5.32408	5.256004	5.10489	5.039617	7.07979	6.989265	9.04434	8.928695	3.66335	3.616509
6.5692	6.43179	5.03897	4.933568	5.11935	5.012267	6.45785	6.322769	9.20884	9.016215	3.86009	3.779347
7.54006	7.377633	5.0522	4.943366	5.28041	5.16666	6.96807	6.817965	8.96114	8.7681	3.56867	3.491794
6.93816	6.843102	5.34922	5.275932	5.24399	5.172144	6.40426	6.316517	8.74004	8.620295	3.45572	3.408374
7.43934	7.317197	5.31893	5.231601	5.28281	5.196074	6.96571	6.851344	9.01361	8.86562	3.56502	3.506488

BRAF 206044_s_at		BRAF 236402_at		BRAF 243829_at		MET 203510_at		MET 211599_x_at		MET 213807_x_at	
6.02199	6.02199	5.30517	5.30517	6.4075	6.4075	11.1928	11.1928	8.18953	8.18953	7.94227	7.94227
5.95788	5.967373	5.42965	5.438302	6.427	6.437241	10.5064	10.52314	8.4198	8.433216	8.035	8.047803
6.25904	6.419963	5.63249	5.777304	6.05408	6.209733	9.63098	9.878597	7.20797	7.39329	7.17301	7.357431
6.74106	6.744567	7.17626	7.179993	6.93799	6.941599	10.4603	10.46574	6.51701	6.5204	6.2211	6.224336
6.08959	6.123568	6.81825	6.856293	6.6172	6.654121	10.474	10.53244	6.68215	6.719434	6.38112	6.416724
6.01852	6.043282	6.15332	6.178637	6.46944	6.496057	9.86034	9.900909	6.56019	6.587181	6.40156	6.427898
6.70691	6.640434	5.76158	5.704473	5.47675	5.422466	9.99063	9.891606	7.83652	7.758847	7.27187	7.199794
6.69178	6.755476	7.80985	7.884189	7.35946	7.429512	10.2467	10.34423	6.57362	6.636192	6.25269	6.312207
6.47544	6.538819	7.24075	7.311619	6.86	6.927143	10.4949	10.59762	6.59544	6.659993	6.42126	6.484108
6.72298	7.078845	7.053	7.426334	7.02343	7.395199	10.9279	11.50634	6.93075	7.297613	6.53676	6.882768
6.21254	6.191782	5.6474	5.62853	5.93893	5.919086	10.8407	10.80448	8.48221	8.453869	7.87272	7.846415
6.34627	6.34627	5.79126	5.79126	5.53869	5.53869	10.7853	10.7853	6.76114	6.76114	6.53379	6.53379
6.32731	6.346024	5.93254	5.950086	5.91049	5.927971	10.386	10.41672	7.68992	7.712664	7.09536	7.116346
6.4529	6.56825	5.72046	5.822717	5.37959	5.475754	11.0307	11.22788	6.78101	6.902225	6.79404	6.915488
6.46282	6.481935	6.06981	6.087762	6.32673	6.345442	10.8116	10.84358	6.50583	6.525072	6.36132	6.380135
7.19027	7.209572	5.69418	5.709466	5.80184	5.817415	12.2832	12.31617	8.62244	8.645587	8.21047	8.232511
6.52072	6.437343	4.92432	4.861356	5.85812	5.783216	10.7985	10.66043	8.30073	8.194593	7.94438	7.8428
6.37795	6.24454	5.78637	5.665334	5.89567	5.772348	11.3471	11.10975	6.60561	6.467438	6.14761	6.019018
6.18889	6.05557	5.08146	4.971996	5.09911	4.989266	11.174	10.93329	9.63712	9.429518	9.15036	8.953244
6.40134	6.313637	5.23608	5.164342	5.41923	5.344983	10.7493	10.60203	8.31784	8.20388	7.74356	7.637468
6.18073	6.079252	5.10461	5.0208	5.64568	5.552987	11.0491	10.86769	7.28635	7.166719	7.23005	7.111344

EML4		EML4		EML4		ERBB2		ERBB2		ERBB2	
223069_s_at		228674_s_at		232587_at		210930_s_at		216836_s_at		234354_x_at	
6.48573	6.48573	8.02424	8.02424	6.65831	6.65831	5.21145	5.21145	10.2394	10.2394	4.52361	4.52361
7.16472	7.176136	7.73401	7.746333	6.48386	6.494191	6.07273	6.082406	10.1589	10.17509	4.57879	4.586086
6.60114	6.770858	8.30356	8.517048	7.34232	7.531094	5.40932	5.548396	10.0493	10.30767	4.46846	4.583346
7.23754	7.241305	7.98674	7.990895	6.93275	6.936357	5.07425	5.07689	9.43326	9.438167	4.69494	4.697382
6.47363	6.50975	7.50604	7.547921	6.44755	6.483525	5.33697	5.366748	10.1609	10.21759	4.91996	4.947411
6.78831	6.816239	7.61726	7.6486	6.92289	6.951373	5.08186	5.102768	9.74023	9.780305	4.76677	4.786382
7.49942	7.425088	8.96651	8.877637	6.58771	6.522415	5.28254	5.230181	9.5175	9.423166	4.17576	4.134371
7.53616	7.607894	8.66662	8.749114	7.30536	7.374897	5.15223	5.201272	9.29234	9.38079	4.79387	4.839501
7.41533	7.487908	8.29663	8.377834	6.96097	7.029101	4.79031	4.837195	9.71744	9.81255	4.86194	4.909527
6.46317	6.805283	6.09983	6.42271	7.03344	7.405738	4.83809	5.094183	9.46005	9.960795	4.8378	5.093877
6.55396	6.532061	7.62876	7.60327	6.41576	6.394323	5.65104	5.632158	9.86882	9.835846	4.52272	4.507608
6.05344	6.05344	8.64125	8.64125	7.06902	7.06902	4.82394	4.82394	10.0919	10.0919	4.51771	4.51771
6.80532	6.825448	8.73155	8.757375	7.08421	7.105163	5.32487	5.340619	9.45013	9.47808	4.38219	4.395151
6.55673	6.673936	9.29139	9.457479	6.33731	6.450593	4.95347	5.042016	10.1178	10.29866	4.64755	4.730628
6.77843	6.798478	7.38949	7.411346	5.81504	5.832239	5.4077	5.423694	10.043	10.0727	4.86688	4.881275
7.18504	7.204328	9.12728	9.151782	7.36436	7.38413	6.13243	6.148893	11.2385	11.26867	4.49499	4.507057
7.04611	6.956015	8.26365	8.157987	6.35744	6.276151	5.52912	5.458422	9.81866	9.693114	4.40492	4.348597
6.54127	6.404444	8.00311	7.835706	5.63846	5.520518	4.90414	4.801558	9.92923	9.721536	4.53508	4.440218
7.56033	7.397466	7.08271	6.930135	5.79815	5.673247	6.94464	6.795039	9.87732	9.664544	4.46846	4.372201
6.97647	6.880887	7.61034	7.506073	6.02023	5.937748	5.73714	5.658537	9.95829	9.821854	4.46761	4.4064
6.51247	6.405545	8.49501	8.355535	6.32907	6.225156	5.36394	5.275872	9.77811	9.617568	4.28179	4.21149

MET		ABCC1		ABCC1		AKT1		PIK3CA		PIK3CA		PIK3CA	
213816_s_at		202804_at		202805_s_at		207163_s_at		204369_at		231854_at		235980_at	
4.58543	4.58543	9.48071	9.48071	7.48265	7.48265	9.90684	9.90684	8.46405	8.46405	5.40326	5.40326	7.18402	7.18402
4.30611	4.312971	9.36536	9.380283	8.12269	8.135633	9.93435	9.950179	8.75912	8.773077	5.77819	5.787397	7.1165	7.127839
4.03535	4.139101	9.31	9.549364	7.68177	7.879272	9.94154	10.19714	8.64879	8.871154	5.92825	6.080668	6.92358	7.101588
4.05966	4.061772	9.54881	9.553777	6.63145	6.6349	8.80533	8.809911	7.69066	7.694661	5.60671	5.609627	6.92437	6.927972
3.99745	4.019754	9.52973	9.582902	7.45402	7.495611	9.45253	9.505271	7.72788	7.770999	5.57647	5.607585	7.08111	7.12062
3.88127	3.897239	9.40368	9.44237	7.57205	7.603204	9.20187	9.23973	7.40438	7.434844	5.9045	5.928793	7.39458	7.425004
4.65374	4.607614	9.1761	9.08515	7.52421	7.449633	10.0612	9.961477	8.59729	8.512077	5.32892	5.276102	6.94572	6.876877
4.08846	4.127376	9.63208	9.723764	7.64741	7.720203	9.26009	9.348233	7.86258	7.937421	5.5383	5.591017	7.18658	7.254986
4.01218	4.051449	9.72014	9.815276	7.43091	7.50364	9.4647	9.557336	7.37535	7.447537	5.52912	5.583237	6.97744	7.045732
4.19086	4.412693	9.87327	10.39589	6.79577	7.155488	7.8742	8.291002	7.59177	7.993622	5.95943	6.274878	7.46696	7.862206
4.75383	4.737946	9.4511	9.419521	7.7886	7.762576	9.81738	9.784577	9.00262	8.97254	6.03724	6.017068	7.1855	7.161491
4.33471	4.33471	9.41767	9.41767	7.18838	7.18838	9.81141	9.81141	7.57482	7.57482	5.05002	5.05002	6.38172	6.38172
4.31147	4.324222	9.47918	9.507216	7.18117	7.202409	9.41948	9.44734	8.30022	8.324769	5.4387	5.454786	6.869	6.889316
4.53362	4.614661	9.25667	9.422139	6.7767	6.897838	9.65393	9.8265	7.77292	7.911866	5.31532	5.410335	6.74412	6.864675
3.60561	3.616274	9.69353	9.7222	7.08584	7.106797	9.55742	9.585688	6.99756	7.018256	5.62152	5.638147	7.01149	7.032228
5.10853	5.122244	9.3781	9.403276	7.40395	7.423826	10.6506	10.67919	7.77356	7.794428	4.82104	4.833982	6.0165	6.032651
4.31694	4.261742	9.22774	9.10975	7.25035	7.157644	9.66173	9.538191	8.78289	8.670588	5.47425	5.404254	7.06092	6.970636
4.12594	4.039636	9.14193	8.950705	6.85037	6.707078	9.26009	9.066393	7.45369	7.297778	5.56144	5.445109	7.13743	6.988134
7.04928	6.897425	9.01085	8.816739	7.44632	7.285912	9.49123	9.286771	8.19884	8.022222	5.74769	5.623874	6.719	6.57426
5.10015	5.030274	9.5183	9.387892	7.67794	7.572747	9.96467	9.828147	7.80073	7.693854	5.24027	5.168474	6.73503	6.642755
4.29191	4.221443	9.3626	9.20888	7.15904	7.0415	9.74157	9.581628	8.46405	8.325083	5.54835	5.457255	6.95025	6.836138

GSM494637	Lung Normal 117N	13.0574		9.92266	9.792409	9.76777	9.639552	10.4627	10.32536
GSM494638	Lung Normal 118N	13.2253		9.47679	9.233659	9.61381	9.367164	9.95543	9.70002
GSM494639	Lung Normal 119N	13.0887		9.63968	9.490394	9.963	9.808707	10.2713	10.11223
GSM494640	Lung Normal 120N	13.073		9.87927	9.737954	9.69988	9.56113	10.6131	10.46129
GSM494641	Lung Normal 121N	13.0493		8.30825	8.20428	9.12728	9.01306	9.3247	9.20801
GSM494642	Lung Normal 122N	12.9043		8.46672	8.454713	9.63155	9.617891	9.03279	9.01998
GSM494643	Lung Normal 123N	12.9607		9.65303	9.597394	9.65226	9.596628	10.1472	10.08872
GSM494644	Lung Normal 124N	13.2565		9.11192	8.857255	9.66889	9.398659	9.87259	9.596665
GSM494645	Lung Normal 125N	13.0026		9.18601	9.103635	9.71281	9.625711	9.90883	9.819973
GSM494646	Lung Normal 126N	13.015		9.31759	9.225237	9.65791	9.562184	10.0265	9.927121
GSM494647	Lung Normal 127N	13.1011		8.49559	8.356105	9.17635	9.025688	9.17472	9.024085
GSM494648	Lung Normal 129N	13.2565		7.35977	7.154075	9.87639	9.600359	8.06907	7.843551
GSM494649	Lung Normal 130N	12.7611		6.48845	6.551956	9.95969	10.05717	7.42891	7.501621
GSM494650	Lung Normal 131N	12.563		9.76559	10.01667	9.87424	10.12811	9.72164	9.971587
GSM494651	Lung Normal 132N	12.6171		9.54395	9.747354	9.75483	9.962728	9.60288	9.80754
GSM494652	Lung Normal 133N	13.0026		8.54846	8.471802	9.95543	9.866155	9.59261	9.506589
GSM494653	Lung Normal 134N	12.8515		8.79814	8.821759	9.79903	9.825336	9.5448	9.570423
GSM494654	Lung Normal 135N	12.7485		9.62675	9.73058	8.71093	8.804882	9.74402	9.849115
GSM494655	Lung Normal 136N	13.073		8.61414	8.490921	9.581	9.443951	9.59261	9.455395
GSM494656	Lung Normal 137N	12.7611		9.35595	9.447522	9.15789	9.247523	9.85324	9.949679

8.74129	5.86332	5.786354	8.56764	8.455176	6.26682	6.184558	4.93631	4.871513	10.1037	9.971072	4.33854
9.783102	6.94915	6.770867	8.90631	8.677815	6.35408	6.191064	5.24812	5.113478	9.71804	9.46872	4.0295
9.345011	6.97546	6.867434	8.09982	7.974381	6.12351	6.028677	5.91964	5.827965	9.92092	9.767278	4.32233
9.028647	6.52676	6.433399	8.80029	8.674408	6.58874	6.494493	4.83489	4.76573	9.73047	9.591283	4.21247
9.410198	7.11069	7.021706	7.27921	7.188117	5.92663	5.852464	6.05377	5.978013	9.95894	9.834313	4.69716
9.193873	7.39997	7.389476	6.59673	6.587375	5.73778	5.729643	6.83856	6.828862	10.0737	10.05941	4.52902
9.185074	5.9672	5.932808	8.08557	8.038968	6.096	6.060865	4.84751	4.819571	9.96533	9.907894	4.05657
9.238396	7.23828	7.035981	8.03411	7.809568	5.69418	5.535036	5.59701	5.440582	9.5646	9.297283	4.46475
9.075539	6.9873	6.924642	7.81001	7.739974	6.12913	6.074167	5.56243	5.512549	9.39745	9.313179	4.19597
9.424988	6.83689	6.769125	8.27748	8.195437	6.11395	6.053351	5.22402	5.172241	9.38247	9.289474	4.3057
9.149207	7.51666	7.393248	7.66495	7.539103	6.00829	5.909643	6.47843	6.372064	9.55151	9.394689	4.46745
9.424855	6.7947	6.604798	7.92333	7.701884	6.31088	6.1345	5.09805	4.955567	9.75456	9.481934	4.72336
10.18229	6.84763	6.914652	7.9101	7.987521	8.08921	8.168384	4.75933	4.805912	9.87603	9.972692	4.41872
10.32439	7.50955	7.702624	8.54567	8.765383	8.81626	9.04293	5.80604	5.955316	9.93078	10.1861	3.9817
10.11553	7.22765	7.381688	7.69273	7.85668	7.48063	7.64006	5.58279	5.701772	9.95302	10.16514	4.05437
8.795682	7.1186	7.054764	6.43552	6.37781	5.84585	5.793428	6.9145	6.852495	10.0123	9.922515	4.47232
9.253214	7.36238	7.382144	6.63592	6.653734	5.63934	5.654479	6.66292	6.680807	10.0297	10.05662	4.56306
9.240976	6.59016	6.661239	9.19506	9.294234	7.13743	7.214411	5.10109	5.156108	10.329	10.4404	4.11323
9.331788	7.1307	7.0287	6.91688	6.817939	5.5597	5.480172	5.66322	5.582212	9.97682	9.834109	4.75701
10.40354	6.45701	6.520208	9.18832	9.278251	7.86921	7.94623	4.81536	4.862491	9.80039	9.896312	3.83757

6.57317	6.486886	5.2985	5.228948	5.43769	5.366311	6.44627	6.361652	8.5315	8.41951	3.6535	3.605542
7.32512	7.137191	5.28928	5.153582	5.23476	5.10046	6.83985	6.664371	8.57278	8.352842	3.58684	3.494818
7.08445	6.974736	5.34755	5.264734	5.3959	5.312336	6.86887	6.762494	9.08938	8.948616	3.62553	3.569383
6.97069	6.870979	5.47296	5.394673	5.46752	5.389311	6.93159	6.832439	8.16813	8.051291	3.37229	3.324052
7.46015	7.366793	5.31598	5.249455	5.49235	5.423618	7.01915	6.931312	8.63285	8.524818	3.494	3.450276
7.97664	7.965328	5.07302	5.065826	5.12959	5.122316	7.50826	7.497612	8.81644	8.803937	3.6975	3.692256
6.95564	6.915551	5.5701	5.537996	5.26786	5.237498	6.64752	6.609207	8.40019	8.351775	3.72683	3.70535
7.25718	7.054352	5.45856	5.306001	5.68731	5.528358	7.21099	7.009453	8.4511	8.214904	3.52743	3.428843
7.41458	7.34809	5.46117	5.412197	5.35192	5.303927	6.97043	6.907923	8.78926	8.710443	3.5586	3.526688
7.40108	7.327723	5.44203	5.388091	5.0471	4.997075	6.89025	6.821956	8.67822	8.592205	3.49943	3.464745
8.10451	7.971446	5.41992	5.330933	5.36223	5.27419	7.70407	7.577581	8.89793	8.75184	3.78416	3.72203
6.63087	6.445547	4.99743	4.857759	5.66364	5.505349	6.34908	6.171632	8.52032	8.282189	4.22507	4.106985
6.55957	6.623772	4.87952	4.927279	5.37044	5.423003	6.4237	6.486572	9.47245	9.565162	3.94617	3.984793
7.64153	7.837997	5.46515	5.605661	5.37534	5.513542	7.35557	7.544685	9.06965	9.302835	3.37618	3.462983
7.64235	7.805226	5.67918	5.800217	5.47675	5.593472	6.96641	7.114881	8.96985	9.161019	3.61256	3.689552
7.09729	7.033645	5.31696	5.26928	5.22013	5.173319	6.93624	6.87404	8.95864	8.878304	3.772	3.738175
7.86807	7.889192	5.22898	5.243017	5.43282	5.447404	7.25572	7.275198	9.03626	9.060518	3.70069	3.710625
7.43047	7.510612	6.15791	6.224327	5.40275	5.461022	7.11403	7.190759	7.15439	7.231554	3.46668	3.50407
7.14409	7.041899	5.21051	5.135977	5.41651	5.339031	6.78474	6.687689	8.97105	8.842725	3.73499	3.681564
6.9031	6.970664	5.5123	5.566252	5.30639	5.358327	6.66371	6.728931	7.70113	7.776505	3.42222	3.455715

5.11143	5.044334	5.29902	5.229462	6.59673	6.510137	6.3591	6.275626	10.9214	10.77804	7.8649	7.76166
5.08898	4.95842	4.87145	4.746471	6.92154	6.743965	6.51018	6.343159	10.5625	10.29152	7.6162	7.420804
5.09366	5.014776	4.9497	4.873046	6.70975	6.605839	6.53882	6.437556	10.312	10.1523	8.55769	8.42516
5.24272	5.167727	4.93792	4.867287	7.57482	7.466468	6.73948	6.643077	10.4457	10.29628	7.62345	7.514402
5.22469	5.159308	5.01495	4.952193	6.10319	6.026814	5.96395	5.889317	9.91232	9.788276	8.18974	8.087253
5.26261	5.255147	4.92203	4.91505	5.85258	5.84428	5.91601	5.90762	9.72533	9.711538	8.50031	8.488255
5.17205	5.14224	4.771	4.743502	7.4451	7.40219	6.78419	6.745089	9.73259	9.676495	8.11394	8.067175
5.21996	5.07407	5.01315	4.87304	6.75708	6.568229	6.00415	5.836343	9.90239	9.625633	7.84022	7.621097
5.03123	4.986113	4.8704	4.826725	7.2242	7.159417	6.46716	6.409166	10.1674	10.07622	8.07091	7.998535
5.07975	5.029401	4.69049	4.644	6.82564	6.757987	6.32338	6.260705	10.3659	10.26316	8.10158	8.02128
5.02946	4.946884	4.77529	4.696887	6.9261	6.812384	6.52862	6.42143	10.3422	10.1724	8.20827	8.073503
4.67007	4.539548	5.27884	5.131304	6.65622	6.470188	6.26826	6.093071	7.97461	7.751731	7.61162	7.398886
4.85398	4.901489	5.32095	5.373029	6.8978	6.965313	6.49211	6.555652	8.52964	8.613124	7.79538	7.871678
5.15425	5.286768	4.89373	5.01955	9.34411	9.584351	8.62717	8.848978	10.3441	10.61005	7.98541	8.190718
5.32449	5.437967	4.84821	4.951537	8.48472	8.665549	8.09998	8.27261	10.7107	10.93897	8.11153	8.284406
5.7451	5.693581	4.99855	4.953726	5.80552	5.753459	5.82468	5.772448	8.64105	8.563562	8.58375	8.506776
5.1299	5.143671	5.49328	5.508027	5.49005	5.504788	5.8731	5.888866	9.83759	9.863999	8.54618	8.569122
5.52009	5.579627	5.16008	5.215734	9.68756	9.792046	8.85537	8.95088	11.0045	11.12319	7.37032	7.449813
5.04436	4.972204	4.96969	4.898602	5.46692	5.38872	5.76766	5.685158	9.9514	9.809052	8.13039	8.014091
5.66242	5.717841	4.81845	4.865611	9.29926	9.390277	8.58569	8.669723	10.4542	10.55652	7.01476	7.083417

4.49747	4.438433	9.41516	9.29157	6.96069	6.869319	9.999	9.867747	7.51649	7.417824	5.69231	5.617589	6.84747	6.757586
4.25753	4.148301	9.07834	8.845432	7.24341	7.057578	9.71495	9.465709	8.52442	8.305723	5.37052	5.232737	6.87026	6.694001
4.6873	4.614709	9.39876	9.253205	7.37317	7.258984	9.6213	9.472298	8.41604	8.285704	5.5927	5.506088	6.76385	6.659101
4.18917	4.129247	9.50113	9.365223	6.80904	6.711642	9.93038	9.788333	6.68337	6.587769	5.05128	4.979025	6.34908	6.258261
5.11006	5.046112	9.105	8.991059	7.75712	7.660047	10.3178	10.18868	8.21778	8.114942	5.67122	5.60025	6.96726	6.880071
5.30806	5.300532	9.61205	9.598419	8.40469	8.392771	10.2502	10.23566	8.52759	8.515497	5.87855	5.870213	7.04337	7.033382
4.2207	4.196374	9.25448	9.201141	6.94944	6.909386	9.75483	9.698607	6.97647	6.936261	5.19855	5.168588	6.41717	6.380184
4.5623	4.43479	9.06579	8.812414	7.18838	6.987475	9.68641	9.415689	7.7005	7.485282	5.14633	5.002498	6.05895	5.889611
4.46601	4.425961	9.06897	8.987645	7.37783	7.31167	9.58552	9.499562	8.60275	8.525605	5.58413	5.534055	6.85037	6.78894
4.26871	4.2264	9.07058	8.980676	7.3067	7.234279	9.49224	9.398156	8.98696	8.897884	5.89939	5.840917	7.28248	7.210299
6.1205	6.020011	8.86056	8.715083	7.16583	7.048178	9.56737	9.410288	8.72834	8.585034	5.60379	5.511784	6.69939	6.589396
4.24505	4.126407	9.41623	9.15306	7.21377	7.012156	9.245	8.986616	7.89064	7.670108	5.49204	5.338545	7.23334	7.031179
3.94496	3.983572	9.68265	9.777419	7.80214	7.878504	9.2259	9.316199	7.28404	7.355333	5.45727	5.510683	7.11039	7.179983
4.2536	4.362962	9.35779	9.598383	7.84565	8.047365	9.77971	10.03115	7.59007	7.785214	5.03617	5.165652	5.96406	6.117398
3.94488	4.028955	9.6561	9.861894	8.02531	8.196348	10.123	10.33874	8.06175	8.233565	5.14522	5.254877	6.45497	6.592541
6.21533	6.159594	9.33082	9.247146	8.27661	8.20239	10.2799	10.18772	8.48146	8.405403	6.28632	6.229948	7.17048	7.106179
6.11106	6.127465	9.40986	9.435121	8.261	8.283177	10.2851	10.31271	8.52562	8.548507	5.83732	5.85299	6.8455	6.863877
4.59494	4.644499	10.004	10.1119	6.44853	6.518081	9.44726	9.549154	4.20174	4.247058	4.4142	4.46181	5.35604	5.413808
4.54794	4.482885	9.1194	8.988953	7.71736	7.606969	10.1585	10.01319	8.3894	8.269396	5.94188	5.856886	6.85944	6.761321
4.01881	4.058144	9.85354	9.949982	7.12604	7.195787	9.77776	9.87346	6.78975	6.856205	4.63093	4.676255	5.89961	5.957353

6.52876	6.443059	10.0224	9.890839	5.41274	5.341689	9.76714	9.63893	6.69925	6.611311	8.85756
6.69226	6.520568	10.1147	9.855204	5.17419	5.041444	9.91746	9.663024	8.04269	7.836352	10.0407
6.53835	6.437093	10.0229	9.867679	4.93078	4.854419	9.7452	9.59428	8.01441	7.890294	9.49201
6.78502	6.687965	9.63482	9.497001	5.71074	5.629052	9.73994	9.600617	5.99918	5.913366	9.15967
6.50987	6.428405	10.3005	10.1716	4.93584	4.874072	9.11258	8.998544	8.56904	8.461806	9.52945
6.52586	6.516605	9.96118	9.947054	4.4575	4.451179	7.95237	7.941092	8.92768	8.915019	9.20693
6.77919	6.740118	10.195	10.13624	6.00461	5.970002	9.69612	9.640236	6.85878	6.819249	9.23832
6.4706	6.289756	9.76522	9.492296	5.40595	5.254862	8.78125	8.535827	8.64292	8.401363	9.50402
6.67199	6.612159	10.0644	9.974148	5.13271	5.086683	9.21528	9.132643	8.13539	8.062436	9.15766
6.72405	6.657404	10.3223	10.21999	5.65336	5.597326	9.82261	9.725252	8.09144	8.011241	9.51934
6.53088	6.423653	10.0961	9.930337	4.78005	4.701569	9.41413	9.259564	9.13698	8.986965	9.30193
6.29139	6.115555	10.4264	10.135	5.5575	5.402176	7.09594	6.897619	6.70865	6.521153	9.69584
6.02075	6.079678	10.3966	10.49836	4.71816	4.764339	6.05699	6.116273	7.60928	7.683756	10.0836
6.91546	7.093259	9.87463	10.12851	4.04243	4.146363	8.31874	8.532618	8.95928	9.189627	10.0656
7.03867	7.188681	9.82096	10.03027	4.28034	4.371564	7.83142	7.998326	8.58354	8.766475	9.90444
6.47013	6.41211	10.01	9.920236	4.25395	4.215803	8.1141	8.041337	8.75992	8.681366	8.87527
6.23369	6.250424	9.97248	9.999251	4.62883	4.641256	8.13256	8.154392	8.64125	8.664448	9.22844
6.82307	6.896661	7.75749	7.841159	4.28763	4.333875	9.13212	9.230615	6.23313	6.300358	9.14237
6.45821	6.36583	10.1254	9.980563	4.79967	4.731014	8.03203	7.917138	8.59992	8.476904	9.46721
6.74915	6.815208	9.71986	9.814994	4.36554	4.408268	9.74365	9.839017	6.81883	6.88557	10.3027

6.39969	6.315683	5.04378	4.977572	5.12125	5.054025	10.6466	10.50685	7.03344	6.941114	6.63843	6.55129
6.36194	6.198722	5.07752	4.947254	5.78667	5.638211	10.9328	10.65231	7.72444	7.526267	7.20252	7.017737
6.20958	6.113414	5.50056	5.415375	5.98187	5.889231	11.0721	10.90063	8.39582	8.265797	7.86258	7.740815
6.33621	6.245575	4.7098	4.64243	5.13281	5.059389	10.3467	10.1987	6.84536	6.747442	6.4634	6.370946
6.54116	6.459303	5.72385	5.652221	5.95583	5.881298	10.7403	10.6059	8.68324	8.574577	8.04091	7.940285
6.28167	6.272762	5.43699	5.42928	5.28673	5.279233	10.1807	10.16626	8.73599	8.723601	8.37606	8.364182
6.80136	6.76216	5.68601	5.653238	5.96497	5.93059	10.7475	10.68556	7.14026	7.099107	6.37341	6.336676
6.29475	6.118821	5.17929	5.034536	5.61528	5.458341	10.4996	10.20615	8.37606	8.141961	7.88765	7.667202
6.40458	6.347147	5.17651	5.13009	5.3061	5.258518	10.1095	10.01884	8.19415	8.120669	7.69936	7.630316
6.41101	6.347466	5.2108	5.159152	5.60608	5.550515	10.6904	10.58444	7.9235	7.844965	7.47805	7.40393
6.32873	6.224822	5.23279	5.146876	5.57096	5.479493	10.6437	10.46895	9.18877	9.037904	8.37641	8.238882
6.28755	6.111822	6.42113	6.241669	6.53049	6.347972	10.6309	10.33378	6.52381	6.341479	6.26958	6.094354
6.07154	6.130966	5.15534	5.205798	6.09842	6.158109	10.4884	10.59106	6.32111	6.382978	5.94699	6.005197
6.03357	6.188696	4.24149	4.35054	5.77325	5.921683	10.5924	10.86474	8.14236	8.351703	7.70295	7.900996
5.81612	5.940075	3.89092	3.973845	6.43866	6.575883	10.1597	10.37623	8.07649	8.248619	7.59891	7.760861
6.1205	6.065615	5.69706	5.645972	5.22045	5.173636	10.7154	10.61931	9.54051	9.454956	8.58446	8.507479
6.01271	6.028851	5.1498	5.163625	5.59067	5.605678	11.0955	11.12529	9.31514	9.340147	8.67625	8.699541
6.36731	6.435985	4.04012	4.083695	4.18391	4.229036	10.3811	10.49307	7.2275	7.305453	6.69226	6.76444
6.11926	6.031728	5.74369	5.661531	5.45908	5.380992	10.9082	10.75217	8.07784	7.962292	7.78844	7.677032
6.47889	6.542303	4.06716	4.106968	4.94997	4.998418	10.2573	10.35769	6.99244	7.060879	6.50038	6.564003

5.7895	5.862382	4.92669	4.98871	9.5233	9.643185	8.96287	9.0757	11.9943	12.14529	8.51229	8.619448
5.09355	5.052226	5.08237	5.041136	5.69336	5.647169	6.00788	5.959138	8.11608	8.050234	7.31462	7.255276
5.10942	5.084876	5.00398	4.979942	5.7357	5.708147	6.04243	6.013404	9.92202	9.874357	8.77155	8.729414
4.98533	5.09283	5.17582	5.287428	6.80532	6.952065	6.34517	6.481993	8.74213	8.93064	8.1669	8.343006
5.3993	5.331733	4.91316	4.851676	8.79593	8.685857	8.27026	8.166765	10.0459	9.920185	8.55367	8.446629
5.14188	5.112244	4.94267	4.914183	5.36174	5.330837	5.78044	5.747124	10.2117	10.15284	7.70407	7.659667
5.25832	5.21261	5.25185	5.206196	6.09092	6.037972	6.08451	6.031617	9.60316	9.51968	7.9153	7.846492
5.25861	5.153234	5.05765	4.956301	5.72385	5.609151	5.47192	5.362269	10.3635	10.15583	7.89804	7.739773
5.06715	4.860704	5.02155	4.816962	5.34218	5.124529	5.16621	4.955728	8.77439	8.416903	7.6781	7.365279
5.27242	5.197002	5.08402	5.011297	5.77164	5.689081	5.88176	5.797626	9.96956	9.826953	7.87935	7.766641
5.00664	5.012085	4.94087	4.946244	5.22167	5.227349	5.31406	5.31984	10.5613	10.57279	8.29525	8.304272
5.37172	5.303035	4.87084	4.808559	6.19279	6.113606	5.95974	5.883536	9.91432	9.787551	8.59807	8.488131
5.37572	5.33827	5.25051	5.213932	5.5867	5.54778	5.96639	5.924825	9.99207	9.92246	8.5027	8.443466
5.34473	5.405556	5.08064	5.138461	5.91435	5.981659	5.79156	5.857471	9.60508	9.714391	8.21494	8.308431
5.27103	5.237538	4.93623	4.904866	5.65962	5.623659	5.95001	5.912204	9.1833	9.12495	8.37119	8.318
5.21098	5.147347	4.80776	4.749051	5.85567	5.784165	5.83691	5.765634	9.15167	9.039916	8.63027	8.524883
5.06536	5.003505	4.97821	4.91742	6.3809	6.302981	6.2871	6.210326	9.999	9.876899	8.67296	8.567052
4.96507	4.899895	4.58983	4.529581	6.57502	6.488712	6.47013	6.385199	10.1455	10.01232	8.46967	8.358492
5.0682	5.017966	4.84143	4.793443	6.13893	6.078083	6.21067	6.149112	7.52968	7.455049	6.82551	6.757858

GSM494657	Lung Normal 139N	12.7258		8.38113	8.486637	6.81213	6.897885	8.04183	8.143065
GSM494658	Lung Normal 142N	12.9914		8.01064	7.945649	9.31835	9.24275	9.06198	8.98846
GSM494659	Lung Normal 143N	12.9482		8.77076	8.728627	9.73443	9.687668	9.52358	9.477831
GSM494660	Lung Normal 144N	12.614		6.65516	6.798667	10.3385	10.56143	7.6888	7.854596
GSM494661	Lung Normal 145N	13.0493		9.14895	9.034459	9.22939	9.113893	9.50498	9.386034
GSM494662	Lung Normal 146N	12.9607		9.31733	9.263629	9.37755	9.323502	9.92336	9.866166
GSM494663	Lung Normal 148N	12.999		9.36183	9.280448	9.60684	9.523328	9.81013	9.724851
GSM494664	Lung Normal 149N	13.1495		8.93074	8.751779	9.76225	9.566626	9.78839	9.592243
GSM494665	Lung Normal 152N	13.4333		8.58569	8.235892	9.45737	9.072057	9.54239	9.153614
GSM494666	Lung Normal 154N	13.073		8.64586	8.522187	9.39662	9.262208	9.62935	9.491609
GSM494667	Lung Normal 156N	12.872		8.20928	8.218209	8.81139	8.820974	8.9807	8.990468
GSM494668	Lung Normal 157N	13.0529		7.41379	7.318994	8.98481	8.869926	8.80333	8.690767
GSM494669	Lung Normal 158N	12.9764		7.80796	7.753566	9.13859	9.074926	9.34557	9.280464
GSM494670	Lung Normal 159N	12.741		8.45166	8.547845	9.10994	9.213616	9.14237	9.246415
GSM494671	Lung Normal 165N	12.9684		7.98428	7.933549	9.27632	9.217379	8.96007	8.903139
GSM494672	Lung Normal 167N	13.0453		7.77371	7.678783	8.95887	8.849471	8.57954	8.474773
GSM494673	Lung Normal 177N	13.0453		8.30972	8.208248	9.52515	9.408836	8.90691	8.798145
GSM494674	Lung Normal 179N	13.0574		8.44226	8.331441	9.25981	9.13826	9.21668	9.095696
GSM494675	Lung Normal 189N	13.015		8.17057	8.089586	8.83252	8.744975	8.63194	8.546383

6.76417	6.849321	9.19224	9.307957	4.55051	4.607795	8.75461	8.864818	6.95422	7.041764	10.3691	10.49963
6.33931	6.287879	10.0586	9.976994	4.71406	4.675815	8.49018	8.421299	8.79471	8.723358	9.86842	9.788357
6.28889	6.25868	9.98954	9.941553	4.47383	4.452339	8.1669	8.127668	9.31123	9.266501	9.27297	9.228425
6.39914	6.537127	10.2812	10.5029	4.69058	4.791725	6.07058	6.201482	7.69142	7.857273	9.88442	10.09756
7.22068	7.13032	9.85382	9.730508	4.20394	4.151332	8.56019	8.453067	8.10502	8.003593	9.12954	9.015292
6.17046	6.134896	9.83128	9.774617	5.02865	4.999667	9.89561	9.838576	6.92466	6.884749	9.19483	9.141835
6.3704	6.315022	10.1254	10.03738	5.11854	5.074045	9.7561	9.67129	7.28097	7.217677	9.79568	9.710526
6.27416	6.148433	9.97847	9.778514	4.76194	4.666517	9.57364	9.381796	8.70881	8.534296	9.44005	9.250883
6.40549	6.144517	9.98195	9.575265	5.16069	4.950433	9.0891	8.718792	9.13544	8.763244	9.96367	9.55773
6.47692	6.384272	9.74737	9.607941	5.22849	5.1537	9.26256	9.130066	8.34149	8.222171	9.30073	9.16769
6.05711	6.063698	10.0419	10.05282	4.90534	4.910675	9.93399	9.944795	9.13698	9.146918	9.30894	9.319065
6.54967	6.465923	10.0973	9.968192	4.101	4.048563	8.57507	8.465425	9.13098	9.014227	9.57586	9.453419
6.23369	6.190263	9.84937	9.780754	4.16825	4.139212	8.28903	8.231285	9.23978	9.175411	9.43816	9.372409
6.80969	6.887188	10.3161	10.4335	4.11558	4.162418	9.14579	9.249874	9.95799	10.07132	10.0904	10.20523
6.37163	6.331145	9.92367	9.860616	4.49699	4.468417	8.43233	8.378752	9.54611	9.485455	9.69201	9.630428
6.37278	6.29496	10.1564	10.03238	4.53334	4.477982	9.03602	8.925678	9.96118	9.839541	10.1658	10.04166
7.04765	6.961589	10.0571	9.93429	4.38829	4.334703	8.73955	8.632829	9.1665	9.054565	9.56901	9.45216
6.65696	6.569576	10.3566	10.22065	4.4	4.342243	8.97386	8.856063	9.48313	9.358648	9.68522	9.558085
7.01915	6.949579	9.76425	9.66747	4.36247	4.319231	8.38594	8.302822	9.93281	9.83436	11.2976	11.18562

7.86552	7.964536	5.84496	5.91854	5.52429	5.593833	7.11012	7.199626	8.2531	8.356995	3.30725	3.348884
7.1156	7.057871	5.40246	5.35863	5.5239	5.479084	6.89449	6.838555	8.44668	8.378152	3.69034	3.6604
8.31728	8.277326	5.35125	5.325544	5.27864	5.253283	7.8929	7.854984	9.13344	9.089565	3.77818	3.760031
6.56274	6.704255	5.09933	5.209289	5.50158	5.620212	6.25777	6.392708	9.80479	10.01621	3.8145	3.896753
7.61162	7.516368	5.54484	5.475451	5.69931	5.627988	6.82088	6.735523	8.85288	8.742094	3.23301	3.192552
6.75088	6.711971	5.12884	5.09928	4.96731	4.938681	6.46644	6.42917	8.12943	8.082575	3.85548	3.833259
6.79736	6.738271	5.26026	5.214533	5.47192	5.424353	6.0405	5.98799	8.2362	8.164603	3.91208	3.878072
7.15641	7.013004	5.19352	5.089448	5.10497	5.002673	6.96584	6.826253	8.76877	8.593055	3.99207	3.912074
6.96038	6.6768	5.40043	5.180405	5.33128	5.114073	6.47232	6.208625	8.43999	8.096128	3.87741	3.719436
7.43376	7.327425	5.29362	5.217899	5.17708	5.103026	6.93133	6.832182	8.60744	8.484317	3.70913	3.656074
8.14607	8.15493	5.16845	5.174071	5.22629	5.231974	7.70991	7.718296	8.52208	8.531349	4.04831	4.052713
7.66264	7.564662	5.38852	5.31962	5.66745	5.594984	7.17145	7.079753	9.10435	8.987938	3.85796	3.80863
7.56173	7.509051	5.2441	5.207567	5.38633	5.348806	7.21192	7.161678	8.90922	8.847154	3.68654	3.660858
8.0879	8.179945	5.3943	5.45569	5.67225	5.736804	7.54623	7.63211	8.54351	8.64074	4.44423	4.494808
7.7063	7.657335	5.29479	5.261147	5.06725	5.035053	7.44424	7.39694	8.58865	8.534079	3.66253	3.639259
7.56811	7.475694	5.48599	5.418999	5.44325	5.376781	7.34652	7.256809	8.57051	8.465853	3.77459	3.728497
7.71505	7.620839	5.27658	5.212146	5.15621	5.093246	7.45076	7.359777	9.09828	8.987178	3.73911	3.693451
7.82548	7.722758	5.27007	5.200892	5.07662	5.009981	7.36639	7.269694	9.06219	8.943234	3.64915	3.601249
6.99639	6.927044	5.26148	5.20933	5.50903	5.454426	6.23155	6.169785	7.47909	7.40496	3.77059	3.733217

6.50049	6.582322	9.33888	9.456443	7.26928	7.36079	5.3595	5.426969	11.139	11.27922	4.09915	4.150753
7.5473	7.486068	6.86498	6.809284	6.19256	6.142319	5.59464	5.54925	9.52945	9.452137	4.41035	4.374569
7.98216	7.943816	6.71355	6.6813	5.60778	5.580842	7.12181	7.087599	10.0965	10.048	4.71714	4.69448
6.72212	6.867071	7.51081	7.672768	7.38602	7.545287	4.91512	5.021106	10.112	10.33005	4.67128	4.772008
7.80262	7.704977	7.99602	7.895957	5.70985	5.638396	5.83711	5.764064	9.75915	9.637023	4.14272	4.090878
6.20166	6.165916	8.34853	8.300413	6.14118	6.105785	5.56243	5.530371	9.93212	9.874875	4.924	4.89562
6.53556	6.478747	9.02632	8.947854	6.72884	6.670346	5.16339	5.118505	9.48559	9.403132	4.58104	4.541217
7.1953	7.051115	7.98303	7.82306	6.10112	5.978861	5.97313	5.853436	9.54799	9.35666	4.64575	4.552655
7.57482	7.266206	7.94438	7.62071	6.45772	6.194619	5.65447	5.424095	9.52783	9.139647	4.79778	4.602309
6.98055	6.880698	7.34405	7.238999	6.16229	6.074143	5.84561	5.761993	9.59375	9.456518	4.74781	4.679896
7.87654	7.885107	7.48614	7.494282	5.71927	5.72549	6.93159	6.939129	10.0953	10.10628	4.63417	4.63921
7.31727	7.223708	6.79238	6.70553	6.39983	6.317999	5.49503	5.424768	9.51295	9.391313	4.35041	4.294784
7.11941	7.069813	6.90024	6.85217	6.03422	5.992183	5.91447	5.873267	10.0563	9.986243	4.59465	4.562641
8.37969	8.475056	7.8432	7.93246	6.28376	6.355273	6.24467	6.315738	8.83235	8.932867	4.6759	4.729114
8.20688	8.154734	7.37425	7.327395	5.78853	5.75175	7.06541	7.020517	9.97355	9.910179	4.34065	4.31307
8.37987	8.277541	7.84407	7.748284	6.05508	5.98114	7.08529	6.998769	10.1484	10.02447	4.41592	4.361996
7.6564	7.562905	7.73485	7.640397	5.95185	5.87917	7.30714	7.21791	10.1398	10.01598	4.1954	4.144169
7.82902	7.726251	7.64772	7.547331	5.79732	5.721221	6.76091	6.672162	9.94052	9.810034	4.41752	4.359533
8.23226	8.150665	8.66398	8.578106	7.97582	7.896767	4.99271	4.943224	7.50006	7.425722	4.3142	4.271439

7.12789	7.21762	4.16253	4.21493	4.90803	4.969815	13.2214	13.38784	7.29565	7.387492	7.24369	7.334878
6.09908	6.049598	6.00394	5.95523	6.07458	6.025297	10.5827	10.49684	8.36351	8.295656	7.8856	7.821624
6.27237	6.242239	5.65631	5.629138	5.72662	5.699111	10.402	10.35203	9.37784	9.332791	8.82014	8.77777
5.71432	5.83754	5.66986	5.792121	5.84486	5.970895	11.4369	11.68352	6.52653	6.667264	6.14182	6.274258
6.40209	6.321974	3.94146	3.892136	4.86968	4.80874	10.2867	10.15797	8.41676	8.311432	7.78605	7.688615
6.32515	6.288695	5.6788	5.64607	5.65164	5.619066	9.41059	9.356351	6.78792	6.748797	6.77244	6.733407
6.56651	6.509427	6.14106	6.087676	6.01747	5.96516	10.1425	10.05433	7.14535	7.083236	6.5871	6.529838
5.76409	5.648585	5.59879	5.486597	5.92429	5.805574	11.1067	10.88414	8.65397	8.480555	7.82658	7.669745
6.30691	6.049954	5.38399	5.164635	6.17321	5.921701	11.0051	10.55673	8.70193	8.347396	8.02191	7.695081
6.29932	6.209213	5.69465	5.613192	6.23292	6.143762	10.7512	10.59741	8.03629	7.921337	7.71784	7.607442
6.55261	6.559737	5.45897	5.464907	5.6608	5.666957	10.1609	10.17195	9.12954	9.13947	8.64276	8.65216
6.7614	6.674946	6.7108	6.624993	6.43008	6.347862	10.3036	10.17185	8.5406	8.431396	7.96326	7.861438
6.22732	6.183937	5.92723	5.885938	6.16982	6.126838	10.2511	10.17969	8.97429	8.911771	8.10502	8.048556
6.79888	6.876255	7.26035	7.342977	7.06352	7.143907	10.2843	10.40134	9.47329	9.581102	8.40433	8.499976
6.31617	6.276038	5.84902	5.811856	5.23949	5.206199	10.8554	10.78643	9.67836	9.616865	9.1077	9.049831
6.45042	6.371652	5.78861	5.717924	5.50456	5.437342	11.1835	11.04693	9.45304	9.337606	9.19696	9.084653
6.54054	6.460672	5.27508	5.210664	6.03379	5.96011	11.0866	10.95122	9.07309	8.962296	8.9254	8.816409
6.32134	6.238362	5.35255	5.282289	6.01111	5.932204	10.8932	10.75021	6.98263	6.890971	8.72261	8.608111
6.5625	6.497455	6.24864	6.186706	5.58854	5.533148	7.01657	6.947024	8.54408	8.459394	6.86026	6.792264

5.46788	5.536713	9.90716	10.03188	6.69707	6.781377	9.09807	9.212602	4.54411	4.601314	4.83662	4.897506	5.50737	5.5767
4.81269	4.773644	9.22123	9.146418	7.82934	7.76582	9.96922	9.888339	8.07007	8.004597	5.28508	5.242202	6.50633	6.453544
6.11979	6.090392	9.42424	9.378968	8.58739	8.546138	10.3621	10.31232	8.49362	8.452819	6.02681	5.997859	6.91844	6.885205
4.06673	4.154422	9.65363	9.861795	7.57944	7.742878	9.17251	9.3703	7.40395	7.563604	5.79006	5.914913	7.51834	7.680461
4.33354	4.27931	9.20529	9.090094	7.47202	7.378515	9.67658	9.555486	8.83965	8.72903	5.04691	4.983753	6.34269	6.263317
4.05211	4.028755	9.29355	9.239986	7.40814	7.365443	10.053	9.995059	8.2338	8.186344	5.46205	5.430569	6.69047	6.651909
4.32758	4.28996	9.43027	9.348293	7.6623	7.595692	9.92642	9.84013	8.12573	8.055093	5.65822	5.609033	7.18704	7.124563
4.77259	4.676953	8.95017	8.770819	7.42466	7.275879	9.71373	9.519079	9.16442	8.980776	6.13824	6.015237	7.11069	6.9682
4.97977	4.776884	9.04499	8.676479	7.85027	7.530434	9.91811	9.514026	8.67916	8.325553	5.58964	5.361907	6.91405	6.632358
4.63337	4.567093	8.99804	8.869329	7.24413	7.140508	9.71462	9.575659	8.88567	8.758567	6.03169	5.945411	7.03628	6.935631
6.02504	6.031593	9.28268	9.292776	8.24524	8.254208	9.98475	9.99561	8.99332	9.003101	6.02395	6.030502	6.82212	6.82954
4.65268	4.593189	9.21644	9.098595	7.81478	7.714857	9.75055	9.625875	8.59881	8.488862	5.77995	5.706045	6.7874	6.700613
4.70845	4.675649	9.09414	9.030786	7.86727	7.812463	9.93654	9.867317	8.67603	8.615588	5.72282	5.682952	7.02617	6.977222
5.32688	5.387503	9.69612	9.806467	8.73955	8.839011	9.8336	9.945512	8.75766	8.857327	5.66253	5.726973	6.7538	6.830662
7.05042	7.005622	8.85682	8.800545	7.79494	7.745412	10.3755	10.30958	8.4357	8.3821	5.55614	5.520837	6.88473	6.840985
7.09965	7.012954	9.24148	9.12863	8.36643	8.264265	10.2947	10.16899	8.45805	8.354766	5.44359	5.377117	6.5365	6.456681
7.1432	7.055972	9.36018	9.24588	7.59191	7.499203	9.5448	9.428246	8.35308	8.251078	5.79245	5.721717	6.54833	6.468366
6.40354	6.319483	9.41674	9.29313	7.5863	7.486717	9.33299	9.210479	8.79009	8.674706	5.81723	5.740869	7.02118	6.929015
4.12162	4.080768	11.2886	11.17671	9.42139	9.328009	9.48177	9.38779	8.39067	8.307505	5.04613	4.996115	6.65819	6.592196

3. Normalizing Gene expression Data from GEO database for Study 2:

Series: GSE10072, Platform: Affymetrix Human Genome U133A Array, Sample number: 107 samples (53 healthy lung and 54 NSCLC)

Patient NO.	Condition	RPS29	DDR2		ALK	ALK	EGFR	EGFR	EGFR	EGFR		EGFR		EGFR	KRAS	
		216570_x_at	205168_at		208211_s_at	208212_s_at	201983_s_at	201984_s_at	210984_x_at	211550_at		211551_at		211607_x_at	204010_s_at	
GSM254626	Normal Lung	12.7485	9.637271	7.001163	6.205506	4.508098	6.951526	5.050057	10.36824	7.532186	8.721795	6.3361	8.449035	6.137948	7.055039	5.125256	6.437509	4.67664	8.416281	6.114154	5.197104	3.775527
GSM254635	Normal Lung	13.073	9.571135	6.780527	6.861165	4.860689	7.197293	5.098814	9.601239	6.801854	8.710017	6.17048	8.843007	6.264695	7.175103	5.083094	6.885917	4.878224	8.792196	6.228699	4.780511	3.386681
GSM254640	Normal Lung	12.7611	9.594097	6.962917	6.521061	4.732661	7.243733	5.25714	9.881953	7.171829	8.766754	6.362473	8.877758	6.443034	7.080365	5.138576	6.699009	4.861807	8.477046	6.152217	4.919469	3.570305
GSM254643	Normal Lung	12.7258	9.379262	6.825883	6.572959	4.783558	7.190062	5.232663	9.764111	7.105962	8.912546	6.486224	8.812259	6.413238	7.010292	5.101833	6.712329	4.884987	8.704246	6.334631	5.681385	4.134704
GSM254649	Normal Lung	12.9914	9.596492	6.841192	6.235605	4.445267	7.088895	5.053565	9.524994	6.790223	8.660024	6.173598	8.628196	6.150908	6.805656	4.851648	6.725081	4.794207	8.351887	5.953932	5.038726	3.592031
GSM254653	Normal Lung	12.9482	9.28233	6.639309	6.045441	4.324081	6.79737	4.861909	10.21754	7.308228	8.668391	6.20018	8.44571	6.040905	6.966995	4.983234	6.57223	4.700874	8.540426	6.108652	4.986172	3.566425
GSM254658	Normal Lung	12.614	8.456651	6.208988	6.491343	4.766032	7.240175	5.315835	7.890757	5.793501	8.894413	6.530399	8.542266	6.271847	7.096791	5.210561	7.04527	5.172733	8.341138	6.124177	4.828609	3.545231
GSM254660	Normal Lung	13.0493	9.231602	6.551867	6.434108	4.566426	7.141145	5.068225	10.06849	7.145827	8.673761	6.155955	8.736345	6.200373	7.164312	5.084667	6.884222	4.885881	8.513929	6.042519	4.906548	3.482283
GSM254673	Normal Lung	12.9607	9.513546	6.798126	6.215731	4.441595	7.169601	5.123205	9.743857	6.9627	8.289554	5.923494	8.432378	6.025552	7.037443	5.028769	6.622651	4.73237	8.266244	5.906838	4.76193	3.402748
GSM254681	Normal Lung	12.999	9.080349	6.469457	6.070856	4.32529	7.330972	5.223082	9.680542	6.897075	8.95065	6.377051	8.496519	6.053497	6.790386	4.837932	6.65376	4.74059	8.433492	6.008593	5.528661	3.938994
GSM254693	Normal Lung	13.1495	9.593057	6.756519	6.251462	4.402989	7.286077	5.131682	9.908775	6.978884	8.783981	6.186676	8.697203	6.125558	7.078151	4.985237	6.794723	4.785615	8.612334	6.065783	4.857435	3.421157
GSM254695	Normal Lung	13.4333	9.316407	6.423045	6.315508	4.354124	7.340687	5.060917	9.788827	6.748748	8.482647	5.848223	8.74163	6.026774	7.20796	4.969411	7.041536	4.854673	8.551643	5.895791	4.804215	3.312188
GSM254702	Normal Lung	13.073	9.88193	7.000705	6.717759	4.759095	7.162102	5.073883	10.40361	7.370284	8.47375	6.003101	8.701593	6.164513	6.939868	4.916445	6.945891	4.920712	8.781756	6.221303	4.745696	3.362017
GSM254719	Normal Lung	12.872	9.546776	6.86888	6.230135	4.482566	7.105274	5.112226	10.44495	7.515115	8.705564	6.26363	8.965422	6.450597	7.12439	5.12598	6.828179	4.912857	8.694803	6.255888	4.755883	3.421846
GSM254727	Normal Lung	13.0529	9.855569	6.992781	6.072125	4.30833	6.77468	4.80681	9.632903	6.834794	8.438018	5.986992	8.640129	6.130395	6.925168	4.913586	6.678339	4.738454	8.606045	6.106212	4.867712	3.453767
GSM254628	Normal Lung	12.9764	9.772315	6.974587	6.248048	4.459286	7.221138	5.153789	10.50208	7.495426	8.754335	6.248045	8.698577	6.208251	7.08839	5.059046	6.72226	4.797736	8.733453	6.233142	5.07301	3.620651
GSM254632	Normal Lun	12.741	9.752796	7.089259	6.478435	4.709143	7.112934	5.170357	10.36824	7.536619	8.544304	6.210812	8.668396	6.301014	7.209784	5.240756	7.05471	5.128034	8.540642	6.20815	4.672198	3.396198
GSM254634	Normal Lung	12.9684	9.077514	6.482698	6.612465	4.722285	7.577445	5.411425	9.601239	6.856716	8.810506	6.292014	9.362531	6.686242	7.566383	5.403525	7.366985	5.261125	9.252613	6.607745	4.615817	3.296382
GSM254638	Normal Lung	13.0453	9.346567	6.635495	6.645153	4.717655	7.157207	5.081182	9.881953	7.015586	8.897645	6.316787	9.028392	6.409609	7.325067	5.200353	6.887622	4.889793	8.851901	6.284312	5.108155	3.62648
GSM254644	Normal Lung	13.0453	10.19462	7.237562	7.006776	4.974385	7.374888	5.235722	9.764111	6.931925	8.73401	6.200616	8.980608	6.375686	7.107762	5.046079	6.839141	4.855374	9.004571	6.392698	4.700291	3.336921
GSM254646	Normal Lung	13.0574	9.637271	6.835536	6.205506	4.401449	6.951526	4.930588	9.524994	6.755901	8.721795	6.186207	8.449035	5.992742	7.055039	5.004007	6.437509	4.566005	8.416281	5.969511	5.197104	3.686209
GSM254651	Normal Lung	13.015	9.571135	6.810743	6.861165	4.88235	7.197293	5.121536	10.21754	7.270718	8.710017	6.197978	8.843007	6.292613	7.175103	5.105746	6.885917	4.899964	8.792196	6.256457	4.780511	3.401774
GSM254655	Normal Lung	12.848	9.594097	6.915822	6.521061	4.700651	7.243733	5.221582	7.890757	5.687984	8.766754	6.319439	8.877758	6.399455	7.080365	5.10382	6.699009	4.828923	8.477046	6.110606	4.919469	3.546157
GSM254662	Normal Lung	12.8515	9.379262	6.759119	6.572959	4.736771	7.190062	5.181483	10.06849	7.25581	8.912546	6.422782	8.812259	6.350511	7.010292	5.051932	6.712329	4.837207	8.704246	6.272672	5.681385	4.094262
GSM254665	Normal Lung	13.0529	9.596492	6.80896	6.235605	4.424323	7.088895	5.029755	9.743857	6.913519	8.660024	6.144511	8.628196	6.121928	6.805656	4.828789	6.725081	4.771619	8.351887	5.92588	5.038726	3.575107
GSM254667	Normal Lung	13.1613	9.28233	6.531809	6.045441	4.254068	6.79737	4.783187	9.680542	6.812023	8.668391	6.099791	8.44571	5.943094	6.966995	4.902549	6.57223	4.62476	8.540426	6.009744	4.986172	3.50868
GSM254669	Normal Lung	13.1697	8.456651	5.946998	6.491343	4.564928	7.240175	5.091531	9.908775	6.968179	8.894413	6.254846	8.542266	6.007205	7.096791	4.990699	7.04527	4.954468	8.341138	5.865765	4.828609	3.395638
GSM254671	Normal Lung	13.065	9.231602	6.543994	6.434108	4.560938	7.141145	5.062135	9.788827	6.938994	8.673761	6.148558	8.736345	6.192922	7.164312	5.078556	6.884222	4.88001	8.513929	6.035258	4.906548	3.478099
GSM254676	Normal Lung	13.1011	9.513546	6.725273	6.215731	4.393996	7.169601	5.068302	10.40361	7.354476	8.289554	5.860014	8.432378	5.960978	7.037443	4.974878	6.622651	4.681655	8.266244	5.843536	4.76193	3.366282

EGFR		EGFR		EGFR		EGFR		EGFR		KRAS	
201984_s_at		210984_x_at		211550_at		211551_at		211607_x_at		204010_s_at	
8.721795	8.721795	8.449035	8.449035	7.055039	7.055039	6.437509	6.437509	8.416281	8.416281	5.197104	5.197104
8.710017	8.429762	8.843007	8.558473	7.175103	6.944236	6.885917	6.664355	8.792196	8.509297	4.780511	4.626693
8.766754	8.81384	8.877758	8.92544	7.080365	7.118394	6.699009	6.734989	8.477046	8.522576	4.919469	4.945891
8.912546	9.128625	8.812259	9.025907	7.010292	7.180253	6.712329	6.875066	8.704246	8.915275	5.681385	5.819127
8.660024	8.389681	8.628196	8.358846	6.805656	6.593202	6.725081	6.515142	8.351887	8.091164	5.038726	4.881431
8.668391	8.292587	8.44571	8.07956	6.966995	6.664952	6.57223	6.287302	8.540426	8.17017	4.986172	4.770005
8.894413	8.945781	8.542266	8.5916	7.096791	7.137778	7.04527	7.085959	8.341138	8.389311	4.828609	4.856496
8.673761	8.482823	8.736345	8.544029	7.164312	7.006601	6.884222	6.732678	8.513929	8.326509	4.906548	4.798539
8.289554	7.99992	8.432378	8.137754	7.037443	6.791558	6.622651	6.391258	8.266244	7.977425	4.76193	4.595549
8.95065	9.03795	8.496519	8.579389	6.790386	6.856615	6.65376	6.718656	8.433492	8.515748	5.528661	5.582585
8.783981	8.694277	8.697203	8.608386	7.078151	7.005867	6.794723	6.725334	8.612334	8.524383	4.857435	4.80783
8.482647	8.192967	8.74163	8.443106	7.20796	6.961811	7.041536	6.80107	8.551643	8.259607	4.804215	4.640153
8.47375	8.334556	8.701593	8.558656	6.939868	6.82587	6.945891	6.831794	8.781756	8.637503	4.745696	4.66774
8.705564	8.314423	8.965422	8.562606	7.12439	6.804291	6.828179	6.521389	8.694803	8.304146	4.755883	4.542202
8.438018	8.22607	8.640129	8.423105	6.925168	6.75122	6.678339	6.510591	8.606045	8.389877	4.867712	4.745444
8.754335	8.690912	8.698577	8.635558	7.08839	7.037036	6.72226	6.673559	8.733453	8.670181	5.07301	5.036257
8.544304	8.32207	8.668396	8.442934	7.209784	7.02226	7.05471	6.87122	8.540642	8.318503	4.672198	4.550676
8.810506	8.914778	9.362531	9.473337	7.566383	7.655932	7.366985	7.454173	9.252613	9.362118	4.615817	4.670446
8.897645	8.906469	9.028392	9.037346	7.325067	7.332332	6.887622	6.894453	8.851901	8.86068	5.108155	5.113221
8.73401	8.656634	8.980608	8.901047	7.107762	7.044793	6.839141	6.778551	9.004571	8.924797	4.700291	4.65865
8.721795	8.721795	8.449035	8.449035	7.055039	7.055039	6.437509	6.437509	8.416281	8.416281	5.197104	5.197104
8.710017	8.429762	8.843007	8.558473	7.175103	6.944236	6.885917	6.664355	8.792196	8.509297	4.780511	4.626693
8.766754	8.81384	8.877758	8.92544	7.080365	7.118394	6.699009	6.734989	8.477046	8.522576	4.919469	4.945891
8.912546	9.128625	8.812259	9.025907	7.010292	7.180253	6.712329	6.875066	8.704246	8.915275	5.681385	5.819127
8.660024	8.389681	8.628196	8.358846	6.805656	6.593202	6.725081	6.515142	8.351887	8.091164	5.038726	4.881431
8.668391	8.292587	8.44571	8.07956	6.966995	6.664952	6.57223	6.287302	8.540426	8.17017	4.986172	4.770005
8.894413	8.945781	8.542266	8.5916	7.096791	7.137778	7.04527	7.085959	8.341138	8.389311	4.828609	4.856496
8.673761	8.482823	8.736345	8.544029	7.164312	7.006601	6.884222	6.732678	8.513929	8.326509	4.906548	4.798539
8.289554	7.99992	8.432378	8.137754	7.037443	6.791558	6.622651	6.391258	8.266244	7.977425	4.76193	4.595549

KRAS		KRAS		EML4		ERBB2		ERBB2		BRAF	
204009_s_at		214352_s_at		220386_s_at		210930_s_at		216836_s_at		206044_s_at	
9.344258	9.344258	10.59069	10.59069	8.016689	8.016689	4.892919	4.892919	9.611819	9.611819	7.223582	7.223582
8.244097	7.978834	10.5624	10.22254	7.471258	7.230862	5.527505	5.349651	9.627641	9.31786	7.911404	7.656845
8.6776	8.724208	11.10638	11.16603	8.043009	8.086208	5.26265	5.290916	9.013744	9.062157	7.598258	7.639068
9.16753	9.389792	10.30457	10.5544	8.395242	8.598779	4.900344	5.01915	9.568784	9.800774	7.45326	7.63396
9.531537	9.233988	10.39933	10.07469	7.923102	7.675764	4.847657	4.696326	9.693794	9.39118	7.093738	6.872291
9.213606	8.814166	10.02106	9.586611	7.536019	7.209307	5.061973	4.842519	9.807965	9.382757	6.953857	6.652384
9.383985	9.438181	8.712564	8.762882	8.128467	8.175412	5.02129	5.05029	9.430051	9.484513	7.256001	7.297907
8.94546	8.748541	10.16687	9.943066	7.781152	7.609864	5.17662	5.062666	9.917498	9.699181	7.398179	7.235321
9.087753	8.77023	10.15358	9.798819	8.057399	7.775876	4.952123	4.779098	9.630976	9.294473	6.878638	6.638301
9.746443	9.841504	10.6386	10.74236	7.713463	7.788695	4.767465	4.813964	8.809415	8.895336	7.264726	7.335582
9.182566	9.088792	10.30026	10.19507	7.886118	7.805584	4.982291	4.931411	9.462323	9.365692	7.181656	7.108315
8.525655	8.234507	10.12738	9.781534	7.877877	7.60885	5.19939	5.021833	9.352205	9.032831	7.397594	7.144969
9.005221	8.857297	10.26454	10.09593	7.89713	7.767407	5.002957	4.920776	9.911157	9.748351	7.357653	7.236792
9.268858	8.852409	10.1953	9.737221	7.940199	7.583446	5.115086	4.885265	10.0403	9.589194	6.874636	6.565759
9.250636	9.018276	9.911418	9.662461	8.238891	8.031945	4.957329	4.83281	9.825489	9.578691	6.798984	6.628206
9.064588	8.998917	10.54032	10.46396	8.220451	8.160896	4.773871	4.739285	9.326943	9.259372	7.457359	7.403332
8.877021	8.646133	10.28666	10.01911	8.406036	8.187398	4.885365	4.758298	9.239789	8.999466	7.172406	6.985854
8.577437	8.678951	9.664138	9.778513	8.007694	8.102465	5.230309	5.29221	9.244657	9.354068	7.236243	7.321884
8.830942	8.8397	10.71658	10.72721	7.391124	7.398455	5.135064	5.140156	9.504999	9.514426	7.925379	7.933239
9.168853	9.087624	10.62088	10.52679	8.241933	8.168916	4.857923	4.814885	8.722555	8.645279	7.321643	7.256779
9.344258	9.344258	10.59069	10.59069	8.016689	8.016689	4.892919	4.892919	9.611819	9.611819	7.223582	7.223582
8.244097	7.978834	10.5624	10.22254	7.471258	7.230862	5.527505	5.349651	9.627641	9.31786	7.911404	7.656845
8.6776	8.724208	11.10638	11.16603	8.043009	8.086208	5.26265	5.290916	9.013744	9.062157	7.598258	7.639068
9.16753	9.389792	10.30457	10.5544	8.395242	8.598779	4.900344	5.01915	9.568784	9.800774	7.45326	7.63396
9.531537	9.233988	10.39933	10.07469	7.923102	7.675764	4.847657	4.696326	9.693794	9.39118	7.093738	6.872291
9.213606	8.814166	10.02106	9.586611	7.536019	7.209307	5.061973	4.842519	9.807965	9.382757	6.953857	6.652384
9.383985	9.438181	8.712564	8.762882	8.128467	8.175412	5.02129	5.05029	9.430051	9.484513	7.256001	7.297907
8.94546	8.748541	10.16687	9.943066	7.781152	7.609864	5.17662	5.062666	9.917498	9.699181	7.398179	7.235321
9.087753	8.77023	10.15358	9.798819	8.057399	7.775876	4.952123	4.779098	9.630976	9.294473	6.878638	6.638301

MET 203510_at		MET 211599_x_at		MET 213807_x_at		MET 213816_s_at		ABCC1 202804_at		ABCC1 202805_s_at		AKT1 207163_s_at		PIK3CA 204369_at	
9.018332	9.018332	7.936651	7.936651	7.778968	7.778968	6.621838	6.621838	9.655212	9.655212	7.106563	7.106563	9.81879	9.81879	8.068703	8.068703
8.608945	8.331942	8.096049	7.835549	7.999747	7.742346	6.662588	6.448212	9.467918	9.163277	6.951024	6.727367	9.756792	9.442856	6.396756	6.190933
8.75255	8.79956	8.056041	8.099309	7.299417	7.338622	6.437211	6.471785	9.492454	9.543438	7.20643	7.245136	9.40262	9.453121	7.837676	7.879772
8.724791	8.936319	7.915797	8.107711	8.034528	8.22932	6.557087	6.71606	9.804341	10.04204	7.225118	7.400286	9.86719	10.10641	7.663871	7.849677
9.311564	9.020882	7.834672	7.590094	7.740874	7.499225	6.157237	5.965025	9.510489	9.213597	7.068836	6.848166	10.12528	9.809195	7.701283	7.460869
9.452081	9.042302	7.825254	7.486003	7.779731	7.442454	6.349367	6.074101	9.664272	9.245294	7.132316	6.823106	10.48058	10.02622	7.58224	7.253525
8.956725	9.008453	7.933109	7.978925	8.084123	8.130811	6.282741	6.319026	9.880728	9.937793	7.209879	7.251519	9.983091	10.04075	7.293225	7.335346
8.880459	8.684971	7.756381	7.585638	7.684869	7.515699	6.399541	6.258666	9.648991	9.436585	7.208196	7.04952	10.11565	9.892974	7.291332	7.130826
9.149979	8.830282	8.109419	7.826078	7.770203	7.498715	6.254401	6.035874	9.508587	9.17636	7.124778	6.87584	10.0898	9.737268	8.346249	8.054634
9.445994	9.538124	7.728422	7.803801	7.613959	7.688221	6.289902	6.35125	9.621553	9.715396	6.68372	6.748909	9.344705	9.435848	8.338715	8.420046
8.642194	8.553938	8.017813	7.935934	7.952566	7.871353	6.216235	6.152754	9.52904	9.431728	7.142998	7.070052	9.882927	9.782001	7.605153	7.527487
8.515657	8.22485	8.054409	7.779354	7.945055	7.673734	6.645141	6.418212	9.560397	9.233913	6.98083	6.742437	9.735466	9.403003	7.06897	6.827567
8.22368	8.088594	7.951019	7.820412	7.630024	7.504689	6.113868	6.013439	9.641838	9.483456	6.974716	6.860146	9.856857	9.694943	7.25909	7.139849
8.673168	8.283482	8.317803	7.944085	7.985513	7.626724	6.369392	6.083215	9.485463	9.059282	7.198428	6.875003	10.25854	9.797621	8.068136	7.705635
8.601036	8.384993	7.758008	7.563141	7.514752	7.325995	5.847082	5.700214	9.618594	9.376993	7.630899	7.439224	10.29503	10.03644	7.762529	7.567548
9.158736	9.092383	8.200218	8.140809	8.065826	8.007391	6.450577	6.403844	9.552101	9.482898	6.896049	6.846089	9.891632	9.819969	8.029991	7.971816
8.640792	8.416048	7.765865	7.563878	7.958592	7.751592	6.454993	6.287101	9.528179	9.280354	7.117541	6.932417	10.23876	9.972458	7.680761	7.480987
8.312351	8.410728	8.355423	8.45431	8.306943	8.405256	6.920105	7.002004	9.277549	9.387349	7.106899	7.191009	9.874824	9.991692	7.21034	7.295674
8.509654	8.518094	7.697681	7.705315	7.740011	7.747687	6.76309	6.769797	9.572697	9.58219	6.96995	6.976862	9.88124	9.89104	7.368253	7.375561
7.791649	7.722621	7.799592	7.730494	7.915454	7.84533	6.953398	6.891796	9.279623	9.197413	6.689822	6.630556	9.528711	9.444294	8.541475	8.465804
9.018332	9.018332	7.936651	7.936651	7.778968	7.778968	6.621838	6.621838	9.655212	9.655212	7.106563	7.106563	9.81879	9.81879	8.068703	8.068703
8.608945	8.331942	8.096049	7.835549	7.999747	7.742346	6.662588	6.448212	9.467918	9.163277	6.951024	6.727367	9.756792	9.442856	6.396756	6.190933
8.75255	8.79956	8.056041	8.099309	7.299417	7.338622	6.437211	6.471785	9.492454	9.543438	7.20643	7.245136	9.40262	9.453121	7.837676	7.879772
8.724791	8.936319	7.915797	8.107711	8.034528	8.22932	6.557087	6.71606	9.804341	10.04204	7.225118	7.400286	9.86719	10.10641	7.663871	7.849677
9.311564	9.020882	7.834672	7.590094	7.740874	7.499225	6.157237	5.965025	9.510489	9.213597	7.068836	6.848166	10.12528	9.809195	7.701283	7.460869
9.452081	9.042302	7.825254	7.486003	7.779731	7.442454	6.349367	6.074101	9.664272	9.245294	7.132316	6.823106	10.48058	10.02622	7.58224	7.253525
8.956725	9.008453	7.933109	7.978925	8.084123	8.130811	6.282741	6.319026	9.880728	9.937793	7.209879	7.251519	9.983091	10.04075	7.293225	7.335346
8.880459	8.684971	7.756381	7.585638	7.684869	7.515699	6.399541	6.258666	9.648991	9.436585	7.208196	7.04952	10.11565	9.892974	7.291332	7.130826
9.149979	8.830282	8.109419	7.826078	7.770203	7.498715	6.254401	6.035874	9.508587	9.17636	7.124778	6.87584	10.0898	9.737268	8.346249	8.054634

GSM254677	Normal Lung	13.0574	9.080349	6.440522	6.070856	4.305945	7.330972	5.199721	10.44495	7.408409	8.95065	6.348529	8.496519	6.026422	6.790386	4.816294	6.65376	4.719387	8.433492	5.981719	5.528661	3.921376
GSM254679	Normal Lung	13.2253	9.593057	6.717795	6.251462	4.377754	7.286077	5.10227	9.632903	6.745698	8.783981	6.151218	8.697203	6.090449	7.078151	4.956665	6.794723	4.758186	8.612334	6.031017	4.857435	3.401549
GSM254683	Normal Lung	13.0887	9.316407	6.592152	6.315508	4.46876	7.340687	5.194161	10.50208	7.431116	8.482647	6.002195	8.74163	6.185448	7.20796	5.100246	7.041536	4.982487	8.551643	6.051016	4.804215	3.399392
GSM254685	Normal Lung	13.073	9.88193	7.000705	6.717759	4.759095	7.162102	5.073883	9.764111	6.917237	8.47375	6.003101	8.701593	6.164513	6.939868	4.916445	6.945891	4.920712	8.781756	6.221303	4.745696	3.362017
GSM254689	Normal Lung	13.0493	9.546776	6.775553	6.230135	4.421661	7.105274	5.042766	9.524994	6.760094	8.705564	6.178527	8.965422	6.362954	7.12439	5.056333	6.828179	4.846106	8.694803	6.17089	4.755883	3.375353
GSM254691	Normal Lung	12.9043	9.855569	7.073306	6.072125	4.357943	6.77468	4.862163	10.21754	7.33309	8.438018	6.055936	8.640129	6.20099	6.925168	4.970168	6.678339	4.79302	8.606045	6.176528	4.867712	3.493539
GSM254699	Normal Lung	12.9607	9.772315	6.983035	6.248048	4.464688	7.221138	5.160033	7.890757	5.638525	8.754335	6.255614	8.698577	6.215771	7.08839	5.065174	6.72226	4.803548	8.733453	6.240693	5.07301	3.625037
GSM254703	Normal Lung	13.2565	9.752796	6.813582	6.478435	4.52602	7.112934	4.969299	10.06849	7.034137	8.544304	5.969295	8.668396	6.055989	7.209784	5.036961	7.05471	4.928622	8.540642	5.966736	4.672198	3.264132
GSM254706	Normal Lung	13.0026	9.077514	6.465647	6.612465	4.709865	7.577445	5.397191	9.743857	6.940263	8.810506	6.275465	9.362531	6.668656	7.566383	5.389313	7.366985	5.247287	9.252613	6.590365	4.615817	3.287711
GSM254708	Normal Lung	13.015	9.346567	6.650943	6.645153	4.728638	7.157207	5.093011	9.680542	6.888597	8.897645	6.331493	9.028392	6.424531	7.325067	5.212459	6.887622	4.901177	8.851901	6.298942	5.108155	3.634923
GSM254710	Normal Lung	13.1011	10.19462	7.206736	7.006776	4.953198	7.374888	5.213422	9.908775	7.004666	8.73401	6.174207	8.980608	6.348531	7.107762	5.024587	6.839141	4.834694	9.004571	6.36547	4.700291	3.322708
GSM254711	Normal Lung	13.2565	9.513546	6.646436	6.251462	4.36745	6.79737	4.748837	9.764111	6.821487	8.668391	6.055986	8.843007	6.177978	7.096791	4.958021	6.712329	4.689425	8.540426	5.966586	4.986172	3.483482
GSM254712	Normal Lung	12.7611	9.080349	6.590064	6.315508	4.583481	7.240175	5.254558	9.524994	6.912766	8.894413	6.455121	8.877758	6.443034	7.164312	5.1995	6.725081	4.880728	8.341138	6.053582	4.828609	3.504364
GSM254713	Normal Lung	12.563	9.593057	7.071945	6.717759	4.952292	7.141145	5.26441	10.21754	7.532308	8.673761	6.394246	8.812259	6.496346	7.037443	5.187962	6.57223	4.845009	8.513929	6.276418	4.906548	3.617079
GSM254715	Normal Lung	12.6171	9.316407	6.838552	6.230135	4.573126	7.169601	5.262725	7.890757	5.792078	8.289554	6.084808	8.628196	6.333382	6.790386	4.984369	7.04527	5.171462	8.266244	6.067698	4.76193	3.495414
GSM254717	Normal Lung	13.0026	9.88193	7.038609	6.072125	4.324997	7.330972	5.221636	10.06849	7.171492	8.95065	6.375285	8.44571	6.015631	7.078151	5.041559	6.884222	4.903429	8.433492	6.006929	5.528661	3.937903
GSM254723	Normal Lung	12.8515	9.546776	6.879837	6.248048	4.502625	7.286077	5.250675	9.743857	7.021863	8.783981	6.330133	8.542266	6.155942	7.20796	5.194381	6.622651	4.772581	8.612334	6.206436	4.857435	3.500487
GSM254725	Normal Lung	13.0026	9.855569	7.019832	6.478435	4.614399	7.340687	5.228556	9.680542	6.895166	8.482647	6.04194	8.736345	6.222642	6.939868	4.943064	6.65376	4.739277	8.551643	6.091084	4.804215	3.421902
GSM254730	Normal Lung	13.015	9.772315	6.953901	6.612465	4.705377	7.162102	5.096495	9.908775	7.051005	8.47375	6.029853	8.432378	6.000413	7.12439	5.069659	6.794723	4.83507	8.781756	6.249028	4.745696	3.376999
GSM254731	Normal Lun	13.1011	9.752796	6.894402	6.645153	4.697562	7.105274	5.022828	9.680542	6.843325	8.705564	6.154098	8.496519	6.00632	6.925168	4.895508	7.041536	4.977771	8.694803	6.146491	4.755883	3.362008

8.496519	8.579389	6.790386	6.856615	6.65376	6.718656	8.433492	8.515748	5.528661	5.582585	9.746443	9.841504	10.6386	10.74236
8.697203	8.608386	7.078151	7.005867	6.794723	6.725334	8.612334	8.524383	4.857435	4.80783	9.182566	9.088792	10.30026	10.19507
8.74163	8.443106	7.20796	6.961811	7.041536	6.80107	8.551643	8.259607	4.804215	4.640153	8.525655	8.234507	10.12738	9.781534
8.701593	8.558656	6.939868	6.82587	6.945891	6.831794	8.781756	8.637503	4.745696	4.66774	9.005221	8.857297	10.26454	10.09593
8.965422	8.562606	7.12439	6.804291	6.828179	6.521389	8.694803	8.304146	4.755883	4.542202	9.268858	8.852409	10.1953	9.737221
8.640129	8.423105	6.925168	6.75122	6.678339	6.510591	8.606045	8.389877	4.867712	4.745444	9.250636	9.018276	9.911418	9.662461
8.698577	8.635558	7.08839	7.037036	6.72226	6.673559	8.733453	8.670181	5.07301	5.036257	9.064588	8.998917	10.54032	10.46396
8.668396	8.442934	7.209784	7.02226	7.05471	6.87122	8.540642	8.318503	4.672198	4.550676	8.877021	8.646133	10.28666	10.01911
9.362531	9.473337	7.566383	7.655932	7.366985	7.454173	9.252613	9.362118	4.615817	4.670446	8.577437	8.678951	9.664138	9.778513
9.028392	9.037346	7.325067	7.332332	6.887622	6.894453	8.851901	8.86068	5.108155	5.113221	8.830942	8.8397	10.71658	10.72721
8.980608	8.901047	7.107762	7.044793	6.839141	6.778551	9.004571	8.924797	4.700291	4.65865	9.168853	9.087624	10.62088	10.52679
8.843007	8.894079	7.096791	7.137778	6.712329	6.751095	8.540426	8.58975	4.986172	5.014969	9.531537	9.586585	10.30457	10.36408
8.877758	8.682329	7.164312	7.006601	6.725081	6.57704	8.341138	8.157522	4.828609	4.722316	9.213606	9.010785	10.39933	10.17041
8.812259	8.504362	7.037443	6.791558	6.57223	6.342599	8.513929	8.216455	4.906548	4.735115	9.383985	9.056112	10.02106	9.670925
8.628196	8.71235	6.790386	6.856615	7.04527	7.113985	8.266244	8.346869	4.76193	4.808375	8.94546	9.032709	8.712564	8.797541
8.44571	8.359461	7.078151	7.005867	6.884222	6.813919	8.433492	8.347368	5.528661	5.472202	9.087753	8.994947	10.16687	10.06305
8.542266	8.25055	7.20796	6.961811	6.622651	6.39649	8.612334	8.318225	4.857435	4.691556	9.746443	9.413605	10.15358	9.806841
8.736345	8.592837	6.939868	6.82587	6.65376	6.544461	8.551643	8.411169	4.804215	4.725299	9.182566	9.031728	10.6386	10.46384
8.432378	8.053512	7.12439	6.804291	6.794723	6.489436	8.781756	8.387192	4.745696	4.532472	8.525655	8.142598	10.30026	9.837467
8.496519	8.283101	6.925168	6.75122	7.041536	6.864666	8.694803	8.476406	4.755883	4.636424	9.005221	8.779026	10.12738	9.872999

7.713463	7.788695	4.767465	4.813964	8.809415	8.895336	7.264726	7.335582	9.445994	9.538124	7.728422	7.803801
7.886118	7.805584	4.982291	4.931411	9.462323	9.365692	7.181656	7.108315	8.642194	8.553938	8.017813	7.935934
7.877877	7.60885	5.19939	5.021833	9.352205	9.032831	7.397594	7.144969	8.515657	8.22485	8.054409	7.779354
7.89713	7.767407	5.002957	4.920776	9.911157	9.748351	7.357653	7.236792	8.22368	8.088594	7.951019	7.820412
7.940199	7.583446	5.115086	4.885265	10.0403	9.589194	6.874636	6.565759	8.673168	8.283482	8.317803	7.944085
8.238891	8.031945	4.957329	4.83281	9.825489	9.578691	6.798984	6.628206	8.601036	8.384993	7.758008	7.563141
8.220451	8.160896	4.773871	4.739285	9.326943	9.259372	7.457359	7.403332	9.158736	9.092383	8.200218	8.140809
8.406036	8.187398	4.885365	4.758298	9.239789	8.999466	7.172406	6.985854	8.640792	8.416048	7.765865	7.563878
8.007694	8.102465	5.230309	5.29221	9.244657	9.354068	7.236243	7.321884	8.312351	8.410728	8.355423	8.45431
7.391124	7.398455	5.135064	5.140156	9.504999	9.514426	7.925379	7.933239	8.509654	8.518094	7.697681	7.705315
8.241933	8.168916	4.857923	4.814885	8.722555	8.645279	7.321643	7.256779	7.791649	7.722621	7.799592	7.730494
7.877877	7.923375	5.061973	5.091207	9.013744	9.065802	6.953857	6.994018	9.149979	9.202823	8.056041	8.102567
7.89713	7.723288	5.02129	4.910755	9.568784	9.358144	7.256001	7.096273	9.445994	9.238056	7.915797	7.741544
7.940199	7.662771	5.17662	4.995751	9.693794	9.355096	7.398179	7.13969	8.642194	8.340238	7.834672	7.560931
8.238891	8.319248	4.952123	5.000424	9.807965	9.903626	6.878638	6.945728	8.515657	8.598713	7.825254	7.901577
8.220451	8.136502	4.767465	4.718779	9.430051	9.333749	7.264726	7.190537	8.22368	8.139698	7.933109	7.852094
8.406036	8.118972	4.982291	4.812148	9.917498	9.578818	7.181656	6.936405	8.673168	8.376982	7.756381	7.491503
8.007694	7.876155	5.19939	5.113982	9.630976	9.472773	7.397594	7.276077	8.601036	8.459751	8.109419	7.976209
7.391124	7.059041	5.002957	4.778174	8.809415	8.413608	7.357653	7.027074	9.158736	8.747234	7.728422	7.381185
8.057399	7.855011	5.115086	4.986604	9.462323	9.224646	6.874636	6.701958	8.640792	8.423751	8.017813	7.81642

7.613959	7.688221	6.289902	6.35125	9.621553	9.715396	6.68372	6.748909	9.344705	9.435848	8.338715	8.420046
7.952566	7.871353	6.216235	6.152754	9.52904	9.431728	7.142998	7.070052	9.882927	9.782001	7.605153	7.527487
7.945055	7.673734	6.645141	6.418212	9.560397	9.233913	6.98083	6.742437	9.735466	9.403003	7.06897	6.827567
7.630024	7.504689	6.113868	6.013439	9.641838	9.483456	6.974716	6.860146	9.856857	9.694943	7.25909	7.139849
7.985513	7.626724	6.369392	6.083215	9.485463	9.059282	7.198428	6.875003	10.25854	9.797621	8.068136	7.705635
7.514752	7.325995	5.847082	5.700214	9.618594	9.376993	7.630899	7.439224	10.29503	10.03644	7.762529	7.567548
8.065826	8.007391	6.450577	6.403844	9.552101	9.482898	6.896049	6.846089	9.891632	9.819969	8.029991	7.971816
7.958592	7.751592	6.454993	6.287101	9.528179	9.280354	7.117541	6.932417	10.23876	9.972458	7.680761	7.480987
8.306943	8.405256	6.920105	7.002004	9.277549	9.387349	7.106899	7.191009	9.874824	9.991692	7.21034	7.295674
7.740011	7.747687	6.76309	6.769797	9.572697	9.58219	6.96995	6.976862	9.88124	9.89104	7.368253	7.375561
7.915454	7.84533	6.953398	6.891796	9.279623	9.197413	6.689822	6.630556	9.528711	9.444294	8.541475	8.465804
7.779731	7.824662	6.157237	6.192797	9.492454	9.547276	7.132316	7.173507	9.86719	9.924177	7.837676	7.882941
8.084123	7.906165	6.349367	6.209597	9.804341	9.588516	7.209879	7.051166	10.12528	9.902388	7.663871	7.495164
7.684869	7.416362	6.282741	6.063225	9.510489	9.178196	7.208196	6.956344	10.48058	10.1144	7.701283	7.432203
7.770203	7.845989	6.399541	6.461958	9.664272	9.758532	7.124778	7.194269	9.983091	10.08046	7.58224	7.656193
7.613959	7.536204	6.254401	6.190529	9.880728	9.779824	6.68372	6.615464	10.11565	10.01235	7.293225	7.218745
7.952566	7.680988	6.289902	6.075104	9.648991	9.319482	7.142998	6.899067	10.0898	9.745239	7.291332	7.042335
7.945055	7.814545	6.216235	6.114124	9.508587	9.352394	6.98083	6.866159	9.344705	9.191204	8.346249	8.209149
7.630024	7.287207	6.645141	6.346575	9.621553	9.189257	6.974716	6.661343	9.882927	9.438887	8.338715	7.964057
7.985513	7.784932	6.113868	5.960299	9.52904	9.289688	7.198428	7.017617	9.735466	9.490928	7.605153	7.414125

		RPS29	DDR2		ALK		ALK		EGFR		EGFR		EGFR		EGFR		EGFR		KRAS	
		216570_x_at	205168_at		208211_s_at		208212_s_at		201983_s_at		201984_s_at		210984_x_at		211550_at		211551_at		211607_x_at		204010_s_at	
GSM254625	Lung Cancer	12.9369	8.90873	6.512376	6.080085	4.444607	6.986887	5.107489	11.90086	8.699656	10.00427	7.313225	9.117993	6.66535	6.720559	4.9128	6.486877	4.741976	8.847607	6.467695	5.077474	3.711688
GSM254629	Lung Cancer	12.2582	8.501505	6.55878	6.556737	5.058422	7.163287	5.526365	10.48194	8.086654	9.517434	7.342553	8.986462	6.932917	7.126759	5.498184	6.825318	5.265627	8.919397	6.881177	4.941142	3.812015
GSM254636	Lung Cancer	12.6482	8.722198	6.521555	6.746213	5.044118	6.892645	5.153605	9.884534	7.390629	8.812866	6.589347	9.078502	6.787962	7.326579	5.478056	6.936971	5.186747	8.931057	6.677718	4.869283	3.640745
GSM254639	Lung Cancer	13.0887	9.290041	6.712357	6.539718	4.725159	6.757956	4.882843	9.067223	6.551364	9.530545	6.886129	9.144321	6.607069	7.088172	5.121435	7.25593	5.242646	9.015467	6.513968	5.34098	3.859032
GSM254648	Lung Cancer	13.1324	9.939094	7.157422	6.462138	4.653568	7.453312	5.36734	9.926185	7.148126	9.185259	6.614564	8.761732	6.30957	7.041447	5.070744	7.003162	5.043174	8.642139	6.223448	5.046569	3.634176
GSM254652	Lung Cancer	13.0767	8.919912	6.450841	7.070889	5.113636	8.434929	6.100103	10.36884	7.4987	8.540407	6.176384	8.787881	6.355357	7.105299	5.138521	6.8506	4.954324	8.734542	6.316782	4.660583	3.370513
GSM254659	Lung Cancer	13.026	9.14693	6.640767	6.640081	4.820768	7.244197	5.259362	11.38306	8.264217	9.954422	7.227014	9.399941	6.824455	7.061748	5.126902	6.810532	4.944517	9.224705	6.697232	4.588444	3.331258
GSM254674	Lung Cancer	12.9914	8.945545	6.511856	6.412272	4.667775	7.190527	5.234301	9.399217	6.842104	8.171105	5.948107	8.628877	6.281339	6.987604	5.086585	6.544827	4.764268	8.42834	6.13536	4.562435	3.321197
GSM254680	Lung Cancer	12.9482	8.713707	6.364254	6.638279	4.848418	7.345104	5.364663	10.51241	7.67798	9.282749	6.779867	8.934418	6.525455	7.069353	5.163263	6.973417	5.093194	8.940985	6.530251	4.753146	3.471568
GSM254686	Lung Cancer	13.2565	8.527245	6.083224	6.602262	4.709966	7.160286	5.108053	10.79775	7.702975	8.888619	6.341023	9.012448	6.429362	7.024172	5.010952	6.8504	4.886984	8.801847	6.279122	4.651129	3.318054
GSM254694	Lung Cancer	12.7319	8.919219	6.625025	6.587899	4.893366	7.157293	5.316301	12.19702	9.05971	9.824943	7.29778	9.572393	7.110191	7.189402	5.340151	6.89972	5.12498	9.301589	6.909042	4.614002	3.427192
GSM254700	Lung Cancer	12.804	8.672386	6.405409	6.319652	4.667684	6.840451	5.052345	10.46496	7.729399	9.020104	6.662233	8.895476	6.570183	7.065519	5.21858	6.751052	4.986315	8.99134	6.640988	4.872999	3.599188
GSM254701	Lung Cancer	13.2565	8.552371	6.101149	6.077868	4.335871	7.150829	5.101307	10.39112	7.41289	8.863014	6.322757	8.890539	6.342393	7.167776	5.113397	7.034202	5.018107	8.559302	6.106093	4.887856	3.486932
GSM254718	Lung Cancer	12.7738	9.609025	7.113988	6.600678	4.886775	7.064987	5.230524	10.97665	8.126501	9.473123	7.013374	9.199635	6.810899	7.105266	5.260344	7.106427	5.261204	9.017366	6.675957	4.80415	3.556726
GSM254726	Lung Cancer	13.5775	9.169518	6.386761	6.276165	4.37148	7.21176	5.023141	10.24562	7.136287	8.357384	5.821092	8.448174	5.884329	6.835278	4.760913	6.885446	4.795857	8.149511	5.676304	4.694149	3.269572
GSM254627	Lung Cancer	13.0808	8.90873	6.440735	6.080085	4.395713	6.986887	5.051302	11.90086	8.603952	10.00427	7.232773	9.117993	6.592025	6.720559	4.858755	6.486877	4.68981	8.847607	6.396545	5.077474	3.670856
GSM254630	Lung Cancer	12.9181	8.501505	6.223735	6.556737	4.80002	7.163287	5.24406	10.48194	7.673561	9.517434	6.967471	8.986462	6.57876	7.126759	5.217319	6.825318	4.996641	8.919397	6.529664	4.941142	3.617284
GSM254631	Lung Cancer	12.353	8.722198	6.677401	6.746213	5.164657	6.892645	5.276761	9.884534	7.567243	8.812866	6.746813	9.078502	6.950174	7.326579	5.608965	6.936971	5.310695	8.931057	6.837295	4.869283	3.727748
GSM254633	Lung Cancer	13.3931	9.290041	6.559798	6.539718	4.617765	6.757956	4.771865	9.067223	6.402464	9.530545	6.72962	9.144321	6.456903	7.088172	5.005035	7.25593	5.12349	9.015467	6.365918	5.34098	3.771323
GSM254637	Lung Cancer	12.9292	9.939094	7.269911	6.462138	4.726705	7.453312	5.451695	9.926185	7.260469	9.185259	6.718521	8.761732	6.408734	7.041447	5.150438	7.003162	5.122435	8.642139	6.321258	5.046569	3.691292
GSM254641	Lung Cancer	13.3135	8.919912	6.336103	7.070889	5.022683	8.434929	5.991604	10.36884	7.365324	8.540407	6.066528	8.787881	6.242317	7.105299	5.047125	6.8506	4.866204	8.734542	6.204429	4.660583	3.310564
GSM254642	Lung Cancer	12.6085	9.14693	6.86066	6.640081	4.980396	7.244197	5.433513	11.38306	8.537867	9.954422	7.466319	9.399941	7.05043	7.061748	5.296667	6.810532	5.108243	9.224705	6.918995	4.588444	3.441565
GSM254645	Lung Cancer	13.1825	8.945545	6.417457	6.412272	4.600108	7.190527	5.158422	9.399217	6.742917	8.171105	5.861881	8.628877	6.190282	6.987604	5.012847	6.544827	4.695203	8.42834	6.046418	4.562435	3.273051
GSM254647	Lung Cancer	13.0967	8.713707	6.292091	6.638279	4.793443	7.345104	5.303835	10.51241	7.590921	9.282749	6.702992	8.934418	6.451465	7.069353	5.104718	6.973417	5.035443	8.940985	6.456206	4.753146	3.432205

EGFR		EGFR		EGFR		KRAS		KRAS		KRAS		EML4	
211550_at		211551_at		211607_x_at		204010_s_at		204009_s_at		214352_s_at		220386_s_at	
6.720559	6.720559	6.486877	6.486877	8.847607	8.847607	5.077474	5.077474	10.85061	10.85061	11.75051	11.75051	8.760082	8.760082
7.126759	6.805739	6.825318	6.517876	8.919397	8.517629	4.941142	4.718572	9.676614	9.240738	10.59684	10.11951	8.981761	8.577184
7.326579	6.998617	6.936971	6.626449	8.931057	8.531273	4.869283	4.651318	8.757186	8.365186	10.07911	9.62794	8.171915	7.806113
7.088172	6.775893	7.25593	6.93626	9.015467	8.618278	5.34098	5.105676	8.963281	8.568391	10.23301	9.782184	8.134388	7.776016
7.041447	6.817632	7.003162	6.780564	8.642139	8.367446	5.046569	4.886162	9.32032	9.024071	10.3304	10.00204	8.401606	8.134558
7.105299	7.42013	6.8506	7.154145	8.734542	9.121563	4.660583	4.867091	9.357854	9.772494	10.79641	11.2748	8.553898	8.932915
7.061748	7.367721	6.810532	7.10562	9.224705	9.624395	4.588444	4.787253	8.44739	8.8134	10.31177	10.75856	8.937836	9.325096
6.987604	6.781784	6.544827	6.352049	8.42834	8.180083	4.562435	4.428048	8.952214	8.688527	10.21743	9.91648	8.476904	8.227217
7.069353	6.964887	6.973417	6.870369	8.940985	8.808861	4.753146	4.682907	8.888587	8.757238	10.45839	10.30385	9.774063	9.629628
7.024172	6.395852	6.8504	6.237623	8.801847	8.014512	4.651129	4.23508	9.628878	8.767564	10.34325	9.418033	9.455237	8.609455
7.189402	6.602522	6.89972	6.336487	9.301589	8.542288	4.614002	4.237355	9.047995	8.309395	10.5641	9.701737	7.993458	7.340941
7.065519	6.397649	6.751052	6.112907	8.99134	8.141431	4.872999	4.412377	8.733204	7.907696	9.535219	8.6339	7.942679	7.191895
7.167776	6.549749	7.034202	6.427692	8.559302	7.821294	4.887856	4.466411	9.332215	8.527563	10.22177	9.340414	8.563933	7.825525
7.105266	7.279866	7.106427	7.281056	9.017366	9.238952	4.80415	4.922204	8.90542	9.124255	10.16764	10.4175	8.301655	8.505655
6.835278	6.5568	6.885446	6.604924	8.149511	7.817489	4.694149	4.502903	8.896034	8.533599	10.11585	9.703722	8.446422	8.102304
6.720559	6.720559	6.486877	6.486877	8.847607	8.847607	5.077474	5.077474	10.85061	10.85061	11.75051	11.75051	8.760082	8.760082
7.126759	6.805739	6.825318	6.517876	8.919397	8.517629	4.941142	4.718572	9.676614	9.240738	10.59684	10.11951	8.981761	8.577184
7.326579	6.998617	6.936971	6.626449	8.931057	8.531273	4.869283	4.651318	8.757186	8.365186	10.07911	9.62794	8.171915	7.806113
7.088172	6.775893	7.25593	6.93626	9.015467	8.618278	5.34098	5.105676	8.963281	8.568391	10.23301	9.782184	8.134388	7.776016
7.041447	6.817632	7.003162	6.780564	8.642139	8.367446	5.046569	4.886162	9.32032	9.024071	10.3304	10.00204	8.401606	8.134558
7.105299	7.42013	6.8506	7.154145	8.734542	9.121563	4.660583	4.867091	9.357854	9.772494	10.79641	11.2748	8.553898	8.932915
7.061748	7.367721	6.810532	7.10562	9.224705	9.624395	4.588444	4.787253	8.44739	8.8134	10.31177	10.75856	8.937836	9.325096
6.987604	6.781784	6.544827	6.352049	8.42834	8.180083	4.562435	4.428048	8.952214	8.688527	10.21743	9.91648	8.476904	8.227217
7.069353	6.964887	6.973417	6.870369	8.940985	8.808861	4.753146	4.682907	8.888587	8.757238	10.45839	10.30385	9.774063	9.629628
7.024172	6.395852	6.8504	6.237623	8.801847	8.014512	4.651129	4.23508	9.628878	8.767564	10.34325	9.418033	9.455237	8.609455

ERBB2		ERBB2		BRAF		MET		MET		MET		MET	
210930_s_at		216836_s_at		206044_s_at		203510_at		211599_x_at		213807_x_at		213816_s_at	
5.019197	5.019197	10.9006	10.9006	6.948721	6.948721	10.73589	10.73589	9.144911	9.144911	8.351561	8.351561	6.681157	6.681157
4.944808	4.722072	9.847991	9.404395	7.525797	7.186802	10.55386	10.07847	8.473156	8.091489	8.258258	7.886271	7.032918	6.716125
5.393191	5.151774	9.822166	9.382493	7.169118	6.848205	7.413054	7.081222	8.081205	7.719464	7.993065	7.635269	6.204503	5.926769
5.537726	5.293753	9.263712	8.855586	7.197049	6.879973	7.787368	7.444284	7.676451	7.338254	7.520839	7.189498	6.33738	6.058178
5.166489	5.002271	9.696516	9.38831	7.255601	7.02498	9.632992	9.326804	8.480273	8.210725	8.344527	8.079293	6.737466	6.523313
5.07408	5.298909	9.698318	10.12804	7.137885	7.45416	9.429521	9.847336	8.394154	8.766093	7.973323	8.326615	6.730629	7.028858
5.17716	5.401477	9.930941	10.36123	7.574476	7.902665	9.72435	10.14569	8.666892	9.042413	8.295478	8.654907	7.168737	7.479345
5.054333	4.905458	10.82697	10.50806	6.982045	6.776389	10.31536	10.01152	8.42711	8.17889	8.06456	7.827018	6.771247	6.5718
5.142453	5.066461	9.999741	9.851971	7.559068	7.447365	11.70842	11.5354	10.57391	10.41766	9.476371	9.336336	8.95982	8.827418
5.098506	4.642439	11.07075	10.08045	7.328531	6.672985	11.53794	10.50586	9.574419	8.717976	9.07343	8.261802	7.343025	6.686183
5.244584	4.816462	10.45461	9.601189	7.130129	6.548088	10.45356	9.600225	8.481408	7.789059	8.355131	7.67309	7.166011	6.58104
5.277328	4.778488	9.586194	8.680056	7.018112	6.354723	9.620457	8.711081	8.219598	7.442638	7.933038	7.183166	6.660558	6.030967
5.092844	4.653724	11.01347	10.06385	7.509894	6.862368	10.9462	10.00239	8.188206	7.482194	8.141018	7.439075	7.489511	6.843743
5.282669	5.412482	9.57775	9.813107	7.342606	7.523038	8.922811	9.142074	7.938638	8.133717	7.901227	8.095387	7.194206	7.370991
5.087779	4.880496	10.10668	9.69492	6.987217	6.702549	9.304811	8.925721	8.147045	7.815124	7.853706	7.533736	6.831689	6.553357
5.019197	5.019197	10.9006	10.9006	6.948721	6.948721	10.73589	10.73589	9.144911	9.144911	8.351561	8.351561	6.681157	6.681157
4.944808	4.722072	9.847991	9.404395	7.525797	7.186802	10.55386	10.07847	8.473156	8.091489	8.258258	7.886271	7.032918	6.716125
5.393191	5.151774	9.822166	9.382493	7.169118	6.848205	7.413054	7.081222	8.081205	7.719464	7.993065	7.635269	6.204503	5.926769
5.537726	5.293753	9.263712	8.855586	7.197049	6.879973	7.787368	7.444284	7.676451	7.338254	7.520839	7.189498	6.33738	6.058178
5.166489	5.002271	9.696516	9.38831	7.255601	7.02498	9.632992	9.326804	8.480273	8.210725	8.344527	8.079293	6.737466	6.523313
5.07408	5.298909	9.698318	10.12804	7.137885	7.45416	9.429521	9.847336	8.394154	8.766093	7.973323	8.326615	6.730629	7.028858
5.17716	5.401477	9.930941	10.36123	7.574476	7.902665	9.72435	10.14569	8.666892	9.042413	8.295478	8.654907	7.168737	7.479345
5.054333	4.905458	10.82697	10.50806	6.982045	6.776389	10.31536	10.01152	8.42711	8.17889	8.06456	7.827018	6.771247	6.5718
5.142453	5.066461	9.999741	9.851971	7.559068	7.447365	11.70842	11.5354	10.57391	10.41766	9.476371	9.336336	8.95982	8.827418
5.098506	4.642439	11.07075	10.08045	7.328531	6.672985	11.53794	10.50586	9.574419	8.717976	9.07343	8.261802	7.343025	6.686183

ABCC1 202804_at		ABCC1 202805_s_at		AKT1 207163_s_at		PIK3CA 204369_at	
9.660216	9.660216	7.475769	7.475769	10.49991	10.49991	7.426923	7.426923
9.244343	8.827938	6.943111	6.630363	9.850881	9.407155	7.379147	7.046758
9.293197	8.877203	7.322345	6.994573	9.863793	9.422257	6.445242	6.156732
9.452996	9.036531	7.392268	7.066592	10.0518	9.608952	5.795668	5.540332
9.651251	9.344483	7.27166	7.040528	9.495192	9.193384	7.249267	7.018847
9.746048	10.17789	7.413753	7.742251	9.812312	10.24709	7.181253	7.499449
9.429029	9.837572	7.252308	7.566538	10.3964	10.84685	7.221355	7.534244
9.24704	8.974669	6.869095	6.666766	9.747402	9.460292	7.45382	7.234268
9.451874	9.3122	6.926194	6.823843	9.728215	9.584457	7.185545	7.079362
9.667411	8.80265	7.194969	6.551371	10.46215	9.526297	7.775797	7.080243
9.672213	8.882658	7.342236	6.74288	10.02931	9.210601	7.422936	6.816992
10.99829	9.958676	9.213701	8.342774	10.03054	9.082404	7.748376	7.015959
9.3223	8.518503	7.048239	6.440519	10.32263	9.432586	7.116289	6.502701
9.754645	9.994349	7.107859	7.282522	9.966737	10.21165	7.238057	7.41592
9.342168	8.961557	6.558639	6.291432	9.702689	9.307389	7.278408	6.981877
9.660216	9.660216	7.475769	7.475769	10.49991	10.49991	7.426923	7.426923
9.244343	8.827938	6.943111	6.630363	9.850881	9.407155	7.379147	7.046758
9.293197	8.877203	7.322345	6.994573	9.863793	9.422257	6.445242	6.156732
9.452996	9.036531	7.392268	7.066592	10.0518	9.608952	5.795668	5.540332
9.651251	9.344483	7.27166	7.040528	9.495192	9.193384	7.249267	7.018847
9.746048	10.17789	7.413753	7.742251	9.812312	10.24709	7.181253	7.499449
9.429029	9.837572	7.252308	7.566538	10.3964	10.84685	7.221355	7.534244
9.24704	8.974669	6.869095	6.666766	9.747402	9.460292	7.45382	7.234268
9.451874	9.3122	6.926194	6.823843	9.728215	9.584457	7.185545	7.079362
9.667411	8.80265	7.194969	6.551371	10.46215	9.526297	7.775797	7.080243

GSM254650	Lung Cancer	13.073	8.527245	6.168611	6.602262	4.776078	7.160286	5.179753	10.79775	7.811098	8.888619	6.430029	9.012448	6.519608	7.024172	5.081288	6.8504	4.955581	8.801847	6.367259
GSM254654	Lung Cancer	12.344	8.919219	6.833211	6.587899	5.047136	7.157293	5.483361	12.19702	9.344404	9.824943	7.527107	9.572393	7.333622	7.189402	5.50796	6.89972	5.286028	9.301589	7.126153
GSM254656	Lung Cancer	13.0067	8.672386	6.305585	6.319652	4.594941	6.840451	4.973608	10.46496	7.608942	9.020104	6.558407	8.895476	6.467791	7.065519	5.137252	6.751052	4.908607	8.99134	6.537493
GSM254657	Lung Cancer	12.4828	8.552371	6.479306	6.077868	4.604614	7.150829	5.417492	10.39112	7.872351	8.863014	6.71465	8.890539	6.735502	7.167776	5.430332	7.034202	5.329135	8.559302	6.484557
GSM254661	Lung Cancer	13.2993	9.609025	6.832891	6.600678	4.693682	7.064987	5.023848	10.97665	7.805395	9.473123	6.736252	9.199635	6.541777	7.105266	5.05249	7.106427	5.053316	9.017366	6.412167
GSM254663	Lung Cancer	12.7196	9.169518	6.817529	6.276165	4.666323	7.21176	5.361937	10.24562	7.617609	8.357384	6.213708	8.448174	6.28121	6.835278	5.082023	6.885446	5.119323	8.149511	6.059154
GSM254664	Lung Cancer	12.9077	8.90873	6.527109	6.080085	4.454662	6.986887	5.119043	11.90086	8.719336	10.00427	7.329769	9.117993	6.680428	6.720559	4.923914	6.486877	4.752703	8.847607	6.482326
GSM254666	Lung Cancer	13.307	8.501505	6.041845	6.556737	4.659739	7.163287	5.090801	10.48194	7.449299	9.517434	6.763845	8.986462	6.386494	7.126759	5.064841	6.825318	4.850614	8.919397	6.338833
GSM254668	Lung Cancer	12.7939	8.722198	6.447286	6.746213	4.986674	6.892645	5.094914	9.884534	7.306463	8.812866	6.514306	9.078502	6.710659	7.326579	5.41567	6.936971	5.127679	8.931057	6.60167
GSM254670	Lung Cancer	13.0574	9.290041	6.728447	6.539718	4.736486	6.757956	4.894548	9.067223	6.567068	9.530545	6.902636	9.144321	6.622907	7.088172	5.133712	7.25593	5.255213	9.015467	6.529583
GSM254672	Lung Cancer	13.3135	9.939094	7.060062	6.462138	4.590267	7.453312	5.29433	9.926185	7.050892	9.185259	6.524588	8.761732	6.223743	7.041447	5.001768	7.003162	4.974573	8.642139	6.138792
GSM254675	Lung Cancer	12.6085	8.919912	6.690384	7.070889	5.303524	8.434929	6.326623	10.36884	7.777154	8.540407	6.405736	8.787881	6.591355	7.105299	5.329333	6.8506	5.138296	8.734542	6.551347
GSM254678	Lung Cancer	13.1825	9.14693	6.561929	6.640081	4.763537	7.244197	5.196924	11.38306	8.166106	9.954422	7.141217	9.399941	6.743436	7.061748	5.066037	6.810532	4.885817	9.224705	6.617724
GSM254682	Lung Cancer	13.0967	8.945545	6.459499	6.412272	4.630245	7.190527	5.192216	9.399217	6.787092	8.171105	5.900283	8.628877	6.230836	6.987604	5.045688	6.544827	4.725962	8.42834	6.08603
GSM254684	Lung Cancer	12.9369	8.713707	6.369813	6.638279	4.852653	7.345104	5.369349	10.51241	7.684686	9.282749	6.785789	8.934418	6.531155	7.069353	5.167773	6.973417	5.097642	8.940985	6.535955
GSM254686	Lung Cancer	12.2582	8.527245	6.578637	6.602262	5.093543	7.160286	5.52405	10.79775	8.3303	8.888619	6.857432	9.012448	6.952965	7.024172	5.419041	6.8504	5.284977	8.801847	6.790489
GSM254688	Lung Cancer	12.6482	8.919219	6.668867	6.587899	4.925748	7.157293	5.351482	12.19702	9.119663	9.824943	7.346073	9.572393	7.157243	7.189402	5.375489	6.89972	5.158895	9.301589	6.954763
GSM254690	Lung Cancer	13.0887	8.672386	6.266081	6.319652	4.566154	6.840451	4.942448	10.46496	7.561272	9.020104	6.517319	8.895476	6.427271	7.065519	5.105068	6.751052	4.877855	8.99134	6.496536
GSM254692	Lung Cancer	13.1324	8.552371	6.158804	6.077868	4.376844	7.150829	5.149514	10.39112	7.482941	8.863014	6.382507	8.890539	6.402328	7.167776	5.161718	7.034202	5.065527	8.559302	6.163795
GSM254696	Lung Cancer	13.0767	9.609025	6.949205	6.600678	4.773581	7.064987	5.109367	10.97665	7.938264	9.473123	6.850921	9.199635	6.653135	7.105266	5.138497	7.106427	5.139337	9.017366	6.521319
GSM254697	Lung Cancer	13.026	9.169518	6.657166	6.276165	4.556561	7.21176	5.235813	10.24562	7.438426	8.357384	6.067548	8.448174	6.133463	6.835278	4.962483	6.885446	4.998906	8.149511	5.91663
GSM254698	Lung Cancer	12.9914	8.90873	6.485057	6.080085	4.425962	6.986887	5.086062	11.90086	8.66316	10.00427	7.282545	9.117993	6.637388	6.720559	4.892191	6.486877	4.722083	8.847607	6.440563
GSM254704	Lung Cancer	12.9482	8.501505	6.209267	6.556737	4.788862	7.163287	5.231869	10.48194	7.655722	9.517434	6.951274	8.986462	6.563467	7.126759	5.20519	6.825318	4.985026	8.919397	6.514484
GSM254705	Lung Cancer	13.2565	8.722198	6.222301	6.746213	4.812659	6.892645	4.917122	9.884534	7.051496	8.812866	6.286982	9.078502	6.476483	7.326579	5.226685	6.936971	4.948743	8.931057	6.371298
GSM254707	Lung Cancer	12.7319	9.290041	6.900465	6.539718	4.857577	6.757956	5.019681	9.067223	6.73496	9.530545	7.079106	9.144321	6.792226	7.088172	5.264959	7.25593	5.389566	9.015467	6.696516
GSM254709	Lung Cancer	12.804	9.939094	7.340998	6.462138	4.772924	7.453312	5.505003	9.926185	7.331463	9.185259	6.784216	8.761732	6.4714	7.041447	5.2008	7.003162	5.172523	8.642139	6.383069
GSM254716	Lung Cancer	13.2565	8.919912	6.363347	7.070889	5.044279	8.434929	6.017367	10.36884	7.396994	8.540407	6.092613	8.787881	6.269158	7.105299	5.068827	6.8506	4.887128	8.734542	6.231107
GSM254720	Lung Cancer	12.7738	9.14693	6.771879	6.640081	4.915947	7.244197	5.363201	11.38306	8.427382	9.954422	7.369701	9.399941	6.959194	7.061748	5.228126	6.810532	5.042139	9.224705	6.829459
GSM254721	Lung Cancer	13.5775	8.945545	6.230759	6.412272	4.466281	7.190527	5.008352	9.399217	6.54675	8.171105	5.691345	8.628877	6.010193	6.987604	4.867012	6.544827	4.558609	8.42834	5.870514

9.572393	8.790986	7.189402	6.602522	6.89972	6.336487	9.301589	8.542288	4.614002	4.237355	9.047995	8.309395	10.5641	9.701737
8.895476	8.054629	7.065519	6.397649	6.751052	6.112907	8.99134	8.141431	4.872999	4.412377	8.733204	7.907696	9.535219	8.6339
8.890539	8.12397	7.167776	6.549749	7.034202	6.427692	8.559302	7.821294	4.887856	4.466411	9.332215	8.527563	10.22177	9.340414
9.199635	9.4257	7.105266	7.279866	7.106427	7.281056	9.017366	9.238952	4.80415	4.922204	8.90542	9.124255	10.16764	10.4175
8.448174	8.103985	6.835278	6.5568	6.885446	6.604924	8.149511	7.817489	4.694149	4.502903	8.896034	8.533599	10.11585	9.703722
9.117993	8.828174	6.720559	6.506944	6.486877	6.280689	8.847607	8.566383	5.077474	4.916085	10.85061	10.50572	11.75051	11.37702
8.986462	9.384646	7.126759	7.44254	6.825318	7.127743	8.919397	9.31461	4.941142	5.160081	9.676614	10.10538	10.59684	11.06638
9.078502	9.471857	7.326579	7.644027	6.936971	7.237537	8.931057	9.318023	4.869283	5.080261	8.757186	9.136619	10.07911	10.51582
9.144321	8.874975	7.088172	6.87939	7.25593	7.042207	9.015467	8.749916	5.34098	5.183662	8.963281	8.699268	10.23301	9.931601
8.761732	8.632257	7.041447	6.937393	7.003162	6.899674	8.642139	8.514431	5.046569	4.971994	9.32032	9.182591	10.3304	10.17774
8.787881	8.001795	7.105299	6.469722	6.8506	6.237806	8.734542	7.953227	4.660583	4.243689	9.357854	8.520783	10.79641	9.830663
9.399941	8.632611	7.061748	6.485288	6.810532	6.254579	9.224705	8.471681	4.588444	4.213883	8.44739	7.757819	10.31177	9.470009
8.628877	7.81323	6.987604	6.327099	6.544827	5.926176	8.42834	7.631649	4.562435	4.13117	8.952214	8.106004	10.21743	9.251628
8.934418	8.570419	7.069353	6.781339	6.973417	6.689311	8.940985	8.576718	4.753146	4.559497	8.888587	8.526455	10.45839	10.0323
9.012448	9.012448	7.024172	7.024172	6.8504	6.8504	8.801847	8.801847	4.651129	4.651129	9.628878	9.628878	10.34325	10.34325
9.572393	9.141211	7.189402	6.865561	6.89972	6.588926	9.301589	8.882605	4.614002	4.406167	9.047995	8.640434	10.5641	10.08825
8.895476	8.497285	7.065519	6.749243	6.751052	6.448853	8.99134	8.588858	4.872999	4.654868	8.733204	8.342277	9.535219	9.108391
8.890539	8.498854	7.167776	6.85199	7.034202	6.7243	8.559302	8.18221	4.887856	4.672515	9.332215	8.921071	10.22177	9.771431
9.199635	8.907222	7.105266	6.879423	7.106427	6.880547	9.017366	8.730746	4.80415	4.651449	8.90542	8.622358	10.16764	9.844462
8.448174	8.822507	6.835278	7.138144	6.885446	7.190535	8.149511	8.51061	4.694149	4.902143	8.896034	9.290211	10.11585	10.56408
9.117993	9.513059	6.720559	7.011749	6.486877	6.767942	8.847607	9.230958	5.077474	5.297472	10.85061	11.32074	11.75051	12.25964
8.986462	8.721766	7.126759	6.91684	6.825318	6.624278	8.919397	8.656677	4.941142	4.795601	9.676614	9.39159	10.59684	10.28471
9.078502	8.944346	7.326579	7.218311	6.936971	6.834461	8.931057	8.799079	4.869283	4.797328	8.757186	8.627778	10.07911	9.930171
9.144321	8.326351	7.088172	6.454127	7.25593	6.606879	9.015467	8.209023	5.34098	4.863223	8.963281	8.161506	10.23301	9.317659
8.761732	8.0465	7.041447	6.466644	7.003162	6.431485	8.642139	7.93667	5.046569	4.634611	9.32032	8.55949	10.3304	9.487114
8.787881	7.957204	7.105299	6.433669	6.8506	6.203045	8.734542	7.908907	4.660583	4.220041	9.357854	8.4733	10.79641	9.775881
9.399941	8.58945	7.061748	6.452863	6.810532	6.223308	9.224705	8.429324	4.588444	4.192814	8.44739	7.719031	10.31177	9.422661
8.628877	8.354605	6.987604	6.765501	6.544827	6.336798	8.42834	8.160442	4.562435	4.417416	8.952214	8.667665	10.21743	9.892669
8.934418	9.330296	7.069353	7.382591	6.973417	7.282404	8.940985	9.337154	4.753146	4.963754	8.888587	9.282435	10.45839	10.9218
9.012448	9.402942	7.024172	7.328517	6.8504	7.147215	8.801847	9.183216	4.651129	4.852654	9.628878	10.04608	10.34325	10.7914
9.572393	9.290439	7.189402	6.977639	6.89972	6.696489	9.301589	9.027611	4.614002	4.478096	9.047995	8.781486	10.5641	10.25293
8.895476	8.764025	7.065519	6.96111	6.751052	6.651289	8.99134	8.858472	4.872999	4.800989	8.733204	8.60415	9.535219	9.394313

7.993458	7.340941	5.244584	4.816462	10.45461	9.601189	7.130129	6.548088	10.45356	9.600225	8.481408	7.789059	8.355131	7.67309
7.942679	7.191895	5.277328	4.778488	9.586194	8.680056	7.018112	6.354723	9.620457	8.711081	8.219598	7.442638	7.933038	7.183166
8.563933	7.825525	5.092844	4.653724	11.01347	10.06385	7.509894	6.862368	10.9462	10.00239	8.188206	7.482194	8.141018	7.439075
8.301655	8.505655	5.282669	5.412482	9.57775	9.813107	7.342606	7.523038	8.922811	9.142074	7.938638	8.133717	7.901227	8.095387
8.446422	8.102304	5.087779	4.880496	10.10668	9.69492	6.987217	6.702549	9.304811	8.925721	8.147045	7.815124	7.853706	7.533736
8.760082	8.48164	5.019197	4.85966	10.9006	10.55412	6.948721	6.727854	10.73589	10.39465	9.144911	8.854237	8.351561	8.086104
8.981761	9.379736	4.944808	5.163909	9.847991	10.28435	7.525797	7.85926	10.55386	11.0215	8.473156	8.848596	8.258258	8.624176
8.171915	8.52599	5.393191	5.626869	9.822166	10.24774	7.169118	7.479743	7.413054	7.734249	8.081205	8.431349	7.993065	8.33939
8.134388	7.89479	5.537726	5.374612	9.263712	8.99085	7.197049	6.98506	7.787368	7.557991	7.676451	7.450341	7.520839	7.299313
8.401606	8.277452	5.166489	5.090142	9.696516	9.553228	7.255601	7.148383	9.632992	9.490642	8.480273	8.354957	8.344527	8.221217
8.553898	7.788742	5.07408	4.620198	9.698318	8.830792	7.137885	6.499393	9.429521	8.586039	8.394154	7.643287	7.973323	7.2601
8.937836	8.208229	5.17716	4.754542	9.930941	9.120265	7.574476	6.956162	9.72435	8.930539	8.666892	7.959402	8.295478	7.618308
8.476904	7.675623	5.054333	4.576571	10.82697	9.803544	6.982045	6.322066	10.31536	9.340294	8.42711	7.630535	8.06456	7.302255
9.774063	9.375856	5.142453	4.932943	9.999741	9.592339	7.559068	7.251102	11.70842	11.2314	10.57391	10.14312	9.476371	9.090292
9.455237	9.455237	5.098506	5.098506	11.07075	11.07075	7.328531	7.328531	11.53794	11.53794	9.574419	9.574419	9.07343	9.07343
7.993458	7.633398	5.244584	5.008345	10.45461	9.983692	7.130129	6.808957	10.45356	9.98269	8.481408	8.099368	8.355131	7.978779
7.942679	7.587138	5.277328	5.041098	9.586194	9.157084	7.018112	6.703959	9.620457	9.189814	8.219598	7.851662	7.933038	7.57793
8.563933	8.186637	5.092844	4.868472	11.01347	10.52825	7.509894	7.179035	10.9462	10.46395	8.188206	7.827463	8.141018	7.782354
8.301655	8.037785	5.282669	5.114758	9.57775	9.273318	7.342606	7.109219	8.922811	8.639196	7.938638	7.686306	7.901227	7.650084
8.446422	8.820677	5.087779	5.313215	10.10668	10.5545	6.987217	7.296816	9.304811	9.7171	8.147045	8.508035	7.853706	8.201698
8.760082	9.139641	5.019197	5.23667	10.9006	11.37291	6.948721	7.249797	10.73589	11.20106	9.144911	9.541144	8.351561	8.71342
8.981761	8.717203	4.944808	4.799159	9.847991	9.557919	7.525797	7.304125	10.55386	10.243	8.473156	8.223579	8.258258	8.015012
8.171915	8.051156	5.393191	5.313494	9.822166	9.67702	7.169118	7.063177	7.413054	7.303509	8.081205	7.961786	7.993065	7.874949
8.134388	7.406758	5.537726	5.04237	9.263712	8.435062	7.197049	6.553265	7.787368	7.090779	7.676451	6.989783	7.520839	6.848091
8.401606	7.715772	5.166489	4.744742	9.696516	8.904977	7.255601	6.663317	9.632992	8.846638	8.480273	7.788017	8.344527	7.663352
8.553898	7.745338	5.07408	4.594452	9.698318	8.781582	7.137885	6.463175	9.429521	8.538193	8.394154	7.600694	7.973323	7.219642
8.937836	8.167189	5.17716	4.73077	9.930941	9.074665	7.574476	6.921382	9.72435	8.885888	8.666892	7.919607	8.295478	7.580217
8.476904	8.207463	5.054333	4.893679	10.82697	10.48283	6.982045	6.760119	10.31536	9.987478	8.42711	8.159252	8.06456	7.808225
9.774063	10.20714	5.142453	5.370311	9.999741	10.44282	7.559068	7.894005	11.70842	12.22721	10.57391	11.04244	9.476371	9.896263
9.455237	9.864915	5.098506	5.319415	11.07075	11.55042	7.328531	7.646063	11.53794	12.03786	9.574419	9.989262	9.07343	9.466566
7.993458	7.75801	5.244584	5.090105	10.45461	10.14667	7.130129	6.920111	10.45356	10.14565	8.481408	8.231588	8.355131	8.10903
7.942679	7.825307	5.277328	5.199344	9.586194	9.444535	7.018112	6.914403	9.620457	9.478293	8.219598	8.098134	7.933038	7.815809

7.166011	6.58104	9.672213	8.882658	7.342236	6.74288	10.02931	9.210601	7.422936	6.816992
6.660558	6.030967	10.99829	9.958676	9.213701	8.342774	10.03054	9.082404	7.748376	7.015959
7.489511	6.843743	9.3223	8.518503	7.048239	6.440519	10.32263	9.432586	7.116289	6.502701
7.194206	7.370991	9.754645	9.994349	7.107859	7.282522	9.966737	10.21165	7.238057	7.41592
6.831689	6.553357	9.342168	8.961557	6.558639	6.291432	9.702689	9.307389	7.278408	6.981877
6.681157	6.468794	9.660216	9.353163	7.475769	7.23815	10.49991	10.16617	7.426923	7.190856
7.032918	7.344542	9.244343	9.653954	6.943111	7.250755	9.850881	10.28737	7.379147	7.706111
6.204503	6.473333	9.293197	9.695855	7.322345	7.63961	9.863793	10.29117	6.445242	6.724503
6.33738	6.150713	9.452996	9.174559	7.392268	7.174529	10.0518	9.755723	5.795668	5.624957
6.737466	6.637904	9.651251	9.508631	7.27166	7.164204	9.495192	9.354878	7.249267	7.142142
6.730629	6.128566	9.746048	8.874253	7.413753	6.750584	9.812312	8.93459	7.181253	6.538881
7.168737	6.583543	9.429029	8.659325	7.252308	6.660293	10.3964	9.547724	7.221355	6.631867
6.771247	6.131193	9.24704	8.372961	6.869095	6.219792	9.747402	8.826026	7.45382	6.749246
8.95982	8.594786	9.451874	9.066793	6.926194	6.644012	9.728215	9.331875	7.185545	6.892797
7.343025	7.343025	9.667411	9.667411	7.194969	7.194969	10.46215	10.46215	7.775797	7.775797
7.166011	6.843223	9.672213	9.236535	7.342236	7.01151	10.02931	9.577542	7.422936	7.088575
6.660558	6.36241	10.99829	10.50597	9.213701	8.801266	10.03054	9.581544	7.748376	7.401533
7.489511	7.15955	9.3223	8.911593	7.048239	6.737719	10.32263	9.867856	7.116289	6.802771
7.194206	6.965536	9.754645	9.44459	7.107859	6.881933	9.966737	9.649941	7.238057	7.007993
6.831689	7.134396	9.342168	9.756113	6.558639	6.849248	9.702689	10.13261	7.278408	7.60091
6.681157	6.970639	9.660216	10.07878	7.475769	7.799681	10.49991	10.95485	7.426923	7.748719
7.032918	6.825764	9.244343	8.972051	6.943111	6.738602	9.850881	9.560723	7.379147	7.161794
6.204503	6.112817	9.293197	9.155869	7.322345	7.214141	9.863793	9.718032	6.445242	6.349998
6.33738	5.770494	9.452996	8.607415	7.392268	6.731021	10.0518	9.152653	5.795668	5.277239
6.737466	6.187478	9.651251	8.863407	7.27166	6.678065	9.495192	8.720087	7.249267	6.6575
6.730629	6.094414	9.746048	8.8248	7.413753	6.712966	9.812312	8.884801	7.181253	6.502443
7.168737	6.550627	9.429029	8.61603	7.252308	6.626992	10.3964	9.499987	7.221355	6.598709
6.771247	6.55602	9.24704	8.95312	6.869095	6.650759	9.747402	9.437577	7.45382	7.216898
8.95982	9.356823	9.451874	9.87068	6.926194	7.233088	9.728215	10.15926	7.185545	7.503931
7.343025	7.661186	9.667411	10.08628	7.194969	7.506715	10.46215	10.91545	7.775797	8.112708
7.166011	6.954936	9.672213	9.387318	7.342236	7.12597	10.02931	9.733893	7.422936	7.204293
6.660558	6.562133	10.99829	10.83577	9.213701	9.077547	10.03054	9.882319	7.748376	7.633876